GEOLOGICAL SURVEY OF CANADA
BULLETIN 506

GEOLOGY AND METALLOGENY OF THE KLUANE MAFIC-ULTRAMAFIC BELT, YUKON TERRITORY, CANADA: EASTERN WRANGELLIA – A NEW Ni-Cu-PGE METALLOGENIC TERRANE

L.J. Hulbert

1997

Natural Resources Canada | Ressources naturelles Canada

Canada

Canada-Yukon economic
development agreement

Contribution to Canada-Yukon Mineral Resource Development Cooperation Agreement (1991-1996),
a subsidiary agreement under the Canada-Yukon Economic Development Agreement

Contribution à l'Entente de coopération Canada-Yukon sur l'exploitation minérale (1991-1996),
entente auxiliaire négociée en vertu de l'Entente Canada-Yukon de développement économique

Yukon
Government

Canada

GEOLOGICAL SURVEY OF CANADA
BULLETIN 506

GEOLOGY AND METALLOGENY OF THE KLUANE MAFIC-ULTRAMAFIC BELT, YUKON TERRITORY, CANADA: EASTERN WRANGELLIA – A NEW Ni-Cu-PGE METALLOGENIC TERRANE

L.J. Hulbert

1997

Catalogue No. M42-506E
ISBN 0-660-16815-4

Available in Canada from
Geological Survey of Canada offices:

601 Booth Street
Ottawa, Ontario K1A 0E8

3303-33rd Street N.W.,
Calgary, Alberta T2L 2A7

101-605 Robson Street
Vancouver, B.C. V6B 1R8

or from

Canada Communication Group — Publishing
Ottawa, Ontario K1A 0S9

A deposit copy of this publication is also available for reference
in selected public libraries across Canada

Price subject to change without notice

Cover illustration

The Kluane Range looking west from the south end of Kluane Lake.
GSC 1996-105

Author's address

Geological Survey of Canada
601 Booth Street
Ottawa, Ontario
K1A 0E8

Original manuscript submitted: 1995–03
Final version approved for publication: 1995–09

CONTENTS

Appendixes

Tables

GEOLOGY AND METALLOGENY OF THE KLUANE MAFIC-ULTRAMAFIC BELT, YUKON TERRITORY, CANADA: EASTERN WRANGELLIA — A NEW Ni-Cu-PGE METALLOGENIC TERRANE

Abstract

Triassic mafic-ultramafic intrusive complexes along the eastern margin of "Wrangellia", adjacent the Denali fault from east-central Alaska to northern British Columbia, constitutes a newly recognized Ni-Cu-PGE metallogenic terrane that can be traced along strike for at least 600 km. These sill-like intrusive centres acted as subvolcanic magma chambers that fed the thick, overlying basalts of the Nikolai Group. Confinement of these olivine-rich ultramafic sills, Ni-Cu-PGE mineralization and more olivine normative and primitive coeval basalts exclusively to the eastern portion of Wrangellia is believed to be a product of melts forming in closer proximity to the hotter axial "jet" of the mantle plume that initiated melting, relative to the cooler more distal portions. Although the parental magmas that gave rise to these intrusive and extrusive rocks are clearly of a tholeiitic origin, the intrusive complexes have striking similarities to Archean and Proterozoic komatiitic ultramafic bodies that host world class nickel sulphide deposits. The unprecedented levels of platinum group elements, the vast extent of this mineralized terrane (second only to the Circum-Superior Belt of North America), the temporal association with Siberian trap magmatism, and the accompanying Noril'sk mineralizing event suggest that mantle plume activity during the Permo-Triassic was unique with respect to the Phanerozoic record.

Because of the potential economic significance of this newly recognized Ni-Cu-PGE metallogenic terrane, and the general absence of vital information pertaining to the intrusions, sulphide deposits and mineralized occurrences, and the surrounding local geology and tectonomagmatic framework, this detailed report provides much needed documentation required for a better understanding of the tectono-stratigraphic and magmatic setting of Wrangellia and Ni-Cu-PGE metallogenic processes during the Triassic.

Résumé

Les complexes intrusifs de roches mafiques-ultramafiques du Trias situés le long de la marge orientale de la «Wrangellie», que l'on peut observer à proximité de la faille de Denali du centre est de l'Alaska au nord de la Colombie-Britannique, ont récemment permis de définir un nouveau terrane métallogénique à minéralisations de Ni-Cu-ÉGP que l'on peut suivre dans une direction longitudinale sur une distance d'au moins 600 km. Ces centres intrusifs qui adoptent la forme de filons-couches sont les témoins de chambres magmatiques subvolcaniques desquelles sont issus les magmas qui ont alimenté les épaisses successions de coulées basaltiques sus-jacentes du Groupe de Nikolai. Le fait que ces filons-couches ultramafiques riches en olivine, que la minéralisation à Ni-Cu-ÉGP et que les basaltes contemporains des intrusions présentant un caractère plus primitif et une concentration d'olivine normative plus élevée soient confinés à la portion orientale de la Wrangellie pourrait s'expliquer par la formation des bains silicatés à plus faible distance du «jet» axial plus chaud du panache mantellique responsable de la fusion, plutôt que dans les portions plus éloignées et plus froides. Même si les magmas parentaux qui ont donné naissance à ces roches intrusives et extrusives sont nettement d'origine tholéiitique, les complexes intrusifs présentent des similarités étonnantes avec les massifs de roches ultramafiques aux affinités komatiitiques de l'Archéen et du Protérozoïque qui recèlent des gisements sulfurés de nickel de classe mondiale. L'existence de concentrations d'éléments du groupe du platine hors du commun, la grande étendue de ce terrane métallogénique (le deuxième en superficie après la ceinture périphérique de la Province du lac Supérieur en Amérique du Nord), l'association dans le temps avec l'activité magmatique à l'origine des trapps en Sibérie et l'épisode minéralisateur associé de Noril'sk nous amènent à penser que l'activité de panaches mantelliques au Permien-Trias a été un événement unique dans l'histoire du Phanérozoïque.

Étant donné la possible importance économique de ce terrane métallogénique à minéralisations de Ni-Cu-ÉGP récemment découvert et étant donné l'absence générale d'informations essentielles sur les intrusions, les gisements sulfurés et les indices minéralisés ainsi que sur la géologie locale et le cadre tectonomagmatique des environs, la présente étude renferme des renseignements indispensables pour bien comprendre le contexte tectonostratigraphique et magmatique de la Wrangellie et les processus métallogéniques responsables des minéralisations de Ni-Cu-ÉGP durant le Trias.

SUMMARY

Investigation of Triassic mafic-ultramafic intrusions along the eastern margin of "Wrangellia" in northern British Columbia, the Yukon, and east-central Alaska has resulted in the recognition of a new Ni-Cu-PGE metallogenic belt that can be traced along strike for at least 600 km. This belt of mineralized mafic to predominantly ultramafic rocks is referred to as the "Kluane Mafic-Ultramafic Belt" and is best developed, mineralized and preserved in the Kluane Mountain Ranges of the Yukon. On a North American scale this belt is second only, in size and extent, to the nickeliferous Circum-Superior Belt (CSB) of Canada, and has many similar features with respect to: lithological zonation, silicate mineralogy, distribution of ores, and Ni-Cu-PGE grades. However, unlike the Circum-Superior Belt intrusions, which are Proterozoic and of a komatiitic origin, the Kluane Belt intrusive complexes are clearly younger, tholeiitic, and generally much larger in size.

Kluane mafic-ultramafic intrusions originally had a well developed internal lithological zonation consisting of a thin gabbroic margin that envelopes the intrusion, and the complex becomes progressively more mafic towards the core of the intrusion giving rise to: mela-gabbro, clinopyroxenite, olivine clinopyroxenite, wehrlite, and dunite zones, respectively. These zoned bodies are sill- and lens-like in form and are believed to represent subvolcanic magma chambers that fed the overlying Triassic Nikolai basalt. On a regional scale, these bodies preferentially intrude the Pennsylvanian to Permian country rock sequence at or near the contact between the Station Creek and Hasen Creek formations. This level marks an important lithostratigraphic break from predominantly volcanic and volcanoclastic rocks to argillite, chert, and carbonate strata. Selective silling of magma at this level probably resulted from a combination of a change in the regional ambient stress field and the mechanical competency and permeability of the strata at this horizon.

Field relationships and geochemical and isotopic studies also suggest that the volatile, sulphur- and Ba-rich Permian strata acted as an important source of magma contamination that subsequently initiated sulphide immiscibility within successive incursions of olivine phenocryst-charged magma. The best mineralization appears to be concentrated as a result of riffling of sulphide-bearing magma flowing over

SOMMAIRE

L'étude des intrusions mafiques-ultramafiques du Trias le long de la marge orientale de la «Wrangellie» dans le nord de la Colombie-Britannique, au Yukon et dans le centre est de l'Alaska a permis d'établir l'existence d'une ceinture métallogénique à minéralisations de Ni-Cu-ÉGP que l'on peut suivre dans une direction longitudinale sur une distance d'au moins 600 km. Cette bande de roches minéralisées de composition mafique et, surtout, ultramafique est appelée «ceinture de roches mafiques-ultramafiques de Kluane» et c'est dans les chaînons Kluane au Yukon qu'elle montre le meilleur développement, contient les plus importantes minéralisations et est le mieux conservée. À l'échelle de l'Amérique du Nord, cette ceinture est la deuxième, par la taille et l'étendue, après la ceinture nickélifère du pourtour de la Province du lac Supérieur (Circum-Superior Belt) au Canada avec laquelle elle partage de nombreuses caractéristiques, dont les suivantes : zonalité lithologique, minéralogie des silicates, répartition des minerais et teneurs en Ni-Cu-ÉGP. Cependant, contrairement aux intrusions de la ceinture périphérique de la Province du lac Supérieur, qui sont d'âge protérozoïque et montrent des affinités komatiitiques, les complexes intrusifs de la ceinture de Kluane sont nettement plus récents, de caractère tholéiitique et généralement de plus grande taille.

Les intrusions mafiques-ultramafiques de la ceinture de Kluane présentaient à l'origine une zonalité lithologique interne bien marquée, définie par une mince bordure gabbroïque enveloppant une succession de zones lithologiques de composition progressivement plus mafique en se dirigeant vers le noyau de l'intrusion : gabbro mélanocrate, clinopyroxénite, clinopyroxénite à olivine, wehrlite et dunite. Ces corps intrusifs zonés adoptent la forme de filons-couches et de lentilles et pourraient représenter les chambres magmatiques subvolcaniques ayant alimenté les successions sus-jacentes du basalte de Nikolai qui se sont mises en place au Trias. À l'échelle régionale, ces corps intrusifs se sont mis en place préférentiellement dans la séquence de roches environnantes du Pennsylvanien-Permien au contact des formations de Station Creek et de Hasen Creek, ou près de celui-ci. Ce niveau coïncide avec une importante discontinuité lithostratigraphique assurant le passage d'une succession de roches à prédominance volcanique et volcanoclastique à une succession d'argilite, de chert et de roches carbonatées. La mise en place préférentielle des filons-couches à ce niveau est probablement le reflet d'un changement dans le champ de contraintes régional combiné à une modification de la compétence mécanique et de la perméabilité des couches.

Les relations établies à partir des observations de terrain combinées aux résultats d'études géochimiques et isotopiques indiquent en outre que les couches permiennes riches en éléments volatils, en soufre et en baryum ont été une source importante de contamination du magma, ce qui a par la suite causé l'immiscibilité des sulfures dans les poussées successives de magma chargé de phénocristaux d'olivine.

irregularities at the base of the intrusion. However, other styles of mineralization such as the Ni-rich "offset" ores that occur well within the footwall strata of the White River Complex, "skarn" ores juxtaposed with the Permian carbonate at the Quill Creek Complex, disseminated sulphides within or above the gabbro-ultramafic zone contact in most intrusions, and PGE+Au-rich zones associated with hydrothermal (metasomatic) quartz-carbonate alteration that envelope the extremities of many intrusions, are also important reserves. In addition, the ultramafic zones of the Kluane intrusions should be re-examined as sizeable Ni-Cu-PGE massive sulphide concentrations can be contained within this zone. Each of these types of mineralization is discussed in detail to provide vital background information necessary for future discoveries and exploitation.

Recent exploration of the Quill Creek Complex has disclosed three major zones and one minor zone of gabbro-hosted massive and disseminated sulphide mineralization. Five types of primary magmatic sulphide have been identified within these zones. In addition, three types of postmagmatic hydrothermal and metasomatic mineralization have been recognized. Some of this mineralization is very rich in gold and platinum-group elements. Mining of the Wellgreen deposit within the complex has demonstrated that basal accumulations of massive sulphides are generally up to 60 m in length, less than 20 m in thickness, and have average mill feed grades of 2.23% Ni, 1.39% Cu, 1300 ppb Pt, 920 ppb Pd, 171 ppb Au, 400 ppb Rh, 420 ppb Ru, 250 ppb Ir, 200 ppb Os, 200 ppb Re. Detailed geochemical profiles through these massive sulphide ores disclosed that the sulphides have experienced considerable PGE+Au fractionation. The lower half of the ore bodies are generally enriched in Os, Ir, Ru, and Rh, with grades of 1000 to 2000 ppb for each. The best values generally occur associated with the most Ni-rich intervals; however, Pt/Pd ratios vary little through these bodies. This PGE+Au fractionation gives rise to a number of diverse chondrite normalized PGE profiles and should sound as a precaution to the exclusive use of these profiles to ascertain the nature of the parental magma from which the sulphides segregated.

Increasing Cu/(Cu+Ni) and Pd/Pt ratios and cobalt content of pentlandite from the centre to western end of the complex suggest that the parental magmas that gave rise to the western zones of mineralization are more fractionated than their eastern counterparts. This chemical and mineralogical association, in conjunction with decreasing numbers of massive sulphide bodies towards the west, implies that the sulphidic magma was transported in a westerly direction before being discharged to surface.

Detailed mineralogical investigations of the massive sulphides disclosed that this type of ore consists mainly of pyrrhotite and pentlandite, followed by chalcopyrite and magnetite. Approximately 70% of

La minéralisation la plus intéressante semble avoir été concentrée par l'écoulement de magma renfermant des sulfures au-dessus d'irrégularités à la base de l'intrusion qui auraient agi à la manière des baguettes transversales dans un sluice. Cependant, d'autres styles de minéralisations fournissent des réserves importantes parmi lesquels on peut mentionner les minerais riches en nickel qui sont associés à des apophyses qui pénètrent sur de grandes distances dans les couches du mur du Complexe de White River, les «skarns» minéralisés qui se situent dans le prolongement des roches carbonatées du Permien qui encaissent le Complexe de Quill Creek, les sulfures disséminés à l'intérieur ou au-dessus du contact entre la zone gabbroïque et les zones ultramafiques dans la plupart des intrusions et, enfin, les zones riches en ÉGP+Au associées à des zones d'altération à quartz-carbonates d'origine hydrothermale (métasomatique) qui enveloppent les extrémités de nombreuses intrusions. De plus, les zones ultramafiques des intrusions de la ceinture de Kluane devraient faire l'objet d'un examen approfondi car elles pourraient contenir des concentrations de sulfures massifs à Ni-Cu-ÉGP. Chacun de ces types de minéralisations est traité en détail afin de fournir les informations de base nécessaires à la découverte de nouvelles ressources et à la leur mise en valeur.

Les récents travaux d'exploration menés au Complexe de Quill Creek ont mis au jour au sein des gabbros trois zones minéralisées principales et une zone minéralisée secondaire recèlant des sulfures massifs et disséminés. Dans ces zones minéralisées, on a reconnu cinq types de minéralisations primaires de sulfures magmatiques auxquels s'ajoutent trois types de minéralisations hydrothermales et métasomatiques postmagmatiques. Une partie de ces minéralisations est très riche en or et en éléments du groupe du platine. Dans ce complexe, l'exploitation du gisement de Wellgreen a révélé que les accumulations basales de sulfures massifs peuvent mesurer jusqu'à 60 m de longueur et atteindre une épaisseur de tout au plus 20 m, et que les teneurs à l'extraction du minerai s'élèvent en moyenne à 2,23 % de Ni, 1,39 % de Cu, 1 300 ppb de Pt, 920 ppb de Pd, 171 ppb de Au, 400 ppb de Rh, 420 ppb de Ru, 250 ppb de Ir, 200 ppb de Os et 200 ppb de Re. Les profils géochimiques détaillés traversant ces amas de sulfures massifs témopignent d'un fractionnement considérable des ÉGP+Au. La moitié inférieure des amas de sulfures est généralement enrichie en Os, Ir, Ru et Rh et les teneurs pour chacun de ces éléments y varient de 1 000 à 2 000 ppb. Les valeurs les plus élevées sont généralement associées aux intervalles les plus riches en Ni; cependant, les rapports Pt/Pd varient peu au sein de ces amas. Ce fractionnement des ÉGP+Au se traduit par une variété de profils des ÉGP normalisés en fonction de leur concentration dans les chondrites et il devrait servir à nous mettre en garde contre l'utilisation exclusive de tels profils pour établir la nature du magma parental à partir duquel les sulfures se sont séparés par ségrégation.

Une augmentation des rapports Cu/(Cu+Ni) et Pd/Pt, ainsi que de la teneur en cobalt de la pentlandite, du centre à l'extrémité ouest du complexe, indique que les magmas parentaux ayant donné naissance aux zones de minéralisation occidentales sont plus différnciés que leurs contreparties orientales. Cette association chimique et minéralogique, combinée à un nombre décroissant d'amas de sulfures massifs vers l'ouest, font supposer que le magma sulfuré s'est déplacé dans une direction ouest avant de s'épancher à la surface.

Des études minéralogiques détaillées des sulfures massifs ont révélé que ce type de minerai se compose principalement de pyrrhotite et de pentlandite, suivies de chalcopyrite et de magnétite. Environ 70 % de la pyrrhotite montre une symétrie du système cristallin hexagonal et le reste, soit 30 %, une symétrie du système

the pyrrhotite is of the hexagonal variety and 30% monoclinic, and generally contains 0.81 wt.% Ni. Platinum-group mineral (PGM) investigations disclosed that more than 90% occur in pyrrhotite and are relatively small (largest 12 x 30 μm). The PGMs, in decreasing order of abundance, are: *merenskyite* (49.3%), *moncheite* (22.0%), *sudburyite* (19.1%), *testibiopalladite* (4.7%), *sperrylite* (4.1%), *Pt-Pd-bearing melonite* (2.0%), and *Au-Ag alloy* (0.68%). Similar details pertaining to the other ore and mineralized types from the Quill Creek Complex provide valuable exploration and metallurgical information.

Sulphur isotope, S/Se ratios, and geochemistry of sulphide mineralization throughout the belt has shown that although crustal contamination is an important prerequisite for sulphide immiscibility and segregation within these Triassic intrusive complexes, excessive crustal contamination only gives rise to barren magmatic sulphides of a local nature. It is envisaged that the barren mineralization with ^{32}S-enriched compositions ($\delta^{34}S$ down to -39‰), and high S/Se ratios (10 000 to 20 000) have not had an opportunity to equilibrate with the same mass of silicate magma as ore grade mineralization had (with its distinctive signature, $\delta^{34}S$ = -5 to -10‰ and S/Se ratios of <5000). This relationship between the mass of silicate magma/sulphide ratio and the metal grades of the mineralization is better known as the R-factor. Calculations suggest that the PGE-rich massive sulphides have R values of about 460, whereas their barren counterparts have values of 0. Similar calculations for ultramafic-hosted disseminated sulphides indicate R values of 40 and 1361 for barren and metalliferous mineralization, respectively.

Petrological investigations indicate that all mafic-ultramafic igneous complexes had the following crystallization order: olivine (±chromite sulphides) : clinopyroxene : plagioclase : orthopyroxene : Fe-Ti-oxides. The scarcity of orthopyroxene within this intrusive suite probably reflects the silica undersaturated nature of these magmas, and the low crystallization pressures operative in this subvolcanic regime. Olivine from ultramafic rocks generally has a limited range in composition ($Mg/(Mg + Fe^{2+})$ or Mg# = 0.870-0.805, with most in the 0.870-0.820 interval). Nevertheless, the Quill Creek and Tatamagouche Creek complexes, both of which are known to have massive sulphide bodies at their intrusive base, display a wider spread in compositions and also more Fe-rich differentiates (i.e. 0.865-0.795 and 0.858-0.707, respectively). In addition, the Ni content of olivine associated with or proximal to disseminated sulphides was approximately half that of olivine from unmineralized ultramafic rocks containing olivine of equivalent Mg#. Thus Ni depletion associated with olivine could be used to assess the exploration potential of certain complexes. The Mg# of clinopyroxene from most ultramafic bodies is generally rather limited (0.895-0.840); however, relatively

monoclinique, et elle renferme en général 0,81 % en poids de Ni. L'analyse des minéraux à éléments du groupe du platine a fait ressortir le fait que plus de 90 % de ceux-ci sont présents dans la pyrrhotite et qu'ils sont relativement de petite taille (au plus 12 x 30 μm). Les minéraux à éléments du groupe du platine sont, par ordre décroissant d'abondance, les suivants : *mérenskyite* (49,3%), *monchéite* (22,0%), *sudburyite* (19,1%), *testibiopalladite* (4,7%), *sperrylite* (4,1%), *mélonite à Pt-Pd* (2,0%) et *alliage d'or-argent* (0,68%). Des données détaillées semblables sur d'autres types de minerais et de minéralisations dans le Complexe de Quill Creek fournissent des informations utiles pour la prospection et le traitement métallurgique.

L'étude de la composition isotopique du soufre, des rapports S/Se et de la géochimie de la minéralisation sulfurée dans l'ensemble de la ceinture a permis de constater que bien que la contamination crustale soit un élément important menant à l'immiscibilité des sulfures et à leur ségrégation au sein de ces complexes intrusifs du Trias, une contamination excessive du magma par des matériaux crustaux ne donne lieu qu'à la formation de concentrations de sulfures magmatiques dépourvus d'éléments utiles de nature locale. On suppose que les sulfures dépourvus d'éléments utiles qui montrent un enrichissement en ^{32}S ($\delta^{34}S$ atteignant jusqu'à -39 ‰) et manifestent des rapports S/Se élevés (entre 10 000 et 20 000) n'ont pas eu la possibilité d'atteindre un état d'équilibre avec la même masse de magma silicaté que les sulfures renfermant des éléments utiles (la signature distinctive de ceux-ci se traduisant par une valeur $\delta^{34}S$ de -5 à -10 ‰ et des rapports S/Se de <5 000). Cette relation entre les proportions relatives (sur une base massique) de magma silicaté et de bain sulfuré et les teneurs en métaux de la minéralisation est mieux connue sous l'appellation de «facteur R». Les calculs indiquent que les sulfures massifs riches en ÉGP affichent des valeurs de facteur R d'environ 460 tandis que leurs contreparties dépourvues d'éléments utiles montrent des valeurs de facteur R proches de zéro. Des calculs semblables portant sur les sulfures disséminés dans des roches ultramafiques donnent des valeurs de facteur R de 40 pour des minéralisations dépourvues d'éléments utiles et de 1 361 pour celles qui en contiennent.

Les analyses pétrologiques révèlent que tous les complexes ignés de roches mafiques-ultramafiques témoignent de l'ordre de cristallisation suivant : olivine (± chromite, sulfures) : clinopyroxène : plagioclase : orthopyroxène : oxydes de Fe-Ti. La rareté de l'orthopyroxène dans cette suite intrusive est le reflet probable de la sous-saturation en silice de ces magmas et des faibles pressions caractéristiques du régime subvolcanique dans lequel a eu lieu la cristallisation. L'olivine des roches ultramafiques affiche généralement un intervalle de composition limité ($Mg/[Mg + Fe^{2+}]$ ou Mg# = 0,870-0,805, mais la majorité des résultats d'analyse tombent dans l'intervalle 0,870-0,820). Néanmoins, les complexes de Quill Creek et de Tatamagouche Creek qui renferment tous deux des amas de sulfures massifs à leur base intrusive, affichent un intervalle de composition plus étendu en plus de présenter des différenciats plus riches en Fe (soit 0,865-0,795 et 0,858-0,707, respectivement). En outre, la teneur en Ni de l'olivine directement associée à des sulfures disséminés ou située à leur proximité était environ la moitié de celle de l'olivine contenue dans les roches ultramafiques non minéralisées renfermant de l'olivine de Mg# équivalent. Par conséquent, l'appauvrissement en Ni de l'olivine pourrait servir à évaluer le potentiel métallifère de certains complexes. Le Mg# du clinopyroxène dans la plupart des massifs de roches ultramafiques montre généralement une variation limitée (0,895-0,840); cependant, des clinopyroxènes

Fe-rich clinopyroxene compositions are also associated with the Fe-rich olivine from the Quill Creek and Tatamagouche Creek complexes. Clinopyroxene associated with massive sulphides and thermally metamorphosed country rock have their own distinctive pyroxene quadrilateral compositions. Gabbroic rocks that have clinopyroxene generally have Mg#s in the 0.875 to 0.825 range, and are continuous with ultramafic-hosted compositions. Regardless, values as low as 0.530 can be found due to zoning and the development of late stage Fe-rich interstitial clinopyroxene crystallization products. Plagioclase from the Kluane Belt is characteristically altered and thus gives rise to a spectrum of compositions (e.g. Ca/(Ca+Na+K) or Ca# = 0.850 to 0.00). Rare barium feldspars have been identified in both mafic and ultramafic rocks. Plagioclase, of a non-cumulate origin, from gabbroic rocks are pervasively altered, whereas those from cumulate rocks are remarkably fresh. This preferential alteration may be the outcome of non-cumulate types being more prone to contamination and ensuing alteration resulting from reaction with the volatile-rich Permian country rock sediments.

The most distinctive mineralogical feature associated with the Kluane Belt is the TiO_2-rich nature of chromite. Samples with up to 10.75 wt.% TiO_2 have been recorded from the Quill Creek Complex. Although there is considerable variation in the investigated complexes, unmineralized intrusions appear to have a greater proportion of samples with low TiO_2 than mineralized intrusions. The only other intrusions known to contain chromite with comparable TiO_2 contents are those hosting the Ni-Cu-PGE ores of the Noril'sk region of Russia. No anomalous Zn values were detected in either mineralized or unmineralized Kluane chromites. Strong correlations between the behaviour of NiO and TiO_2, and their enrichment in zones of anomalous sulphides have been detected. Mineralized ultramafic rocks and intrusions also contain a greater frequency of chromites with elevated $Fe^{3+}/(Cr+Al+Fe^{3+})$ ratios than their unmineralized counterparts. The high TiO_2 chromites from the Kluane Belt, plus elevated values associated with and/or proximal to mineralized horizons and the recognition of similar features from the near age-equivalent Noril'sk Ni-Cu-PGE camp of Russia, suggest that this association should be persued further as a possible exploration tool. In addition, the refractory nature of chromite also makes it very amenable to regional stream geochemical and heavy mineral surveys.

Geochemical investigations of mineralized and unmineralized intrusions throughout the belt have revealed some rather interesting trends and associations pertinent to mineral exploration. Macroscopically unmineralized ultramafic lithologies, from known mineralized intrusions, contain approximately twice the background levels of Ni as their barren counterparts from other intrusions in rocks with

relativement riches en Fe sont également associés à des olivines riches en Fe dans les complexes de Quill Creek et de Tatamagouche Creek. Dans un diagramme quadrilatère servant à représenter la composition des pyroxènes, les clinopyroxènes associés à des concentrations de sulfures massifs montrent des compositions distinctes de ceux contenus dans des roches ayant été soumises à un métamorphisme thermique. Lorsqu'ils sont présents dans des roches gabbroïques, les clinopyroxènes montrent des valeurs du paramètre Mg# qui varient généralement entre 0,875 et 0,825, valeurs qui se situent dans la continuité de celles associées aux clinopyroxènes dans les roches ultramafiques enveloppées par les gabbros. Néanmoins, des valeurs aussi basses que 0,530 peuvent être reconnues et sont attribuables à la zonation lithologique et à la formation de produits de cristallisation de stade tardif riches en fer occupant une position interstielle dans les cristaux de clinopyroxène. Dans les roches de la ceinture de Kluane, les plagioclases sont de façon générale altérés ce qui donne lieu à toute une gamme de composition (p. ex. Ca/[Ca+Na+K] ou Ca# s'étendant de 0,850 à 0,00). Tant dans les roches mafiques qu'ultramafiques, des feldspaths barytifères de caractère peu commun ont été identifiés. Dans les roches gabbroïques, les plagioclases qui ne sont pas apparus sous la forme de phases cumulus sont intensément altérés, tandis que ceux contenus dans des cumulats sont remarquablement non altérés. Cette altération différentielle peut être due au fait que les plagioclases qui ne constituent pas des phases cumulus sont dérivés de magmas plus susceptibles d'avoir été contaminés et que leur altération résulterait de la réaction du magma avec les sédiments riches en éléments volatils du Permien de la succession lithologique encaissante.

Dans la ceinture de Kluane, la principale caractéristique d'ordre minéralogique reconnue tient à la forte teneur en TiO_2 de la chromite. Des phases minérales pouvant contenir jusqu'à 10,75 % en poids de TiO_2 ont été identifiées dans le Complexe de Quill Creek. Même si cette teneur varie considérablement dans les complexes étudiés, les intrusions non minéralisées semblent se distinguer des intrusions qui le sont par une plus grande proportion d'échantillons à faible teneur en TiO_2. Les seules autres intrusions que l'on sait contenir des chromites à teneur comparable en TiO_2 sont celles logeant les minerais à Ni-Cu-ÉGP de la région de Noril'sk en Russie. Dans la ceinture de Kluane, aucune concentration anomale de Zn n'a été décelée dans les chromites provenant tant d'intrusions minéralisées que non minéralisées. Dans les zones renfermant des concentrations anomales de sulfures, de fortes corrélations ont été établies entre le comportement de NiO et de TiO_2 qui sont tous deux enrichis. Les roches ultramafiques et les intrusions minéralisées contiennent en outre une plus forte fréquence de chromites àrapport $Fe^{3+}/(Cr+Al+Fe^{3+})$ élevé que leurs contreparties non minéralisées. La forte teneur en TiO_2 des chromites et les valeurs élevées associées directement aux horizons minéralisés ou à leurs environs immédiats dans la ceinture de Kluane, de même que la reconnaissance de caractéristiques semblables dans le camp minier de Noril'sk en Russie où les minéralisations de Ni-Cu-ÉGP remontent à un âge assez proche des précédentes, incitent à approfondir cette association qui pourrait s'avérer un outil d'exploration utile. De plus, le caractère réfractaire de la chromite en fait un minéral qui se prête bien aux levés géochimiques régionaux basés sur l'échantillonnage des sédiments de ruisseau et de la fraction des minéraux lourds.

Les analyses géochimiques des intrusions minéralisées et non minéralisées dans toute la ceinture ont mis en évidence des tendances et des associations plutôt intéressantes pour l'exploration minérale. Au sein d'intrusions que l'on sait être minéralisées, les lithologies ultramafiques qui apparaissent non minéralisées d'après un examen

equivalent amounts of S. As the marginal gabbro intrusions are seldom exposed this geochemical relationship with the more voluminous ultramafic rocks could prove to be a useful exploration guide. This relationship also holds for Pt and Pd. One of the most characteristic and unique geochemical features of this belt is the high concentrations of the rarer platinum-group elements Os, Ir, Ru and Rh and the high Pt/Pd ratios relative to other magmatic sulphide occurrences in Canada and abroad, particularly for sulphides of a tholeiitic affinity. Se demonstrates a strong chalcophile trend in all intrusions, but noticeably higher concentrations are associated with metalliferous sulphides relative to their barren equivalents. Highly anomalous amounts of Ba occur in ultramafic and mafic intrusive lithologies and in mineralized equivalents, but the coeval Nikolai, Chilkat, and Karmutsen basalts do not appear to have anomalous Ba contents relative to this and other basaltic suites. Evidence is presented to show that the Kluane intrusive suites have inherited anomalous Ba concentrations as a consequence of crustal contamination by Ba-rich Permian sediments, and are not a geochemical characteristic of their mantle source melt.

Mineralogical, petrological, geochemical, and isotopic investigations of the gabbroic chilled margins to the mafic-ultramafic complexes, coeval hypabyssal sills, dykes, and Nikolai basalt clearly indicate derivation from tholeiitic parental magmas. Corroborating studies suggest that the initial pulse of magma that formed the thin chilled marginal zone gabbroic envelope was relatively fractionated (MgO = 6.2 wt.%, Mg# = 0.523) and contained about 12.7% normative olivine. The more evolved nature of the earlier magma pulse may have resulted from the initial injection of magma being tapped off the top of a density-stratified, fractionating, master magma chamber at depth. Ensuing crustal contamination accompanying intrusion would also modify this composition to a more evolved state. Subsequent ingressions of more representative and progressively more primitive, olivine phenocryst-bearing magma (MgO = 8.53 wt.%, Mg# = 0.679) containing about 20.6% normative olivine, were probably repeatedly injected into the magma chamber and gave rise to the remaining portion of the marginal gabbro and ultramafic zones. The Mg# of the primitive chills are compatible with the computed Mg# of the magma from which the associated olivine crystallized, based on a $K_D(Mg/Fe^{2+})_{olivine\text{-}melt}$ of 0.30 ± 0.03. Chilled margins from subsequent hypabyssal dykes that cut the intrusive complexes and feed overlying basalt, as well as Nikolai basalt compositions, believed to be representative of the melt, suggest that some of these later magmas may have been as fractionated as 0.581. Nikolai basalt from the Chilkat Peninsula of Alaska have Mg#s that range from 0.638 to 0.4810.

macroscopique contiennent des concentrations de fond en Ni deux fois plus élevées que leurs contreparties stériles dans d'autres intrusions qui contiennent une teneur équivalente en S. Comme les bordures gabbroïques des intrusions sont peu représentées en affleurement, cette relation géochimique qui s'applique aux roches ultramafiques qui occupent un beaucoup plus grand volume des intrusions pourrait s'avérer un guide d'exploration utile. Cette relation s'applique aussi à Pt et Pd. Quand on les compare aux autres occurrences de sulfures d'origine magmatique au Canada et à l'étranger, et plus particulièrement à celles contenues dans des roches aux affinités tholéiitiques, l'une des caractéristiques géochimiques les plus frappantes et les plus distinctives des minéralisations de cette ceinture tient à leur contenu élevé en éléments du groupe du platine plus rares (Os, Ir, Ru et Rh) et aux rapports Pt/Pd élevés. Le sélénium affiche une forte tendance chalcophile dans toutes les intrusions, mais les concentrations nettement plus élevées de cet élément sont associées aux concentrations de sulfures renfermant des éléments utiles par rapport à leurs équivalents dépourvus d'intérêt économique. De fortes teneurs en Ba de caractère anomal s'observent dans les lithologies ultramafiques et mafiques des intrusions, ainsi que dans leurs équivalents minéralisés, mais les basaltes de Nikolai, de Chilkat et de Karmutsen qui sont contemporains de ces intrusions ne semblent pas contenir de teneurs anomales en Ba lorsqu'on les compare aux intrusions de cette ceinture ou aux autres suites basaltiques. Les données présentées démontrent que les concentrations anomales de Ba dans les intrusions de la ceinture de Kluane proviennent d'une contamination du magma par des matériaux crustaux, en l'occurrence des sédiments riches en Ba du Permien, et qu'elles ne résultent en rien de caractéristiques géochimiques particulières de la source du magma dans le manteau.

L'analyse minéralogique, pétrologique, géochimique et isotopique des bordures figées de composition gabbroïque des complexes mafiques-ultramafiques, de même que celle des filons-couches hypabyssaux, des dykes et du basalte de Nikolai qui sont contemporains de ces complexes, indique clairement que ces diverses lithologies dérivent de magmas parentaux aux affinités tholéiitiques. Des études complémentaires révèlent que la poussée initiale de magma, à partir de laquelle a cristallisée la mince enveloppe gabbroïque à grain fin de la zone marginale, montrait un certain degré de fractionnement (MgO = 6,2 % en poids, Mg# = 0,523) et contenait environ 12,7 % d'olivine normative. Le caractère plus évolué de la poussée de magma la plus ancienne peut être attribuable au fait que l'injection initiale de magma s'est faite à partir du sommet d'une chambre magmatique principale située en profondeur dans laquelle opérait un processus de différenciation magmatique et qui montrait une stratification témoignant d'un gradient de densité. La contamination du magma par des matériaux crustaux qui a accompagné la mise en place des intrusions aurait également participé à la modification des compositions originelles concourrant ainsi à la définition d'un caractère plus évolué. Des poussées subséquentes d'un magma à phénocristaux d'olivine de composition plus représentative et de caractère progressivement plus primitif (MgO = 8,53 % en poids, Mg# = 0,679), contenant environ 20,6 % d'olivine normative, se sont probablement injectées en succession dans la chambre magmatique située à moins grande profondeur, ce qui a formé par cristalisation la partie restante de la zone marginale gabbroïque et les zones ultramafiques. Le Mg# des bordures figées de caractère primitif est compatible avec le Mg# calculé du magma à partir duquel les olivines associées ont cristallisé, en utilisant une valeur de $K_D(Mg/Fe^{+2})_{olivine\text{-}bain\ silicaté}$ de 0,30 ± 0,03. Les bordures figées des dykes hypabyssaux de formation ultérieure qui ont recoupé les complexes intrusifs et servi de conduits nourriciers

The most striking regional differences between the eastern and western portion of Wrangellia are the distribution of mafic-ultramafic bodies and associated Ni-Cu-PGE mineralization, the extrusive volcanic environment, and varying degrees of fractionation and metal depletion associated with different volcanic areas. Triassic basalt from the western and eastern portion of Wrangellia erupted under different extrusive conditions (i.e. subaqueous and subaerial environments, respectively). Basalt from the western portion is both more fractionated (Mg# = 0.638-0.481, $\overline{X}$ = 0.555) and less olivine normative (0-18.8% olivine; $\overline{X}$ = 10%) than its eastern counterpart with Mg# of 0.676-0.581, $\overline{X}$ = 0.629, and normative olivine content of 15.9-20.7%, $\overline{X}$ = 19.1%. Zr contents are also noticeably lower in the eastern suite. Comparison of Ni and Cu values for the different basalt suites clearly demonstrates that the eastern suite (from the Yukon) has 30 to 50% lower metal concentrations than their western counterparts with similar Mg#s. This metal depletion could only be a product of prior segregation of Ni-Cu sulphides from these or earlier magmas. Explanation of this metal depletion is corroborated by the fact that sulphidic, subvolcanic, mafic-ultramafic intrusive complexes, through which these basaltic liquids passed, only occur in the eastern portion of Wrangellia and underlie the Ni- and Cu-depleted volcanic rocks. In addition, the elevated normative olivine content of the eastern volcanic rocks is not surprising when one considers the olivine-rich nature of the underlying predominantly ultramafic subvolcanic sills which fed them.

A U-Pb age determination of 232.3 ± 1.0 Ma on zircon from a hypabyssal sill that cuts the upper portion of the Tatamagouche Creek Mafic-Ultramafic Complex and feeds the proximal Nikolai basalt, provides a minimum age for this and other such complexes in the belt, and a precise age for the onset of Triassic volcanism in Wrangellia. This age determination not only corroborates earlier less precise K-Ar ages determined for two of the complexes, but also demonstrates that volcanism began in the Carnian and not Norian stage of the Triassic, as previously believed.

Rb-Sr, Nd-Sm, and Re-Os isotopic studies were conducted on a variety of samples from the Quill Creek Complex. The isotopic systematics in some of the samples have been modified by magmatic and postmagmatic fluids which have passed through the rocks. However, the remaining samples, in conjunction with available Nd isotope information from other studies in Wrangellia, demonstrate that Permian and not Pennsylvanian sediments are the only viable contaminants when the ε_{Nd} signature of each group is considered. It also demonstrates that the ultramafic portion of the complex has a more chondritic signature (+2.89 to +4.49) than the marginal gabbro (+2.02 to +3.46) when compared to the values of the mantle

aux basaltes sus-jacents, ainsi que les compositions du basalte de Nikolai que l'on croit représentatives de celle du bain silicaté, indiquent que certains de ces magmas tardifs témoignent d'une différenciation poussée se traduisant par un Mg# pouvant atteindre 0,581. Le Mg# du basalte de Nikolai dans la péninsule Chilkat en Alaska varie de 0,638 à 0,4810.

À l'échelle régionale, les différences les plus frappantes entre les portions orientale et occidentale de la Wrangellie ont trait à la répartition des massifs de roches mafiques-ultramafiques et de la minéralisation de Ni-Cu-ÉGP associée, à l'environnement volcanique dans lequel les laves se sont épanchées et aux degrés variables de fractionnement et d'appauvrissement en métaux associés des lithologies dans les différentes régions volcaniques. Les basaltes triasiques des portions occidentale et orientale de la Wrangellie ont fait éruption dans des conditions d'épanchement différentes (respectivement subaquatiques et subaériennes). Les basaltes de la portion occidentale sont à la fois plus fifférenciés (Mg# = 0,638-0,481, moyenne = 0,555) et moins riches en olivine normative (0-18,8 % d'olivine; moyenne = 10 %) que leurs contreparties de la portion orientale qui montrent un Mg# de 0,676-0,581 (moyenne = 0,629) et une concentration d'olivine normative de l'ordre de 15,9-20,7 % (moyenne = 19,1%). Les concentrations de Zr sont aussi nettement plus faibles dans la suite orientale. La comparaison des teneurs en Ni et en Cu des différents suites de basalte fait ressortir que les basaltes de la suite orientale (au Yukon) contiennent des concentrations de métaux de 30 à 50 % moins élevées que celles de la suite occidentale pour des valeurs équivalentes de paramètre Mg#. Cet appauvrissement en métaux ne peut être attribuable qu'à un épisode antérieur de ségrégation des sulfures de Ni-Cu à l'intérieur de ces magmas ou à un processus similaire dans les magmas plus anciens. Cette explication de l'appauvrissement en métaux est corroborée par le fait que les complexes intrusifs subvolcaniques de composition mafique-ultramafique montrant une minéralisation sulfurée qui ont été traversés par ces liquides basaltiques, ne sont présents que dans la portion orientale de la Wrangellie où ils apparaissent sous des roches volcaniques appauvries en Ni et en Cu. De plus, la concentration élevée d'olivine normative dans les roches volcaniques de la suite orientale n'est pas étonnante lorsqu'on considère la forte concentration d'olivine dans les filons-couches subvolcaniques sous-jacents de composition principalement ultramafique qui ont servi de conduits nourriciers.

Un âge U-Pb sur zircon de 232,3 ± 1,0 Ma déterminé sur un filon-couche hypabyssal qui recoupe la portion supérieure du complexe de roches mafiques-ultramafiques de Tatamagouche Creek et qui sert de conduit nourricier à la succession proximale dsu basalte de Nikolai, établit une limite d'âge minimale pour ce complexe et d'autres complexes semblables dans la ceinture et un âge précis quant au début du volcanisme triasique dans la Wrangellie. Cette datation corrobore non seulement les résultats de datations K-Ar précédentes moins précises, effectuées sur deux des complexes, mais également que le volcanisme a débuté au Carnien plutôt qu'au Norien (Trias), comme on l'avait d'abord établi.

Des analyses de la composition isotopique des couples Rb-Sr, Nd-Sm et Re-Os ont été effectuées sur divers échantillons du Complexe de Quill Creek. Dans certains d'entre eux, la systématique isotopique a été modifiée par le passage de fluides magmatiques et postmagmatiques dans les roches. Cependant, l'information tirée de tous les autres échantillons, combinée à celle provenant d'autres études sur la composition isotopique du Nd dans la Wrangellie, permet d'établir que ce sont les sédiments permiens et non pennsylvaniens qui sont les seuls contaminants possibles des magmas

(i.e. +6.2 to +7.3; Karmutsen and Chilkat basalts from western Wrangellia) at 232 Ma. This also corroborates other evidence which suggests that the marginal gabbro is more contaminated than the more weakly mineralized ultramafic rocks. Os isotope magma mixing models confirms other presented models which suggest that as little a 5% contamination of the Quill Creek Complex magma can give rise to ores with isotopic systematics similar to those observed in the Wellgreen deposit of this complex.

A number of tectonomagmatic geochemical discriminant diagrams were examined with the objective that they could be used to reconstruct the Triassic paleotectonic environment of this rather enigmatic terrane. These diagrams served little practical use particularly when cryptic contamination is present in samples that otherwise appeared to be pristine. The erroneous paleotectonic settings inferred from these diagrams can only serve as a caution against the "blind" use of such diagrams in the absence of acceptable tectono-stratigraphic analysis based on a knowledge of field relations, structure, and petrology of epiclastic and volcaniclastic rocks.

Previous proposals to explain the origin of Triassic magmatism in Wrangellia shared a common rifting property; however, inadequate evidence for such rifting has led to a petrotectonic interpretation based on a modification of the 1991 "mantle plume" initiation model. The proposed model adequately explains variations in volcanic chemistry, thickness, environment of deposition, and the occurrence of mafic-ultramafic intrusions and normative olivine-enriched basalt in the eastern portion of Wrangellia relative to the west.

This study clearly demonstrates that eastern Wrangellia is a new and unique Ni-Cu-PGE+Au metallogenic terrane with impressive exploration potential.

lorsqu'on s'appuie sur la signature ε_{Nd} de chaque groupe. Ils permettent en outre d'établir que la portion ultramafique du complexe montre une signature qui se rapproche davantage de celle des chondrites (+2,89 à +4,49) que celle du gabbro de la zone marginale (+2,02 à +3,46) lorsqu'on les compare aux valeurs mantelliques (soit +6,2 à +7,3; basaltes de Karmutsen et de Chilkat dans la Wrangellie occidentale) à 232 Ma. Cela corrobore également d'autres indices qui incitent à penser que le gabbro de la zone marginale est plus contaminé que les roches ultramafiques plus faiblement minéralisées. Les modèles de mélange de magmas basés sur la composition isotopique de Os vont dans le même sens que d'autres modèles présentés voulant qu'une contamination du magma du Complexe de Quill Creek qui s'éleverait à aussi peu que 5 % puisse être à l'origine de minerais dont la systématique isotopique est semblable à celle observée dans le gisement de Wellgreen logé dans ce complexe.

Un certain nombre de diagrammes géochimiques servant à discriminer les différents cadres tectonomagmatiques ont été utilisés afin de reconstituer le milieu paléotectonique de ce terrane plutôt énigmatique au Trias. Ces diagrammes se sont avérés d'une utilité limitée, en particulier lorsqu'une contamination cryptique existait dans des échantillons qui à tout autre égard apparaissaient représentatifs des conditions originelles. Les cadres paléotectoniques erronés établis à partir de ces diagrammes ne peuvent servir qu'à mettre en garde contre une utilisation aveugle de ces diagrammes en l'absence d'une analyse tectonostratigraphique acceptable basée sur des observations de terrain, des interprétations structurales et des données sur la pétrologie des roches épiclastiques et volcanoclastiques.

Les propositions antérieures formulées pour expliquer l'origine du magmatisme dans la Wrangellie au Trias partageaient la même hypothèse d'un épisode de rifting; cependant, des indices insuffisants de l'existence d'un tel épisode de rifting ont mené à l'élaboration d'une interprétation pétrotectonique basée sur une modification du modèle de «panache mantellique» de 1991. Le modèle proposé dans la présente étude explique convenablement les variations de composition chimique, d'épaisseur et de milieu d'épanchement des coulées volcaniques, de même que la présence d'intrusions mafiques-ultramafiques et de basaltes riches en olivine normative dans la portion orientale de la Wrangellie par comparaison à ce que l'on observe dans la portion occidentale.

La présente étude établit de manière non équivoque que la Wrangellie orientale est un nouveau et exceptionnel terrane métallogénique à minéralisations de Ni-Cu-ÉGP+Au offrant un potentiel impressionnant en matière d'exploration minérale.

INTRODUCTION

An investigation of mafic-ultramafic rocks and associated Ni-Cu-PGE mineralization within the Kluane Ranges, Yukon, and its lateral extensions in northern British Columbia and Alaska, was undertaken to better understand Triassic plutonic activity in this portion of the Cordillera: age and tectonic setting, petrology of the intrusive rocks and relationship to the overlying volcanic rocks, and the economic potential. The study area encompasses a belt of mafic-ultramafic rocks that extends in a southeasterly direction from 63°20′N, 145°45′W in east-central Alaska to 57°55′N, 137°00′W in northwestern British Columbia (Fig. 1, 2). The best known mineralization is at the Wellgreen deposit, which occurs in the central portion of the area (61°28′N, 139°32′W), and was mined from 1972-73. Prior to this study a number of mafic-ultramafic intrusions was known immediately to the west of the Denali fault; however, little if anything was known about their age, petrology and economic potential. This study investigates these bodies, both in detail and on a regional scale, and documents this information on a site by site basis, emphasizing the economic potential of this newly recognized metallogenic terrane.

The Denali fault marks the eastern boundary of the area. In the Yukon, the mafic-ultramafic intrusive complexes are generally confined to a continuous chain of foothills along the northeast flank of the St. Elias Mountains known as the

Kluane Ranges (see Muller, 1967). This series of intrusive bodies has been coined by the author as the Kluane Mafic-Ultramafic Belt. The area also falls within the eastern branch of "Wrangellia", the largest allochthonous tectonostratigraphic terrane along the northwest margin of North America (Fig. 1, 2). Although the largest and best preserved complexes and associated mineralized occurrences occur in the Kluane Ranges in the Yukon, sites from northern British Columbia and east-central Alaska were also investigated for a more complete understanding of the eastern portion of this rather enigmatic terrane. Proving that these intrusive bodies are part of Wrangellia, coeval with Triassic volcanism, lithologically zoned, intrude along a common stratigraphic horizon, and have diagnostic geochemical and isotopic signatures is fundamental to understanding their origin, development, and potential.

The findings of this study unequivocally demonstrate that this belt constitutes one of the largest tracts of Ni-Cu-Platinum Group Elements (PGE) mineralized mafic-ultramafic rocks in North America, second only to the nickeliferous intrusions from the Proterozoic Circum-Superior Belt of Canada (i.e. Thompson Ni-Belt, Manitoba and Raglan Horizon, Cape Smith Belt, Quebec). Furthermore, similarities between the morphology of the Kluane Belt intrusions and those of the economic Circum-Superior deposits, and the consanguineous development of world-class Cu-Ni-PGE deposits in the Siberian Traps, Russia, lend additional support to the potential significance of this belt. Comparisons with the western branch of Wrangellia (along the Pacific margin) are presented, and an explanation for the lack of Ni-Cu-PGE mineralization and ultramafic intrusions is proposed.

Although most of the intrusive bodies are poorly exposed and some are highly deformed and altered due to faulting, an opportunity to investigate fairly well preserved and continuous cumulate stratigraphic intervals and mineralized zones was presented by the ongoing mineral exploration in the area during this study. Access to diamond-drill core, and underground workings at the Wellgreen and Canalask deposits provided the author with an unprecedented opportunity to study these intrusions and deposits. This information is used to unravel the geology of similar yet more poorly exposed and/or highly deformed intrusions elsewhere in the belt.

The first part of the report is a thorough description and documentation of all representative mafic-ultramafic complexes and affiliated sulphide occurrences in the belt, including: location, history and physiography, structure and stratigraphy, petrology, and Ni-Cu±PGE mineralization. Descriptions and discussions related to all aspects of the geology and the different types of mineralization from the Quill Creek Intrusive Complex (which hosts the Wellgreen deposit) and other complexes are presented. The second part is devoted to igneous silicate and oxide mineral chemistry, geochemistry of selected mafic-ultramafic intrusions, petrology and geochemistry of the temporal Nikolai basalt, Maple Creek gabbro dykes and selected chilled margins, geochronology, radiogenic and stable-isotope investigations, tectonostratigraphic comparisons, and tectonomagmatic and metallogenic modelling. This publication, therefore, describes specific mineralized and unmineralized mafic-ultramafic complexes within eastern Wrangellia, and investigates all important aspects of Triassic magmatism, metallogeny, and geological setting in this region.

Access to most of the area is readily available from the Alaska Highway which tends to follow the Denali fault zone (Shakwak Trench, Muller, 1967). Many of the better known and explored bodies are accessible by dirt and gravel roads which are intermittently maintained by exploration and placer mining activity. Other more remote and elevated bodies are accessible from the highway by arduous day-long hikes or short flights from helicopter bases located on the Alaska Highway. Services, accommodation, and, in some places, airstrips, are also located along the entire length of the highway and were used during this study.

The topography of the Kluane Ranges rises steeply from the Denali fault to a maximum of 2500 m. They are deeply dissected by V-shaped transverse valleys, and are broken by major gaps marked by Duke River and adjoining Burwash Uplands, and Slims, Donjek, Koidern, and White rivers. Parts between Duke and Slims rivers contain several alpine glaciers (Muller, 1967). Intrusive complexes may be found above the tree line in rugged alpine terranes as much as 2091 m above sea level, or in areas of lower elevation (757 m) consisting of rolling spruce forested hills separated by swampy depressions with interspersed birch and alder growths.

Topography has a pronounced influence on the climate in locations on and beyond the northeast slopes of the St. Elias Mountains, which lie to the west of the Kluane Ranges. These mountains act as a barrier to the relatively warm and moist Pacific Ocean air, and give rise to a continental climate, despite proximity to the sea. During the summer months of June and July temperatures in the 12° to 16°C are common and maximum temperatures of 31° have been recorded, and the sun is above the horizon for a maximum of >19 hours (Muller, 1967). Temperatures cool during August, and towards September night frost is common. Annual precipitation is generally light, in the 25 to 40 cm range; however, it is high to extreme in southern portion of the area (northern British Columbia) because of the increased elevation of the confining mountains and closer proximity to the ocean. Unlike other areas, unpredictable rain and cloud conditions in the extreme southern portion of the area often impede field work. Snow can be present all year round on some of the north facing slopes in areas of high elevation. Strong winds are common to all areas particularly at increased elevations. Long winters with daylight shortening to less than six hours and mean daily temperatures below freezing from October through April can be expected. Minima of -51°C have been recorded from November through March. The cold winters make exploration drilling particularly difficult since most sources of water freeze to bottom.

Although parts of the area received geological note as far back at 1891, mapping by the Geological Survey of Canada did not begin until 1904 by R.G. McConnell in the Kluane Lake area (McConnell, 1905). Detailed mapping was undertaken in the White River area in 1913 by D.D. Cairnes (1915), and in the Steele Creek area in 1943 by R.P. Sharp (1943). Reconnaissance mapping along the Alaska Highway

commenced in 1945 by H.S. Bostock (1952), but it was not until 1951 that Ni-Cu mineralization was discovered on a tributary of Quill Creek. This and subsequent discoveries were undoubtedly the result of enhanced activity of prospectors and mining companies resulting from the improved access provided by the Alaska Highway after the Second World War. An ensuing staking rush occurred in 1952 and 1953 and as a result several exploration companies took up claims along the Kluane Ranges and the area has been intermittently explored to the present.

During this study the author had an opportunity to experience working conditions within the Kluane Mafic-Ultramafic Belt under spring, summer, fall and winter conditions. Based on experience in mafic-ultramafic terranes elsewhere in Canada, the Kluane Belt is one of the most attractive areas to explore when one considers the geology, normal climatic conditions, exposure, ease of access, accommodations, and the readily available infrastructure.

Field work for the present study was conducted in 1988. Detailed petrological, geochemical, and isotopic laboratory investigations were conducted between 1988 to 1991; some radiogenic isotope data, however, were not available until 1993.

Acknowledgments

The author would like to acknowledge the hard work and dedication of M. Fayak who assisted with the field work in 1988. Also, members of the analytical chemistry section of the Geological Survey of Canada deserve special thanks for persevering patiently with the large number of samples submitted during this project, and analytical problems associated with the sulphide-rich material (B. Williamson is thanked for completing the microprobe analyses that were critical to many of the interpretations made in this report). Without these superior quality analyses, many of the insights gained from this geochemically oriented project would not have been possible. Also, C. Grégoire is thanked for the low-level, isotope-dilution-ICP platinum-group analyses of intrusive chilled margins and the Nikolai basalt. Laboratory identification and analyses of the ore minerals by L. Cabri (CANMET) and D. Paktunc (GSC) (partially funded under this project) added vital information concerning the mineralogy and metallurgy not only of the Quill Creek Complex (Wellgreen) ores, but also many other similar types of mineralization present throughout the belt. J. Mortensen (GSC) is thanked for his assistance in the geochronological study of material from Tatamagouche Creek. This provided the first unequivocal age constraint for the onset of Triassic magmatism, and the emplacement of mafic-ultramafic and related Ni-Cu-PGE mineralization. F. Marcantonio and staff at the Lamont-Doherty Earth Observatory of Columbia University are thanked for their participation in the Re-Os, Nd, and Sr-isotopic studies. I am also very grateful to G. Abbott, J. Morrison, and T. Bremner of the Geological Services Division, Department of Indian and Northern Affairs, Whitehorse, Yukon, for financial assistance under the Canada-Yukon Economic Development Agreement and their continued patience awaiting the final report. The Geological Survey of Canada also provided considerable financial support for this project. Logistical support and access to geological and geophysical data pertaining to the Tatamagouche Complex was provided by L. Halferdahl and Associates, Edmonton and is greatly appreciated. The United States Geological Survey in Alaska is also thanked for assistance in providing the author with mineralized material from east-central Alaska for re-analyses and use in this study.

During the course of this study the author had the good fortune of supervising M. Fayak (1989) and S. Miller (1991), both of whom conducted thesis projects on different aspects of Quill Creek Complex geology. These exemplary students provided many hours of stimulating geological dialogue which has undoubtedly helped to shape many of the concepts presented in this report.

I would like to thank Dick Bell and Tucker Barrie for their detailed and expeditious reviews of the original version of the manuscript, and Kim Nguyen for his care and patience with me during the preparation and editing of the geological figures.

Finally, the success of this project is in a large part due to the enthusiasm, logistical support, access to company exploration records, and the Kluane Belt geological expertise provided the author by Robert Carne of Archer, Cathro & Associates (1981) Limited, Vancouver.

GEOLOGICAL SETTING

Tectonostratigraphic setting

Within the Cordillera of western North America large tracts of land with internally consistent stratigraphy have been identified and referred to as distinct terranes (Berg et al., 1972; Monger, 1984). Berg et al. (1972) working in southern and southeastern Alaska were the first to introduce the term "terrane" and identified three distinctive pre-mid Jurassic terranes now referred to as Wrangellia, Alexander, and the Yukon-Tanana (Fig. 1). Subsequently, new terranes were recognized (Fig. 1), and Jones et al. (1977) showed that Wrangellia could be traced discontinuously southward along the Pacific margin of North America, from the Wrangell Mountains area of southern Alaska, to the Queen Charlotte Islands and Vancouver Island and possibly as far south as the Hells Canyon area of eastern Oregon and western Idaho (Fig. 2), a distance of over 2000 km. Type sections throughout this terrane have remarkably similar stratigraphy, structure, position of unconformities, fossil faunas, and overall geological characteristics and are discussed in other sections. The most diagnostic feature of Wrangellia is a similar sequence of Triassic rocks, including a thick pile of tholeiitic flows and pillow lavas (Nikolai Group ("Greenstone") and Karmutsen Formation) capped by inner platform carbonate. Where exposed, older parts of the terrane consist dominantly of sediments and arc-related volcanic units no older than Pennsylvanian. Paleomagnetic, paleobiogeographical, and lithological evidence independently suggest that during the Triassic Wrangellia was situated near the equator and subsequently drifted northward to collide with the west coast of North America. Paleomagnetic studies and tectonic reconstructions indicate that the Triassic basalt erupted at a latitude of about 10° to 17° in the eastern or western Pacific Ocean, and that Wrangellia accreted onto the continental margin

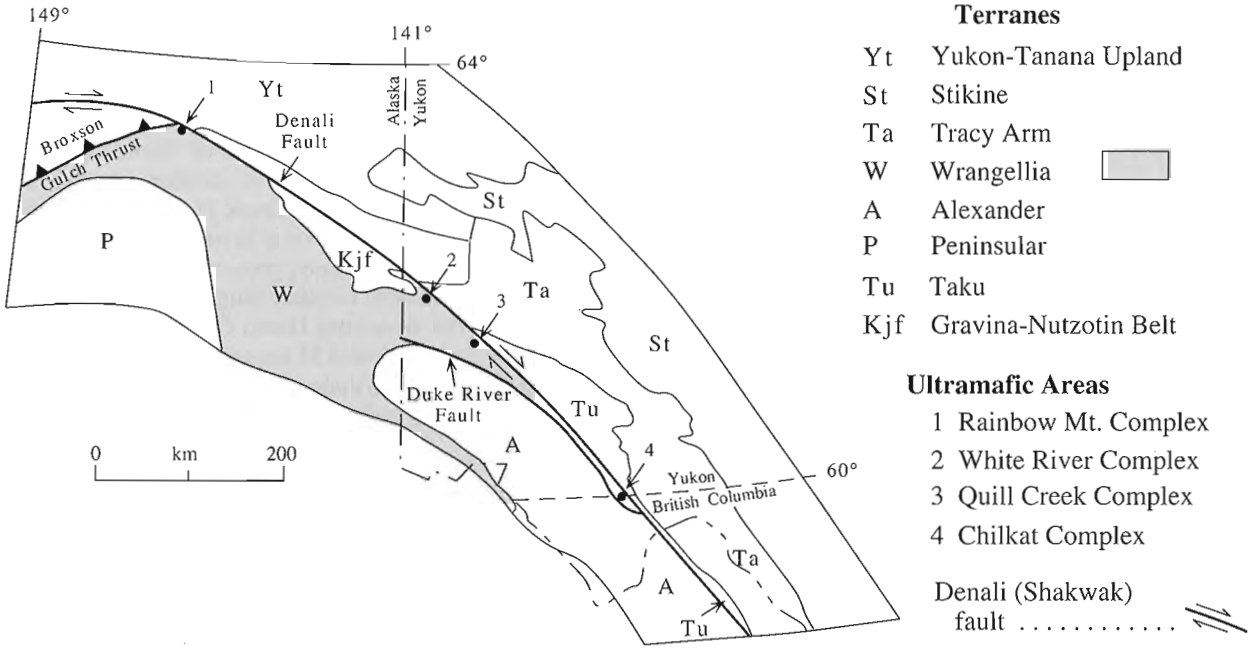

Figure 1. *Map illustrating the tectonic framework of eastern Wrangellia and surrounds, and the lateral confines of Triassic mafic-ultramafic bodies extending from northern British Columbia (Chilkat Complex) to east-central Alaska (Rainbow Mt. Complex).*

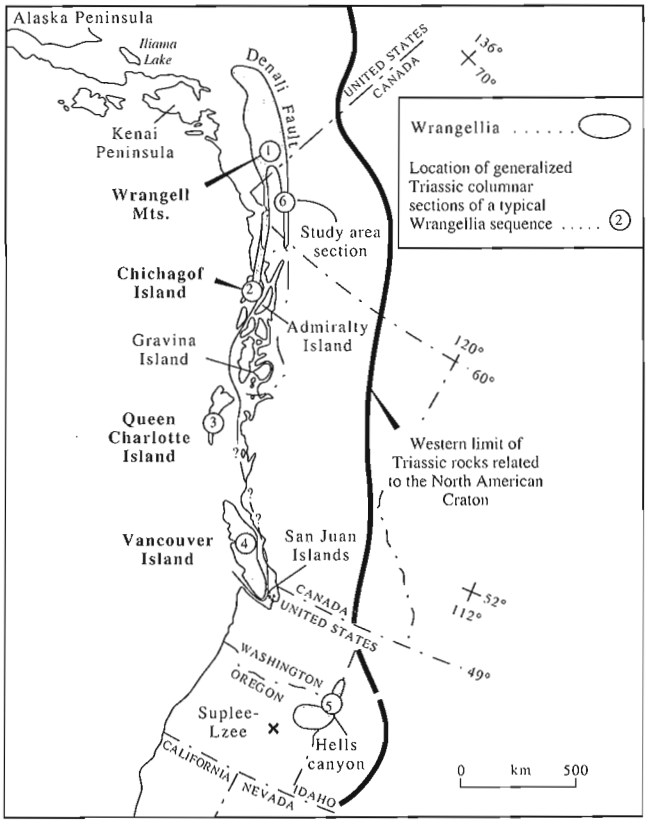

Figure 2.

Map showing the distribution of Wrangellia and position of generalized stratigraphic sections (modified from Jones et al., 1977).

during the Middle Cretaceous or Jurassic. However, ambiguity with respect to the hemisphere of origin results from a lack of knowledge concerning the polarity of the geomagnetic field during magnetization of the rocks. A northern hemisphere origin requires a minimum northern transport of approximately 3100 km and nearly 90° counterclockwise rotation, whereas, a southern hemisphere origin requires a northward displacement of 6200 km and about 90° clockwise rotation with respect to North America (Jones et al., 1977).

These paleomagnetic-determined movements are corroborated by paleobiogeographical analyses conducted by Tipper (1981) and Tozer (1982). They found that the low-latitude, tropical Triassic faunas of Wrangellia were consistently shifted northward with respect to similar low-latitude faunas that are bound to the North American Craton. The presence of sabkha deposits in the Triassic limestone also corroborates the tropical climatic environs and the lack of quartzose detritus substantiates a non-pericratonal setting.

This evidence, in addition to the juxtaposition of the terrane (Wrangellia) against an unlike sequence of Triassic and older rocks throughout its extent, is further evidence for the allochthonous nature of this terrane.

The northern part of Wrangellia occupies a large tract of central and southeastern Alaska and has two southward extending branches which are separated by the Alexander terrane (Fig. 1, 2). The western branch extends along the Pacific margin, whereas, the eastern branch borders the Denali fault and extends southward tapering through the Yukon and into northern British Columbia. The study area is confined to the eastern branch, and to a limited extent the northern portion (Rainbow Mountain, Alaska) of the terrane.

The vast thickness and extent of Triassic basalt, its essentially uniform composition, and the rapidly erupted nature of the flows bound by marine sedimentary formations have no obvious analogue or explanation in terms of plate boundary volcanism such as island arc formation or sea-floor spreading. Although it has been proposed that Triassic magmatism within Wrangellia occurred in a rifted island arc (Davis and Plafker, 1985) to back-arc with frontal-arc component (Barker et al., 1989) environments, these hypotheses are challenged in more detailed discussions concerning the tectonostratigraphic and magmatic character of the terrane based on detailed field relations, and geochemical and isotopic studies.

Regional setting

Stratigraphy and lithologies

The investigated area comprises Pennsylvanian and Permian volcanic and sedimentary units of the Skolai Group, Triassic volcanic sequences of the Nikolai Group, and Upper Triassic to Lower Jurassic strata of the Nizina and Chitistone limestones and McCarthy Formation. They have been correlated with map units of the "Taku-Skolai" (Smith and MacKevett, 1970; Mackevett, 1971) or "Wrangellia" terrane (Read and Monger, 1976) of eastern Alaska. A generalized stratigraphic section for the study area is shown in Figure 3.

Skolai Group

The Skolai Group comprises the oldest rocks in the area and was defined by Smith and MacKevett (1970) from a thick sequence of predominantly volcanic and volcaniclastic rocks exposed along the upper reaches of Skolai Creek, near McCarthy, Alaska. The group is divided into the Station Creek Formation and Hasen Creek Formation. The Station Creek Formation consists of a lower member of basic to intermediate plagioclase and pyroxene phyric volcanic rocks and an upper volcanic member ranging from coarse breccia to fine tuff. The overlying Hasen Creek Formation, named after Hasen Creek, located 35 km east northeast of McCarthy, consists of chert, black shale, sandstone, limestone, and minor conglomerate, and contains Early Permian fossils.

Station Creek Formation. The Station Creek Formation is about 1000 m thick and underlies all other map units in the area. Although the base of the formation is not exposed, Read and Monger (1976) described a gabbroic complex west of Donjek River which may represent basement to the Station Creek Formation. Potassium-argon age determinations suggest that the complex is 475 Ma (Read and Monger, 1976).

The lower section of the formation consists of basaltic and andesitic volcanic flows that grade upwards into fine- to medium-grained tuff. Volcanic agglomerate and breccia may overlie the tuff locally. Discontinuous beds of argillite and limestone occur within these units.

Volcanic flows are aphanitic to fine grained, medium grey-green, and may contain phenocrysts of plagioclase ranging in size from 1 x 3 mm to 2 x 16 mm. Pillows are commonly 30 to 60 cm across and contain augite phenocrysts and sparse 0.3 to 1.0 mm chlorite amygdules.

Pyroclastic rocks, consisting of lapilli and lapilli crystal tuff, are fine to medium grained, massive to thinly bedded, and generally attain thicknesses of 10 to 20 cm. Some beds display size and colour sorting from coarser-grained darker material to finer-grained medium green tuff. Massive to poorly bedded pyroclastic rocks consist of pale to dark-green fragments in a medium-green, fine-grained matrix. Both the thinly bedded and massive pyroclastics contain agglomerate horizons. Crystal fragments within the tuff include plagioclase, augite, hornblende, and sparse pseudomorphs of serpentine after olivine. Commonly, the volcanic flows, pillows, and pyroclastic rocks have been propylitized.

The Station Creek Formation is generally unfossiliferous; however, two new conodont localities (Campbell, 1981) from limestone beds within the volcanic sequence suggest a Late Mississippian to Early Permian age for this portion of the Station Creek Formation. In eastern Alaska, sparse fossil evidence in correlative rocks of the Tetelna Volcanics (Richter and Dutro, 1975) suggests that the Station Creek Formation is probably Pennsylvanian.

The upper 400 m of Station Creek Formation is characterized by interbedded black shale, siltstone, argillaceous limestone, and cherty argillite with intercalations of very fine-grained tuff horizons that decrease in abundance upward. Campbell (1981) designated this section of the Station Creek Formation as the

"Transition zone" and noted that it forms a gradational contact with the overlying Hasen Creek Formation. The contact of the Station Creek Formation with the overlying sediments of the Hasen Creek Formation is placed at the cessation of pyroclastic rocks.

Pillow basalt with a sparse vesicle content, massive thinly bedded tuff with interlayered siltstone and shale, and interbedded limestone units within the flow and tuffaceous sections, suggest deposition of the Station Creek Formation volcanic rocks under subaqueous conditions. The organic-rich nature of the shale and argillaceous content of the limestone beds in the upper 400 m or "Transition zone" suggest a restricted basin environment of deposition.

Hasen Creek Formation. Hasen Creek Formation strata outcrop extensively in the Kluane Ranges and attains a maximum thickness of approximately 800 m (Fig. 3). It comprises grey to black shale, cherty argillite and chert, and siltstone in the lower portion with an upward gradation to shaley limestone, buff-coloured, massive limestone, and discontinuous beds of reddish-brown conglomerate, massive greywacke, and sandstone (Campbell, 1981).

Shale in this sedimentary sequence commonly contains pyrite crystals giving rise to oxidized exposures with a rusty appearance. Black shale locally grades to slate and both shale and siltstone are commonly interbedded with individual laminae between 0.5 to 1.0 cm in thickness. Chert and cherty argillite are pale grey-green to pale grey and thinly bedded (≤0.5 cm). Limestone may be fine and medium grained, white to buff-coloured argillaceous, crystalline, and massive with chert bands. Thin-bedded bioclastic limestone and calcarenite occur in the upper part of the Hasen Creek Formation on the southwest side of the terrane.

Sill-like gabbroic bodies invade the entire Hasen Creek Formation, however, ultramafic rocks of a cumulate origin preferentially occur near the contact between the Station

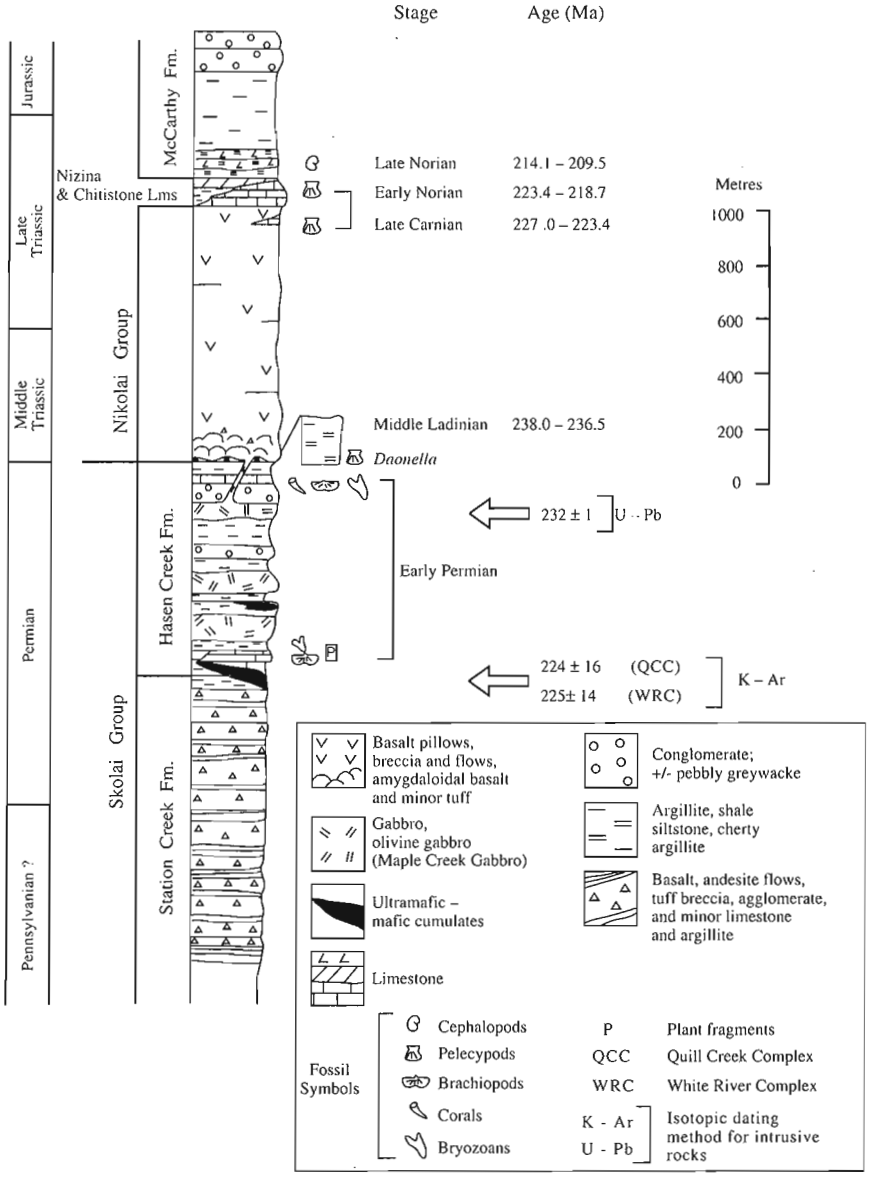

Figure 3.

Generalized stratigraphic section of Paleozoic and Mesozoic strata in the study area (modified from Read and Monger, 1976).

Creek and Hasen Creek formations. This intrusive activity has been dated at 232 Ma and is coeval with the onset of Nikolai volcanism during the Middle Triassic.

Diagnostic fauna within the Hasen Creek Formation indicate an Early Permian age (Read and Monger, 1976; Muller, 1967). This sedimentary assemblage (interlayering of shale, greywacke, and distinct limestone units) suggests deposition in a subaqueous basin under conditions of considerable fluctuation in water depth.

Nikolai Group

The Nikolai Group is a sequence of basalt flows, with minor interbedded limestone, which attains a thickness of approximately 1000 m and unconformably overlies the Hasen Creek Formation. At some localities a fossiliferous (*Daonella*) horizon separates the Hasen Creek Formation from the overlying Nikolai volcanic rocks. Where present this horizon can be up to several hundred metres thick and occurs as lens-shaped bodies consisting of argillite, carbonaceous shale, phyllite, and some thin grey limestone. Although no obvious break separates the buff-weathering, cherty argillite of the Hasen Creek Formation from this grey-weathering, *Daonella*-bearing horizon, the presence of *Daonella* demonstrates that these strata are Middle Triassic and form the base for the Nikolai Group.

The base of the volcanic pile consists of a thin, discontinuous maroon to dark green volcanic breccia and pillow breccia that reaches a maximum of 100 m in thickness (Read and Monger, 1976). Nikolai flows are thin (2 to 10 m), vesicular to amygdaloidal, and commonly have gently undulating flow tops. Locally, hematite-rich tuff and breccia or amygdule-rich zones separate flows. The lower portion of flows is dark green. Nikolai volcanic rocks are characteristically enriched in amygdules (10 to 30%) that are commonly 1 to 5 mm in diameter. Although they are scattered throughout the flows, amygdules generally increase upward and show a slight enrichment towards the centre of flows.

Thin (≤30 m) discontinuous bioclastic limestone and greenish-grey shale are interbedded within the flows. Faunas from interbedded limestone indicate a Late Carnian age for the cessation of volcanism.

Petrographically the Nikolai volcanic rocks can be divided into: (1) fine diabasic-textured flows, (2) porphyritic to glomerophyric flows with or without amygdules, and (3) very fine-grained amygdaloidal lava flows (Campbell, 1981). Groundmass mineral constituents include plagioclase, augite, magnetite, ilmenite, and glassy material. Phenocrysts include plagioclase, augite, olivine, and hornblende. Burial metamorphism to the prehnite-pumpellyite facies has given rise to chlorite, epidote, albite, quartz, laumontite, prehnite, and calcite.

The basal part of the formation appears to have been deposited subaqueously. However, the hematitic nature of most of the overlying flow tops, abundance of vesicles, and presence of interbedded limestone suggest that the remaining sequence was deposited under subaerial conditions.

Mafic-ultramafic intrusions

Mafic and ultramafic intrusions are common throughout the study area but are generally confined, particularly the ultramafic-dominated complexes, to or near the contact between the Station Creek and Hasen Creek formations. A significant number of these intrusive complexes are associated with anomalous magmatic sulphide concentrations, and some have proven to be of economic potential with respect to Ni-Cu±PGE+Au. The mafic-ultramafic complexes generally have a thin gabbroic marginal zone at their base and are overlain successively by mela-gabbro, clinopyroxenite, olivine clinopyroxenite, peridotite, and dunite. These complexes vary in thickness from <10 m to 600 m and may attain strike lengths up to 20 km. Coeval with these complexes and the overlying Nikolai volcanic rocks are varied-textured hypabyssal sills and dykes of a gabbroic composition and referred to henceforth as the Maple Creek gabbro. These sills generally overlie the mafic-ultramafic complexes and in some cases act as feeders to the Nikolai volcanic flows. Precise dating of these bodies at 232 ± 1 Ma by the U-Pb zircon method (Mortensen and Hulbert, 1991) constrains the earlier, less precise, K-Ar dates (≈224 ± 16 Ma) for the Quill Creek and White River complexes (Campbell, 1981) and the middle Triassic age for the Nikolai volcanism. Description of these mafic and ultramafic lithologies are discussed in conjunction with detailed descriptions of each complex.

Nizina and Chitistone limestone. Massive light grey limestone with bioclastic layers conformably overlie the Nikolai Group and underlie the McCarthy Formation throughout the Kluane Ranges. The thickness varies from several hundred metres to thin discontinuous lenses (≤30 m), but regionally the formation thins northeastward (Read and Monger, 1976).

Although the Chitistone and Nizina limestones are nearly devoid of macrofauna, locally abundant microfauna have been identified and indicate deposition during the Late Carnian to Early Norian stages of the Late Triassic (Read and Monger, 1976).

Gypsum and anhydrite forms a lens 7 km long and up to 1 km in width and could represent deposition in a sabkha environment similar to that postulated by Armstrong et al. (1969) for the lower part of the Chitistone Limestone at McCarthy, Alaska.

McCarthy Formation. Thin-bedded limestone of the McCarthy Formation usually overlies Chitistone Limestone only where the Chitistone is thick. The McCarthy limestone is light to dark-grey argillaceous, interbedded with dark-grey argillite, and gives rise to a distinctive striped "pajama rock" that ranges from tens to hundreds of metres thick. Within the lower 100 m of the McCarthy Formation thin shell beds containing *Monotis subcircularis* have been recorded and yield a Late Norian age (Late Triassic).

The upper grey argillite to phyllite section of the McCarthy Formation grades imperceptibly into Jurassic rocks. Minor conglomerate and greywacke occur near the top of the sequence. The few fossil localities indicate a Late Jurassic or early Cretaceous age.

Granitic intrusions

Granitic plutons outcrop in the north, central, and southern portions of the study area and were referred to by Muller (1967) as the "Kluane Ranges Intrusions". These bodies consist of medium-grained, massive hornblende granodiorite and diorite. Details of these plutonic rocks are given by Muller (1967). Potassium-argon dating for hornblende from a granitic body on Burwash Creek, in the central portion of the study area, gave an age of 117 to 115 ± 4 Ma and corresponds to an Early Cretaceous age (Christopher et al., 1972). The age of granitic intrusions in the Wrangellian terrane of the Yukon probably corresponds to the 117 to 105 Ma range established for granitic intrusions within the same terrane in eastern Alaska (Richter et al., 1975).

A few granitic dykes intrude the terrane at Burwash Creek. These thin bodies are commonly referred to as "felsite" and have a latite to quartz latite porphyry petrographic character. A potassium-argon date for biotite from this material gave an age of 26 Ma (Read and Monger, 1976) which corresponds to the Oligocene epoch.

Tertiary strata

In the study areas comprising the Duke River and Dickson Creek intrusive complexes significant thicknesses of Tertiary continental clastic sedimentary rocks and basaltic to andesitic volcanic flows have been deposited, and are designated as the Amphitheatre Formation and Wrangell lava, respectively.

Amphitheatre Formation. Lithologies comprising this formation are, in order of abundance: sandstone, siltstone, conglomerate, sand, gravel, shale, coal, clay, and tuff, but only the first three were encountered in the study area (Duke River Complex). Sandstone and conglomerate merge in places, both laterally and vertically, into unconsolidated equivalents (Muller, 1967). The arenite and rudite are light coloured with the harder beds being light yellow, orange, and brown, but the softer beds have been leached white. The coarser components of the clastic units consist of volcanic, intrusive, and minor sedimentary rocks derived from older formations from the Kluane and Donjek ranges, whereas the metamorphic rocks were probably derived from the Yukon Plateau to the east. Thin grey, laminated to poorly bedded shale beds locally contain fossil leaves suggestive of a Paleocene to Eocene age.

The Amphitheatre strata were clearly deposited in fresh water lakes and rivers within an intermontane basin environment. These sedimentary rocks may originally have been deposited over a wide area west of the Denali fault, but at present are generally confined to areas of higher elevation along the "Duke Depression", which is a chain of valleys and plateau surfaces west of the Kluane Ranges. The sedimentary succession appears cyclical with conglomerate at the base, ranging through pebbly sandstone and sandstone, to shale with clay and coal near the top. The thickness varies from 60 m to 575 m.

Wrangell lava. Miocene to Pliocene basalt, andesite, and minor acid pyroclastic rocks were deposited on a land surface formed in the Late Cretaceous to Early Tertiary. Study areas containing Wrangell lava are underlain by Amphitheatre Formation. The flows are distinguished by their reddish-brown to rusty-brown colour, and degree of freshness relative to the greenish and maroon colour of the more altered Triassic volcanic strata. The flows are mainly basaltic, ranging in thickness from 3 to 65 m, and are generally massive, but in places are columnar jointed in the lower part, and vesiculated to amygdaloidal near the tops. Flow tops are brick red and highly brecciated. The thickness of this extrusive sequence varies from 430 to 1400 m.

Structure and metamorphism

Apart from subsidence and minor warping the structural history of the Alaskan and Yukon tract of Wrangellia was relatively simple from the Pennsylvanian to Early Cretaceous and lacks evidence for any strong orogenic activity. During the Late Jurassic and Early Cretaceous conditions changed with the initiation of strong folding and northerly and westerly directed thrust faulting. It would appear that the first pulse of deformation occurred during the Late Jurassic (≈150-140 Ma) and the second during the Aptian (≈115 Ma). The first deformation may be the result of a Late Jurassic collision that amalgamated Wrangellia, Alexander, and Peninsular terranes into a composite super terrane called "Talkeetna" (Csejtey et al., 1982). The second deformation may record the initial contact of amalgamated Wrangellia to North America. Although less information is available for the Yukon portion of Wrangellia, Read and Monger (1976) suggested that deformation and accompanying low grade metamorphism are bracketed to being younger than unmetamorphosed Cretaceous fossiliferous strata (135 to 131 Ma) and older than the Kluane Ranges granitic plutons (117 to 115 Ma). Therefore, deformation and metamorphism must have occurred within the 131 to 117 Ma interval (Read and Monger, 1976).

Within the study area, two major northwest-trending faults, the Duke River fault and Denali fault, separate Wrangellia tectonostratigraphic assemblages from those of the western Alexander Terrane and the eastern Gravina-Nutzotin Belt.

The Denali fault marks the northeastern and eastern boundary of Wrangellia. After obduction, slicing of the continental margin by the ancestral Denali fault took place during the Tertiary and Wrangellia migrated northwards along the continental margin. Movements of hundreds of kilometres have been postulated during the Cenozoic (Forbes et al., 1974; Eisbacher, 1976). Displacement along the Denali fault continues today. The fault is steeply dipping and begins in eastern Alaska, continues through the Yukon and northern British Columbia as the Shakwak fault and Dalton fault. In this report the names Shakwak fault and Dalton fault are abandoned in preference for the regionally accepted name Denali fault. In the southeast portion of the study area the vertical to nearly vertical Duke River fault appears to join the Denali fault and together define the southeastern boundary of the Wrangellia. In the McCarthy Quadrangle of Alaska, the Duke River fault continues to separate Wrangellia from Alexander Terrane.

Smaller-scale faulting is present along the length of the Kluane Ranges. These faults strike northwesterly and appear to be steeply dipping to vertical. The density of faults increases to the southeast as the Duke River fault approaches the southern portion of the Denali fault.

Major fold axes strike parallel to the major northwest-trending faults mentioned above. These folds are tight to isoclinal, inclined to the southwest, and in turn have been folded about northeast axes into a series of culminations and depressions extending along the length of the Kluane Ranges.

A summary of the important geological events in Wrangellia and the study area is presented in Table 1.

GEOLOGY OF SELECTED KLUANE MAFIC-ULTRAMAFIC INTRUSIVE COMPLEXES

Eight exposed Triassic mafic-ultramafic intrusive complexes from the Yukon, two from northern British Columbia, and one from Alaska were selected for detailed geological, petrological, mineralogical, isotopic, and mineral deposit

Table 1. Summary of geological events in Wrangellia and the study area.

CENOZOIC	Quaternary	• Deposition of glacial silts, sands and gravels.
	Tertiary	△ Extrusion of Wrangell basaltic to andesitic flows during Miocene to Pliocene. ¤ Emplacement of quartz latite porphyry dykes during the Oligocene (26 Ma). • Deposition of continental clastic sediments of the Amphitheatre Formation. Fossil leaves suggest the formation is Paleocene to Eocene age.
MESOZOIC	Cretaceous	¤ Intrusion of granitic plutons ("Kluane Range Intrusions") between 117 and 105 Ma (Aptian-Albian stage).
	Jurassic	» Deformation during the Aptian stage due to the initial contact of amalgamated Wrangellia with North America. » Deformation related to Late Jurassic collision that amalgamated Wrangellia, the Alexander and Peninsular terranes into "Talkeetna". • Minor conglomerate and greywacke sedimentation near the top of the McCarthy Formation. Fossils suggest a Late Jurassic to Cretaceous age. • Terminal subsidence produced grey argillite and phyllite in the upper section of the McCarthy Formation. This horizon grades imperceptibly from the underlying Triassic age McCarthy Formation sediments into the overlying basal Jurassic rocks.
	Late Triassic	• Continued crustal subsidence gives rise to deep water basinal limestone of the McCarthy Formation during the Late Norian (*Monotis subcircularis*). • Gradual thermal subsidence of lithosphere, following cessation of volcanism, led to marine sedimentation of tidal (sabhka facies) and inner and outer platform carbonate of the Nizina and Chitistone Limestones during the Late Carnian to Early Norian (223.4 to 218.7 Ma).
	Middle Triassic	△ Extrusion of thick subaqueous (Karmutsen) and subaerial (Nikolai) basalts in western and eastern Wrangellia, respectively, continued until the Late Carnian (227-223.4 Ma). △ Commencement of widespread flood basalt volcanism throughout Wrangellia, and emplacement of mafic and Ni-Cu-PGE-bearing mafic-ultramafic subvolcanic sills at precisely 232 ± 1 Ma. ⇒ The mafic-ultramafic bodies preferntially intrude pyritic strata at or near the contact between the Permian Hasen Creek Formation and Pennsylvanian Station Creek Formation △ Initiation of a hot diapir of deep mantle material (plume) that rose beneath the oceanic lithosphere and caused rapid uplift of the ocean floor preceeding the onset of partial melting. • Deposition of a thin discontinuous, deep water, unit of black shale, siltstone and minor limestone with bivalves of *Daonella* during Middle Ladinian (238 to 236.5 Ma).
PALEOZOIC	Permian	• Postarc cooling and gradual subsidence led to the deposition of sedimentary rocks consisting of Lower Permian shallow water fossiliferous limestone, sandstone, shale and locally Middle to Upper Permian deep water argillite and radiolarian chert of the Hasen Creek Formation.
	Pennsylvanian	• The upper 400 m of the Station Creek Formation is characterized by thin interbedded black shale, siltstone, argillaceous limestone and cherty argillite with intercalations of very fine-grained tuff horizons that decrease in abundance upward. This section has been designated as the "Transition Zone" and forms a gradational contact with the overlying Hasen Creek Formation. This zone is noteably enriched in sedimentary sulphides. △ Development of an island arc complex consisting of a thick sequence of predominantly basaltic and andesitic volcanic and volcaniclastic rocks of the Station Creek Formation. This formation is generally unfossiliferous; however, two new conodont localities from limestones beds within the volcanic sequence suggest a late Mississipian to Early Permian age in the study area. Fossil evidence from Alaska suggest that the formation is probably Pennsylvanian.

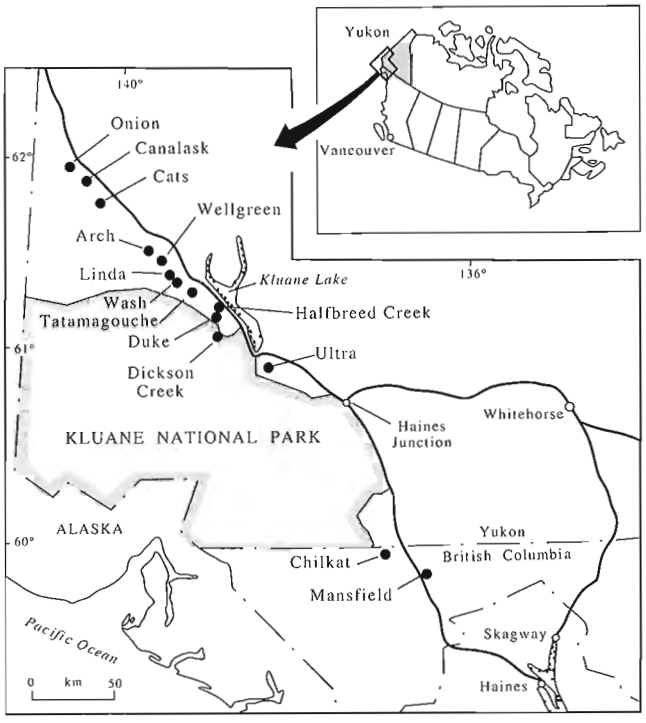

Figure 4. *Map showing the location of some of the better known mafic-ultramafic intrusive complexes in the Yukon and northern British Columbia, and most of those investigated during the course of this study.*

studies. The greatest concentration, best preserved, and economically most significant intrusions occur within the Kluane Ranges of the Yukon. In the Yukon and northern British Columbia, the belt has been divided into a Northern section (White River Complex), North-central section (Quill, Arch, and Linda Creek complexes), Central section (Tatamagouche, Duke River, Halfbreed Creek, and Dickson Creek complexes) and a Southern section (Chilkat and Mansfield Creek complexes). The Alaskan section deals with intrusive bodies from the Rainbow Mountain Complex, Alaska, and points out similarities with those from the Yukon, as well as new metallogenic features not yet fully appreciated (but of significant future potential) in the Canadian occurrences. The greatest concentration of these igneous bodies is in the northern and central sections of the belt (Fig. 4, 5). Potential hidden complexes, based on aeromagnetic data, are also shown. In addition, some mineralized properties associated with these complexes are also described. Since many of these localities are better known by their property or claim names (i.e. Canalask rather than White River Complex) their traditional claim names are also often used in conjunction with the name of the intrusive complex. Many of these historical claim names are synonymous with the complex name (Linda, Arch, Tatamagouche), however, others are not (Onion and Canalask properties of the White River Complex). Most of the properties discussed are shown in Figure 4, whereas the associated intrusive complexes are shown in Figures 1 and 5.

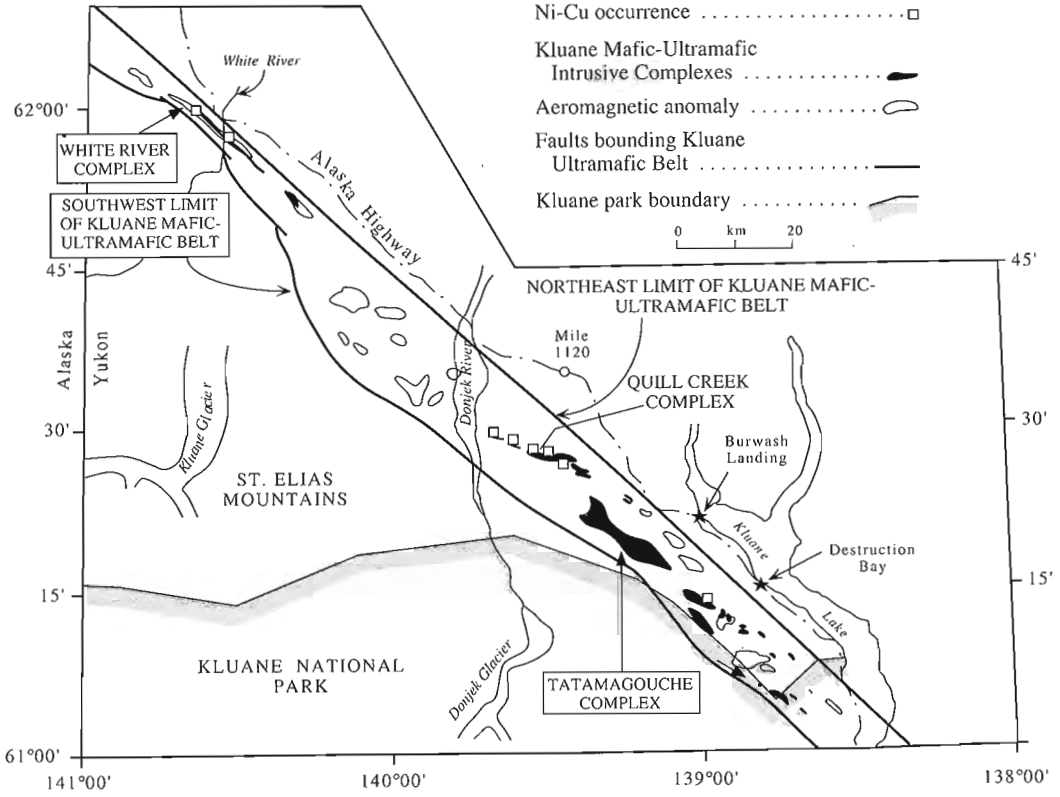

Figure 5. *Map showing the distribution and size of known Triassic intrusions, and the outlines of similar bodies inferred from aeromagnetic anomalies, within the Kluane Mafic-Ultramafic Belt in the central and northern portion of the Kluane Ranges, Yukon.*

Cumulate terminology, as defined by Wager and Brown (1968) and Irvine (1982), has been employed throughout this study because of the cumulate-like textural features present in the ultramafic lithologies. However, the lack of layering and associated mineralogical features (i.e. graded layering, cryptic layering, etc.), and the symmetrical distribution of similar lithologies about ultramafic cores in some subsidiary sills and apophyses raise considerable doubt concerning the origin of these textures by classical cumulate processes. Nevertheless, a semi-quantitative cumulate classification (where the cumulus minerals are listed in order of decreasing abundance, e.g. olivine-chromite cumulate) is used to describe the rocks, and a mafic-ultramafic rock nomenclature (Sabine, 1974) for mapping purposes.

Northern section

White River Intrusive Complex

The White River Intrusive Complex occurs in the southwest portion of the Yukon Territory and represents the second largest mafic-ultramafic body in the Kluane belt. It is 16 km long and attains an average width of approximately 275 m (Fig. 6). The complex characterizes the structure, internal magmatic stratigraphy, petrology, mineralogy, economic sulphide mineralization, late magmatic alteration zones, and the invaded Paleozoic strata associated with Kluane mafic-ultramafic intrusions. Investigations of the complex are based on studies conducted at the Onion and Canalask properties.

Onion property

Location, history, and physiography. The Onion property is located in the southwest Yukon Territory about 20 km east of the Alaska-Yukon border. It is situated on Miles Ridge, 3 km south of the Alaska Highway, at latitude 62°00'N and longitude 140°37'W and straddles the boundary between NTS claim maps 115F/15 and 115K/2 (Fig. 4, 6). The property covers the western end of the White River Intrusive Complex and occurs 7 km along strike from the Canalask nickel deposit. Access is either by helicopter or on foot from the highway. Accommodation is available at several nearby highway lodges.

Prospectors working in the vicinity of the Canalask nickel deposit discovered a nickel-copper occurrence along the northwest margin of the White River Intrusive Complex approximately 300 m east of Onion Creek. The occurrence was staked as the Beth claims in July 1952 for Prospectors Airways Ltd. and was referred to as the Discovery showing. The showing was subsequently held by P. Johnson and W. Abraham in 1956 (Ellik, Glacier, and Possible claims), G. Harris in 1957 (Success claims), Conwest Exploration Co. Ltd. in 1960 (Onion claims), Cominco Ltd. in 1966 (Hawk, etc. option), J. Enoch in 1967 (Porky claims), D. Backstrom in 1968 (Sparky claims), and by P. Versluce and C. Gibbons in 1969 as part of the neighboring Canalask property (Micro claims). Work consisted of prospecting, mapping, and hand trenching to evaluate the nickel potential of the property. The Onion property was staked by Archer, Cathro & Associates in 1986 on behalf of Kluane Joint Venture. In 1987 the Joint Venture optioned the property to Rexford Minerals Ltd. which conducted a program (managed by Archer, Cathro & Associates) of mapping, sampling, geophysical and geochemical grid surveys, and hand trenching (Main and Davis, 1989).

Most of the property lies above the treeline and covers a steep northeast-facing hillside, the main area of which occurs at approximately the 1220 m elevation, and is situated about midway above the 770 m White River valley and the crest of Miles Ridge which attains elevations of 1650 m.

Structure and stratigraphy. The western end of the White River Intrusive Complex is relatively well exposed on the Onion property and displays a number of important structural and stratigraphic, as well as petrological, features characteristic of the Kluane mafic-ultramafic intrusions. However, direct observations of these features at other localities in the Kluane Belt are not possible due poor exposure and structural deformation.

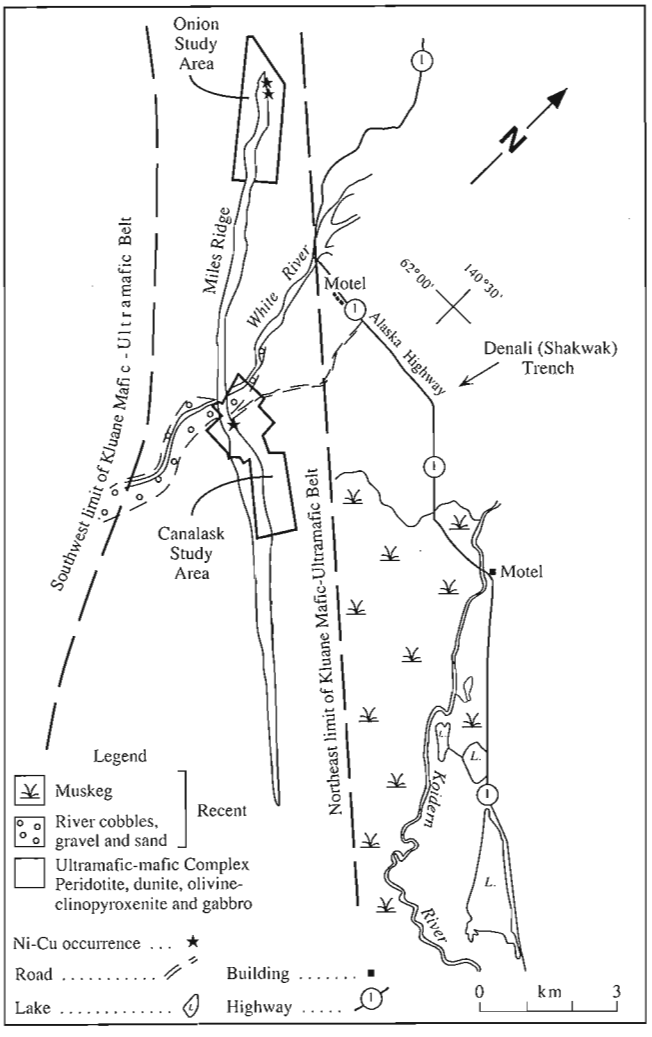

Figure 6. *Location of the White River Intrusive Complex and the Onion and Canalask properties and study areas.*

At the Onion property the White River Intrusive Complex consists of a sill-like body of ultramafic and mafic rocks exposed along strike for approximately 3000 m (Fig. 7). The intrusion normally varies in thickness from 100-150 m and dips to the southwest (≈50°). It intrudes the Pennsylvanian Station Creek Formation volcanic breccia and tuff that are, in turn, overlain conformably by the Permian Hasen Creek Formation limestone and clastic sedimentary strata and unconformably by the Upper Triassic Nikolai Group amygdaloidal basalt flows (Fig. 7).

The northern margin of the complex represents the original intrusive basal contact zone, whereas the southern margin delineates the upper intrusive contact. The ultramafic zone grades abruptly into a marginal quartz-carbonate alteration zone. This enveloping alteration zone occurs at the footwall and hanging wall contacts where it is developed over a width of approximately 50 m. Contacts are poorly exposed with highly variable dips ranging from vertical to shallow. The intrusion appears to pinch out near the western portion of the property (Fig. 7), however, it may extend farther north under the Nikolai Group volcanic cover. Stratigraphically all intrusive, extrusive, and sedimentary lithologies face in a southwesterly direction.

The youngest rocks in the area are the Cretaceous Kluane Ranges Intrusions. These intrusions consist of hornblende-diorite and granodiorite and are mainly confined to the area north of the White River Complex where they intrude Station Creek Formation strata. A small body of this type intrudes the Hasen Creek Formation adjacent the southern margin near the central portion of the ultramafic complex. Thin dyke-like bodies of this material intrude the ultramafic rocks of the complex.

A ground magnetic survey conducted over the property clearly outlines this predominantly ultramafic complex. As the magnetic contact closely coincides with that of the observed contact in areas of good exposure (which are limited due to extensive areas of talus and vegetation cover) the intrusive outline delineated in Figure 7 is based on the results of the magnetic survey. The complex and surrounds do not appear to have been folded, however, the magnetic survey did detect a number of small offsets along the contact due to faulting.

The most intriguing morphological features of this portion of the White River Intrusive Complex are embayments associated with the basal intrusive contact. The most unequivocal embayment occurs along the 600 m of strike length defining the northern (basal) contact southeast of Onion Creek. The northern contact in the central portion of the area also has similar characteristics, however, the influence of Cretaceous intrusives in this area cannot be ruled out. Similar features occur along the northern contact of the White River Complex at the Canalask property where Cretaceous Kluane Range intrusions are absent.

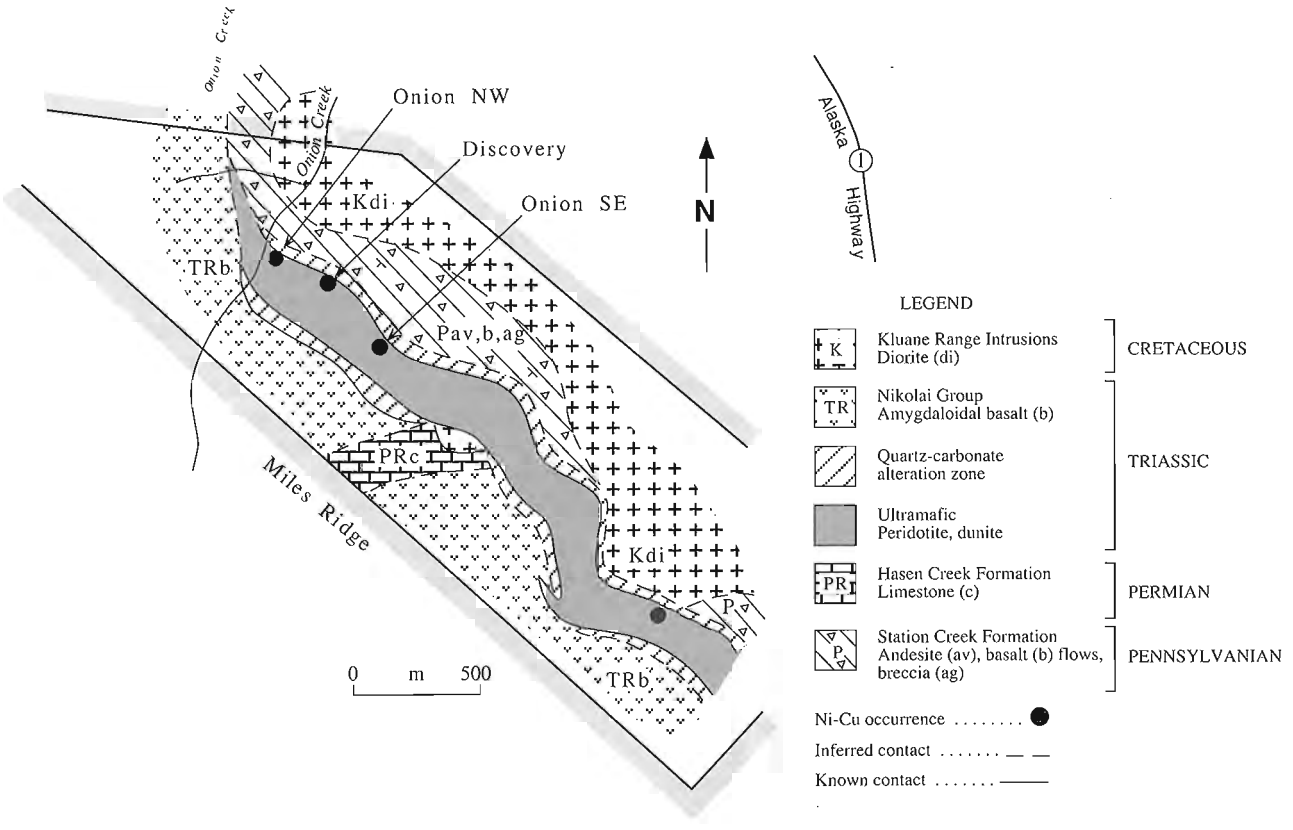

Figure 7. *Simplified geological map of the Onion property and study area.*

Petrology. The White River Intrusive Complex at the Onion property is dominated by ultramafic rock types. However, a thinly developed (0.3-3.0 m) zone of marginal gabbro occurs in two trenches through the basal contact and is assumed to be present along the entire base of the intrusion and possibly the upper contact zone as well.

Gabbro. Marginal gabbro is medium to coarse grained and highly oxidized. It contains the following phases: clinopyroxene (45-65%), plagioclase (30-50%), sulphides (0-5%), phlogopite (0-1.0%), and chromite (0-0.2%). Relict clinopyroxene displays both hourglass and undulose zoning, whereas plagioclase pseudomorphs consist of a turbid mosaic of albite, saussurite, kaolinite, and calcite. Orthopyroxene and olivine have not been observed, however, chemical analyses of the freshest specimens indicate that they are normatively present in terms of their Cross-Iddings-Pearson-Washington (CIPW) cation constituents. The highly decomposed nature of this rock type is due to the oxidized nature of the disseminated sulphides within and that of underlying massive and semi-massive Ni-Cu sulphide concentrations.

Ultramafic. All ultramafic lithologies are medium to coarse grained and are a dark green to black due to extensive serpentinization. The gabbroic marginal facies changes upward, over a distance of <0.5 m, into an ultramafic facies consisting of peridotite and dunite as the result of the onset of cumulate-like crystallization conditions. The underlying gabbroic rocks had a plagioclase-clinopyroxene (Pl:Cpx) crystallization order that passed into the overlying peridotite (wehrlite) as a consequence of the magma progressing to a compositional field conducive to clinopyroxene-olivine± chromite (Cpx:Ol:Chr) crystallization conditions. The clinopyroxene-olivine-chromite and olivine-clinopyroxene-chromite cumulate character of these lithologies is well displayed in the photomicrographs in Figure 8 (A, B). Chadocrysts of cumulus olivine are included in intercumulus clinopyroxene, and in clinopyroxene overgrowths on cumulus clinopyroxene. Olivine may display a strong elongated idiomorphic habit with the subsequent development of a pronounced igneous lamination (Fig. 8B) due to magmatic flow or postcumulate current action, whereas, other phases have a xenomorphic habit due to subsolidus peritectic reactions (Fig. 8C). Cumulates from this level of the intrusion are referred to as poikiolitic peridotite due to the development of large (10-20 mm) intercumulus crystals of clinopyroxene with included olivine and chromite. Subsequent alteration of the samples commonly gives rise to serpentinized olivine included in relatively unaltered clinopyroxene as shown in Figure 8C. Accessory orthopyroxene occurs as an intercumulus phase.

Approximately 50 m above the base of the complex a phase change is present where clinopyroxene disappears as a cumulus phase and the volume of intercumulus clinopyroxene, and its distinctive poikiolitic texture, decrease noticeably. Subsequent lithologies are more olivine-rich than those from the underlying cumulate stratigraphy and have a higher proportion of intercumulus plagioclase. In cumulate terminology lithologies from this horizon are olivine±chromite cumulates with a high proportion of intercumulus plagioclase. A non-cumulate designation for lithologies from this horizon would classify them as dunite or feldspathic dunite. Altered dunite usually occurs in the form of serpentinite (Fig. 8D) which still preserves their original textural features regardless of the degree of serpentinization of olivine and alteration of plagioclase to a dark turbid mass of clay minerals. Stratigraphic and petrological profiles of the remaining stratigraphic interval were not conducted in the same detail as in the underlying ultramafic rocks, however, field relations suggest that the upper half of the complex is the mirror image of the lower half, with the possible absence of the upper gabbroic margin.

At a few localities on the property, peridotite with disseminated sulphides was noted immediately above the gabbro-ultramafic transition zone (Fig. 8E). Unfortunately, this portion of the complex is mostly covered with talus and its continuity along strike is uncertain. Other ultramafic rocks within the belt contain significant enrichments of disseminated sulphides at this stratigraphic level and there is no reason to believe that it is absent from the Onion property.

Quartz-carbonate alteration. This zone of quartz-carbonate alteration is derived from the marginal mafic-ultramafic intrusive rocks, plus some of the adjacent Pennsylvanian and Permian wallrocks. Representative samples of this alteration have a fine-grained waxy grey to buff coloured matrix that weathers to orange. The samples are commonly laced with thin quartz and carbonate veins. Fine disseminations of pyrite are present locally.

Ni-Cu±PGE mineralization.

Immiscible magmatic sulphide segregations. At the Onion property Ni-Cu-PGE mineralization has been noted at four localities along the northern or basal contact zone of the complex. Three of these occurrences are situated within the 700 m "Onion zone", southeast of Onion Creek (Fig. 7). The second zone is the 500 m long "Sax zone" near the southern end of the property. Although no additional surface Ni-Cu sulphide mineralization has been discovered, coincident geochemical and geophysical anomalies suggest a third zone. This anomalous area is referred to as the "Rex zone" and occurs along the basal contact between the Onion and Sax zones for about 400 m. Additional exploration may demonstrate that the Sax and Rex zones are continuously mineralized or that all three zones are continuous at depth.

The Onion zone contains the Discovery showing, plus two smaller showings, one 200 m to the northwest and the other 300 m to the southeast (Fig. 7). The Discovery and Onion Northwest showing contain semi-massive to massive, slightly foliated, pyrrhotite-pentlandite-chalcopyrite bands up to 10 cm thick. The Onion Southwest showing, discovered in 1987, consists of strongly sheared and altered mafic-ultramafic rocks containing malachite and minor limonite staining but no apparent sulphides. However, samples of this mineralization assayed up to 19.2% Ni, 0.02% Cu, 100 ppb

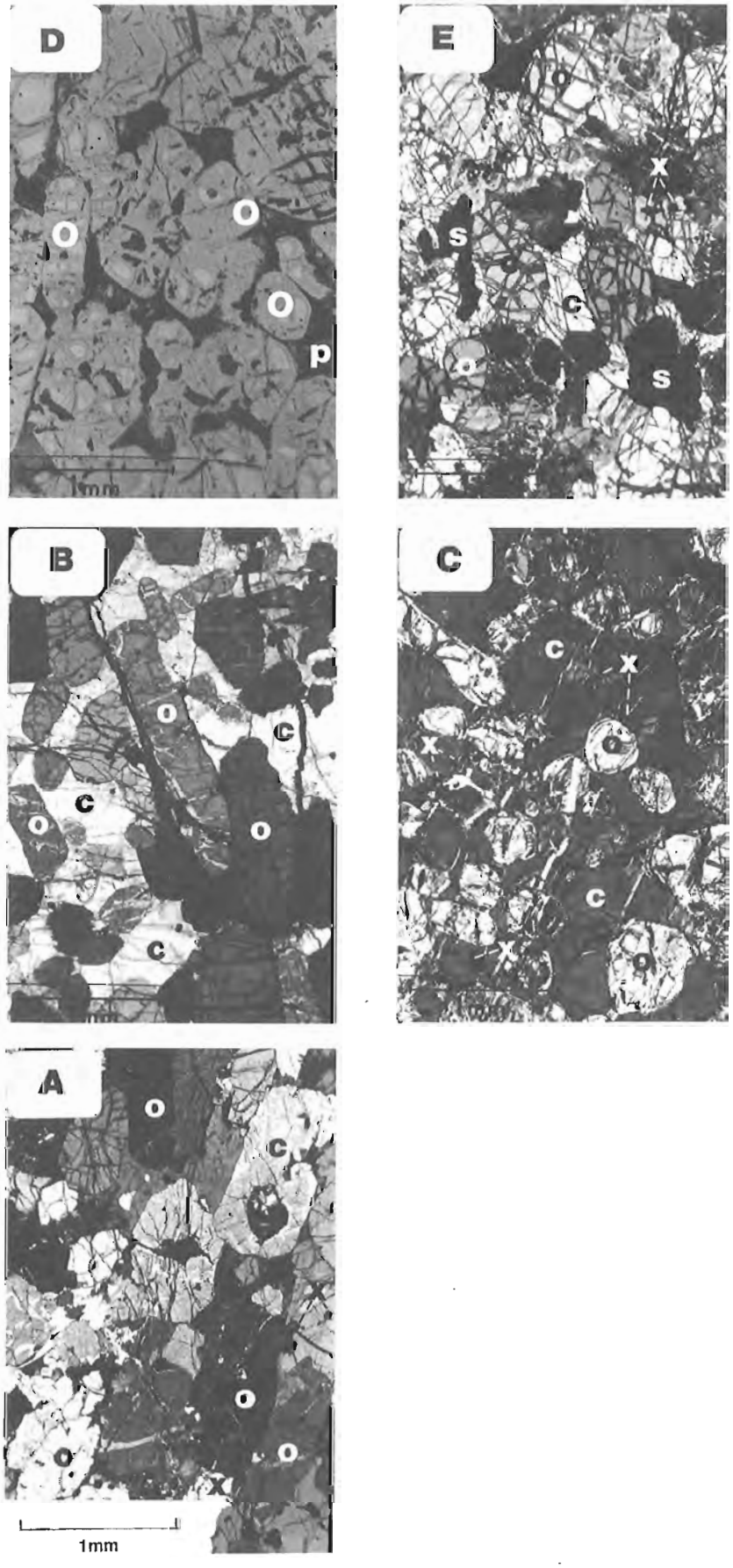

Figure 8.

*Photomicrographs of representative ultramafic lithologies from the Onion property. GSC 1995-106B (**A**) HDB-88-On-8. Olivine-clinopyroxene cumulate with chadocrysts of cumulus olivine included in cumulus clinopyroxene overgrowths. Note the igneous lamination defined by the elongation of minerals. Cross-polarized light. (**B**) HDB-88-On-8a. Olivine±chromite cumulate with elongated cumulus olivine grains included in large oikocrysts of intercumulus clinopyroxene. Cross-polarized light. (**C**) HDB-88-On-9. Olivine± chromite cumulate with rounded, subrounded and embayed cumulus olivine grains resorbed by the intercumulus melt. Many of the olivine grains are cross-cut by serpentine minerals. Cross-polarized light. (**D**) HDB-88-On-15. Olivine±chromite cumulate with intercumulus plagioclase. Olivine is completely serpentinized and plagioclase is altered to a dark turbid mosaic of clay minerals and carbonate. Rock types of this character have been mapped as dunite or feldspathic dunite (now serpentinized). Plane-polarized light. (**E**) HDB-88-On-12. Olivine-clinopyroxene-sulphide cumulate. Cross-polarized light. o = olivine, c = clinopyroxene, x = chromite, p = plagioclase, s = sulphide.*

Pd, 50 ppb Pt, and 4100 ppb Au. The high Ni and low Cu content is believed to be due to the presence of niccolite rather than Ni-Cu sulphides.

The Discovery showing represents the best mineralization discovered to date on the Onion property. The mineralization consists predominantly of pyrrhotite, pyrite, pentlandite, chalcopyrite and minor heazlewoodite, niccolite, and magnetite which occurs at or near the base of the marginal gabbro. Assays of this massive sulphide mineralization range from: Ni (3.1-4.5%), Cu (0.73-0.91%), Co (0.09-0.15%), As (60-983 ppm), Pd (750-1700 ppb), Pt (50-2000 ppb), Au (26-56 ppb), Rh (700-780 ppb), Os (760-1000 ppb), Ir (640-840 ppb), and Ru (1900-2500 ppb). Disseminated sulphide mineralization in the hanging wall gabbro contains up to 0.32% Ni, 0.24% Cu, and 1100 ppb PGE+Au. For a summary of compositional ranges for respective elements and lithologies from the Onion property see Figures 73, 85, 96, 107, and 119.

The basal outline of the White River Intrusive Complex reveals a number of important structural controls on the distribution of the primary immiscible magmatic sulphides within this complex. The best mineralization in the Onion zone (i.e. Discovery showing) occurs in the trough or axial zone of the most westerly floor embayment. If these are primary magmatic controls the two pronounced embayments associated with the Rex zone should be high priority future exploration targets.

Hydrothermal (remobilized ?) mineralization. The quartz-carbonate alteration appears to be a metasomatic front in which Mg and Fe are removed and Si, Ca, and CO_2 are introduced. In general, this rock type has high precious metal contents: 510, 330, and 10 ppb Pd, Pt, and Au, respectively, for relatively S-poor (0.37 wt.%) samples with <1400, 1600, and 2600 ppm Cr, Ni, and Cu, respectively. These samples are also characteristically As-rich (≈413 ppm).

Canalask property

Location, history, and physiography. The Canalask property is located in the southwestern Yukon Territory, approximately 375 km northwest of Whitehorse. It occurs on the east bank of White River at latitude 61°57′, longitude 140°32′, within NTS claim map 115F/15. The property is accessible from the Alaska Highway (km 1880) by a 4 km all-weather road. Accommodation, service, and supplies are available within a few kilometres at White River Lodge and Koidern Motel (Fig. 4, 6).

In 1952, Ni-Cu sulphide mineralization was discovered near the east bank of the White River by P. Eiklund, W. Theriault, and F. Hickey. The claim was optioned in 1953 by Prospectors Airways Ltd., Noranda Mines Ltd., and Kerr Addison Gold Mines Ltd. syndicate, which drilled 14 diamond-drill holes (S1A-S14) for a total of 1622 m. Canalask Nickel Mines Ltd. optioned the property from 1954-1958 and completed 518 m of drifting on two levels connected by a 107 m winze, and 16 surface (2677 m) and 14 underground (402 m) diamond-drill holes, in addition to metallurgical testing. P. Versluce and associates remapped and sampled the property from 1964-1966. From 1967-1968 the property was optioned by Discovery Mines Ltd., Rayrock Mines Ltd., and Consolidated Canadian Faraday Mines Ltd. The syndicate completed a geophysical survey (IP, magnetometer, EM-16), trenching, surface drilling (999 m), and underground drilling (371 m). A joint venture between Canadian Superior Exploration Ltd., Aquitane Co. Canada Ltd., Home Oil Ltd., and Getty Mines Ltd. optioned the ground in 1972-1973 and drilled 7 surface holes (643 m) and a conducted a geophysical survey (magnetometer and EM). In 1987 Kluane Joint Venture purchased the ground from P. Versluce and associates and in turn optioned it to Rockridge Mining Corporation. During this time 603 m of surface diamond drilling and geophysical (magnetometer and VLF) programs were conducted. In 1988 a underground chip sampling program was conducted. The 1987 and 1988 programs were managed by Archer, Cathro and Associates. The 1952 to 1968 work concentrated on a small area of high grade nickel sulphide mineralization referred to as the "Main zone" located north of the complex. However, exploration during the 1972-1987 period was primarily directed at larger areas of lower grade Ni-Cu-PGE mineralization within the ultramafic portion of the complex.

The topography of the property consists of rolling hills, forested by spruce stands, and local interspersed birch and alders growths separated by swampy depressions.

Structure and stratigraphy. Due the scarcity of natural exposures on the property the intrusive contacts have been outlined with the aid of geophysical surveys, diamond-drill hole data, and trench contact mapping (Fig. 9).

The study area covers about 2.7 km of strike length in the central portion of the White River Intrusive Complex where it has an average width of 430 m but may be as much as 600 m wide. The northern outline defines the basal contact of the intrusion whereas the southern outline marks the upper intrusive contact. Geophysical and geological data suggest that the intrusion has an average dip of 45° to the southwest and has not been significantly affected by faulting or folding.

As at the Onion property, the basal contact is juxtaposed Station Creek Formation and the upper contact borders Hasen Creek Formation strata. However, unlike the Onion property, the Canalask property lacks a marginal quartz-carbonate alteration zone and locally exhibits a thin (<2.0 m) contact metamorphic (thermal) aureole in the footwall Station Creek Formation tuff.

The property also contains a proximal massive sulphide deposit in the footwall of the intrusion and has been referred to by the various exploration geologists working the property as the "Main zone" mineralization. Associated with this mineralization is a 20 m thick mixed mineralized gabbro-sedimentary rock unit that has in the past been informally referred to as the "Chert" unit. It occurs north of the Main zone massive sulphide deposit and extends eastwards for a strike length of >1.0 km, and appears to converge with the base of the ultramafic complex in the vicinity of diamond-drill hole VQ7 (Fig. 9).

It would appear from the examination of old drill records, and of limited telescoped core from two of these intersections, that the ultramafic complex possesses a crude cumulate stratigraphy. A marginal contact gabbro facies was not observed during this study; examination of the logs from the 1972-73 drilling program, however, suggests that a gabbroic to feldspathic ultramafic marginal facies exists near DDH-VQ7. Feldspathic peridotite commonly occurs near the basal contact of the intrusion and in turn grades upwards into non-feldspathic peridotite and dunite. With the exception of one limited exposure along the east bank of White River, the stratigraphic succession for the remaining upper half of the complex is unknown due to lack of exposure and drilling in the area. Nevertheless, the presence of feldspathic peridotite near the southern boundary and of similar internal magmatic stratigraphy in other intrusions elsewhere in the belt suggests that a mirror image of the stratigraphy in the lower half of the intrusion can be expected in the upper half. If this is the case the lower and upper 20% of the stratigraphy is predominantly feldspathic peridotite (±gabbro) with the remaining central portion of the intrusion occupied by olivine-rich cumulates of dunitic character. A distinctive mineralized peridotite horizon is associated with the basal contact zone of the intrusion. This horizon has a strike length of >2.0 km, a width of 7 to 12 m, and is generally found 30 to 50 m south of the basal contact (Fig. 10).

A large footwall embayment along the central portion of the northern contact, and a congruent depression along the southern hanging wall contact represent primary basinal structures which may have significant exploration implications.

Petrology. Five ultramafic and two sulphide associations have been identified on the property (Fig. 11).

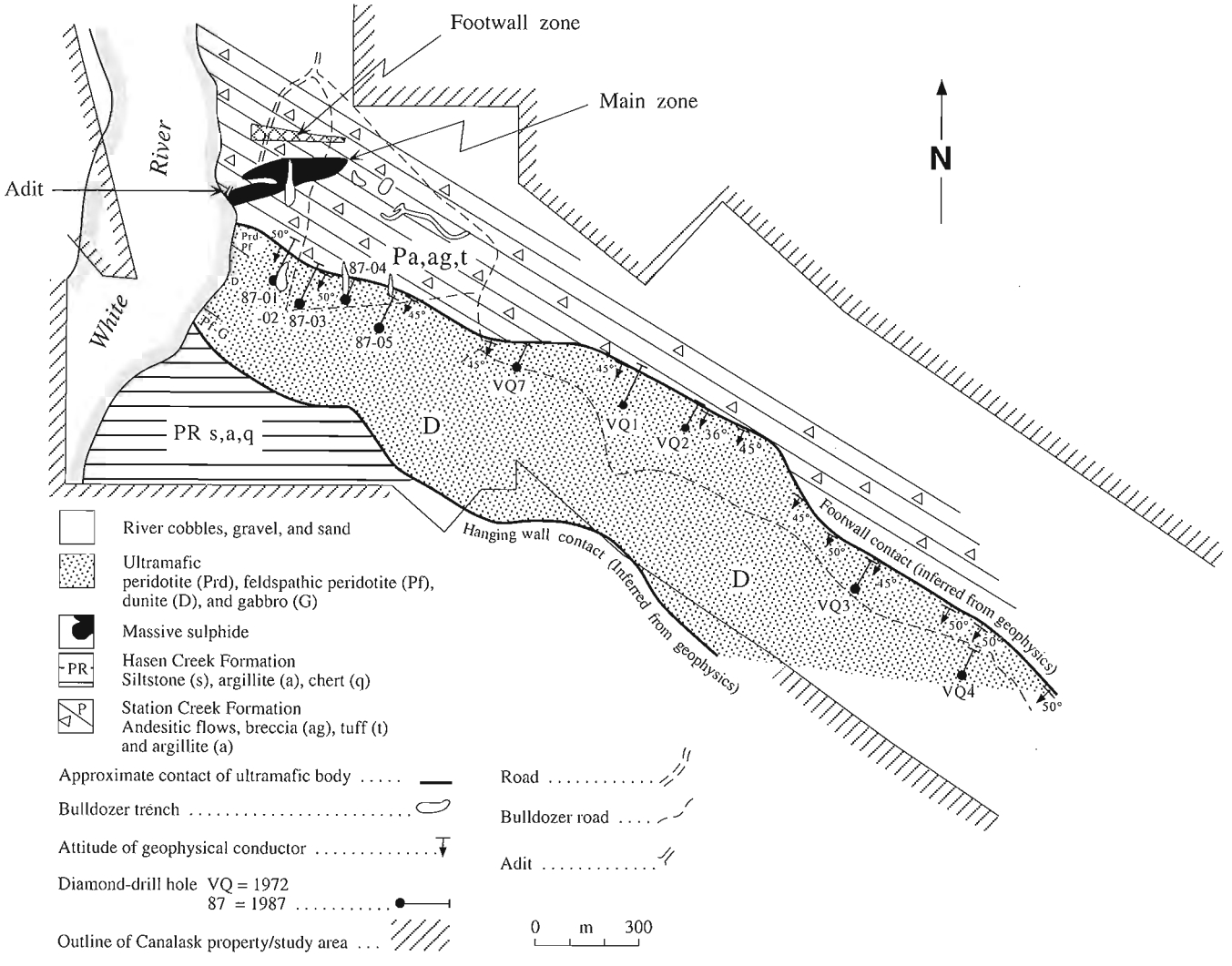

Figure 9. *Simplified geological map of the Canalask property with the hanging wall and footwall contacts inferred from geophysical surveys.*

Sulphides. The most common sulphide-rich lithology from the Main zone mineralization (north of the ultramafic complex) is that of a brecciated clinopyroxene-sulphide cumulates. Semi-massive mineralization displays large, somewhat fractured, cumulus clinopyroxene supported in a matrix of pyrrhotite, pentlandite, and chalcopyrite. The matrix sulphides commonly contain smaller fragments of compositionally similar pyroxene. Mineralized gabbro from the thin gabbro-sedimentary rock or so-called "Chert" unit is shown in the Figure 11B. The rock is fine grained and consists of a microcrystalline, cataclastic matrix of amphibole, pyroxene, epidote, plagioclase, clay minerals, and sulphides. Porphyroblastic albite and relict gabbro domains are visible in thin section. Macroscopically this rock type is similar to some Station Creek Formation rocks.

Ultramafic. Clinopyroxene cumulates (clinopyroxenite), similar to that shown in Figure 11C, occur both near the base of the complex and interlayered with peridotite in the overlying ultramafic cumulate succession. Cumulus clinopyroxene generally alters to uralite, and intercumulus plagioclase commonly occurs as a turbid mosaic of clay minerals and Fe-oxide dusting. Large intercumulus grains of phlogopite are local. The introduction of cumulus olivine±chromite introduces clinopyroxene-olivine±chromite cumulates or wehrlite (Fig. 11E). The proportion of intercumulus plagioclase is quite variable at this horizon (Fig. 11D), however it increases in volume up section at the expense of intercumulus clinopyroxene. Olivine from this level of the intrusion commonly has a pronounced elongate growth habit (Fig. 11D) which has subsequently been influenced by either magmatic flow, currents, or stratified chemical (nutrient) gradients in the overlying magma column. The increasing proportion of intercumulus plagioclase and cumulus olivine up section is clearly demonstrated in Figure 11F. This serpentinized olivine cumulate has near dunitic olivine concentrations. Note the dark turbid character of the altered intercumulus plagioclase (Fig. 11F). For some unknown reason plagioclase minerals from the Kluane Mafic-Ultramafic Belt are extremely unstable and are generally completely altered, even in the presence of fresh olivine and pyroxene. Elimination of the intercumulus liquid from the cumulate in Figure 11F would produce true olivine adcumulates or dunite similar to that represented in Figure 11I.

Macroscopic examinations of a number of mineralized peridotite or olivine-sulphide-chromite cumulates suggest that these sulphide-enriched samples have relatively higher proportions of intercumulus plagioclase than do unmineralized

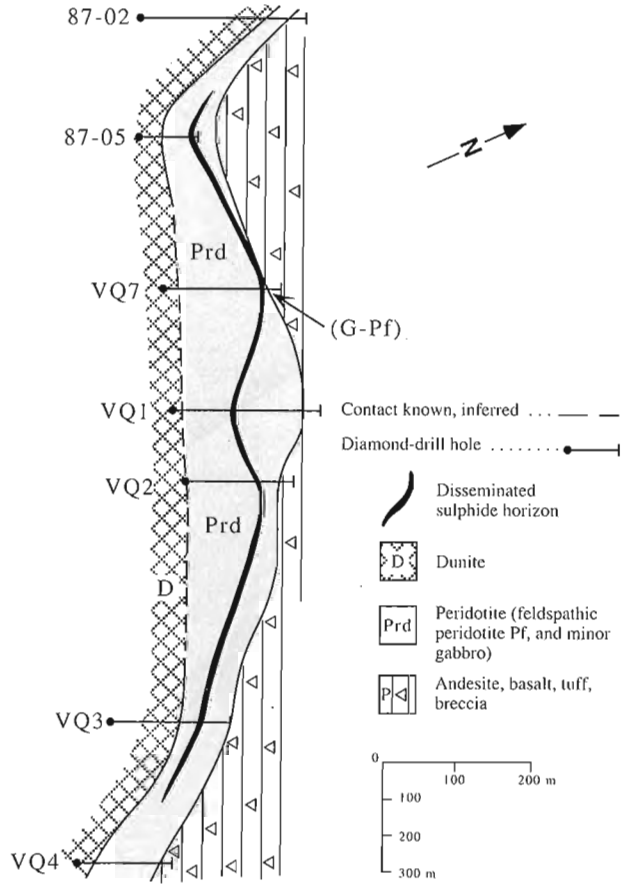

Figure 10. *Generalized geological plan of the lower third intrusive stratigraphy of the Canalask property and the underlying footwall strata based on diamond-drill hole projections from DDH-87-02 to DDH-VQ 4. Note how the basal peridotite member passes into dunite towards the core of the intrusion, and the conformable and dis-conformable attitude of the undulating disseminated sulphide zone.*

Figure 11 *(opposite). Photomicrographs of representative lithologies from the Canalask property. GSC 1995-106M* ***(A)*** *HDB-88-CAN-19b. Main zone semi-massive sulphide ore. Brecciated clinopyroxene-sulphide cumulate with numerous small clinopyroxene fragments in a consolidated sulphide matrix. Plane-polarized light.* ***(B)*** *HDB-CAN-4. Highly altered mineralized gabbro protolith from the thin gabbro-sediment or so-called "chert unit". Note relict igneous clinopyroxene. Plane-polarized light.* ***(C)*** *DDH-87-05-74.9. Coarse clinopyroxene cumulate with intercumulus plagioclase (now altered). Plane-polarized light.* ***(D)*** *HDB-88-CAN-23a. Clinopyroxene-olivine± chromite cumulate with some intercumulus plagioclase. Cross-polarized light.* ***(E)*** *HDB-88-Can-10a. More closely packed and laminated clinopyroxene-olivine±chromite cumulate. Cross-polarized light.* ***(F)*** *DDH-87-02-139.67. Serpentinized olivine±chromite cumulate or dunite with altered intercumulus plagioclase. Plane-polarized light.* ***(G)*** *HDB-87-CAN-9b. Olivine-sulphide cumulate, or net-textured sulphides in peridotite. Plane-polarized light.* ***(H)*** *HDB-87-CAN-9a. Olivine-sulphide cumulate, or net-textured sulphides in peridotite. Plane-polarized light.* ***(I)*** *YQ3-66.6. Olivine adcumulate or dunite. Note the olivine grain boundary triple point junctions, lack of intercumulus material and the fresh, unaltered nature of this rock. Cross-polarized light. o = olivine, c = clinopyroxene, x = chromite, p = plagioclase, s = sulphide.*

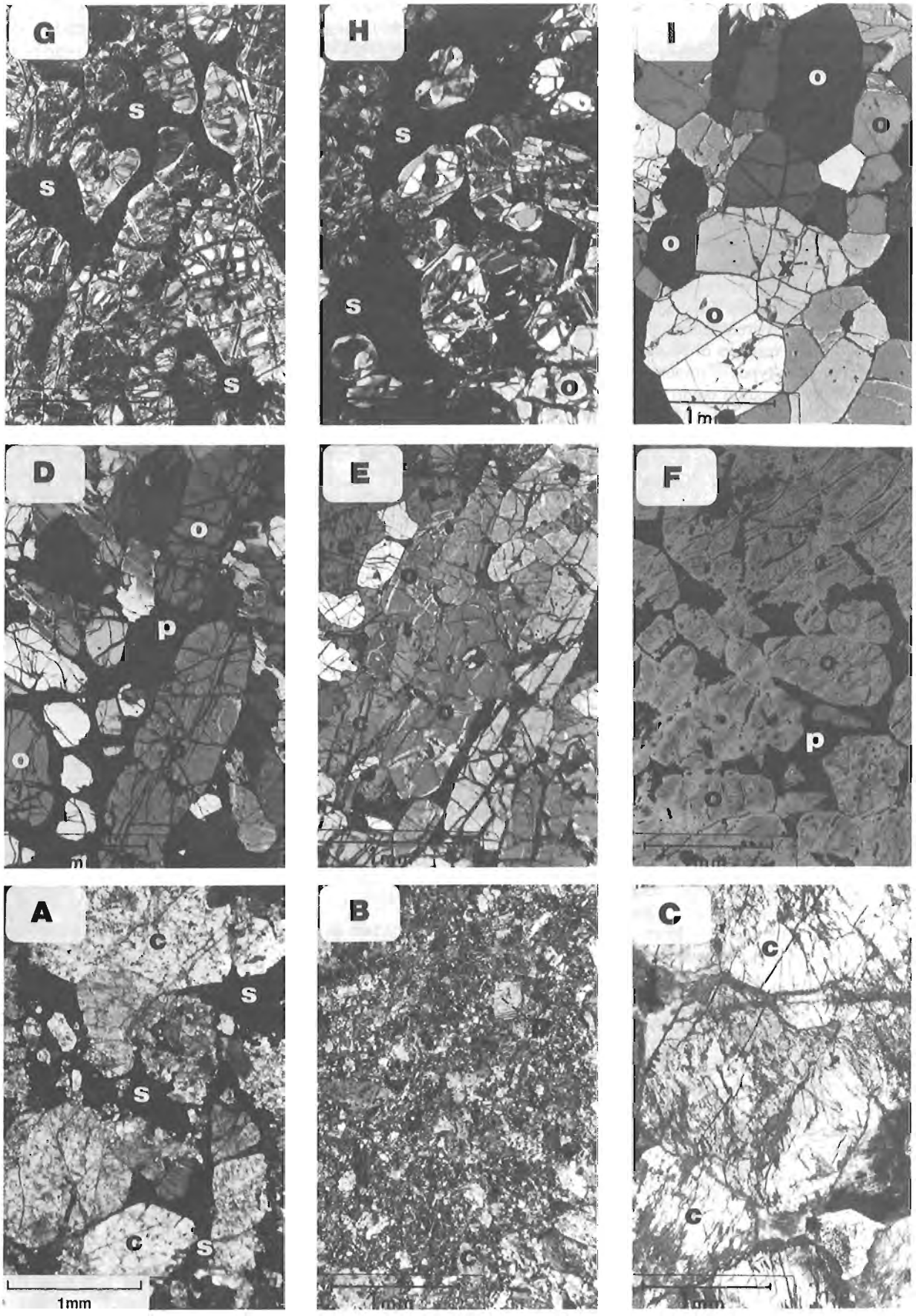
G
S
S
S
H
S
S
O
I
O
O
O
O
1m
D
O
P
O
m
E
O
O
F
O
P
O
A
C
S
S
C
S
1mm
B
C
C
C
C

peridotite. Typical peridotite on the Canalask property generally contains <0.50% sulphides whereas mineralized samples contain 5.0 to 8.0% sulphides. Sulphide-enriched portions of the mineralized peridotite display classic olivine-sulphide net texture fabrics (Fig. 11G, H).

Ni-Cu±PGE mineralization. Economically significant concentrations of Ni-Cu±PGE+Au mineralization occur both within the ultramafic cumulate strata of White River Intrusive Complex and in the proximal footwall Station Creek Formation strata at the Canalask property. The latter type is unique within the Kluane Belt, nevertheless it represents the largest proven single reserve of directly exploitable high-grade Ni-Cu sulphide mineralization in the Yukon. In addition, it also serves as a model for a new environment within the belt in which to explore for additional reserves of Ni-Cu sulphide mineralization. Research on both types of mineralization suggests some interesting primary structural controls on the distribution of magmatic sulphides and the role of footwall embayments on the distribution of mineralization. Possible future discoveries of massive sulphides within these floor embayments and their influence on the distribution of "Offset"-type mineralization must be considered. For a graphical summary of the base, precious, semi-metal concentrations as well as sulphur-isotope compositions and metal ratios for the various lithologies and mineralization see Figures 74, 86, 97, 108, and 120.

Immiscible magmatic sulphide segregations.

Ultramafic. On the Canalask property a 5 to 8 m thick strata-bound horizon of mineralized peridotite occurs within the basal portion of the White River Intrusive Complex. This mineralized horizon is continuous along strike for over 2.0 km. Although the mineralized horizon was not intersected in diamond-drill holes 87-01 to 87-04 and VQ4 on the western and eastern ends of the property, this horizon may be present at other localities farther along strike (Fig. 9, 10). The mineralized peridotite generally contains 5 to 8% disseminated sulphides with sporadic patches of net-textured sulphides.

The Ni and Cu grades within this horizon range from 4000-7800 ppm and 700-2700 ppm respectively. Chalcophile metal concentrations within the ultramafic members generally display a coherent trend with respect to the amount of sulphide or sulphur in the samples. Unlike the semi-massive and massive "Main zone" Ni-Cu sulphide mineralization in the footwall, the mineralized ultramafic rocks contain high PGE+Au concentrations (800-1600 ppb) relative to the amount of sulphide in the sample (see Fig. 130A). The figure indicates that unmineralized ultramafic rocks contain high background PGE+Au concentrations. Plots of the various noble metals also demonstrate coherent trends with respect to the amount of sulphide (Fig. 108A, B, D, 120A, B, C), but a weaker correlation exists for Au (Fig. 108C). With the exception of five samples falling in the 0.03-0.1 wt. % S range, all of the ultramafic rocks have S/Se ratios of <5000 (Fig. 97A). The ratio for the mineralized samples fall in the 2000-5000 range. The abnormally low values (<1000) associated with the S-poor samples may be the result of S loss due to serpentinization. Eckstrand and Hulbert (1987) have suggested that Ni-Cu sulphide mineralization with S/Se values <5000 are commonly enriched in PGE+Au. Although there is no correlation between the S/Se x 1000 ratio and PGE+Au content of the ultramafic units (Fig. 130D) a strong statistical correlation exists between the amount of noble metals associated with the sulphides (S/PGE+Au) and the S/Se ratio of the sulphides in the samples (Fig. 130C).

The western half of the mineralized peridotite horizon has an unusual undulating character relative to the eastern half. The most remarkable feature of this horizon is that it forms a topographic high over an area underlain by a structural depression due to an embayment along the basal contact. Similar structures are common to ultramafic bodies hosting Ni deposits in komatiitic terranes. Although an adequate explanation for this feature must await future drilling, it does explain the localization of the best magmatic sulphide mineralization recorded within the ultramafic portion of the complex. The 1972 diamond-drill hole VQ7 intersected a 0.12 m concentration of semi-massive Ni-Cu mineralization in gabbro at the basal contact. The average grade was 1.32% Ni and 0.32% Cu, and a minimum of 2.0 ppm PGE+Au. Mineralized feldspathic peridotite assaying 0.66% Ni and 0.28% Cu over 1.4 m overlies this semi-massive sulphide concentration.

It would appear that a cryptic cumulate stratigraphy and topography exist within similar cumulate lithologies in the ultramafic zone of the Canalask property. The accumulation of semi-massive concentrations of immiscible magmatic sulphides at this horizon is the result of sulphide immiscibility followed by gravitation settling and accumulation in topographic depressions. These paleo-topographic highs may have riffled sulphides from magma flowing over these sites.

Offset mineralization. Three separate areas of nickel, copper, and PGE mineralization occur in a 200 m wide and >1000 m long section of intense alteration (albitization) in the footwall of the ultramafic body. The section is bounded on the west by the White River and disappears to the east under heavy overburden cover and swampy ground.

"Main zone". The Main zone Ni sulphide deposit occurs on the east bank of White River. This discordant ore deposit is located from 50 to 125 m in the footwall of the ultramafic body. It occurs in the form of a steeply dipping, southwest plunging, Ni sulphide zone that is approximately 130 m long and 23 m wide. In plan the Main zone appears as a northern appendage of massive sulphide projecting from the base of the ultramafic body beneath White River. The sulphide body is enclosed by bedded andesitic tuff and volcanic breccia. Unfortunately all records of the 1953-1968 work on the body were lost and the only available information was obtained from page-sized summary maps prepared by consultant P.H. Sevensma for the property owners in 1966. These maps indicate that most of the mineralized intervals average about 1.5% Ni but individual values as high as 6.0% have been noted. Discovery Mines Ltd. suggested (1968) that this zone contains 390 235 tonnes of ore grading 1.35% Ni. However, this calculation did not consider dilution, thus a more realistic

value based on a 0.0% Ni value for unassayed or recovered intervals over this 23 m average width suggest a ore reserve of 1 800 000 tonnes of 0.86% Ni. This grade is considered conservative, as the average grade of sections on the 2700 Level, where complete assays were carried out and no dilution is necessary, is 1.10% Ni (Carne, 1989). It is believed that the Main zone converges, down-plunge to the southwest, with the footwall contact of the ultramafic complex and provides extensions to the outlined tonnage.

"Footwall zone". A poorly defined sulphide domain known as the Footwall zone occurs approximately 30 m north of the Main zone. This zone has been intersected by seven drillholes and by the 2700 Level crosscut. Most of the intersections consist of narrow intervals of moderate copper and nickel grade, with the exception of a near surface intersection grading 0.58% Ni (Carne, 1989).

"Gabbro-sedimentary rock unit". A relatively steeply dipping, 20 m thick, mineralized unit consisting of altered gabbro and tuffaceous sediments occurs immediately north of the footwall zone in the vicinity of the main showing area. The unit appears to converge with the floor of the ultramafic complex to the southeast, in the vicinity of diamond drill hole VQ7, and thus defines a new mineralized body with a strike length in excess of 1 km. Earlier workers noted the "heavy" sulphide mineralization but little record of the assays from diamond-drill intersections or bulldozer trenches remains. A 1966 record indicates that a sample taken from a bulldozer trench (Fig. 9) returned a value of 0.92% Ni and 0.22% Cu over 20 m. Similar "heavy" mineralization was also reported from the bank of White River, 140 m to the west. The sulphide mineralization consists of pyrrhotite, pentlandite, and chalcopyrite in a brecciated host consisting of altered fine grained gabbro (originally mapped as "chert" by company geologists). This horizon may be a narrow gabbro sill-like extension (apophyses) from the ultramafic body.

Metallurgical tests of the Main zone mineralization indicate that an exceptionally high value, clean nickel concentrate can be produced with moderate grinding using conventional floatation techniques. A full analysis of one of the concentrates gave the following: 19.7% Ni, 0.28% Co, 0.34% Cu, 31.10% Fe, 10.90% S, 0.10% As, 0.858 ppm Pt, 0.543 ppm Pd, 0.572 ppm Au, and 14.8 ppm Ag.

Due to the inaccessible nature of most semi-massive and massive sulphides on the Canalask property, a limited chemical database exits for this type of mineralization. Nevertheless, it is apparent from Figure 74(A, B) that a wide spectrum of Ni (<3.5%) and Cu (<3.1%) values is associated with this style of mineralization. The chalcopyrite-rich and pyrrhotite-pentlandite-rich mineralogy of some samples, in conjunction with relict magmatic and flow-foliation textures, suggest both a primary and secondary influence on the distribution of these elements. The coherent extension of the magmatic (ultramafic) trend for Co (Fig. 74C) is in striking contrast to the Ni and Cu trends. The low concentrations of As (Fig. 74D) associated with these samples and the dearth of Co minerals suggest relatively high concentrations of Co in sulphides other than pentlandite. Zn and Pb concentrations seldom exceed 350 ppm and 4 ppm, respectively. All footwall sulphide mineralization is characteristically depleted in PGEs (<18 ppb) relative to that from the ultramafic body (Fig. 108, 120, 130), and other Ni-rich massive sulphide occurrences in the belt.

The lack of normal magmatic trends, the low noble metal contents, and scarcity of gabbroic or ultramafic lithologies in this proximal environment may help explain the rather unique nature of this mineralization. The PGE-poor, and in some cases base metal-poor, nature of this mineralization may be the result of sulphur saturation being attained in a thin sill-like body of gabbroic parental magma invading and assimilating sulphur-rich Station Creek Formation strata. The limited mass of magma from which the separating sulphides equilibrated and sequestered transition and noble metals would control the metal endowment of the segregating sulphides. Sulphide mineralization in the Gabbro-sedimentary rock unit may represent the earliest immiscible sulphide mineralization associated with the initial pulse of magma that gave rise to the intrusive complex. The geometry and precious metal grades of this zone, and other zones of sulphide mineralization in the footwall environment, suggest that the parental magma from which the sulphides segregated was of relatively limited volume. Subsequent ingressions of magma(s) that produced the ultramafic zone of the White River Complex would have exerted considerable force on the surrounding floor and roof rocks as the sill thickened. This could in turn have filter-pressed semi-molten sulphides from a gabbroic, marginal zone into dilation zones resulting from the ingressive intrusive forces (i.e. breccia zone now occupied by the Main zone Ni-deposit and possibly even the Gabbro-sedimentary rock unit). The plastic nature of these displaced sulphides may explain the foliated character of some of the mineralization within the Main zone.

A sulphur-isotope investigation of the Ni-Cu sulphide mineralization in the White River Intrusive Complex indicates that a significant amount of crustal sulphur has been assimilated by the intrusion (Fig. 97C). The mineralized peridotite from the Canalask property is the least contaminated with $\delta^{34}S$ values ranging from -6.9 to -12‰. The latter value is similar to that of massive sulphides from the Discovery showing, Onion property (-10.9‰) (Fig. 97C). The $\delta^{34}S$ isotopic compositions of the sulphides from the Onion gabbro (-15.9 to -16.7‰) are strikingly similar to those of the semi-massive and massive sulphides from the footwall mineralization at the Canalask property which range from -14.5 to -17.2, $\overline{X}$ = 16.0‰ (n = 12). Sulphide from the bordering Pennsylvanian Station Creek Formation, the inferred source of the sulphur contamination, has an isotopic composition of -26.5‰. It would appear that the parental magmas that gave rise to the Onion basal gabbroic rocks and the Canalask footwall Ni-Cu ores have been contaminated to a similar degree. These findings, in conjunction with the restricted isotopic range of the Canalask footwall mineralization and the known composition of the Station Creek Formation contaminant, preclude the origin suggested by Campbell (1981). Campbell hypothesized that the Main zone Ni-Cu ore represented an original syn-sedimentary or volcanogenic

pyrrhotite-pyrite-chalcopyrite body that was subsequently replaced by Ni-rich (hydrothermal) eminations derived from the White River Intrusive Complex. Low Zn and Pb concentrations, relatively low S/Se ratios, and similar Ni/Cu ratios of the sulphide fraction (100% sulphide) in both ultramafic and footwall-hosted mineralization negate the origin proposed by Campbell. Also, nickel is relatively inert in hydrothermal fluids and when present it is only precipitated under extremely oxidizing conditions similar to those responsible for the formation of unconformity-type uranium deposits (Hulbert et al., 1992b).

North-central section

Five separate sill-like mafic-ultramafic intrusions – Donjek, Arch Creek, Quill Creek, Linda Creek, and Wash – are located in the north-central portion of the Kluane Mafic-Ultramafic Belt (Fig. 4, 5, 12). These intrusions trend in a southeast direction for approximately 20 km and are confined by Pennsylvanian to Permian strata. The structure and form of these intrusions are progressively more complicated along strike from northwest to southeast. Economically, the greatest concentration of Ni-Cu-PGE mineralization and the most promising prospects occur in this portion of the belt.

Arch Creek Intrusive Complex

Of the many mafic-ultramafic intrusions in the belt, the Arch Creek Complex could be considered the type model of Kluane Mafic-Ultramafic Intrusive Complex. This relatively small intrusion retains most of its original magmatic features.

Location, history, and physiography

The Arch Creek Intrusion Complex is located in the southwestern Yukon, approximately 320 km northwest of Whitehorse; at latitude 60°27'N and longitude 139°25'W on NTS claim map 115G/6. Access to the area is by an intermittently maintained road that extends 7.3 km northwest of the Wellgreen Mine site which is linked to the Alaska Highway by a 14 km gravel road. Road access to this and other similar intrusions varies from year to year and is dependant on exploration activity in the area.

The complex covers parts of two drainages: Arch Creek, a west-northwest-flowing tributary of Donjek River, and Swede Johnson Creek, a north-flowing tributary of Kluane River. Elevations range from 1070 m along creek beds to 1980 m along ridge crests. Outcrop is poor due to black spruce and poplar vegetation on the floors of creeks giving way to buckbrush and slide alder on the lower slopes, and moss and lichen at higher elevations.

Disclosure of ultramafic and mafic rocks at this locality resulted from the discovery of the Airways Ni-Cu showing (Fig. 13) in 1952. The property (complex) was staked as the Enger (etc.) claims by a syndicate composed of Prospector Airways Ltd., Noranda Mines Ltd., and Kerr Addison Gold Mines Ltd. Prospecting, mapping, geophysical surveys, and 143 m of drilling were conducted between 1953 and 1955. J. Brown (1964) and P. Versluce and C. Gibbons (1966) restaked the property and carried out geophysical and mapping programs and trenching between 1967 and 1970. In 1972 the property was optioned by the Nickel Syndicate which conducted mapping, geochemical, geophysical, and trenching programs. Between 1977 and 1980 the Airways showing and surrounds was investigated by W. Green who held the AMC claim over the complex. The Arch property was acquired by staking and option in 1986 by Archer, Cathro & Associates (1981) Ltd. on behalf of Kluane Joint Venture to cover the extension of the Quill Creek Complex west of the Wellgreen property. Between 1986 and 1989 the joint venture conducted an extensive mapping, geophysical, and geochemical program, in addition to grid layout, road construction, drilling of three diamond-drill holes totalling 173 m, and bulldozer trenching.

Structure and stratigraphy

The Arch Creek intrusion is an 80 to 100 m thick, northwest-trending, unconformable to nearly conformable mafic-ultramafic sill-like body that has been traced intermittently in creek sections and trenches for 750 m along strike. It has also been extended along strike an additional 500 m to the west based on geophysical surveys. The body has a steep to moderate (50°) southwest dip, and appears to have intruded near the contact between the Station Creek and the Hasen Creek formations. Stratigraphic evidence suggests that the southwest

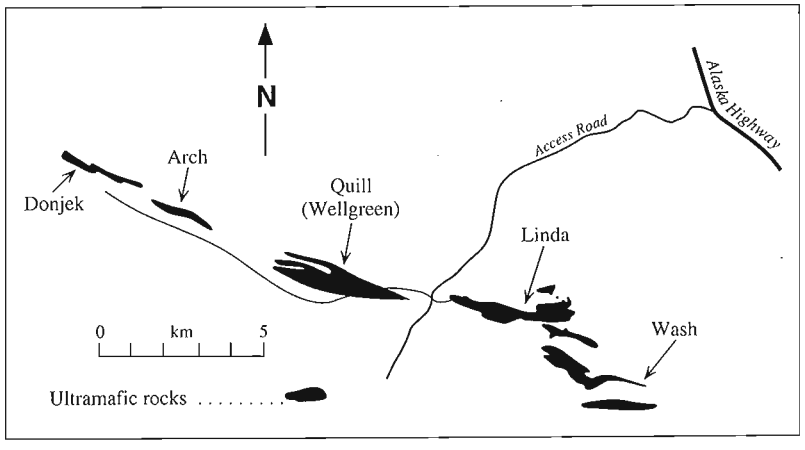

Figure 12.

Location of sill-like mafic-ultramafic intrusive complexes from the north-central portion of the Kluane Belt.

dip of the intrusion represents the true facing direction. The southeast extremity of the intrusion terminates by bifurcating from the main tabular body (Fig. 13).

Magmatic stratigraphy within the intrusion is relatively simple. The northern boundary of the intrusion demarcates the basal contact (Fig. 13). Bordering the contact on the hanging wall, a 2 to 5 m thick marginal gabbro facies is developed adjacent Station Creek Formation tuffaceous sediments. This contact zone is also the site of intermittent Ni-Cu massive sulphide accumulations that pass expeditiously into overlying weakly mineralized peridotite. The remaining stratigraphy consists exclusively of ultramafic rocks. However, the proportion of olivine in the successive ultramafic rocks appears to increase up section to the point where strata 70 m above the basal contact have a distinctive dunitic and feldspathic peridotite character. Coarse, discontinuous areas of pegmatitic gabbro occur along the southern contact of the intrusion in the vicinity of a solitary Permian argillite screen. Stoping of these wet sediments and subsequent reaction with the magma gave rise to localized areas of pegmatitic gabbro, some of which are enriched in disseminated sulphides. The southern outline of the intrusion (Fig. 13) borders Station Creek Formation andesitic flows and marks the upper intrusive contact.

A second but distinctively different variety of gabbro, called the Maple Creek gabbro, occurs as dykes and rarely sills on the property. The gabbro is interpreted as feeders to the Upper Triassic Nikolai Group volcanic rocks. The Nikolai Group basaltic flows and related sediments unconformably overlie other units and are limited to a few outcrops in the southern part of the property.

A series of strong, near vertical faults trend northwesterly across the property and cut all units, but they do not appear to have significantly affected the mafic-ultramafic intrusion. Compelling evidence suggests that the property is situated on the limb of a northwest-trending fold.

Petrology

Gabbro. The thin basal gabbro from the marginal zone is an equigranular, fine- to medium-grained rock. All samples are waxy-green due to the pervasive development of alteration phases: chlorite, uralite, serpentine, saussaurite, and albite. Fine-grained "chilled" material is best preserved in the presence of heavily disseminated sulphides (Fig. 14A). Semi-massive and massive basal sulphide accumulations commonly contain resorbed inclusions of coarser-grained gabbro displaying relict sub-ophitic (Fig. 14B).

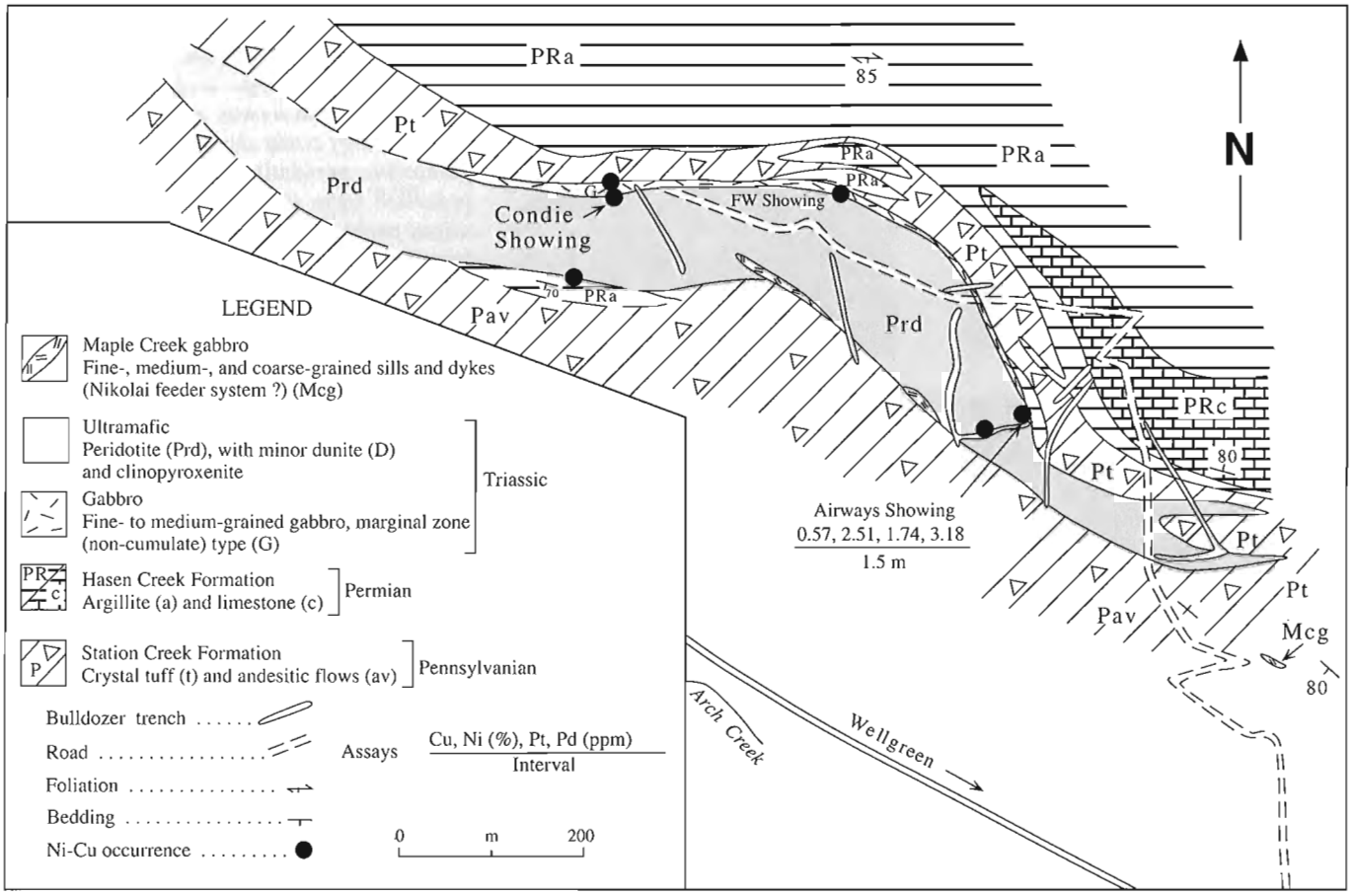

Figure 13. *Simplified geological map of the Arch Creek Intrusive Complex.*

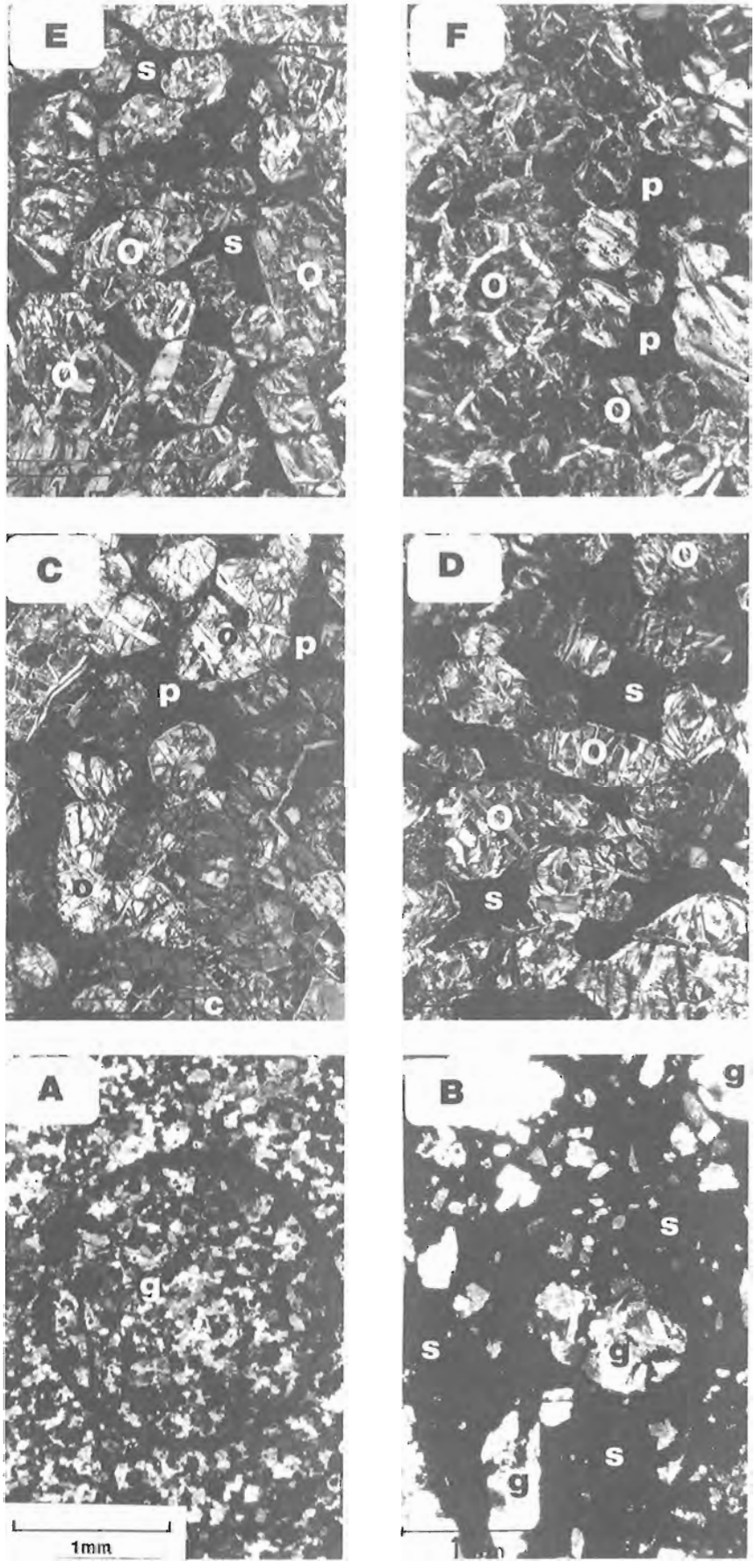

Figure 14.

*Photomicrographs of selected lithologies from the Arch Creek Intrusive Complex. GSC 1995-106E (**A**) HDB-ARC-3c. Fine-grained "chilled margin" material with fine disseminated sulphides. The silicate fraction of this sample is highly altered. Plane-polarized light. (**B**) HDB-ARC-3b. Semi-massive to massive basal sulphide accumulations with inclusions of gabbroic material, some of which retains their primary ophitic texture. Plane-polarized light. (**C**) HDB-ARC-7a. Cumulus olivine and chromite chadocrysts included in large intercumulus oikocrysts of clinopyroxene. This lithology could also be referred to as a poikiolitic peridotite or wehrlite. Cross-polarized light. (**D**) HDB-ARC-11. Mineralized peridotite with pronounced igneous lamination. Plane-polarized light. (**E**) HDB-ARC-7b. Serpentinized net-textured peridotite. Plane-polarized light. (**F**) HDB-ARC-4b. Feldspathic peridotite (altered). Plane-polarized light. o = olivine, c = clinopyroxene, x = chromite, p = plagioclase, s = sulphide, g = gabbro.*

Ultramafic. The thin gabbroic marginal zone is overlain by ultramafic cumulate strata consisting almost exclusively of mineralized and non-mineralized peridotite (wehrlite). This lithology is a dark greenish-black, medium-grained, highly serpentinized poikiolitic peridotite. The initial 10 m of the ultramafic sequence is generally composed of strongly mottled poikiolitic wehrlite containing up to 35% intercumulus clinopyroxene and 2 to 5% disseminated pyrrhotite. The proportion of intercumulus pyroxene decreases to 10 to 20% in the overlying 15 m of cumulate strata, and marks the introduction of a plagioclase (5-10%) as a prominent intercumulus crystallization product. This horizon also contains 2 to 4% disseminated pyrrhotite. The next 20 m of ultramafic strata differ from that of the underlying sequence in that they lack the distinctive mottled and poikiolitic texture due to the gradual upward increase in the amount of intercumulus plagioclase at the expense of clinopyroxene. The volume of intercumulus plagioclase varies from 15-25% within this interval and is aptly referred to as feldspathic peridotite. Correspondingly, the proportion of disseminated sulphide within this interval declines to 1-2%. The remaining ultramafic strata above this level consist of feldspathic peridotite and dunitic cumulates. Pervasive serpentinization is present in all ultramafic lithologies.

The olivine-chromite±sulphide cumulates shown in Figure 14(C, D, E) are representative of the mineralized ultramafic strata. In Figure 14C, cumulus olivine and chromite chadocrysts are included in large oikocrysts of intercumulus clinopyroxene. The intercumulus space occupied by this phase, and to a lesser degree plagioclase, decreases as the amount of sulphide in the sample increases (Fig. 14D, E). Sulphide-enriched peridotite commonly contains olivine with an elongated habit. In thin section the elongated olivine generally imparts a preferred orientation or igneous lamination to the specimen (Fig. 14D). Intercumulus pyroxene is almost exclusively Mg-rich clinopyroxene, but grains of intercumulus orthopyroxene have been observed locally. Increased proportions of intercumulus plagioclase are associated with feldspathic peridotite and dunitic rocks similar to that in Figure 14F. Although the clinopyroxene appears to have experienced little alteration, olivine and plagioclase from the same sample are generally altered to serpentine and opaque pseudomorphs consisting of a mosaic of turbid clay minerals, iron dusting, and epidote, respectively (Fig. 14C, F).

Ni-Cu±PGE mineralization

Prospecting, trenching, and geophysical surveys have revealed three different zones within the intrusion where economically significant concentrations of immiscible magmatic Ni-Cu sulphides have accumulated.

Immiscible magmatic sulphide segregations.

Marginal gabbro. Three major Ni-Cu sulphide showings occur within the basal gabbroic marginal zone of the complex (Fig. 13), in addition to a number of lesser occurrences. The Airways showing is located in a shallow hand trench, and old bulldozer trench, near the east end of the intrusion. It consists of a 10 m long and up to 1.5 m wide lens of massive pyrrhotite-pentlandite-chalcopyrite. A chip sample taken across the lens in 1987 assayed 2.51% Ni, 0.57% Cu, 1740 ppb Pt, 3180 ppb Pd, and 68 ppb Au over 1.5 m (Eaton, 1988b). Detailed investigation of this same lens, by the author, subsequently disclosed that this sulphide concentration contains a thin semi-massive sulphide interval within the central portion. Nevertheless, the base, semi- and noble metal concentrations recorded for this massive and semi-massive sulphide occurrence confirm the earlier high-grade metal assays. Analytical data for this mineralization and other from the complex are summarized graphically in Figures 75, 87, 98, 109, 121, and 131. Metal contents of nine samples from this showing have the following ranges: Ni (1.4-4.3%), Cu (0.45-2.0%), Co (0.06-0.16%), Pt (800-1800 ppb), Pd (1400-4500 ppb), Au (52-130 ppb), Rh (220-770 ppb), Os (260-680 ppb), Ir (150-410 ppb), Ru (300-900 ppb), and PGE+Au (3330-6900 ppb).

The FW showing is approximately 320 m northwest of the Airways showing and comprises two limonitic gabbro outcrops developed where a small creek has eroded through the footwall contact of the sill. A 2.0 m chip sample from the east side of the creek assayed 0.47% Ni, 0.80% Cu, 925 ppb Pt, and 1405 ppb Pd, whereas, the west side assayed 0.34% Ni, 0.23% Cu and 5588 ppb Pt, and 2091 ppb Pd over 1.0 m.

The Condie showing, the most westerly of the showings, is also located in a creek cut, 260 m west of the FW showing. It consists of several mineralized exposures developed in marginal gabbro. Chip samples over 1.0 m returned values of 0.97% Ni, 0.38% Cu, 1645 ppb Pt, and 1200 ppb Pd.

In addition, a number of other minor showings (two east of the Airways showing, one midway between the Airways and FW showings, and one between the FW and Condie showings) with relatively respectable grades also occur in the marginal gabbro adjacent the basal contact. Eaton (1988b) calculated the average grade of chip samples from showings in the marginal gabbro zone to be 0.81% Ni, 0.66% Cu, 1165 ppb Pt, and 2022 ppb Pd over a width of 2.0 m.

Ni-Cu-PGE mineralization has only been noted at one locality from the upper contact of the intrusion. This mineralization occurs 120 m south-southwest of the Condie showing (Fig. 13). The mineralization is disseminated in a pegmatitic gabbro and assays up to 0.60% Ni, 0.76% Cu, 925 ppb Pt, and 3600 ppb Pd have been recorded over a width of 1 m. This locality represents the first confirmed magmatic Ni-Cu-PGE mineralization from the upper contact zone of a Kluane mafic-ultramafic intrusions.

Ultramafic. Peridotite forms the hanging wall to the mineralized marginal gabbro zone, and is weakly mineralized with disseminated sulphides for widths of 20 to 40 m. A 1987 exploration chip sample of this material assayed 0.36% Ni, 0.25% Cu, 411 ppb Pt, 548 ppb Pd and 68 ppb Au (Eaton, 1988b). A 46 m diamond-drill hole intersection through the lower half of the Arch Complex subsequently revealed that the highest values are associated with a 10 m intersection of poikiolitic wehrlite: 0.35% Ni, 0.28% Cu, 685 ppb Pt, and 788 ppb Pd. The remaining 36 m comprise weakly poikiolitic

peridotite, feldspathic peridotite, and dunitic ultramafic rocks averaging 0.29% Ni, 0.15% Cu, 411 ppb Pt, and 445 ppb Pd. Sporadic net-textured patches (<3.0 cm) containing up to 8.0% sulphides have been noted.

Ultramafic rocks demonstrate coherent geochemical trends with respect to Ni, Cu, Co, Se, Bi, S/Se, Pt, Pd, Au, Ru, Rh, Os, Ir, and PGE+Au (Fig. 75, 87, 98, 109, 121, and 131). These smooth chalcophile element trends demonstrate a comagmatic origin for all intrusive lithologies analyzed. These diagrams indicate that weakly mineralized and unmineralized samples from the Arch Creek Complex have high background PGE concentrations.

The isotopic composition ($\delta^{34}S$) of the sulphur associated with these samples is approximately -6.5‰ which is not significantly different than that of the gabbro (-5.7‰) and the massive sulphide (-8.1 to -8.9‰). The isotopic signature of the Arch mineralization clearly indicates that the parental magma, from which the immiscible sulphides segregated, was contaminated by crustal sulphur. Erratic S/Se, As, and Sb etc. trends for country rock lithologies clearly reflect the influence of postmagmatic hydrothermal fluids.

Hydrothermal (remobilized ?) mineralization. A 3.0 m wide, malachite-stained fracture zone containing 3 to 10% sulphides is developed in the footwall tuff adjacent the Ni-Cu sulphide lens at the Airways showing. A chip sample taken across this zone assayed 1.25% Ni, 0.44% Cu, 34 ppb Pt, 137 ppb Pd, and 34 ppb Au (Eaton, 1988b). Investigation of the first metre of this zone during the present study disclosed similar Ni (0.50-1.40%) and Cu (0.53-0.63%) values, but the PGE+Au concentration is significantly higher (3928-4035 ppb). The As content of this footwall mineralization is considerably enriched (66-79 ppm) compared to that from within the massive sulphide lens (<4.0 ppm). The isotopic composition of sulphur ($\delta^{34}S$) from this footwall fracture zone is -5.3‰ and is indistinquishable from that of the marginal gabbro (-5.7‰ confirming that the sulphides originated from the Arch mafic-ultramafic intrusion. The fractured nature of the footwall, the high Ni (1.4%), As (79 ppm), and PGE+Au (4035 ppb) content, and the presence of other hydrothermal related elements in weakly mineralized samples (<11.0% sulphides) suggest an origin due to postmagmatic remobilization of base, semi and noble metals into the country rock from the overlying intrusion. This mineralization may represent the migration of late stage deuteric fluids.

Quill Creek Intrusive Complex

The Quill Creek Complex is the largest and most deformed mafic-ultramafic body in the north-central section of the belt (Fig. 12). It hosts the partially exploited Wellgreen Mine, the only past producer of Ni-Cu in the Yukon. Additional newly discovered reserves indicate that it contains the largest single proven concentration of Ni, Cu, and PGE mineralization in the Cordillera of western North America. It is also the most extensively explored intrusion in the belt and thus provides an excellent geological and exploration reference base for the various types of magmatic and postmagmatic mineralization, cumulate and non-cumulate igneous stratigraphy, country rock-intrusive stratigraphic relationships, and internal and external morphological features of Kluane mafic-ultramafic intrusions. The complex has been used as a laboratory to monitor the magmatic behavior of mineralogical, chemical, and isotopic constituents during the evolution of this intrusion, and as a site for the discovery and development of new exploration tools and models for this and other intrusive complexes within the belt.

Location, history, and physiography

The Quill Creek Intrusive Complex is approximately 317 km west of Whitehorse at latitude 61°28'N and longitude 139°32'W on NTS map 115G/5 (Fig. 4, 5, 12). The Wellgreen Mine is located in the centre of the complex, approximately 3.2 km west of the junction of Quill and Nickel creeks in the Quill Creek area of the Kluane Ranges (Fig. 15, 32). A 14 km gravel road which joins the Alaska Highway near kilometre post 1788 provides access to the mine. Services, accommodation, and the nearest airstrip are available at Burwash Landing, 30 km east of kilometre 1788. A motel-cafe-garage facility located at the Kluane Wilderness Village on the Alaska Highway, 8 km north of the Wellgreen access road junction, provides year-round services. The property lies within the Kluane Game Sanctuary, and the Kluane National Park lies 25 km to the south.

Topography of the area is relatively rugged; slopes are usually in the 25 to 30° range with the highest peaks exceeding 2000 m. The main mineralized trend on the property lies between elevations 1295 and 1707 m on a moderate to steep south-facing slope. Small cirque glaciers accumulated on the north-facing slopes and coalesced to form localized glacial valleys in the area.

The Wellgreen surface showing was discovered in 1952 by prospectors Wellington Green, C.A. Aird, and C.E. Hankins. The property was optioned by Hudson Bay Exploration and Development Company Limited in 1952 and held since 1955 through a subsiduary, Hudson-Yukon Mining Co. Between 1953 and 1956 a total of 19 812 m of surface and underground drilling was conducted, in addition to the development of 4267 m of underground excavations in the form of four levels and two internal shafts. In 1968 ground geophysical (Turam EM and magnetometer) and geochemical surveys were conducted and supplemented by 762 m of surface diamond drilling (13 holes). A production decision was announced in March 1970 and development work consisting of slashing an exploration drift, sinking an internal shaft, and driving sublevels in preparation for stoping started in February 1970. Milling of ore began on May 1, 1972 but ceased on July 6, 1973 due to falling metal prices and excessive dilution due to weak peridotite hanging wall and the unexpectedly erratic distribution of the massive sulphide lenses. Of the initially outlined 669 150 tonnes of ore, only 171 652 tonnes were mined. The mined ore had an average grade of 2.23% Ni, 1.39% Cu, 0.073% Co, and 2.15 ppm Pt and Pd.

Kluane Joint Venture (Chevron Minerals Ltd. and All-North Resources Ltd.) optioned the Wellgreen property from Hudson-Yukon Mining Co. Ltd., for the period 1986-1990. An extensive program of prospecting, grid mapping, geochemical (soil and rock) and geophysical (VLF-EM, magnetometer, IP, MaxMIN) surveys, road construction, bulldozer trenching, surface and sub-surface diamond drilling and underground rehabilitation work was performed during this period. Metallurgical and mineralogical tests on composite samples of all types of mineralization were carried out by Chevron, Lakefield Research, and CANMET (Carne, 1987).

Campbell (1981) investigated the Wellgreen Ni-deposit as part of a Ph.D thesis which focused on the genesis of copper deposits and associated host rocks in the Quill Creek area.

Structure and stratigraphy

The area is underlain by a series of intrusive, volcanic, and sedimentary rocks ranging from Pennsylvanian to Triassic. The oldest rocks are correlated with the Pennsylvanian Station Creek Formation, a predominantly volcanic sequence of light- to medium-green, intermediate andesitic flows, crystal and lapilli tuff, tuff breccia, agglomerate, and conglomerate.

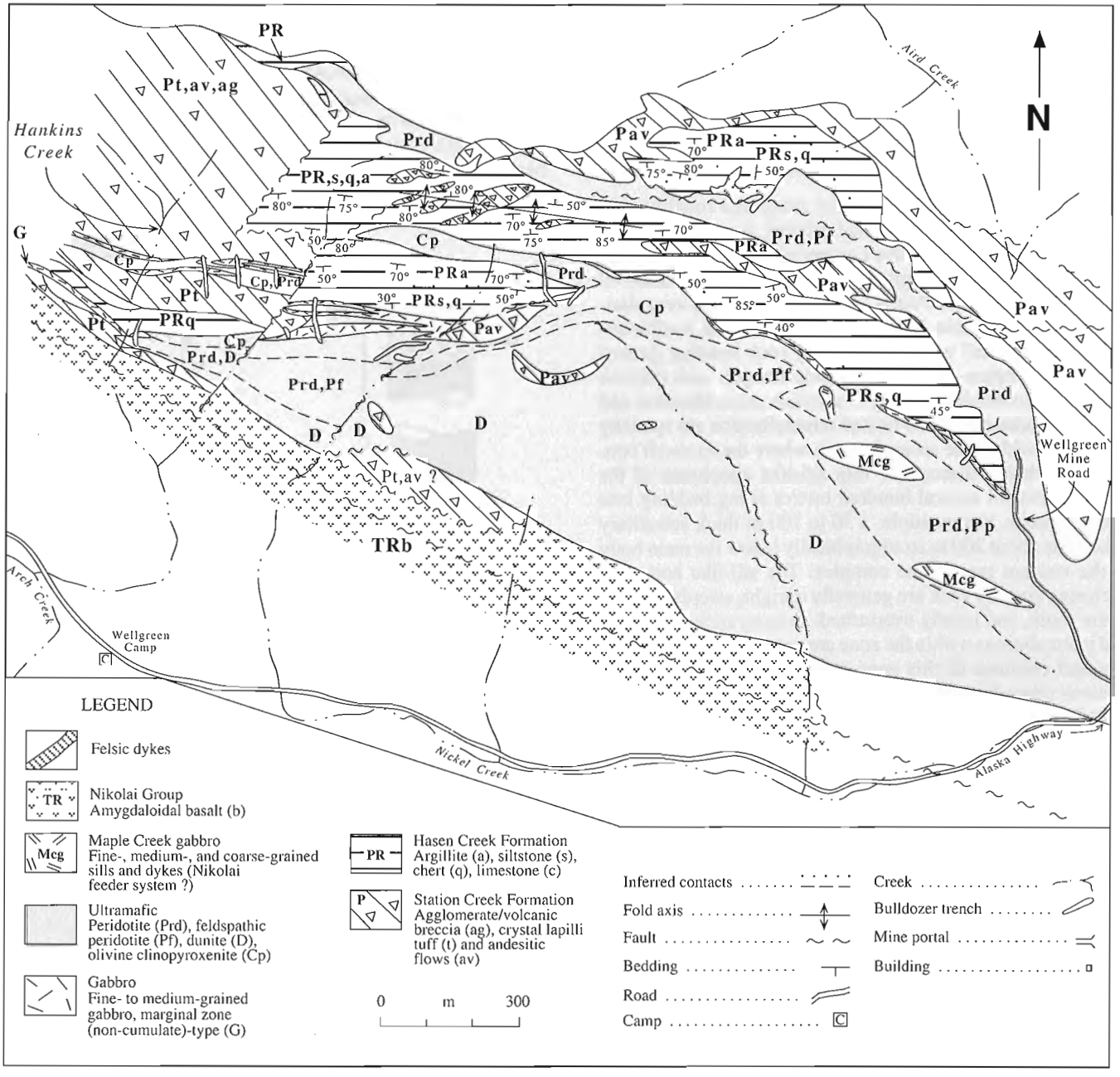

Figure 15. *Generalized geological map of the Quill Creek Intrusive Complex.*

Conformably overlying this formation is a sequence of thin-bedded grey to black argillite, olive-grey volcanic derived siltstone, and white to grey chert and recrystallized limestone of the Permian Hasen Creek Formation. These older rocks are unconformably overlain by dark-green to maroon amygdaloidal basalt, volcanic breccia, and conglomerate with minor thin-bedded limestone, chert, and argillite of the Upper Triassic Nikolai Group. The geological map shown in Figure 15 is a compilation based on surface mapping of creek sections, slope exposures, roadcuts, and bulldozer trenches, in addition to information gained from geophysical and geochemical surveys, diamond drilling, and underground workings. Due to the poor exposure over intrusive rocks information gained from indirect methods had to be heavily relied upon.

The Quill Creek Intrusive Complex is a highly serpentinized and moderately deformed 4.2 km long sill-like mafic-ultramafic body that varies in thickness from 10 to 600 m, but no complete section is exposed (Fig. 12). The complex is emplaced near or at the stratigraphic contact between the Station Creek and Hasen Creek formations.

Intrusive contacts are generally sharp and roughly conformable with bedding; detailed studies, however, demonstrate that the lower intrusive contact cuts downsection from west to east over a stratigraphic interval of several hundred metres. The floor of the sill is uneven and contains irregularities of varying scale. These irregularities are southwest-plunging "shelves" where the country rock bedding flattens and "rolls" where intrusive contacts steepen and become orthogonal to bedding. Massive sulphide mineralization and elevated grades of gabbro-hosted mineralization are spatially associated with these areas. In areas where the footwall contact is markedly discordant, thin sill-like apophyses of the intrusion extend several hundred metres along bedding into the host rocks. For example, a 30 to 100 m thick subsidiary sill occurs about 200 m stratigraphically below the main body in the western part of the complex. The sill-like body and enclosing country rock are generally upright, steeply dipping to the south, and locally overturned. Country rock inclusions and intercalations within the zone are common. The morphology and confines of this zone are discussed in subsequent sections related to marginal zone mineralization.

Although the footwall of the complex is highly variable, the main mass is crudely layered with laterally distinct lithological zones. This crude magmatic stratigraphy, of both cumulus and non-cumulus origin, is best represented with the aid of the geological map of the complex (Fig. 15) and the generalized stratigraphic column (Fig. 16). The base of the complex is occupied by gabbro, mineralized gabbro, massive sulphide lenses, or a mixture of all three. When massive sulphide forms the basal member, it varies in thickness from 0.1 to 6 m and transgresses along strike into mineralized and unmineralized gabbro.

This marginal gabbro zone is present along the entire length of the complex and is as variable in thickness as it is in texture. Generally the zone varies in thickness from 9 to 33 m and commonly has a fine-grained chilled margin developed at the contact. The thickness of the aphanitic chilled interval can be as little as 1.0 cm or as thick as several metres. Successive internal chill related textural variants have been noted up section at a few localities within the marginal zone and suggest the introduction of more than one batch of basaltic magma during the evolution of this zone.

The remaining portion of the marginal zone consists of massive mineralized and non-mineralized gabbro displaying a wide variety of textures. The most common lithology is that of a medium-grained, equigranular gabbro that becomes pegmatitic in the vicinity of calcareous floor rocks, intercalations, or inclusions. Near the top of the zone the gabbro is increasingly more mafic and grades from gabbro to mela-gabbro and clinopyroxenite over short intervals. These clinopyroxene-rich rocks are laterally discontinuous along strike, but nevertheless they introduce the beginning of cumulate crystallization activity in the complex. The frequency and thickness of this lithology generally increase near the top of the zone and may contain dark green serpentinized pseudomorphs after olivine. The introduction of cumulus olivine at this stratigraphic level signifies the onset of ultramafic cumulus activity and the beginning of the ultramafic zone. This distinctive olivine- and clinopyroxene-rich ultramafic member has been referred to as

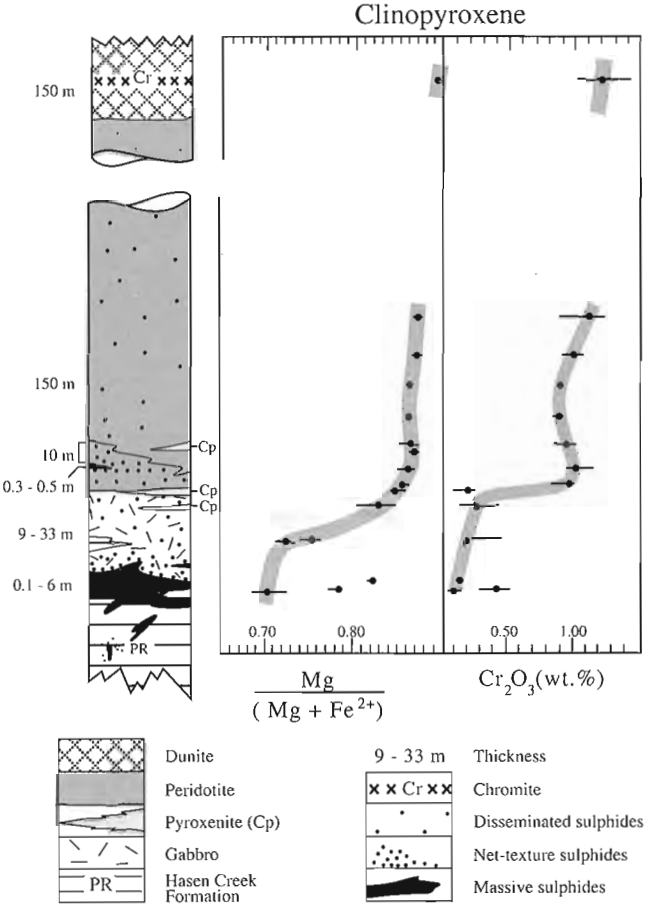

Figure 16. *Simplified stratigraphic column and associated clinopyroxene compositions through the mafic-ultramafic members, basal massive sulphide bodies, and footwall sedimentary rocks.*

"clinopyroxenite" (Fig. 15). However, by definition (Sabine, 1974) this mapped lithological subdivision consists of both wehrlite and olivine clinopyroxenite and varies in thickness from 10 to 50 m. The clinopyroxene-rich lithologies occur along the entire basal portion of the ultramafic zone. Disseminated Ni-Cu sulphides, and to a much lesser extent localized (centimetre scale) net-textured and semi-massive sulphide lenses, are also characteristic features of this lithological member.

Typically, the proportion of clinopyroxene decreases upward in this member to the level where it occupies <50% by volume of the rock and true clinopyroxenite ceases to exist. This change denotes the base of the peridotite and feldspathic peridotite members. Although this member has a very irregular width, it occurs along the entire strike length of the complex (Fig. 15). Field observations reveal that the lower half of this member is occupied by true peridotite (wehrlite) with only trace amounts of intercumulus plagioclase (<5%). The amount of intercumulus plagioclase appears to increase upwards through the member to the point where the peridotite is best referred to as "feldspathic" and contains between 10 and 25% intercumulus plagioclase. The uppermost member of the ultramafic zone, and volumetrically most prominent part of the complex, has a dunitic character. These fine- to medium-grained, light- to medium-green rocks are confined to the southern portion of the complex where the member attains a maximum thickness of 400 m. Although most of the lithologies within this member are not a true dunite by definition (>90% olivine), they have nevertheless been mapped as dunite or dunitic because of the high olivine content relative to other ultramafic rocks in the complex and their similarity to what has been referred to as dunite, and feldspathic dunite in other large stratiform mafic-ultramafic intrusions (i.e. Bushveld and Stillwater igneous complexes). These olivine-rich rocks are more serpentinized than other ultramafic strata within the complex and this tends to accentuate their dunitic character. Rocks within this member characteristically lack the mottled texture (due to poikiolitc clinopyroxene) common in other members. Cumulate layering was not observed.

"Skarn" rocks occur in the floor of the complex adjacent to the marginal zone gabbro. In the eastern portion of the complex these rocks are associated with a complicated interfingering of gabbro and limestone, whereas, near the western extremities it occurs with gabbro and calcareous tuffaceous siltstone. Where best developed (eastern portion) this contact metamorphic/metasomatically derived calc-silicate sequence extends for at least 30 m from the intrusive contact and can be subdivided into lithological zones. Based on a detailed investigation of the skarn rocks, on the 1235 L of the Wellgreen Mine, Fayak (1989) divided the skarn into seven contact metamorphic/metasomatic zones based on distinctive index minerals. With increasing distance from the contact, these zones and their approximate thickness are: white skarn zone (3.5 m), feldspar-garnet skarn zone (4 m), first axinite-bearing augite skarn zone (2.5 m), garnet skarn zone (7.5 m), second axinite-bearing skarn zone (3.5 m), quartz skarn zone (3.5 m), and the carbonate skarn zone (12.1 m).

Elongated pipe- or plug-like bodies of Maple Creek gabbro intrude the dunitic member in the eastern portion of the complex. These bodies generally strike southeast to east-southeast and have moderate southerly dips (50°). The eastern bodies are the largest encountered in the complex, and attain widths of up to 65 m and can be traced along strike for over 280 m. These intrusive bodies all have well developed peripheral chilled margins and coarsen to medium-grained porphyritic varieties as the intrusion cools towards the centre of the body. An irregular thin envelope of baked and sheared ultramafic rock encloses this body.

In the central portion of the complex isolated lens-shaped bodies of material of a questionable origin have been mapped. Propylitic and carbonate alterations mask primary diagnostic features in these rocks. Nevertheless, this fine-grained material contains some relict features which suggest that it is assimilated Station Creek Formation strata. The possibility that it represents altered Maple Creek gabbro cannot be overlooked as the Maple Creek gabbro plugs to the east were originally mis-identified as Station Creek volcanic flows.

The final intrusive event in the area occurs in the form of felsic dykes. These white to light-green bodies are generally 0.05 m to 5.0 m thick but may attain a thickness of up to 25 m. The wider bodies contain phenocrysts of feldspar set in a fine-grained matrix. These dykes form resistant exposures, especially in contrast to the sheared serpentinite, and develop thin chilled margins with a "skin" of baked peridotite. An increased frequency of occurrence of these bodies tends to be associated with the northwest-trending faults cutting through the centre of the complex. Although the origin of these felsic dykes remains uncertain they may be related to the Oligocene felsic magmatism or represent escaped felsic melts derived from partial melting of country rock.

The Quill Creek Complex contains the most complicated structural geology in the Kluane Mafic-Ultramafic Belt. Much of the area is underlain by Pennsylvanian and Permian strata that strike approximately 100 to 110° and dip 60 to 80° to the south. The sequence has been modified by folds and faults. The southern edge of the mapped area (Fig. 15) is bounded by a west-northwest-trending fault zone of regional extent and probably represents a splay of the much larger Denali (Shakwak) fault, 12 km north of the property (Fig. 1). Graded bedding in sedimentary strata demonstrates that the sequence is upright and generally homoclinal. A minor anticlinal fold occurs north of the main portion of the intrusive complex.

Longitudinal structures are common in the ultramafic rocks either as shear zones within peridotite cores to narrow subsidiary sills, or as serpentinized faults along the contacts between relatively competent gabbro and incompetent peridotite. Sense of movement along these structures is uncertain.

Three northerly trending fault zones are associated with the complex. The two major faults in the western part of the complex are west-dipping reverse faults. The third fault is confined to the dunite member in the central portion of the complex. At present the sense of movement along this fault is unknown.

Petrology

A wide variety of mafic-ultramafic lithologies are associated with the gabbroic marginal zone and ultramafic zone of the complex. Most of the mafic rocks from the marginal zone are of a non-cumulate origin, whereas, those from the ultramafic zone are cumulates of olivine and clinopyroxene±chromite and sulphides. The appearance of cumulus clinopyroxene near the top of the marginal zone, and subsequent development of thin discontinuous clinopyroxenite, marks the onset of the first cumulus activity in the Quill Creek Complex. The ensuing introduction of cumulus olivine, in addition to clinopyroxene, gives rise to the olivine clinopyroxenite member, which actually consists of both olivine clinopyroxenite and wehrlite (Fig. 15). Above this member, variations in the amount and mineralogical character of the intercumulus porosity have given rise to a crude "intercumulus" macro layering within the ultramafic zone.

Gabbro. Extensive exploration drilling and underground development work in the marginal zone of the Quill Creek Complex presented an unprecedented opportunity to study the petrological character of this zone. Petrological variation of gabbroic rocks within the zone is greater than that observed for other marginal zone gabbro in the belt. Therefore, the petrological features discussed here could be considered representative of marginal zone gabbro from the belt.

One of the most characteristic petrological features of gabbro from this zone, as well as similar zones elsewhere in the belt, is the mineralogical absence of both olivine and orthopyroxene, the ubiquitous alteration of plagioclase, and the marked textural variations. The extensive alteration of plagioclase, in the presence of relatively unaltered clinopyroxene and in some cases even olivine, is unusual relative to mineralogical susceptibility to alteration observed in similar lithologies outside the belt.

Regardless of textural variations, marginal gabbro is massive, light- to medium-green, and weathers to a rusty-brown with increasing sulphide content. The textural variants range from microcrystalline to phanerocrystalline and are typically hypidiomorphic inequigranular rocks. Grain size varies from cryptocrystalline-microcrystalline in the chilled gabbro (representative of initial quenched basaltic magmas), to very coarse-grained and pegmatitic gabbro in areas of the so-called skarn rock mineralization. Although unaltered specimens of chilled margins are rare, representative specimens do exist and are discussed in the section related to the nature of the parental magmas that gave rise to the mafic-ultramafic rocks within the belt.

On average, marginal zone gabbro consists of fine- to medium-grained mesocratic rocks similar to those displayed in Figure 17 (A, C). Fine-grained gabbro in the vicinity of the basal contact commonly displays an ophitic to ophimottling texture. Figure 17A displays a well developed ophimottling texture; patches of ophitic texture separated by areas with intergranular textures. The coarser grained intergranular plagioclase and finer grained included plagioclase chadocryst laths are extremely altered (saussurite) relative to that of the poikilitic clinopyroxene crystals. Most fine-grained gabbro is mesocratic with respect to colour index, but melanocratic varieties similar to that in Figure 17B are present. Interstitial sulphides are present in all gabbro, even those considered unmineralized (Fig. 17B). Medium-grained gabbro generally occurs farther away from the intrusive contact, or is localized within areas of higher volatile content within the chilled facies. It commonly displays cumulophyric textures consisting of segregations of three to five twinned and/or zoned clinopyroxene crystals (Fig. 17C), and occasionally glomerophyric texture with segregations consisting of clinopyroxene and subordinate plagioclase. The groundmass of these medium-grained rocks is more allotriomorphic (anhedral) and sulphide enriched relative to their finer-grained equivalents. The colour index of these rocks covers the same range

Figure 17. *Photomicrographs of selected lithologies from the Quill Creek Intrusive Complex. GSC 1995-106L (**A**) U492-71.6. Fine-grained marginal gabbro with subophitic texture. Note the mottling due to the alteration of plagioclase in the groundmass. Plane-polarized light. (**B**) U492-92.35. Fine-grained, granular mela-gabbro to feldspathic clinopyroxenite typical of the upper portion of the marginal gabbro zone. Plane-polarized light. (**C**) U492-86.8. Medium-grained gabbro with cumulophyric clinopyroxene patches and interstitial sulphide. Cross-polarized light. (**D**) DDH-87-98-120. Thin isomodal laminae of clinopyroxenite, one to two crystals thick, alternating with equally thin laminae of gabbro and mela-gabbro demarcating the introduction of the first significant ultramafic cumulate activity near the marginal gabbro/ultramafic zone contact. Cross-polarized light. (**E**) DDH-87-98-120. Coarser-grained clinopyroxenite lacking gabbroic laminae introduced 6 mm above previous level in the same thin section. This laminae marks the disappearance of plagioclase as a primary mineralogical (cumulus) constituent. Crossed-polarized light. (**F**) DDH-87-98-120. "Form contact" marking the introduction of cumulus olivine resulting in clinopyroxene-olivine cumulates or olivine clinopyroxenite. Note that anomalous amounts of sulphide are also introduced with this lithology, and that it is more highly altered than its predecessors, even within the same thin section. Cross-polarized light. (**G**) DDH-87-98-120. Less altered and more equigranular clinopyroxene-olivine-chromite-sulphide cumulate 4 mm above the previous level. Note the fractures cutting olivine are parallel to the cumulate stratification. Cross-polarized light. (**H**) U492-103.3. Net-textured sulphide with serpentine pseudomorphs after olivine. Plane-polarized light. (**I**) U492-81.8. Massive sulphide ore with clinopyroxenite and gabbro fragments. Plane-polarized light. o = olivine, c = clinopyroxene, x = chromite, p = plagioclase, s = sulphide.*

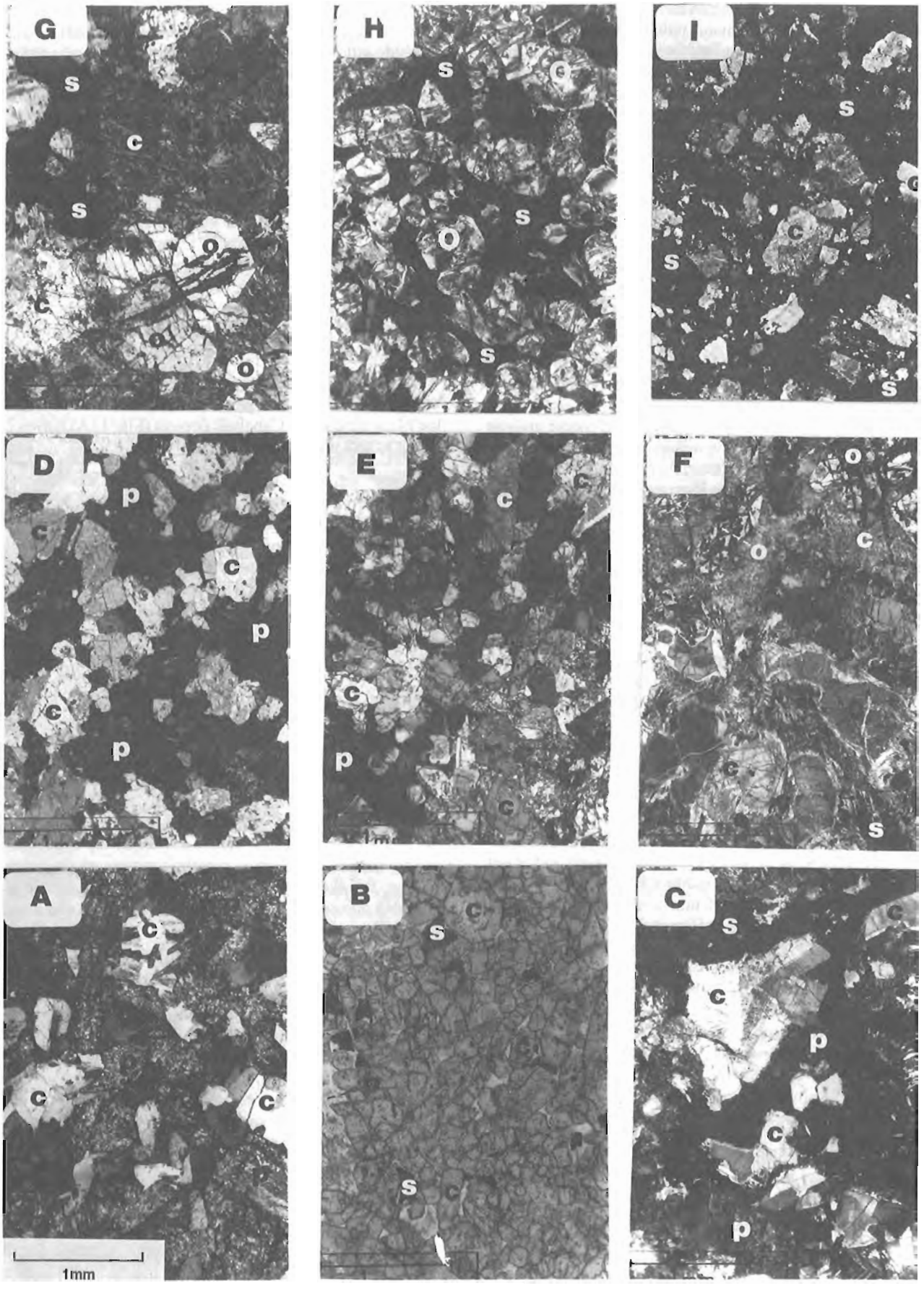
G
H
I
D
E
F
A
B
C
1mm

as that of their finer-grained equivalents, but as they become coarser the amount of magmatic phlogopite also increases. Accessory minerals include minor intergranular quartz, phlogopite, orthoclase, apatite, monazite, sphene, ilmenite, rutile, and rare baddelyite and zircon. When altered, clinopyroxene commonly breaks down to uralite±chlorite (clinochlore)± carbonate, whereas plagioclase alters to saussurite included with a fine opaque dusting. Orthopyroxene has been reported from previous petrological investigations (Campbell, 1981; Carne, 1987), but the present study demonstrates that it is a rather rare phase.

The proximal association of "pegmatitic gabbro" with areas of calc-silicate skarn development and so-called "skarn"-type Ni-Cu-PGE mineralization gives rise to this unique gabbroic facies. Because of the close association of the pegmatitic gabbro with calc-silicate rocks, Hudson-Yukon Mining Ltd. exploration staff used the term "skarn" collectively to describe areas containing either one or both of these lithologies. Pegmatitic gabbro is highly irregular and inequigranular with grain sizes ranging from fine to coarse grained over distances as little as a few metres. Panidiomorphic and allotriomorphic textures are generally characteristic of these grey-green to dark-green rocks. Pyroxene and feldspar grains are generally in the 0.5 to 1.0 cm or greater size range. Mineralogically, this gabbroic facies is composed primarily of clinopyroxene (30-60%), plagioclase (20-30%), calcite (5-10%), and sulphides (10-30%). Accessory quantities of prehnite, axinite, garnet, and apatite are also present. Carbonate veinlets, approximately 0.2 mm in thickness, typically cut the mafic and felsic mineral constituents. Pyrrhotite and chalcopyrite commonly occur as intergranular fillings associated with calcite, and as sulphide veinlets. Less commonly they occur as 0.5 to 1.0 cm immiscible sulphide-looking globules. The sulphide minerals from this type of gabbro characteristically have higher chalcopyrite:pyrrhotite ratios than other comparably mineralized gabbro.

Clinopyroxene in the pegmatitic gabbro commonly occurs as euhedral to subhedral crystals of both short prismatic habit (Fig. 26E) and elongate columnar aggregates. Compositionally the pyroxene falls in the diopside-augite field and is not unlike others from the marginal gabbro; it is discussed in the section on the mineralogy of mafic-ultramafic intrusions within the belt. Large euhedral grains usually occur in a fine-grained matrix of sericitized feldspar and prehnite. Plagioclase appears to be even more prone to alteration in this type of gabbro than others. What appears to be remnant plagioclase patches within sericite pseudomorphs generally turns out to be albite formed as a result of alteration. Prehnite may constitute 3 to 10% of the mode and commonly replaces plagioclase. In strongly altered intervals it also replaces clinopyroxene. Axinite occurs in veinlets cutting large pyroxene grains in a manner similar to that observed in the axinite-bearing augite skarn in the calc-silicate country rocks. Garnet occurs in minor amounts (≈3%) and is typically associated with calcite. Sporadic concentrations ranging from 5-15% have been noted locally. Fine-grained aggregates and larger crystals seldom exceed 1.5 mm in size. Electron microprobe analyses indicate a garnet composition of $Ad_{20}Gr_{80}Uv_{0}$.

Massive and semi-massive sulphides display a number of primary magmatic textural features reminiscent of immiscible sulphide-silicate segregations. Unfortunately, primary igneous mineralogy is seldom preserved in this environment. Some sulphide masses also contain a very fine-grained microbreccia fabric (Fig. 17I). This inequigranular fabric consists of clinopyroxene fragments ranging from 0.5 to 0.001 mm in diameter. Gabbroic fragments are less common. Some of the larger fragments appear to have a relict cumulophyric and glomerophyric texture. Inclusions of gabbroic material are common to the massive and semi-massive sulphide ores, but are not amenable to transmitted light photomicroscopy because of the extensive alteration and pervasive opaque sulphide dusting. Nevertheless, photographs of slabbed core adequately demonstrate these sulphide-silicate (gabbro) textural and relict mineralogical features (Fig. 26A, B, C, D) and are discussed in the next section.

Comparison of the texture of the sulphide-pyroxene ore in Figure 17I with that of pyroxene-sulphide "offset" ore from the Main zone at the Canalask deposit (Fig. 11A) leaves little doubt as to a magmatic origin.

Ultramafic. Thin lenses and discontinuous laminae of melanocratic gabbro and clinopyroxenite occur near and at the top of the marginal zone (Fig. 16) and marks the first cumulate crystallization activity developed during the evolution of the marginal zone. Thin isomodal laminae of clinopyroxene, one to two crystals thick, alternate with equally thin laminae of gabbro and mela-gabbro to form thin pyroxenitic or feldspathic horizons similar to that in Figure 17D. The thickness of the pyroxenitic laminae (Fig. 17E) increases towards a "form contact" defining the introduction of cumulus olivine at the base of the ultramafic zone (Fig. 17F). These two photomicrographs come from a thin section of a sample that represents the basal contact of the ultramafic zone. The base of the olivine-bearing cumulate strata is a clinopyroxene-olivine-chromite±sulphide cumulate. Note the increased grain size of the cumulus clinopyroxene due to overgrowths, the high proportion of irregular (anhedral) intercumulus clinopyroxene, the highly resorbed nature of the cumulus olivine, and the relatively high content of discernable intercumulus porosity. The form of cumulus olivine and clinopyroxene becomes more regular in outline, and is accompanied by enhanced levels of cumulus sulphides within as little as 10 mm above the contact (Fig. 17G). Parallel fractures (Fig. 17G) and serpentinization are common along this contact zone due to marked ductility contrasts between the hanging wall and footwall rocks. The clinopyroxene-rich basal portion of the ultramafic zone is due to both an increase in the proportion of cumulus clinopyroxene and associated postcumulus enlargement, and the high proportion of clinopyroxene in the intercumulus space. In addition to designating this as a pyroxenitic member of the ultramafic zone, it also imparts a pronounced mottled appearance to the rocks because of the poikiolitic textural habit of the clinopyroxene. Olivine content of this clinopyroxene-rich member varies from 12-45% and in non-cumulate nomenclature would be referred to as olivine clinopyroxenite. At some localities

anomalous mineralization occurs in the form of net-textured sulphides (Fig. 17H) and thin (40-50 mm) massive sulphide lenses.

The peridotite member is identical to that described previously from other intrusions. In most cases it has a poikiolitic texture and consists of cumulus olivine and chromite enclosed in large areas of intercumulus clinopyroxene and/or plagioclase similar to that in Figure 14C. The volume of intercumulus plagioclase appears to increase at the expense of clinopyroxene up section within this member. This phenomenon also occurs laterally along strike. All peridotite from this member contains between 30-70% olivine, 10-35% clinopyroxene, and 5-15% plagioclase and falls in the wehrlite and feldspathic wehrlite fields. Primary accessory phases in this and other ultramafic rocks include chromite, sulphide, phlogopite, monazite, orthoclase, hyalophane (K-Na-Ba-feldspar), barite, ilmenite, rutile, and rare zircon. Orthopyroxene is a rare phase within this zone and has frequently been misidentified (Campbell, 1981) for pinacoidal [100] sections of clinopyroxene.

Serpentinized feldspathic peridotite (Fig. 11F) is not unlike feldspathic peridotite from the Quill Creek Complex, particularly in the vicinity of the dunite member. Feldspathic peridotite is an olivine-chromite cumulate and contains approximately 70-85% cumulus olivine and 15-30% intercumulus plagioclase. As these rocks have insufficient quantities of pyroxene and olivine to be classified as true peridotite or dunite (*sensu stricto*) and compositionally fall between these two extremes, they have been coined "feldspathic peridotite" mainly for mapping purposes.

Fresh specimens of dunite, similar to that shown in Figure 11I, have not been found within the dunite member of the Quill Creek Complex. However, serpentinite displaying relict olivine adcumulate and olivine cumulate textures is abundant. The serpentinite appears to originally have been fine- to medium-grained equigranular olivine-chromite± sulphide cumulate. This light-green serpentinized dunite is distinguished on the basis of colour alone from the dark-green to greenish-black serpentinite derived from the underlying peridotite member. Serpentized dunite is characteristically devoid of mottling due to the absence of oikocrystic clinopyroxene. The light colour of serpentinized dunite tends to accentuate the black refractory chromite. Chromite is present in the form of disseminations or weakly developed "chain"-texture and may attain concentrations up to 10% (by volume). Although this light coloured serpentinite gives the impression that there is significantly more chromite than in the darker peridotite, chemical and modal analyses suggest the contrary. Average dunitic rocks contain approximately 3-5% chromite whereas peridotite contains 1-3% chromite. Feldspathic peridotite similar to that shown in Figure 11F also occurs within the dunite member. The olivine-chromite cumulate has been mapped as dunite, dunitic, and originally contained 85-98% olivine and 2-15% intercumulus plagioclase.

Ultramafic rocks from the complex are extensively serpentinized, and represent the most altered and deformed olivine-rich rocks investigated in the belt. Olivine alters to serpentine (antigorite and slip-fibre chrysotile), magnetite, clinochlore, carbonate±talc. Magnetite veinlets, scattered grains, rimming of sulphide and chromite, and outlinings of original olivine crystals are the most common manifestations of iron released from olivine during serpentinization. Clinopyroxene is relatively resistant, but when altered it breaks down to uralite and chlorite. Plagioclase is ubiquitously altered to saussurite and a fine opaque (Fe-oxide) dusting.

Skarn. In the eastern portion of the complex a 30 m sequence of calc-silicate country rock was produced by contact-metasomatic reactions between the Quill Creek intrusion and the underlying calcareous floor rocks. Detailed mapping and petrological studies by Fayak (1989) have shown that this area of "skarn" rock can be divided into zones. The terminology used here is based on that used by Fayak (1989). It employs his classification based on distinctive contact metamorphic/metasomatic lithologies and index minerals, and nomenclature inherited from past exploration and mining records. The contact metasomatic zones, with increasing distance from the intrusive contact, are: (1) white skarn, (2) feldspar-garnet skarn, (3) first axinite-bearing augite skarn, (4) garnet skarn, (5) second axinite-bearing augite skarn, (6) quartz skarn, (7) carbonate skarn. With the exception of the axinite-bearing augite skarn rocks, contact metamorphic/metasomatic index minerals like grossularite-enriched garnet and Fe-rich clinopyroxene (hedenbergite) are common throughout the skarn zones. In addition to zonation, the skarn interval is characterized by an increase in grain size towards the intrusive contact. Unfortunately, this textural feature is commonly masked by fault-related deformation.

The white skarn zone (Hudson-Yukon Mining terminology) is adjacent to the intrusive contact. It is fine grained, extensively fractured, and composed predominantly of lime-green patches of uralite after clinopyroxene (60%), white calcite (35%), and sulphides (5%). Chalcopyrite and pyrrhotite occur in approximately equal amounts. The feldspar-garnet skarn zone rocks are fine grained consisting of garnet (65%), calcite (20%), feldspar (5%), and sulphides (10%). Sulphide patches range from 1 mm to 1 cm and tend to be associated with calcite. Pyrrhotite is significantly more abundant than chalcopyrite. The first axinite-bearing augite skarn zone rocks display a granoblastic texture and are primarily composed of clinopyroxene (i.e. augite-salite, 50%) with plagioclase (10%) and sulphides (40%). Ferro-axinite generally occurs in veins that range in thickness from 0.30 to >2.0 mm and consist of small interlocking grain aggregates. In places it may constitute up to 40% of the rock. Sulphides occur in the fine-grained pyroxene-plagioclase matrix. Pyrrhotite occurs as large (1 to 6 cm) rounded globules, which appear to have formed from the coalescence of smaller sulphide droplet-like bodies. Chalcopyrite occurs as disseminations in the matrix of the host. The sulphide textures, similar clinopyroxene compositions and whole rock Cr levels (four to ten fold that of calc-silicate background levels) similar to those from the marginal gabbro, and relict textural features suggest the axinite-augite skarn rocks are metasomatically altered early sill-phases related to the main body of the Quill Creek Intrusive Complex.

Garnet skarn zone rocks are fine- to medium-grained and consist primarily of reddish-brown garnets (75-80%), pyroxene (1-25%), calcite (2-10%), and sulphides (1-15%). Sulphides are almost exclusively associated with interstitial calcite. Chalcopyrite generally occurs in minor amounts relative to pyrrhotite. Samples from the second axinite-bearing augite skarn zone are green to dark-green and consist of augite-salite (40%), calcite (20%), feldspar (30%), and sulphide (10%). The mode and irregular veining of axinite is similar to that of the first zone. Sulphides occur as small blebs and cross-cutting veins. Sulphides are generally 1-2 mm in size and consist of equal proportions of chalcopyrite and pyrrhotite. Due to the rather simple mineralogy of this relatively pure intercalated quartzite, referred to as quartz skarn by past mine and exploration geologists, this horizon was not sampled. The carbonate skarn zone displays a strong porphyroblastic texture and consists primarily of a creamy pink calcite (60%) and yellowish green garnets (35%). Sulphides occur as fine disseminations.

Garnet occurs in all skarn lithologies, with the exception of the axinite-bearing augite skarn lithologies. It ranges from 0.05 mm near the intrusive contact, to 1.2 mm in the garnet zone. Garnets near the intrusive contact are zoned, whereas those in the carbonate skarn are unzoned and lack inclusions. Electron microprobe analyses indicate that the garnets belong to the ugrandite series with an average composition of $Ad_{72}Gr_{27}(Uv+Sp)_1$. In most lithologies the Fe-content of zoned garnet increases towards the periphery of the grain; in garnet from the carbonate skarn, however, it decreases from core to rim.

Clinopyroxene is found in all skarn zones with the exception of the carbonate skarn zone. Those associated with garnet generally occur in open spaces as elongated lath-like crystals. Electron microprobe analyses and optical identification distinguish the clinopyroxene as hedenbergite with an average composition of $Wo_{50}En_{0.5}Fs_{49.5}$. When altered, particularly near the intrusive contact, this Fe-rich clinopyroxene breaks down to a chlorine-rich ferro-actinolite. Clinopyroxene from the axinite-bearing augite skarn zones are both texturally and

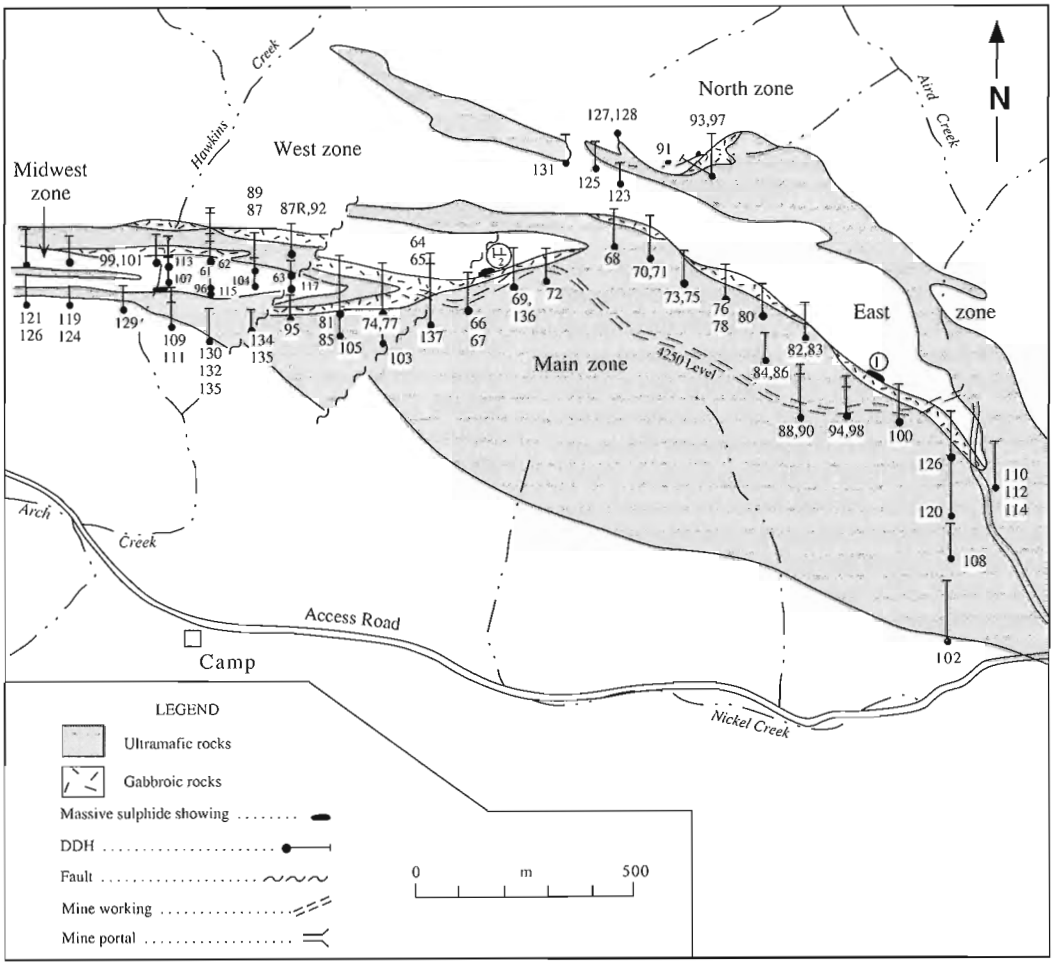

Figure 18. *Generalized map showing location of known mineralized zones within the Quill Creek Complex (QCC), distribution of ultramafic and gabbroic rocks, and the location of surface diamond-drill holes investigated during this study.*

compositionally distinct and most likely reflect their original igneous parentage. These clinopyroxenes are fine grained (0.10-1.0 mm) with a subhedral to anhedral habit and are evenly dispersed with altered plagioclase. Microprobe analyses identified the pyroxene as a member of the augite-salite series with an average composition of $Wo_{45}En_{41}Fs_{14}$. When altered it breaks down to a white uralitic amphibole.

Ni-Cu±PGE mineralization

To date, three major, and one minor, areas of gabbro-hosted massive and disseminated sulphide mineralization have been discovered in the Quill Creek Complex. In order of decreasing importance the East zone, West zone, and North zone are the most significant areas of mineralization (Fig. 18). The Midwest zone is a recently discovered extension of the West zone. A laterally continuous zone of lower grade disseminated sulphide mineralization in the olivine clinopyroxenite, and to a lesser extent peridotite and dunite members, is known as the Main zone. Five types of primary mineralization due to segregation of immiscible magmatic sulphides have been identified in the marginal and ultramafic zones from within these mineralized areas. In addition, three types of late stage proximal (hydrothermal and/or remobilized and metasomatic) mineralization have been recognized in the footwall and extremities of the complex. A detailed description of the various types and zones of Ni-Cu-PGE mineralization are discussed with respect to: areas of delineated mineralization, host rock, style, origin, and geochemical character. The results of a detailed mineralogical investigation of the opaque phases are discussed in considerable detail and are summarized in Tables 2 and 3.

Mineralized zones. East zone mineralization has been extensively explored since its discovery in 1952. To date geological information obtained from 4267 m of underground development on seven levels, including three internal shafts, and over 500 surface and underground drillholes, indicate that Ni-Cu-PGE mineralization occurs near the base of the complex as discontinuous massive sulphide lenses, disseminations in gabbro, "skarn"-hosted disseminations and massive sulphides, quartzite-hosted fracture, vein and breccia sulphide fillings, and replacement zones in the footwall quartzite. The gabbro-hosted mineralization is the most significant and comprises over 90% of the volume of mineralized rock from this zone. In general, the grade of the zone decreases upward from the mineralized contact, through heavily disseminated sulphides in gabbro to barren gabbro, near the top of the marginal gabbro zone. Sections illustrating the geology of the East zone marginal gabbro-hosted (ƞ "skarn"-type) mineralization and its relationship with the overlying ultramafic-hosted (Main zone) mineralization are summarized in Figures 19 to 23.

Mineralization in the East zone has been outlined by extensive underground drilling over a strike length of 900 m, and an average vertical extent of 200 m. The gently

Table 2. Opaque minerals observed in the Quill Creek Intrusive Complex**.

Major Minerals			
pyrrhotite	Fe_7S_8-Fe_9S_{10}*	pyrite	FeS_2
pentlandite	$(Fe,Ni)_9S_8$	magnetite	Fe_3O_4
chalcopyrite	$CuFeS_2$	ilmenite	$FeTiO_3$
Less Common to Rare Minerals			
violarite	$FeNi_2S_4$	galena	PbS
sphalerite	(Zn,Fe)S	altaite	PbTe
chromite	$FeCr_2O_4$	nickeline	NiAs
cobaltite***	CoAsS/NoAsS	undefined	Cu-Fe-Ba-S‡
arsenopyrite	FeAsS	covellite	CuS
ullmannite	NiSbS	breithauptite	NiSb
siegenite	$(Ni,Co)_3S_4$	barite	$BaSO_4$
argentopentlandite	$Ag(Fe,Ni)_8S_8$	titanite (sphene)	$CaTiSiO_5$
gold/electrum	(Au,Ag)	hessite	Ag_2Te
melonite	$NiTe_2$	matildite (?)	$AgBiS_2$
bismuth telluride (s)	Bi-Te(?)		

* ideal formula given for all minerals
*** unidentified members of the cobaltite-gersdorffite series
‡ probably a new Cu-Fe-Ba sulphide
** from Cabri et al., 1991, 1993

west-plunging zone has a moderate to steep dip to the south, and is open along strike at both ends and at depth. The base of this zone coincides with the depth at which the base of the complex cuts abruptly downsection through the chert to a limestone-argillite sequence. Massive sulphide lenses along the gabbro-chert contact give way below this structure to a mixed zone of pegmatitic gabbro and calc-silicate skarn rocks collectively referred to as "skarn" (Fig. 23). Sulphide mineralization in this latter environment consists of erratic sulphide veins, segregations, and disseminations. The highest PGE+Au grades associated with this mineralization, re-assaying of remaining Hudson-Yukon Mining Company Inc. core (DDH-U432), returned values of 1.03% Ni, 1.52% Cu, 1920 ppb Pt, and 1817 ppb Pd over a true width of 10.6 m. These sulphide lenses enclosed within gabbro also have chilled contacts and appear to represent immiscible sulphide segregations related to subsequent injections of new magma.

East zone ore estimates (based on a 0.5% Cu cutoff over a minimum horizontal width of 1.5 m) using underground drill intersections suggest proven and probable reserves of 3.1 million tonnes grading 1.10% Cu, 0.51% Ni, 1337 ppb Pt, and 925 ppb Pd over an area weighted average horizontal width of 5.6 m (Carne, 1987). Analyses of Wellgreen ore conducted during this study suggest that had Rh, Ru, Os, Ir, Ru, and Au assays been available, the precious metal content of this ore would be approximately twice that of the combined Pt and Pd values given above.

West and midwest zones mineralization was discovered during the course of the 1987 drilling program which was designed to test geophysical anomalies. Mineralization occurs within and adjacent a narrow east-trending ancillary sill to the main body of the intrusive complex.

The attitude of the sill is variable, dipping steeply south at the east end of the zone and steepening through vertical to steeply north-dipping and overturned along the west end. The dip also changes from south to north down dip. Footwall rocks

Table 3. PGMs and PGE-bearing minerals observed in the Quill Creek Intrusive Complex**.

PGMs in relative order of abundance			
sperrylite	$PtAs_2$	undefined	$(Pd,Ni)_2(Te,Sb)_3$
sudburyite	PdSb	undefined	$(Pd,Ni)_3(Te,Sb)_4$
testibiopalladite	PdSbTe	undefined	Pd(Bi,Te)
merenskyite	$PdTe_2$	undefined	$Pd_3Ni(Sb,Te,Bi)_5$
moncheite	$PtTe_2$	laurite	RuS_2
michenerite	PtBiTe	kotulskite	PdTe
stibiopalladinite	Pd_5Sb_2	Pt-Fe alloy (s)	Pt_3Fe or PtFe(?)
mertiete II	Pd_8Sb_3	undefined	Re>Ir>Os>Ru alloy
geversite	$PtSb_2$	undefined	Pd-Hg
hollingworthite	RhAsS	iridium	Ir
froodite	$PdBi_2$	undefined	Re sulphide (?)
PGE-bearing minerals			
melonite	$(Ni,Pd,Pt)Te_2$	up to 15.1% Pd; up to 9.37% Pt	
undefined	$(Ni,Pd)_2(Te,Sb)_3$	up to 22.8% Pd	
undefined	$(Ni,Pd)_3(Te,Sb)_4$	up to 15.9% Pd	
breithauptite	(Ni,Pd)Sb	up to 18.9% Pd	
hexatestibio-panickelite	$(Ni,Pd)_2SbTe$	up to 15.9% Pd	
ullmanite	(Ni,Pd)SbS	up to 0.09%	
cobaltite	(Co,Rh)AsS	up to 2.7% Rh, in zones	
pentlandite	(Pd,Rh,Ru)†	up to 34 Pd, 12 Rh, 13 Ru (ppm)	
chalcopyrite	(Ru,Rh,Pd)†	up to 10 Ru, 10 Rh, 9 Pd (ppm)	
pyrrhotite	(Pd)†	up to 5.6 ppm Pd	

† trace levels as determined by proton microprobe
** from Cabri et al., 1991, 1993

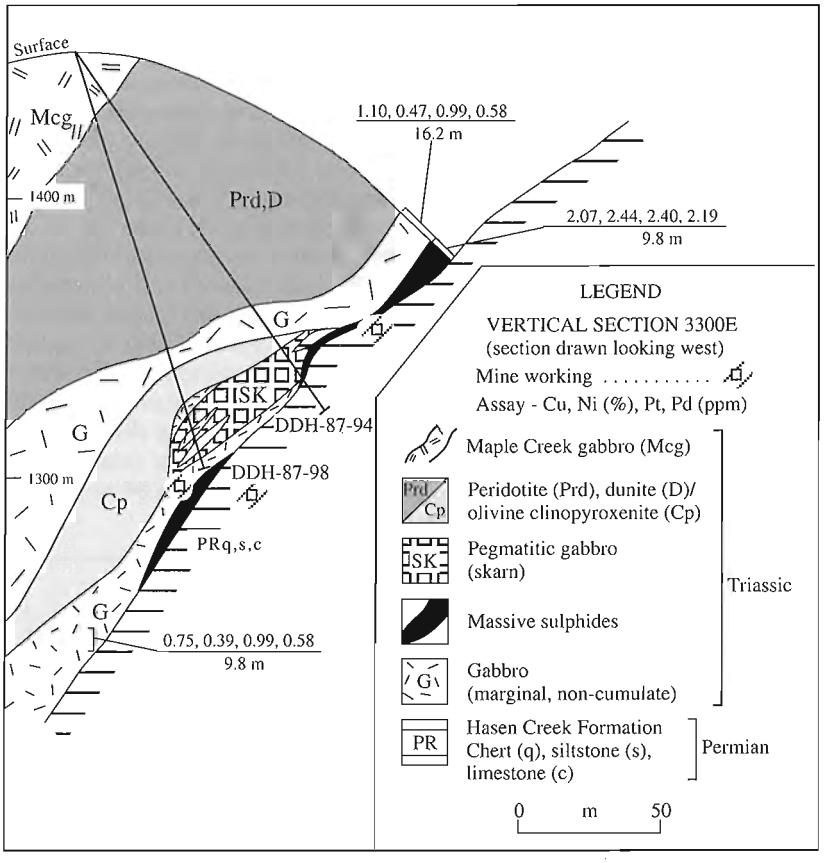

Figure 19.

Generalized geological section of East zone (Quill Creek Complex) massive sulphide, mineralized gabbro and "skarn-type" mineralization and its relationship with the overlying ultramafic-hosted Main zone mineralization. Grades and widths are also shown for certain intervals. The intersection of DDH-87-94 is also shown as reference for later detailed geochemical discussions.

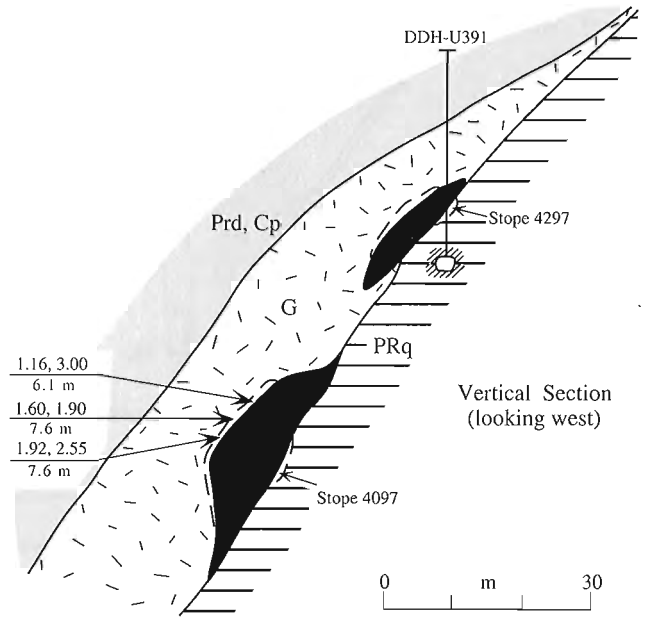

Figure 20. *Generalized geological section of massive sulphide concentrations from the East zone (Quill Creek Complex) illustrating the form and grade of some mined bodies. Refer to Figure 19 for legend.*

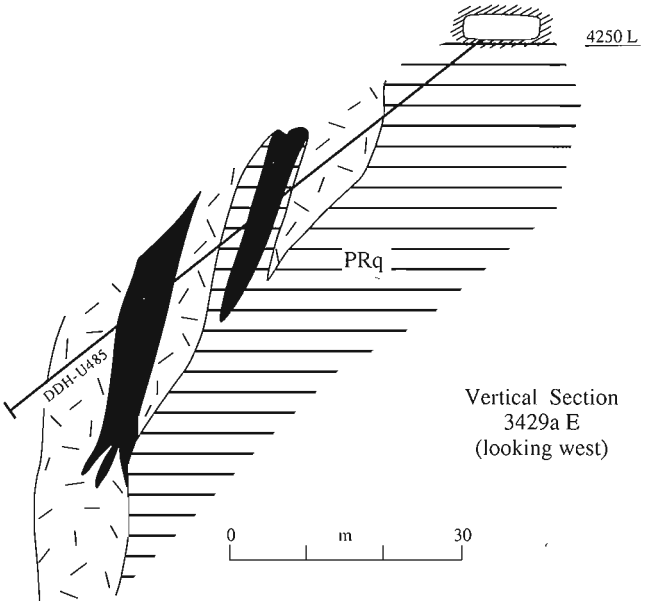

Figure 21. *Generalized geological section showing the form and grades of massive sulphide bodies from the East zone (Quill Creek Complex) and the confinement of these bodies to both gabbro and country rock at this locality. The intersection of DDH-U485 is also shown as reference for later detailed geochemical discussions. Refer to Figure 19 for legend.*

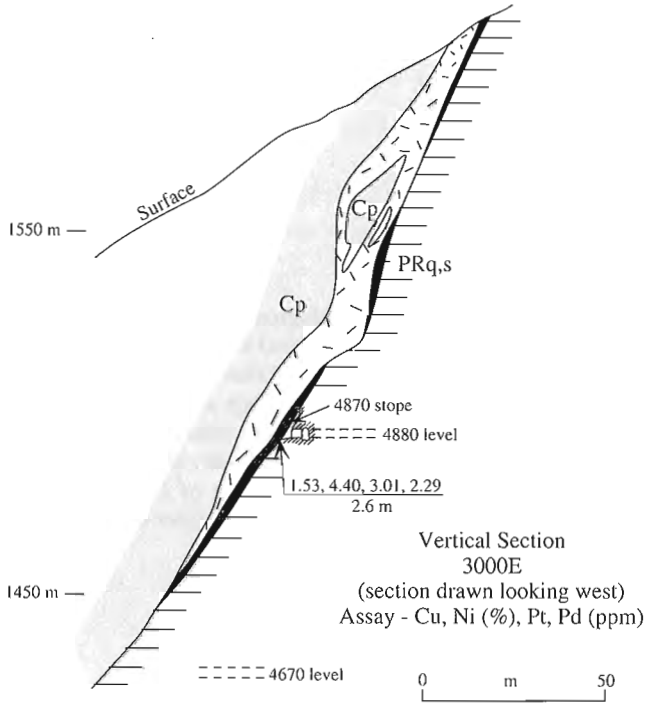

Figure 22. *Generalized section showing the form and grade of a thin massive sulphide horizon along the base of the intrusion from the East zone (Quill Creek Complex). Refer to Figure 19 for legend.*

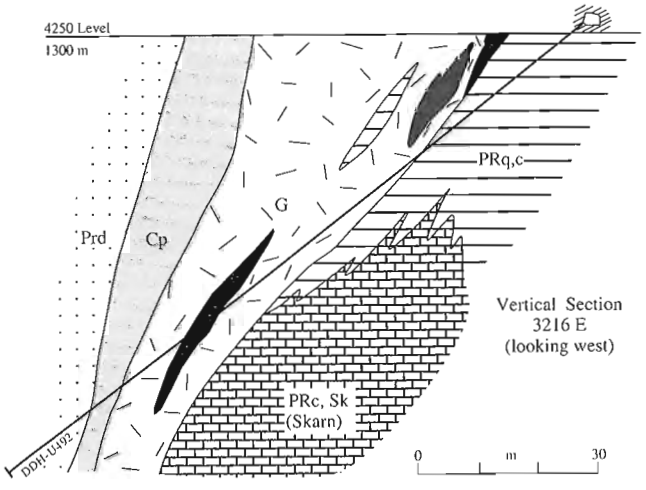

Figure 23. *Simplified geological section of massive sulphide bodies from the base of the marginal gabbro (Quill Creek Complex), and its relationship with proximal "skarn-type" mineralization and the overlying olivine clinopyroxenite and peridotite-hosted Main zone mineralization. The intersection of DDH-U492 is also shown as reference for later detailed geochemical discussions. Refer to Figure 19 for legend.*

are tuffaceous calcareous siltstone, tuff breccia, and agglomerate; the hanging wall at the east end of the zone consists of the main ultramafic body which cuts obliquely upsection to the west (Fig. 24). Midway along the West zone, the sill narrows and splits off the main body along bedding in the host volcaniclastic rocks. The sill has a thin marginal gabbro facies adjacent both walls and grades abruptly to an olivine clinopyroxenite, and minor wehrlite, core (Fig. 25). The dip of the sill has been noted to change from a steeply south-dipping to north-dipping attitude along strike. Gabbro and ultramafic-hosted mineralization is associated with this feature, in addition to volcanic-hosted sulphides of a possible late magmatic hydrothermal origin. The highest grade mineralization occurs in the ultramafic core where thin lenses of massive sulphide alternate with sections of moderate to heavily disseminated and net-textured sulphides. One of the best intersections occurred in DDH-87-87 (Fig. 18) which cut a 84 m interval

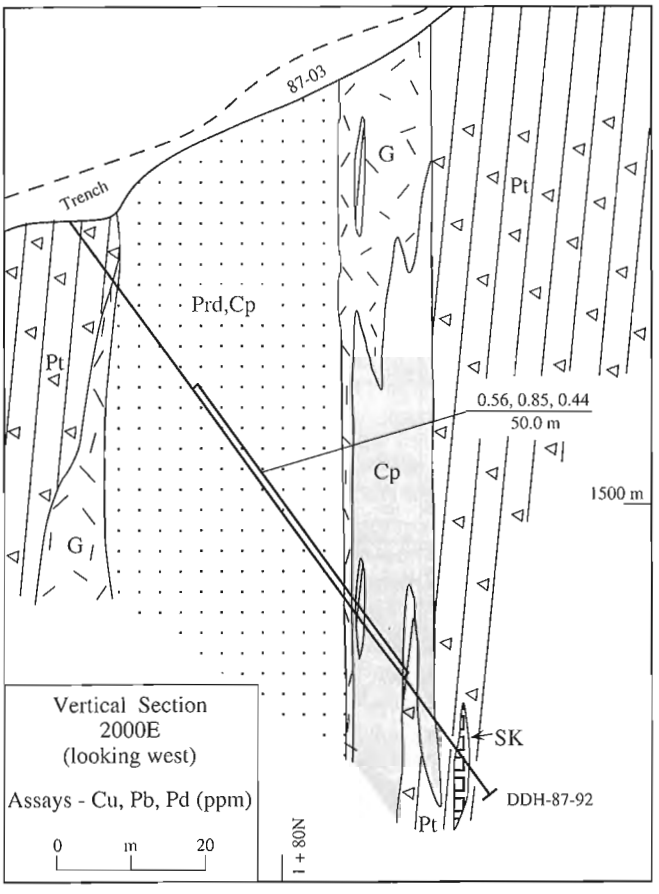

Figure 24. *Generalized geological section of an ancillary sill from the main mass of the Quill Creek Complex. The best sulphides are confined to the central portion of the ultramafic part of the sill (Prd, Cp) and occur as part of the West zone of mineralization. Note the enveloping gabbro and the unusual association of ultramafic material (Cp) in contact with the country rock along the north side of the body. The intersection of DDH-87-92 is also shown as reference for later detailed geochemical discussions. Prd = peridotite, Cp = clinopyroxenite. Refer to Figure 19 for legend.*

(≈50 m true thickness) grading 0.27% Ni, 0.77% Cu, 960 ppb Pt, and 445 ppb Pd, and included an 11 m interval containing 0.50% Ni, 1.62% Cu, 2125 ppb Pt, and 1062 ppb Pd. Similar mineralization also occurs in the thinner symmetrically layered (zoned) sill-like bodies where grades of 0.45% Ni, 1.03% Cu, 1165 ppb Pt, and 582 ppb Pd over 16 to 18 m intervals are not uncommon (Fig. 25). Unlike the East zone, marginal zone gabbro from the West zone is only weakly mineralized and devoid of massive sulphides. Mineralized propylitic, quartz-carbonate, and garnet-diopside metasomatic (skarns) alteration zones are frequently developed in the wall rock adjacent the sill(s).

West zone mineralization, not including the Midwest zone, has been outlined by drilling over a 600 m strike length and to a depth of about 200 m. It is calculated to contain 2.6 million tonnes grading 0.37% Ni, 0.77% Cu, 1131 ppb Pt, and 377 ppb Pd over an average weighted width of 11 m, using a 0.5% Cu cutoff grade (Carne, 1987). Unfortunately Rh, Ru, Os, Ir, and Au were not routinely assayed for during the exploration program; however, analyses conducted during this research indicate relatively high concentrations are present. Preliminary findings suggest that Cu/Cu+Ni ratios in mineralized ultramafic rocks from the West zone are considerably higher than from the East zone.

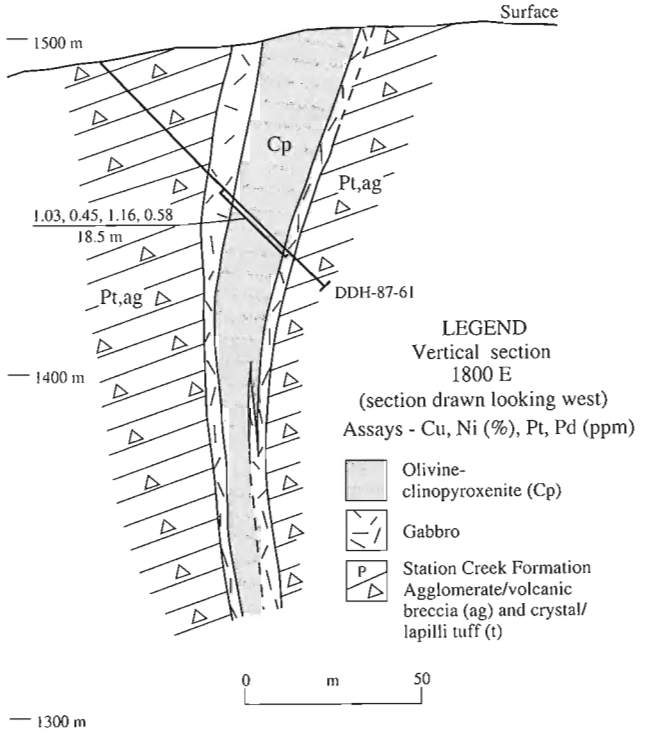

Figure 25. *Vertical section of a thin mafic-ultramafic sill or West zone apophysis (Quill Creek Complex). Note the thin gabbroic envelope about the olivine clinopyroxenite core of the intrusion, and that the best grades are generally confined to the ultramafic core, although mineralization begins near the gabbro-ultramafic contact. Refer to Figure 19 for legend.*

North zone mineralization is located in the east-central portion of a narrow 1200 m long sill-like body that lies 150 m stratigraphically below the main mass of the Quill Creek Complex. The geology of this zone bears similarities to both the West and East zones. Mineralization consists of massive sulphide lenses, disseminations in gabbro and ultramafic rocks, and as fracture fillings in footwall cherts. Although four small isolated massive sulphide lenses where explored and trenched by Hudson-Yukon Mining Company in the 1950s; only one significant massive sulphide lens was intersected during the 1987 program. This 35 cm thick lens assayed 5.79% Ni, 2.07% Cu, 6480 ppb Pt, and 1014 ppb Pd. The entire 1200 m length of the North zone sill is characterized by moderately to strongly anomalous geochemical and geophysical response (Carne, 1987). Due to the steep terrain, frozen north-facing slopes, thick talus cover over most of the strike length and poor ground conditions, exploration of this zone was severely hampered.

Main zone mineralization is confined to the ultramafic members from the thick central mass of the complex between the West zone and mineralized ultramafic rocks from the Main zone or eastern portion of the ultramafic mass. This mineralization is essentially the same as that from the ultramafic lithologies in the West zone. Grades over this 70 to 80 m wide zone average 0.29% Ni, 0.32% Cu, 617 ppb Pt, and 306 ppb Pd.[1]

Other areas of potential are inferred on the bases of results from geochemical and geophysical surveys. A 600 m long, predominantly ultramafic sill, that lies stratigraphically between the West zone and the western half of the North zone has geochemical and geophysical responses similar to these of other mineralized zones. Due to limited exposure the eastern portion of the complex (>2 km) is relatively unknown (Fig. 12). However, a number of relatively strong multi-element geochemical responses occur in this area and warrant testing. If the mineralized Linda Complex were once physically part of the Quill Creek Complex, then significant mineralization could be expected along this unexplored portion of the Quill Creek Complex.

Immiscible magmatic sulphide segregations.

Marginal gabbro-hosted mineralization.

Massive and semi-massive sulphides. Lenses of massive and semi-massive sulphide occur primarily at the gabbro-sediment contact, and less frequently within gabbro (15-20 m above the basal contact). These accumulations are best and most frequently developed when the gabbro is in contact with Hasen Creek Formation sediments, rather than Station Creek Formation volcanic and volcaniclastic rocks (Fig. 15, 18). In the East zone, where massive sulphides are best developed, these concentrations can attain a maximum thickness of 20 m; however, those in the 1-2 m range are the norm. These bodies tend to be elongate, striking up to 60 m in length and generally not attaining a height of more than 20 m. Under exceptional circumstances thicknesses may vary rapidly down-dip to the

[1] News Release Galactic Resources Ltd. and All-North Resources Ltd., July 27, 1988.

extent that some of the thinner sub-economic concentrations may extend up to 200 m (Fig. 22). Locally, enhanced massive sulphide concentrations are controlled by pre-ore joints and faults which form irregularities along the base of the complex. Massive sulphides at the gabbro-country rock interface usually have sharp basal contact with the underlying sediment, but in some sections a diffuse, irregular boundary is more typical. Locally thin gabbro chills and chert xenoliths with thin (2-10 cm) hornfelsed rims are associated with the massive sulphides. Accumulation of massive sulphides along the basal contact is clearly the result of segregation of immiscible magmatic sulphides due to a decrease in the sulphide carrying capacity of the magma in response to a drop in temperature. The form, distribution, and grade of some of these bodies are illustrated in Figures 19 to 23.

Macroscopically the massive, semi-massive, and associated disseminated sulphides display classic sulphide-silicate melt immiscibility features (Fig. 26A, B, C, D). Relatively unmodified accumulations of immiscible magmatic sulphides in the form of massive basal accumulations are illustrated in Figure 26A. The photograph shows massive pyrrhotite-rich sulphides, with small included chalcopyrite and exsolved pentlandite blebs, and irregular globule-like gabbroic inclusions with fine disseminated chalcopyrite in the groundmass. These globular bodies can be isolated (Fig. 26A; left and centre) or in clusters (Fig. 26A; centre-right), and are commonly near much larger isolated gabbro inclusions (Fig. 26A; right). The macroscopic texture of these samples, the high concentration of disseminated chalcopyrite in fine-grained gabbro, and the relatively Cu-impoverished nature of the pyrrhotite-pentlandite domains are supporting evidence for a magmatic origin due to high temperature monosulphide (MSS)-silicate (gabbroic) melt immiscibility, with Cu being preferentially partitioned into the silicate melt.

Overlying samples with semi-massive concentrations of sulphides commonly display coarse interconnected accumulations of immiscible sulphide globules and coalesced globules (Fig. 26B; centre). Above this horizon weaker concentrations of sulphides appear to be separated from the underlying accumulations by irregular downward connecting patches of interstitial sulphide (Fig. 26B; top). These sulphides appear to have collapsed through this once rather plastic gabbro melt.

The "frozen-in" character of the earliest immiscible magmatic sulphides in the Quill Creek Complex are best preserved in the fine-grained chill gabbro (Fig. 26C). In this environment, globular and elongated globular bodies of immiscible magmatic sulphide have been quenched in a very fine-grained gabbroic groundmass. Elongated globules probably reflect the settling direction of the segregating sulphide melts. In a slower cooling magmatic environment such immiscible sulphide segregations would accumulate and coalesce into massive sulphides similar to the example in Figure 26A.

Locally, massive sulphide lenses display evidence of tectonic remobilization. These samples have a pronounced planar fabric, outlined by alternating bands of pyrrhotite-pentlandite and chalcopyrite-silicate. Silicate inclusions tend to be aligned in planer aggregates of augen-shaped particles enveloped by foliated sulphides which wrap around them.

Opaque mineralogy. The major opaque minerals identified in the massive sulphide lenses are pyrrhotite and pentlandite, followed by chalcopyrite and magnetite. Trace amounts of cobaltite/gersdorffite, arsenopyrite, ullmannite, chromite, violarite, galena, Au-Ag alloy, and altaite are present. Approximately 70% of the pyrrhotite is of the hexagonal variety and 30% monoclinic. Randomly selected pyrrhotite grains contain 0.81 wt.% Ni. Electron microprobe analyses of pentlandite selected at random varied little from 34.8-36.0 ($\overline{X}$ = 35.5) wt.% Ni and 1.2-1.5 ($\overline{X}$ = 1.3) wt.% Co (Cabri et al., 1991).

A platinum-group mineral (PGM) investigation of the massive sulphide mineralization disclosed that >90 vol.% occur in pyrrhotite and are relatively small (largest 12 x 30 μm). The PGMs, in decreasing order of relative abundance, are: merenskyite (49.3%), moncheite (22.0%), sudburyite (19.1%), testibiopalladite (4.7%), and sperrylite (4.1%). Three grains of Pt-Pd-bearing melonite (2.0%) in pyrrhotite and one inclusion of Au-Ag alloy (0.68%) in cobaltite/gersdorffite were found (Cabri et al., 1991).

The opaque mineralogy of the semi-massive sulphide from the East zone is essentially the same as that reported above for the massive sulphide. Nevertheless, some coarse grains of sperrylite range from 15 x 75 and 70 x 110 μm in size, and 61 vol.% of these grains were totally liberated, whereas 39 vol.% had minor attached chalcopyrite and pyrrhotite. Sudburyite was also found in nickeline and cobaltite/gersdorffite.

*Figure 26. Photographs of different types of ores and sulphide mineralization from the Quill Creek Complex. See text for detailed descriptions. GSC 1995-106A (**A**) Typical basal pyrrhotite-rich massive sulphides with irregular, chalcopyrite-rich, globular gabbroic inclusions. This textural relationship is reminiscent of sulphide-silicate liquid immiscibility. (**B**) Overlying semi-massive sulphides with coarse interconnected accumulations of immiscible sulphide globules, and coalesced globules, in a gabbroic matrix. (**C**) Early immiscible magmatic sulphide globules and elongated globules quenched in a fine-grained chill gabbro. (**D**) Mineralized fine- to medium-grained gabbro with disseminated sulphides in the form of blebs and intergranular fillings. (**E**) Coarse-grained to pegmatitic gabbro lacking sulphides. (**F**) Mineralized pegmatitic gabbro. (**G**) Mineralized olivine clinopyroxenite to wehrlite (serpentinized). Note the even disseminations of sulphide and the localized net-textured patches. (**H**) Fine-grained disseminated sulphides in dark serpentinized peridotite. c = clinopyroxene, p = plagioclase, s = sulphide, g = gabbro, pn = pentlandite, cp chalcopyrite, m = magnetite.*

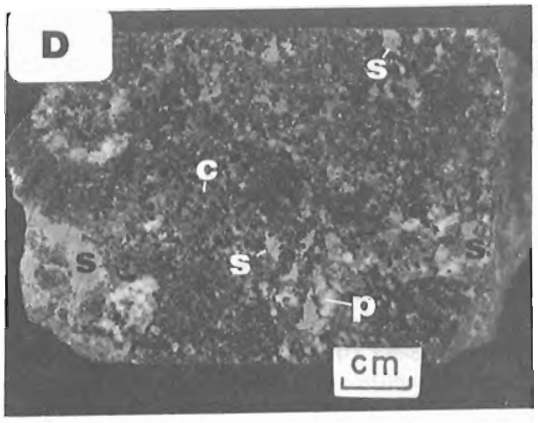
D
s
c
s
s
s
p
cm

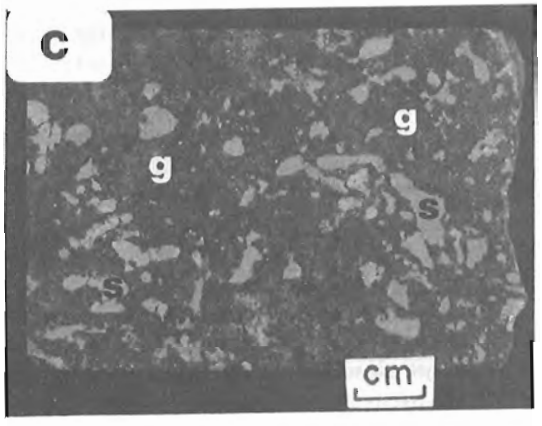
C
g
g
s
s
cm

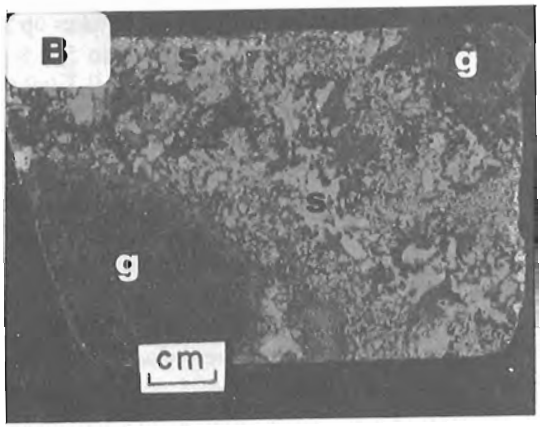
B
s
g
s
g
cm

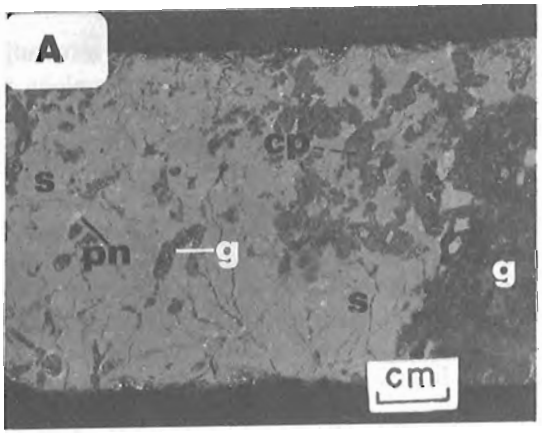
A
cp
s
pn
g
g
s
cm

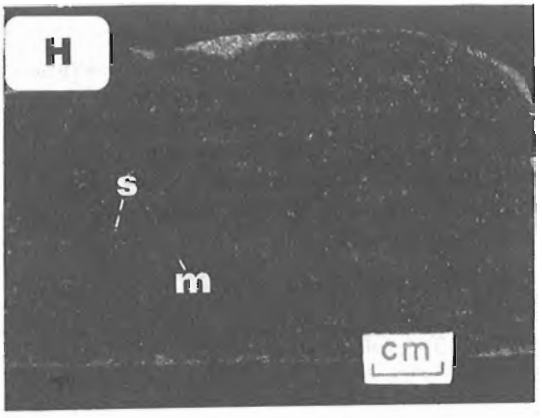
H
s
m
cm

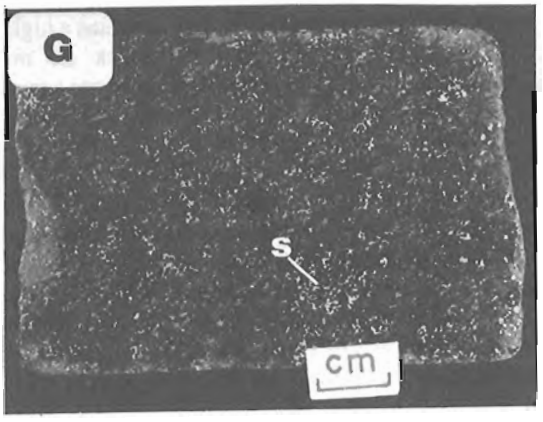
G
s
cm

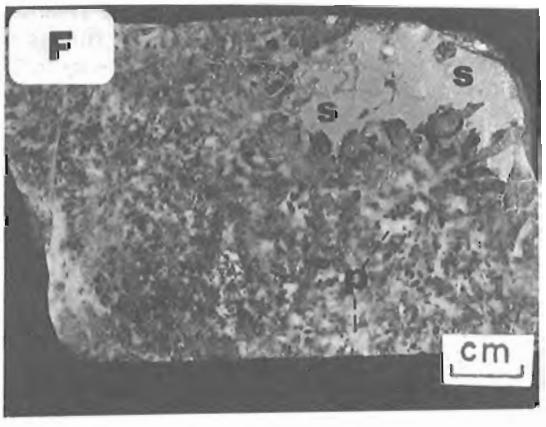
F
s
s
p
cm

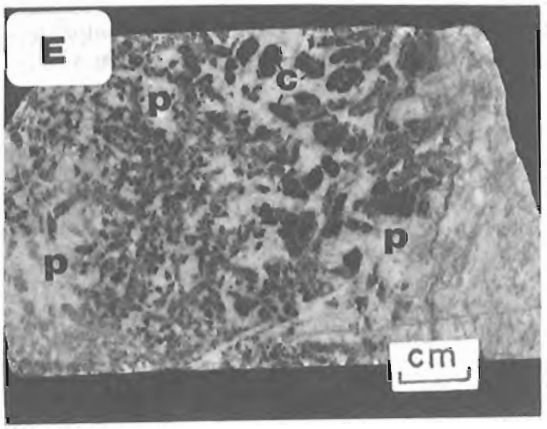
E
p
c
p
p
p
cm

Mineralized gabbro. Gabbro-hosted disseminated sulphides are volumetrically the most abundant type of mineralization in the Quill Creek Complex. Intergranular and bleb-like sulphides, principally pyrrhotite with lesser chalcopyrite and pentlandite, are common throughout the marginal gabbro. The intensity of mineralization increases generally towards the base of the marginal gabbro, with the highest overall grade of Ni, Cu, and PGEs being concentrated near the massive sulphide lenses.

Texturally, two different varieties of mineralized gabbro are present. The most common variety is that of a fine- to medium-grained gabbro containing disseminated sulphides in the form of blebs and intergranular fillings (Fig. 26D). Subordinate amounts of coarse- to very coarse-grained and pegmatitic gabbro (Fig. 26E and 26F) also occur within this zone. Mineralogically, the pegmatitic variety contains a higher proportion of plagioclase and consists of mottled plagioclase-rich domains. Figure 26E represents an unmineralized pegmatitic gabbro. Pegmatitic gabbro tends to have high Cu/Ni ratios (4 to 8) relative to other mineralized gabbro. Accumulating analytical data suggest that the pegmatitic gabbro also contains higher levels of precious metals, especially Au, than comparably mineralized non-pegmatitic gabbro. Average mineralized pegmatitic gabbro samples with approximately 4.0% sulphides contain 840 ppm Ni, 5200 ppm Cu, 561 ppb Pt, 245 ppb Pd, and 427 ppb Au. Opaque mineralogy and sulphide textures of these two different types of gabbro are essentially the same and are treated as such in subsequent discussions.

Disseminated sulphides in the marginal gabbro range from 2 to 16% and occur as intergranular fillings and as bleb-like bodies. In addition, sulphide patches up to 2 cm in size are frequently associated with this mineralization. Less frequently, larger irregular patches of massive sulphide are scattered throughout the gabbro with no apparent control on their distribution. Most of the blebs and larger patches appear to have been immiscible sulphide globules, or coalesced globules that have settled on and around partially crystallized gabbroic silicate phases. The highly irregular shape and size of some of these blebs, and the sharp triangular-shaped intergranular sulphide fillings in others suggest that the bulk of the sulphides (even the interstitial mineralization) represent immiscible sulphides that percolated downwards through a partially crystalline gabbroic (basaltic) magma. Enhanced accumulations of such mineralization impart a sulphide net-texture to the rock in areas bordering massive sulphide lenses. Complex intergrowths with interstitial amphibole and chlorite occur as a result of reaction with late stage deuteric fluids, and in certain cases, contact metasomatic fluids.

Opaque mineralogy. Pyrrhotite is by far the most abundant sulphide phase and contains variable amounts of pentlandite exsolutions in the form of flames, subhedral inclusions, and as partial rims adjacent pyrrhotite-silicate boundaries. Chalcopyrite occurs in the gangue as discrete grains near or adjacent, and locally within, pyrrhotite. Preliminary studies suggest that gabbro-hosted low grade mineralization is chalcopyrite-rich relative to the higher grade disseminated mineralization. The low-grade mineralization (with higher Cu/Ni ratio) may represent sulphides segregated from a more evolved parental magma.

High-grade gabbro-hosted disseminated mineralization (>0.63% Cu). Pyrrhotite and pentlandite are the major opaque minerals in this type of mineralization, with minor quantities of chalcopyrite, pyrite, cobaltite/gersdorffite, arsenopyrite, ullmanite, nickeline, violarite, sphalerite, magnetite, and argentopentlandite. Trace amounts of breithauptite, covellite, marcasite, galena, rutile, Au-Ag alloy, and an undefined Cu-Fe-Ba sulphide were also identified (Cabri, et al., 1991). Electron microprobe analyses of pentlandite show very little compositional variation; the average Ni content is 35.2% and Co is 1.5%. Twenty random grains of pyrrhotite were analyzed, twelve of which are the hexagonal variety, and have a mean Ni content of 0.60 wt.% and Co content of 0.025 wt.%.

Eighty-six discrete grains of PGMs were identified in what is believed to be material representative of this type of mineralized gabbro. Sperrylite ranges in size from <2 to 40 x 55 μm and comprises 24% of this PGM population. Approximately 99 vol.% of identified sperrylite grains are associated with or included in silicate gangue, and 1 vol.% included in pyrrhotite. An undefined (Ni,Pd)2(Te,Sb)3 mineral was identified and constitutes 43% of the total PGM population. All of these grains are closely associated with pyrrhotite, either as inclusions in pyrrhotite or in sulpharsenides, themselves attached or completely enclosed in pyrrhotite, and range from <2 to 12 x 22 μm. Pd-melonite [(Ni,Pd) Te_2] makes up 22% of the PGM population and ranges from <2 to 5 x 8 μm, 97 vol.% of which are included in pyrrhotite, 0.3 vol.% in cobaltite (also included or associated with pyrrhotite), and 2.5 vol.% in pentlandite. Testibiopalladite is closely associated with pyrrhotite or cobaltite and gangue, and ranges from 3 to 6 x 10 μm and constitutes 4.6% to the total PGM population. Sudburyite ranges from <2 to 4 x 5 μm, 87 vol.% of which occurs in cobaltite/gersdorffite and 13 vol.% in ullmannite. Several grains of Pd-bearing breithauptite (generally <40 μm), are associated with ullmannite and cobaltite/gersdorffite. Au-Ag alloys are included in cobaltite/gersdorffite (<2 to 5 x 10 μm) and are approximately one tenth as abundant as PGMs (Cabri et al., 1991, 1993).

Low-grade gabbro-hosted disseminated mineralization (≤0.63% Cu). The opaque base metal mineralogy consists of chalcopyrite, pentlandite, pyrrhotite, ilmenite, and pyrite. Minor to trace amounts of barite, chromite, magnetite, cobaltite/gersdorffite, arsenopyrite, siegenite, violarite, argentopentlandite, galena, altaite, hessite, and Au-Ag alloy were identified. The major sulphides are quite variable in grain size, but there appears to be two populations: relatively coarse-grained sulphides (up to 1-1.5 mm) and fine-grained sulphides (<5 μm) dispersed in the gangue. Electron microprobe analyses of 15 randomly selected pentlandite grains showed little compositional variation; the mean Ni content is 35.45 wt.% and Co content is 2.45 wt.%. The Co-rich nature of pentlandite from this group, relative to that

of the previous group, confirms the earlier suggestion that the magma from which these sulphides segregated was more evolved (fractionated) than that which gave rise to the higher grade gabbro-hosted disseminated mineralization. The lower average Ni content in pyrrhotite (0.32 wt.%) may also be related to the more evolved nature (Ni-depleted) of this magma.

One hundred and forty-five discrete PGMs were identified during the investigation of this material. The most abundant is an undefined $[(Ni,Pd)_2(Te,Sb)_3]$ mineral (44.8%) that ranges from <2 to 25 x 80 μm, with 87.8 vol.% occurring in chalcopyrite, 7.7 vol.% in pyrrhotite, and 4.5 vol.% in pentlandite; the average Pd content is 11.8 wt.%. Sperrylite is the second most abundant PGM (20.7%) and ranges from <2 to 60 x 60 μm and 92 vol.% are liberated, 4 vol.% are included in chalcopyrite and <1 vol.% occurs in pyrrhotite and <1 vol.% in other PGMs. Testibiopalladite makes up 15.2% of the total PGMs and ranges from <2 to 20 x 25 μm; 91 vol.% occur in chalcopyrite, 6 vol.% in pyrrhotite, and 3 vol.% in pentlandite. Michenerite (6.8%) ranges from <2 to 9 x 11 μm with 74 vol.% included in pyrrhotite, 26 vol.% in cobaltite/gersdorffite, and <1 vol.% in chalcopyrite. Hollingworthite (1.3%) occurs as very small grains (<2 μm) disseminated equally in cobaltite, pentlandite, and pyrrhotite. Sudburyite (0.68%) and a Re>Ir>Os>Ru alloy (0.68%) of approximately equal size (≤2 x 3 μm) occur in chalcopyrite. Rhenium sulphide, an exceptionally rare mineral, occurs as a small grain (1 x 3 μm) in pentlandite. Palladian-platinian melonite, at 8.9% of the total PGMs, ranges from <2 to 10 x 10 μm; its distribution is: 54.7 vol.% in pentlandite, 44.7 vol.% in pyrrhotite, and 0.6 vol.% in chalcopyrite. Two small grains of Au-Ag alloy were found in pyrrhotite and cobaltite, and one small (1 x 3 μm) euhedral Rh-bearing cobaltite in pentlandite. The dominance of sperrylite, apart from its highly liberated character (92 vol.%) in ground specimens, over other PGMs, is very striking when one converts the relative abundance 20.7% to volumetric abundance (82%).

Ultramafic-hosted mineralization.

Olivine clinopyroxenite. The olivine clinopyroxenite member forms a 3 to 30 m thick conformable horizon, that overlies the marginal gabbro zone, and is particularly well developed and mineralized in the western portions of the complex.

Sulphide mineralization ranges from scattered irregular disseminations, 0.2 to 1 mm in size, to moderately heavy disseminations with localized net-textured patches (Fig. 26G). Sulphide mineralization is best developed in the lower-central portions of the ultramafic core in the West zone. Massive sulphide lenses up to 1-2 cm thick are developed locally. Where present, massive sulphides occur near the middle or lower-middle portions of the mineralized domain and are enclosed within an area of heavily disseminated sulphides. Massive sulphide breaks in pyroxenites from the West zone can contain relatively pure chalcopyrite concentrations within pyrrhotite-rich assemblages similar to those from the marginal gabbro zone. The geology of this lithological environment and mineralized domain is illustrated in Figures 24 and 25. Detailed discussions pertaining to geochemistry associated with this style of mineralization are presented with the aid of the geological section and geochemical data presented in Figures 24 and 31, respectively.

Opaque mineralogy. Previously, it was noted that the mineralized clinopyroxenite is relatively Cu-rich compared to the gabbro-hosted mineralization, and that the West zone clinopyroxenite appears to have a higher Cu/Ni ratio than counterparts from the Main zone or eastern portion of the ultramafic zone. Investigation of opaque minerals from these zones reveals a distinctive zone-dependant base metal mineralogy which corroborates the different Cu/Ni ratios associated with each zone. Representative West zone and Main zone material has Cu/Ni ratios of 0.885 and 0.362, respectively. Results of a detailed mineralogical investigation of the opaque minerals from the various zones follows.

"West zone". Chalcopyrite, ilmenite, magnetite, pentlandite, and violarite are the major opaque base metal minerals. Minor to trace amounts of pyrite, chromite, pyrrhotite, sphalerite, barite, arsenopyrite, cobaltite-gersdorffite, argentopentlandite, galena, altaite, breithaupite, hessite, and Au-Ag alloy were identified (Cabri et al., 1991). The sulphides are quite variable in grain size, and once again there appears to be two populations: relatively coarse-grained sulphides (up to about 1 mm) and fine-grained sulphides (<5 μm) dispersed in gangue. Very little grain to grain chemical variation is present in pentlandite ($\overline{X}$ = 33.35 wt.% Ni and 2.3 wt.% Co). Pyrrhotite contains about 0.62 wt.% Ni. Sulphides are usually hosted in a serpentine, and to a lesser extent chlorite matrix. The mean Ni content of the serpentine based on 50 electron microprobe analyses is 0.066 wt.%.

Although extremely fine-grained (<9 x 10 μm), a number of diverse PGMs or PGE-bearing minerals occur in this material. They are in decreasing order of relative abundance: sperrylite (32.7%), sudburyite (25.7%), michenerite (10.4%), Pt-Fe-alloy (2.2%), hollingworthite (1.6%), testibiopalladite (1.1%), stibiopalladinite (1.1%), laurite (1.1%), moncheite (0.65%), undefined Pd-Hg mineral (0.65%), geversite (0.65%), iridium (0.65%), undefined $[(Ni,Pd)_2(Te,Sb)_3]$ and $[(Ni,Pd)_3(Te,Sb)_4]$ minerals and Pd-melonite $[(Ni,Pd)\ Te_2]$ (2.7%), and breithauptite (1.1%). All PGMs are strongly associated with magnetite produced during serpentinization. Volumetrically the Pt minerals are distributed in magnetite (60%), pentlandite/violarite (23%), silicates (14%), and chalcopyrite (3%), whereas the Pd minerals occur in magnetite (37%), chalcopyrite (34%), pentlandite (33%), and silicate (4%) (Cabri et al., 1991, 1993).

"Main zone". Chalcopyrite, pyrrhotite, and magnetite are the main opaque minerals associated with this zone. Minor to trace amounts of pentlandite, violarite, pyrite, chromite, ilmenite, sphalerite, barite, arsenopyrite, cobaltite-gersdorffite, covellite, galena, ullmanite, and Au-Ag alloy are present. As in the West zone, the major sulphides are variable in grain size

demonstrating two populations: relatively coarse-grained sulphides (up to 0.5 mm) which are generally associated with magnetite and fine-grained sulphides (<5 μm) dispersed in serpentine. Fifteen randomly selected pentlandite grains revealed only minor grain to grain compositional variation with a mean Ni and Co concentration of 35.7 wt.% and 1.8 wt.%, respectively. Pyrrhotite contains 0.57 wt.% Ni. The Ni-content of the serpentine from the groundmass is nearly identical to that from the West zone member. The pentlandite has approximately 2.3 wt.% more Ni and 0.50 wt.% less Co than in the West zone. This in conjunction with the high Cu/Ni ratios from the West zone substantiates the suggestion that magma that segregated the West zone mineralization was more evolved (differentiated). Under normal magmatic fractionation conditions Ni content decreases and the Co content of pentlandite increases with differentiation (Merkel, 1986). Even small differences, as noted above, require relatively large degrees of evolution of the parental magma from which the sulphide melt segregated.

The PGMs and PGE-bearing minerals from this material are extremely fine grained. In order of decreasing relative abundance they are: sudburyite (35.6%), sperrylite (27.4%), stibiopalladinite (4.1%), undefined $[(Pd,Ni)_3(Te,Sb)_4]$ mineral (2.7%), merenskyite (1.4%), unknown $[(Ni,Pd)_3(Te,Sb)_4]$ mineral (27.4%), and Pd-melonite $[(Ni,Pd)\ Te_2]$ (1.4%). Au-Ag-alloys range from <2 to 7 x 20 μm, occur in sulphides, and are about one-quarter as abundant as the total PGMs and PGE-bearing mineral population. Volumetrically, the Pt-minerals are distributed in magnetite (77%), pentlandite/violarite (14%), and chalcopyrite (10%) and the Pd-minerals in pentlandite/violarite (33%), pyrrhotite (31%), chalcopyrite (24%), and magnetite (12%).

Peridotite. Very fine-grained Ni-Cu-sulphide mineralization occurs throughout most of the peridotite member of the Quill Creek Intrusive Complex, particularly in the western portion. The scattered sulphides range from the micrometre size to 1-2 mm across as partial rims and interstitial fillings to serpentinized olivine. Due to the dark greenish-black colour of the host rock, the pyrrhotite-rich mineralization in the sample is difficult to appreciate (Fig. 26H). Its appearance is even further masked by the development of replacement magnetite rims and veins in the sulphide. Material similar to that shown in Figure 26H and used for the opaque mineralogical investigation, contained approximately 0.40% Ni, 0.15% Cu, 290 ppb Pt, 450 ppb Pd, and 31 ppb Au. (Cabri, et al., 1991, 1993).

Opaque mineralogy. Pyrrhotite and pentlandite are the major opaque phases followed by chalcopyrite and magnetite. Much smaller amounts of pyrite, cobaltite/gersdorffite, an undefined Cu-Fe-Ba sulphide mineral, arsenopyrite, ilmenite, chromite, galena, hessite, Au-Ag alloy, and argentopentlandite have been noted. Electron microprobe analyses of randomly selected grains demonstrate little variation; mean Ni and Co contents are 33.6 and 1.8 wt.%, respectively. All pyrrhotite grains analyzed were of the hexagonal variety and had a mean Ni content of 0.49%.

Two hundred and thirty-eight PGM grains where identified from this material (Cabri et al., 1991). They are in order of decreasing relative abundance: sperrylite (36.4%), sudburyite (30.1%), moncheite (12.3%), michenerite (4.7%), kotulskite (7.2%), mertieite II (4.2%), stibiopalladinite (3.4%), undetermined Pd(Bi,Te) mineral (1.3%), geversite (0.3%), undetermined $[Pd_3Ni(Sb,Te,Bi)_5]$ mineral (0.3%), undetermined $[(Pd,Ni)_3(Te,Sb,Bi)_4]$ mineral (0.3%). A Au or Au-Ag alloy accounts for approximately 1.0% of the total precious metal minerals. The most frequent distribution of the PGMs is in magnetite>>pyrrhotite>chalcopyrite≥silicate> pentlandite. Magnetite contains approximately twice the number of PGMs as any of the other associated phases.

Hydrothermal (remobilized ?) mineralization.

Volcanic-hosted sulphide mineralization. Volcanic-hosted sulphide mineralization is restricted to the West zone where andesitic tuff and tuffaceous siltstone are intruded by the Quill Creek Complex. Sulphides occur as randomly distributed, relatively coarse patches up to 2 cm across, or as areas of moderate to heavy disseminations. Sulphides generally rim or partially replace altered hornblende crystals set in a propylitic altered (carbonate-chlorite-epidote) rock. Mineralization may also occur in quartz-carbonate altered country rock adjacent to the floor of the main sill and as discontinuous envelopes or "flanges" around the narrow subsidiary sills.

Six representative samples of this disseminated mineralization returned the following assays: Cu (0.67-1.57 wt.%, $\overline{X}$ = 1.28 wt.%), Ni (0.26-0.69 wt.%, $\overline{X}$ = 0.36 wt.%), Pt (1410-2780 ppb, $\overline{X}$ = 2200 ppb), Pd (410-1000 ppb, $\overline{X}$ = 668 ppb), Au (180-360 ppb), Ag (2.6-14.4 ppm). The average Cu/Ni and Pt/Pd ratios are 3.55 and 3.29, respectively. This Ni-poor sulphide mineralization is believed to represent the product of a hydrothermal discharge emanating from the complex. This intense hydrothermal alteration is associated with the extremities of the complex as it is with the White River Intrusive Complex (i.e. quartz-carbonate envelope at the Onion property). The East zone of the Quill Creek Complex probably represents the intrusive centre from which magma migrated in a westerly direction. Volatiles associated with the magma(s) would also follow the same course and ultimately accumulate near the extremities of the intrusion and develop an extensive hydrothermal alteration zone.

Opaque mineralogy. The principal opaque minerals are chalcopyrite, pyrite, pyrrhotite, ilmenite, and pentlandite. Minor to trace quantities of the following were also identified: violarite, cobaltite, bismuth-tellurides, covellite, sphalerite, siegenite, melonite, altaite, and galena. Two varieties of pyrite were detected: a low-Ni cobaltoan pyrite (1.1 to 3.3 wt.% Co; low Ni <0.09 wt.%) species and a Ni-enriched pyrite (0.67 to 1.5 wt.% Ni). Pyrrhotite is exclusively of the monoclinic variety and carries between 0.60 to 2.9 wt.% Ni.

Pt and Pd are the only two PGEs that form discrete PGMs in this type of mineralization. The PGMs, in decreasing order of relative abundance, are: sperrylite (73.9%), merenskyite (12.2%), Pd-melonite $[(Ni,Pd)\ Te_2]$ (7.1%), michenerite/ testibiopalladite (5.5%), froodite (0.79%), and sudburyite

(0.39%). Pt is present only as sperrylite which occurs as large euhedral to subhedral grains ranging from 5 x 10 to 145 x 145 μm. Minor substitution of Pt by Os or Ir, or both (up to 0.23 wt.% Ir and 0.13 wt.% Os) occurs in some grains. Crushed samples (-65 and +270 mesh) reveal that 30.2 vol.% of the sperrylite grains are associated with chalcopyrite, 10.5 vol.% with silicates or ilmenite, and the rest of the grains are liberated. Merenskyite forms a complete solid solution with melonite (i.e. $PdTe_2$-$NiTe_2$). Semi-quantitative electron microprobe analyses indicate that melonite contains substantial Pd (5.5 to 13.9 wt.%). Approximately 75% of the merenskyite/melonite grains occur as inclusions in pyrrhotite and the balance in chalcopyrite. Michenerite/testibiopalladite grains are commonly associated with chalcopyrite and sulpharsenides.

The principal carrier of Ag is argentopentlandite, found closely associated with pentlandite. Rare grains (<5 μm) of matildite (?) and hessite occur as complex intergrowths with other minerals including Bi-tellurides. Silver is also present as an alloy of gold. The main source of Au is in the form of argentian gold and as electrum. The gold/electrum grains mainly occur as inclusions in various sulphides (mainly chalcopyrite and pyrite) and sulpharsenides and range from <2 x 2 to 70 x 110 μm.

Chert-hosted sulphides. Sulphides occur in footwall chert and cherty sediments within 2-3 m of the basal contact. The mineralization occurs as fracture fillings (stringers), breccia matrix, veins, or irregular patchy replacements rimmed by fine-grained hornfels (Fig. 16). The dominant ore minerals are chalcopyrite followed by pyrrhotite and pentlandite. Arsenopyrite and lesser amounts of Co-arsenides may also be present within Fe-carbonate-quartz veins in chert adjacent to massive sulphide stringers. Investigation of a 2 m wide stringer interval from the East zone revealed some interesting mineralogical and PGE distribution patterns associated with this remobilized sulphide. Massive sulphide fracture fillings in the immediate (1 m) sequence are pyrrhotite- and pentlandite-rich with an average grade of: Ni (2.3%), Cu (2.0%), As (1.83 ppm), Pt (1633 ppb), Pd (880 ppb), Au (383 ppb), Rh (206 ppb), Os (149 ppb), and Ir (363 ppb). The Ni-rich (pyrrhotite-pentlandite-chalcopyrite) mineralized interval is commonly underlain by a weakly mineralized section (Cu ≤ 0.50%, Ni ≤ 0.08%) containing thin chalcopyrite veinlets and fracture coatings. This interval demarcates the introduction of a Cu-rich facies (chalcopyrite) with the following grade: Ni (1.5%), Cu (4.4%), As (12.2 ppm), Pt (2300 ppb), Pd (1030 ppb), Au (77 ppb), Rh (110 ppb), Os (29 ppb), and Ir (74 ppb). The introduction and enduring nature of this chalcopyrite-rich facies suggest that there is a preferential mobilization of the Cu-rich phase relative to others. It is apparent that Ir, Os, and to a lesser extent Rh are significantly less mobile than Pt or Pd in such an environment. Similar Co contents in the presence of a marked depletion of modal pentlandite suggest that the Co balance has been taken up by Co arsenides derived at the expense of pentlandite from the Ni-rich interval. Although localized massive and semi-massive concentrations have significant grades and geochemical features associated with them, lower grades (≤4000 ppm Ni and ≤10000 ppm Cu) are characteristic of this zone.

Skarn-hosted sulphides. As mentioned previously, contact metasomatic reaction zones (skarns) are developed in the calcareous sequences bordering the complex in both the East and West zones. Sulphide mineralogy is the same in both zones, but the diverse nature of the different styles of mineralization in East zone skarns is not present in the West zone.

A detailed study of the skarn mineralization in the East zone (Fayak, 1989) showed that the calcareous country rock has been metasomatically transformed over a distance of at least 30 m from the intrusive contact. The sulphide mineralization is distributed heterogeneously, and commonly constitutes 3 to 40% of a sample. However, irregular replacement patches, veins, and fracture fillings of sulphides occur in scattered zones, spatially related, but not necessarily in contact with the complex. Sulphide mineralization is, in decreasing order of abundance: pyrrhotite, chalcopyrite, pyrite, pentlandite, magnetite, and minor amounts of sphalerite and galena. Galena occurs as small anhedral grains (≈0.1 mm) at the extremities of larger chalcopyrite grains. Although chalcopyrite and pyrrhotite are spatially associated, chalcopyrite generally occurs along the periphery of the larger pyrrhotite grains. Pentlandite occurs as exsolution lamellae within and rimming pyrrhotite. The size of the area of sulphide mineralization is generally dependent on the size of the available open space.

The sulphides generally occur in three different forms: (1) interstitial to garnet and pyroxene, (2) in veins closer to the intrusive contact, and (3) as globules and matrix disseminations in axinite-augite skarns. Generally, the sulphides are anhedral and associated with carbonate either as veins or open space fillings in the calc-silicate lithologies.

The following is a summary of the respective Ni (ppm), Cu (ppm), Pt (ppb), Pd (ppb), Au (ppb) values associated with each zone: (1) white skarn: 1100 Ni, 670 Cu, 761 Pt, 469 Pd, 39 Au; (2) feldspar-garnet skarn: 350-1900 Ni, 71-180 Cu, 291-1392 Pt, 119-1097 Pd, 46-303 Au; (3) first axinite-bearing augite skarn: 1800-8600 Ni, 8700-9900 Cu, 672-1265 Pt, 620-748 Pd, 69-124 Au; (4) garnet skarn: 380-1000 Ni, 550-1200 Cu, 361-622 Pt, 217-748 Pd, 69-579 Au; (5) second axinite-bearing augite skarn: 4100 Ni, 11000 Cu, 1152 Pt, 1184 Pd, 25 Au; and (6) carbonate skarn: 2100 Ni, 3100 Cu, 167 Pt, 152 Pd, 13 Au.

The highest values associated with sulphides of an unequivocal metasomatic origin are associated with semi-massive concentrations (≈44%) found outside the 1235 level study area of Fayak (1989). This mineralization is hosted in a coarse-grained, clinopyroxene-rich calc-silicate and returned the following values: 1300 ppm Ni, 2200 ppm Cu, 2009 ppb Pt, 1629 ppb Pd, and 119 ppb Au. The Rh, Os, Ir, and Ru levels are relatively low, 10, 8, 7.1, and 10 ppb, respectively, when compared to gabbro-hosted basal sulphides. It is interesting to compare these values with those from the best mineralization (35% sulphides) in the second axinite-bearing augite

skarn zone: 8600 ppm Ni, 8700 ppm Cu, 672 ppb Pt, 620 ppb Pd, 69 ppb Au, 74 ppb Rh, 49 ppb Os, 89 ppb Ir, 50 ppb Ru. Once again the relatively immobile geochemical character of Ir, Os, Ru, and Rh is apparent. The high concentrations and background levels of Pt and Pd in this contact metamorphic/metasomatic front confirm that Pd as well as Pt are very mobile in this type of geological environment. The fact that trace amounts of axinite have been identified in all calc-silicate skarn lithologies, as well as the axinite-bearing augite skarn lithologies, mainly as veins and veinlets and hedenbergite alters to a Cl-rich amphibole, suggest that "chloro-complexes" were the most probable transporting agents of Pt and Pd.

Average Ni, Cu, Pt, Pd, and Au values are: 3247 ppm Ni, 3000 ppm Cu, 730 ppb Pt, 470 ppb Pd, and 131 ppb Au (Fayak, 1989). The Pt/Pd ratio for this entire 30 m interval varies little (1.04 to 1.79) relative to the mafic-ultramafic-hosted mineralization.

As, Bi, Sb, and Te analyses of the calc-silicate material also revealed some interesting levels and trends. The As content increases away from the contact, where a low value of 4.3 ppm was recorded, to attain its highest concentration (165 ppm) at the location farthest from the contact. The average As concentration for the calc-silicates from this interval is 58 ppm. Massive Ni-Cu sulphides from the basal contact only contain 1.2 ppm As. The axinite-bearing augite skarn material, believed to have been of an igneous origin, had levels that ranged from 1.6 to 26.4 ppm. Bi and Sb concentrations are considerably higher than that of the gabbro-hosted massive sulphide, average 1.1 and 2.6 ppm, respectively, which is about twice that found in the massive sulphide. The Te content of the calc-silicate ranges from 0.2 to 2.4 ppm, with an average of 0.51 ppm. This is approximately one third the concentration found in the massive sulphides and in the axinite-bearing augite skarn. It would appear that in this environment anomalous Te concentrations can be related to mineralization of an igneous origin.

Geochemistry of the Quill Creek Intrusive Complex

Ni, Cu, Co, As, Sb, Bi, Te, PGE+Au and $\delta^{34}S$ geochemical trends and associations. A detailed geochemical investigation, based on 323 samples from the Quill Creek Intrusive Complex was conducted on material from country rock, gabbro, and ultramafic-hosted dissemination mineralization. Massive and semi-massive sulphide mineralization from this population is almost exclusively gabbro hosted, but a limited number of samples have been obtained from footwall and ultramafic lithologies. Ni, Cu, Co, Se, and (PGE+Au) concentrations recorded for various lithologies span a wide range in composition and demonstrate a strong chalcophile character. Anomalous barium concentrations and distinctive sulphur-isotope signatures characterize mineralized and unmineralized lithologies from this complex. Other salient features revealed by this survey are summarized graphically in Figures 88, 89, 100, 101, 110, 111, 122 ,123, 132, 133, 143, and 144. The findings of more detailed investigations based on metre- and centimetre-scale sample intervals for gabbro- and ultramafic-hosted massive, semi-massive, and disseminated mineralization are illustrated in Figures 27 to 31.

Nickel content of massive and semi-massive sulphides commonly ranges from 10 000-43 000 ppm, but values as high as 53 000 ppm were recorded during this study. The two metal impoverished samples represent remobilized pyrrhotite-rich footwall mineralization. Ni-rich (>30 000 ppm) massive sulphides, retaining unmodified primary magmatic textures generally have significantly lower Cu contents than average ore, and thus give rise to a secondary near vertical S:Cu trend. The graphical mean Ni and Cu contents of massive and semi-massive sulphides (Fig. 76A, B) from this study are similar to the average mill feed grade recorded for the 1972-1973 mine production (i.e. 2.23% Ni and 1.39% Cu, Carne, 1987).

Ultramafic rocks demonstrate two divergent chalcophile related trends with respect to Ni (and to a lesser degree Co), and both are continuous with the semi-massive and massive sulphide trends. The steeper Ni depleted trend (Fig. 76A) is co-linear with the Ni:S trend established by the semi-massive and massive sulphides, whereas, the shallower Ni-enriched trend is curvi-linear. Ni-depleted samples containing between 0.60-2.0 wt.% S demonstrate a 1300-800 ppm Ni depletion, respectively, relative to Ni-enriched samples with comparable S contents. The Ni-depleted trend comprises almost exclusively mineralized and non-mineralized samples from the olivine-clinopyroxenite member whereas the Ni-enriched trend consists of similarly mineralized samples from the overlying peridotite and dunite members. Due to the compatible partitioning of Co and Ni in both sulphide and olivine (and to a lesser degree in clinopyroxene), the trend(s) established for Co (Fig. 77A) are comparable to those of Ni, but not as pronounced due to lower absolute concentrations. Depletion trends are clearly the result of sulphides crystallizing from a magma impoverished in these elements due to prior segregation of significant quantities of immiscible magmatic Fe-Ni-Cu-Co sulphide melt that gave rise to the marginal zone massive sulphide and gabbro-hosted mineralization.

Copper assays for semi-massive and massive sulphide typically fall in the 10 000 to 50 000 ppm range. Maximum values of 127 000 ppm are associated with Cu-rich footwall mineralization. The relatively well defined Cu:S trends for ultramafic and gabbroic rocks (Fig. 76B) demonstrate the strong chalcophile behaviour of Cu and its exclusion from solid-solutions in silicates.

Selenium demonstrates a very strong chalcophile behaviour (Fig. 88A) and occurs exclusively as a solid solution component in sulphide. Quantitative proton microprobe analyses indicate partitioning of Se in the following mineralogical order: pyrrhotite≥pentlandite>>chalcopyrite (Cabri et al., 1991, 1993). The Se content of pyrrhotite and pentlandite in gabbro-hosted mineralization is two to three times that found in ultramafic-hosted mineralization.

Arsenic (Fig. 77B) and bismuth (Fig. 88B) display an erratic behaviour with high concentrations in almost all lithological groupings. This behaviour is believed to result from the irregular distribution of arsenopyrite, cobaltite, and bismuth

tellurides. Gabbroic and ultramafic rocks have relatively coherent antimony and tellerium chalcophile groupings (Fig. 89A, B). Massive and semi-massive sulphides also display this feature with respect to Te. This association is undoubtedly controlled by the preponderance of Sb- and Te-based PGM, and to a lesser extent Ni minerals.

Sulphur/selenium ratios of mineralized and non-mineralized samples from the Quill Creek Complex regularly fall between 1500-5000, and display a coherent weakly increasing S enrichment trend towards the massive sulphide grouping (Fig. 99A). Values >5000 are mainly associated with massive, semi-massive, and sulphide fracture fillings in the country rock. The low ratios (<1500), primarily associated with ultramafic rocks, may be the result of S-loss accompanying serpentinization.

Barium is present in anomalous concentrations in all lithological groupings from the Quill Creek Complex. Mineralogically, the anomalous Ba content can be attributed to the presence of K- and Ba-feldspars in the unmineralized rocks, and Cu-Fe-Ba sulphide and barite in the massive sulphides. High Ba concentrations associated with both mineralized and unmineralized magmatic lithologies is a diagnostic geochemical trait of the Quill Creek Complex, in particular the marginal gabbro and associated mineralization.

Sulphur-isotope studies were conducted on various types of sulphide mineralization from the Quill Creek Complex. Mineralization from this complex records the narrowest isotopic ($\delta^{34}S$) range encountered in the belt. Unmodified magmatic sulphides fall in the range -2 to -8‰, $\overline{X}$ = -5‰ and are independent of host rock and modal sulphide concentration (Fig. 100). Sulphides remobilized into the country rock generally fall in the -2.5 to -0.7‰ range, regardless of sulphide concentration. The limited isotopic range of the magmatic sulphides clearly demonstrates the high degree of homogenization (blending) of crustal sulphur, and a greater proportion of mantle sulphur associated with these sulphides. The $\delta^{34}S$ composition of pegmatitic gabbro ranges from -1.9 to -4.0, $\overline{X}$ = -3.0‰.

A detailed sulphur-isotope investigations conducted on material (11 samples) from the calc-silicate skarn rocks disclosed a rather limited range of $\delta^{34}S$ compositions (-0.6 to -4.9‰, $\overline{X}$ = -1.8‰). The maximum $\delta^{34}S$ spread encountered in a particular skarn zone was 3.8‰. The mean value of -1.8‰ is not far removed from that of -2.8‰ for massive Ni-Cu sulphide ore with classic immiscible magmatic sulphide segregation features. The S/Se ratios within this skarn environment have a greater range (2823 to 9268) although the mean values are fairly similar. Unlike the gabbro-hosted mineralization, and in some cases, ultramafic hosted, the skarn-hosted mineralization has relatively low Ba contents. Nevertheless, the axinite-bearing augite skarn, of a probable igneous parentage, has Ba contents that range from 1100-2300 ppm, and the calc-silicate has values that range from 30-170 ppm, $\overline{X}$ = 75 ppm. This, in conjunction with the above, clearly demonstrates that S and anomalous Ba contents associated with the intrusive phases were not the product of local assimilation of Ba-rich country rock sediments (sulphates) juxtaposed the intrusion. It also demonstrates that the bulk of the S in the skarn rocks has been derived from the Quill Creek Intrusive Complex through metasomatic exchange.

Platinum group element and gold concentrations in the various lithological groups (Fig. 110, 111, 122, 123, 132, 133) demonstrate that anomalous background concentrations are present in weakly mineralized and unmineralized samples, the strong chalcophile character of most of these noble metals, and the remarkable concentrations associated with the Ni-Cu ores. The $PGE+Au_{(t)}$ concentrations of average massive and semi-massive Ni-Cu ores from the Quill Creek Complex are outstanding, by any standard, particularly with respect to the rarer and more valuable elements – Rh, Os, Ir, and Ru. Massive Ni-Cu ores from the complex not only have $PGE+Au_{(t)}$ grades equivalent to that of the Merensky Reef, but also contain approximately twice the levels of Rh. At present the Merensky Reef is the western world's main source of Rh.

The upper and lower limits of the gabbro and ultramafic trends with respect to sulphur constrain the range of platinum values associated with unmodified magmatic massive and semi-massive sulphides (Fig. 110A). Massive and semi-massive sulphides containing <800 ppb Pt are either associated with unusually Rh-Ru-Os-Ir-rich samples or remobilized sulphides in the footwall. Average Pt grade for primary magmatic massive sulphide mineralization sampled during this study is approximately 2000 ppb. This value is a bit higher than the 1300 ppb Pt grade reported for the proven reserves announced in 1972 (Carne, 1987), but considering the analytical advancements made for PGEs since then, the values agree quite well. The small degree of scatter associated with gabbro containing <20 ppb may be the result of alteration or analytical error. Nevertheless, this well-defined chalcophile trend is most instructive with respect to grade predictability for various hosts and metallogenetic modelling. The pyroxenite, peridotite, and dunite members of the ultramafic grouping have their own distinctive Pt and Pt/Pd characteristics. The following compositional range and mean Pt/Pd ratios characterize the ultramafic members sampled during this study: olivine clinopyroxenite (149-1070 ppb, $\overline{X}$ = 1.5), peridotite (100-1800 ppb, $\overline{X}$ = 1.1) and dunite 16-260, $\overline{X}$ = 0.6). Although the absolute range of Pt concentrations is greater for gabbro than olivine clinopyroxenite, both have similar Pt/Pd ratios (i.e. ≈1.5). The decreasing Pt/Pd ratio in the overlying ultramafic differentiates is probably the consequence of noble metal fractionation (due to a period of prolonged sulphide crystallization in the underlying differentiates) in the parental melt from which the sulphides segregated.

Palladium also displays a chalcophile trend (Fig. 110B). The breadth of this trend is less confined than that for Pt and broadens considerably toward the sulphur-rich end. The spread, which is mainly confined to samples with <300 ppb Pd, can once again be attributed to either the remobilized footwall mineralization, or the abnormally enriched Rh-Ru-Os-Ir samples. Pd appears to be more depleted in some of the Rh-Ru-Os-Ir-rich samples than Pt, and may be a function of the more primitive nature of early sulphide melts. Exclusion of these samples would define a rather strong chalcophile trend in which the typical magmatic Pd contents of the massive

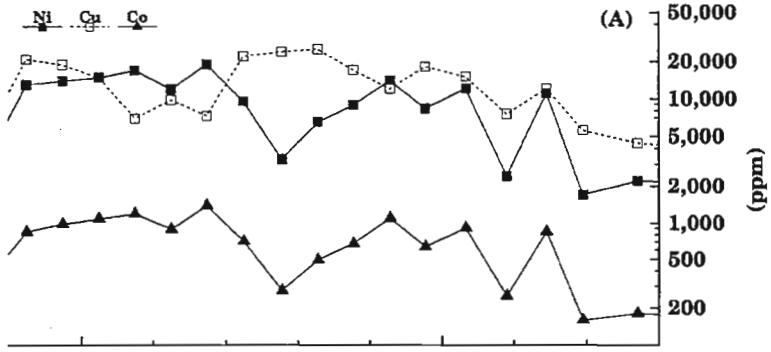
Ni Cu Co
(A)
50,000
20,000
10,000
5,000
2,000
1,000
500
200
(ppm)

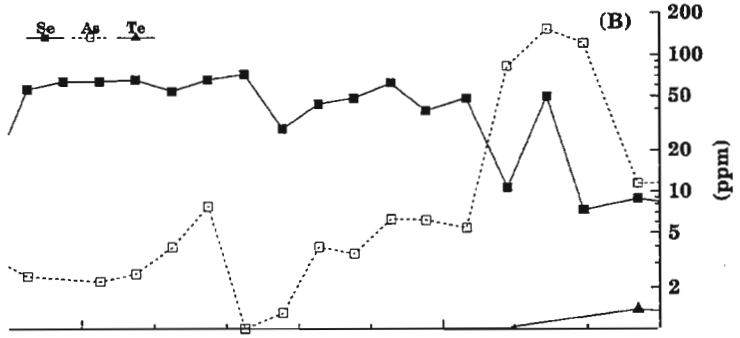
Se As Te
(B)
200
100
50
20
10
5
2
(ppm)

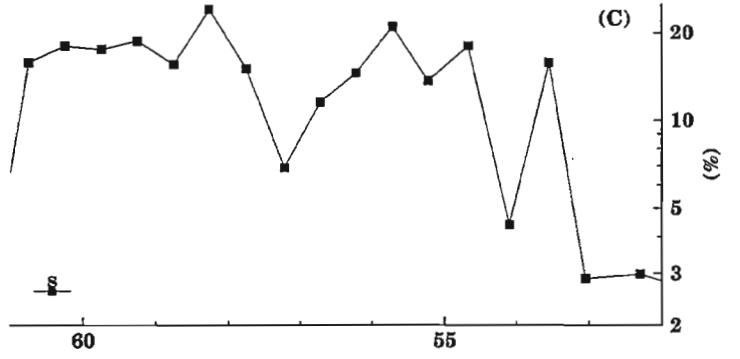
(C)
20
10
5
3
2
(%)
S
60
55

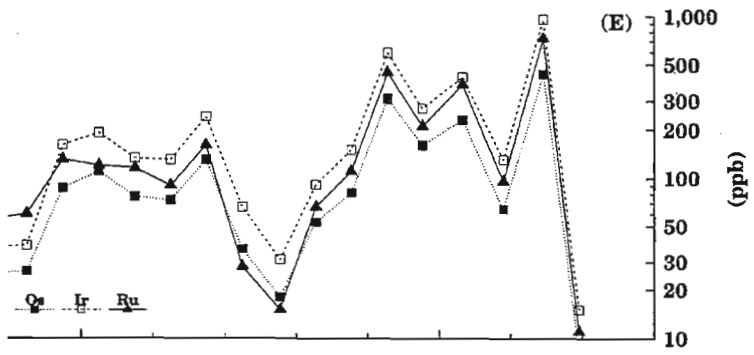
(E)
1,000
500
300
200
100
50
30
20
10
(ppb)
Os Ir Ru

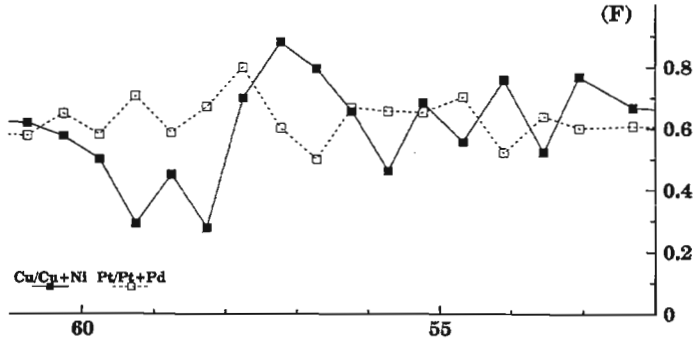
(F)
0.8
0.6
0.4
0.2
0
Cu/Cu+Ni Pt/Pt+Pd
60
55

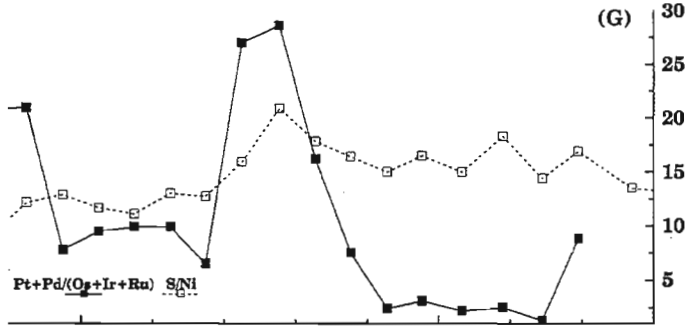
(G)
30
25
20
15
10
5
Pt+Pd/(Os+Ir+Ru) S/Ni

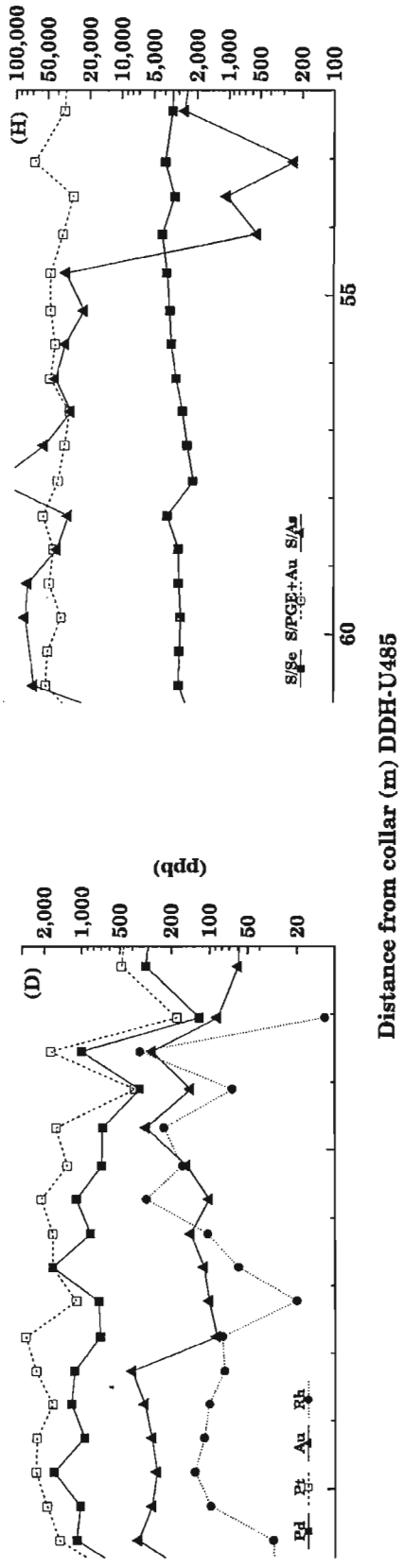

Figure 27 (A-H). *Ni, Cu, Co, Se, As, Te, S, Pd, Pt, Au, Rh, Os, Ir, Ru concentrations and elemental ratios in the 52 to 61 m interval of core from DDH-U485 (Quill Creek Complex). See Figure 21 for reference.*

and semi-massive sulphides would probably be continuous with that established by the gabbro and ultramafic rocks. The average Pd content of massive and semi-massive sulphides sampled in this survey is approximately 1000 ppb, which is close to the 1972 proven ore reserve value of 920 ppb Pd. Maximum values up to 11 800 ppb have been recorded in Cu-rich segregations (12.7% Cu) associated with Ni-Cu mineralization (1.1% Ni). Samples with Pd values in the 4000-6600 ppb range are generally confined to material with >24 000 ppm Ni and containing normal to low Cu contents.

Gold is clearly the least chalcophile of the noble metals (Fig. 111A). The highest Au value (11 700 ppb) comes from the same Cu-rich (12.7%) segregation mentioned above, whereas, the next highest value (1600 ppb) is associated with normal Ni-Cu mineralization with Cu (10 000 ppm) slightly in excess of Ni (9000 ppm). The macroscopic appearance and low levels of As, Sb, Te, and Bi confirm that these are primary chalcopyrite-rich segregations and not hydrothermally induced or late stage fracture filling features. The breadth of the Au vs. S trend outlined by the gabbro and ultramafic rocks suggest that Au is considerably more mobile than the other noble metals. Unlike other noble metal vs. S patterns, the mid-point maxima trend established by the ultramafic rocks project an order of magnitude above the maxima established by the massive sulphides. As the average for unmodified massive sulphides best represents magmatic concentrations of Au, it is most likely that some Au enrichment associated with the ultramafic rocks is the result of serpentinization. Massive sulphides containing low Au concentrations (<50 ppb) are usually associated with Ni-rich samples with higher than normal Ni/Cu ratios. The 1972 ore reserve calculations for the Wellgreen deposit suggested that the average Ni-Cu ore contained 171 ppb Au. Excluding the high and low outliers (Fig. 111A), this value is reasonably close to that established for the massive sulphides during this study.

Rhodium is present in anomalous concentrations compared to other Canadian Ni-Cu ores. In fact, the only other Ni-Cu ores with comparable values are the near age equivalent Noril'sk ores in Russia. Average massive sulphides (excluding remobilized material) contain ≈400 ppb Rh. The Rh-rich mineralization generally occurs in the basal portion of the massive sulphide bodies, where values in the 300-1000 ppb range are not uncommon (Fig. 111B). Rh concentrations in the 100-300 ppb range generally occur in the upper portions of the massive sulphide bodies. Values from these levels are also relatively high when compared with other Ni-Cu ores (Hulbert et al., 1988). Massive and semi-massive sulphides with Rh levels <100 ppb are generally associated with remobilized sulphides in the footwall, the concentrations being a function of distance from the gabbro-chert contact. If one excludes the samples containing <5 ppb Rh (analytical limit of detection is 5 ppb), the ultramafic and gabbroic rocks define a moderate to strong chalcophile trend that is continuous with the unmodified semi-massive and massive magmatic trend. The upper limit of the trend is particularly well defined. Unlike the previously mentioned noble metals, Rh occurs in both higher absolute and background concentrations in the

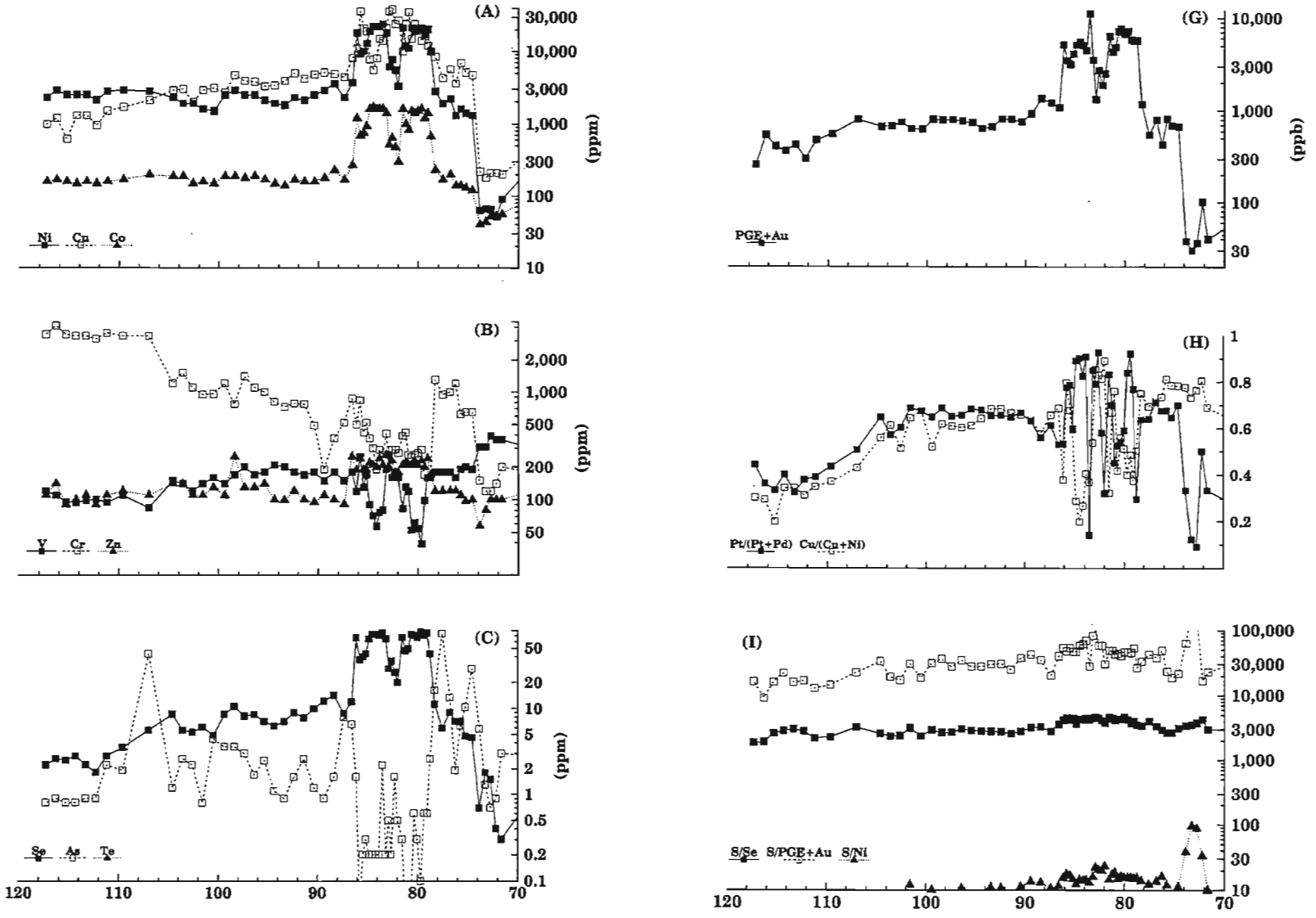
(A)
30,000
10,000
3,000
1,000
300
100
30
10
(ppm)
Ni Cu Co
(B)
2,000
1,000
500
200
100
50
(ppm)
V Cr Zn
(C)
50
20
10
5
2
1
0.5
0.2
0.1
(ppm)
Se As Te
120
110
100
90
80
70
(G)
10,000
3,000
1,000
300
100
30
(ppb)
PGE+Au
(H)
1
0.8
0.6
0.4
0.2
Pt/(Pt+Pd) Cu/(Cu+Ni)
(I)
100,000
30,000
10,000
3,000
1,000
300
100
30
10
S/Se S/PGE+Au S/Ni
120
110
100
90
80
70

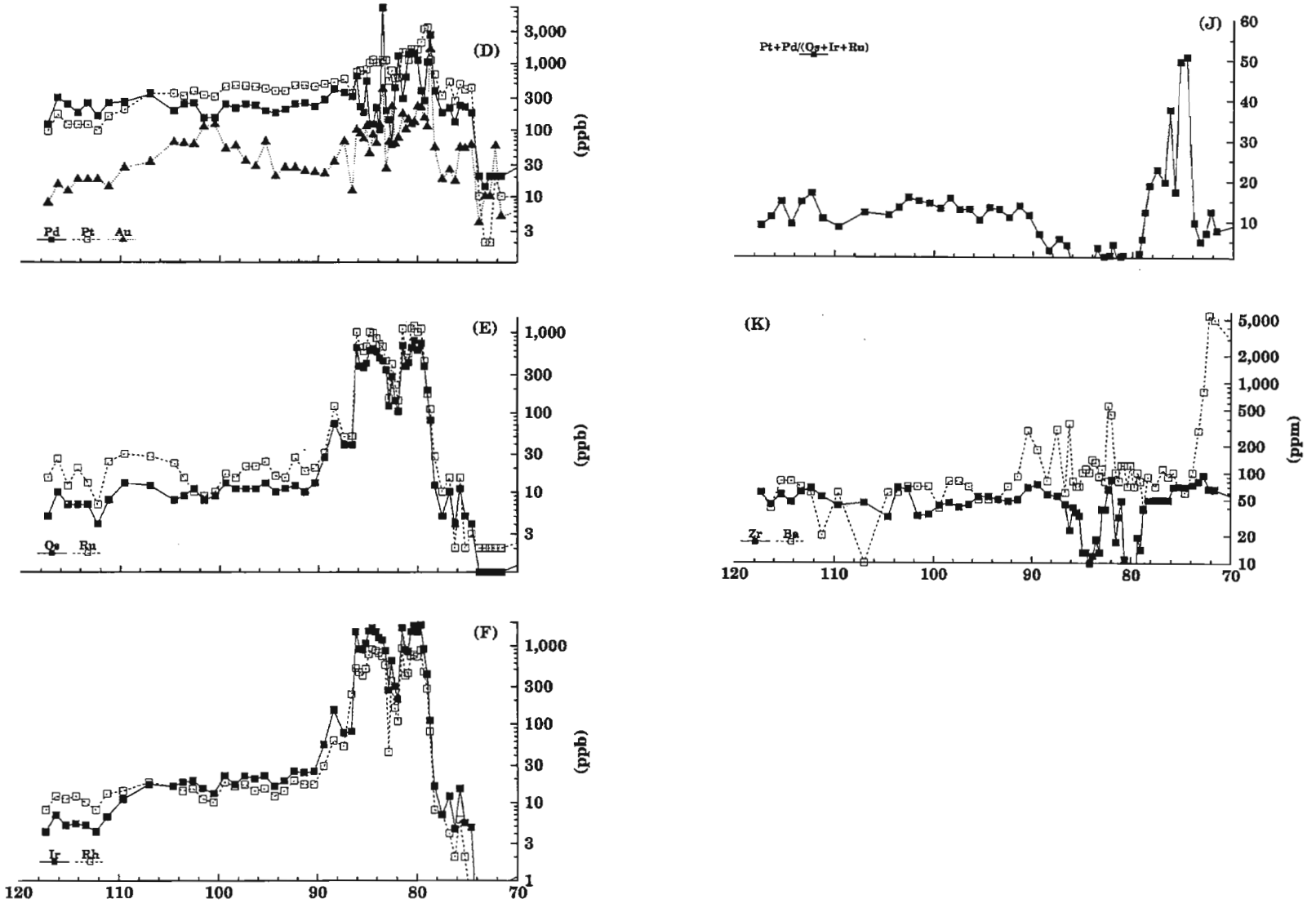

Figure 28. (A-K). *Ni, Cu, Co, V, Cr, Zn, Se, As, Te, Pd, Pt, Au, Os, Ru, Ir, Rh, PGE+Au, Zn, Ba concentrations and elemental ratios in the 70 to 120 m interval of core from DDH-U492 (Quill Creek Complex). See Figure 23 for reference location.*

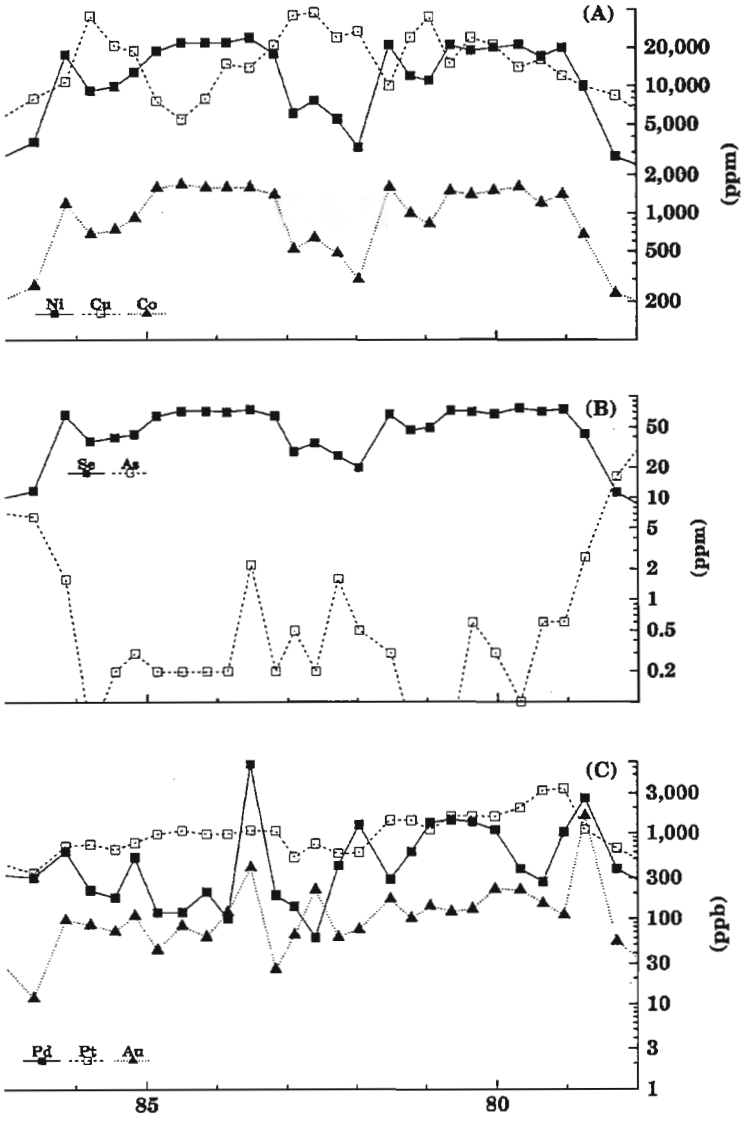
(A)
20,000
10,000
5,000
2,000
1,000
500
200
(ppm)
Ni Cu Co
(B)
50
20
10
5
2
1
0.5
0.2
(ppm)
Se As
(C)
3,000
1,000
300
100
30
10
3
1
(ppb)
Pd Pt Au
85
80

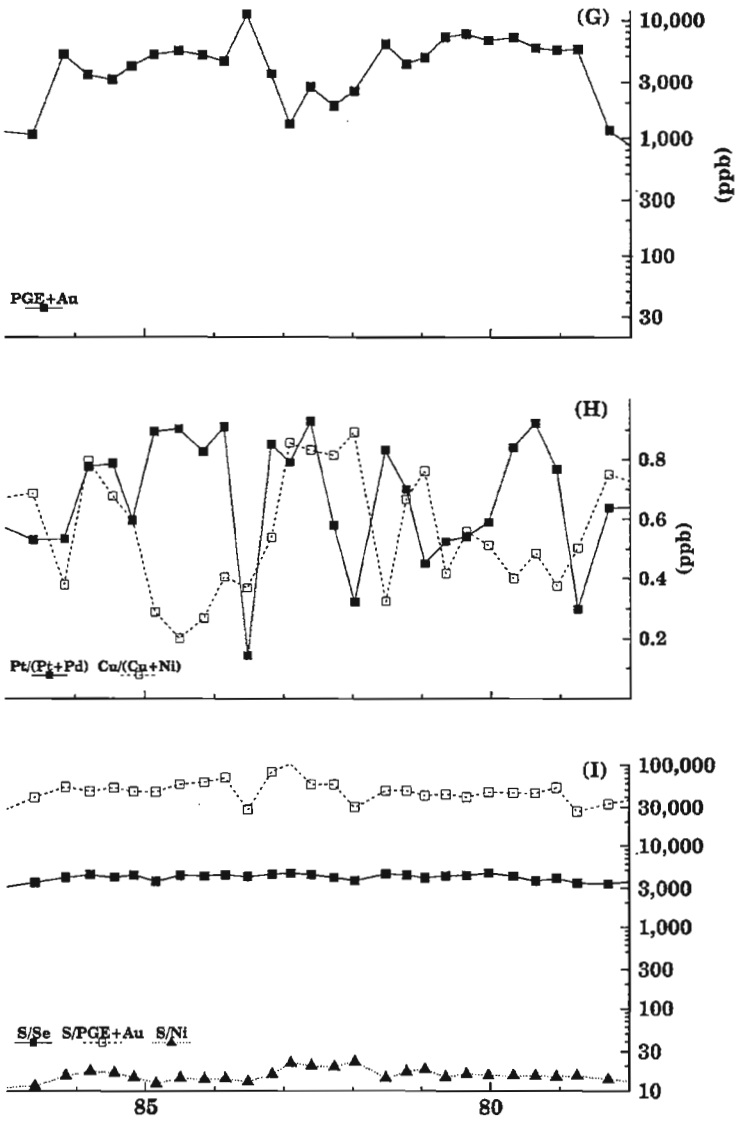
(G)
10,000
3,000
1,000
300
100
30
(ppb)
PGE+Au
(H)
0.8
0.6
0.4
0.2
(ppb)
Pt/(Pt+Pd) Cu/(Cu+Ni)
(I)
100,000
30,000
10,000
3,000
1,000
300
100
30
10
S/Se S/PGE+Au S/Ni
85
80

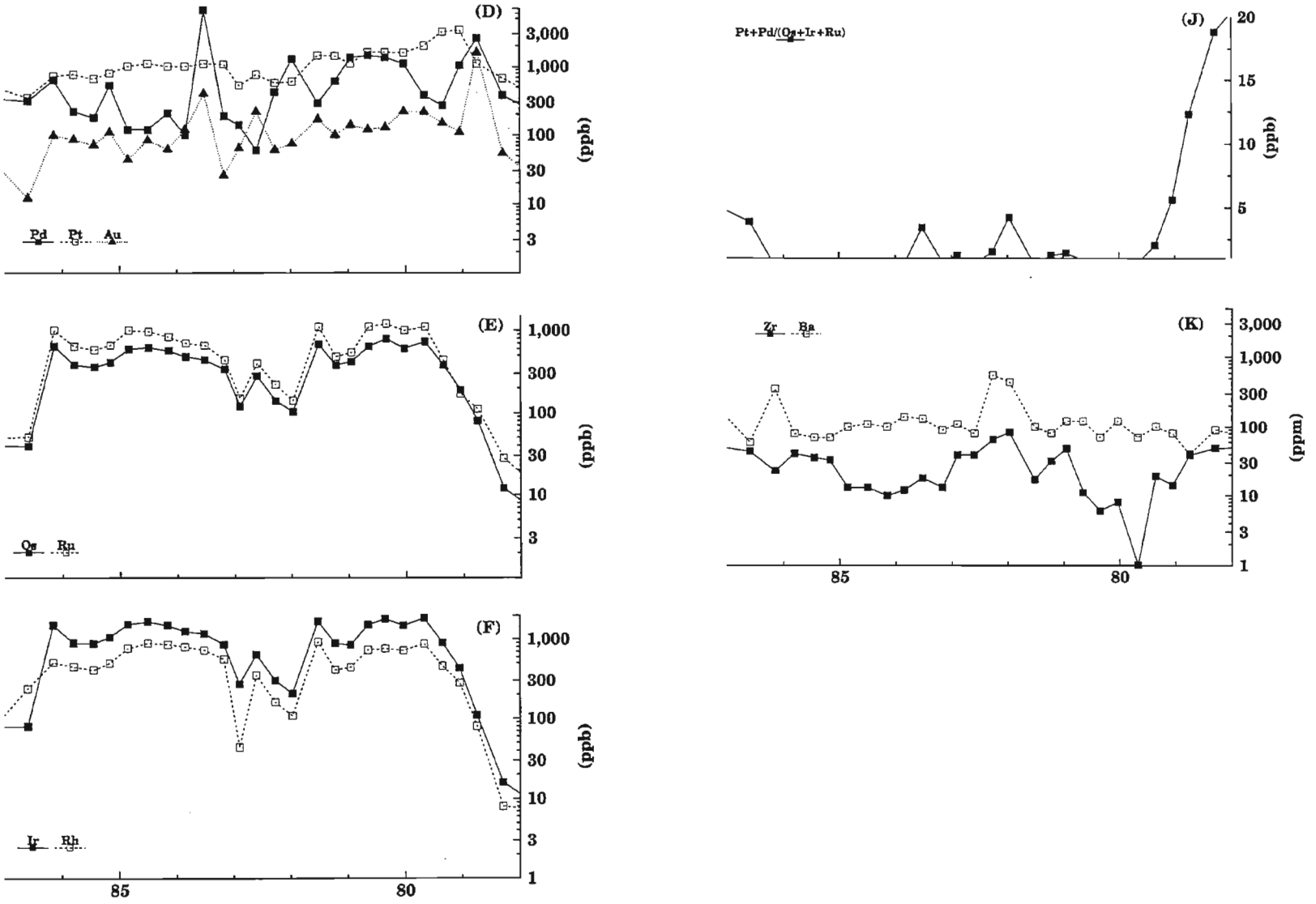

Figure 29. (A-K). *Ni, Cu, Co, Se, As, Pd, Pt, Au, Os, Ru, Ir, Rh, PGE+Au, Zn, Ba concentrations and elemental ratios in the detailed interval 78 to 87 m from the collar of DDH-U492 (Quill Creek Complex). See Figure 23 for reference location.*

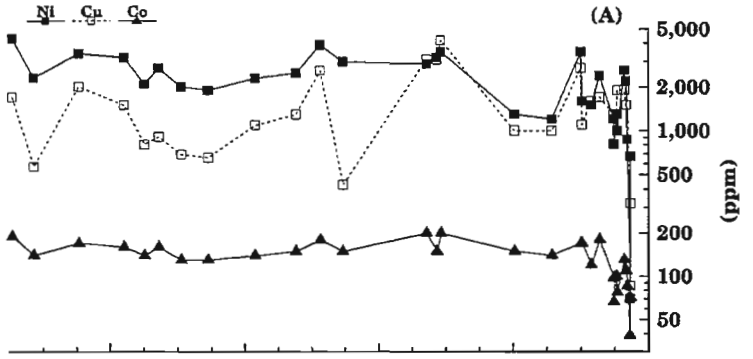
Ni Cu Co
(A)
5,000
2,000
1,000
500
200
100
50
(ppm)

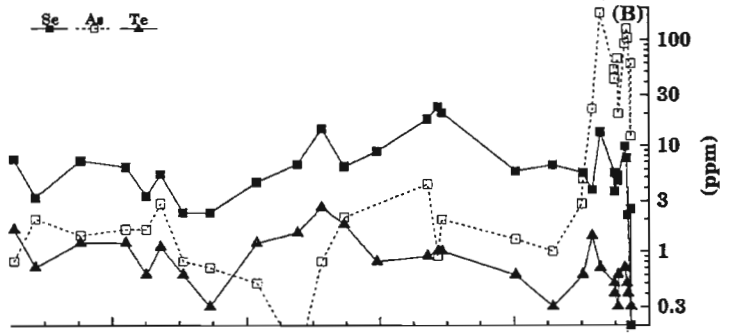
Se As Te
(B)
100
30
10
3
1
0.3
(ppm)

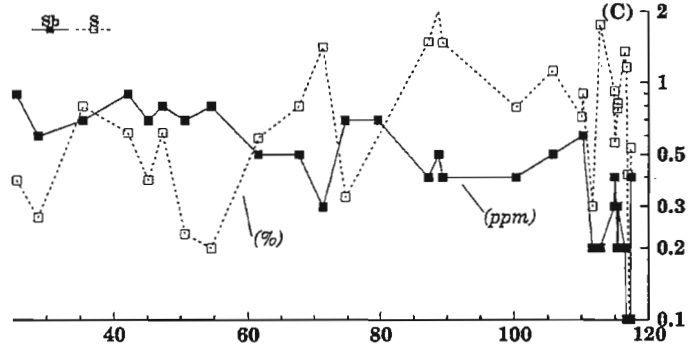
Sb S
(C)
2
1
0.5
0.3
0.2
0.1
(%)
(ppm)
40
60
80
100
120

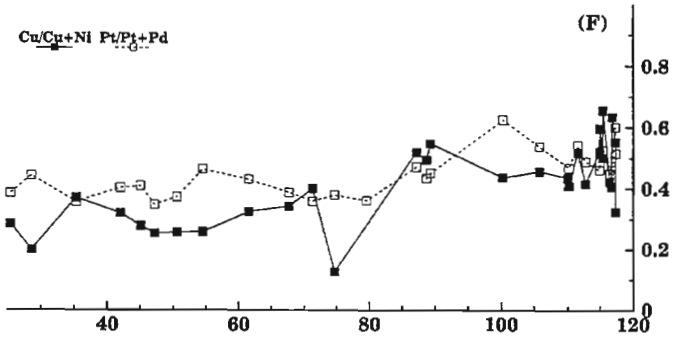
Cu/Cu+Ni Pt/Pt+Pd
(F)
0.8
0.6
0.4
0.2
0
40
60
80
100
120

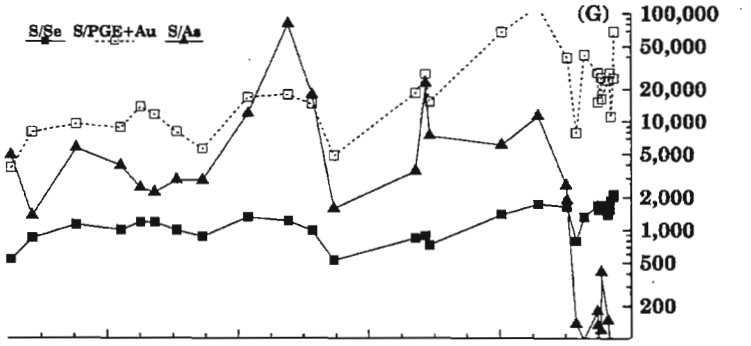
S/Se S/PGE+Au S/As
(G)
100,000
50,000
20,000
10,000
5,000
2,000
1,000
500
200

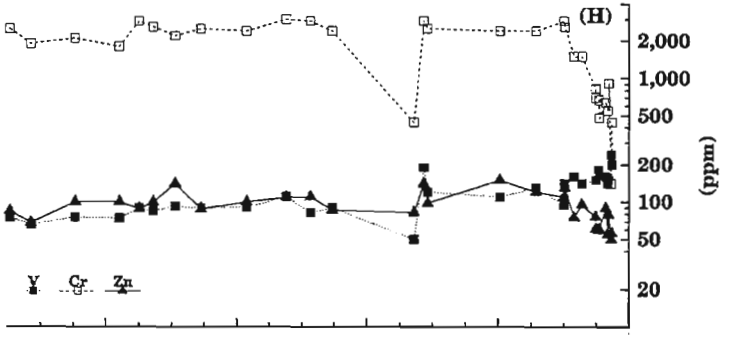
(H)
2,000
1,000
500
200
100
50
20
(ppm)
Y Cr Zn

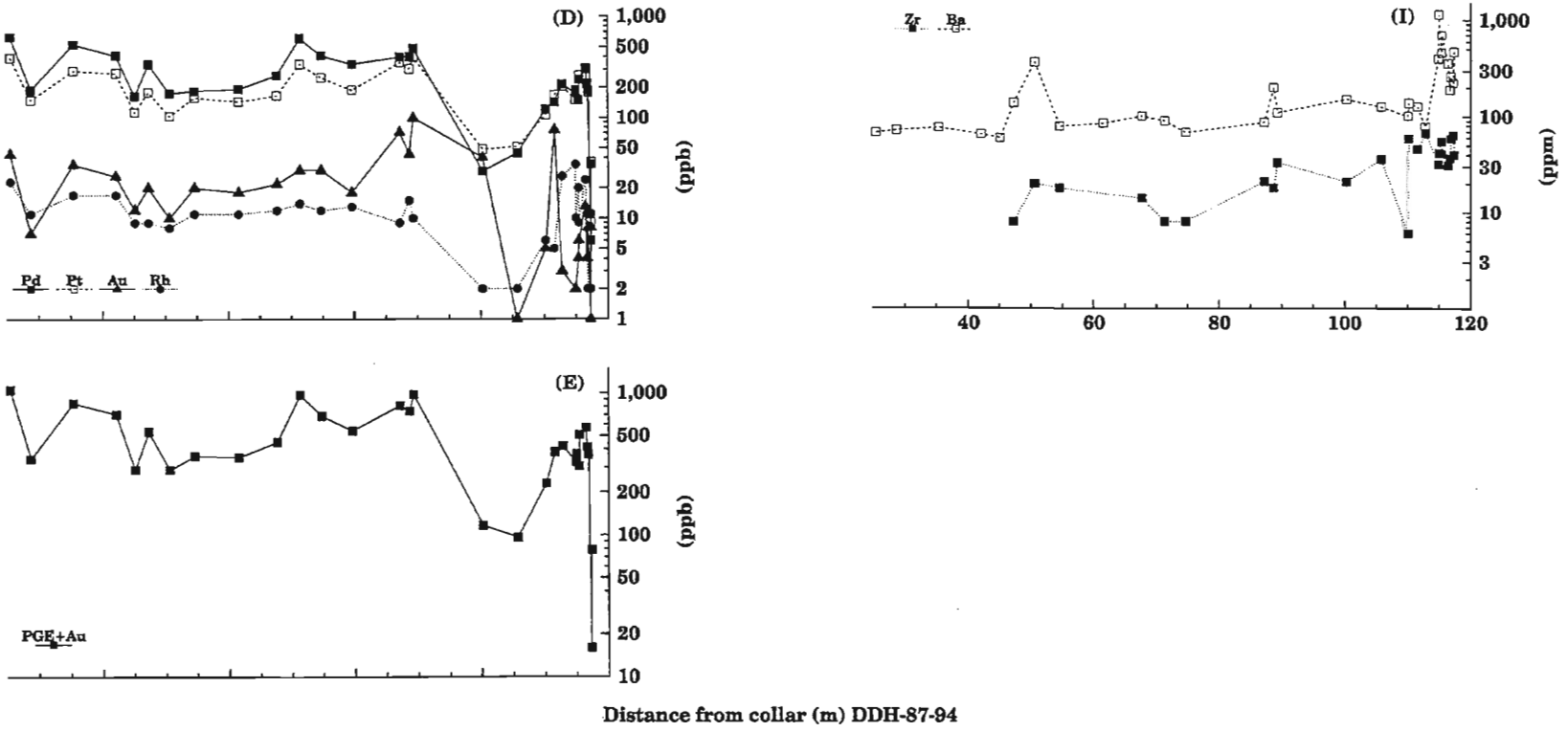

Figure 30. (A-I). *Ni, Cu, Co, Se, As, Te, Sb, S, Pd, Pt, Au, Rh, PGE+Au, V, Cr, Zn, Zr, Ba concentrations and elemental ratios in the 25 to 120 m interval of core from DDH-87-94 (Quill Creek Complex). See Figure 19 for reference location.*

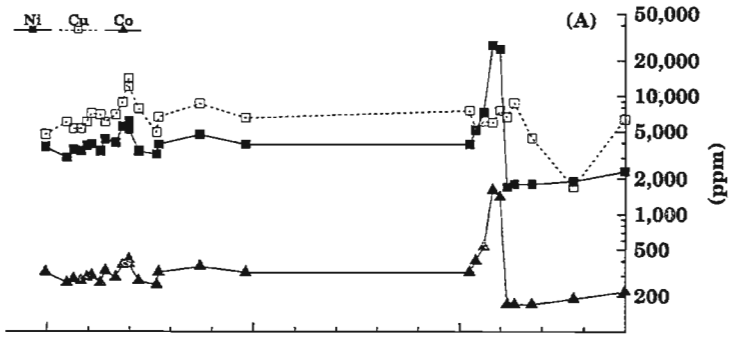
Ni Cu Co
(A)
50,000
20,000
10,000
5,000
2,000
1,000
500
200
(ppm)

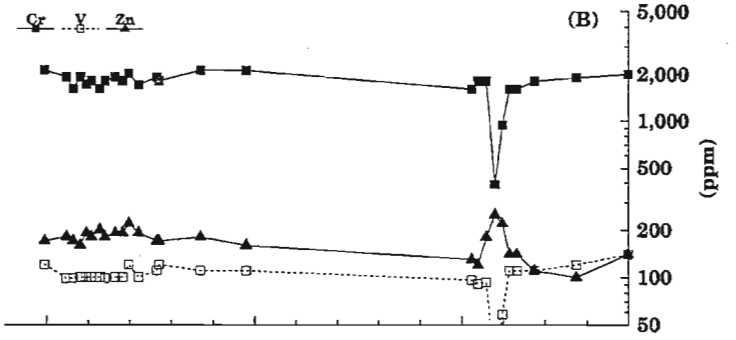
Cr V Zn
(B)
5,000
2,000
1,000
500
200
100
50
(ppm)

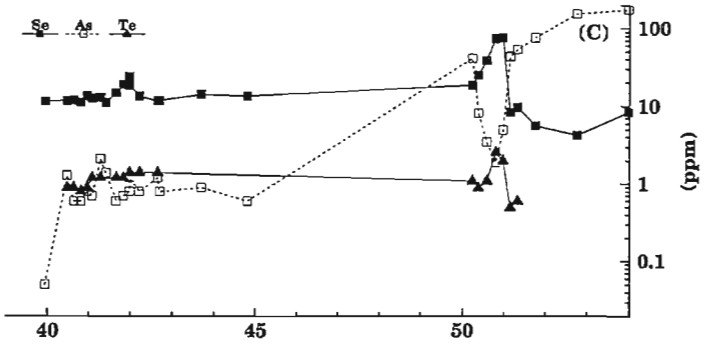
Se As Te
(C)
100
10
1
0.1
(ppm)
40
45
50

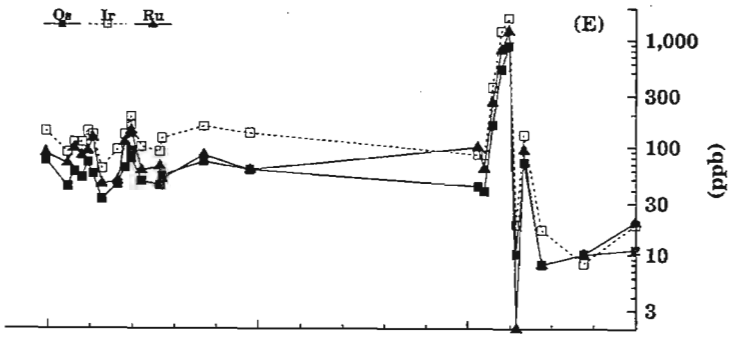
Os Ir Ru
(E)
1,000
300
100
30
10
3
(ppb)

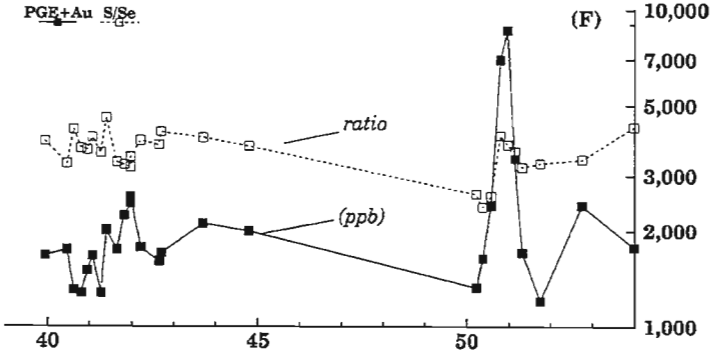
PGE+Au S/Se
(F)
10,000
7,000
5,000
3,000
2,000
1,000
ratio
(ppb)
40
45
50

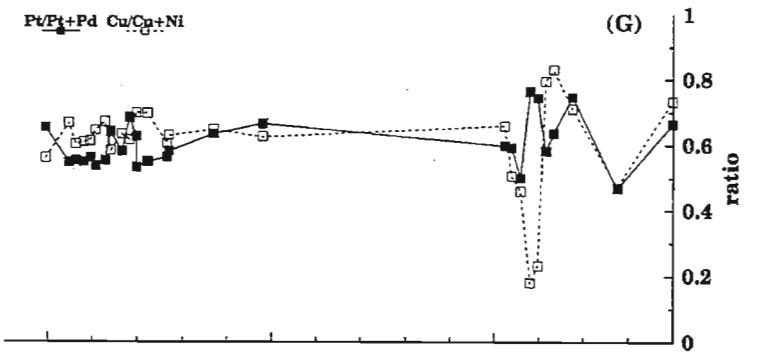
Pt/Pt+Pd Cu/Cu+Ni
(G)
1
0.8
0.6
0.4
0.2
0
ratio

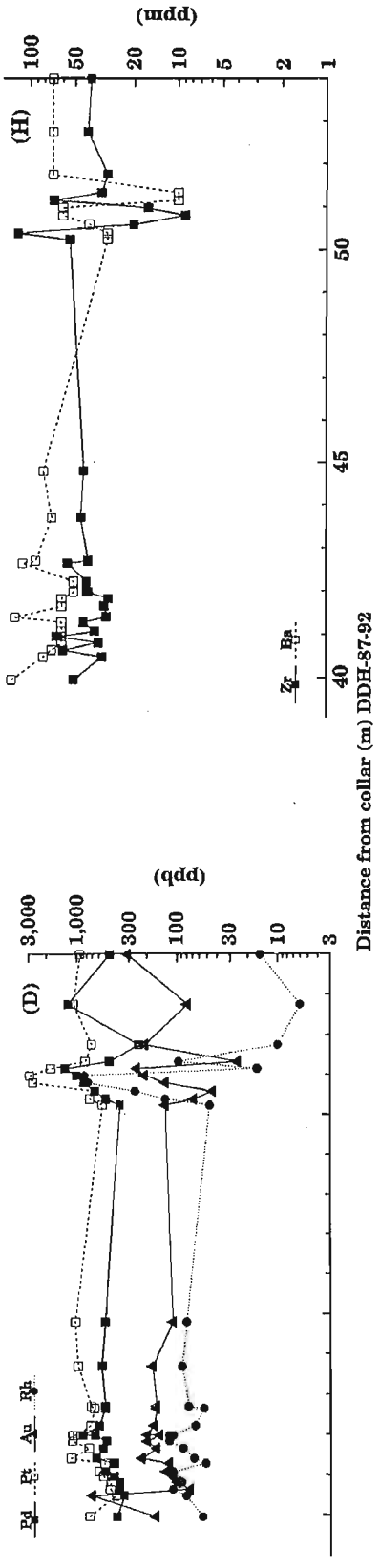

Figure 31. (A-H). Ni, Cu, Co, Cr, V, Zn, Se, As, Te, Pd, Pt, Au, Rh, Os, Ir, Ru, PGE+Au, Zr, Ba concentrations and elemental ratios in the 40 to 54 m interval of core from DDH-87-92 (Quill Creek Complex). See Figure 24 for reference location.

peridotite than the olivine clinopyroxenite member. This may be a function of the higher modal chromite contents in the peridotite member.

Ruthenium also displays a chalcophile trend (Fig. 122A) particularly when one excludes the remobilized material, and samples containing less than the analytical detection limit (5 ppb). Ru-rich samples invariably co-exist with Rh-, Os-, and Ir-rich material, thus controls mentioned above for Rh also apply to this element. Geochemically, Ru is believed to be rather immobile and this inertness probably accounts for the low values (<12 ppb) associated with remobilized sulphides in the footwall. Average Ru content for unmodified accumulations of massive and semi-massive sulphide is approximately 420 ppb. Values in excess of 1000 ppb are not uncommon and maximum values of 1500 ppb have been recorded.

Iridium not only demonstrates a strong chalcophile trend, but is also present in remarkably high concentrations for Ni-Cu-PGE ores (Fig. 122B). The upper and lower bounds of the gabbro and ultramafic trends are somewhat continuous with the massive sulphide trend which ranges from 250-1900 ppb. Anomalously high and low values can be explained along the same lines as that previously mentioned for Rh and Ru. It should be stressed that these Ir-rich massive sulphides, along with their high associated Os, Ru, and Rh concentrations, are unprecedented in the geological literature. Similar mineralization elsewhere in the belt characterizes this unique metallogenic terrane.

Osmium displays trends and features similar to that of Rh, Ru, and Ir (Fig. 123A) and thus warrants no further discussion.

Rhenium does not behave like the PGEs or Au in the either ultramafic or gabbroic rocks since large concentrational variations occur for comparably mineralized samples (Fig. 123B). The best values occur in massive sulphides where a maximum value of 970 ppb was recorded. The average Re content for primary magmatic massive sulphides is approximately 200 ppb. Most Canadian Ni-Cu ores contain <10 ppb Re. The Re content of this ore is unprecedented in the literature and these anomalous concentrations are an additional geochemical characteristic of this belt of intrusions and associated Ni-Cu-PGE mineralization. There is a suggestion that Re-rich samples are preferentially associated with the Ni-rich samples or sulphides with relatively high Ni/Cu ratios. If this proves to be the case, Re, which occurs both as a Re>Ir>Os>Ru alloy and Re sulphide, may in fact be restricted to the early sulphide segregations that commonly occur near the base of the sulphide intervals. Low values (<40 ppb) are associated with remobilized sulphides. Enhanced Re concentrations associated with Ir-, Os-, and Ru-rich sulphides confirm the importance of the unidentified Re>Ir>Os>Ru alloy identified in samples from the Quill Creek Complex.

$PGE+Au_{(t)}$ concentrations, associations, and trends are summarized in Figure 132A. When the other more rare and valuable elements Rh, Os, Ru, and Ir are considered, which was not the case in past reserve calculations, the precious metal content of the mineralization (especially the massive ores) more than doubles in quantity and appreciably increases the

value of the mineralization. As a group the PGE+Au demonstrate one of the strongest chalcophile trends noted during the course of this study. The average PGE+Au grade for massive and semi-massive mineralization is approximately 5000 ppb. Pt/(Pt+Pd) vs. Cu/(Cu+Ni) relationships illustrated in Figure 132B demonstrate a high degree of scatter for the various groupings. Interpretation of clustering and vague trends within this plot are further complicated by the influence of silicate Ni in the unmineralized and sparsely mineralized gabbroic and ultramafic samples. The noteworthy features in this plot are the clustering of massive sulphide samples in the 0.2-0.5 Cu/(Cu+Ni) and 0.4-0.9 Pt/(Pt+Pd) range and the variable composition of semi-massive samples. Naldrett (1981b) suggested that this plot could be used to characterize parental magma types (i.e. tholeiitic flood basalt, komatiite, etc). However, this is clearly not the case for any of the Kluane mineralized intrusions.

S/PGE+Au, PGE+Au vs. S/Se x 1000 relationships were investigated to ascertain if the PGE-rich sulphides from this complex substantiate the hypothesis of Eckstrand and Hulbert (1987) that PGE-enriched mineralization is associated with Se-enriched sulphides. Figure 133A demonstrates clearly that as the sulphides become enriched in PGE+Au (decreasing S/PGE+Au), the associated Se-content increases relative to sulphur (decreasing S/Se x 1000). The ordinate scale values represent increments of 1000 (i.e. scale value 5 is actually 5000). The well-defined negative trend bounded by decreasing S/Se ratios from 5000 to 2000 demonstrates the significance of the geochemical trend and association. The unusually low S/Se ratios (≤1000) and the low S/PGE+Au ratios may actually be exaggerated due to S-loss accompanying serpentinization. If one tries to apply the S/Se ratio to PGE+Au concentrations that have not been normalized to account for the modal variation in sulphides, a relationship similar to that depicted in Figure 133B arises. Nevertheless, this diagram clearly demonstrates the S/Se ratios of <5000 are restricted to PGE-rich sulphides.

Geochemical profiles through selected mineralized environments. To fully appreciate the geochemical behaviour of the important base, semi-, and precious metals within and outside the complex, and the various styles, zones, and host rock associations, a detailed investigation was conducted through gabbro-hosted horizons containing massive, semi-massive, and disseminated sulphide mineralization. The graphically illustrated geochemical data represent that obtained from continuous diamond-drill core intervals and not individual grab samples. As a rule all detailed sample intervals were ≤0.33 m long in the mineralized zone. In some cases shorter intervals were sampled within noteworthy sections. In areas of weak mineralization, near the outer limits of a mineralized zones, the sample interval may increase to 1.0 m. The geochemical profiles for gabbro-hosted mineralization have been obtained on core samples from diamond-drill holes DDH-U485 and DDH-U492 and are illustrated in Figures 27, 28, and 29. Ultramafic-hosted profiles have been obtained from core in holes DDH-87-94 and DDH-87-92 (Fig. 30, 31). The axis representing the distance from collar in the geochemical profiles can be referenced relative to the geology in Figures 21 and 23 for gabbro-hosted, and in Figures 19 and 24 for ultramafic-hosted mineralization.

Gabbro-hosted.

DDH-U485. Semi-massive to massive sulphide lens and mineralized footwall gabbro interval were investigated over a 9 m length in this diamond-drill hole (Fig. 21, 27). The weakly mineralized immediate footwall interval from 52 to 53.3 m contains approximately 8% disseminated sulphides, and the remaining 7.7 m interval contains >45% sulphides, with the exception of a sulphide depleted gabbroic segregations at the 54.25 and 57.25 m intervals. These gabbroic segregations tend to contain anomalous concentrations of fine disseminated chalcopyrite in the silicate matrix.

Nickel grades for the mineralized interval varies from 10 000 to 20 000 ppm, with the highest values occurring in the remaining 2 m interval (Fig. 27A). Copper increases in concentration rather steadily from the weakly mineralized footwall gabbro to the 57.7 m position where it attains the 20 000 ppm level. Over the next 2 m the values fall to one-quarter of their previous value, and once again steadily rise toward the 20 000 ppm level at the end of the mineralized zone. The Cu enrichment associated with the S-, Ni-, Co-, and Se-depleted interval from the 55.75 to 57.75 m is most unusual. In this interval the gabbro host contains fine chalcopyrite disseminations and dustings in the silicate matrix. This Cu-rich style of mineralization is identical to that in the silicate fractions associated with sulphide-silicate immiscibility textures discussed previously in relation to Figure 26 (A, B, C). Cobalt displays a chemical profile identical to Ni but at significantly lower concentrations (<1200 ppm). Selenium (Fig. 27B) concentrations remain relatively constant throughout the sulphide-rich intervals and vary in concert with S (Fig. 27C) which is a reflection of the amount of sulphide in the rock. The drop in Se concentration associated with the central area of Cu enrichment can also be attributed to the lower (50%) Se content in chalcopyrite relative to pyrrhotite and pentlandite. Arsenic haloes (90-150 ppm) occur in the thin gabbroic intervals underlying the first semi-massive to massive sulphide segregation in the 53 and 54 m interval (Fig. 27B). High As levels associated with the footwall, and to lesser extent footwall contacts of massive sulphide lenses, have been observed elsewhere within the complex. Within the sulphide-rich intervals As contents are generally in the 1 to 9 ppm range. Sulphur content of the various intervals (Fig. 27C) nicely outlines the sulphide-rich areas, gabbroic segregations, and footwall contact.

$PGE+Au_{(t)}$ display the pronounced metal trends and associations (Fig. 27 D, E). Platinum grades range from 1000 to 2500 ppb in the semi-massive and massive sulphide intervals, and in the central Cu-rich segregation. There is a suggestion that the grades associated with the upper half of the mineralized interval are slightly higher than that of the lower half. Palladium is somewhat more erratic than Pt and is generally about 50% lower in absolute concentration. Gold is significantly enriched in upper portion of this sulphide-rich interval relative to other levels. Osmium, iridium, ruthenium,

and to a lesser extent rhodium, have a strong geochemical affinity as is demonstrated in Figures 27D and E. These higher melting point noble metals are preferentially associated with the initial sulphide segregations in the lower portion of these sulphide bodies. These elements also demonstrate the greatest impoverishment in areas of Cu enrichment, and high Cu/Cu+Ni ratios although the Pt/Pt+Pd ratio is not significantly different (Fig. 27F). The S/Ni, S/Se and S/PGE+Au ratios (Fig. 27G, H) demonstrate that sulphur/metal ratios in the sulphide fraction vary little across this mineralized interval. However, with respect to the preferential distribution of Pt and Pd relative to Os, Ir, and Ru, there is a pronounced fractionation demonstrated by the Pt+Pd/(Os+Ir+Ru) variation across the mineralized interval. This study demonstrates the influence of sulphide melt fractionation on the distribution and abundance of PGEs and Au.

DDH-U492. Nobel metal fractionation described above is not present in all massive sulphide bodies. The more massive, Ni-enriched sulphide bodies commonly contain high concentrations of all PGE+Au throughout the entire mineralized interval. The geochemical character of this type of massive sulphide mineralization, and that of the surrounding mineralized gabbro and overlying weakly mineralized olivine clinopyroxenite and peridotite members, is examined using the data obtained from 50 m of continuously sampled core from DDH-U492. The geochemical profiles from this interval are presented in Figures 28 and 29, and the geology in Figure 23.

Sulphide-poor interval. The footwall gabbro is barren as little as 5 m below the base of the massive sulphide lens (79 m) and contains 60 to 100 ppm Ni, 40 to 60 ppm Co, and 200 ppm Cu (Fig. 28A). The intervening gabbro, between the barren material and the base of the massive sulphide lens, becomes increasingly enriched in Ni, Cu, Co, Cr, Se, As, Pt, Pd, Os, Ir, Ru, and Rh by more than an order of magnitude. The massive sulphide intersection, which occurs in the 79 to 86 m interval, individually contains >20 000 ppm Ni and Cu and ≥4000 ppb PGE+Au. Although the Zn content has doubled within the massive sulphide interval, it is only 2x background. The geochemical profiles of this 7 m massive sulphide width are discussed with reference to the more detailed sections illustrated in Figure 29.

Nickel, copper, and cobalt grades drop off sharply at the upper contact of the massive sulphide lens and maintain an average of about 2500, 3500, and 175 ppm, respectively, up to the gabbro/clinopyroxenite contact (99 m). The Cu concentration decreases marginally in the clinopyroxenite member ($\overline{X}$ = 2500 ppm) and significantly in the peridotite ($\overline{X}$ = 1300 ppm). The Ni content decreases with the introduction of the pyroxenite member and immediately begins to increase towards the peridotite contact at the 107.5 m mark, whereupon it levels out to approximately the 2500 ppm level. This trend is strongly influenced by increasing amounts of modal olivine.

Chromium demonstrates an unexpected chemical behaviour. In gabbroic rocks it attains relatively high concentrations in the immediate footwall of the sulphide lens, and also demonstrates an increasing trend from the centre to top of the lens. With the exception of the Cr depletion in the 86 to 90 m interval, Cr increases for the duration of the gabbro intersection. However, it only increases marginally through most of the clinopyroxenite member (99-107.5 m) and then more than doubles in the overlying peridotite member (which starts at 107.5 m) due to the introduction of cumulus chromite. Vanadium displays a general decreasing trend from the lowest to highest stratigraphic levels. Selenium concentrations and profiles shown in Figure 28C are an accurate reflection of the modal sulphide content in the 50 m investigated interval. Arsenic shows an affinity for the silicate rather than sulphide-rich mineralized intervals, in particular that of the footwall environment.

Platinum (Fig. 28D) displays an exceptionally smooth and coherent decreasing trend from the base of the massive sulphide body (79 m) to the lower portion of the peridotite member (114 m). Palladium is more erratic in profile and lower in concentration within the massive sulphide and decreases towards the gabbro/clinopyroxenite contact (99 m). The Pd values generally increase from the base of the clinopyroxenite member to the clinopyroxenite/peridotite contact (107.5 m) where the Pt and Pd trends cross over. From this point onwards Pd concentration exceeds that of Pt and clearly demonstrates the Pd-enriched nature of the peridotite member relative to others. Gold profiles a concave trend centred in the middle of the gabbro horizon. This also corresponds to the convex As and Se profiles established within this interval (Fig. 28C). The Au grades drop constantly from near the base of the clinopyroxenite member (101 m) well into the peridotite member (117 m) and are somewhat sympathetic to the Se trend associated with this interval and most likely reflect the modal sulphide trend. Osmium and ruthenium (Fig. 28E) decrease rapidly and rather systematically in the hanging wall, away from the massive sulphide interval, and attain levels only marginally higher than that found in the mineralized footwall. The 30 ppb convex trend centred about the clinopyroxenite/peridotite contact at 107.5 m is difficult to explain. Iridium and rhodium display sympathetic trends with Ir concentrations exceeding that of Rh in all samples except for the peridotite member. A cross over of these trends occurs at the clinopyroxenite/peridotite boundary (Fig. 28F). The Ir and Rh depletion trends in the hanging wall of the massive sulphide lens (86-120 m) are recording fractionation trends of these elements in the evolving and fractionating sulphide melts.

The PGE+Au profile (Fig. 28G) through this 50 m interval reveals the high noble metal content associated with the massive sulphide ores ($\overline{X}$ = 5000 ppb) and the high background values associated with gabbro (750 ppb), clinopyroxenite (500 ppb), and peridotite (350 ppb). The Pt/(Pt+Pd) is relatively constant in the footwall and hanging wall gabbro sequences about the massive sulphide horizon, but a slight depletion does occur in the 3 to 4 m interval above the upper contact of the sulphide lens. A rapid decrease in this ratio commences in the middle of the pyroxenite member and continues well into the overlying peridotite member. Affiliated Cu/(Cu+Ni) trends are similar to that for Pt/(Pt+Pd) in the silicate-rich rocks, but an antipathetic relationship is present within the massive sulphide width. The S/Se, S/PGE+Au, and S/Ni (Fig. 28I) ratios are very constant within this interval.

The metal-poor anomalies with respect to the last two ratios occur in the barren footwall gabbro. A slight S enrichment is present in the massive sulphide interval as is suggested by the slight inflection of the ratios at this location. In decreasing order of intensity the Pt+Pd/(Os+Ir+Ru) ratios are the highest in the mineralized footwall gabbro, hanging wall gabbro, clinopyroxenite, peridotite, and massive sulphide, respectively (Fig. 28J). Zirconium concentrations through this diamond-drill hole intersection are believed to represent changes in the volume of interstitial or intercumulus material present in the sample. Barium concentrations are extremely high but display a decreasing trend in the barren footwall gabbro. The anomalous Ba levels found in the Cu-rich gabbroic segregations, within the massive sulphide horizon, and in the 6 m hanging wall interval, are remarkable. The anomalous Ba and Zr concentrations associated with the late crystallizing intercumulus phases suggest that relatively high concentrations of these incompatible elements were present in the parental melts from which they crystallized.

Massive sulphide interval. Metal trends and concentrations within the massive sulphide lens in DDH-U492 are examined in closer detail with the aid of the expanded scale illustrated in Figure 29. Nickel and cobalt contents within this interval are generally about 20 000 and 1500 ppm, respectively. However, in areas where the copper content exceeds 20 000 ppm the Ni content is noticeably depleted (i.e. in the 80.5-81.5 m, 82-83.5 m, and 85-86 m intervals, Fig. 29A). These Ni-depleted intervals consist of gabbro with a fine-grained silicate matrix consisting of disseminated chalcopyrite similar to that contained in the gabbroic fraction shown in Figure 26 (A, B, C) and ascribed to sulphide-silicate immiscibility. The generally increasing Cu trend in the 78 to 83 m interval (where it culminates) is additional evidence for the immiscibility hypothesis. Selenium demonstrates a depletion trend in the Cu-rich intervals due to a lower modal sulphide content and lower concentrations of this element in chalcopyrite (Fig. 28B). Arsenic decreases in concentration from the upper and lower contacts of the massive sulphide lens towards the central portion of the body by about two orders of magnitude.

Platinum follows a well defined decreasing concentrational trend in the 79 m to 87 m interval. However, it and all other noble metals are depleted in the central Cu-enriched interval (Fig. 29C). Palladium, with only a few exceptions, is always lower in concentration than Pt and has a very erratic concentrational range. Excluding the two concentrational spikes in the 82 to 84 m interval, gold displays a decreasing (33%) trend from the base to top of the massive sulphide lens. Osmium, ruthenium, iridium, and rhodium (Fig. 29E, F) display both extraordinary absolute concentrations and coherent inter-element correlations with each other. These profiles also correlate strongly with both Ni and Co (Fig. 29A) and to a lesser degree Pt (Fig. 29D). In addition to the coherent geochemical trends, the high levels of Ir, Os, Ru, and Rh are unequalled by other terrestrial Ni-Cu ores, with the possible exception of selected Noril'sk ores, and have concentrations similar to that of meteorites. The $PGE+Au_{(t)}$ content in the massive sulphide interval (Fig. 29G) also displays an overall decreasing trend (≈1500 ppb) from the base to top of the lens.

The Pt/(Pt+Pd) and (Cu/(Cu+Ni) profiles (Fig. 29H) are erratic. Nevertheless, the S/Se, S/PGE+Au and S/Ni ratios in Figure 29I are strikingly constant. The S/Se ratio deviates little from an average value of approximately 3500, and the S/PGE+Au demonstrates that the noble metal content of the sulphide fraction is the same throughout the mineralized interval, except within and adjacent to the Cu-rich central portion. The same relationship also exists for the Ni content of the sulphide fraction. The Pt+Pd/(Os+Ir+Ru) ratio is the lowest (most primitive) in the Ni-rich interval and highest in the weakly mineralized footwall gabbro and central Cu-rich segregation (Fig. 29J). The highest concentrations of Ba within the sulphide lens occur associated with the Cu-rich gabbroic segregation and may be due to the increased silicate fraction and/or possibly anomalous amounts of the rare Cu-Fe-Ba sulphide.

Ultramafic-hosted.

DDH-87-94. The geochemical behaviour of selected base, semi-, and precious metals in an ultramafic environment was investigated in diamond-drill hole 87-94 and are represented in Figure 30. Continuous diamond-drill core was sampled through the ultramafic interval and the top 7 m of the marginal gabbro which was intersected 111 m from the collar. The geology of this interval is shown in Figure 19. Nickel, copper, and cobalt trends (Fig. 30A), excluding the isolated Cu-depletion at the 79 m mark, are similar along the entire 95 m length of sampled core. A 10 m length of Ni depleted ultramafic rocks occurs immediately above the gabbro/ultramafic contact and represents an alternating wehrlite to olivine clinopyroxenite interval with relatively low modal olivine content relative to the ultramafic rocks in the 25 to 90 m section. Selenium and sulphur (Fig. 30B, C) reflect an overall decreasing modal sulphide trend from the 90 m level towards the collar. Tellerium behaves similar to Se and thus is controlled by the distribution and composition of the evolving sulphide phase. Both arsenic and antimony have ill-defined trends.

Platinum, palladium, gold, and rhodium concentrations and trends are remarkably conformable and anomalously rich for ultramafic rocks that contain well less than 5.0% sulphides, and are underlain by Ni-Cu-PGE ore bodies. The similarity between these trends and that of Se, and to a lesser extent S, clearly demonstrates the strong chalcophile or sulphide control on the distribution of these elements. The Pd-rich nature of most peridotite and the Pt enrichment in the basal olivine clinopyroxenite and wehrlite portions of the ultramafic member, as well as in the gabbro, are apparent from the trends shown in Figure 30D. The concave noble metal depletion trend associated with the basal portion of the ultramafic member is perplexing as this interval is endowed in sulphides as well if not better than most other samples from the ultramafic interval. The high background $PGE+Au_{(t)}$ trend and absolute concentrations (Fig. 30E) demonstrate the anomalous noble metal background values in these rocks, and depletion trends associated with the basal portion of the ultramafic member. It is the author's opinion that the mineralized olivine clinopyroxenite horizon formed in response to mixing of residual basaltic magma from the marginal gabbro facies with new and more primitive magma introduced at or

near a level now defined by the base of the ultramafic zone. As a result of the blending of these two rather diverse magmas, sulphide saturation and segregation occurred. However, due to the extensive development of disseminated and massive sulphides in this eastern portion of the complex (relative to other areas), the residual melt and derived sulphides are depleted in metals.

The Pt/(Pt+Pd) and Cu/(Cu+Ni) ratios through the investigated interval display decreasing metal ratios up section (Fig. 30F). Although the former ratio can only be accounted for by variation in metal phases, the latter can be influenced by the silicate Ni and thus renders interpretation more difficult. S/Se, S/PGE+Au, and S/As profiles (Fig. 30G) suggest a slight increase in the Se and PGE+Au metal content of the sulphide fraction at higher stratigraphic levels than those found at lower levels. Conversely, arsenic enrichment occurs associated with the late stage differentiates in the marginal gabbro relative to the ultramafic horizons. Chromium concentrations vary little through this ultramafic interval, and with the exception of the one sample at 88 m, and average about 2100 ppm. The increasing Cr-content over the final 7 m of the marginal gabbro depicts the nature of the gabbro/ ultramafic transition. As clinopyroxene is the only Cr-bearing phase (unlike the overlying member in which Cr is hosted by both chromite and clinopyroxene) in this interval, increasing Cr concentrations record increasing amounts of modal clinopyroxene as the ultramafic contact is approached. Vanadium and zinc vary little through this interval and both are restricted to chromite and ilmenite. Barium and zirconium decrease in concentration from the top of the gabbro interval, through the ultramafic member. Again, high Ba contents are associated with the gabbro and the ultramafic rocks.

DDH-87-92. A 50 m length of mineralized peridotite and clinopyroxenite from the West zone has a combined grade of 5600 ppm Cu, 857 ppb Pt, and 445 ppb Pd. A detailed geochemical investigation of a 14 m length of this mineralized peridotite was conducted on diamond-drill core obtained from the 40 to 54 m interval in DDH-87-92. The geochemical data are discussed with reference to Figure 31, and the geology shown in Figure 24. The mineralized interval consists of heavily disseminated to net-textured sulphides that culminated with the development of a massive sulphide lens at 50.5 m. The footwall consists of weakly to moderately disseminated sulphides. Unfortunately, core from the 46-50 m length had previously been sampled and the remaining material was not suitable for the needs of this study. Examination of this material, however, indicated that it was similar to that sampled in the 40-45 m length and would produce the same geochemical trend.

Nickel and copper display similar geochemical trends in the disseminated hanging wall interval as the massive sulphide lens (Fig. 31A). Cu is generally 1500 to 2000 ppm higher in concentration than Ni. There is a weak depletion trend for both elements from the disseminated hanging wall of the massive sulphide lens to the 40 m mark. Average values for this 10.5 m length are 5500 ppm Cu and 3700 ppm Ni. Anomalous sections containing up to 13 000 ppm Cu and 5200 ppm Ni occur within this mineralized length. Ni assays in the 22 000 to 25 000 ppm range occur within the massive sulphide lens; however, the Cu concentrations are not elevated much above those in the 40 to 50 m disseminated interval. Nevertheless, Cu demonstrates a depletion trend from the immediate footwall (0.5 m), to the top of the sulphide lens. The rapid increase in Ni content from 1800 ppm to 22 000 ppm over a matter of a few centimetres (Fig. 31A) reflects the sharp lower contact of the massive sulphide accumulation. The massive sulphides have high Ni/Cu ratios whereas the disseminated mineralization has low Ni/Cu ratios. Geochemically, cobalt behaves in a manner similar to Ni. The constant chromium content of the investigated interval (Fig. 31B) reflects the relatively consistent modal proportions of clinopyroxene and chromite, with the exception of the massive sulphide interval. The similarity between the vanadium trend and that of Cr suggests this element is substituting in both chromite and intercumulus clinopyroxene. The *zinc* trend is very similar to that of selenium (Fig. 31C) which reflects variations in the modal Fe-Ni-Cu and Zn sulphide content. The systematic decrease in Se content in the hanging wall of the massive sulphide lens reflects an incremental decrease in sulphide content in this interval. Tellerium also follows a chalcophile trend. However, arsenic once again displays its footwall enrichment and massive sulphide depleted trend. The massive sulphide horizon displays a symmetrically disposed concave profile with respect to the sulphide lens, with high values located adjacent the upper and lower contact.

Platinum, palladium, and gold have similar geochemical trends in the mineralized interval from 40-50 m (Fig. 31D). Pt is consistently higher than Pd through the entire 14 m interval. Combined Pt and Pd values >1000 ppb characterize the entire width. High Pt grades are symmetrically distributed about the massive sulphide and net-textured hanging wall mineralization attaining values as high as 3000 ppb in the massive sulphide lens. Pd does not behave in the same manner as Pt in this interval. It demonstrates a marked depletionary trend through this same interval. Au displays a similar trend as Pd through most of this interval except near the upper portions where it shows an increasing trend (Fig. 31D). Rhodium, osmium, iridium, and ruthenium (Fig. 31D, E) are remarkable in that they display identical geochemical patterns and occur in exceptionally high concentrations within the massive sulphides. These elements are also preferentially enriched in the basal accumulations and decline in the higher levels (50-51.5 m). The geochemical character of this peridotite-hosted mineralization is similar to that of the massive and disseminated gabbro-hosted mineralization and are rather unique relative to all other known Ni-Cu deposits. The $PGE+Au_{(t)}$ profile in Figure 31F clearly indicates the anomalous noble metal content of the disseminated, net-textured, and massive sulphide mineralization. The S/Se ratio of this PGE-rich mineralization clearly demonstrates the Se-rich nature of the sulphides, regardless of modal sulphide content, and favourable ratios of <5000. The significance of the Pt/(Pt+Pd), Cu/(Cu+Ni), Ba, and Zr profiles in Figures 31G and H is not immediately apparent, however, anomalous Ba contents are associated with the disseminated mineralization in the 40 to 43 m length.

Linda Creek Intrusive Complex

Mafic-ultramafic intrusive rocks that constitute this complex are complicated in intrusive form and distribution. However, diamond-drill hole intersections of flanking apophyses, similar to the so-called "subsidiary sills" from the West zone of the Quill Creek Complex, have confirmed a similar distribution of lithological zones within this complex. Ni-Cu-PGE mineralization discovered to date is limited in extent, however, some of the highest metal grades and best recorded skarn-type mineralization are from this complex. The complex appears to be physically separate from the Quill Creek Intrusive Complex (Fig. 32), but it is probable that it once was part of this larger complex to the west. If this were the case, the unexposed eastern half of the Quill Creek Complex (i.e. southeast of Wellgreen Mine Road, Fig. 12, 15) would now be a high priority exploration area for additional reserves of high grade Ni-Cu-PGE mineralization.

Location, history, and physiography

The Linda Creek Intrusive Complex is located approximately 3.2 km southeast of the Wellgreen Mine, which occurs in the east-central portion of the Quill Creek Intrusive Complex. The complex occurs at latitude 60°27′ and longitude 139°25′ on NTS claim map 115G/6 (Fig. 4). The access road to the former Wellgreen Mine passes near the west end of the complex (Fig. 12, 32) at a point approximately 11 km from the Alaska Highway. A bulldozer road suitable for four-wheel drive vehicles was built 2.5 km up Linda Creek in 1972. In 1987 and 1988 the road was extended an additional 7 km to provide four-wheel drive access to all of the complex and to the adjacent "Wash Intrusive Complex" (Fig. 12).

The complex is mainly confined to the drainage basin of a westerly flowing tributary of Quill Creek, known as Linda Creek. The terrain is characterized by long steep (≈25°) slopes cut by numerous dry creeks, particularly at the higher elevations. Elevations range from 1980 m along the ridge crests to 1070 m on the floor of Quill Creek. Outcrops in the area are rare and confined to ridge crests and eroded creek cuts. Landslide activity has been recognized in the area (Fig. 32). Mature black spruce vegetation occurs on the floor of Quill Creek and gives way to scattered, stunted black spruce, buchbrush, and slide alder on the lower slopes. At higher elevations the slopes are covered by moss and lichen.

The presence of mafic and ultramafic rocks and their potential to host Quill Creek Complex (Wellgreen)-type mineralization was first recognized at this locality in 1952 by Yukon Mining Company Limited who staked the area as the Jeep claims. It was subsequently optioned to Hudson Bay Mining and Smelting Company Limited and explored in conjunction with the "Wellgreen" exploration on the Quill Creek Complex. Prospecting, mapping and geophysical surveys were conducted in 1953 and four holes drilled in 1953-54. The area was restaked and prospected in 1965 by H. Versluce and P. Versluce. Quill Creek Copper Mines was formed in 1966 to develop the property in conjunction with a copper showing in the Nikolai volcanic rocks on adjoining claims to the south. This company in turn optioned the property to Newmont Mining Corporation of Canada Ltd. who performed mapping and sampling in 1967-68. The Nickel Syndicate (Aquitaine Co. Canada Ltd., Canadian Superior Exploration Ltd., Home Oil Limited, and Getty Mines Ltd.) conducted mapping, sampling, and bulldozer trenching in 1972.

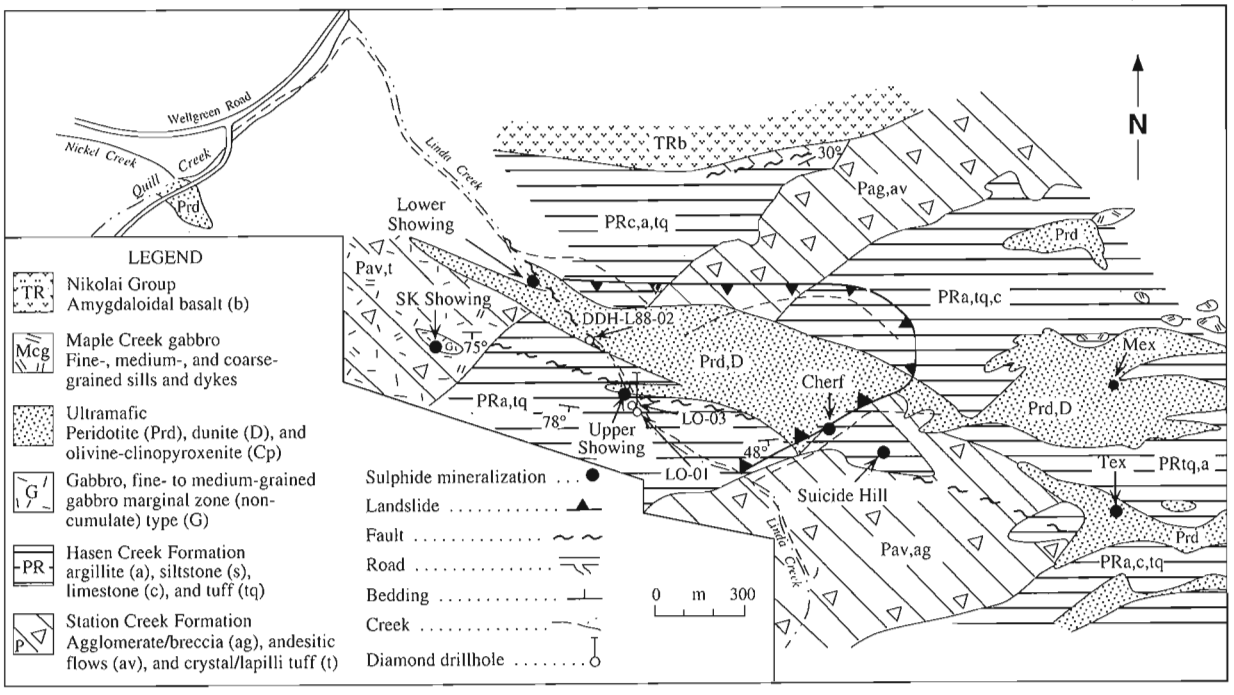

Figure 32. *Generalized geological map of the Linda Creek Intrusive Complex, location of mineralized zones, and position diamond-drill holes referred to in text.*

The Linda property was staked as the Klu claims in May 1986 by Archer, Cathro & Associates (1981) Limited on behalf of the Kluane Joint Venture (Chevron Minerals Ltd. and All-North Resources Ltd.) to cover extensions of the Quill Creek Complex to the west. In December 1986, the joint venture optioned the property to 2001 Resources Ltd. and Rockridge Mining Corporation. In 1987 and 1988 work consisted of additional claim staking, grid layout, geological mapping, geochemical soil sampling, rock sampling, geophysical surveys (magnetics and EM), road construction, bulldozer trenching, and diamond drilling (three holes totalling 246.2 m)

Structure and stratigraphy

A number of semi-conformable mafic and ultramafic sill-like bodies cut a westerly trending sequence of Permian and Pennsylvanian sedimentary and volcanic rocks. The geological interpretation presented in Figure 32 is based on geochemical and geophysical signatures, diamond-drill core and records (7 holes), bulldozer trenches, roadcuts, and mapping of limited natural exposures. The outlines of the discordant-looking Station Creek Formation may in fact be fault bounded blocks. The geological outlines of the ultramafic bodies can be accurately located based on its distinctive soil geochemistry. In addition, faulting, folding, and recent landslide activity further complicate the true geological framework of the area.

The main ultramafic body occurs in the centre of the study area and is approximately 3 km long and up to 350 m wide (Fig. 32). At the west end it appears to be steeply dipping and gradually pinches out in the surrounding sedimentary rocks. The peridotite underlying the Quill Creek road may be an isolated satellite body or a detached portion of the Linda Creek Complex. A 55 m thick subsidiary sill-like body or apophyse, similar to those from the West zone of the Quill Creek Complex, occurs along the central portion of the southern intrusive contact. Toward the east the body narrows to 30 m, then abruptly widens; here, the sill encloses a number of large country rock xenoliths and forms several complex lobes and interdigitations. The exact orientation, shape, and internal magmatic stratigraphy of the body has not been determined due to poor bedrock exposure. Nevertheless, investigation of diamond-drill hole intersections through the subsidiary sill demonstrates lithologies and distribution patterns similar to those in the Quill Creek Complex.

Several smaller satellite bodies occur north, south, and southeast of the main body in the eastern part of the area. The largest of these is at least 1500 m in length and extends outside the study area. At present it is not certain whether this complex is an extension of the adjacent "Wash Intrusive Complex" (Fig. 12), or is a separate body.

Mafic-ultramafic sill-like bodies are commonly in contact with argillite, siltstone, quartzite, limestone, and tuff of the Permian-age Hasen Creek Formation. Less commonly, the intrusions are in contact with the volcanic rocks of the Station Creek Formation. The country rock generally dips moderately to steeply toward the south. Hasen Creek Formation limestone occurs as a 10 m thick bed along the north side of Linda Creek near the Upper showing and as a thermally metamorphosed xenolith or roof pendant within the ultramafic near the eastern end of the study area. Quartz-carbonate alteration zones are prominently developed within this formation in areas adjacent to some ultramafic sills and in large fault zones. Contacts between the Hasen Creek Formation and Station Creek Formation are rarely exposed. In some cases the Station Creek Formation is difficult to distinquish from the fine-grained Maple Creek dykes and the thin marginal gabbro associated with the intrusive complex.

Triassic Nikolai Group basalt is confined to the northern edge of the area and appears to unconformably overlie the older units.

The youngest mafic intrusion in the area is the Triassic Maple Creek gabbro. These fine- to medium-grained dykes and sills intrude close to the ultramafic bodies. Apart from their crosscutting relationships these bodies are difficult to discern from the fine- to medium-grained marginal gabbro facies associated with the main body of the complex. As mentioned previously, the Maple Creek gabbro may represent the feeder system to the Nikolai volcanic rocks.

A number of large west-northwest-trending, steeply dipping faults cut all units and commonly form geological contacts.

Direct evidence for folding in the area was not observed from outcrop mapping; however, indirect evidence suggests that all or part of the area has been folded or overturned. The first line of evidence is the location of the subsidiary sill along the southern contact rather than the northern contact, as is the case with the Quill Creek Complex; second, diamond-drill holes LO-01 and LO-03 (Fig. 32) encountered massive sulphide near what would be the upper contact of the subsidiary sill. If the sill and country rock strata are correctly facing, then this would be the first occurrence of massive sulphide forming near the roof of an intrusion in the entire belt. It is difficult to envisage how a (0.83 m x ŋ100 m) Ni-rich massive sulphide layer could form near the roof zone of an intrusion and not gravitate to the floor of the sill. Thirdly, one would have expected the Nikolai volcanic rocks to be confined to the area south, rather than north, of the intrusive complex, as is the case at the Quill Creek Complex to the west.

Petrology

Although mafic and ultramafic bedrock in the area is sparse, critical exposures within the complex and drillhole intersections at crucial localities clearly indicate that similar lithologies and distribution patterns in the Quill Creek Complex are also present in the Linda Creek Complex. Two diamond-drill hole intersections (DDH-88-L01, -L03) through the subsidiary sill hosting the "Upper showing" (Fig. 32) are described to elucidate the nature and distribution of various lithologies within the sill and complex in general. Details of the two diamond-drill hole intersections are illustrated in Figure 34. The sequence, however, is believed to be overturned and the massive sulphide intersections represent the original base of the sill. As there is a symmetrically zoned

distribution of similar lithologies about the central portion or core of the sill, folding or overturning only affects the position of the basal sulphide accumulations.

Gabbro. The basal contact of the sill (and probably the complex in general) consists of a 1.0 to 1.5 m thick gabbroic chilled margin. Gabbroic material in contact with the Hasen Creek Formation sediments is very fine grained and displays a variety of classic "quench" textures. The photomicrographs in Figure 33 (A, B) display these textures and provide unequivocal evidence for the quenched nature of the initial basaltic magma that gave rise to this intrusive complex. The microcrystalline to weakly hypocrystalline quenched gabbro has a hypidiomorphic-inequigranular texture and consists of approximately equal amounts of plagioclase and clinopyroxene. Accessory amounts of opaque minerals in the form of ilmenite laths or sulphides occur in the groundmass. Trace amounts of altered basaltic glass are present in some material. Orthopyroxene and olivine are absent in these rocks although they are present with respect to their normative chemical composition. Clinopyroxene normally displays two different growth habits. The most common habit is that of singular acicular crystals that grow at acute angles to each other and define triangular crystallization domains within the rock. Smaller equant grains of clinopyroxene and plagioclase subsequently grow within this wedge-shaped intergranular area. Elongated pyroxene bundles, and local individual acicular crystals, are generally curved due to impingement during rapid unidirectional growth. Many of these acicular pyroxene crystals are also skeletal in habit and contain dark opaque cores consisting of devitrified and altered basaltic glass (Fig. 33B). The quenched groundmass supporting the pyroxene is dark to opaque in nature and consists of altered plagioclase and basaltic glass, both of which are charged with included opaque minerals and dustings. Clinopyroxene less commonly occurs as small (0.25-0.33 mm in diameter) euhedral micro-phenocrysts.

This very fine-grained quenched marginal facies passes upwards into a coarser-grained variety microcrystalline gabbro similar to that shown in Figure 33C. Clinopyroxene within this lithology is generally irregular to equant anhedral crystals, some of which containing numerous opaque inclusions. The pyroxene may also display weak twinning and zoning crystallographic features. Plagioclase is commonly anhedral in outline and turbid in appearance due to alteration and opaque dusting. Unexsolved ilmenite laths up to 0.75 mm long are not uncommon in this rock type. A fine- to medium-grained, weakly mineralized, ophitic to sub-ophitic gabbro (Fig. 33D) occurs in the immediate footwall and hanging wall of the massive sulphide horizon shown in Figure 34. Plagioclase from this environment tends to be of a more euhedral habit, but is generally altered to a mosaic of sericite, albite, and a fine opaque dusting. Clinopyroxene occurs as large, irregular, intergranular poikiolitic crystals with included or partially included plagioclase chadocrysts. Large 1.0 to 1.5 mm cumulophyric patches of clinopyroxene occur throughout this environment. Cumulophyric pyroxene is commonly zoned; however, zoning is not as common in the ophitic and sub-ophitic varieties. Sulphides in the form of pyrrhotite, pentlandite, and chalcopyrite seldom occur in concentrations greater than 7%.

Massive and semi-massive Ni-Cu sulphide accumulations up to 0.83 m thick generally occur within the chilled marginal gabbro (1-2 m above the base) or at the gabbro-sediment contact. Inclusions of highly altered ophitic gabbro within the sulphide (Fig. 33E) are common, particularly in mineralization that occurs above the gabbro-sediment contact. Similar gabbroic inclusions are also present in massive sulphides from the Arch Creek Intrusive Complex (Fig. 14B).

Pegmatitic gabbro and feldspathic pyroxenite lithologies occur near Hasen Creek Formation limestone on the north side of Linda Creek, near the Upper showing. These inequigranular rocks display a variety of textures and become pegmatitic in areas of sulphide enrichment. In many respects they are analogous to the "skarn" related pegmatitic gabbro and associated mineralization found in the Quill Creek Complex; however, they generally contain more clinopyroxene and lack garnets. Plagioclase is present only as an intergranular phase and seldom exceeds 40% of the rock. When present it also is extremely altered. Anomalous concentrations of sphene

Figure 33. *Photomicrographs of selected lithologies from the Linda Creek Intrusive Complex. GSC 1995-106J (**A**) DDH-88-LO3-98.7. Upper chilled margin with microphenocrysts of clinopyroxene. Cross-polarized light. (**B**) DDH-88-LO1-34.7. Gabbroic chilled margin with elongated and curved clinopyroxene quench features due to rapid clinopyroxene growth in an impinging environment. Plane-polarized light. (**C**) DDH-88-LO3-97.3. Fine-grained marginal gabbro, with skeletal ilmenite, that underlies the aphanitic to very fine-grained upper chill. Cross-polarized light. (**D**) DDH-88-LO1-34.8. Fine- to medium-grained subophitic gabbro that occurs in the hanging wall of massive sulphides. Cross-polarized light. (**E**) DDH-88-LO1-34.45. Massive sulphide with resorbed inclusions of subophitic gabbro. Plane-polarized light. (**F**) HDB-88-L-5. Feldspathic pyroxenite associated with pegmatitic gabbro. Note the well developed igneous lamination due to alignment of clinopyroxene. Cross-polarized light. (**G**) HDB-88-L-1c. Finer-grained feldspathic pyroxenite to mela-gabbro with sulphides. Cross-polarized light. (**H**) HDB-88-L-1a. Pegmatitic gabbro with coarse sulphide globules partially engulfing clinopyroxene. Clinopyroxene in these samples are generally highly altered. Plane-polarized light. (**I**) DDH-88-LO3-64.3. Net-textured sulphides in serpentinized peridotite. Plane-polarized light. o = olivine, c = clinopyroxene, x = chromite, p = plagioclase, s = sulphide, g = gabbro, i = ilmenite.*

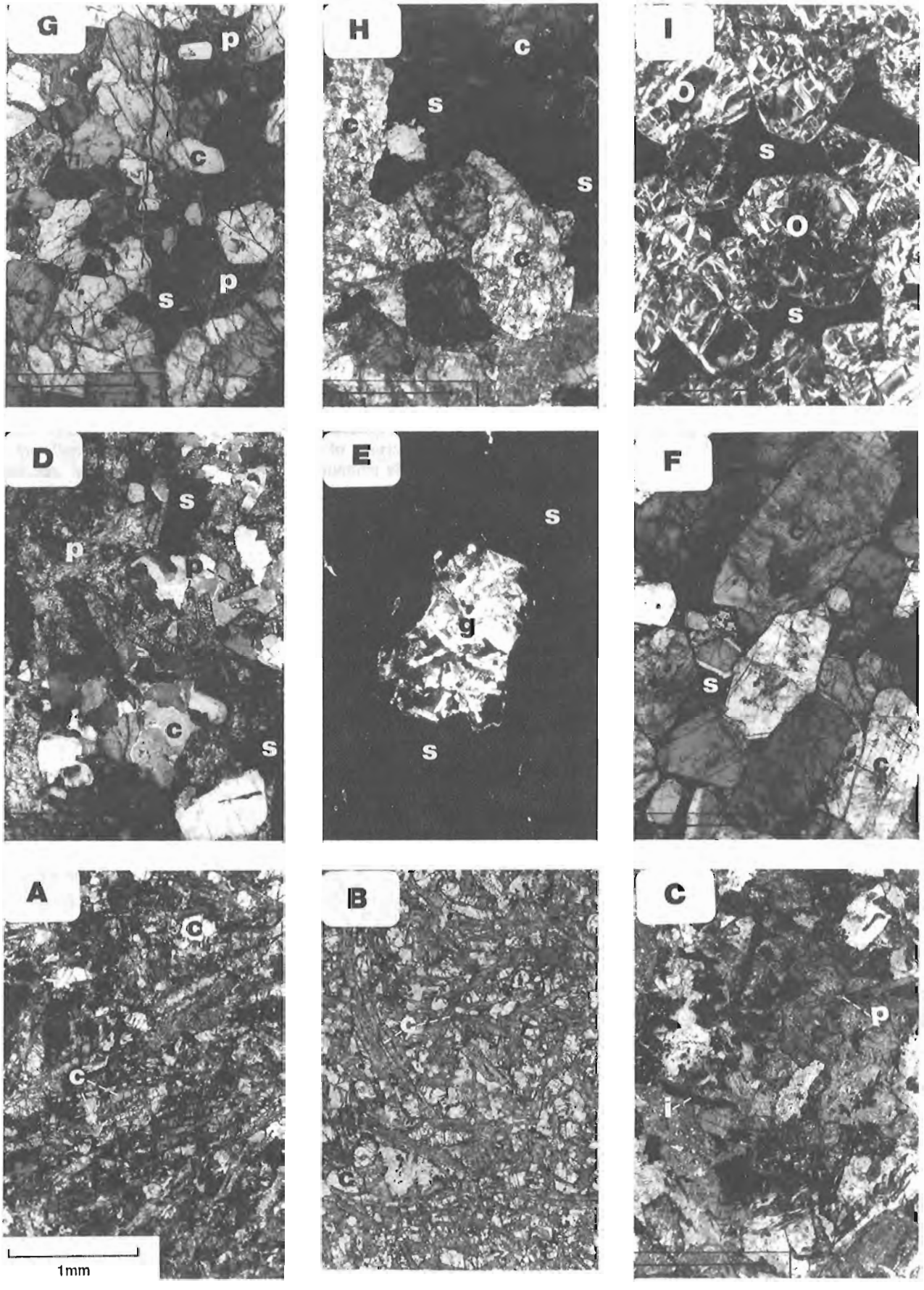
G
p
c
s
p
H
c
s
s
I
O
s
O
s
D
s
p
p
c
s
E
s
g
s
F
s
c
A
c
c
1mm
B
c
C
p
i

(titanite) are also associated with this material, as is the case for the Quill Creek pegmatitic gabbro. Some clinopyroxene-rich samples develop a pronounced igneous lamination defined by oriented clinopyroxene crystals with very little interstitial plagioclase (Fig. 33F); others have more of an equigranular habit with intergranular plagioclase and sulphides (Fig. 33D). The coarse-grained pegmatitic samples usually contain anomalous concentrations of both immiscible sulphide globules and interstitial fillings. Samples containing 1-2 cm size sulphide globules are associated with this type of material (Fig. 33H). All of these mineralized samples also contain anomalous amounts (<10%) of calcite and relatively altered clinopyroxene. At present, the extent and thickness of this pegmatitic material are uncertain.

A similar fine-grained chilled marginal gabbro occurs at the 100 m mark near the bottom contact of the core in DDH-88-L03. This chilled marginal gabbro is less than half as thick as that associated with massive sulphide in the 45 to 58 m interval and is believed to represent the original upper intrusive contact. Marginal chill facies gabbroic intervals are seldom preserved in the roof of magma chambers due to the combined effects of magmatic stoping and gravity. For this reason upper intrusive chill margins are at least thinner, if preserved at all. This observation is additional evidence that the complex has been overturned.

Ultramafic. Clinopyroxenite and/or olivine-clinopyroxenite overlies the medium-grained gabbro (Fig. 34). However, clinopyroxenite occurs only in DDH-88-L01, where it attained a thickness of about 5 m. Petrologically, these two members are similar to their counterparts previously described from other intrusive complexes within the belt, and thus no further discussion concerning their petrological features is necessary. Nevertheless, the rapid changes in thickness of the olivine-clinopyroxenite member from DDH-88-L01 to L03 and the limited degree of macro layering within this interval, relative to that in the other drillhole, is remarkable. In addition, this pyroxenite-rich drillhole contains numerous thin peridotite (wehrlite) intercalations, the thickest of which attains widths of ≤5.0 m. The thickness of this pyroxenitic intersection is equivalent to that of the entire ultramafic zone in the other hole.

In contrast, DDH-88-L03 records a rather systematic distribution of ultramafic members from the marginal gabbro to the centre of the sill. The main control on the distribution of the various ultramafic lithologies is the result of modal variations in the proportions of cumulus olivine and intercumulus clinopyroxene; modal olivine increases towards the centre of the sill at the expense of intercumulus clinopyroxene. The accompanying textural and mineralogical changes give rise to the succession olivine clinopyroxenite, poikiolitic peridotite, and peridotite (Fig. 34). The peridotite can be classified as wehrlite, the poikiolitic variety contains large (≤1 cm) oikocrysts of intercumulus clinopyroxene enclosed in a matrix containing 40 to 60% cumulus olivine, whereas the non-poikiolitic variety generally contain 60 to 80% olivine. The entire ultramafic interval averages 1 to 2% disseminated sulphides. Occasionally, short intervals (1-2 cm) of net-textured sulphides (Fig. 33I) occur within the peridotite member.

Ni-Cu±PGE mineralization

To present, the mineral potential of the Linda Mafic-Ultramafic Complex has virtually been untested because of the limited bedrock exposure. Nevertheless, limited diamond

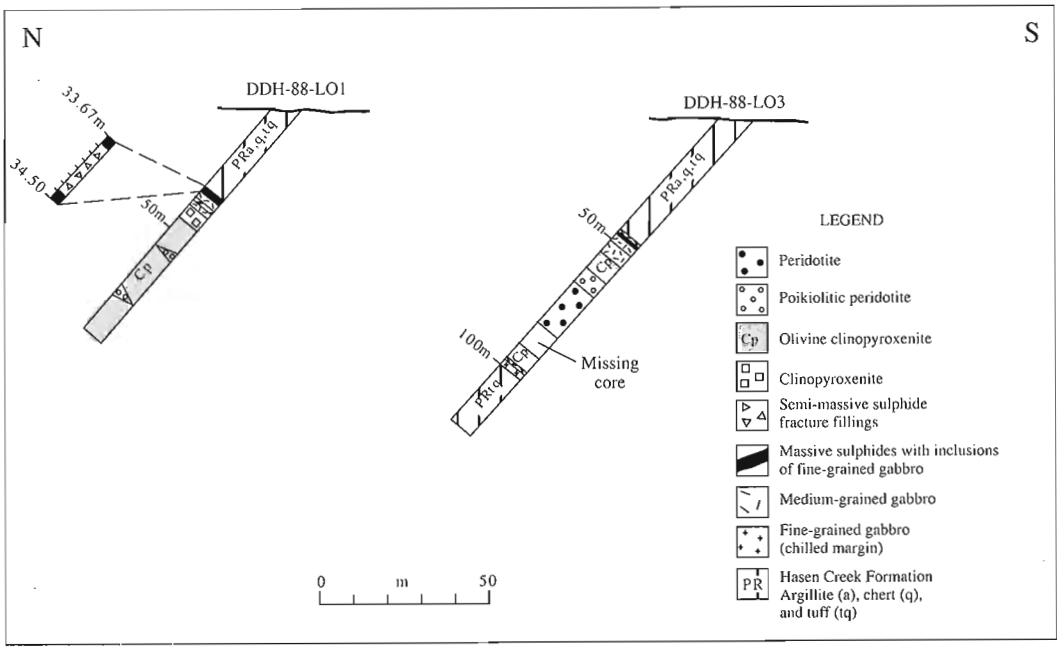

Figure 34. *Diamond drill hole sections representative of DDH-88-LO1 and LO3 in the Linda Creek Intrusive Complex.*

drilling along the south-central portion of the main body, and the discovery of seven surface showings has confirmed the presence of several different styles of gabbro and ultramafic-hosted magmatic immiscible sulphide concentrations. In addition, late to post-magmatic hydrothermal mineralization in the country rock has been recognized. The range in grade of the various metals, metal ratios, and sulphur-isotope compositions with respect to the various lithological groupings are summarized graphically in Figures 78, 90, 101, 112, 124, and 134.

Immiscible magmatic sulphide segregations.

Marginal gabbro. Sulphide occurrences associated with this environment occur as disseminations within gabbro and as massive and semi-massive sulphide accumulations near or at the base of the complex. These represent the most important types of mineralization on the property. The main sulphides consist of pyrrhotite, chalcopyrite, pentlandite, and trace amounts of sphalerite and galena. Although a detailed opaque mineralogical study was not conducted on this mineralization, evidence suggests that the mineralogical findings obtained from the study of the Quill Creek Intrusive Complex also apply to this complex.

Four gabbro-hosted surface showings ("Cherf", "Sk", "Tex", and "Mex"; Eaton, 1988a) were discovered as a result of prospecting and soil geochemical surveys during the 1987 and 1988 field season. The Mex showing is the best exposed, has the greatest width and highest grade, and occurs in a highly sheared limonitic gabbro. A 6 m chip sample assayed 5100 ppm Ni, 5400 ppm Cu, 1451 ppb Pt, and 1611 ppb Pd, whereas, a shorter chip sample (2 m) contained 9900 ppm Ni, 9200 ppm Cu, 3300 ppb Pt, and 7600 ppb Pd (Eaton, 1988a). However, most of the examined gabbro-hosted mineralization was not as high grade and is similar to that in the 36.13 to 37.13 m interval of DDH-88-L01 (Fig. 34). This medium-grained gabbro interval contains about 4.7% disseminated sulphides which occur mainly as wedge-shaped interstitial fillings and sparsely dispersed globular bodies consisting of mixtures of pyrrhotite, chalcopyrite, and pentlandite. Average grades for this interval are: 3100 ppm Ni, 2000 ppm Cu, 900 ppm Cr, 380 ppb Pt, 520 ppb Pd, 51 ppb Au, 92 ppb Rh, 200 ppb Ru, 130 ppb Ir, and 110 ppb Os. With the exception of the Mex showing normal marginal gabbro generally contains 0.7 to 4.7% disseminated sulphides and relatively high background Cr (900 ppm) and $PGE_{(t)}$ (200 ppb) levels.

Pegmatitic gabbro occurs proximal to calcareous country rock and is enriched in sulphide mineralization. This style of gabbro-hosted mineralization generally contains 9-13% disseminated sulphides in the form of relatively coarse interstitial fillings and large sulphide globules, reminiscent of classic magmatic immiscible sulphide segregations. The sulphide globules have smooth outlines and drape around and over existing clinopyroxene (Fig. 33H). Only one occurrence of this material was discovered but its proximity to calcareous Hasen Creek Formation strata and similarity to the so-called skarn-associated pegmatitic gabbro and related mineralization in the Quill Creek Complex leaves little doubt that the two are genetically related. Based on five samples the grade has the following ranges: Ni (3300-4000 ppm), Cu (3100-4200 ppm), Pt (820-900 ppb), Pd (1100-1500 ppb), Au (5-35 ppb), Rh (43-60 ppb) Os (95-140 ppb), Ir (39-55 ppb), and Ru (130-170 ppb). PGE+Au concentrations range from 2194-2600 ppb. Chemically, this gabbro-hosted mineralization differs from that of the normal medium-grained gabbro (mentioned above) in that it has higher Cu/Ni ratios, and much lower concentrations of Ir, Os, Ru, and Rh relative to the amount of sulphide. The pegmatitic variety also has much higher levels of Ba (350-4800 ppm) than the normal fine- to medium-grained gabbro (<160 ppm), and is represented by the different concentrational ranges shown in Figure 101B.

Massive sulphide mineralization has only been discovered at the "Upper showing" (Fig. 32). Other zones of similar mineralization could be present elsewhere, but are difficult to find because of their highly oxidized and recessive surface expressions. On surface the Upper showing consists of a mixture of pyrrhotite, chalcopyrite, limonite, and azurite-malachite patches within a 10 cm to 1 m wide shear at the gabbro-sediment contact. A chip sample taken in 1987 returned a grade of 1.80% Ni, 1.02% Cu, 2199 ppb Pt, and 1611 ppb Pd over 1.3 m. A 1954 drillhole (W-1), which tested downdip from the surface exposure, intersected a 36 cm wide massive sulphide band that assayed 4.19% Ni, 1.80% Cu, 4114 ppb Pt, and 4800 ppb Pd. Two additional holes explored the showing in 1988 (DDH-88-L01, -L03) and were investigated during this study. The massive sulphides occur directly at the gabbro-sediment contact or within 1 m above it. A shear zone developed at the gabbro-sediment contact in DDH-88-L01 bifurcates the original massive sulphide band into two thinner bands separated by an interval of semi-massive sulphide fracture fillings (Fig. 34). Assays for the massive sulphide intervals from both drillholes record the following values: Ni (3.9-5.6%), Cu (0.08-.87%), Pt (3200 ppb), Pd (800 ppb), Au (210 ppb), Ru (2100 ppb), Os (1300 ppb), Rh (1100 ppb), Ir (1800 ppb), and $PGE+Au_{(t)}$ (10400 ppb).

The semi-massive fractured interval contains 25 to 33% sulphides. Sulphides within this interval have been remobilized from the massive sulphides and are characterized by numerous cross-cutting chalcopyrite veinlets. The following grades represent the range encountered within this interval: Ni (1.2-2.2%), Cu (0.54-1.6%), Pt (1000-2100 ppb), Pd (1000-2000 ppb), Au (100-140 ppb), Ru (93-620 ppb), Os (80-440 ppb), Rh (84-320 ppb), Ir (92-600 ppb), and $PGE+Au_{(t)}$ (2349-6000 ppb).

Ultramafic. Fine-grained disseminated pyrrhotite generally comprises 1 to 2% of the ultramafic lithologies within the complex, but macroscopic chalcopyrite is rare. The average grade for the entire pyroxenitic ultramafic interval in DDH-88-L01 (Fig. 34) is 1455 ppm Ni, 607 ppm Cu, 159 ppb Pt, and 150 ppb Pd, whereas, in the more peridotitic intersection in DDH-88-L03, it is 1408 ppm Ni, 615 ppm Cu, 213 ppb Pt, and 156 ppb Pd. It is remarkable that these two lithologically diverse intersections are so similar in terms of their Cu and Pd content. Nevertheless, it is clear that the more peridotitic intersection is enriched in Pt. Corresponding Au, Rh, Os, Ir, and Ru concentrations in this ultramafic interval are 15, 20, 38, 19, and 75 ppb, respectively. The sulphide content of these

rocks is not unlike that of other peridotites in the literature, but their background PGE concentrations are exceptionally high. The best mineralized ultramafic material found in the complex contains approximately 5% disseminated sulphide. The average grade for this type of material is: Ni (2300 ppm), Cu (1500 ppm), Pt (630 ppb), Pd(1200 ppb), Au (31 ppb), Rh (61 ppb), Os (120 ppb), Ir (52 ppb), and Ru (220 ppb). The $PGE+Au_{(t)}$ for five samples of this material with sulphide contents in the 3-5% range is 1902 to 2283 ppb. These ultramafic rocks contain remarkably high concentrations of PGEs relative to the amount of sulphide in the rock.

During the road construction phase of the Linda exploration program, routes were designed to cross the ultramafic bodies and attempts were made to ensure that the inside bank was cut well into bedrock. This in effect, produced a series of long trenches. The roadcuts were mapped and wide interval reconnaissance chip sampling was performed over the ultramafic bodies. A near continuous profile was obtained across the eastern and southeastern ultramafic bodies hosting the Mex and Tex showings, respectively. Most samples were collected over 25 to 75 m widths and consisted of three to four rock fragments from each metre and weighed between 5 to 10 kg. The average grade of these ultramafic bodies is: 1916 ppm Ni, 159 ppb Pt, and 173 ppb Pd. The nickel concentrations in these two bodies is marginally higher than that of the ultramafic intersection overlying the massive sulphide lens at the Upper showing in the central portion of the complex. Although, the average Pt and Pd levels are similar, they are also anomalously high ($(Pt+Pd)_t$ = 332 ppb) with respect to the amount of contained sulphide mineralization, and typical values for other non-Kluane ultramafic rocks.

Geochemically, the magmatic rocks display rather coherent metal vs. sulphur trends with respect to: Ni, Cu, Co, Se, Bi, S/Se, Pt, Rh, Ru, Ir, Os, $PGE+Au_{(t)}$ and thus demonstrate the chalcophile nature of these elements (Fig. 78A,B,C, 90A,B, 101, 112, 124, 134). Pd and Au demonstrate a higher degree of scatter which may be a consequence of their more mobile geochemical behaviour. Other late magmatic (deuteric) and hydrothermal associated elements (As, Sb, Te) also demonstrate irregular metal distribution patterns in both the magmatic and hydrothermal environments (Fig. 78D, 90C,D) and attest to the mobile character of these elements. Also, note the high Cu and As concentrations associated with the country rock-hosted mineralization (Fig. 78B,D). The S/Se ratio of magmatic rocks demonstrates a weakly decreasing trend, particularly for the sulphide-poor ultramafic samples. Sulphur loss due to serpentinization may have contributed towards these low values. Regardless, all of the samples have a S/Se ratio of <5000, the cutoff value associated with PGE-enriched sulphide mineralization. The S/Se ratio for country rock-hosted mineralization is highly variable. The S/PGE+Au vs. S/Se plot indicates that the sulphide fraction associated with the ultramafic rocks contains the highest PGE+Au concentrations, whereas, the gabbro contains the lowest and the massive and semi-massive sulphides fall between these two defined ranges.

The isotopic composition of sulphur ($\delta^{34}S$) associated with sulphides from the Linda Creek Complex varies from -4 to -11.3‰. The greatest variation occurs with the pegmatitic gabbro which ranges from -4 to -10.7‰. The lower value is associated with a sample containing significantly less sulphide. This smaller volume of sulphide may have communicated with a larger reservoir of mantle derived magmatic sulphur than its ^{32}S enriched counterparts. Ultramafic-hosted sulphide mineralization ranges in composition from -7.6 to -11.3‰. No significant difference in composition was recorded in various ultramafic members (i.e. olivine clinopyroxenite and wehrlite from the same locality, -11.0 and -11.3‰). A chalcopyrite-rich sample containing remobilized stringer mineralization contained the lightest sulphur (-11.7‰). Sulphides associated with massive, semi-massive and overlying gabbro-hosted disseminations are confined to the -5.0 to -5.6‰ range. The isotopic composition of this mineralization is very similar to that of comparable mineralization from the Quill Creek Complex.

Hydrothermal (remobilized ?) mineralization. Fracture fillings and disseminated mineralization are common in the volcanic and sedimentary rocks adjacent the main body, in particular where the rocks are strongly sheared. The best example is the Lower showing where sulphides occur in a limonitic shear zone between chlorite schist and silicified mudstone, about 20 m from the main ultramafic body. Both pyrrhotite-rich and chalcopyrite-rich mineralization occurs within the shear zone as either sulphide patches or stringers. A pyrrhotite-rich specimen collected in 1986 assayed 4.1% Ni, 0.08% Cu, 925 ppb Pt, 4388 ppb Pd, 1062 ppb Ir, 2708 ppb Os, 3291 ppb Ru, and 994 ppb Rh (Eaton, 1988a). In contrast, semi-massive chalcopyrite-rich mineralization collected during this investigation contained approximately 29% sulphide and assayed: 0.26% Ni, 7.2% Cu, 0.11% Zn, 65 ppm Pb, 232 ppm Se, 1900 ppm As, 200 ppb Ag, 1700 ppb Pd, 2200 ppb Pt, 34 ppb Au, 1 ppb Rh, 9 ppb Os, 13 ppb Ir, 11 ppb Ru. The chalcopyrite-rich mineralization is depleted in the higher melting point platinum-group elements Os, Ir, Ru, and Rh. This same inert geochemical character of these PGEs in the Cu-rich remobilized sulphides was also noted in the footwall quartzite at the base of the Quill Creek Complex. The Suicide Hill showing occurs in sheared, malachite-stained quartz-carbonate alterated Station Creek Formation strata near the main body of the ultramafic complex, and contains 0.07% Ni, 0.39% Cu, 1542 ppb Pt, and 2022 ppb Pd. This mineralization is characteristically Cu rich and Ni depleted, and contains very high noble metal contents for the amount of associated sulphides. This style of mineralization is believed to be of a hydrothermal origin.

Central section

Four mafic-ultramafic intrusive complexes occur in the central section of the Kluane Mafic-Ultramafic Belt. They are from northwest to southeast: Tatamagouche Creek Complex, Duke River Complex, Halfbreed Creek Complex, and Dickson Creek Complex (Fig. 4). These bodies differ from those in the Northern and North-central sections in that they are significantly less altered, the ultramafic zone is more fractionated, and contains an additional cumulate crystallization order not previously recorded in the northern sections, i.e. olivine-plagioclase cumulates, and some contain

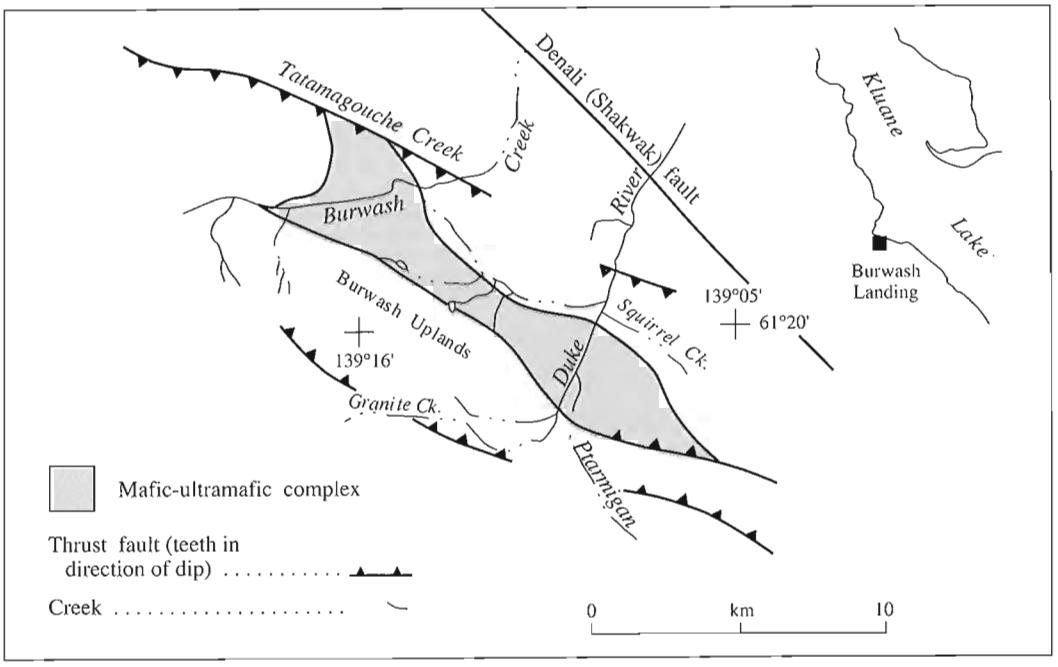

Figure 35. *Geological outline of the Tatamagouche Creek Intrusive Complex and surrounds.*

sulphides with the lightest isotopic character and the most metal-depleted compositions recorded in the belt. In addition, these mafic-ultramafic intrusions become increasingly confined to Permian age strata as they progress towards the southeast (rather than Pennsylvanian strata or the Pennsylvanian-Permian contact zone as in the northern sections) and the complexes are associated with a greater volume of contemporaneous but relatively younger high level mafic intrusions associated with the Nikolai volcanism.

Tatamagouche Creek Intrusive Complex

The Tatamagouche Creek Intrusive Complex is the largest mafic-ultramafic intrusive complex in the belt, but it is also one of the most poorly exposed. Since the turn of the century the Tatamagouche Creek and Burwash Creek (Fig. 5, 35, 36) areas have been well known for their placer gold production and high-grade copper mineralization (Muller, 1967). However, the Ni-Cu-PGE potential of this area has never been fully appreciated let alone tested. Data gained during this investigation suggest that this body would make an excellent target for future exploration of Quill Creek-type Ni-Cu-PGE+Au mineralization. If size and structure of an intrusive complex are proportional to the amount of segregated magmatic sulphide, then the Tatamagouche Complex could potentially host some of the largest and least deformed Ni-Cu-PGE orebodies in the belt.

Location, history, and physiography

The study area is located approximately 14 km west of Burwash Landing, Kluane Lake. The centre of the complex is located 40 km southeast of the Wellgreen Mine, and is at latitude 61°21′ longitude 139°16′ on NTS reference 115G/6. The area is partially accessible from the Alaska Highway by four-wheel drive vehicle along dirt roads adjacent Burwash Creek and Duke River. Access may also be gained from the north along the Quill Creek road which branches into the Tatamagouche Creek road at the junction of the Nickel Creek road which serviced the Wellgreen Mine site. Accessibility of these roads is dependant on placer mining and exploration activity in the area. Services, accommodation, and fixed wing airfield facilities are available at Burwash Landing.

The complex was first staked for its Ni-Cu potential in 1952 by Hudson Bay Mining and Smelting Co. Ltd. The area was staked as the Bert claims and was part of a large block of claims extending southeast from the Wellgreen discovery site. After prospecting and geophysical surveys, Hudson Bay Mining and Smelting drilled five holes, for a total of 210 m, on claim Bert #19 in 1954. The area was restaked as the Glen claims in December 1966 by Alice Lake Mining Ltd. The company conducted magnetic and electromagnetic geophysical surveys and drilled two holes in 1967 for a total of 218 m. It restaked the showing in September 1972 as the Mary claims and conducted further geophysical, geochemical, and geological surveys. In August 1978 these claims were restaked as the Wen, Jo, claims etc. by L.B. Halferdahl & Associates (BUR Syndicate) which explored, mapped, and conducted deep soil geochemical surveys and magnetometer surveys in 1979-80. Trenching and five drillholes (297 m) were completed in 1981, three holes (273 m) in 1982, and more sampling and mapping was conducted in 1983 and 1984. The property was transferred to Tatam Resources Ltd., which drilled the Wen and JV 40 claims in 1985. In 1986, trail construction, stripping, trenching, and geological and

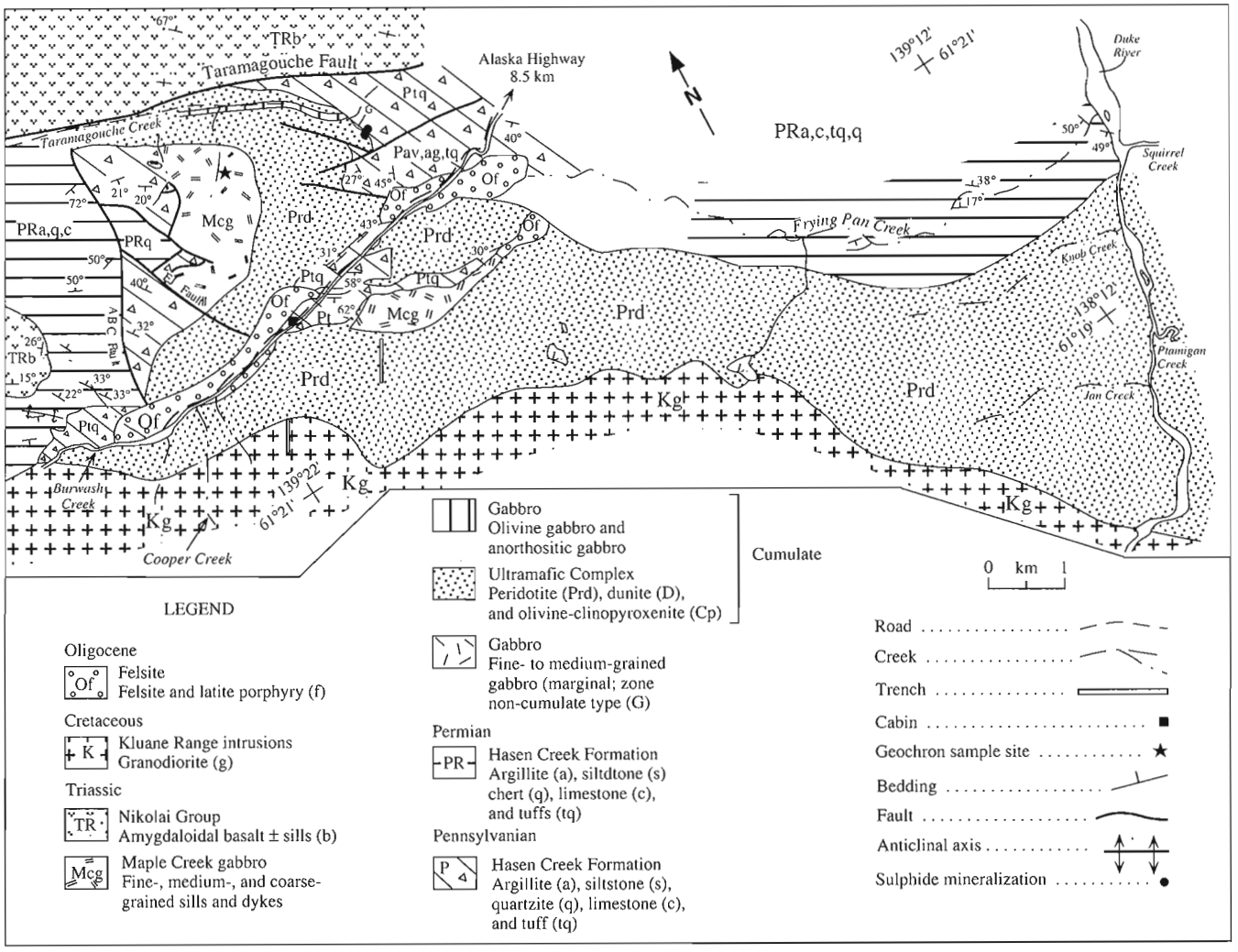

Figure 36. *Generalized geological map of the Tatamagouche Creek Intrusive Complex west of Duke River.*

geochemical surveys were conducted on the JY claims.[1] The filed assessment work suggests that most of the exploration subsequent to 1978 was directed towards non-magmatic base metals and precious metal (Au) associations as Ni, Cu, Cr, and PGE analyses were not conducted, and only very limited mention of gabbroic or ultramafic rocks occurs in the drill logs.

As the best exposure of the complex occurs north and northwest of Burwash Creek (Fig. 35, 36) essentially all past exploration was conducted in this area. The sparsely exposed portion of the complex in the area between Burwash Creek and Duke River was investigated by J.S. Vincent Ltd., for the Nickel Syndicate, in 1973. The Nickel Syndicate conducted limited mapping and magnetometer surveys. The area east of Duke River has not been investigated but the presence of mafic and ultramafic intrusive rocks are known from regional mapping (Muller, 1967) and airborne geophysical surveys.

[1] Mineral Policy Sector, Dept. of Energy, Mines and Resources, Ottawa, #506481, REF. NI 1 and Northern Cordillera Mineral Inventory, Archer, Cathro & Associates Ltd., Occurrence No. 16.

Most of the complex occurs in a physiographic area known as the "Burwash Uplands" (Muller, 1967). This flat to gently sloping tract of land rises towards the Donjek Range to the south and the Kluane Range to the southeast and northwest. This glacially eroded upland consists of thick Quaternary glacial and alluvial deposits created by the Ruby Ice-Sheet (Muller, 1967). Major water courses are Duke River and Burwash Creek. These glacially fed drainages (with their headwaters in the Donjek Range) and tributaries (i.e. Tatamagouche Creek, Ptarmigan Creek, etc.) dissect the complex and provide the only bedrock exposures of ultramafic rocks. The best exposure and most actively explored area north of Burwash Creek has a maximum elevation of approximately 550 m above the creek bed. Timber cover is limited in the area because of shallow permafrost conditions, and where present it is generally black spruce. The upland area is covered by a boggy meadow consisting of grass ("tussocks" and "bunchgrass") and willows. This "uplands" environment is difficult to traverse both on foot and by tracked vehicle.

Structure and stratigraphy

The virtual absence of exposure over most of the complex and limited exploration directed towards gabbro- and ultrabasic-hosted mineralization has presented one of the most difficult impediments in preparing a geological map of this complex. Nevertheless, it was felt that the knowledge gained from other complexes in the belt, and the geological information obtained from multiple exposure mapping in the Burwash Creek-Tatamagouche Creek area could be coupled with the geophysical results and data from other exploration programs to compile generalized geological maps of the Tatamagouche Creek Intrusive Complex (Fig. 35, 36). A schematic stratigraphic section based on available information from the Tatamagouche Creek area is also presented in Figure 37.

The inferred intrusive contacts and boundaries of the Tatamagouche Creek Complex, and proximity to the Denali (Shakwak) fault, are presented in Figure 35. A more detailed map of the complex between Tatamagouche Creek and Duke River is presented in Figure 36.

The oldest mafic-ultramafic intrusive rocks in the area constitute the bulk of the Tatamagouche Creek Complex and middle Triassic mafic sills and dykes related to Nikolai volcanism. It is believed that the original intrusive complex was a rooted sill-like body with a feeder centred along the Duke River section. In its present form the body attains a length of 17 km and widths of 1.4 km in the central part of the complex and up to 3.0 km near the northwest and southeast extemities. Along the northern boundary of the complex the intrusive rocks appear to have been emplaced near the contact between Station Creek Formation and Hasen Creek Formation or within these formations. Generally these Pennsylvanian and Permian age rocks strike in a northwesterly direction and have moderate to shallow southwest dips. Members of the Station Creek Formation and Hasen Creek Formation are similar to those previously described, and thus warrant no further discussion. Granitic intrusive rocks demarcate the southern contact of the complex. These Cretaceous age granodiorite and diorite belong to a group of granitic rocks known as the "Kluane Range Intrusions". Fine-grained granitic chilled margins and zones of ultramafic xenoliths occur near the southern contact along the Duke River section.

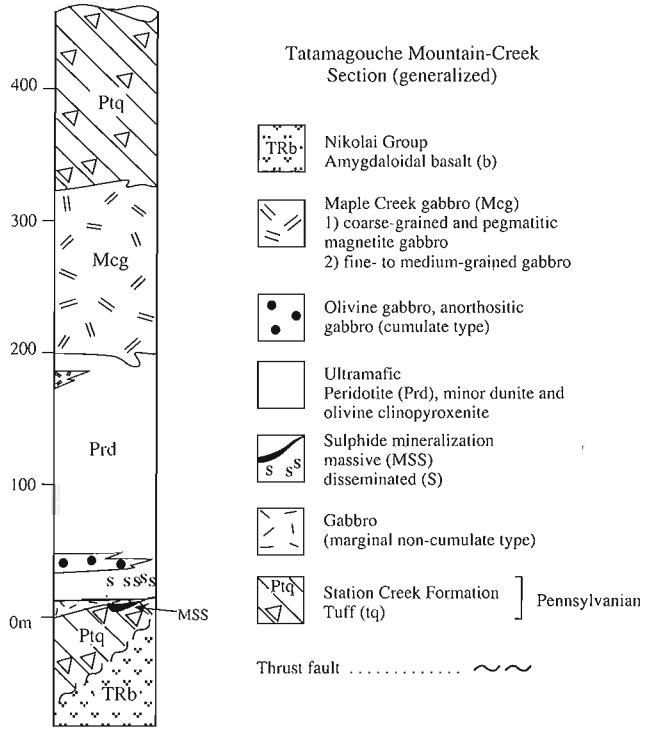

Figure 37. *Schematic stratigraphic section through the Tatamagouche Creek Intrusive Complex and surrounds.*

The geological map of the complex (Fig. 36) suggests that the mafic and ultramafic rocks belonging to the main intrusive event appear not to be as varied as in other complexes. However, this lack of lithological diversity may be a consequence of sparse exposure. Marginal zone gabbroic rocks were only observed along Tatamagouche Creek near the northwestern intrusive contact. Here, highly decomposed, medium-grained mineralized gabbro hosts semi-massive sulphide concentrations and is in contact with Station Creek Formation tuff. This locality is also the site of one of the two known massive Ni-Cu sulphide occurrences recorded for the complex (Fig. 36). Unfortunately, since the showings discovery in 1952, an access road had been built over the site by placer miners. In 1988, this site was partially unearthed as a result of unseasonal torrential flooding along Tatamagouche Creek. This gabbroic marginal zone is a minimum of 15 m thick. Similar gabbroic material is believed to be present along the basal intrusive contact elsewhere in the complex. Two diamond-drill holes collared in Station Creek Formation tuff to the north and south of the above mentioned mineralized locality recorded a highly faulted gabbro sill-tuff sequence. The gabbro varies in width from 0.69 m to 19 m and generally intrudes thin tuffaceous horizons. Only one thin (2.2 m) basic volcanic interval was recorded. The scarcity of volcanic flow material and absence of black shale, siltstone, and argillaceous material at this locality suggest that the complex has intruded middle Station Creek Formation strata. The abundance of Hasen Creek Formation strata along the north-central and northeastern contacts suggests the intrusion has cut down-sequence as it transgressed westward from its eastern feeder zone in the Duke River area. The presence of these sills confirms that there was an early "sill phase" associated with the initial emplacement of the Tatamagouche Complex, and other similar intrusive complexes in the belt.

The ultramafic zone of the Tatamagouche Complex overlies the marginal gabbro zone and is a minimum of 180 m thick in the western part of the area (along the Tatamagouche Creek section, Fig. 37). The basal portion of this zone contains sporadic pockets (<2 m) of sulphide-enriched (≤2%) peridotite. This mineralized locality is in the vicinity of the gabbro-hosted semi-massive sulphide showing at the gabbro-tuff contact (Fig. 36). Ultramafic rocks within the exposed portion of the complex cannot be subdivided into pyroxenitic, peridotitic, and dunitic members due to lack of exposure. However, most of these lithological varieties have been observed in the Tatamagouche Creek area, and there is no

reason to believe that an olivine enrichment trend does not occur up-section as in the other intrusions within the belt. Unfortunately, most of the ultramafic bedrock exposures are confined to seasonal drainages controlled by faults. Also, in the vicinity of these faults, ultramafic rocks are commonly transformed to serpentinite and their original petrological character is lost. As in other intrusions, the ultramafic rocks in this complex display no evidence of rhythmic layering, large scale macro layering, or other planar cumulate features that could be used to interpret the internal structure and attitude of the complex. Nevertheless, based on the shallow to moderate dips (20-45°) in the country rock, it is assumed that the internal magmatic stratigraphy has a similar attitude. A layer of olivine gabbro, anorthositic gabbro, and gabbro of a cumulate origin was initially disclosed along the north side of Tatamagouche Creek, approximately 1.3 km upstream from the confluence with Burwash Creek. The layer continues for an additional 2.2 km west, mainly in the bed of Tatamagouche Creek. Many of these creek bed exposures have a chalky appearance due to shearing. The presence of this feldspathic lithology is inferred at other localities where large boulders of similar, but fresher, material occurs on the grassy south slopes of Tatamagouche Creek. The exact thickness of this olivine gabbro member is not known but it is at least 16 m thick and is confined to the basal portion of the ultramafic zone.

Unfortunately, due to poor weather conditions, time did not allow for detailed examination of outcrops along Duke River. However, J.S. Vincent Ltd. examined this interval in 1972-73.[1] He found rather systematic textural variations within the peridotite in a section from the northern to southern contact. From the northern contact a 150 m wide medium-grained peridotite passes into a coarse-grained variety of equal width. This in turn passes into a 25 m wide so-called "picrite" horizon. This picrite may be the equivalent of the olivine gabbro horizon from the western part of the complex. A 300 m width of pyroxenite occurs adjacent to the southern contact, and passes northward into coarse and very coarse peridotite attaining widths in excess of 500 m. Medium- and coarse-grained peridotite and mica-rich peridotite intervals occur in the central portion of the section. Vincent noted that the highest sulphide contents (2x background) occur in this interval. The textural and grain size variations within this ultramafic section are probably monitoring the volume of intercumulus clinopyroxene. The coarser-grained variety is most likely olivine clinopyroxenite, particularly in the southern intervals where it overlies a wide pyroxenite interval. The medium-grained variety is probably the more equigranular olivine-rich peridotite.

The youngest mafic intrusive rocks in the area are the middle Triassic Maple Creek gabbro sills and dykes. These bodies are best exposed in the western part of the area where a large sill is centred on Tatamagouche Mountain (Fig. 36). The sill is approximately 1.3 x 2.3 km in surface extent and attains a thickness of about 130 m. The sill intrudes near the top of the ultramafic zone (Fig. 37) of the complex. Similar material, of unknown attitude, occurs within the ultramafic rocks east of Burwash Creek. Most of this gabbro has a distinctive greyish-black, pegmatitic texture, relatively high Fe-Ti-oxide content, and has been coined "magnetite gabbro" for the convenience of field mapping, although it is not true magnetite gabbro by definition (i.e. ≥10% magnetite). Thin sills and dykes of this material occur throughout the western portion of the complex, and the fine- to very fine-grained varieties are indistinguishable from some of the Nikolai sills and volcanic rocks. There is strong field evidence from the Tatamagouche Creek section showing that these hypabyssal rocks represent subvolcanic feeders to the overlying Nikolia basalt.

Nikolai volcanic rocks are restricted to the area north of the Tatamagouche fault and along the western margin of the study area. These volcanic rocks are predominantly made up of fine-grained diabasic-textured flows and minor sills. They commonly are maroon and have a pronounced amygdaloidal texture, but areas of glomorophyric plagioclase and pyroxene have also been noted.

The youngest intrusive rocks in the area are granitic. The oldest of these, and by far the most abundant, are the Cretaceous "Kluane Ranges" granitic rocks. They are mainly medium-grained equigranular hornblende granodiorite and quartz diorite with minor biotite, and are restricted to the area along the southern contact of the complex. Marginal areas and smaller bodies of diorite, gabbro, and hornblendite are also common along the contact zone. Younger east-northeast-trending felsite and latite porphyry dykes of Oligocene age intrude the complex in an area that generally straddles Burwash Creek. The largest of these bodies is about 3.3 km long and 0.4 km wide. These rocks are conspicuous due to their white colour. They are generally creamy white, pink, or light reddish-brown and contain andesine or oligoclase phenocrysts up to 2 mm in size.

The study area has been highly dissected by faults. The most pronounced of these is a southerly dipping thrust fault occurring along most of the length of Tatamagouche Creek, and thus coined the Tatamagouche fault (Fig. 35, 36). This thrust brings Nikolai volcanic rocks in fault contact with the northwest contact of the complex. The southeast contact of the complex is also in thrust contact with Station Creek Formation strata (Fig. 35). A major northerly trending reverse fault ("ABC") occurs in the western part of the area and brings Pennsylvanian volcano-sedimentary rocks in contact with Permian strata (Fig. 36). Subsidiary faults (i.e. "EJ fault") with sinistral movement are also present. The easterly trending faults transecting the ultramafic rocks and the Station Creek Formation strata in the vicinity of the recorded sulphide mineralization also appear to be reverse faults with associated subsidiary faults. These faults may be related to the emplacement of the Oligocene felsite intrusions. The association of these felsite bodies with similarly trending slices of Station Creek Formation tuff within the ultramafic portion of the complex suggests that these older tuffaceous strata faulted into their present position accompanying the intrusion of the felsite bodies.

[1] John S. Vincent Ltd. mapped this section for the Nickel Syndicate in 1973.

Folding was only recognized in the southwest part of the study area where a single northwest-trending anticline is developed. The localized nature of this fold may be due to either the emplacement of the bordering Kluane Ranges granitic intrusions, or to the influence of the Duke River Thrust to the south.

Petrology

Petrologically, most of the mafic and ultramafic lithologies within the Tatamagouche Complex differ little from those in other complexes. However, the introduction of a new cumulate crystallization order (i.e. olivine:clinopyroxene:plagioclase) and the frequency of consanguineous hypabyssal Maple Creek gabbro sills within the ultramafic zone present two important changes not noted in the northern section of the belt.

Gabbro. Three different varieties of gabbro occur within this complex: (1) marginal zone gabbros; (2) olivine gabbro, gabbro, and anorthositic gabbro cumulates that occur in the basal portion of the ultramafic zone; and (3) Fe-Ti-oxide-rich hypabyssal ("Maple Creek") gabbro.

Material representative of marginal zone gabbro was only discovered at one locality, therefore it is difficult to elaborate on the petrological character of gabbroic rocks from this zone. Although this unearthed gabbroic material is in a partially decomposed state, it is not unlike that of many other mineralized marginal zone gabbro in surface exposures from the Quill Creek Intrusive Complex. It consists primarily of a greenish-white to green, medium-grained, hypidiomorphic granular gabbro. In terms of original igneous constituents the material consisted of plagioclase, clinopyroxene, and sulphide with trace amounts of phlogopite, apatite, and ilmenite. The plagioclase content generally varied between 40 to 60% of the sample with the remainder being made up of pyroxene and sulphides. Sulphide content varied from 1.3 to 13%. In the weaker mineralized samples, sulphides occurred as wedge-shaped interstitial fillings of pyrrhotite and chalcopyrite, and with increasing sulphide the samples tend to contain increasing amounts of globular sulphides (≤0.7 cm). Due to surface weathering many of the more mineralized samples are porous, friable, and have an ochreous appearance from the presence of limonite development in this gossanous environment.

A thin horizon consisting of olivine gabbro, anorthositic gabbro, and gabbro was discovered in the lower portion of the ultramafic zone. The olivine gabbro is a classic olivine-clinopyroxene-plagioclase cumulate consisting of approximately equal amounts of cumulus olivine crystals (0.5-1.5 mm) and cumulus clinopyroxene of equal dimensions (Fig. 38F). These mafic cumulus phases coexist with smaller (0.4-1.0 mm) euhedral to subhedral cumulus plagioclase laths. This rock type may also be referred to by some as "picritic". The plagioclase and clinopyroxene commonly display zoning, and thus this cumulate is best thought of as a mesocumulate (cumulate rock retaining part of its original magmatic porosity). The new crystallization sequence differs only from that of the olivine:clinopyroxene crystallization order, that constitutes most olivine clinopyroxenite and wehrlite, by the introduction of a new cumulus phase-plagioclase. It is not difficult to visualize the comagmatic relationship of the olivine-clinopyroxene cumulate in Figure 38A with that of the olivine-clinopyroxene-plagioclase cumulate in Figure 38F. The composition (Mg# = $Mg/(Mg+Fe^{2+})$) of olivine and clinopyroxene from this horizon is also compatible with some of the more fractionated peridotite within the Tatamagouche Complex. The disappearance of cumulus olivine from the crystallization sequence gives rise to clinopyroxene-plagioclase cumulates within this horizon; the proportion of these two cumulus phases determines whether anorthositic (Fig. 38G) or gabbroic (Fig. 38H) cumulates develop. Accessory levels of intercumulus orthopyroxene (bronzite) occur in some samples. The anorthositic gabbro may also contain intercumulus patches of sulphide mineralization, as is represented by the opaque patches in Figure 38G. In addition, these plagioclase-rich cumulates, particularly sulphide-bearing samples, are altered relative to other cumulates from this horizon. The anorthositic cumulates are coarser grained, particularly the cumulus plagioclase crystals, than other cumulates and can contain small amounts of intercumulus quartz.

Maple Creek gabbro, in particular the coarser-grained varieties, differs petrologically from the other gabbro in the complex by: a darker colour due to anomalous concentrations of Fe-Ti oxides, diverse textures and extreme grain size variations, and the presence of late stage magmatic amphibole and granophyric crystallization products. The coarse- to very coarse-grained variety associated with the sill on Tatamagouche Mountain is the most distinctive variety (Fig. 38I). Samples with plagioclase and clinopyroxene crystals exceeding 3 cm in length are not uncommon. These two phases are generally present in near equal proportions. The large plagioclase crystals commonly contain fine opaque inclusions, and are almost always sausseratized with clear albite patches. Clinopyroxene is of the augite-ferroaugite variety and may contain rims of late magmatic amphibole. Composite magnetite-ilmenite granules and skeletal crystals characterize this coarse-grained variety, as do interstitial granophyric patches. The Fe-Ti oxide concentration generally ranges from 3 to 9% but local oxide-enriched pockets (9-20%) occur. Apatite concentrations up to 1.2% may also be present associated with these granophyric areas as well as trace amounts of biotite, pyrite, and zircon. This coarser-grained variety has a pegmatitic character which generally occurs as irregular patches and lenses within medium-grained "diabasic" or ophitic-textured gabbro.

The medium-grained variety consists of approximately equal amounts of plagioclase and clinopyroxene, but may contain up to 9% disseminated Fe-Ti oxides. The finer-grained varieties are not unlike similar grain size marginal gabbro elsewhere in the belt. Had it not been for the crosscutting relationships and slightly darker colour due to anomalous Fe-Ti oxide concentrations, these finer grained varieties would be difficult to tell apart in the field. These fine-grained marginal zone gabbro and Maple Creek gabbro are discussed in the section dealing with the nature of the parental magmas associated with Triassic magmatism.

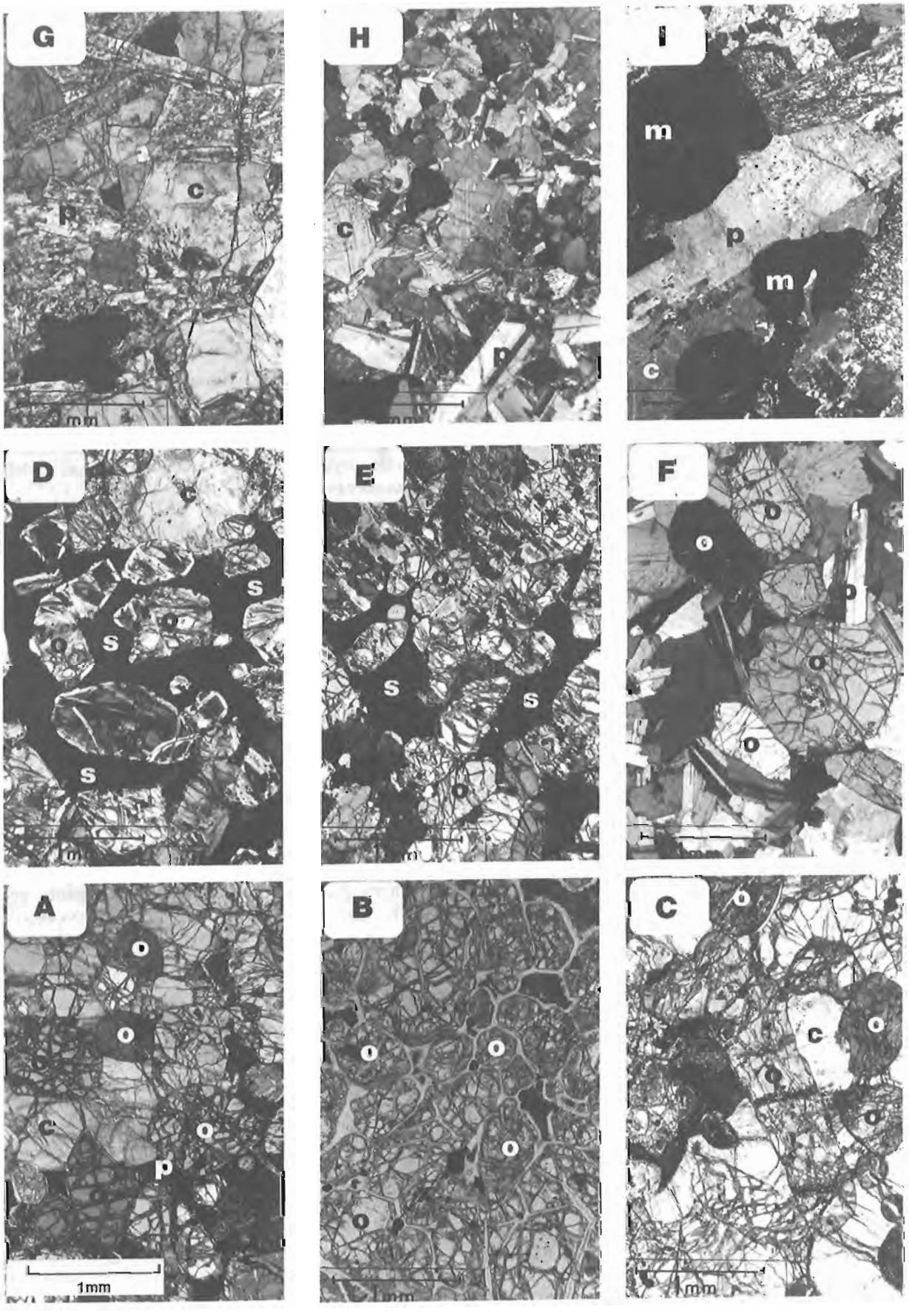
G
c
p
mm
H
c
p
I
m
p
m
c
D
c
s
o
s
o
s
E
o
s
s
o
F
o
o
o
o
A
o
o
c
o
p
1mm
B
o
o
o
o
C
o
c
o
o
o

Ultramafic. Members of the ultramafic zone consist of olivine clinopyroxenite, wehrlite, and feldspathic dunite. Olivine clinopyroxenite occurs in the basal portion of the ultramafic section. This rock type consists of olivine-clinopyroxene cumulate, with the crystallization order olivine:clinopyroxene±chromite. The relationship between cumulus olivine and clinopyroxene, and that of secondarily enlarged cumulus and intercumulus clinopyroxene, are illustrated in Figure 38A, as well as the presence of turbid intercumulus plagioclase. With an increasing proportion of cumulus olivine up section, the olivine clinopyroxene cumulate passes into the peridotite (wehrlite) field (Sabine, 1974) and the olivine takes on a distinctive elongated habit.

Some of the basal ultramafic rocks in the Tatamagouche Creek section are more fractionated than those from higher elevations in the ultramafic section. This up section Mg-enrichment is analogous to that recorded in the Quill Creek Complex (Fig. 16). Feldspathic dunite is also present in the basal portion of the ultramafic zone (Fig. 38B). This olivine-chromite cumulate contains only plagioclase as an intercumulus phase, and reflects the amount of original porosity (intercumulus space). Similar olivine cumulates with net-textured sulphides filling part of the intercumulus volume also occur in the basal portion of the ultramafic zone (Fig. 38D,E). Clinopyroxene is sparse in these sulphide enriched specimens. Accessory amounts of orthopyroxene (bronzite) occur in some samples.

Ni-Cu±PGE Mineralization

This mafic-ultramafic complex is one of the least explored and most underestimated intrusive complexes in the belt with respect to its potential to be a major repository of Ni-Cu-PGE+Au mineralization. Two significant Ni-Cu showings were discovered in the marginal zone gabbro during the early 1950s and confirm that the Ni-Cu-PGE metallogenic process, active in the northern section of the belt, was also operative within this complex. Unfortunately, most of the past Ni-Cu related exploration was confined to the portion of the complex west and northwest of Burwash Creek. Showings in this area occur at the gabbro-tuff (Station Creek Formation) contact and are somewhat similar to the sporadic semi-massive showings from the West zone of the Quill Creek Complex. Previous discussions related to marginal zone massive and semi-massive sulphide mineralization have clearly shown that this style of mineralization is best developed when the intrusion is in contact with the Permian Hasen Creek Formation sediments. Therefore, the development of this style of mineralization, even under these adverse contact conditions, and the extensive area of more favourable Hasen Creek Formation sediments along the northern intrusive contact east of Burwash Creek suggest that this body has significant economic potential. An exploration model based on the different styles of sulphide mineralization, their geographic distributions, and favourable contact relationships established at the Quill Creek Complex should be applied to the Tatamagouche Creek Complex.

Immiscible magmatic sulphide segregations.

Marginal gabbro. Due to the limited width and recessive nature of the marginal gabbro, material from this zone was discovered at only one locality during this investigation. In addition, the zone has only been uncovered twice since the early 1950s, and on both occasions it has been at the discovery site of Ni-Cu sulphide mineralization. The "Burwash Creek showing" is the most significant sulphide discovery to date, and occurs along the north bank of Burwash Creek, about 183 m upstream from the mouth of Tatamagouche Creek[1]. Unfortunately the presence of this showing could not be confirmed during this study and is thus not shown on Figure 36. Exploration records suggest that the previously exposed showing was approximately 6.1 by 1.5 m and occurred between "sill-like gabbroic bodies and latite porphyry bodies that intrude volcanoclastic rocks of the Station Creek Formation". The mineralization consisted of a narrow zone of disseminated sulphides and small lenses and patches of semi-massive pyrrhotite-pyrite-chalcopyrite-pentlandite. A grab sample of material containing approximately 50%

[1] CANMINDEX File – Burwash Creek Ni-Cu occurrence (Glen Group), NMI accession #115/G/06/Ni/001 and Northern Cordillera Mineral Inventory-1972 – Archer, Cathro & Associates Ltd.

Figure 38. *Photomicrographs of selected lithologies from the Tatamagouche Creek Intrusive Complex. GSC 1995-106K (**A**) HDB-88-TAT-20a. Olivine clinopyroxenite or olivine-clinopyroxene±chromite cumulate. Cross-polarized light. (**B**) HDB-88-TAT-41. Feldspathic dunite or olivine± hromite cumulate with a groundmass of intercumulus plagioclase. Plane-polarized light. (**C**) HDB-88-TAT-18a. Peridotite (wehrlite) with elongated olivine and discrete crystals of clinopyroxene of both a cumulus and intercumulus origin. Cross-polarized light. (**D**) HDB-88-TAT-53a. Peridotite with coarse net-textured sulphide domains. Plane-polarized light. (**E**) HDB-88-TAT-54b. Peridotite with interstitial sulphides giving rise to localized net-texture. Plane-polarized light. (**F**) HDB-88-TAT-16a. Olivine gabbro or olivine-clinopyroxene-plagioclase cumulate from the lower portion of the ultramafic zone. Cross-polarized light. (**G**) HDB-88-TAT-60c. Altered gabbro or clinopyroxene-plagioclase cumulates from the lower portion of the ultramafic zone. Cross-polarized light. (**H**) HDB-88-TAT-21. Fresh gabbro or clinopyroxene-plagioclase cumulate from the lower portion of the ultramafic zone. Cross-polarized light. (**I**) HDB-88-TAT-24b. Coarse-grained Maple Creek gabbro or magnetite gabbro. Note the large magnetite crystals. Cross-polarized light. o = olivine, c = clinopyroxene, x = chromite, p = plagioclase, s = sulphide, m = magnetite.*

sulphides assayed 3.6% Ni and 0.7% Cu. The high Ni/Cu ratio of this mineralization and grade suggest that it is similar to the high-grade Ni-sulphide ores from the Quill Creek Complex, and will undoubtedly have the same anomalous PGE concentrations, in particular the high melting point elements: Os, Ir, Ru, and Rh. Three diamond-drill holes were put on this showing by Hudson Bay Mining and Smelting Ltd. in 1954, but the results of the intersections are not available. In 1967, Alice Lake Mines carried out geological mapping, ground magnetometer and electromagnetic surveys over the property and showing. Several anomalies were indicated including anomaly "A" which extends west from the showing. Traces of chalcopyrite with pyrite and pyrrhotite were also found 184 m west and 180 m northwest of the main showing and also have EM conductors located near them. Two diamond-drill holes (totalling 183 m) were drilled in anomaly "A", with disappointing results, in September of that year.

The "Tatamagouche Creek showing" is the second most important site of gabbro-hosted mineralization and occurs along the south bank of Tatamagouche Creek, approximately 1100 m north of the creek mouth. An EM conductor is also located near this showing. A limited geochemical soil survey, carried out in 1972 by Alice Lake Mines Ltd., outlined a Cu-Ni zone 427 m by 752 m. Four grab samples of this gossaned material assayed from 0.01 to 0.58% Cu and 0.01 to 0.13% Ni. Halferdahl & Associates found that the conductor and geochemical anomaly coincided with the basal contact of the intrusion.

A portion of this showing, unearthed and sampled in 1988, contains a basal concentration of semi-massive sulphides overlain by gabbro with 1.3 to 13% disseminated sulphides. Ni grades for gabbro and semi-massive sulphide mineralization range from 200-3200 ppm and 7000-11 000 ppm, respectively. Corresponding Cu values vary from 45 to 8000 ppm and 8500 to 20 000 ppm (Fig. 79A, B). These grades are significantly higher than that of grab samples taken by Alice Lake Mines Ltd. It is possible that the Alice Lake Mines Ltd. samples came from mineralized country rock tuff directly opposite this location, on the north side of Tatamagouche Creek. This volcanogenic country rock mineralization is Cu-rich and Ni-poor and also occurs at one locality on the north side of the creek near the inferred base of the complex.

Ultramafic. Ultramafic-hosted mineralization was only observed at a couple of localities as sporadic net-textured sulphide patches within peridotite (Fig. 38D, E), and seldom exceeded 2% by volume. These net-textured patches are also sporadic and attain maximum dimensions of 3 cm in diameter.

Geochemically, gabbroic and ultramafic rocks demonstrate some interesting trends and associations. The Ni vs. S trend for all non-cumulate gabbro and gabbro-hosted mineralization displays a strong chalcophile pattern. The one noted exception is the weakly mineralized anorthositic gabbro from the cumulate gabbro horizon. Ni enrichment associated with the cumulate gabbro horizon is undoubtedly a function of increasing amounts of modal olivine and clarifies the discordant trend associated with the ultramafic rocks. Although present in much lower concentrations, Co (Fig. 79C) displays a similar trend to Ni, with respect to the various rock types, and similarly demonstrates both the chalcophile and lithophile character of these elements. The chalcophile character of Cu with respect to all rock types is evident from Figure 79B. The As content (Fig. 79D) of the various rock types is highly variable and ranges from 0.15 to 100 ppm. Se demonstrates the strongest affinity for S of all the elements investigated (Fig. 91A), and could apart from the sulphur content be used as a reliable measure of the amount of sulphide in the respective samples. The elements Bi, Sb, and Te display no discernable trends (Fig. 91B, C, D) with respect to S and are not obviously chalcophile in nature.

The S/Se ratios for most of the investigated samples are in the 1000 to 5000 range. The extreme S/Se ratios (≥20 000) associated with the mineralized country rock with >1.0% S clearly demonstrate that little if any of this country rock sulphur was assimilated by the Tatamagouche Creek magma(s). The possible contribution of this volcanoclastic-derived country rock sulphur is further diminished on the basis of the sulphur-isotope compositions associated with the marginal gabbro and ultramafic-hosted mineralization. As the isotopic composition of the country rock sulphur is generally heavier than that of sulphides hosted by intrusive rocks, assimilation of extreme amounts of this sulphur would not result in compositions associated with sulphides in the magmatic rocks (Fig. 102C).

Although the number of mineralized specimens from the Tatamagouche Creek Complex is limited, it appears that the PGE+Au levels (Fig. 113, 125, 135A) in analyzed samples are low compared to that from other intrusions. All of the mineralized samples, however, are from the recently unearthed Tatamagouche Creek showing. This mineralization is unlike most other Ni-Cu occurrences in the belt in that it is Cu-rich and has high Cu/(Cu+Ni) ratios (Fig. 135B). The Cu-rich nature of this noble metal depleted mineralization and the presence of Ni-rich mineralization elsewhere in the complex (i.e. Burwash Creek showing, 3.6% Ni, 0.70% Cu), suggest that this Cu-rich variety may be related to the immiscible chalcopyrite-rich segregations associated with some of the Quill Creek ores. The S/PGE+Au vs. S/Se x 1000 plot (Fig. 135C) once again demonstrates that the PGE+Au content of sulphides increases in concert with Se enrichment in the sulphides.

Duke River Intrusive Complex

This complex differs from those previously described in that it contains a greater thickness of gabbroic rocks along the upper, northern margin of the complex, and it contains the first significant concentration of stratiform magmatic sulphides in gabbroic rocks which are believed to be related to the Maple Creek gabbro magmatic suite.

Location, history, and physiography

The centre of the complex is located at latitude 61°12'N and longitude 139°00'W on NTS map sheet 115G/2 (Fig. 4, 5, 39). Only the eastern half of the complex was investigated during

this study (Fig. 39). The southern and western boundaries of the complex adjoin the Kluane National Park and an Indian Land Claim, respectively, both of which are closed to mineral exploration at the present time. The nearest road access lies 13 km to the northeast at Destruction Bay, a small community on the Alaska Highway, 261 km by road from Whitehorse. Access during the present study was by helicopter operating from a seasonal base at Burwash Landing, 13 km north of the property.

To date only limited exploration has been conducted on this body. The complex was staked as part the Duke claims (#Y18454) in June 1967 by Newmont Mining Limited on the basis of GSC aeromagnetic data. Limited prospecting and silt sampling was conducted later in that year. On July 22, 1987 20 claims were staked by Kluane Joint Venture (Chevron Minerals Limited and All-North Resources Ltd.) The property was optioned to Rockridge Mining Corporation which subsequently added another 24 claims and conducted a prospecting and soil geochemistry survey in 1987 under the direction of Archer, Cathro & Associates (Eaton, 1987).

The study area (Fig. 39) covers most of two south-facing drainages that flow into Duke River. Both drainages were occupied by glaciers until recently and have near vertical cirques at their heads, step talus slopes on their flanks, and thick deposits of glacial till on their floors. Outcrop is limited to ridge tops, actively eroding creek cuts and cirque faces. Elevations range locally from 1700 m in creek bottoms to 2250 m on ridge tops. Vegetation is restricted to scattered clumps of slide alder in creek bottoms and grass, moss, and lichen on glacial terraces and lower slopes.

Structure and stratigraphy

The oldest rocks in the area belong to the Permian Hasen Creek Formation and include thin-bedded argillite and minor basalt flows in the lower portion with an upward change toward limestone. The Hasen Creek Formation is intruded by rocks of the Duke River Intrusive Complex. This sill-like body consists of a basal ultramafic zone and an overlying gabbroic zone that strikes northwesterly and dips 50-60° northeast. The ultramafic zone is composed mainly of dark green to black, partially to totally serpentinized peridotite that attains a thickness of at least 200 m. A 20-70 m thick screen (roof pendant ?) of Permian sediments appears near the top of the ultramafic zone in the central portion of the area (Fig. 39, 40). This material is similar to that of the country rock associated with the major intrusive bifurcation adjacent the western boundary of the study area and the basal zone of the complex. Sedimentary rocks adjacent the ultramafic rocks commonly exhibit moderate to intense degrees of quartz-carbonate alteration.

Marginal zone gabbro was not observed in the footwall of the ultramafic zone, but due to poor exposure, this is not unexpected and Quill Creek-type marginal gabbro and associated mineralization may occur along the base of the complex. Nevertheless, the thickest section of gabbroic rocks in the belt is associated with horizons overlying the ultramafic zone of this complex. Field and laboratory evidence suggest that this zone consists of three different generations of coeval gabbro complexly intermingled due to multiple intrusive and assimilation events.

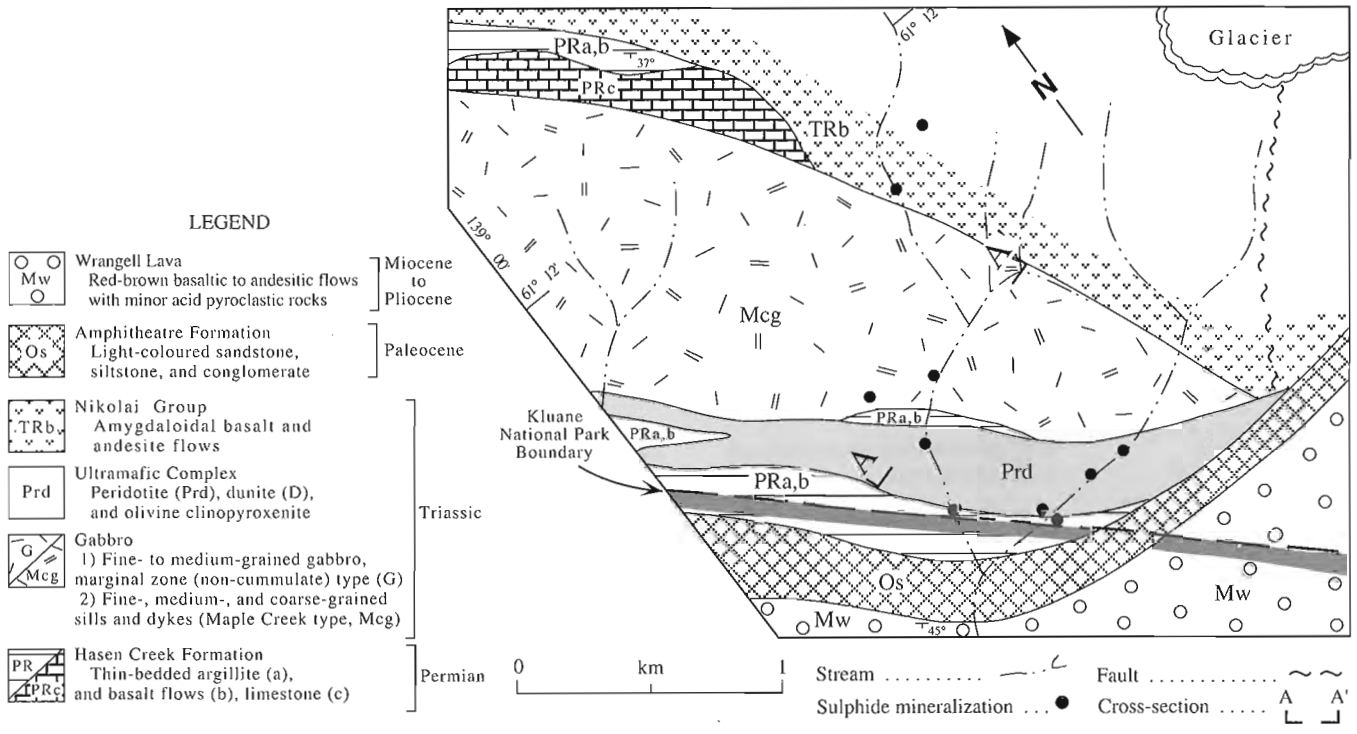

Figure 39. *Generalized geological map of the Duke River Intrusive Complex.*

To the east the intrusive units extend beneath the younger volcanic and sedimentary cover, whereas to the west the gabbroic portion becomes thicker and the ultramafic portion appears to pinch out (Fig. 39).

The intrusive complex, and enveloping Permian strata, are unconformably overlain to the north and east by dark green and maroon amygdaloidal basaltic rocks of the Triassic Nikolai Group. To the south, the area consists of a Tertiary sequence that is floored by Amphitheatre Formation light coloured sandstone, siltstone, and conglomerate. These strata are in turn capped by Wrangell Lava consisting of red-brown basaltic to andesitic flows with minor white to yellow acidic pyroclastic horizons.

Structural modifications due to faulting have not affected this complex to the degree that it has in most other comparable bodies in the belt. However, regional scale mapping (Muller, 1967) suggests that the complex occupies the southern limb of a northwest-trending syncline whose axis is centred 2 km to the north. The more northerly Halfbreed Creek Intrusive Complex may represent the folded and eroded remnants of the northern extension of the Duke River Igneous Complex (Fig. 4, 43).

Petrology

The ultramafic zone of this complex differs little from others in the belt; the gabbro zone, however, contrasts significantly in that it appears to consist of three different generations of multiply intruded, and complexly intermingled coeval gabbro. The youngest gabbroic intrusive event, believed to be related to late-stage Maple Creek gabbro magmatism, gave rise to multiple intrusions in the form of sill-like (and occasionally dyke-like) bodies consisting of fine- to medium-grained ophitic gabbro. This later intrusive event can be distinguished from earlier events by the ubiquitous plagioclase alteration and ophitic texture associated with this new lithological group, and the unequivocal crosscutting field relations. These voluminous, late stage gabbroic rocks are believed to be related to middle Triassic Nikolai volcanism, and have not been recognized in the previously described complexes to the northwest. All remaining mafic-ultramafic complexes in the belt north and east of this locality contain this late stage gabbroic phase.

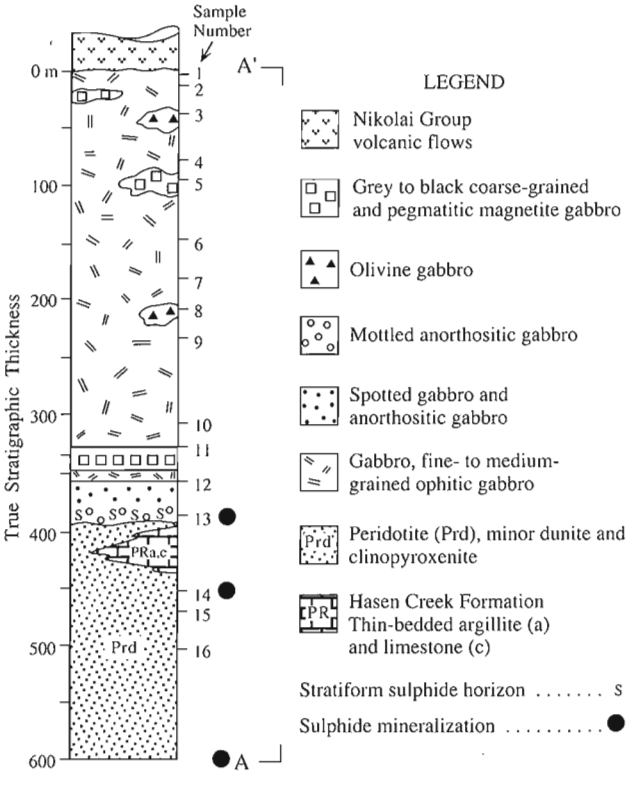

Figure 40. *Schematic stratigraphic section of the Duke River Intrusive Complex.*

Gabbro. Marginal zone gabbro was not directly observed near the base of the complex due to inadequate exposure. Nevertheless, quenched and highly inequigranular specimens reminiscent of Quill Creek Complex marginal gabbro occur locally near the top of the gabbroic section, suggesting that an upper marginal zone may once have been present with sporadic inclusions of this material throughout the gabbroic section. The fine-grained marginal zone specimens appear similar to the textural equivalents associated with late-stage Maple Creek gabbro magmatism and thus the two are sometimes indistinguishable in the field.

The greatest volume of gabbroic rocks in the complex consists of fine-, medium-, and coarse-grained ophitic gabbro, magnetite gabbro, and subordinate anorthositic differentiates, all believed to be represent different stages and products of Maple Creek gabbro magmatism.

The lower half of the gabbro zone (200-390 m) contains the most orderly distribution of basic lithologies (Fig. 40). The basal 35 m interval of this zone consists of a mixture of medium-grained gabbroic and anorthositic differentiates, and a thin stratiform sulphide-enriched horizon. Although contact relations are rather poorly exposed, the cumulate-like mottled anorthositic gabbro and gabbro may represent the earliest differentiates, and pass upwards into spotted varieties subsequent to the development of a thin intervening sulphide-enriched horizon. The mottled anorthositic gabbro is medium-grained plagioclase cumulates containing chadocrysts of plagioclase (1-2 mm laths) enclosed in much larger clinopyroxene oikocrysts of an intercumulus origin (Fig. 42G).

The stratiform sulphide horizon demarcates an important phase and form contact (Irvine, 1982) cumulate horizon. At this level the cumulate crystallization order changes from that of predominantly plagioclase cumulates to plagioclase-clinopyroxene-sulphide cumulates (Fig. 42H). The sulphide content of this horizon varies from 5 to 8%, and occurs mainly as intergranular fillings and as coarse irregular segregations. This horizon marks not only the brief introduction of sulphide as a new cumulate phase but also clinopyroxene as a permanent cumulate phase in the overlying strata. The spotted texture in the overlying anorthositic gabbro is the result of clinopyroxene crystallization under cumulate rather than intercumulus conditions.

A 12 m thick medium-grained gabbro interval separates the top of the cumulate-derived spotted gabbro, sulphide-enriched gabbro, and anorthositic gabbro horizon from that of the overlying grey to black, coarse-grained, and pegmatitic magnetite gabbro of a non-cumulate origin. This intervening gabbro is fairly representative of the bulk of the overlying (0-330 m) gabbroic section of the complex and is discussed briefly. This gabbroic lithology is generally a fine- to medium-grained hypidiomorphic inequigranular rock consisting of approximately equal amounts of plagioclase and clinopyroxene. Magnetite generally comprises only 2 to 3% of the mode (Fig. 42D), but is accentuated by its light coloured altered matrix. Macroscopically the rock has a distinctive ophitic texture and chalky greenish-white hue due to pervasive alteration of plagioclase. One of the most pronounced microscopic features is the marked degree of zoning (undulous, normal, hourglass) and twinning of the clinopyroxene, and the general absence of orthopyroxene; nonetheless, it should be noted that rare grains of orthopyroxene have been identified (with the aid of the electron microscope) and the relative lack of alteration of clinopyroxene compared to that of coexisting plagioclase. Plagioclase is always extensively altered to albite and clay minerals, whereas associated clinopyroxene demonstrates only mild degrees of marginal uralitization, if present at all.

Grey to black, coarse-grained, and pegmatitic magnetite gabbro occurs within the stratigraphic column in two forms: as a thin stratiform horizon in the 330 to 347 m interval and as irregular segregation and inclusion-like bodies within the upper portion of the magmatic stratigraphic succession (Fig. 40). This magnetite gabbro is identical to that previously described from the Tatamagouche Complex and may be related to Maple Creek gabbro magmatism. This lithology has a hypidiomorphic inequigranular texture and consists of equal amounts of zoned (normal) clinopyroxene (Mg# = 0.7-0.5), plagioclase (Ca# = 0.58-0.40), and contains 4 to 9% Fe-Ti oxides. In the coarser grained lithologies the oxides generally occur as large skeletal crystals associated with interstitial spaces (Fig. 42I). Anomalous concentrations of interstitial granophyre (up to 12%) are also found near these oxide-rich areas (Fig. 42F). The pegmatitic rocks also contain higher concentrations of apatite, zoisite, phlogopite, amphibole, and zircon as interstitial crystallization products, than their medium-grained lithological equivalent. In most samples plagioclase is extensively altered to albite; however, associated clinopyroxene is only marginally altered to uralite.

The upper half of the gabbro interval (0-200 m) contains strong evidence for multiple intrusive events during its magmatic history. Within this stratigraphic interval numerous field localities contain fine-grained quenched horizons with chilled material similar to Figure 42A. These crudely conformable horizons seldom exceeded 10 m in thickness and are separated by wide stratigraphic intervals of medium-grained gabbro similar to those described above. Inclusions of olivine gabbro, as well as irregular bodies of grey to black coarse-grained and pegmatitic magnetite gabbro several metres in diameter, are present (Fig. 40) in this interval. At some localities these bodies look like inclusions of material similar to that from the 347 to 350 m level, whereas, at others they appear as pegmatitic in situ crystallization products. The olivine gabbro inclusions are similar to the olivine gabbro cumulates previously described from the Tatamagouche Complex (Fig. 38F). Associated picritic material (Fig. 41B) also occurs as inclusions within this interval. The olivine and pyroxene content of these medium-grained lithologies is approximately 35% each, with plagioclase making up the remainder. Both olivine and pyroxene have a distinctive cumulate character, whereas, plagioclase is clearly of a cumulus origin in the gabbro and intercumulus in the picrite. It is clear from the textures, mineralogy, and cryptic compositions that the olivine gabbro and picritic lithologies represent cognate zenoliths derived from the ultramafic zone by subsequent ingressions of new magma. It would appear that most of these new magmatic pulses intruded as sill-like bodies, however, thin dykes of compositionally similar material are present.

Ultramafic. Olivine-rich cumulates in the form of peridotite (wehrlite) and feldspathic dunite comprise the bulk of lithologies in the ultramafic zone. Field mapping and the pyroxene-poor nature of the ultramafic cumulates within this zone suggest that the exposed portion represents the top of the ultramafic zone. Peridotite is commonly black to dark-green and has a marked poikiolitic texture due to the development of large (0.5-2 cm) oikocrysts of clinopyroxene (Fig. 41H). Some samples also contain cumulus olivine with a pronounced igneous lamination (Fig. 41I). The more olivine-rich ultramafic rocks tend to be more green and lack oikocrysts. Serpentinization, which is pervasive in all the ultramafic rocks, also tends to accentuate the greenish colour of the more olivine-rich rocks. Net-textured sulphide mineralization is sporadically developed through the ultramafic sequence and provides one of the few mineralogical and textural variants (Fig. 41G). A slight pyroxene enrichment occurs in lithologies towards the base of the ultramafic sequence.

Ni-Cu±PGE mineralization

The Duke River Complex contains a number of interesting sulphide showings within gabbro, ultramafic, and the adjacent country rock. However, unlike the gabbro-hosted mineralization from the previously mentioned complexes in the belt, the Duke River gabbro contains a new type of immiscible magmatic sulphide mineralization not described previously. It is believed to be the product of crustally contaminated cumulates derived form Maple Creek gabbro magma. Assays, metal ratios, and sulphur-isotope data for a range of mineralized and unmineralized samples from the complex have been graphically summarized in Figures 80, 92, 103, 114, 126, and 136. Highly anomalous stream sediment sample containing 791 ppm Ni, 254 ppm Cu, and 74 ppm Co was recorded from drainage covering this area by the Geological Survey of Canada Reconnaissance Stream Sediment Survey (Open File 1362). Nickel and cobalt values are higher, and copper is slightly lower, than values obtained from a sample taken directly downstream from the Main zone at the Wellgreen Ni-Cu-PGE deposit. This in conjunction with the discovery of moderate to strong geochemical anomalies in the soil, and sulphide occurrences are encouraging and justify further exploration of this complex.

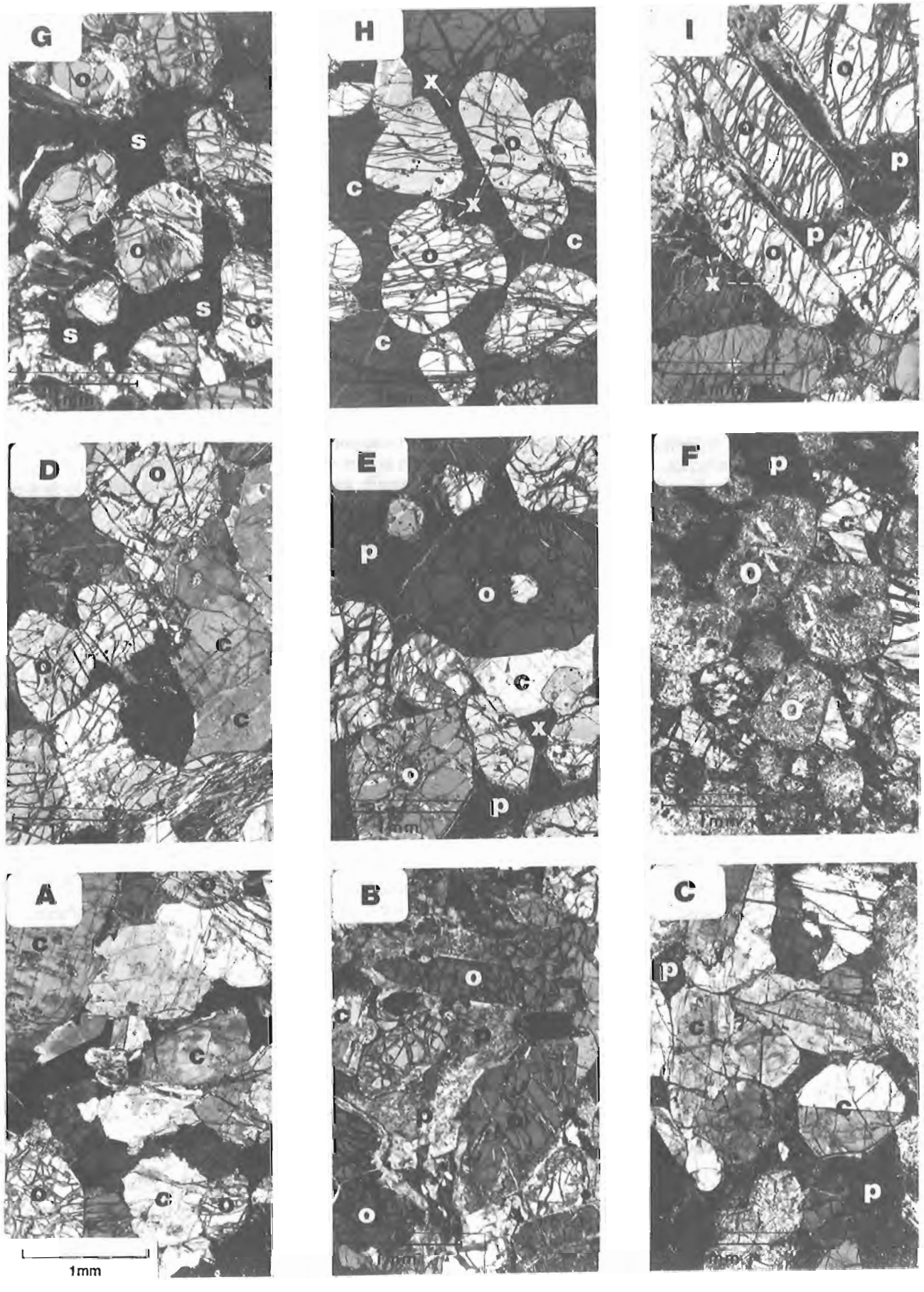
G
H
I
D
E
F
A
B
C
1mm

Immiscible magmatic sulphide segregations.

Marginal gabbro. Due to lack of exposure, this style of mineralization was not observed directly within the Duke River Complex, but its presence is inferred based on the geology of the complex and the discovery of "marginal zone"-type gabbro "float" containing malachite, chalcopyrite, and pyrrhotite on fractures and as disseminations.

Maple Creek gabbro. The presence of stratiform sulphides at the interface between spotted and mottled gabbroic cumulates is a distinctive new type of sulphide mineralization and cumulate stratigraphic marker. This mineralization was discovered by the author in 1988. Generally the horizon contains 5 to 8% disseminated sulphides and can be traced along strike for over 400 m. The initial discovery was made at the site marking the location of the most southerly gabbro-hosted sulphide showing west of the stream cutting the central portion of the study area (Fig. 39). Unfortunately, the true thickness of this mineralization was difficult to ascertain due to limited exposure and time spent exploring the area. Nevertheless, intersection with the stream cut in the central portion of the area indicates that it is a minimum of 3 m thick.

Unlike the marginal zone gabbro mineralization, this new style of mineralization is very rich in pyrite. The sulphide mineralogy is in decreasing order of abundance: pyrite, chalcopyrite, pyrrhotite, pentlandite, galena, and sphalerite. In outcrop, macroscopic grains of galena 1-2 mm in diameter occur in some coarser-grained sulphide segregations.

Assays of the mineralized material with 1 to 3 wt.% S contain 40-72 ppm Ni, 27-150 ppm Cu, ≤6 ppb Pt, ≤5 ppb Pd, and ≤7.9 ppb Au. Mineralized samples are poor in metals (Fig. 80, 92, 114). The $\delta^{34}S$ composition of the sulphides ranges from -6.2 to -15.2‰ (Fig. 103). The wide range and high mean S/Se ratio ($\overline{X}$ = 12 822) along with the ^{32}S-enriched isotopic composition and range demonstrates that the bulk of the sulphur in these samples has been derived from a crustal rather than mantle source. There is a relatively strong correlation between the S/Se content of a specimen and the associated PGE+Au content (Fig. 136D) and the S/PGE+Au ratio (Fig. 136C).

Ultramafic. Sporadic patches of net-textured sulphide mineralization have been noted in peridotite at five localities within the ultramafic zone. These patches are very irregular in size, form, and distribution. They comprise areas that seldom exceed a few centimetres in width and generally occur in samples containing about 0.5% background sulphide. In thin section, the more sulphide-enriched portions appear to consist of olivine-sulphide-chromite cumulates (Fig. 41G). Inspection of the S vs. metal plots (Fig. 80, 92, 103, 114) reveals the following range of concentrations: Ni (1100-1400 ppm), Cu (38-320 ppm), Co (110-130 ppm), Cr (1500-4000 ppm), Pd (3-48 ppb), Pt (1-11 ppb), and Au (<1 to 2.2 ppb).

Hydrothermal (remobilized ?) mineralization. Hydrothermal mineralization was not observed by the author in the Duke River Complex during the course of his reconnaissance investigation of this body, but during the 1987 field season Archer, Cathro and Associates (1981) Limited discovered a lens of massive pyrrhotite, up to 1 m wide, at the base of a creek bed within intensely quartz-carbonate-altered sedimentary rocks some 50 m below the southern boundary of the ultramafic zone (Fig. 39). Up to 5% disseminated arsenopyrite is present in some of the quartz-carbonate-altered rocks occurring between the lens and the inferred base of the complex (Eaton, 1987).

Halfbreed Creek Intrusive Complex

The Halfbreed Creek Complex is rather unique in that it is the only complex in the belt that provides an opportunity to investigate a thick succession of ultramafic cumulates that have been relatively unaffected by serpentinization. Also, it is one of the few intrusive centres that furnishes unequivocal field evidence for the late stage Maple Creek gabbro magmatic event.

Location, history, and physiography. The Halfbreed Creek Complex is located at latitude 61°15'N and longitude 139°00'W on NTS map sheet 115 G/2 (Fig. 4, 43). The centre of the area is approximately 11 km west-southwest of the

Figure 41. *Photomicrographs of representative mafic and ultramafic cumulates from the Duke River, Halfbreed Creek and Chilkat intrusive complexes. GSC 1995-106F (**A**) HDB-88-HB-18. Olivine clinopyroxenite or clinopyroxene-olivine cumulate. Halfbreed Creek Complex. Cross-polarized light. (**B**) HDB-88-DK-3. Picrite to olivine gabbro. Olivine-clinopyroxene-plagioclase cumulate. Duke River Complex. Cross-polarized light. (**C**) HDB-88-CHI-3b. Mela-gabbro to feldspathic pyroxenite. Chilkat Complex. Cross-polarized light. (**D**) HDB-88-HB-18b. Fresh wehrlite or olivine-clinopyroxene±chromite cumulate. Halfbreed Creek Complex. Cross-polarized light. (**E**) HDB-88-HB-13. Feldspathic peridotite (wehrlite) or olivine-clinopyroxene±chromite cumulate with abundant intercumulus plagioclase. Halfbreed Creek Complex. Cross-polarized light. (**F**) HDB-88-CHI-11. Serpentinized peridotite. Note that the olivine is completely serpentinized, but clinopyroxene is affected little by the alteration. Chilkat Complex. Plane-polarized light. (**G**) HDB-88-DK-15x. Fresh olivine in net-textured peridotite. Duke River Complex. Cross-polarized light. (**H**) HDB-88-HB-10a. Poikiolitic peridotite with cumulus olivine and chromite included in large intercumulus clinopyroxene grains. Halfbreed Creek Complex. Cross-polarized light. (**I**) HDB-88-HB-12. Elongated olivine crystals in fresh peridotite. Halfbreed Creek Complex. Cross-polarized light. o = olivine, c = clinopyroxene, x = chromite, p = plagioclase, s = sulphide.*

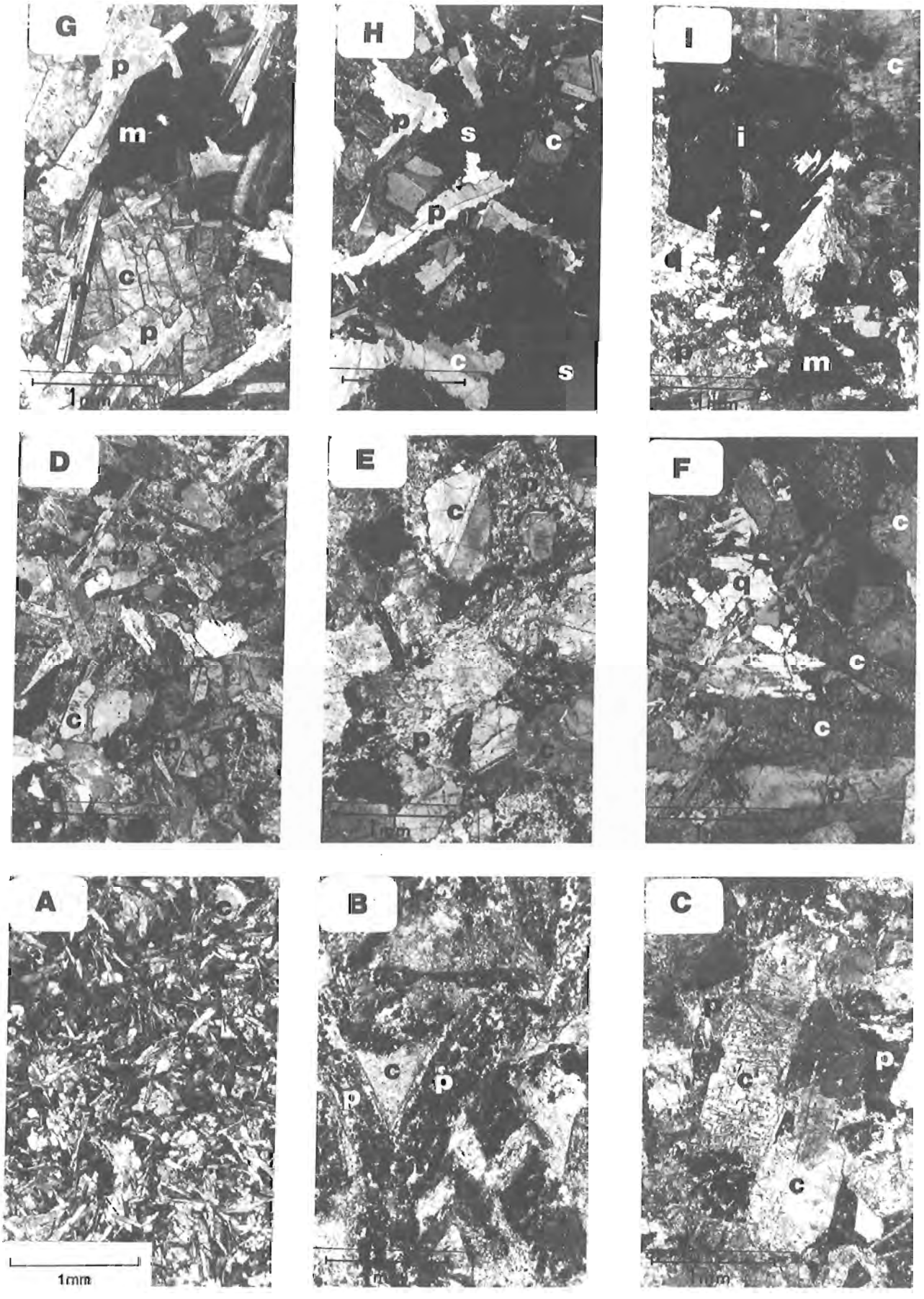
G
p
m
c
p
1mm
H
p
s
c
p
c
s
I
c
i
q
m
D
c
E
c
p
1mm
F
c
q
c
c
A
c
1mm
B
c
p
p
C
p
c
c

community of Destruction Bay. The nearest road access lies 10 km to the north at mile post 1080 on the Alaska Highway. Access to the area can be made on foot along either Lewis Creek or Halfbreed Creek or by helicopter from Burwash Landing.

Initial interest in the ultramafic-mafic complex resulted in staking of the RAM claims (# 63758) in November 1952 by Yukon Exploration and Development Corp., which optioned the property to Conwest. The Halfbreed Creek area was mapped by J.R. Woodcock in 1953 at a scale of 1 inch = 2500 feet (Department of Indian and Northern Affairs, Geological Services Division, unpublished map). Newmont Mines Limited staked three blocks of claims (Duke #Y18454) in June 1967 on the basis of Geological Survey of Canada aeromagnetic data. The claims were situated 3.2 km northeast, immediately south, and 4 km northwest of the RAM property. Prospecting and silt sampling were carried out later in the same year[1].

The complex is confined to a rugged northwest-trending ridge crest and north-facing slope of near continuous outcrop and talus flanks, in an area stretching from near the headwaters of Lewis Creek in the east to Halfbreed Creek in the west (Fig. 43). Local elevations range from 1500 m in creek bottoms to 2325 m at ridge crests. Vegetation is restricted to moss and lichen on the lower slopes.

Structure and stratigraphy. The bulk of the area is underlain by moderate to steeply dipping, northwest-trending folded sediments of the Permian Hasen Creek Formation (Fig. 43). Units of this formation consist almost exclusively of argillite, tuff, and chert and may represent strata from the lower portion of the Hasen Creek Formation. These sediments have been intruded by a somewhat conformable, northerly dipping (55-60°), irregular shaped sill-like body of ultramafic rocks of Triassic age. The main mass has a strike length of at least 5.0 km and attains a maximum thickness of 800 m in the western portion of the complex, west of Lewis Creek. Contact relations with the enclosing chert are obscured by talus cover. Lateral continuity of the ultramafic rocks becomes ambiguous within 0.5 to -1.0 km of Lewis Creek due to Pleistocene and Recent moraine cover. Nevertheless, it is inferred that the ultramafic outcrop east of Lewis Creek is a continuation of the western mass.

The ultramafic portion of the complex generally appears as a black to greenish-black, blocky, massive, poikolitic peridotite (wehrlite) with subordinate olivine clinopyroxenite. The poikiolitic variety characteristically contains large (1.0-2.0 cm in diameter) oikocrysts of clinopyroxene set in a highly pocked matrix of recessively weathered olivine. Crude layering in the form of 2 to 3 m wide alternating bands of feldspathic peridotite (10-15% intercumulus plagioclase) and peridotite to weakly dunitic rocks occur locally. The more dunitic areas are accentuated by a greenish hue imparted by a greater volume of serpentinized olivine. Olivine-clinopyroxenite appears to be more abundant near and along the ridge crest (basal portion of ultramafic zone ?) and decreases in frequency towards the north (up section ?). Faults and rock slides commonly contain slickensided surfaces of antigorite.

Discordant gabbroic bodies intrude the ultramafic mass in the eastern and central portion of the complex. These younger intrusions are particularly abundant in the eastern portion of the main mass of the complex where they intrude as dyke and plug-like bodies. Lithologically these bodies are identical to what has previously been referred to in the Duke River Complex as Maple Creek gabbro. A number of textural varieties of this gabbroic material occurs in a single outcrop. The fine- to medium-grained variety tends to be ophitic near the intrusive margins and grades into more feldspathic lithologies farther from the contact. The more feldspathic varieties have a distinctive spotted, and in some cases mottled, appearance resulting from the crystallization of round ophitic clinopyroxene crystals that may obtain diameters of up to 5 mm. Some of the dykes contain fairly well-defined core zones of pegmatitic gabbro and granophyric patches. Most specimens

[1] Mineral Policy Sector, Department of Energy, Mines and Resources, Ottawa, #150640, REF. NI 3 and Archer, Cathro & Associates; Northern Cordillera Mineral Inventory, 1977, 115 F, G, Occurrence No. 6.

Figure 42. *Photomicrographs of representative gabbroic rocks from the Duke River, Halfbreed Creek and Chilkat intrusive complexes. GSC 1995-106C (**A**) HDB-88-HB-1a. Quenched gabbro. Halfbreed Creek Complex. Cross-polarized light. (**B**) HDB-88-CHI-4. Highly altered medium-grained, weakly ophitic gabbro with clinopyroxene crystallizing in the interstitial space between plagioclase laths. Chilkat Complex. Plane-polarized light. (**C**) HDB-88-CHI-3. Altered mela-gabbro or plagioclase-clinopyroxene cumulate. Chilkat Complex. Cross-polarized light. (**D**) HDB-88-DK-2a. Fine- to medium-grained magnetite gabbro. Cross-polarized light. Duke River Complex. (**E**) HDB-88-CHI-4b. Altered subophitic gabbro with relatively fresh equant and twinned clinopyroxene. Cross-polarized light. Chilkat Complex. (**F**) HDB-88-DK-2b. Coarse-grained magnetite gabbro with interstitial granophyre. Cross-polarized light. Duke River Complex. (**G**) HDB-88-DK-1a. Medium-grained anorthositic gabbro with a spotted and mottled texture imparted by clinopyroxene. Note the abundance of cumulus-looking plagioclase laths. Cross-polarized light. Duke River Complex. (**H**) HDB-88-DK-19c. Mineralized gabbro or plagioclase-clinopyroxene-sulphide cumulate. Cross-polarized light. Duke River Complex. (**I**) HDB-88-DK-5b. Coarse-grained magnetite gabbro with skeletal ilmenite and a relatively altered groundmass. Cross-polarized light. Duke River Complex. c = clinopyroxene, p = plagioclase, s = sulphide, q = granophyre, m = magnetite, i = ilmenite.*

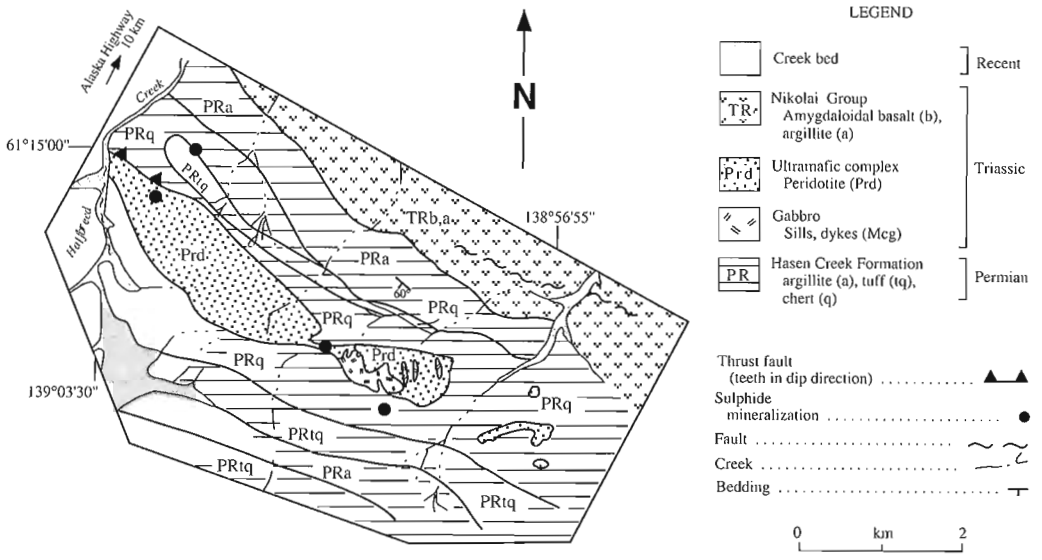

Figure 43. *Generalized geological map of the Halfbreed Creek Intrusive Complex and surrounds (modified from unpublished map by J.R. Woodcock, 1953).*

contain visible interstitial magnetite (2.0-3.0%) accentuated by the altered, chalky greenish-white feldspathic matrix. Although most of the gabbro is discordant to the trend of the ultramafic body, it is seldom found outside the confines of the intrusive complex and attests to late but coeval origins.

Permian and Triassic strata in the area are all unconformably overlain to the north by maroon and dark-green amygdaloidal basalt and andesite of the Triassic Nikolai Group.

Regional scale mapping (Muller, 1967) suggests the presence of a northwardly dipping thrust fault along the northern contact of the complex (Fig. 43). The highly irregular structural trends in the intervening area between the intrusive complex and the Nikolai Group to the north suggest the presence of folding in this area, however it is not shown in Figure 43. As was previously mentioned, the Halfbreed Creek Complex may represent the northern equivalent of the hidden portion of the ultramafic zone not exposed in the Duke River Complex.

The geological map in Figure 43 represents a generalized compilation of the Halfbreed Creek Intrusive Complex and its surrounds based on mapping of the area by J.R. Woodstock (unpublished map, 1953), Muller (1967), and by the author in 1988.

Petrology

Gabbro. The majority of gabbroic lithologies from this complex are of the fine- and medium-grained ophitic variety. Very fine-grained quenched varieties (Fig. 42A) occur along intrusive contact zones and pass into fine-grained (magnetite-bearing) gabbro (Fig. 42B). This variety quickly passes into medium-grained ophitic gabbro which is also magnetite bearing (Fig. 42G). Numerous spotted, mottled, and pegmatitic varieties have been noted proximal the intrusive contact zone. Since this gabbro is identical to that previously described from the Duke River Intrusive Complex no further discussion is necessary.

Ultramafic. As a result of the relatively unaltered nature of this intrusion, primary ultramafic cumulate mineralogical and textural features can be observed directly for the first time. Examination of the photomicrographs in Figure 41 reveals that the ultramafic cumulate sequence consists almost exclusively of olivine-chromite cumulates, olivine-clinopyroxene cumulates, and clinopyroxene-olivine cumulates and thus represents a number of ultramafic rock types. Orthopyroxene is very rare and never occurs as a cumulus phase. The clinopyroxene-olivine cumulate crystallization sequence displayed in Figure 41A gives rise to true olivine-clinopyroxenite. These medium-grained cumulates are the fresh equivalent of the olivine-clinopyroxenite horizon in the Quill Creek Complex that marks the introduction of the ultramafic zone. Note the high proportion of well defined cumulus clinopyroxene. As the proportion of cumulus olivine increases and clinopyroxene decreases, peridotite (wehrlite) develops (Fig. 41D). The disappearance of cumulus clinopyroxene is associated with the appearance of cumulus chromite and olivine-chromite cumulates (Fig. 41E, H, I). Variations in the mineralogical proportions, and volume of intercumulus material give rise to olivine-chromite cumulates and a number of different peridotitic lithologies. The abundance of intercumulus plagioclase (Fig. 41E) gives rise to what is referred to in the field as feldspathic peridotite, whereas, elsewhere a high proportion of intercumulus clinopyroxene (Fig. 41H)

produces poikolitic peridotite. Feldspathic peridotite may in turn pass into feldspathic dunite as the volume of intercumulus material decreases and olivine increases as a result of packing and subsequent postcumulus growth. In some cases the olivine crystals have been rotated and secondarily enlarged along the plane of bedding due to compaction (Fig. 41I).

Ni-Cu±PGE mineralization

No significant Ni-Cu-PGE mineralization has been discovered to date in this complex. The best mineralization recorded during this study returned assays of 6100 ppm Cu, 1 ppm Ni, 6 ppm Cr, 140 ppm Zn, 3.9 ppm Se, 13.9 ppm As, 3 ppb Pd, 11 ppb Pt, and 1 ppb Au. The mineralization is confined to a 5 m wide gossan in a fine- to medium-grained gabbro dyke in the central portion of the complex where the ultramafic body necks-out. The sulphide mineralization is of a disseminated nature and does not exceed 5% by volume. This mineralization is exceptionally depleted in the transitional metals Ni and Cr as adjacent unmineralized equivalents contain 59-91 ppm Ni and 270-280 ppm Cr. The relative similarity in major element chemistry but marked depletion of the transitional elements suggest that this mineralization is the direct result of localized crustal contamination of this Maple Creek gabbro magma by the surrounding Permian strata. This localized contamination gave rise to sulphides in a magma with a very low *R-factor* (mass ratio of sulphide to silicate magma).

Sulphide mineralization in ultramafic rocks, found at only one locality, occurs as sparse localized disseminations attaining a maximum concentration of 0.45%. Maximum metal concentrations associated with this mineralization are: 1200 ppm Ni, 130 ppm Cu, 11 ppb Pd, 17 ppb Pt, and 6 ppb Au.

A graphical summary of the geochemical data obtained from the Halfbreed Creek Intrusive Complex is provided in Figures 81, 93, 104, 115, and 137.

Dickson Creek Intrusive Complex

The Dickson Creek Complex contains a wide variety of mineralized mafic and ultramafic intrusive rocks and enclosing Permian sediments. Each of these mineralized lithological groups contained a characteristic geochemical association in terms of their base, noble, semi-metal, and sulphur-isotope compositions. Although this complex was only studied briefly (two days) and on a very limited scale, due to sparse exposure, poor weather conditions and the restrictive access to the park, it is clearly one of the most informative study areas in the entire belt with respect to the metallogeny of mafic and ultramafic rocks.

Location, history, and physiography

The centre of the complex is located at latitude 61°07'N and longitude 138°57'W on NTS map sheet 115 G/2 and occurs within the Kluane National Park (Fig. 4, 44). Access to the area may be made on foot along a rough trail beginning at the Duke River bridge, Milepost 1098 of the Alaska Highway, and following the general course of the river for approximately 40 km. During the dry season it may be possible to access the area by tractor following the gravel bars left during flood conditions along the river valley. Helicopter access may be obtained from a year round base at Haines Junction, 90 km to the southeast, and it may also be possible from a seasonal operation based at Burwash Landing, 28 km north of the property.

Sulphide mineralization was first discovered in August 1952 by G. Dickson and staked as the Kane claims (#63584) for Barymin Mines Ltd. Mapping, sampling and limited geophysical surveys were conducted by Barymin in 1953 and by Inco, under option, in 1954. Some diamond drilling is believed to have been carried out on the complex in 1958 by Prospectors Airways Ltd. The property was restaked as the Castille claims (#Y11782) in January 1967 by J.B. O'Neill and as the DC claims (#Y24753) in May 1968 by P. Versluce and H. Versluce, who built an access road and conducted trenching and mapping in 1969. The property was later included within the Kluane National Park and sold to the crown in October 1978[1].

The intrusive complex underlies a northwest-trending glacial terrace that parallels the Duke River valley (Fig. 44). The terrace has a gentle southerly slope, with elevations varying from 1470 to 1370 m in the study area, and is covered by moss and willow swales. The closest stands of timber are 4 km downstream along the Duke River. The study area is incised by a number of southerly draining streams and gullies that have cut through a mantle of overlying volcanic, sedimentary, and intrusive rocks. These glacial streams have created narrow gullies and valleys with precipitous walls and floors strewn with glacial fill, boulders, and volcanic ash, created by spring run-off conditions. Along the extreme southeastern margin of the complex, the erosive action of Dickson Creek and an unnamed northerly trending tributary, provides an excellent cross-section of this portion of the complex (Fig. 45). Dickson Creek, its tributaries, and all other water courses in the study area flow into the Duke River flood plain which generally occurs at an elevation of 1060 to 1220 m in the area (Fig. 44).

Structure and stratigraphy

The Dickson Creek Intrusive Complex is Triassic and confined to the Permian Hasen Creek Formation. This northwest-trending Permian formation consists primarily of argillite, limestone, tuff, and minor basaltic flows (Fig. 44) and dips steeply (80°) to the northeast. Along the northeast extremity of the complex gabbroic rocks are in contact with tuffaceous members of this formation. The tuffaceous rocks are dense, fine grained, and pale-green with a cherty appearance. Cliff faces exposed along the creek gulch have been weathered to a rusty almost red alteration product. Considerable oxidation has taken place along these faces.

[1] Mineral Policy Sector, Department of Energy, Mines and Resources, Ottawa, #506479, REF. NI 1 and Northern Cordilleran Mineral Inventory 1972; Archer, Cathro & Associates Ltd., Occurrence No. 5.

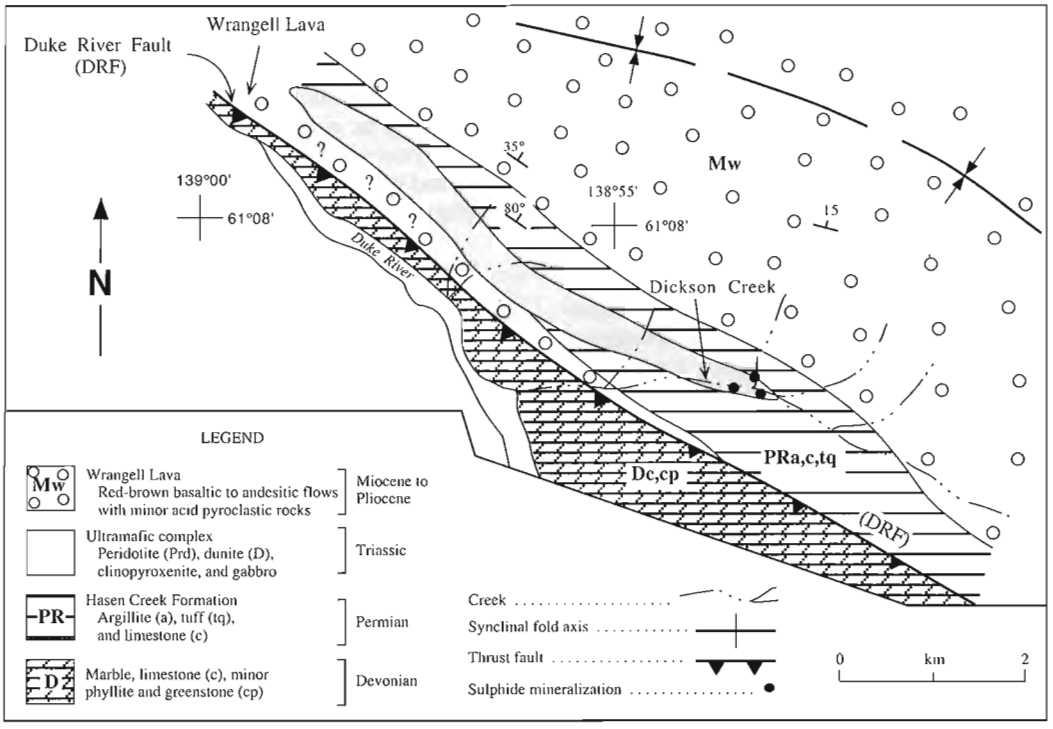

Figure 44. *Generalized geological map of the Dickson Creek Intrusive Complex and surrounds.*

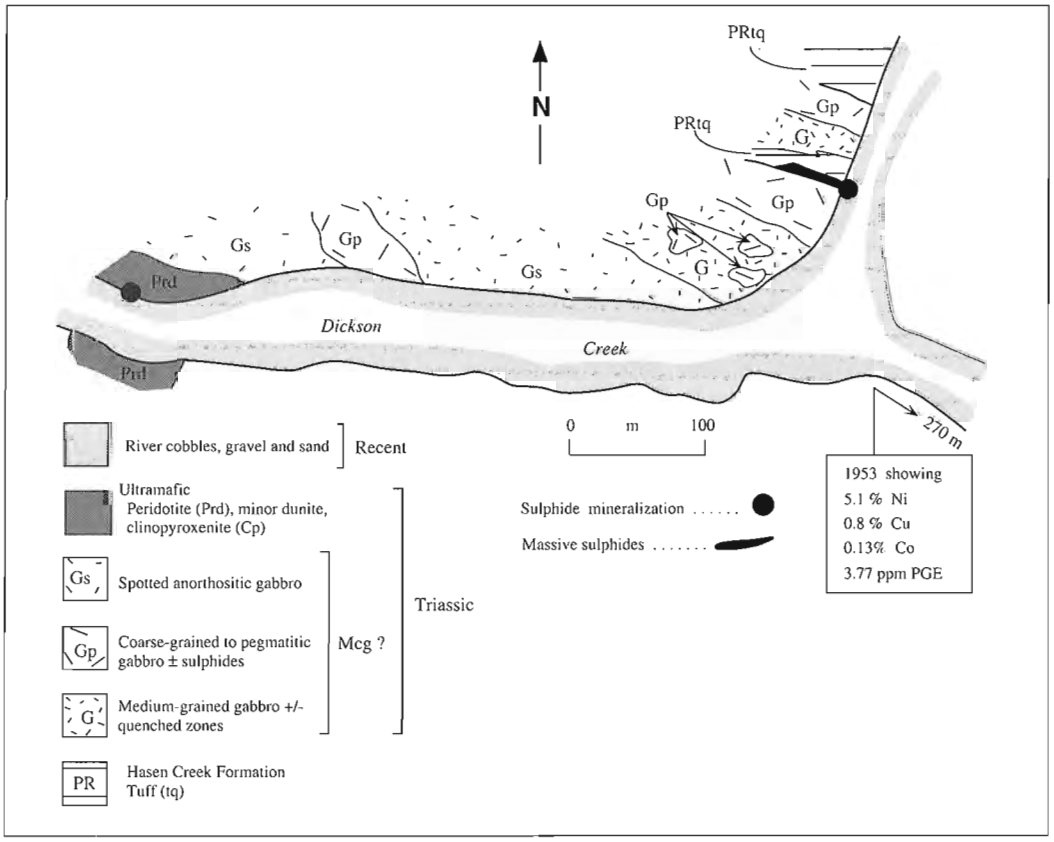

Figure 45. *Simplified geological map of the eastern extremity of the Dickson Creek Intrusion Complex as exposed along the north bank of Dickson Creek.*

The intrusive complex is a thin (≤280 m) northwest-trending, steeply dipping (80° north-northeast) mafic-ultramafic body that has been traced along strike for 6 km (Muller, 1967). Unfortunately, most of the complex is overlain by moss covered glacial terrace material, and thus creek channels provide the only exposures of the intrusive complex. In the past, mineral exploration assessment records have referred to the body as a "peridotite dyke" because of its near vertical attitude. However, it clearly represents a Triassic sill-like complex that has attained its present steep northerly dip due to post intrusive regional scale structural deformation. The assessment files also refer to the host intrusion as being of "strictly ultrabasic composition" (Department of Indian Affairs and Northern Development; Assessment File: Barymin Mines Ltd., 1953, 115 G/3), but detailed mapping by the author along the southeast extremity of the complex disclosed a significant volume of gabbroic material associated with this portion of the complex (Fig. 45). Based on these findings and the lack of first hand experience with most of the other areas of the complex, it is difficult to ascertain the true proportion of ultramafic material associated with this complex. Barymin Mines Ltd. reported that the peridotite is approximately 76 m thick, which is in accord with the thickness estimates based on the authors field work. This and Muller's (1967) represented thickness of 280 m are in accord with the thickness measured along the eastern periphery of the complex (Fig. 45) by the author, and suggests that the entire northern portion of the complex may contain a significant volume of gabbroic rocks. More field work in the western portion of the complex is necessary to resolve this enigma.

The ultramafic zone is made up almost exclusively of peridotite (wehrlite), feldspathic dunite, and subordinate olivine clinopyroxenite. These lithologies are conspicuous by their dark greenish-black, waxy appearance resulting from serpentinization, poikiolitic texture, and ubiquitous disseminated pyrrhotite. The ultramafic zone is overlain by gabbroic rocks attaining a thickness of 200 m near the eastern extremity of the complex.

Based on the field relations illustrated in Figure 45, ultramafic zone of the complex appears to be overlain by a complicated sequence of gabbroic rocks similar to those observed in the Duke River and Halfbreed Creek intrusive complexes and equated with Maple Creek gabbro magmatism. This being the case, one could also expect to find a thin basal layer of older Quill Creek-type marginal zone gabbro (and associated Ni-Cu-PGE mineralization) beneath the ultramafic zone.

Three different textural variants of gabbroic rocks have been observed to date (Fig. 45): spotted anorthositic gabbro, coarse-grained to pegmatitic gabbro, and medium-grained gabbro with quenched marginal sections. The spotted anorthositic variety preferentially occurs above the ultramafic zone and is identical to that from the Duke River and Halfbreed Creek complexes. Irregular-shaped and sporadically distributed areas of coarse-grained to pegmatitic gabbro occur within the spotted anorthositic gabbro and the overlying medium-grained gabbro. However, near the upper contact of the complex the frequency and continuity of the pegmatitic gabbro increase with proximity to Hasen Creek Formation. Such bodies may contain disseminated sulphides and appear to have crystallized *in situ* in response to increased volatile activity resulting from country rock contamination of the magma. Medium-grained gabbro with quenched zones also appear to be more abundant in the upper reaches of the complex. Very fine-grained quenched gabbro is best developed along the west bank of a northerly trending gully at a locality where the intrusion has come into contact with Hasen Creek tuff that hosts massive sulphides of a volcano-sedimentary exhalative origin.

Permian and Triassic units are unconformably overlain to the north and south by Miocene to Pliocene (Tertiary) Wrangell Lava consisting of red-brown basaltic to andesitic flows and minor acid pyroclastics. These gently dipping lava flows have been folded about a west-northwest to northwest-trending axis.

The oldest rocks in the study area occur south of the Duke River thrust fault (Fig. 44). This middle and upper Devonian sequence consists of marble, argillite, minor phyllite, and greenstone of the Kaskawulsh Group (Muller, 1967).

The Duke River fault is the most significant fault in the area. The fault forms a structural contact between a block with pre-Permian rocks (south) and a block of Permian to Tertiary rocks (north). On and above Duke River a recumbent anticline of Kaskawulsh limestone has been thrust over Permian Hasen Creek Formation rocks and Triassic peridotite and gabbro, along with folded and disturbed Tertiary volcanic rocks. The fault has been active since eruption of the Tertiary lavas and was probably active during an earlier Tertiary or late Cretaceous date. Compression of Tertiary and other beds near the fault suggests a northeast thrust direction. Muller (1967) suggested that the fault plane has a southwest inclination.

Petrology

Gabbro. Medium-grained gabbro with quenched marginal zones demonstrates the greatest degree of lithological variability. Quenched rocks represent specimens from the chilled margins of the gabbroic bodies. They are microcrystalline and contain approximately equal quantities of equant to acicular plagioclase and clinopyroxene set in a dark turbid groundmass of devitrified glass, microlites, Fe-Ti oxides, and sulphides (Fig. 46A). Unfortunately, the best quenched specimens were found in the vicinity of the exhalative massive sulphide lens shown in Figure 45, and consequently are contamination and contain an abnormal quantity of sulphides (≈4.0%). The quenched variety irregularly passes into a fine-grained, weakly ophitic type (Fig. 46B). Skeletal plagioclase crystals containing dark devitrified glass cores are not uncommon in these rocks. Coarsening away from the contact gives rise to medium-grained gabbroic rocks, some of which possess an ophitic texture. This medium-grained variety may contain fine- to medium-grained melanocratic types similar to that shown in Figure 46C. On average they contain; 19% plagioclase, 78% pyroxene, and 2% Fe-Ti oxides. These melanocratic types are panidiomorphic to hypidiomorphic, and display fairly well-developed crystal outlines with respect to the mafic phases. The euhedral to subhedral nature of the clinopyroxene and the interstitial or intercumulus-like nature of plagioclase suggest that this variety may represent localized cumulate activity. This variety may also be present within the spotted anorthosite gabbro.

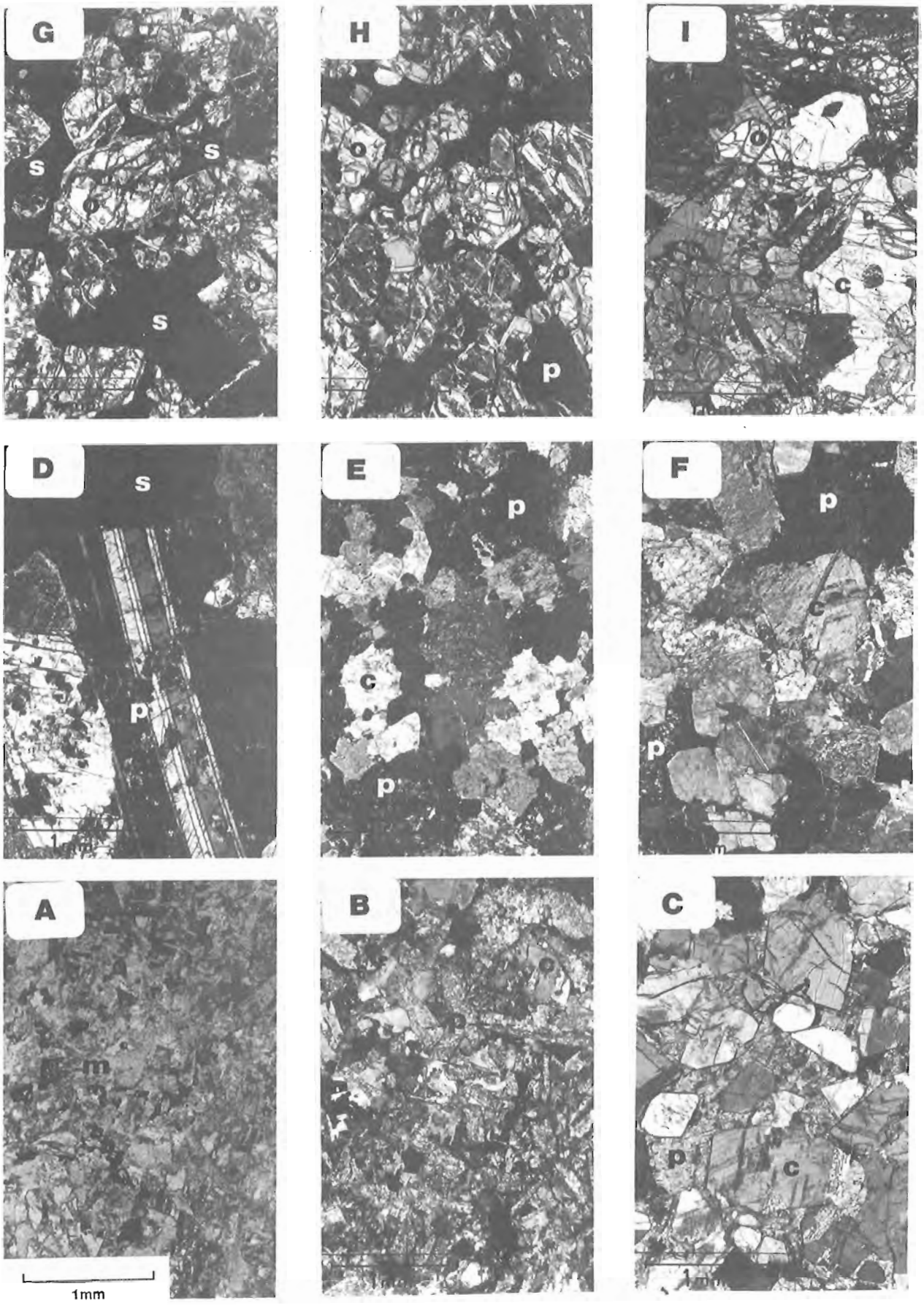
G
S
S
S
H
p
I
c
D
S
p
E
p
c
p
F
p
c
p
m
A
m
1mm
B
p
C
p
c
1mm

Coarse-grained to pegmatitic gabbro (Fig. 46D) occurs as irregular shaped pockets in the spotted anorthositic gabbro, the medium-grained gabbro (Fig. 46F), and in areas adjacent the upper contact of the complex. The following represents the general range of the mode: plagioclase (24-37%), clinopyroxene (49-74%), Fe-Ti oxides (1.9-2.4%), apatite (0.06-.15%), sulphides (2-3%). These mesocratic to melanocratic rocks contain clinopyroxene and plagioclase crystals up to 1.2 cm in length (Fig. 46D). Sulphides, when present, usually occur as medium- to coarse-grained intergranular patches or as areas containing fine-grained disseminated sulphides. These coarse-grained sulphide-enriched patches are always accompanied by coarse crystals (5-8 mm) of Fe-Ti oxides.

The spotted anorthositic gabbro group essentially consists of anorthositic gabbro and gabbro with a distinctive spotted appearance resulting from the crystallization of coarser equant clinopyroxene (Fig. 46E). The gabbro contains 47-53% plagioclase, 41-46% clinopyroxene, 1.3-1.5% Fe-Ti-oxides, 0.06% apatite, and 0.19-.32% sulphides. The anorthosite members, which are slightly more abundant, contain approximately 75% plagioclase and 23% clinopyroxene. This group generally appears to be more leucocratic than it actually is because of the crystallization of light coloured alteration products on both the mafic and felsic phases (ie. clinozoisite, albite, calcite, chlorite, uralite (tremolite-rich variety) and serpentine).

Ultramafic. Apart from the sulphide-rich nature of this zone, the ultramafic members of the complex differ little from those observed elsewhere in the belt. Wehrlite is the most abundant peridotite but subordinate olivine clinopyroxenite has been recognized. The wehrlite is poikiolitic, containing coarse intercumulus clinopyroxene oikocrysts (Fig. 46I). Most of the ultramafic members are moderately to heavily serpentinized. The sulphide-rich samples are classic olivine-sulphide cumulates similar to that in Figure 46G. Proximal to these sulphide-enriched cumulates are weakly mineralized and barren ultramafic rocks that can contain up to 25% intercumulus plagioclase, and are best referred to as feldspathic peridotite and dunite. Intercumulus feldspars are always replaced by a dark turbid alteration product similar to that shown in Figure 46I. These sulphide-enriched ultramafic rocks are discussed in considerable detail in the next section.

Orthopyroxene is seldom present in the Dickson Creek Complex and plagioclase is generally highly altered.

Ni-Cu±PGE mineralization

Sulphide mineralization consisting of pyrrhotite and chalcopyrite is relatively abundant both within the mafic-ultramafic intrusive complex and the surrounding Permian strata. Although assays from these mineralized localities returned disappointing grades (specifically when the high modal sulphide contents are considered) the resulting geochemical and isotopic database has contributed significantly to an understanding of Ni-Cu-PGE metallogenic process in the Kluane Mafic-Ultramafic Belt. Geochemical and isotopic data are presented in Figures 82, 94, 105, 116, 127 and 138.

Immiscible magmatic sulphide segregations.

Marginal gabbro. Lack of exposure in the basal portion of the complex impeded discovery of marginal zone gabbro, but its presence is inferred in the area immediately south of the southern gully wall of Dickson Creek (Fig. 45).

Maple Creek gabbro. Gabbro, equated to Maple Creek gabbro magmatism, contains irregular areas of disseminated sulphide mineralization. These areas are generally associated with the coarse-grained to pegmatitic gabbro, and the medium-grained gabbro containing quenched marginal zones. Adjacent the west bank of a north-trending gully, above the confluence with Dickson Creek, mineralized medium-grained gabbro, coarse-grained to pegmatitic gabbro, and localized zones of quenched gabbro are present. They are best developed in the interval between the massive sulphide locality and the Hasen Creek tuff, 50 m to the north (Fig. 45).

The medium-grained gabbro has a characteristic subophitic to ophitic texture and contains 4.7 to 6.0% disseminated sulphides consisting almost exclusively of pyrrhotite

Figure 46. *Photomicrographs of representative gabbroic and ultramafic rocks from the Dickson Creek Intrusive Complex. GSC 1995-106D* ***(A)*** *HDB-88-DIC-2i. Quenched marginal gabbro from northern (upper) intrusive contact. Fine opaques are sulphide and magnetite. Plane-polarized light.* ***(B)*** *HDB-88-DIC-2h. Fine-grained subophitic marginal gabbro. Note skeletal plagioclase with dark devitrified glassy cores. Plane-polarized light.* ***(C)*** *HDB-88-DIC-4. Medium-grained mela-gabbro with fresh clinopyroxene and pervasively altered plagioclase. Cross-polarized light.* ***(D)*** *HDB-88-DIC-6b. Coarse-grained pegmatitic gabbro from near the upper contact. Cross-polarized light.* ***(E)*** *HDB-88-DIC-8. Spotted anorthositic gabbro. Spotted appearance due to round to equant clinopyroxene grains in a plagioclase-rich matrix. Cross-polarized light.* ***(F)*** *HDB-88-DIC-18. Typical medium-grained gabbro adjacent the upper intrusive contact, and host to pegmatitic gabbro masses. Cross-polarized light.* ***(G)*** *HDB-88-DIC-12a. Net-textured peridotite or olivine-sulphide cumulates from mineralized ultramafic zone. Plane-polarized light.* ***(H)*** *HDB-88-DIC-12b. Net-textured feldspathic peridotite overlying the previous horizon. Cross-polarized light.* ***(I)*** *HDB-88-DIC-10. Weakly mineralized poikiolitic peridotite from upper 10 m of the mineralized ultramafic horizon. Cross-polarized light. o = olivine, c = clinopyroxene, p = plagioclase, s = sulphide, m = magnetite.*

and chalcopyrite. The mineralization can be traced along strike for at least 30 m. This gabbro is represented by three samples occurring in the 1.77 to 2.26 wt. % sulphur range in Figures 82, 94, 105, 116, 127, and 138. The highest modal sulphide content occurs in these rocks, but they contain amongst the lowest Ni (48-61 ppm), Co (46-67 ppm), Cr (130-320 ppm) Pt (2 ppb), Pd (3 ppb), Au (2 ppb), and Rh (<0.5 ppb) values encountered in the complex. However, elements like Se (1.4-2.8 ppm), As (0.3-6.1 ppm), Cu (210-370 ppm), Zn (39-46 ppm), and Ba (1300-2000 ppm) are present in relatively high concentrations. The elevated elements and the association of isotopically light sulphur from this group ($\delta^{34}S$ = -26.4‰) show that the gabbro has been extensively contaminated by crustal material. The Cu/(Cu+Ni) ratio for this group is in the 0.75 to 0.81 range.

Immediately overlying this medium-grained group, and above the massive sulphide horizon, is a coarse-grained to pegmatitic variety developed adjacent the upper intrusive contact. Although these samples generally have a much coarser sulphide fraction, the modal sulphide content is generally lower (2.7-3.8%). These samples fall in the 1.02 to 1.43% S range. Figures 82, 94, 105, 116, 127, and 138 show that the pegmatitic group generally has slightly higher Ni (100-110 ppm) and Cr (330-810 ppm) contents, marginally lower Se (1-1.3 ppm), As (1.6-2.2 ppm), Cu (92-190 ppm), Zn (24-40 ppm) and Ba (860-1100 ppm) values, and similar PGE+Au levels. The Cu/(Cu+Ni) is significantly lower (0.45-0.65) than that of the medium-grained group. The coarse-grained to pegmatitic gabbro beneath the massive sulphide horizon (Fig. 45) is identical in appearance and sulphide content (up to 3.7%) to that above it, but is significantly depleted in Ni (28 ppm), Cr (27 ppm), and Ba (480 ppm) whereas the concentrations of the other elements are approximately at the same level. The proximity to the massive sulphide horizon (believed to be of a volcano-sedimentary exhalative origin), the isotopic composition of the pegmatite-hosted sulphides ($\delta^{34}S$ = -26.6‰) and the high Cu/(Cu+Ni) ratio of 0.75 indicate that the significant crustal contamination of the magma resulted in the pegmatitic association. Quench-textured gabbro, adjacent the Hasen Creek tuff near the upper contact, contains 3.6 to 5.0% disseminated, groundmass sulphides and is represented by the three gabbro samples in the 1.35 to 1.87% S range on plots in Figures 82, 94, 105, 116, 127, and 138. This quenched gabbro is geochemically identical to the medium-grained variety, particularly when the slight differences in sulphide content are taken into consideration.

Coarse-grained to pegmatitic gabbro from the lower half of the gabbro zone is remarkably enriched in transition and noble metals (by approximately an order of magnitude for most of these metals) compared to its lithological and petrological equivalent from the upper half of the intrusion. The lower half comprises all gabbro units south of the mixed horizon containing both medium-grained and coarse-grained to pegmatitic gabbro exposed near the confluence of Dickson Creek and the unnamed northerly trending gully (Fig. 45). These mineralized pegmatitic lithologies are represented by three samples in the 0.82 to 1.00 wt.% S range on plots in Figures 82, 94, 105, 116, 127, and 138. Although they have marginally lower sulphide content (i.e. 2.2-2.7% in the lower half vs. 2.7-3.8% in the upper half) the petrological character is analogous to that in the previously mentioned mineralized pegmatitic gabbro. The range in values in these representative specimens, with the higher ones almost always being associated with the southernmost samples, is: Ni (1400-1900 ppm), Co (78-97 ppm), Cr (700-890 ppm), Cu (2800-3200 ppm), Zn (75-100 ppm), Pd (170-260 ppb), Pt (190-270 ppb), Au (29-110), Rh (4-6 ppb). The lower and less variable Cu/(Cu+Ni) ratio (0.62-0.66), S/Se ratio (1429-3125) and heavier isotopic composition of sulphur ($\delta^{34}S$ = -6.8 to -5.5‰) clearly indicate a much higher proportion of mantle-derived sulphur in the sulphides associated with the lower gabbro. This in turn suggests a much larger magmatic reservoir from which the sulphides scavenged transition and noble metals.

In Figures 82, 94, 105, 116, 127, and 138 the unmineralized to weakly mineralized spotted anorthositic gabbro, gabbro, and to a lesser extent, the medium-grained gabbro (all from the lower half of the gabbroic portion of the complex) contain samples with sulphur contents in the range 0.06 to 0.5 wt.% S. These samples are also significantly enriched in Ni, Cr, and PGE+AU relative to mineralized gabbro from the upper half of the gabbro zone.

Ultramafic. To date, all exploration activity and interest in the complex have been directed at the ultramafic zone. The ultramafic zone contains extensive widths of low grade disseminated and localized semi-massive pyrrhotite and chalcopyrite mineralization. The best exposure of the mineralization in this zone occurs at and in the vicinity of the most westerly site of sulphide mineralization (Fig. 45). Four contiguous channel samples taken by Barymin Mines Ltd. across a 15.6 m width of continuously mineralized peridotite (referred to as the Main zone) returned the following grades (wt. %) from south to north: 4.3 m (0.35 Ni, 0.63 Cu); 5.8 m (0.30 Ni, 0.20 Cu); 1.06 m (0.60 Ni, 0.37 Cu); and 4.5 m (0.30 Ni, 0.22 Cu), respectively. A 15.25 m by 6.1 m chip sample across this zone by R.J. Cathro of Archer, Cathro and Associates revealed an average grade of 0.3% Ni and 0.2% Cu[1].

A 10.4 m wide channel sample of similar but lower grade mineralization (0.25% Ni, 0.22% Cu) occurs south of the Main zone in peridotite on the opposite side of Dickson Creek, along the southern face and accompanying slope of the creek (Department of Indian Affairs and Northern Development; Assessment File: Barymin Mines Ltd., 1953, 115 G/3). The assessment files suggest, but could not confirm, that the highest concentration of sulphide mineralization is in the central portion of the ultramafic zone and not near the base.

The following is a brief account of the author's interpretation of the ultramafic zone, and associated mineralization, based on field observations and subsequent laboratory studies conducted on material obtained from a traverse along

[1] Mineral Policy Sector, Department of Energy, Mines and Resources, Ottawa, #506479, REF. NI 1 and Northern Cordilleran Mineral Inventory 1972; Archer, Cathro & Associates Ltd., Occurrence No. 5.

the north face of Dickson Creek. The traverse starts at the top of the ultramafic zone and works its way down section to a level equivalent to the base of the Main zone mineralization.

The contact between the top of the ultramafic zone and the overlying spotted anorthositic gabbro is not exposed at this locality. The top 10 m width of the ultramafic zone consists essentially of weakly mineralized poikiolitic peridotite (Fig. 46I). The peridotite is, in terms of cumulate nomenclature, best referred to as olivine-chromite±sulphide cumulates. Olivine generally makes up 50 to 75% of the mode with the intercumulus space being occupied by poikiolitic clinopyroxene crystals. Sulphide content of this interval averages of 0.9%. A representative sample for this interval contains the following metal grades: S (0.34%), Cu (590 ppm), Ni (1700 ppm), Se (1 ppm), As (0.4 ppm), Pd (51 ppb), Pt (19 ppb), Au (2.6 ppb), Rh (4 ppb), and Cr (4000 ppm). The sample also has a low Cu/(Cu+Ni) ratio of 0.25 and S/Se ratio (3400) (Fig. 82, 94, 105, 116, 127, and 138). Near the bottom of this poorly mineralized interval the sulphide content increases to 3 to 4% over the next 5 m width. Sulphides occur as disseminated pyrrhotite and chalcopyrite composite blebs and intercumulus fillings. Average metal concentrations within this interval are in proportion to the increased sulphide concentration: S (1.18-1.50%), Cu (1300-1800 ppm), Ni (2000-2100 ppm), Se (2.3-2.8 ppm), As (0.4-0.8 ppm), Pd (190-230 ppb), Pt (56-83 ppb), Au (24-33 ppb), Rh (7-8 ppb), and Cr (4300-4400 ppm). Comparatively low Cu/(Cu+Ni) ratios (0.39-0.46), S/Se ratios (5130-5337), and sulphur-isotope compositions ($\delta^{34}S$ = -4.6 to -4.9‰) suggest a rather limited degree of crustal contamination of the magma that gave rise to this mineralized interval.

Ultramafic lithologies become increasingly feldspathic and enriched in sulphides in the underlying 5 m width. Within this more feldspathic interval the sulphide content ranges from 6.5 to 8.4% and occurs primarily as heavily disseminated and locally net-textured sulphides. The net-textured concentrations are represented by the olivine-sulphide cumulates (Fig. 46G). In the field, these net-textured areas appear as globular to lozenge-shaped sulphide bodies, 1 to 2 cm in diameter, within feldspathic dunite and peridotite. These ultramafic rocks are olivine-chromite-sulphide cumulates with up to 25% intercumulus plagioclase (Fig. 46H). The metal contents associated with this horizon are: S (2.4-3.2%), Cu (2400-2800 ppm), Ni (2800-3300 ppm), Se (7.7-8.3 ppm), As (1.1-1.2 ppm), Pd (380-460 ppb), Pt (210-220 ppb), Au (56-57 ppb), Rh (11-13 ppb), and Cr (1300 ppm). The ratios of Cu/(Cu+Ni) (0.45-0.46) and S/Se (3182-3887) and sulphur-isotope signature ($\delta^{34}S$ = -4.9‰) again indicate limited crustal contamination, and geochemical congruence with the overlying mineralized interval.

Disseminated sulphide concentration decreases to 4.8% in the next 5 to 7 m width of poikiolitic peridotite underlying the above horizon. This interval contains the following metal content: S (1.8%), Cu (1100 ppm), Ni (2400 ppm), Se (4.3 ppm), As (1.5 ppm), Pd (15 ppb), Pt (7 ppb), Au (13 ppb), Rh (7 ppb), and Cr (1500 ppm). The S/Se ratio is 4186 and the Cu/(Cu+Ni) ratio is 0.31.

The above metal-enriched disseminated interval is separated from the underlying barren, semi-massive sulphide break within the ultramafic rocks, by a 3 to 4 m width of highly brecciated and oxidized (Fe-stained) tuffaceous break. It is not certain if this tuffaceous break represents a xenolith or fault juxtaposition of country rock, but the former appears more probable.

Semi-massive concentrations of immiscible magmatic sulphides occur in a 2 to 3 m interval within peridotite adjacent the north bank of Dickson Creek, in the western part of the study area (Fig. 45). This locality represents the lowest portion of the ultramafic zone examined during this study; however, peridotite with low grade disseminated sulphide mineralization similar to that described above has also been reported by Barymin Mines Ltd. along the south bank of the creek (Fig. 45). Sulphides within this interval generally constitute 32 to 40% of the rock and are very pyrrhotite rich. Net-textured sulphide relationships predominate in this interval but massive sulphide (50-90%) concentrations occur locally. Stubby olivine and prismatic clinopyroxene crystals within a sulphide-rich matrix characterize these samples. In addition, feldspathic ultramafic to mela-gabbroic patches have been found within this interval. The metal contents of this sulphide-rich interval are: S (11.9-14.7%), Cu (2100-2700 ppm), Ni (91-131 ppm), Se (18.6-19.7 ppm), As (0.8-1.2 ppm), Pd (3 ppb), Pt (4 ppb), Au (<1 ppb), Rh (<1 ppb), Cr (35-110 ppm). This mineralization has the highest S/Se and Cu/(Cu+Ni) ratios in the complex (i.e. 6398-7462 and 0.94-0.96, respectively). Sulphur-isotope signatures of associated sulphides are the lightest or most ^{32}S-enriched magmatic sulphides encountered in the Kluane Belt. The composition ranged from -29.9 to -28.4‰. The classic magmatic sulphide-silicate textural relationships, the impoverished transition and noble metal content of the mineralization, and the extremely light isotopic composition of the sulphur in the immiscible sulphides suggest localized sulphur saturation resulting from contamination of the magma by Permian tuff with an isotopic composition in the -39.6 to -34.3‰ range. The sudden overwhelming and localized sulphur saturation limited the volume of parental magma and time in which the immiscible sulphide segregations could communicate with the magma (low *R-factor*) and thus gave rise to metal-poor sulphide accumulations with the bulk of the sulphur being derived from the assimilated tuff.

Hydrothermal (remobilized ?) and exhalative mineralization.

Exhalative mineralization. One of the best examples of sulphide-rich country rock mineralization and the role of such assimilated material on the metallogenic evolution of Triassic magmas within the Kluane Belt, are well illustrated at this locality. Therefore, it is important to document the geology and geochemistry of one of these external sources of sulphur.

A steeply dipping (75° north-northwest) pyrrhotite-rich massive sulphide body occurs at the base of a thin intercalation or inclusion of Permian tuff, adjacent the west bank of a north-trending gully, near the western edge of the complex (Fig. 44, 45). This lens-shaped body has a true thickness of

3 m and consists of rectangular blocks (20 x 40 cm, with the long axis parallel the dip) of dark, fine-grained, massive unlaminated sulphides set in a dark-grey to greenish brecciated siliceous matrix. The degree of brecciation appears to be slightly greater near the base of the lens (i.e. adjacent the upper intrusive contact). The sulphide content of five equally spaced channel samples across the width of the body ranges from 35 to 51% and the associated metal contents fall within the following ranges: S (13-17.7%), Cu (1500-4900 ppm), Ni (21-54 ppm), Se (1-19.5 ppm), As (1.1-4.6 ppm), Pd (2 ppb), Pt (3 ppb), Au (10 ppb), Rh (1 ppb), and Cr (77-110 ppm). The S/Se ratio ranged from 6872-15 391 through the lens; however, a low Se value of 1 ppm in the top 10 cm gave rise to a very high ratio of 166 000. The low transition and PGE metals, the high Cu/(Cu+Ni) ratio (0.98-0.99), and the extremely light isotopic composition of the sulphur ($\delta^{34}S$ = -39.6 to -34.3‰) characterize this country rock, volcano-sedimentary "exhalative"-type of Permian sulphide mineralization. This mineralization also contains relatively high Ba contents of 250 to 770 ppm ($\overline{X}$ = 600 ppm) as do many mineralized Kluane intrusions within the belt.

Other areas of country rock mineralization as much as 61 m away from the sill have been noted in siliceous argillite and minor limestone of the Permian Hasen Creek Formation, but it is best developed at the contact (Northern Cordilleran Mineral Inventory 1972; Archer, Cathro & Associates Ltd., Occurrence No. 5).

Hydrothermal (remobilized ?) mineralization. During the author's limited investigation of this property no obvious signs of hydrothermal mineralization or remobilized sulphides were noted. However, more extensive ground surveys conducted in the past have reported that narrow stringers of chalcopyrite and pyrrhotite (up to 5 cm in width) occur in the adjacent tuff (Mineral Policy Sector, Department of Energy, Mines and Resources, Ottawa, #506479, REF. NI 1).

Sulphide samples picked from stringers near the extreme eastern intrusive contact with the tuff, approximately 270 m southeast of the confluence of Dickson Creek and the unnamed north-trending gully (Fig. 44, 45), returned the following values: 5.1% Ni, 0.8% Cu, 0.13% Co, and 3.8 ppm (0.11 oz./ton) PGE[1,2].

Southern section

Triassic intrusions from the Southern section of the Kluane Mafic-Ultramafic Belt are located in northwestern British Columbia (Fig. 1, 4, 47). The greatest volume of gabbroic material encountered in the belt is associated with one of these intrusions (i.e. Chilkat Complex). The bulk of the Chilkat gabbroic material is believed to be related to Maple Creek gabbro magmatism, and supports earlier suggestions that the volume and frequency of this magma type increase towards the southern portion of the belt. Near the extreme southern end of the belt, the Mansfield Creek mafic and ultramafic bodies take on a sinuous form and occur associated with Paleozoic greenstone. These irregularities and the extensive quartz-carbonate alteration in this area may be a direct result of proximity to the Denali fault which occurs as little as 100 to 500 m to the northeast. Nevertheless, both areas have striking geochemical signatures that characterize them as belonging to the Kluane Mafic-Ultramafic Belt.

Chilkat Intrusive Complex

The Chilkat Intrusive Complex differs from other coeval Kluane Belt complexes in that it consists of two, irregular northwest-trending, sinuous, mafic-ultramafic zones present throughout the entire length of the complex. In addition, Nikolai volcanic rocks appear to be more removed from the mafic-ultramafic intrusions than usual (1-2 km to the west), the intrusive bodies occur at a higher stratigraphic level (juxtaposed with the Upper Triassic McCarthy Formation) inconsistent with their Middle Triassic age, the Nikolai volcanic rocks unconformably overlie the younger McCarthy Formation calcareous sediments, the absence of Hasen Creek Formation strata, and the sinuous nature of the intrusions, suggest that thrusting has been very active in this area.

Location, history, and physiography

The Chilkat Complex straddles the British Columbia – Yukon border and is centred at latitude 59°55'N and longitude 137°00'W on NTS map sheet 114P/15 (Fig. 47). The northwest portion of the study area is near the headwaters of Squaw (Dollis) Creek which is accessible by a rough (4-wheel drive vehicle) road when the Tatshenshini River is fordable. This 25 km access road connects with the Haines Road, approximately 140 km north of the deep sea port at Haines, Alaska. Access during this study, and the limited exploration program conducted in 1988, was by helicopter based out of the Mansfield Creek exploration camp (established by Archer, Cathro & Associates) located 11 km east-southeast of the centre of the complex. The nearest permanent helicopter base is located at Haines Junction, 95 km to the north.

Once again the economic significance of the mafic-ultramafic intrusive rocks in this area has been greatly overshadowed by the placer mining activity. The Squaw Creek area has a long history of exploration, mainly for placer gold, beginning in 1924. Placer mining has been in operation since that time, and as recent as 1987 a 2605 ppm (76 ounce) nugget was discovered. Prior to 1987 all other exploration in the area focused on copper in Nikolai volcanic rocks. In 1967, Rouge Point Mines Ltd. explored for Cu in Nikolai volcanic rocks west of the study area, and in 1983 Noranda Exploration Ltd. explored the eastern fringe of the area and conducted an airborne geophysical survey. In 1984, Arbor Resources Ltd. performed prospecting, mapping, and geochemical surveys

[1] Department of Indian Affairs and Northern Development; Assessment File: Barymin Mines Ltd., 1953, 115 G/3.

[2] Mineral Policy Sector, Department of Energy, Mines and Resources, Ottawa, #506479, REF. NI 1 and Northern Cordilleran Mineral Inventory 1972; Archer, Cathro & Associates Ltd., Occurrence No. 5.

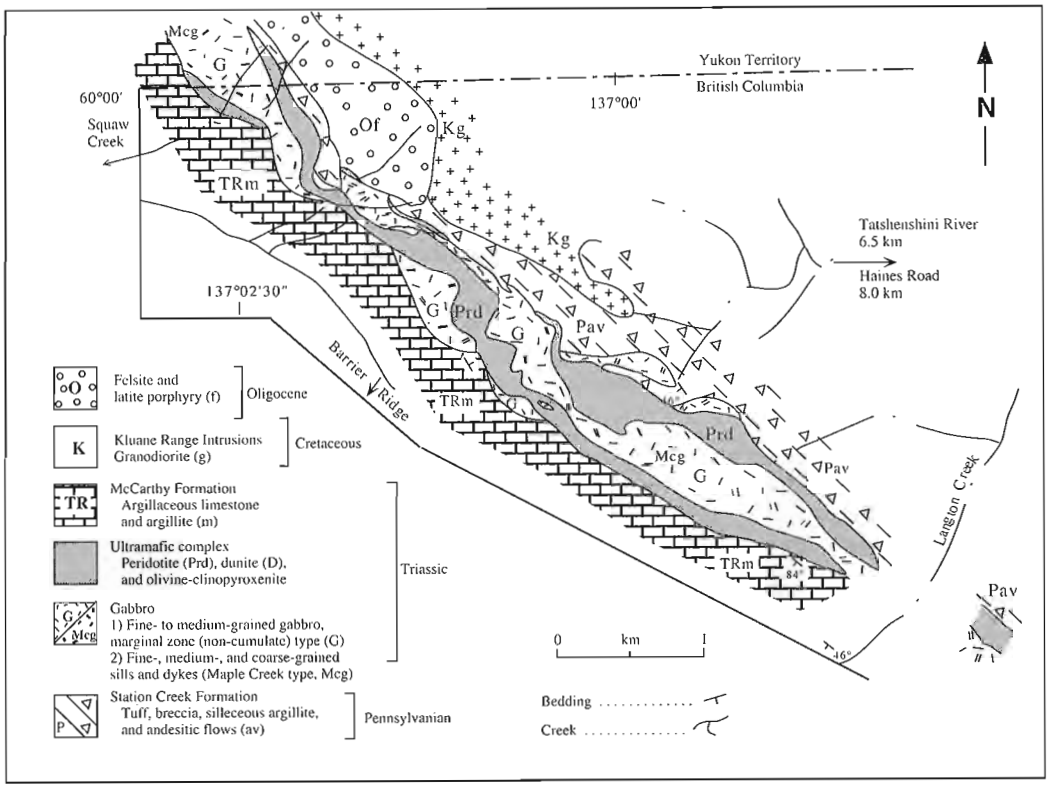

Figure 47. *Simplified geological map of the Chilkat Intrusive Complex and environs.*

in the area immediately west of the study area to explore for the lode source of the gold in Squaw Creek (Davis and Main, 1988).

It was not until May 1987 that the Chilkat Complex became the focus for Quill Creek Complex-type Ni-Cu-PGE exploration when Archer, Cathro & Associates (1981) Ltd. staked 71 units in six claims, collectively known as the Chilkat property, on behalf of W6 Joint Venture. During September 1987, an airborne geophysical survey was flown over the property and surrounding area by Dighem. The survey showed magnetic and EM anomalies which compared favourably with those at the Quill Creek Intrusive Complex. Reconnaissance soil geochemical surveys, prospecting, and mapping was conducted in 1988.

The intrusive complex is situated in the Alsek Range which is surrounded by the Tatshenshini River to the west, north, and east. Climate is strongly influenced by the height of the mountain ranges as well as by proximity to the ocean. Precipitation is high to extreme, particularly at higher elevations. Snow is present all year round on some of the north-facing ridges. Most of the area lies above treeline which is at an elevation of 1000 m. Some of the lower slopes are covered with dense slide alder and buckbrush. Topography is generally rugged (attaining elevations of 2091 m along ridge crests) and north- and east-facing slopes are commonly unnavigable. South- and west-facing slopes are more moderate and are accessible for most types of exploration. Most of the study area is covered by talus and outcrops are largely restricted to ridge crests, north-facing slopes, and actively eroding creek cuts. The intrusive complex cuts obliquely across the main ridge of the Alsek Range so that the northwest half of the complex is exposed on the southwest-facing slopes which are moderate and accessible, whereas the southeastern half is on precipitous northeast-facing slopes which are more difficult to explore but have much better exposures.

Structure and stratigraphy

Strata within this study area occur near the extreme southeastern end of the eastern arm of Wrangellia (Fig. 1, 2). This allochthonous, accreted material is bounded to the west (2 km) and east (6 km) by the Duke River and Denali faults, respectively.

The oldest rocks in the study area belong to the northwest-trending Station Creek Formation (Fig. 47). This Pennsylvanian formation is composed mainly of fine-grained ash tuff and siltstone, commonly silicified, and greenish-grey massive volcanic breccia and agglomerate. Andesitic flow units occur locally. This so-called "island arc volcaniclastic and volcanic assemblage" occurs in the footwall of the Chilkat Intrusive Complex and dips steeply (≈60°) to the southwest.

Intrusive into the upper part of this formation are irregular bodies of gabbroic and ultramafic rocks. Collectively these bodies form what is referred to as the Chilkat Intrusive Complex, and can be traced for at least 8 km along strike and generally attain surface widths of about 500 m. The true

lateral extent of this complex is not established. Ultramafic rocks are on average 200 m wide, and occur in two bands separated by gabbro of variable composition and texture. The ultramafic rocks have the same lithological character as elsewhere in the belt, and consist mainly of medium- to coarse-grained poikiolitic peridotite (wehrlite), olivine clinopyroxenite, and clinopyroxenite. Some of the peridotite contains conspicuous concentrations of phlogopite and a high proportion of interstitial plagioclase. The olivine-bearing lithologies are usually dark-green and generally exhibit a high degree of serpentinization. Some outcrops are highly sheared and have localized quartz-carbonate alteration along the margins of the ultramafic rocks. Isolated patches of disseminated pyrrhotite (1-2%) are fairly common.

Sill-like gabbroic bodies intrude along the centre of the complex and divide the ultramafic mass into the two separate bands described above. Intrusion of this gabbroic material appears to have been controlled by a pre-existing structure, or relict cumulate stratigraphy within the ultramafic mass. In addition to the sills, lobate-shaped gabbroic bodies occur along the footwall and hanging wall contacts near the central portion of the complex. Although some of these gabbroic lithologies look very similar to the "marginal zone" varieties, it is clear that they are younger than the ultramafic members. The gabbroic rocks within this complex are very similar to those in the Duke River, Halfbreed Creek, and Dickson Creek complexes, and are related to Maple Creek gabbro magmatism. Texturally the gabbroic lithologies range from fine-grained chilled varieties to coarse-grained, pegmatitic types, with the latter generally being developed as bands up to 40 cm thick within a medium-grained equigranular gabbro containing calc-silicate inclusions. Rhythmic banding of medium-grained gabbro, anorthositic gabbro, and melanocratic gabbro over widths as narrow as 1.0 m are not uncommon.

The Chilkat Intrusive Complex is unconformably overlain to the west and southwest by the Triassic age McCarthy Formation (Fig. 47). This formation consists of thin, interbedded light to dark-grey argillaceous limestone and argillite. The limestone is commonly recrystallized and intercalations of chert and ash are present. It is possible that members of the underlying Triassic Chitistone and Nazina formations may occur in the area designated as McCarthy Formation in Figure 47.

Kluane Range intrusive rocks, consisting of granodiorite to the north and diorite to the south, invade the Pennsylvanian strata in the north-central part of the study area. These granodioritic rocks are in turn intruded to the west by Oligocene felsite. The felsites generally form dyke, sill and plug-like bodies composed primarily of latite porphyry. The porphyry is a fine-grained, pinkish-white siliceous rock with blebs of epidote and chlorite.

Rock units in the area have been affected by strong transcurrent movements along the boundary Duke River and Denali faults during the Cretaceous and Tertiary. Although thrust faults are difficult to observe in this area, their presence is inferred based on the mentioned inconsistencies in the stratigraphic record.

Petrology

Gabbro. The greatest lithological variation within this complex occurs near the periphery of the intrusive bodies. Contact specimens are very fine-grained, microcrystalline, equigranular chill rocks containing on average: 57.5% plagioclase, 39.5% clinopyroxene, 2.5% Fe-Ti oxides, and 0.21% apatite. The Mg# of the chill facies gabbroic rocks is 0.70. The microcrystalline variety evolves away from the contact into a medium-grained, weakly ophitic gabbro containing plagioclase laths, arranged in a triangular fashion, with the interstitial space occupied by clinopyroxene (Fig. 42B). Intergranular growth and enlargement of the clinopyroxene demonstrate the progressive textural development from weakly sub-ophitic and ultimately ophitic textured gabbro. Further crystallization of this magma gives rise to medium-grained hypidiomorphic granular gabbro similar to that in Figure 42E. This medium-grained variety is by far the most abundant lithology in the Chilkat Complex and normally contains approximately: 36% plagioclase, 61% clinopyroxene, 1.9% Fe-Ti oxides, 0.15% apatite. The medium-grained gabbroic members generally have a Mg# of approximately 0.81 and a normative plagioclase composition of Ca# of about 0.60.

Melanocratic varieties are not uncommon within the medium-grained gabbro, and frequently display cumulate or quasi-cumulate textures similar to those in Figures 41C and 42C. The more melanocratic varieties generally contain 29% plagioclase, 69% clinopyroxene, and 2% Fe-Ti oxides and have a Mg# of approximately 0.79 and normative Ca# of approximately 0.61. Clinopyroxene has a well developed euhedral form, and appears to be a cumulus or primocryst phase within these rocks, whereas plagioclase is clearly of an intercumulus or interstitial origin. Plagioclase is ubiquitously recrystallized to a turbid, fine-grained mosaic of alteration products, even in the presence of extremely fresh clinopyroxene (Fig. 41C). Orthopyroxene has not been observed in these rocks; it is present, however, as a normative constituent in all of the gabbroic rocks. Coarse-grained pegmatitic gabbro, with clinopyroxene crystals up to 1.5 cm in length, also occurs within the medium-grained gabbro lithologies, particularly in the vicinity of calc-silicate xenoliths. Apart from the obvious textural difference there is also a noticeable increase in the quartz, Fe-Ti oxide, and plagioclase content of the pegmatitic variety: 49% plagioclase, 45% clinopyroxene, 2.4% quartz, and 3.2 % Fe-Ti oxides. The Mg# is significantly lower ($\approx$0.63), and reflects the more Fe-rich nature of the associated clinopyroxenes in this textural variety. The normative Ca# of contained plagioclase (0.58) is similar to that of the host medium-grained gabbro.

Ultramafic. Ultramafic lithologies within the Chilkat Intrusive Complex differ little from those previously described for other complexes, therefore further discussions are not warranted. Serpentinization of ultramafic lithologies is prevalent and has completely pseudomorphosed olivine in most cases (Fig. 41F); however, primary textural features of the rock are relatively unchanged and aided in establishing the lithological character of this zone.

Ni-Cu±PGE mineralization

The Chilkat Intrusive Complex has only been superficially explored and clearly warrants an extensive exploration program based on its size, similarity to other mineralized intrusions within the belt, anomalous reconnaissance geochemical responses over the complex, and the sulphide-rich nature of the intruded Pennsylvanian strata. Only a limited number (12) of gabbroic and ultramafic samples were analyzed by the author during the course of this rather brief investigation of this complex. They are represented on the chemical plots illustrated in Figures 83, 95, 106, 117, and 139. Many of the investigated samples contain sulphur concentrations <0.01 wt.% and thus do no appear on the plots.

Immiscible magmatic sulphide segregations.

Marginal gabbro. True marginal zone-type gabbro was only observed at one locality within the complex. Although this material was unmineralized (<0.01 wt.% S), gabbro of a similar origin elsewhere in the complex may host economic concentrations of Ni-Cu-PGE mineralization similar to those in the Quill Creek Complex 200 km to the northwest.

Maple Creek gabbro. All gabbroic material analyzed during the course of this investigation is believed to be related to Maple Creek gabbro magmatism. With only one known exception all gabbro contains ≤0.06 wt.% S. One weakly mineralized sample contained 0.31 wt.% S; however, it is accompanied by an inappreciable enrichment in Ni, Cu, Co, and Se. The highest Pd, Pt, and Au contents occur in unmineralized samples which contain 10, 14, and 1 ppb, respectively. In addition the gabbroic rocks contain unusually high Cr contents (i.e. $\overline{X}$ = 1040 ppm).

Davis and Main (1988) noted that the disseminated sulphide is commonly associated with the margins of the gabbroic sills, and a specimen containing approximately 2% sulphides contained 0.23% Ni, 400 ppb Pt, and 95 ppb Pd. Prospecting in 1988 located samples containing up to 45% Cu and 0.23% Ni.

Ultramafic. Ultramafic material analyzed during this investigation contained ≤0.30 wt.% S. The highest Pd, Pt, and Au contents were 24, 33, and 5 ppb, respectively. Davis and Main (1988) noted that the ultramafic rocks contained up to 100 ppb Pt and 130 ppb Pd. These reconnaissance values are anomalous and considering the complex has only been lightly prospected these results should encourage future exploration.

Mansfield Creek Intrusive Complex

Apart from being the most southerly of the Triassic mafic-ultramafic complexes within the Kluane Belt, the Mansfield Creek Intrusive Complex is also the most highly altered and deformed. The modified nature of the magmatic material, and the uncharacteristic country rock enclosing parts of the complex dramatically illustrate the influence of the Denali (Shakwak) fault system on these Kluane mafic-ultramafic intrusions. Significant Ni-Cu-PGE sulphide and "lithwanitic"-related mineralization (affiliated with primary magmatic and Cretaceous hydrothermal activity, respectively), discovered in the complex, and the pronounced geophysical and soil geochemical anomalies associated with this complex warrant a better understanding and further exploration of the "Mansfield-type" of modified Kluane mafic-ultramafic intrusions.

Location, history, and physiography

The Mansfield Complex is situated in northwest British Columbia, approximately 15 km south of the British Columbia-Yukon border (Fig. 4). The area is centred at latitude 59°55′N and longitude 136°47′W, on map sheet 114 P/15, on land between the Haines Road to the southwest and Mt. Mansfield to the northeast. The complex spans a narrow width of ground, roughly paralleling the Haines Road (which connects to the Alaska Highway), in an area stretching from Stanley Creek in the west to an area 4.3 km to the east of the junction of Kwatinick Creek and the Haines Road, for a total strike length of at least 13 km (Fig. 48).

In 1957, radioactive float was reported along the Haines Road, near the bridge over Stanley Creek. A reconnaissance heavy metal geochemical survey was conducted by the British Columbia Department of Mines on drainages which cut the strong quartz-carbonate altered zone upstream from the bridge (Davis and Main, 1988). The Stanley Creek showing was discovered in 1965 by C.J. Curzon and W.M. Erwin during a soil geochemical survey. Electromagnetic and magnetic geophysical surveys were also conducted in the same year over the showing and adjacent area.

In May 1987, Archer, Cathro and Associates (1981) Ltd. staked nine claims (95 units) collectively known as the Mansfield property on behalf of W6 Joint Venture. The claims covered the original Stanley Creek Ni-Cu showing plus a 9.0 km strike length of favourable ground. During September 1987, an airborne geophysical survey was flown over the property and surrounding area by Dighem. The survey outlined magnetic and EM anomalies, similar to those over the Quill Creek Complex, and seven addition claims (113 units) were staked to cover the southeastern extension of the anomalies. In 1988, a camp was established, three grids were cut to coincide with airborne geophysical anomalies. Once cut the grids were tested by ground geophysical and soil geochemical surveys, mapping, and prospecting. In addition a total of six trenches were cut by an excavator on two of the grids (Davis and Main, 1988).

The study area lies within the Tatshenshini River valley between the Alsek Range to the west and the Boundary Range to the east. Local climate is strongly influenced by the presence of these mountain ranges, as well as proximity to the coast. Rain and fog cover appears to be the climatic norm for this area. Topography within the valley is subdued and consists of low glaciated hills. Local elevations range from 885 m on the valley floor to 1800 m on the surrounding ridges. The area has been extensively glaciated and most of it is blanketed by up to 5 m of till. Relatively continuous bedrock exposures

are restricted to deeply incised tributary drainages. Vegetation consists of closely spaced slide alder over most of the area, with black spruce at lower elevations.

Structure and stratigraphy

The Mansfield Complex occurs at the extreme southern tip of the Wrangellia Terrane (Fig. 2, 4, 48), near the vergence of the Denali and Duke River fault systems. Parts of the eastern and northeastern edge of the area overlap into the adjacent Taku Terrane and demonstrate the proximity of the complex to a major regional structural and stratigraphic discontinuity.

The oldest rocks in the study area consist of northwest-trending, steeply dipping (vertical to 80° east-northeast) basic volcanic rocks, greenstone and amphibolite, believed to be of Paleozoic age, representing transformed Pennsylvanian Station Creek Formation volcanic rocks. This volcanic material is light-green and contains local interbeds of related sediments. However, due to faulting and accompanying dynamothermal metamorphism in the area, it is possible that some of the volcanic material may be Mesozoic in age (Nikolai volcanic rocks ?). The distribution of material of this character on either side of the Denali fault demonstrates the complexity of the area. The lower quarter of the study area consists of similar trending Permian sediments belonging to the Hasen Creek Formation, the bulk of which consists of argillite and siltstone, and subordinate limestone (Fig. 48).

In the part of the study area, that straddles and is east of Kwatinick Creek (Fig. 48), a relatively thin, discontinuous sill of sheared peridotite, commonly about 50 m wide, was identified in four widely spaced and roughly linear outcrops. In addition, three excavator trenches, sited on the basis of geophysical anomalies, also confirmed the presence of the sill at other localities. The outcrops extend over a length of 4 km in a northwesterly direction. At two localities the sill has a thin margin of gabbro associated with it. The trace of the sill shown in Figure 48 is based on proven surface exposures and trenches coinciding with a magnetic anomaly that is periodically offset by west-trending faults. Quartz-carbonate alteration zones are commonly associated with or near known ultramafic bodies. The presence of a large (1700 x 125 m) quartz-carbonate zone, northeast of the ultramafic body in the area cut by Kwatinick Creek, suggests the possibility of another ultramafic body within the core of this zone. The only other exposures of similar material occur 8.0 km to the west of Kwatinick Creek, along the creek bank which hosts the Stanley Creek showing. The massive quartz-carbonate zone at Stanley Creek is exposed for over 1200 m along the creek.

The youngest rocks in the area occur within the Taku Terrane, north and east of the Denali fault, and consist of upper Jurassic to lower Cretaceous light to dark-buff grey lithic greywacke, sandstone, and siltstone of the Dezadeash Group (Campbell and Dodds, 1983).

The main tectonic feature in the area is the northwest-trending Denali fault which strikes subparallel to most of the rock units. Very few contacts between units are exposed, and

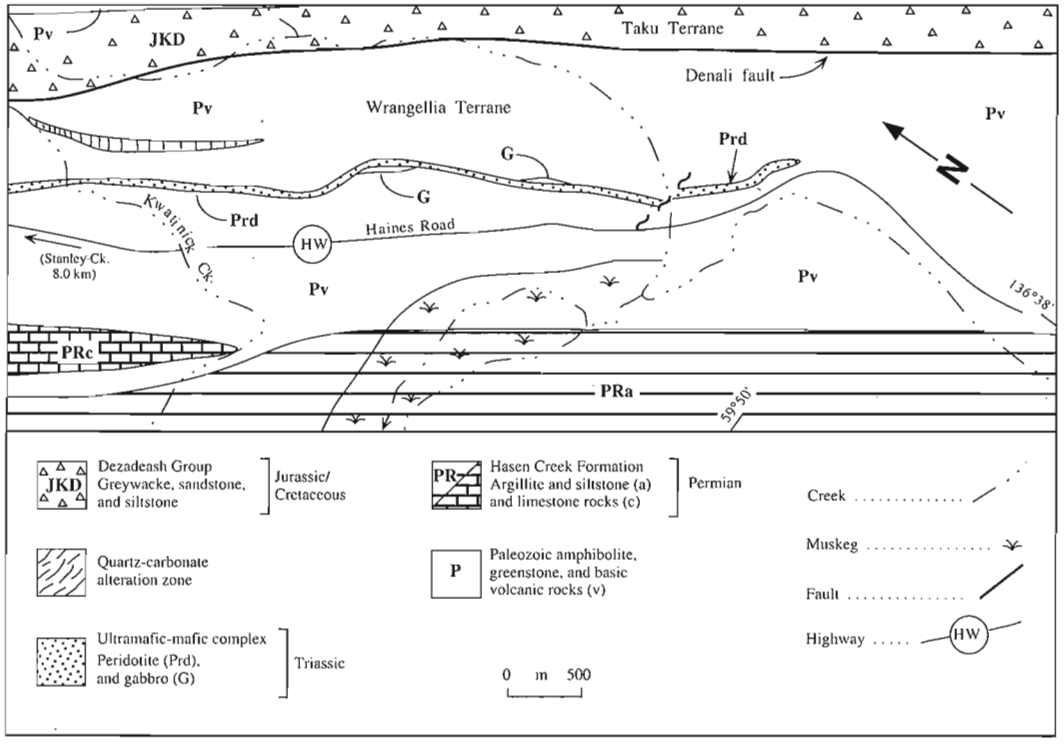

Figure 48. *Generalized geological map of the Mansfield Creek Intrusive Complex and surrounds.*

it is not known if they are conformable or formed by faults paralleling the Denali fault. The abrupt change in course of Stanley Creek, which is coincident with the occurrence of the strongly quartz-carbonate-altered rock unit (hosting the Stanley Creek showing), suggests the presence of a strong west-striking splay off the Denali fault. This westerly orientation is the same as the strike of the fault that hosts the showing (Davis and Main, 1988). Displacement of magnetic and EM anomalies that outline the ultramafic body in Figure 48 also suggests a second west-striking fault system, and is further supported by the presence of a 080° trending shear zone exposed in one of the trenches in this area.

Petrology

Gabbro. Although the gabbro is highly sheared and altered, it is clearly more melanocratic than most marginal gabbro, and is transitional in composition between mela-gabbro and feldspathic olivine clinopyroxenite. These rocks are dark grey to greenish black and appear to have consisted primarily of clinopyroxene, lesser amounts of olivine, and up to 30% interstitial plagioclase. The pyroxene and olivine constituents are totally altered to a felted aggregate of uralite and serpentine, respectively, whereas, the feldspar is completely decomposed to a dark fine-grained turbid mosaic of chlorite, epidote, and calcite. All gabbroic intervals are highly sheared and generally display some degree of foliation. Small lenses of serpentinite within these gabbroic intervals are not uncommon.

A trench cut in the central portion of the ultramafic body (Fig. 48) revealed that a north-flanking marginal zone gabbroic interval had a gradual contact with the adjacent peridotite. This contact relationship suggests that the sub-vertical to vertical dipping body may have had a primary southerly facing direction.

Ultramafic. This group consists primarily of medium- to coarse-grained dark greenish-black serpentinized peridotite (wehrlite) and olivine pyroxenite. Isolated patches containing 0.5 to 2.0% sulphides are not uncommon. The rock is generally competent and massive in areas not overprinted by shearing, but adjacent to and within shear zones the rocks are strongly foliated and commonly contain repetitive intervals of greenish-yellow serpentinite and/or clay. Brecciated intervals within the ultramafic rocks can contain quartz-carbonate veinlets and epidote veinlets all of which may be overprinted in a subsequent silicification event which appears to reseal the host environment.

Ni-Cu±PGE mineralization

Immiscible magmatic segregations.

Ultramafic. The only examples of immiscible magmatic mineralization observed in this complex were found in the serpentinized ultramafic rocks with isolated patches containing 0.5 to 2.0% disseminated sulphides.

Hydrothermal (remobilized ?) mineralization.

Hydrothermal sulphide mineralization. The best known occurrence of Ni-Cu mineralization in the area is that of the Stanley Creek showing. This oxidized vein mineralization was exposed in a narrow fault cutting the quartz-carbonate zone along the southern side of Stanley Creek. At the time of its discovery (1965) it was reported to assay 4.6% Ni and 4.0% Cu over a width of 1.2 m. Since then, Stanley Creek has eroded the base of the showing and there is no evidence of the old trench sites. However, detailed examinations at the locality showed that the showing is hosted in a narrow fault, striking approximately 100° and cuts quartz-carbonate material exhibiting "lithwanitic" alteration (i.e. fuchsite staining), but no obvious Ni or Cu sulphide or carbonate was observed. Well mineralized material selectively picked from the showing, in 1987, assayed 1.10% Ni, 0.23% Cu, 700 ppb Pt, and 760 ppb Pd (Davis and Main, 1988). Oxidized outcrops 100 m south of the showing contain disseminated sphalerite as well as trace amounts of Sb, Sr, and Pb-carbonate. A second showing containing sphalerite was found 1000 m to the south.

Quartz-carbonate mineralization. Cream to orange coloured, silicified, amorphous alteration zones are commonly developed adjacent fault zones in the area. These rocks are included as a separate unit as they form a nearly continuous exposure for over 1200 m along the south bank of Stanley Creek, suggesting that they may be of regional extent. As similar quartz-carbonate alteration zones are associated with the contacts of many known mafic-ultramafic intrusions elsewhere in the Kluane Belt and locally in this area, it is assumed that this material generally represents alteration zones associated with Triassic magmatism. Nevertheless, the extensive development with west-striking splays off the Denali fault implies that this alteration can also be developed in the mafic volcanic rocks. In thin section, the rock displays a fabric consisting of thin ribbons of quartz and calcite set in a finer-grained siliceous Fe-stained matrix. Locally, fuchsite (Cr-mica) is developed.

Quartz-carbonate rocks from the Stanley Creek area have the following compositional ranges: 34-40% SiO_2, 6.8-9.8% $Fe_2O_{3(t)}$, 10.5-16.3 % CaO, 17.6-25.8% CO_2, 0.4-0.7 % S, 260-1700 ppm Cr, 36-500 ppm Cu, 70-1200 ppm Ni, 118-675 ppm As, 2-177 ppb Pd, 12-295 ppb Pt, and 5-23 ppb Au. The most PGE-enriched samples have the highest levels of As and Sb and lowest S and Se concentrations, but similar levels of Ni, Cu, Co, Cr, F, and Cl.

Alaskan section

Rainbow Mountain Intrusive Complex

In the vicinity of Rainbow Mountain, Alaska, an ultramafic complex consisting of dismembered sill-like bodies are exposed along the south side of the Broxson Gulch thrust and the Denali fault, and host Ni-Cu sulphide occurrences similar to those previously described from the Kluane Belt in the Yukon. Although these bodies are confined to the same tectonostratigraphic terrane (Wrangellia) and are also

believed to be co-magmatic with the Triassic Nikolai volcanic rocks, there are minor but important metallogenic differences that have not been observed in the Yukon. The most notable difference is that significant massive sulphide accumulations tend to be hosted within the ultramafic zone of the complex, and gabbro dykes (probably the equivalent of the Maple Creek gabbro) may contain significant Ni-Cu mineralization. A brief discussion of the Alaskan occurrences completes the remaining Ni-Cu-PGE associations related to Triassic magmatism in the Kluane Belt. In addition it provides documented evidence of Kluane-style Ni-Cu-PGE sulphide mineralization in the northernmost part of Wrangellia, and corroborates the great lateral extent of this mineralized belt of mafic-ultramafic rocks throughout the eastern portion of Wrangellia.

Location, history, and physiography

The centre of the Rainbow Mountain study area is located at 63°20'N latitude and 145°45'W longitude, in the east-central Alaska Range of mountains, and is approximately 208 km south-southeast of Fairbanks, Alaska (Fig. 2, 49). The ultramafic complex has been informally named after the prominent nearby Rainbow Mountain (Barker, 1988).

Ni-Cu sulphide occurrences were first staked in the Miller Creek, Ann Creek, and Glacier Lake intrusions by R. Emerick in the early 1950s about the same time as the staking and exploration was in progress on similar bodies in the Yukon. The U.S. Bureau of Mines conducted Ni-Cu investigations in the area between 1959 and 1962 and PGE-related studies between 1981 and 1984. The results of the PGE investigation have been documented by Barker (1988). No production from these bodies or thorough exploration of the prospects has been conducted, but several tonnes of massive sulphide were stockpiled in 1971.

For further details concerning the Rainbow Mountain Complex the reader is referred to Barker (1988).

Structure and stratigraphy

The Rainbow Mountain Complex occurs as a dismembered sill-like body which occurs along the south side of the Broxson Gulch thrust and the Denali (Shakwak) fault, both of which demarcate the northernmost extent of Wrangellia (Fig. 2, 49). The complex is part of a 112 km long trend of mafic-ultramafic rocks that continues along the Denali fault to Gillette Pass in the southeast and along the south side of the Broxson Gulch thrust towards the MacLaren Glacier to the west. These dismembered ultramafic bodies are elongated parallel to the Denali fault and other major faults that cut the east-central Alaska range.

The Denali fault is a major structural feature of the northern Cordillera and extends in an arc for 2000 km from Chatham Strait in the southeastern Alaska panhandle, across southern Alaska and the Yukon Territory and into northwestern British Columbia. At least 400 km of displacement has occurred along the Denali fault which remains active to present. South of the Denali fault, in the Rainbow Mountain area, north- and northeast-trending wrench faults are a common feature and have dismembered the ultramafic complex due to related movements along the Denali fault. The northwest-trending intrusions (i.e. Miller Creek, Glacier Lake, and Canwell Glacier bodies) occur along an escarpment resulting from strike and dip-slip movement along a prominent northeast-trending wrench fault. The Broxson Gulch thrust is a major suture that represents a zone of Mesozoic accretion onto the Wrangellia terrane by rocks to the north. The thrust consists of a series of imbricate north-dipping thrust faults. The west-trending ultramafic bodies in the area are subparallel to and thus likely related to the Broxson Gulch Thrust.

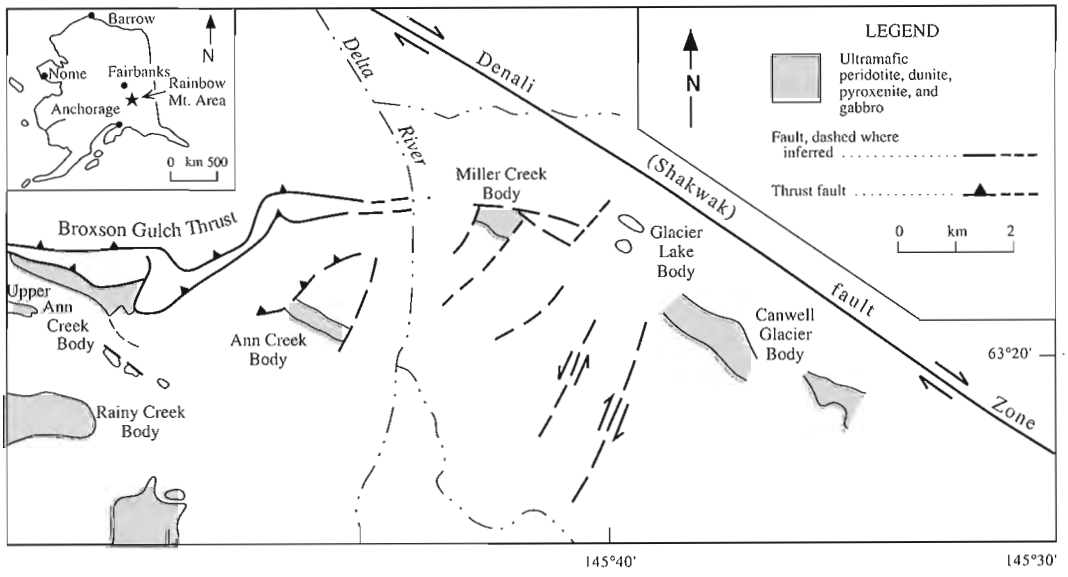

Figure 49. *Generalized geological map of the Rainbow Mountain Complex, Alaska.*

Contacts between the ultramafic bodies and the Permian and Pennsylvanian strata are both intrusive and faulted. West of Delta River, the Ann Creek body intrudes andesite along its northern contact. The Canwell Glacier, Upper Ann Creek, and Rainy Creek ultramafic bodies all demonstrate intrusive contacts with the surrounding andesite.

The Rainbow Mountain Complex is composed principally of peridotite grading into dunite, but locally the dunite grades into plagioclase peridotite, pyroxenite, "light coloured gabbro" (anorthositic gabbro ?), and diorite (gabbroic anorthosite ?). The Canwell Glacier bodies and the Ann Creek body exhibit macro layering that grades from gabbro along the southern margin, to plagioclase peridotite (feldspathic peridotite), followed by peridotite grading to dunite as the succession progresses towards the north (Barker, 1988). This progressively more mafic succession of lithologies away from the southern margin is identical to the mafic-ultramafic bodies in the Kluane Belt of the Yukon and suggests a northerly facing direction. Unfortunately many of the ultramafic intrusive bodies in the Rainbow Mountain area have been intruded by younger granitic bodies, particularily along or near the primary contacts thus obscuring the stratigraphic relationships. Gabbroic dykes have cut the ultramafic strata in the Miller Creek and Canwell Glacier bodies; however, mafic dykes generally occur near the periphery of these bodies, but may also cut both ultramafic and Paleozoic volcanic rocks.

Petrology

Gabbro. Gabbroic rocks are restricted to the so-called "gabbronorite dykes" and "gabbronorite sills". Care should be taken in interpreting these bodies in a true genetic and lithological sense as experience with similar looking bodies from the Yukon ultimately turned out to be faulted marginal zone gabbro. Due to competency differences, fault-emplaced gabbro within ultramafic sequences commonly has very fine-grained aphanitic contacts that coarsen away from the faults, and commonly are mistaken for chilled margins. Also, the modal content of orthopyroxene in these rocks generally fell well short of that required to be classified as *bonafide* gabbronorite in the true sense of the word. Electron microprobe investigation of similar material from the Yukon, previously identified as containing orthopyroxene generally turned out to be [100] pinacoidal sections of diopside with low birefringence and straight extinction, which optically is easily mistaken for orthopyroxene.

Very little petrological information is available for the gabbroic rocks from this area. Barker (1988) documented that the "gabbronorite sill" consists of orthopyroxene, clinopyroxene, olivine, plagioclase, clay minerals, magnetite, and sulphide minerals. The mineralized "gabbronorite dyke" consists of orthopyroxene, with lesser amounts of diopsidic clinopyroxene, serpentinized olivine, feldspar (altered to sericite and clay minerals), chloritized biotite, tremolite, and magnetite.

Ultramafic: Serpentinization has affected all of the Rainbow Mountain Complex ultramafic rocks to some degree and where pervasive the rock displays a distinctive recessive weathering. Completely serpentinized rocks are aphanitic and commonly contain 3 to 5% secondary magnetite disseminated through the rock. The serpentinite is derived from peridotite, feldspathic peridotite, and dunite, and as a rule is greyish to black. Local iron staining due to weathering of sulphide-enriched samples is fairly common in the serpentinite. Serpentinized peridotite consists primarily of antigorite with minor amounts of clinopyroxene, chlorite, epidote, actinolite, magnetite, chromite, biotite, and hornblende. Coatings on weathered surfaces consist of calcite, hematite, malachite, goethite, and garnierite (Barker, 1988).

Ni-Cu±PGE mineralization

Immiscible magmatic sulphide segregations. Ultramafic and mafic rocks from this complex host four different styles of Ni-Cu-PGE sulphide mineralization: (1) disseminations, wisps, and small blebs in the ultramafic rocks, (2) massive sulphide lenses at the lower contact of the ultramafic zone, (3) economically significant disseminations in the gabbroic portions of the complex, and (4) remobilized (hydrothermal) Ni-Cu sulphide mineralization near the contacts of younger intrusive granitic bodies that cut the ultramafic rocks. Unlike comparable ultramafic rocks from the Yukon, the ultramafic zone in the Rainbow Mountain Complex hosts significant lens-like accumulations of massive sulphide mineralization of a primary magmatic origin. This mineralization may contain up to 7055 ppb $PGE+Au_{(t)}$ and differs from the gabbro-hosted mineralization in that the levels of Ru, Ir, and Os generally exceed that of Pt and Pd. The available geochemical data for this complex are summarized graphically in Figures 84, 118, and 128. Data presented in these plots are a compilation of that derived from Barker (1988) and the author's analyses. Unfortunately, Barker's data set did not contain sulphur analyses, and for this reason Cu was chosen as the relative measure of the amount of sulphide in the samples. The plots nicely illustrate the range, and graphical average of metal values associated with each rock type and the relatively coherent geochemical trends.

Gabbro. Gabbro-hosted mineralization occurs in the form of disseminated sulphides in "gabbronorite" dykes and sills which cut the complex (Barker, 1988). The best example of a mineralized "gabbronorite dyke" (?) is associated with the Miller Creek body. Here a steep north-dipping, 4 m wide, dyke strikes west-northwest along a fault plane that has a slickensided and mylonitized fabric along the contact. The mineralized dyke was exposed for <7 m along strike. The metal content of the dyke averages 11455 ppm Ni, 8289 ppm Cu, 189 ppm Co, 989 ppb Pt, 977 ppb Pd, 17 ppb Rh, 4 ppb Os, 16 ppb Ir, and 193 ppb Au, based on nine channel samples across the body (Barker, 1988, Table II). Hand specimen and polished sections contain about 10% disseminated sulphides. The sulphides are commonly 1 mm anhedral interstitial grains consisting, in decreasing order of abundance, of: pyrrhotite, pyrite, pentlandite, chalcopyrite, and traces of bornite.

Disseminated Ni-Cu sulphide mineralization has also been found in an east-northeast-trending, 35 m wide, gabbronorite sill exposed for 75 m near Ann Creek. Geophysical surveys suggest that the sill extends at least 100 m to the east, dips 70° to the north and varies in thickness from 30 to 60 m. Sulphides comprise 3 to 5% of the sill and occur as ≤2 mm interstitial composite grains of pyrrhotite, pentlandite, pyrite, and chalcopyrite. Varying concentrations of sulphides tend to impart a layering to parts of this body. Ni and Cu contents seldom exceed 2000 ppm each with associated maximum Pt and Pd values of 273 and 340 ppb, respectively. Data from the gabbroic bodies suggest a slight enrichment of Pd compared to Pt and lower Ni:Cu ratios (1 to 1.5) compared to other types of Ni-Cu occurrences.

The dimensions and attitude of the sill-like body, the metal grades, and ratios associated with both the so-called dyke and sill-like gabbroic bodies, are remarkably similar to that of the marginal zone gabbro and associated mineralization at the Quill Creek Complex, Yukon.

Samples of mineralized gabbronorite from Miller Creek contain merenskyite $(Pd,Pt)(Te,Bi)_2$ and smaller grains of altaite (PbTe). Grains of a Pt-Pb-As mineral (palarstanide ?) were also found at the boundary of pyrrhotite and silicate as well as native Au particles in silicate. In the Ann Creek body sperrylite ($PtAs_2$) was detected at a pyrrhotite-silicate grain boundary. It would appear that most platinum-group minerals range in size from 0.5 μm to several micrometres, and all occur within, or at the interstices of the silicate minerals rather than in the sulphide grains (Barker, 1988).

Ultramafic. Ni-Cu sulphide mineralization occurs within the ultramafic rocks in the form of: (1) sparsely disseminated sulphide grains, wispy segregations, and small sulphide blebs, and (2) massive sulphide lenses.

The first type of ultramafic-hosted sulphide mineralization is generally developed in proximity to massive sulphide lenses. The sparsely disseminated sulphide minerals consist of pyrrhotite, pentlandite, chalcopyrite, and pyrite in decreasing order of abundance. The average Ni, Cu, and Co content, based on 28 representative samples are: 2929 ppm, 217 ppm and 124 ppm, respectively, whereas, the average Pt and Pd values are 59 and 48 ppb, respectively (Barker, 1988, Table I). The average PGE content of these rocks, which contain rare or no visible sulphide mineralization, is high when compared to typical background levels of similar ultramafic lithologies quoted in the literature (i.e. 10-20 ppb Pt and 2-10 ppb Pd, Crocket, 1981). The ultramafic rocks are characteristically enriched in Pt relative to Pd and have an average Pt:Pd ratio of 1.5.

Massive Ni-Cu sulphide lenses occur within the serpentinized ultramafic sequence in the Miller Creek, Ann Creek, and Canwell Glacier ultramafic bodies. Lenses exposed in trenches in the Miller Creek body range in width from 0.1 to 1.0 m and commonly have strike lengths equal to 10 times their width. Limonitic gossan zones up to 2.0 m in width also occur, and suggest that wider lenses were present. Sulphides compose ≥50% of the rock and have a gangue consisting of serpentine minerals, fine- and medium-grained clinopyroxene, and minor magnetite. The sulphide minerals include pyrrhotite, pentlandite, chalcopyrite, and minor pyrite. Pyrrhotite typically comprises 70% of the mode with pentlandite and chalcopyrite each making up 15%. The average metal content of these lenses, based on 10 samples from the Ann Creek body, is: 45 500 ppm Ni, 7950 ppm Cu, 1237 ppm Co and 724 ppb Pt, 934 ppb Pd, 349 ppb Rh, 880 ppb Ru, 290 ppb Os, 1292 ppb Ir, and 80 ppb Au (Barker, 1988, Table IV). The average Pt:Pd ratio for this type of mineralization is 0.88, and has the highest Ni:Cu ratio (≈6:1).

Exceptionally high concentrations of Ir (3090 ppb), Rh (620 ppb), Ru (2180 ppb), Pt (2380 ppb), and Pd (1680 ppb) have been recorded in samples of this type of mineralization, but are not necessarily associated with the highest Ni or Cu contents. Of particular interest are the levels of Os, Ir, Ru, and Rh, which are considerably higher than in the other types of Ni-Cu sulphide mineralization. Values of Ru, Ir, and occasionally Os, exceeding those of Pt and Pd are not uncommon. Total PGE concentrations as high as 7510 ppb are associated with this type of Ni-Cu mineralization.

A number of Ir-rich arsenide grains were detected at boundaries of pyrrhotite and silicates in the Miller Creek massive sulphides. The grains are 1 to 5 μm in size and have the approximate composition (Ir,Ru,Rh,Pt)AsS and may be irarsite. These grains appear to be zoned, some of which contain Ir-deficient rims.

Based on silicate-sulphide textural relationships and geochemical associations, it is clear that the above mentioned disseminated and massive sulphide mineralization formed under magmatic conditions in response to sulphide-silicate liquid immiscibility in sulphide saturated basic melt. The sulphur-isotope signature of the gabbro and ultramafic-hosted massive sulphide (Fig. 84B) indicate that the Rainbow Mountain Complex is probably the least contaminated complex in entire belt; nevertheless, it is apparent that crustal contamination initiated sulphide immiscibility. The gabbro has a very limited range, $\delta^{34}S$ = -2.7 to -3.0‰. The lowest value is associated with the massive sulphide, $\delta^{34}S$ = -1.2‰. These isotopic compositions are only marginally heavier (≈1.5‰) than those associated with the Quill Creek Complex.

Hydrothermal (remobilized ?) mineralization. The best example of remobilized Ni-Cu-PGE mineralization occurs in the Glacier Lake body where sheared serpentinite is intruded by two dykes of granodioritic to dioritic composition. Sulphide mineralization is associated with the contact of the granodiorite and comprises disseminated, fracture-filling, and semi-massive sulphide minerals occurring over a width of 1.5 to 2 m. Sulphide minerals comprise 10 to 50% of the mineralized zone, and in order of decreasing abundance consist of pyrrhotite, pyrite, pentlandite, cubanite, chalcopyrite, and bornite. The average grade, based on nine representative samples, is 28 900 ppm Ni, 14 600 ppm Cu, 687 ppm Co, 410 ppb Pt, 495 ppb Pd, 57 ppb Rh, 29 ppb Ru, 90 ppb Ir, and 25 ppb Au. Similar, but poorly exposed, occurrences are located in the Canwell Glacier and Rainy Creek bodies. This style of massive sulphide mineralization contains

significantly more Cu than the immiscible magmatic accumulations occurring as massive sulphide lenses in ultramafic rocks.

SILICATE AND OXIDE MINERAL CHEMISTRY

A detailed electron microprobe investigation of silicate and oxide mineral compositions from the White River (Onion, Canalask properties), Arch, Quill Creek (Wellgreen), Linda, Tatamagouche, Duke River, Halfbreed Creek, Dickson Creek, and Chilkat complexes, and to a lesser extent the comagmatic Nikolai volcanic rocks was conducted to: (1) establish the degree of differentiation and the chemical signature associated with mafic and ultramafic members of each complex within the belt, (2) test for compositional features that may distinguish mineralized from non-mineralized bodies, and (3) use the mineral chemistry to help constrain the nature and degree of fractionation (primitiveness) of the basaltic parental magmas and the tectonomagmatic environment in which Kluane magmatism took place during the Middle Triassic. The compositional data are summarized in Figures 50 to 72. Due to the relatively small concentration of ferric iron in mafic silicates, and large uncertainties associated with procedures designed to calculate it, all electron microprobe iron analyses have been treated as ferrous concentrations.

Olivine

Originally, olivine was the most abundant mafic silicate phase in the Kluane mafic-ultramafic intrusions, and thus its composition should help assess the degree of differentiation associated with each intrusive complex. In addition it may also detect Ni depletion associated with mineralized intrusions. Unfortunately, many of the ultramafic members have been highly serpentinized due to local and regional tectonism. Nevertheless, a dedicated search for fresh olivine-bearing lithologies within the belt has resulted in compositional data for all bodies except the Dickson Creek and Chilkat complexes. Compositional data for olivine, expressed in the form of the $Mg/(Mg+Fe^{2+})$ ratio and $Mg/(Mg+Fe^{2+})$ vs. Ni are represented in Figures 50 and 51 respectively. Core to rim compositional zoning is negligible (approximately 1.0%).

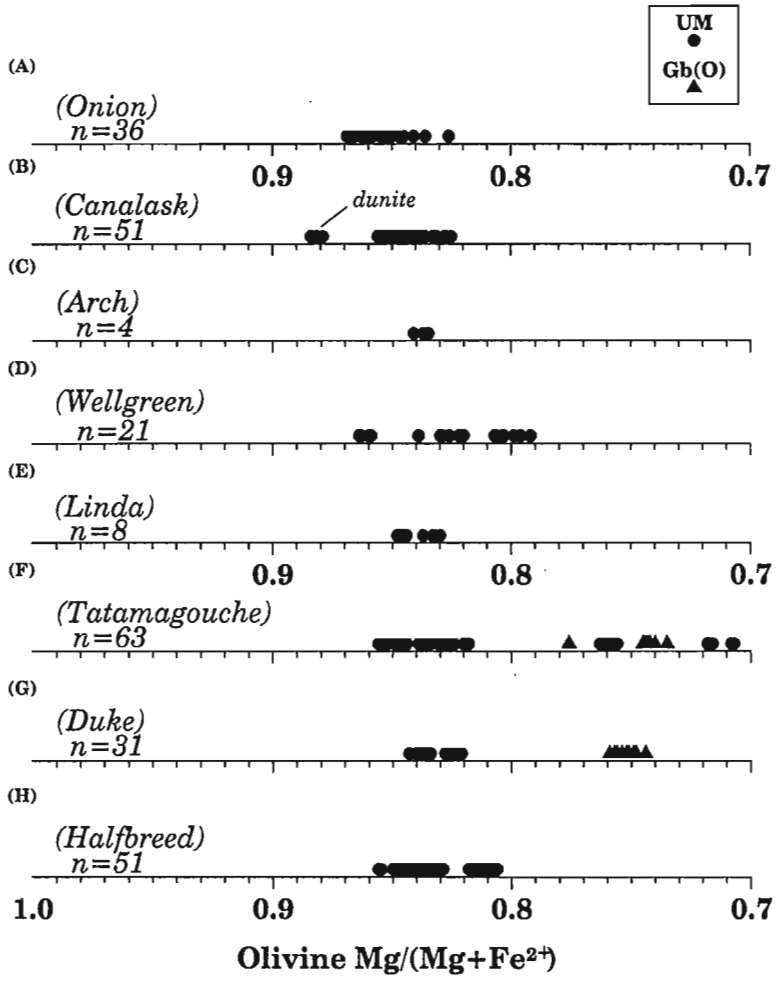

Figure 50 (A-H).

Olivine compositions associated with igneous complexes (or properties) from the Kluane Mafic-Ultramafic Belt. UM = ultramafic, Gb(O) = olivine gabbro.

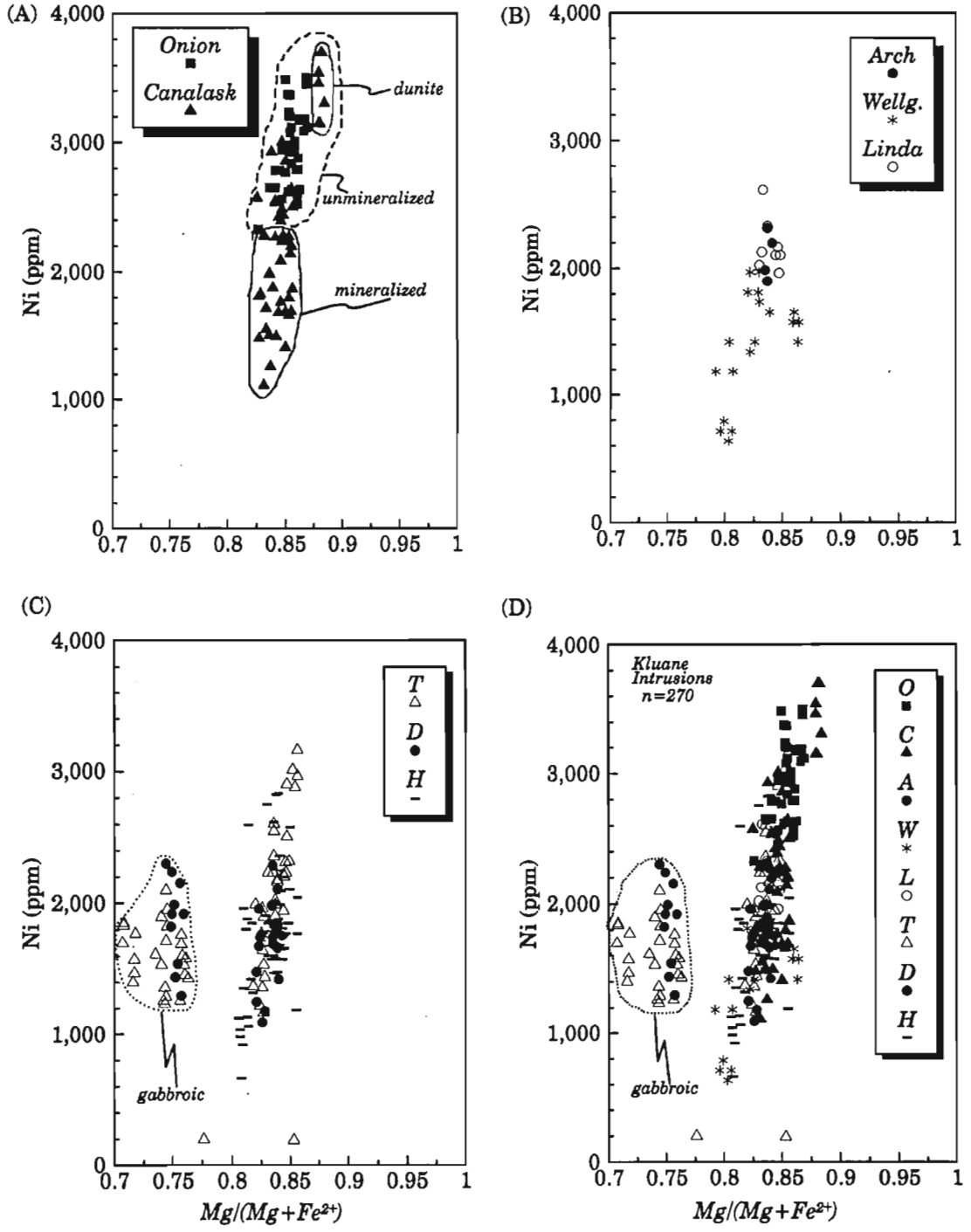

Figure 51 (A-D). *Ni vs. Mg/(Mg+Fe^{2+}) compositional data for olivine from the different igneous complexes or respective properties. O = Onion, C = Canalask, A = Arch, W = Wellgreen, L = Linda, T = Tatamagouche, D = Duke, H = Halfbreed. Note the Ni-depleted olivine associated with or proximal to disseminated sulphides in Canalask samples from the White River Complex (Fig. 51A). Samples from mineralized ultramafic rocks from the Arch, Wellgreen (Wellg.) and Linda complexes also demonstrate significant Ni depletion.*

The $Mg/(Mg+Fe^{2+})$ of olivine (Fig. 50) from all complexes, with the exception of the Quill Creek (Wellgreen) and Tatamagouche Creek complexes has relatively limited ranges: Onion (0.827 to 0.870), Canalask (0.825 to 0.858), Arch (0.835 to 0.842), Linda (0.830 to 0.848), Duke (0.820 to 0.844), and Halfbreed (0.805 to 0.855) for peridotite and olivine clinopyroxenite ultramafic rocks. Fresh olivine from dunite was only obtained from the Canalask property of the White River Complex where the $Mg/(Mg+Fe^{2+})$ was restricted to the range 0.880 to 0.885 which is about 2.3% more magnesian (primitive) than that of associated peridotite from Canalask. Higher $Mg/(Mg+Fe^{2+})$ ratios associated with the dunite relative to peridotite is a common feature in many layered intrusions, especially those associated with anomalous concentrations of chromite as is the case for the Canalask dunite. The increase in Mg is attributed to subsolidus re-equilibration.

The only fresh olivine encountered in the Quill Creek Complex (Wellgreen) is associated with the mineralized olivine clinopyroxenite member. Within this member the $Mg/(Mg+Fe^{2+})$ varied from 0.795 to 0.865. With the exception of the Tatamagouche Complex, this is the largest compositional range encountered in the belt. The most probable explanation for this range is attributed to olivine equilibrating with varying amounts of Fe-Ni sulphides.

The greatest range in $Mg/(Mg+Fe^{2+})$ of olivine was encountered in samples from the Tatamagouche Complex (0.707 to 0.858). The most common compositions occur in the 0.819 to 0.857 range; however, two minor populations are in the 0.707 to 0.718 and 0.755 to 0.764 ranges. In hand specimen the more fractionated samples appear similar to those with the more primitive compositions. Olivine gabbro, inferred to be from a similar stratigraphic level, generally has compositions (0.734 to 0.746 and 0.775) close to those associated with fractionated ultramafic rocks. The wide compositional range of cumulus olivine in both the ultramafic and gabbroic rocks demonstrates that cumulates from the Tatamagouche Complex are the products of more fractionated magmas. The only other occurrence of olivine-bearing gabbroic rocks was discovered in the Duke River Complex. Here the olivine gabbro and lesser amounts of picritic material occur as inclusions in finer-grained Maple Creek gabbro. The $Mg/(Mg+Fe^{2+})$ of olivine from these rocks ranged from 0.743 to 0.760 and falls within the range established for olivine gabbro from Tatamagouche.

The nickel content of olivine is from 3800 ppm in dunite from the Canalask property, to a low of 650 ppm in the mineralized olivine clinopyroxenite member from the Quill Creek Complex (Wellgreen). The relationship between the $Mg/(Mg+Fe^{2+})$ of olivine and the associated nickel content of olivine from various complexes is shown in Figure 51. Data for mineralized and unmineralized ultramafic rocks from the Onion and Canalask properties (Fig. 51A) of the White River Complex display some interesting trends. It is apparent that olivine of similar composition, with respect to the $Mg/(Mg+Fe^{2+})$, has a wide range in Ni contents. Olivine associated with peridotite containing disseminations of sulphides (5-8%) and denoted as "mineralized" contains approximately half the Ni concentration found in "unmineralized" peridotite and dunite. The Ni-depletion in olivine, therefore, is a consequence of equilibration with anomalous amounts of sulphide. Similar Ni depletion is also present in olivine from weakly mineralized ultramafic rocks of the Arch, Linda, and Quill Creek (Wellgreen) complexes (Fig. 51B); the Wellgreen (Wellg.) samples, however, demonstrate even greater Ni depletion than that recorded from the Onion and Canalask properties of the White River Complex. This metal depletion may also be the result of subsequent olivine crystallization from a Ni impoverished magma remaining after segregation of large quantities of immiscible sulphides at the base of the complex.

Olivine compositional data from the Tatamagouche, Duke River, and Halfbreed Creek complexes (Fig. 51C) demonstrate compositional relationships suggesting olivine crystallizing in both environments. Approximately half of the analyzed olivine from the Tatamagouche Complex falls within the established "mineralized" field. The presence of anomalous localized disseminated sulphides in ultramafic rocks, and the existence of at least two basal massive Ni-Cu sulphide bodies in this portion of the Tatamagouche Complex may explain the Ni-depleted nature of many of the olivines. Although less apparent than in the Tatamagouche Complex, disseminated sulphides are visible in many ultramafic rocks from the Duke River Complex suggesting that olivine from this complex crystallized in the presence of anomalous quantities comagmatic Fe-Ni sulphides, thus accounting for the Ni-depleted nature of most olivine from this complex. Approximately two-thirds of the analyzed olivine from the Halfbreed Creek Complex falls in the "mineralized" field; however, no anomalous Ni-Cu sulphide mineralization has been discovered in this complex to date.

The Ni content of olivine from the more differentiated gabbroic lithologies is the result of fractional crystallization. It is apparent that the Ni-depleted olivine associated with the so-called "mineralized" field of the ultramafic rocks cannot be due to fractional crystallization (Duke and Naldrett, 1978; Duke, 1979) and visible sulphides are usually present; it is proposed that this approach may be used to discriminate mineralized from unmineralized intrusions in the Kluane Belt.

A plot of all olivine compositional data (270 analyses) with respect to Ni concentration and $Mg/(Mg+Fe^{2+})$ is given in Figure 51D. Although pseudomorphs of iddingsite after olivine occur in the co-magmatic Nikolai volcanic rocks, thus confirming its presence in the original magmas, representative olivine compositions could not be obtained due to the pervasive alteration.

Pyroxene

Clinopyroxene is present as both a cumulus and intercumulus phase in the ultramafic rocks. Little if any compositional difference exists between cumulus and intercumulus clinopyroxene within the same sample, indicating that postcumulus re-equilibration has taken place. Optical and compositional zoning is seldom present in ultramafic-hosted clinopyroxene, but is one of the most striking optical features in gabbroic rocks, and accounts for part of the broad compositional range

encountered in these rocks. Although present, orthopyroxene is generally of accessory status and crystallizes only as a late stage intercumulus phase in ultramafic rocks and as a late interstitial phase in the gabbro. Clinopyroxenes within semi-massive sulphide concentrations, magnetite-rich Maple Creek gabbroic bodies, and those associated with thermally metamorphosed country rock sediments fall within distinctive compositional fields. Pyroxene compositional data from the belt are summarized in Figures 52 to 60.

The $Mg/(Mg+Fe^{2+})$ for ultramafic, olivine gabbro, magnetite gabbro, anorthositic gabbro, and typical Kluane marginal zone gabbro-hosted clinopyroxene for the respective intrusions are shown in Figures 52 and 53(A, B). Ratios for semi-massive sulphide and country rock-hosted lithologies are also shown for the Arch and Canalask properties (Fig. 52).

Ultramafic-hosted clinopyroxene from all complexes, except Tatamagouche and Quill Creek (Wellgreen), demonstrate a rather tight $Mg/(Mg+Fe^{2+})$ grouping in the 0.840 to 0.895 range (Fig. 52). The high $Mg/(Mg+Fe^{2+})$ ratios and limited range attest to the relatively primitive nature and limited degree of fractionation of the magmas that gave rise to the ultramafic lithologies within these complexes. Clinopyroxene from the Quill Creek (Wellgreen) Complex (Fig. 53A) shows a wider range consisting of two groups (0.805 to 0.830 and 0.845 to 0.880). The latter group appears to fall in the general range established for other bodies in the belt. The more Fe-rich clinopyroxene group is associated with the more Fe-rich olivine encountered in the Quill Creek Complex. Ultramafic rocks from the Tatamagouche Complex contain clinopyroxene (Fig. 53B) with the widest range of $Mg/(Mg+Fe^{2+})$ ratios encountered in the belt (0.570 to 0.915). Although there is considerable range, most clinopyroxene group in the 0.805 to 0.890 and 0.730 to 0.790 ranges. Outliers occur at 0.900, 0.912, 0.662, and 0.570, with the last value being attributed to zoning. The more Fe-rich group represents clinopyroxene core compositions from the more evolved ultramafic cumulates which also contain Fe-rich olivine. This distinctive silicate Fe-enrichment is only associated with the two largest complexes in the belt, and also those that have the best recorded basal massive sulphide accumulations. This feature may imply that the broader compositional range is a consequence of a higher degree of differentiation experienced by the larger subvolcanic magma chambers. Nevertheless, the influence of sulphides on this chemical relationship cannot be overlooked.

Gabbroic rocks have $Mg/(Mg+Fe^{2+})$ ratios (Mg#) that range from 0.530 to 0.875 (Fig. 52, 53). Most of the marginal zone type gabbroic rocks have clinopyroxene with core compositions that fall in the 0.875 to 0.825 range. Iron-enriched compositions (Mg# ≤0.80) are generally attributed to zoning and minor late stage Fe-rich interstitial clinopyroxene

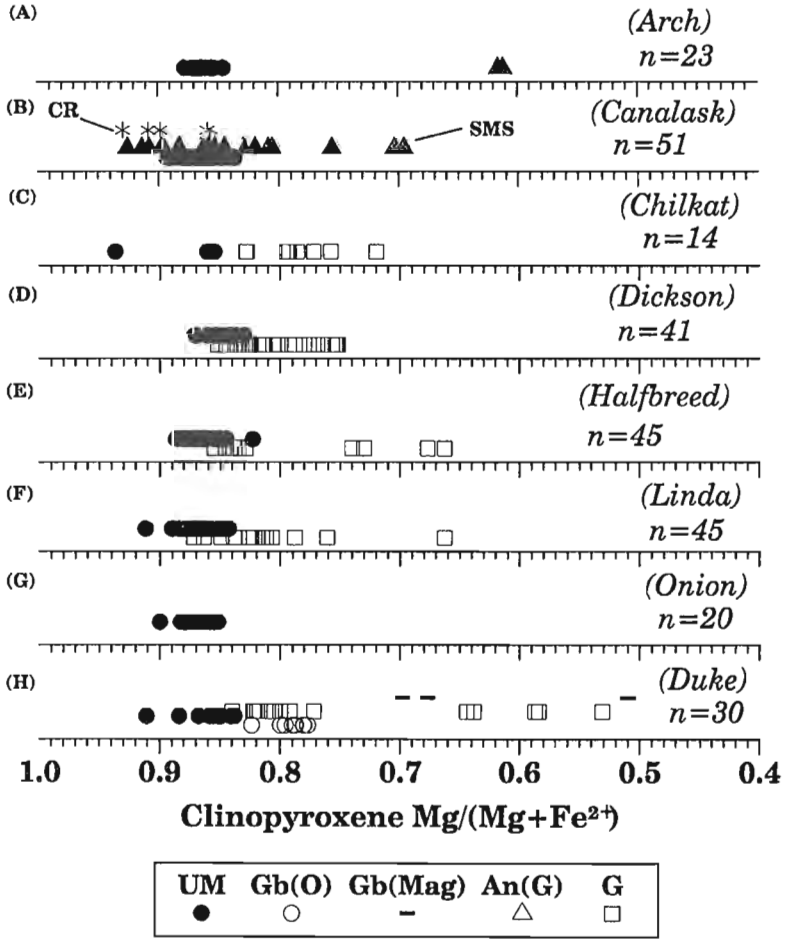

Figure 52 (A-H).

Clinopyroxene compositions associated with various igneous complexes (or properties) and respective lithologies. UM = ultramafic, Gb(O) = olivine gabbro, Gb(Mag) = magnetite gabbro, An(G) = anorthositic gabbro, G = gabbro, CR = country rock (asterisk), SMS = semi-massive sulphide (filled triangle).

crystallizing products. The main gabbro trend overlaps the dominant ultramafic compositional grouping, and suggests compositional continuity, similar to that observed in a detailed study conducted (Fig. 16) in the Quill Creek Complex. The $Mg/(Mg+Fe^{2+})$ trend displayed by the Quill Creek Complex pyroxene is expected for a marginal zone that forms under non-equilibrium chill facies conditions towards hotter equilibrium conditions as the fractional crystallization and cumulate activity is approached and new ingressions of magma take place. Unlike ultramafic-hosted clinopyroxene, those from gabbro have core compositions that can vary by 5 per cent. Compositional variability appears to decrease as the magma evolves from the basal contact towards the ultramafic horizon. Therefore, mineral core composition variations and pronounced normal zoning in the marginal gabbro clinopyroxene are believed to be a manifestation of rapidly and locally changing crystallization conditions (T, f_{O2}, aFe) in an evolving marginal zone sequence. By far the greatest observed near continuous spread in the $Mg/(Mg+Fe^{2+})$ of clinopyroxene is in the Quill Creek (Wellgreen) Complex (Fig. 53A). The highest values fall in the 0.780 to 0.700 range. Samples with values from the upper end of this range, and outliers with even higher Mg-contents, represent mela-gabbro with cumulate-like features that appear to be continuous with the overlying feldspathic clinopyroxenite and feldspathic olivine clinopyroxenite. The more Fe-rich compositions (≤0.700) are generally due to normal zoning, and the occasional Fe-rich interstitial clinopyroxene crystallization products. Quenched samples from the basal portion of the marginal zone gabbro reveal even larger core to rim compositional variations resulting from zoning.

Clinopyroxene from gabbro of cumulate origin (i.e. Gb(O) from the Duke River (Fig. 52H) and Tatamagouche (Fig. 53B) complexes) display a compositional continuity and overlap, respectively, demonstrating the common petrogenetic link between cumulate and marginal gabbroic rocks and the overlying ultramafic rocks. Clinopyroxenes from related anorthositic gabbro cumulates at Tatamagouche fall in the compositional range established by the olivine gabbro cumulates.

Magnetite gabbro from the Duke River and Tatamagouche complexes shows the greatest range in $Mg/(Mg+Fe^{2+})$ ratios (0.840-0.470). The most common range for clinopyroxene from both complexes is 0.700 to 0.640. The range in composition is a consequence of variable T-f_{O2} crystallization conditions, also corroborated by a variety of textures, grain size, and anomalous amounts of magnetite, and mineralogical zoning.

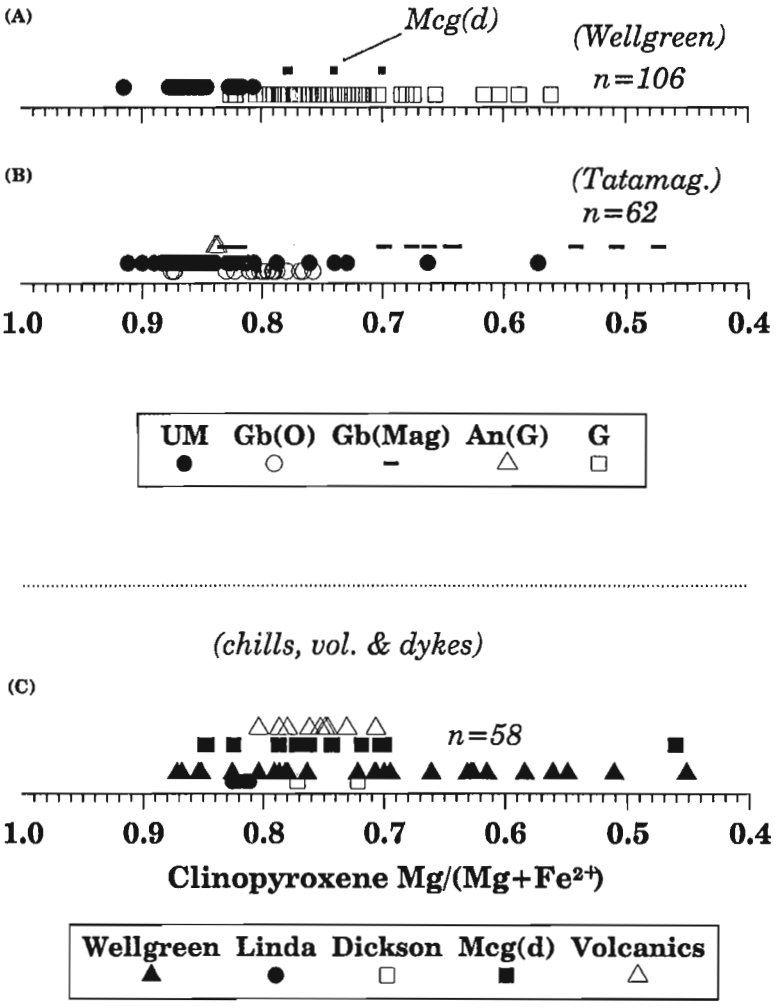

Figure 53 (A-C).

Clinopyroxene compositions associated with respective lithologies from various igneous complexes (or properties), and (C) for the associated quenched facies. UM = ultramafic, Gb(O) = olivine gabbro, Gb(Mag) = magnetite gabbro, An(G) = anorthositic gabbro, G = gabbro, Mcg(d) = Maple Creek gabbro dyke.

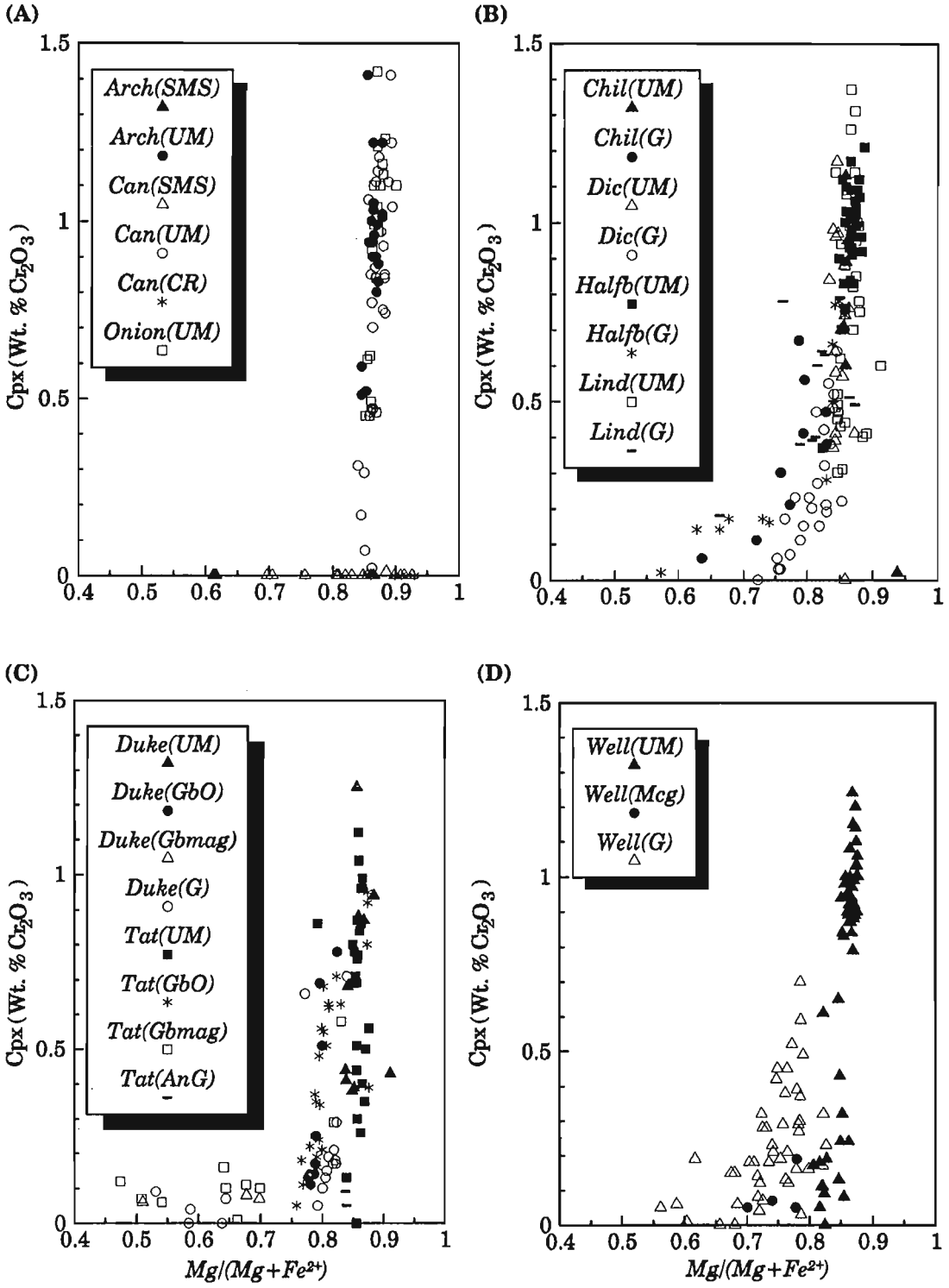

Figure 54 (A-D). *Cr_2O_3 (wt.%) vs. Mg/(Mg+Fe^{2+}) plot of clinopyroxene compositions with respect to associated intrusive complex (or property) and host lithology. Complexes or properties: Arch = Arch, Can = Canalask, Onion = Onion, Chil = Chilkat, Dic = Dickson, Halfb = Halfbreed, Lind = Linda, Duke = Duke, Tat = Tatamagouche, Well = Wellgreen. Lithologies: UM = ultramafic, SMS = semi-massive sulphide, GbO = olivine gabbro, Gbmag = magnetite gabbro, AnG = anorthositic gabbro, G = gabbro, Mcg = Maple Creek gabbro dyke, CR = country rock.*

The $Mg/(Mg+Fe^{2+})$ of clinopyroxene hosted in semi-massive sulphide concentrations is extremely variable. Samples from the Arch Creek Complex are confined to the range 0.620 to 0.610, whereas those from the Canalask property of the White River Complex cover the interval 0.930 to 0.695 (Fig. 52A,B). This wide range, relative to that established for other lithologies, could only be attributed to varying degrees of subsolidus re-equilibration with Fe-sulphides.

Clinopyroxene from thermally metamorphosed country rock is readily distinguishable from its magmatic counterparts on the basis of its high $Mg/(Mg+Fe^{2+})$ ratio (0.860 to 0.930). This compositional characteristic could be used to distinguish the origin of certain ambiguous clinopyroxene-bearing lithologies associated with the footwall Ni sulphide mineralization (i.e. "Gabbro-Sediment Zone").

Clinopyroxene compositions from a number of chilled margins associated with the Quill Creek (Wellgreen), Linda, and Dickson Creek complexes, and samples of Maple Creek gabbro dykes and Nikolai volcanic rocks were examined (Fig. 53C). The degree of $Mg/(Mg+Fe^{2+})$ variability appears to decrease in the following order: Quill Creek Complex (Wellgreen chills), Maple Creek gabbro dykes, Nikolai basalt, Dickson Creek and Linda Complex chilled margins. Although all samples retain their primary igneous compositions, the variation encountered should sound as a precaution in interpreting the primary composition of the initial magma(s) based on pyroxene compositions from mineralized intrusions. Significant core compositional variations (up to 10%) were noted within a single polished thin section and were dependent on proximity of the pyroxene to sulphide grains. Extreme normal zoning occurs in the clinopyroxene from the Quill Creek chilled gabbro (0.710 to 0.460). However, clinopyroxene from sulphide-poor chilled gabbro generally have core compositions in the 0.780 to 0.710 range, with an average core $Mg/(Mg+Fe^{2+})$ value of 0.720, and rim compositions that are 10% richer in iron. The most common $Mg/(Mg+Fe^{2+})$-rich clinopyroxene falls in the 0.788 to 0.764 range and generally has rims slightly enriched in iron (1 to 2 %). These values are similar to those in clinopyroxene cores in chilled margins of Maple Creek gabbro dykes (0.787) that cut the complex. The rims of these same pyroxenes are generally enriched in iron (2.0%) due to normal zoning, but rim compositions with 6-7% more iron have been noted. Similar dykes cutting the Arch complex have clinopyroxene with noticeably higher $Mg/(Mg+Fe^{2+})$ core compositions (0.847 to 0.825) and less than 0.5% Fe enrichment in the rim compositions. These initial clinopyroxene compositions based on quenched margins of Maple Creek gabbro dykes from the Arch Complex are similar to those measured in the chilled margin from the Linda Complex (0.827 to 0.815) and to a Mg-rich group from the Quill Creek Complex ($Mg/Mg+Fe^{2+}$= 0.870 to 0.805). Differences in composition of clinopyroxene from chilled margins of both dykes and the intrusive complexes suggest that at least two batches of basaltic magma were involved in the emplacement and crystallization history of many of these mafic-ultramafic complexes. A similar suggestion was made earlier based on the distribution of chilled gabbroic facies rocks within the Quill Creek Complex marginal gabbro, and also the position of some massive sulphide accumulations relative to the basal contact (Fig. 21, 23).

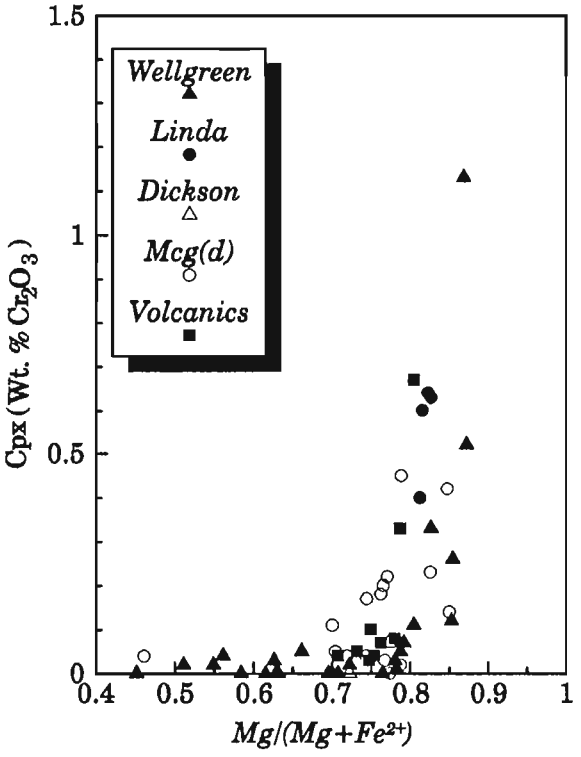

Figure 55. *Cr_2O_3 (wt.%) vs. $Mg/(Mg+Fe^{2+})$ plot of clinopyroxene compositions with respect to quenched facies clinopyroxenes from the Wellgreen property of the Quill Creek Complex, Linda and Dickson Creek complexes, Maple Creek gabbro dykes (Mcg(d)), and coeval Nikolai volcanic rocks.*

Limited investigation of the Nikolai volcanic rocks also suggests two groups of clinopyroxene based on their $Mg/(Mg+Fe^{2+})$ ratios. Those with ratios in the 0.805 to 0.750 range represent the compositions of glomerophyric phenocrysts, whereas compositions in the 0.750 to 0.705 range are indicative of clinopyroxene groundmass compositions.

The Cr_2O_3 content of clinopyroxene was investigated relative to its $Mg/(Mg+Fe^{2+})$ ratio (Fig. 54, 55) to: (1) establish the chromium contribution to the rock by this phase, (2) demonstrate a continuity between ultramafic and gabbroic-hosted clinopyroxene to corroborate the petrogenetic link between these two different lithological groups, and (3) look for chemical discontinuities or irregularities associated with particular lithologies. One of the most apparent trends reflected in these plots (in particular Fig. 54B, C, D) is the exponential curve-like relationship showing the sympathetically decreasing Cr_2O_3 and $Mg/(Mg+Fe^{2+})$ content. This trend monitors the diadochy between Mg and Cr in clinopyroxene from ultramafic and gabbroic rocks within the Kluane Belt. A detailed investigation of this relationship was also established in the Quill Creek Intrusive Complex (Fig. 16). From here and other localities the Cr_2O_3 content of the

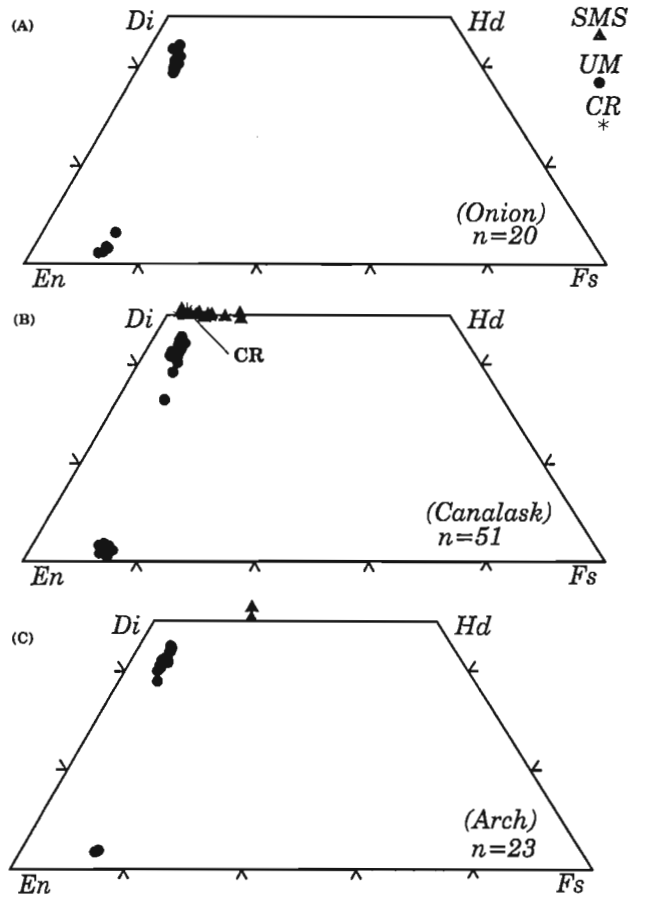

Figure 56 (A-C). *Pyroxene quadrilateral compositions of clino- and orthopyroxenes from the Onion and Canalask properties of the White River Intrusive Complex, and the Arch Creek Intrusive Complex, with respect to host lithology. Note the diopsidic character of clinopyroxenes associated with semi-massive sulphides (SMS) and country rock (CR) hornfels; UM = ultramafic rocks.*

clinopyroxene appears to increase in the following order: chilled gabbro, fine- to medium-grained gabbro, melagabbro, clinopyroxenite, olivine clinopyroxenite, peridotite, and dunite. Many of the coarser-grained gabbro and pyroxenite compositions overlap in the zone marking the transition from mafic to ultramafic rocks.

Low Cr_2O_3 (<0.5 wt.%) content in some ultramafic rocks, particularly those from areas containing abnormally thin gabbroic marginal rocks, may be a consequence of a more limited volume of magma for the pyroxene to sequester Cr_2O_3. Clinopyroxene hosted by semi-massive concentrations of sulphides (i.e. Arch, Canalask, Fig. 54A) are relatively barren in terms of their Cr_2O_3 content. Although substantial subsolidus Fe-Mg exchange has taken place between the clinopyroxene and Fe-sulphide, this alone does not explain the Cr_2O_3 depletion. As sulphide immiscibility would have been a rapid and short-lived event, any cotectic clinopyroxene caught up by the sinking sulphide melt would have been rapidly carried to the base of the magma chamber and thus not allowed to communicate and scavenge chromium from the melt to the degree experienced by normal cumulates. Country rock clinopyroxene has only trace amounts of Cr_2O_3 due to the low levels present in the calc-silicate precursor.

A similar relationship between $Mg/(Mg+Fe^{2+})$ and Cr_2O_3 was found in clinopyroxene from Quill Creek, Linda, and Dickson Creek chills and Maple Creek gabbro dykes and Nikolai volcanic rocks (Fig. 55).

Compositional data for pyroxene from the Kluane Belt have been plotted on the pyroxene quadrilateral in terms of Wo-En-Fs components, and are represented in Figures 56, 57, 58 and 59 with respect to the complex or property and lithological host. Due to the fine scale nature of exsolutions within the pyroxene, and the large number of analyses required to investigate compositions throughout the belt, defocus broad beam electron microprobe analyses were not conducted to obtain bulk pyroxene analyses. Nevertheless, a high density or maxima of Wo-En-Fs compositional data points for various lithologies and localities is a reasonably accurate representation of their bulk composition. To facilitate comparison Figure 60 illustrates pyroxene compositional

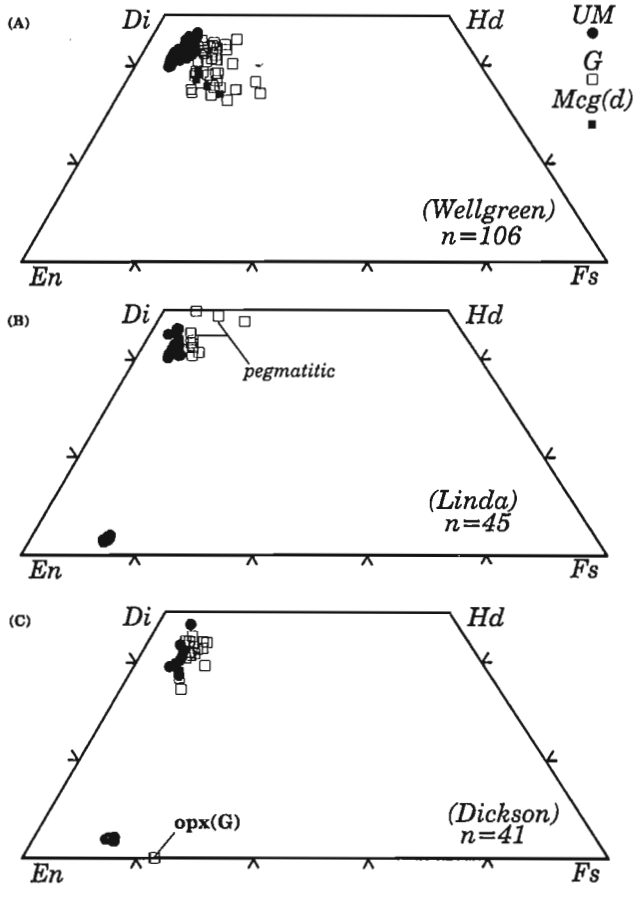

Figure 57 (A-C). *Pyroxene quadrilateral compositions of clino- and orthopyroxenes (opx) from the Wellgreen property of the Quill Creek Complex and the Linda and Dickson Creek complexes with respect to host lithology. UM = ultramafic, G = gabbro, Mcg(d) = Maple Creek gabbro dyke.*

trends for other mafic-ultramafic complexes (i.e. Sudbury, Naldrett et al., 1970; Bushveld, Atkins, 1969, Hulbert and Sharpe, 1981, Buchanan, 1979; Bjerkrem-Sogndal, Duchesne, 1972; Jimberlana, Campbell, 1973; Dufek, Himmelberg and Ford, 1976; Skaergaard, Brown and Vincent, 1963; Stillwater, McCallum et al., 1980).

Clinopyroxene in ultramafic rocks from the Kluane Belt generally plots within the "endiopside" field (Wo_{25-45}, Fs_{0-10}) along the left side of the pyroxene quadrilateral (Onion, Dickson, Tatamagouche, Duke, Halfbreed, and Chilkat, Fig. 56A, 57C, 58A, B, C, 59, respectively). Clinopyroxene from Arch (Fig. 56C), Canalask (Fig. 56B), Linda (Fig. 57B), and Quill Creek (Wellgreen) (Fig. 57A) also have a high proportion of their compositions within the "endiopside" field, but an increasing number demonstrate compositional excursions into the "diopside" field (Wo_{45-50}, Fs_{0-10}), respectively. Those with diopsidic compositions are associated with economically significant concentrations of Ni-Cu-PGE sulphide mineralization arising from contamination of the magma by calcareous Hasen Creek Formation and "Transitional zone" sediments. The influence of calcareous contamination on the wollastonite (Wo) component of proximal igneous pyroxene is best illustrated by the "pegmatitic" samples from

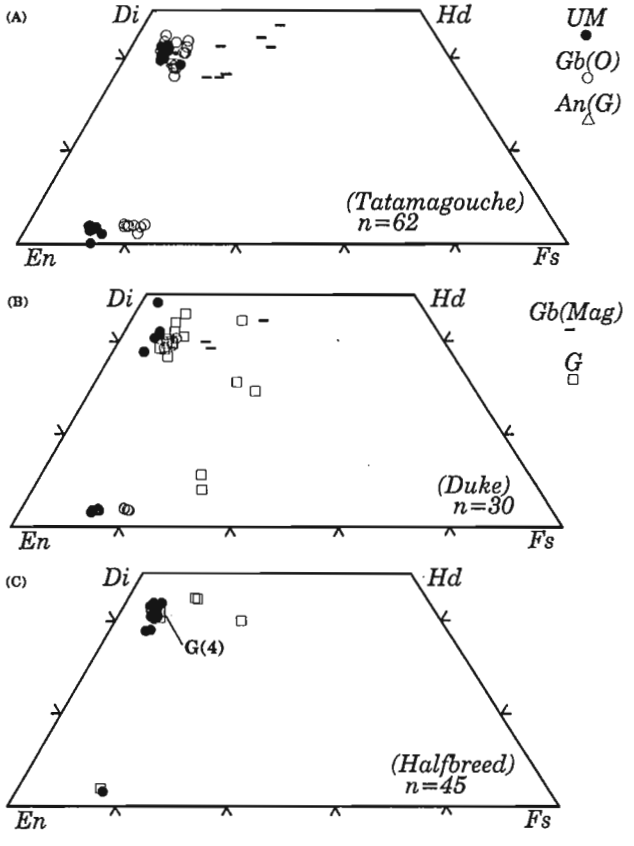

Figure 58 (A-C). *Pyroxene quadrilateral compositions of clino- and orthopyroxenes from the Tatamagouche Creek, Duke River and Halfbreed Creek complexes. UM = ultramafic, Gb(o) = olivine gabbro, An(G) = anorthositic gabbro, Gb(Mag) = magnetite gabbro.*

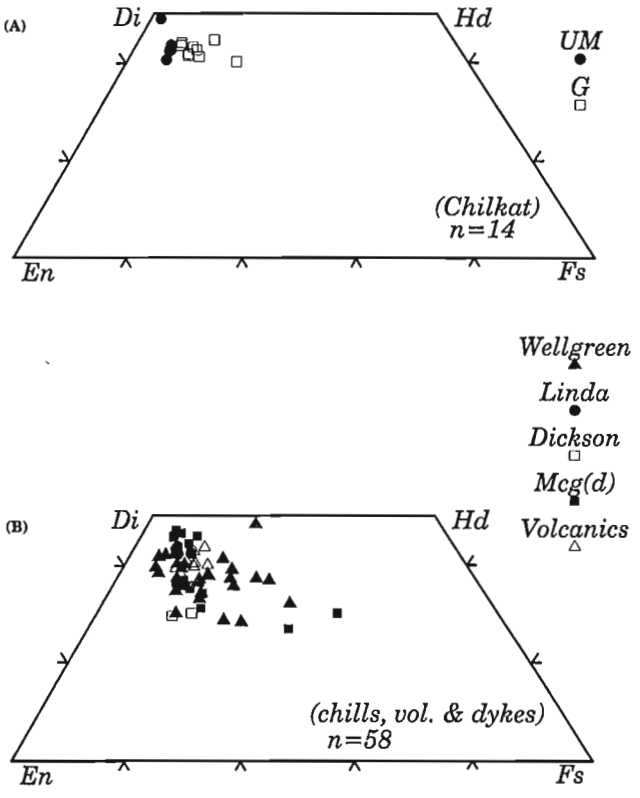

Figure 59. *(A) Pyroxene quadrilateral compositions of clino- and orthopyroxenes from the Chilkat Igneous Complex, and (B) quenched facies from the Wellgreen property of the Quill Creek Complex, the Linda Creek Complex, Maple Creek gabbro dykes (Mcg(d)), and Nikolai volcanics. UM = ultramafic, G = gabbro.*

the Linda Complex (Fig. 57B). The pegmatitic gabbro has formed from intrusion of gabbroic magma capable of crystallizing pyroxene compositions similar to the gabbro samples (i.e. with a *Wo* component less than 45%) to the right of the ultramafic field. Reaction of this magma with calcareous sedimentary rocks has resulted in varied-textured rocks with pegmatitic gabbro pockets, some of which contain coarse interstitial sulphide patches. The mode of these rocks indicates higher abundances of calcium-bearing minerals: plagioclase and clinopyroxene with lesser amounts of sphene, calcite, and locally grossularite, relative to other gabbro. Clinopyroxene from this environment is abnormally enriched in calcium or the pyroxene *Wo* component (Fig. 57B), and thus it is apparent how the more diopsidic ultramafic-hosted clinopyroxene compositions are influenced by contamination. The same reasoning can explain the diopsidic to salitic compositions of clinopyroxene hosted by semi-massive sulphides at Canalask and Arch. Calcareous contamination resulting in sulphide immiscibility would clearly give rise to calcium- or wollastonite-enriched early pyroxene caught up within the basal sulphide concentrations. The most diopsidic pyroxene encountered in this study is from the thermally metamorphosed calcareous country rock adjacent the White River Complex at the Canalask property (Fig. 56B).

With the exception of the pegmatitic gabbro from Linda and the magnetite gabbro from the Tatamagouche and Duke River complexes, clinopyroxene from gabbroic rocks generally occurs immediately to the right of the associated ultramafic domain, within the confines of the "endiopside" field or overlaps into the "augite" field. With progressive Fe-enrichment the samples evolve towards the Fs component. The most evolved igneous compositions are associated with the Quill Creek (Wellgreen) and Duke River complexes.

Orthopyroxene (bronzite) associated with ultramafic rocks generally fall in the En_{84-86} range, but compositions as low as En_{82} have been discovered. Bronzite was also detected in olivine gabbro from Tatamagouche and Duke River and typically falls in the En_{76-81} range. Orthopyroxene is an extremely rare phase in non-cumulate gabbro. The only example of this phase found were one grain (En_{83}) in the Halfbreed Creek Complex, two grains (En_{76}) in the Dickson Creek Complex, and two grains of pigeonite (En_{65}) in the Duke River Complex.

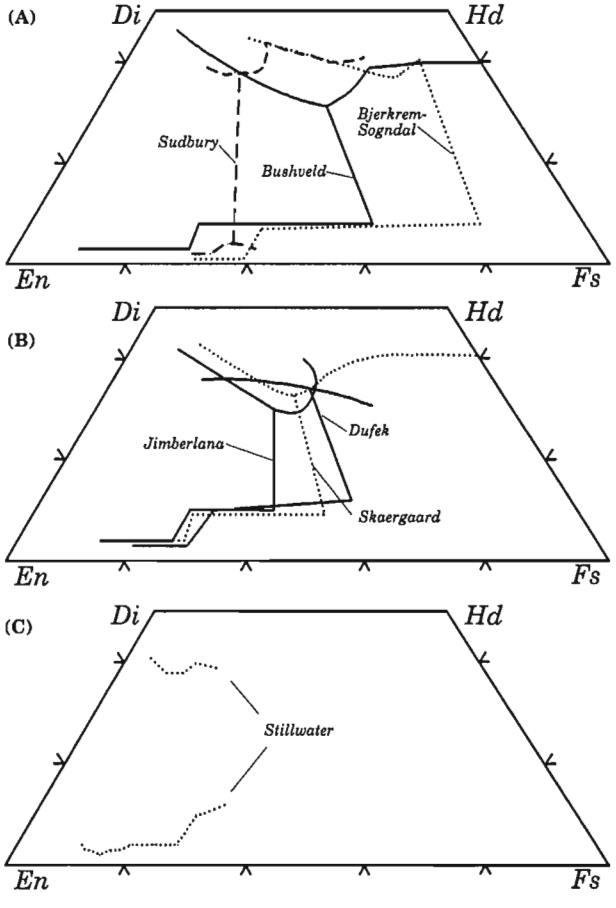

Figure 60 (A-C). *Pyroxene compositional trends of other well studied mafic-ultramafic complexes for comparison with those from the Kluane Belt. Sudbury (Naldrett et al., 1970); Bushveld (Atkins, 1969, Buchanan, 1979, Hulbert and Sharpe, 1981); Bjerkrem-Sogndal (Duchesne, 1972); Jimberlana (Campbell, 1973); Dufek (Himmelberg and Ford, 1975); Skaergaard (Brown and Vincent, 1963); Stillwater (McCallum et al., 1980).*

Pyroxene from the fine-grained chilled margins at Quill Creek (Wellgreen), Linda and Dickson properties, Maple Creek gabbro dykes, and Nikolai volcanic rocks demonstrate greater compositional range than that of the intrusive complexes (Fig. 59B).

With exception of pyroxene from the magnetite gabbro (Fig. 58A, B), Kluane mafic-ultramafic bodies have pyroxene compositional trends similar to those of other large mafic-ultramafic complexes (Fig. 60) of a tholeiitic origin (i.e. Bushveld, Jimberlana, Skaergaard). The trend associated with the magnetite gabbro is similar to that established for Sudbury.

Feldspar

As previously mentioned, plagioclase from the Kluane Belt is unusually susceptible to alteration and as a result compositions (Ca/(Ca+Na+K)) ranging from pure albite (0.0) to bytownite (0.85) occur. The compositional range for plagioclase from different lithologies and intrusive complexes expressed in terms of the Ca/(Ca+Na+K) ratio, henceforth referred to as the Ca#, are summarized in Figure 61. Plagioclase compositions expressed in terms of their An-Ab-Or components are given in Figure 62.

Due to the pervasive alteration of plagioclase and the general absence of marginal zone gabbro in some complexes, primary igneous plagioclase compositions of a non-cumulate origin are very difficult to obtain. What appear to be a optically clear, relict igneous cores in plagioclase, commonly are albite resulting from alteration of primary plagioclase. Nevertheless, exhaustive petrographic examinations of thin sections, and subsequent microprobe analyses from the Quill Creek Complex (Fig. 61A) have revealed that primary core compositions from the marginal zone of this complex have Ca# ratios ranging from 0.57 to 0.33. Relict core compositions in plagioclase from non-cumulate gabbro from the Duke River Complex (Fig. 61C) fall in the 0.667 to 0.578 range. Normal zoning gives rise to intermediate and rim compositions of 0.570 to 0.430. The highest Ca# (0.67) is very similar to the composition recorded for intercumulus plagioclase from a peridotite sample (0.685), and further strengthens the case for the chemical and mineralogical continuum between the gabbro and ultramafic rocks. All sulphide mineralized gabbro, magnetite gabbro, and many Maple Creek gabbro from the Duke River Complex fall in the albite field. These albitic compositions are clearly the result of alteration resulting from late magmatic (dueteric) fluids. By contrast cumulus plagioclase from the olivine gabbro samples (cumulates) is extremely fresh with core compositions (Ca#) in the 0.64 to 0.60 range. Limited normal zoning is present. The high degree of plagioclase alteration associated with the marginal zone gabbro and Maple Creek gabbro, relative to gabbroic cumulates, may be a consequence of higher volatile activity associated with the gabbroic magmas more prone to contamination from volatile-rich sediments.

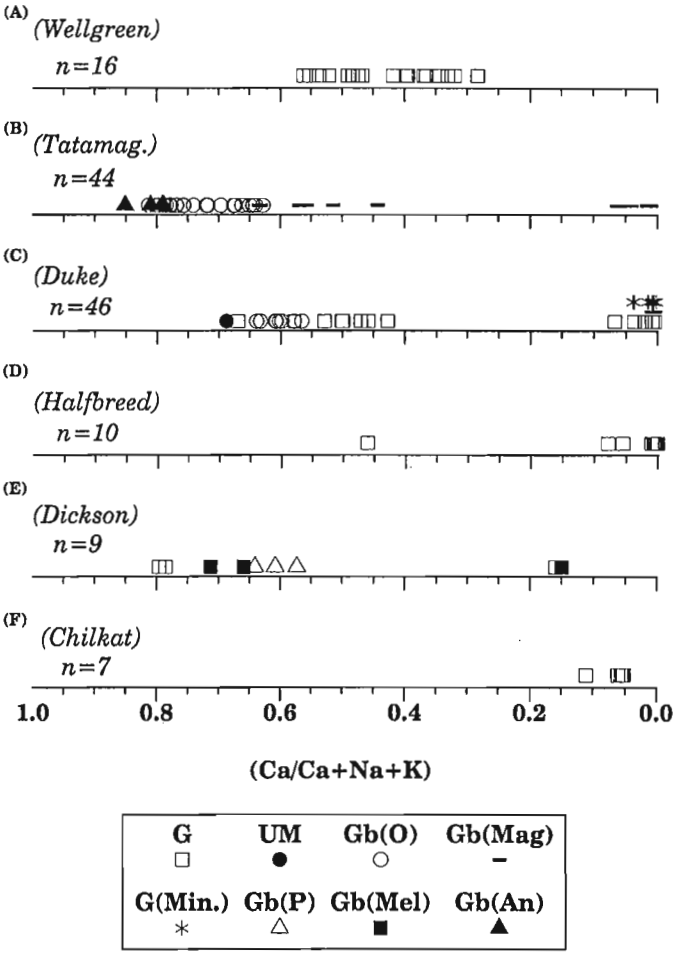

Figure 61(A-F).

Plagioclase compositional ranges associated with various intrusive complexes, related properties, and lithologies. UM = ultramafic, Gb(O) = olivine gabbro, Gb(Mag) = magnetite gabbro, Gb(An) = anorthositic gabbro, G = gabbro, G(Min.) = mineralized gabbro, Gb(Mel) = melanocratic gabbro, Gb(P) = pegmatitic gabbro.

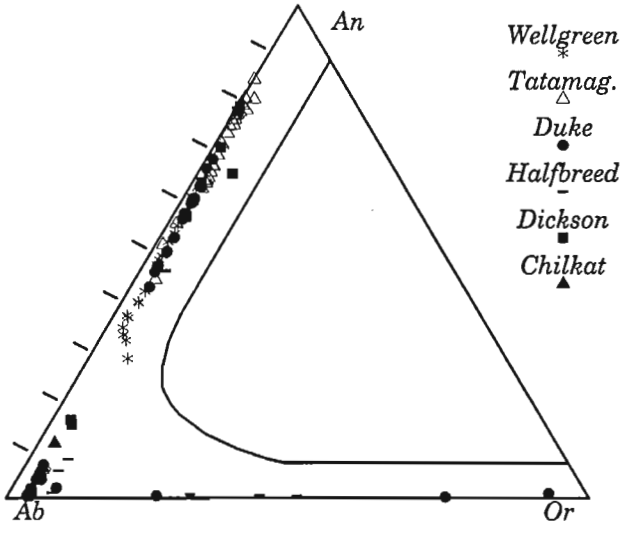

Figure 62. *Kluane plagioclase compositions in the ternary system An-Ab-Or.*

With the exception of one sample from Halfbreed Creek (Ca# = 0.46) containing magmatic plagioclase, all examined primary plagioclase grains from this complex and the Chilkat Complex, have been altered to more albitic compositions (Ca#) ranging from 0.12 to 0.06 (Fig. 61D, F). Primary plagioclase compositions from normal marginal zone gabbro and included melanocratic and pegmatitic varieties from the Dickson Creek Complex have primary compositions (Ca#) that range from 0.80 to 0.59. Alteration of plagioclase in these lithologies has also resulted in more albitic (0.15) compositions but not to the degree found in other complexes. The higher Ca# of plagioclase from this complex may be a reflection of higher prevailing water fugacity of these magmas as inferred from the noticeably higher proportion of magmatic amphibole in these samples and pegmatitic textures. Quenched plagioclase from the Dickson Creek chill has been altered to a 0.15.

The Tatamagouche Complex demonstrates the greatest range in plagioclase compositions (Fig. 61B) encountered in the Kluane Belt. Had samples of nondecomposed marginal zone gabbro been available it is believed that a compositional range similar to that for the Wellgreen property (Fig. 61A) would have been found. As in the Duke River Complex, plagioclase of a cumulate origin from olivine gabbro and gabbroic anorthosite lithologies of the Tatamagouche Complex are remarkably fresh and relatively anorthositic

compared to marginal gabbro. Cumulus plagioclase from gabbroic anorthosite (adcumulates) has reverse zoning with core compositions in the 0.791 to 0.789 range, and rim compositions of 0.851 to 0.810, respectively. In contrast associated olivine gabbro (ortho- to mezocumulates) contain plagioclase with core compositions (Ca#) in the 0.810 to 0.760 range, and typically contain normally zoned rim compositions in the 0.690 to 0.620 range. Where fresh the magnetite gabbro from the Maple Creek gabbro suite has core compositions in the 0.635 to 0.557 range with rim compositions in the 0.560 to 0.515 range, respectively. Plagioclase from chilled Maple Creek gabbro dykes at Wellgreen has core compositions of 0.555 to 0.460 with rim compositions generally 0.10 lower. Only three Nikolai volcanic samples with fresh plagioclase were found. They contain core compositions in the 0.476 to 0.440 range. Figure 62 presents the wide spectrum of feldspar compositions disclosed by this study.

Chromite

Chromite is an early cumulate phase in ultramafic rocks from the Kluane Belt. Therefore, compositional characteristics of Kluane chromites were investigated in considerable detail to gain a better understanding of the petrogenetic nature and evolution of these ultramafic rocks, and to investigate the possibility that distinct chromite compositional groupings may be associated with mineralized and unmineralized complexes. Chromite is not present in the marginal zone nor cumulate-type gabbroic rocks due to the presence of primary clinopyroxene, and the existence of a peritectic reaction between silicate melt and chromite to form Cr_2O_3-enriched clinopyroxene. Kluane Belt chromite compositional data with respect to the various complexes are summarized in Figures 63 to 68 and 70 to 72. Similar compositional plots related to other ultramafic associations are presented in Figure 69 for comparison.

Chromite compositions have been recast into cation ratios and plotted with respect to $Mg/(Mg+Fe^{2+})$ vs. $Cr/(Cr+Al)$, and $Mg/(Mg+Fe^{2+})$ vs. $Fe^{3+}/(Cr+Al+Fe^{3+})$ in Figures 63 to 68. The nature of the host silicate that encloses the analyzed chromite grain (i.e. olivine, clinopyroxene, intercumulus material other than olivine, and not recorded) has also been designated. In many cases the distinction between chromite in clinopyroxene and other intercumulus phases is difficult as many of the clinopyroxene are also of an intercumulus origin (Fig. 65B). Inspection of these plots reveals that there is generally a distinctive compositional grouping associated with each complex based on the nature of the host silicate in which the analyzed chromite resides. Chromite included in olivine generally has $Mg/(Mg+Fe^{2+})$ ratios less than 0.40, whereas those included in clinopyroxene commonly have ratios greater than 0.30 to 0.35. The greatest overlap of these two fields tends to be associated with ultramafic rocks that contain anomalous amounts of comagmatic immiscible sulphides. The degree of overlap associated with the known mineralized ultramafic cumulates appears to increase as the quality of the associated sulphide mineralization increases (i.e. Canalask > Arch > Linda > Onion); however, chromite from unmineralized ultramafic complexes (Chilkat, Halfbreed) clearly falls into distinct fields with little overlap. A further distinction occurs with respect to chromite compositions associated with the sulphide-enriched Dickson Creek samples (Fig. 63D). Although the ultramafic-hosted chromite is associated with anomalous sulphide concentrations, the sulphides are essentially barren with respect to Ni, Cu, Co, PGE, Se, As, Te, Sb, and Bi relative to similar looking mineralization from the other complexes. Not only do the Dickson Creek silicate-hosted fields fail to overlap but the $Cr/(Cr+Al)$ ratios of olivine-hosted chromite are significantly lower than those from their metal-enriched lithological counterparts from other complexes. This lower ratio corroborates earlier suggestions that the metal-poor nature of these sulphides reflects the limited degree of magma mixing and metal scavenging experienced by segregating (sulphides and oxide) phases.

With the exception of dunite (olivine adcumulates) from the Canalask property all investigated ultramafic lithologies have pronounced ortho-to mesocumulate textures. The interdependence of chromite chemistry and host silicate compositions is a common phenomenon in ultramafic cumulates, and is believed to reflect subsolidus re-equilibration of the chromite grains with the enclosing silicate and intercumulus liquid. Chromite in dunite has the highest $Mg/(Mg+Fe^{2+})$ and lowest $Cr/(Cr+Al)$ ratios for olivine-hosted grains encountered in the study, and in many cases for those included in clinopyroxene as well. The associated low $Fe^{3+}/(Cr+Al+Fe^{3+})$ ratio (Fig. 66B) indicates that this grouping is the result of chromite re-equilibrating with olivine under subsolidus conditions, resulting in Mg enrichment of chromite due to Mg and Fe^{2+} exchange with this Mg-rich silicate host. Similar host-silicate dependant chromite compositions occur in other ultramafic cumulate bodies (Cameron, 1975; Henderson, 1975; Clark, 1978; Wilson, 1982). The $Mg/(Mg+Fe^{2+})$-poor compositions (0.0 to 0.07) illustrated in Figures 64C and 65B are believed to be ferritchromite reaction zones resulting from low temperature alteration and serpentinization processes. The higher $Mg/(Mg+Fe^{2+})$ and lower $Cr/(Cr+Al)$ ratios of clinopyroxene-hosted chromite may also indicate postcumulus $Mg\text{-}Fe^{2+}$ exchange resulting in Mg enrichment of chromite. Although postcumulus chemical exchange of both Cr and Al also took place between chromite and its clinopyroxene host, the generally lower $Cr/(Cr+Al)$ ratios suggest greater exchange with the aluminum – (i.e. from pyroxene to chromite) bearing clinopyroxene than in the case of olivine which essentially contains no aluminum.

$Fe^{3+}/(Cr+Al+Fe^{3+})$ ratios of the various silicate-hosted chromite appear to separate the olivine- and clinopyroxene-hosted groups somewhat better than $Cr/(Cr+Al)$ (Fig. 66 to 68). Chromite included in olivine generally has lower $Mg/(Mg+Fe^{2+})$ and higher $Fe^{3+}/(Cr+Al+Fe^{3+})$ ratios. The highest $Fe^{3+}/(Cr+Al+Fe^{3+})$ ratios for chromite are associated with those hosted in olivine, but mineralized ultramafic rocks appear to have a greater frequency of elevated $Fe^{3+}/(Cr+Al+Fe^{3+})$ ratios. As chromite and olivine are both of a cumulus origin, the olivine may be isolating the original cumulus chromite from reacting with intercumulus liquid more than chromite enclosed in intercumulus phases. If this were the case, then the iron-enriched nature of olivine-hosted chromite, and its preferential association with mineralized

ultramafic rocks, could indicate equilibration or re-equilibration in an Fe-rich environment at a cumulus or postcumulus stage in the presence of Fe-sulphides. Roeder and Campbell (1985) suggested that chromite in olivine from the Jimberlana Intrusion appears to have equilibrated with intercumulus liquid until late in the intrusions magmatic history, except where the olivine enclosing chromite is itself surrounded by bronzite. They suggested that chromite can exchange elements with intercumulus liquid through olivine by either diffusion through the olivine structure, or by direct contact with the melt along fine fractures produced by the differential thermal contraction between olivine and chromite.

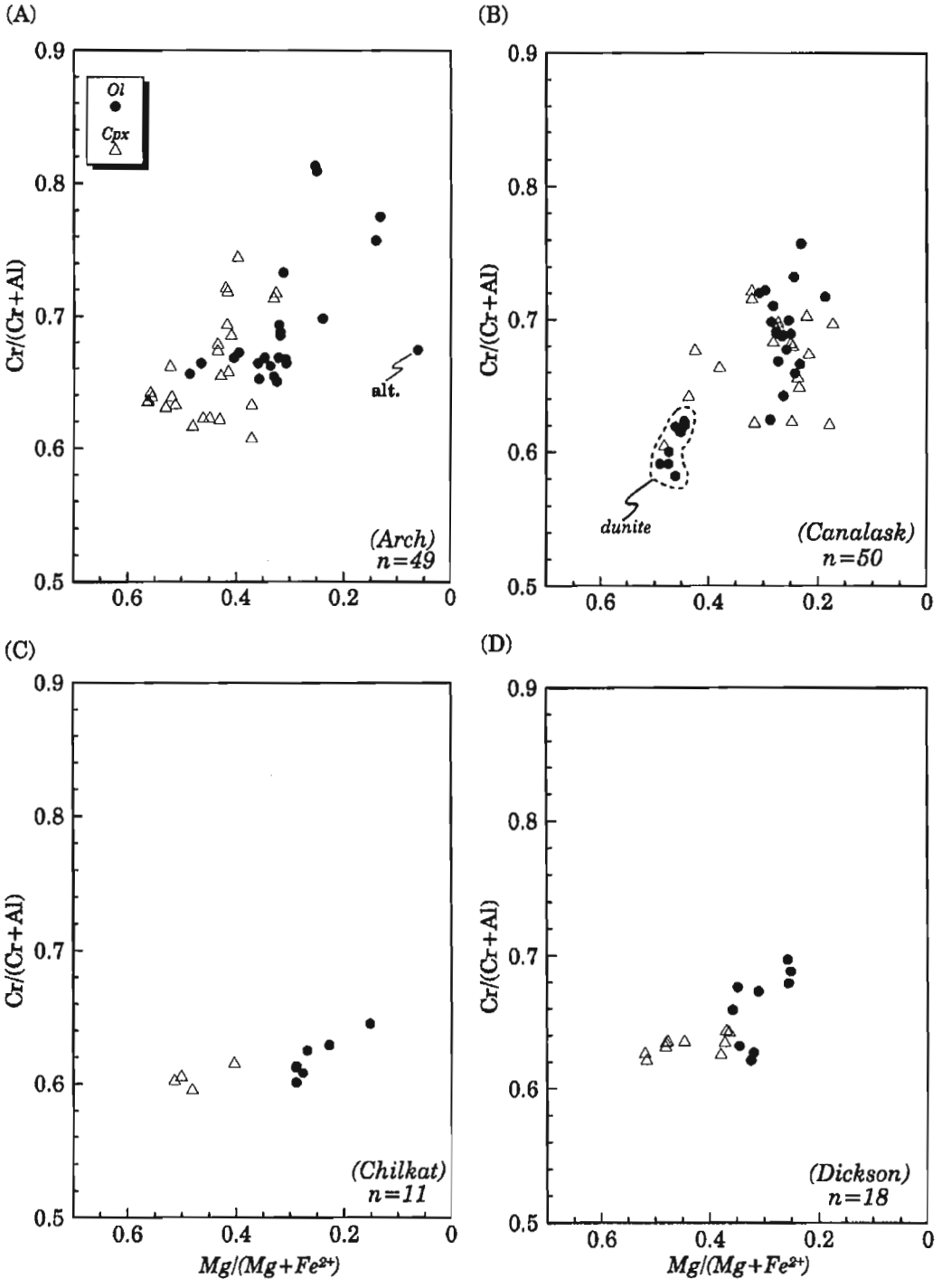

Figure 63 (A-D). *Cr/(Cr+Al) vs. Mg/(Mg+Fe^{2+}) compositional data for chromite from the Arch, Canalask, Chilkat, and Dickson Creek complexes and property with respect to the host silicate. Ol = olivine, Cpx = clinopyroxene.*

Semi-molten cumulus sulphides would migrate and infill the porosity and certainly add to the already Fe-rich nature of the intercumulus material. Regardless of the cumulus or intercumulus origin for this Fe enrichment, it is clear that there is a preferential association between the most Fe-rich samples in terms of their $Fe^{3+}/(Cr+Al+Fe^{3+})$ and $Mg/(Mg+Fe^{2+})$ ratios and sulphide associations. The most $Fe^{3+}/(Cr+Al+Fe^{3+})$-rich chromites are associated with Quill Creek samples from the Wellgreen property (Fig. 68B).

Compositional fields of chromite from other ultramafic environments are shown in Figure 69. The $Mg/(Mg+Fe^{2+})$ ratios of disseminated chromite from ultramafic rocks in the

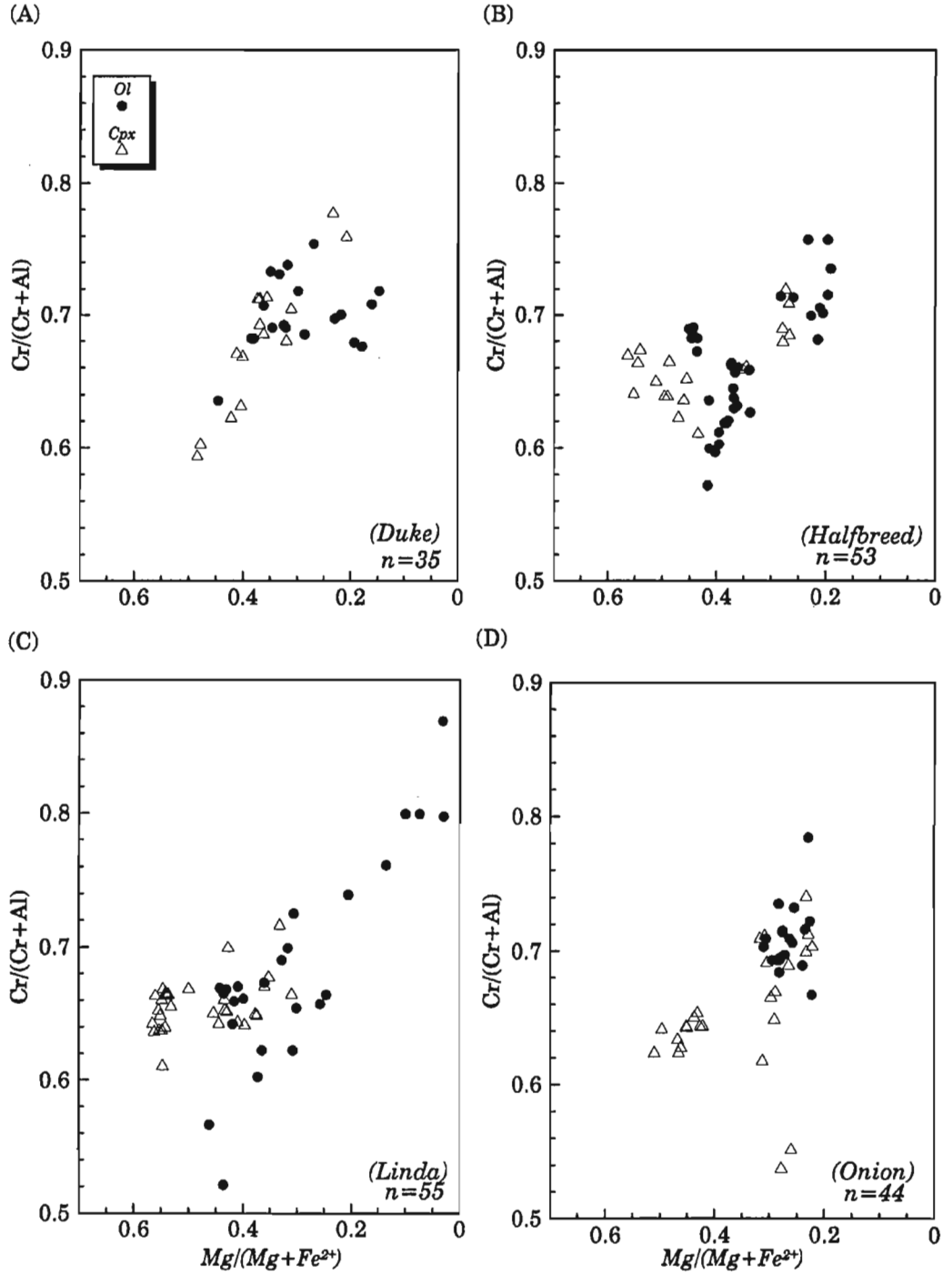

Figure 64 (A-D). *Cr/(Cr+Al) vs. $Mg/(Mg+Fe^{2+})$ compositional data for chromite from the Duke River, Halfbreed, Linda, and Onion intrusive complexes and property with respect to host silicate. Ol = olivine, Cpx = clinopyroxene.*

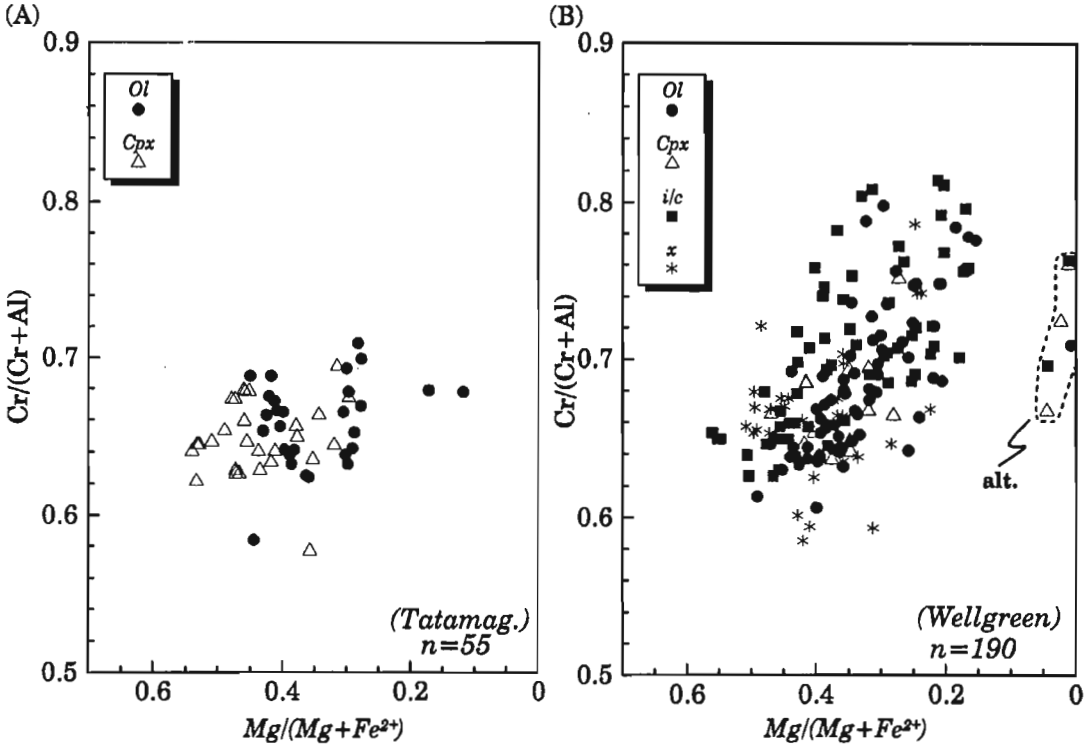

Figure 65 (A-B). *Cr/(Cr+Al) vs. Mg/(Mg+Fe^{2+}) compositional data for chromite from the Tatamagouche Creek Complex and Wellgreen property of the Quill Creek Intrusive Complex with respect to host silicate. Ol = olivine, Cpx = clinopyroxene, i/c = intercumulus, x = not recorded.*

Kluane Belt are similar to those of disseminated chromite from the Eastern Bushveld and Potgietersrus Limb of the Bushveld Complex. However, Kluane samples clearly attain higher Cr/(Cr+Al) ratios and overlap the Great Dyke and Eastern Bushveld chromitite fields (Fig. 69A). The Kluane chromites also have appreciably higher $Fe^{3+}/(Cr+Al+Fe^{3+})$ ratios than their Bushveld counterparts. Chromite from the sulphide-enriched Merensky Reef has noticeably higher $Fe^{3+}/(Cr+Al+Fe^{3+})$ ratios than other lithologies from the Bushveld and Great Dyke. A similar $Fe^{3+}/(Cr+Al+Fe^{3+})$ enrichment has also been observed in the sulphide mineralized cumulates of Cyclic Unit 1 of the Rhum Complex, Scotland (Hulbert et. al., 1992a). From this it may be inferred that $Fe^{3+}/(Cr+Al+Fe^{3+})$ enrichment in chromite is governed by the same parameters that control the sulphide distributions within a magma chamber. Reference to Figure 69C demonstrates that the Kluane chromite is more akin to layered intrusion varieties than those from 'Alpine, Alpine-Alpine, and Abyssal' peridotite (Dick and Bullen, 1984). This chemical distinction may prove to be a useful exploration tool in discriminating 'Kluane-type' ultramafic intrusions from the many so-called 'Alpine-type' (Whittaker, 1982, 1984; Whittaker and Watkinson, 1981) ultramafic bodies within the Cordillera of British Columbia and the Yukon.

The most striking chemical characteristic of Kluane chromite is its anomalous TiO_2 (wt.%) content (Fig. 70). TiO_2 contents range from 0.75 to 10.75 wt.%. The average content of all investigated chromite is approximately 4.0 wt.% TiO_2. Although considerable variations within each complex exist, unmineralized intrusions like Chilkat and Halfbreed appear to have a greater proportion of samples with low TiO_2 than do the sulphide mineralized intrusions. Kluane chromite is very TiO_2-rich relative to that of 'Alpine-type' chromite (0.01 to 0.23 wt.%) (Whittaker, 1984).

The degree of Fe^{3+} and Ti^{4+} enrichment in Kluane ultramafic rocks, particularly the sulphide-rich varieties, is unprecedented for Cr-spinels from both layered and unlayered intrusions, and appears to be independent of host silicate. Cameron (1977) and Hulbert (1983) noted that the TiO_2 content of chromite increases upwards in the Critical Zone of the eastern Bushveld Complex and in the Lower zone and Critical zone cumulates of the Potgietersrus Limb of the Bushveld Complex. Average TiO_2 contents of disseminated chromite from ultramafic cumulates in the lower, middle, and upper portions of the Lower zone from the Potgietersrus Limb are 0.47, 0.87, and 1.00 wt.%, respectively; whereas, the TiO_2 content of disseminated chromite from the lower half of the critical zone is 2.98 wt.% (Hulbert, 1983). Disseminated chromite in olivine, orthopyroxene, plagioclase, and clinopyroxene from the Jimberlana Intrusion averages 1.61, 0.77, 3.48, and 2.40 wt.% TiO_2, respectively (Roeder and Campbell, 1985). The values from the Potgietersrus Limb and Jimberlana are believed to be amongst the highest TiO_2 contents recorded in chromite from layered intrusions lacking economic or near

economic concentrations of Ni-Cu ores, and thus provide a reference base to appreciate how enriched Kluane chromite is with respect to its TiO_2 content. Recently, Roach (1992) found that the main chromitite from the Muskox intrusion generally contained chromite with 3 to 9 wt.% TiO_2, but individual grains contain over 10 wt.% TiO_2. Both disseminated and massive chromite from this sulphide-enriched chromitite is enriched in Fe^{2+}, Fe^{3+}, and Ti relative to chromite in similar chromitite from the Stillwater and Bushveld Complex. Hulbert et al. (1992a) discovered a similar enrichment in Fe^3 and TiO_2 (up to 7.2 wt.%) in disseminated chromite hosted in mineralized peridotite from Cyclic Unit #1 of the Rhum Complex, Scotland. TiO_2-enriched chromite compositions have been recorded in other mafic-ultramafic bodies associated

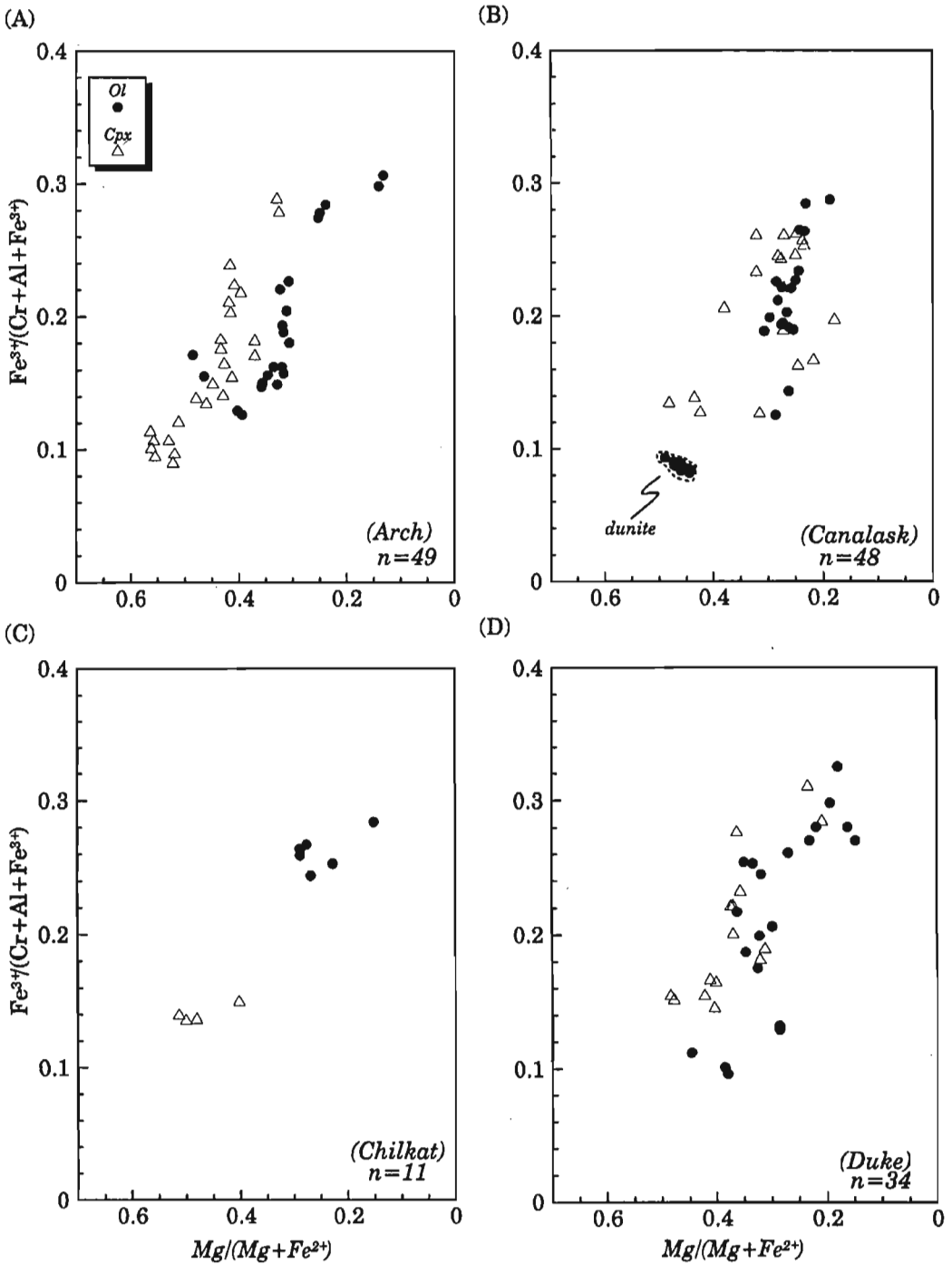

Figure 66 (A-D). *$Fe^{3+}/(Cr+Al+Fe^{3+})$ vs. $Mg/(Mg+Fe^{2+})$ compositional data for chromite from the Arch, Canalask, Chilkat, and Duke River intrusive complexes and property relative to host silicate. Ol = olivine, Cpx = clinopyroxene.*

with massive and semi-massive Cu-Ni sulphide accumulations: i.e. Duluth Complex, USA (Mainwaring, 1975); Pechenga, Russia (Smol'kin and Pakhomovskiy, 1985); Insizwa Complex, Southern Africa (Lightfoot and Naldrett, 1983); Kitdlît Lens, Disko Island, Greenland (Ulff-Møller, 1985) and Noril'sk-Talnakh camp Russia (Genkin et al., 1981).

Evans and Wright (1972) showed that the more fractionated the host basalt the more TiO_2-rich are its chrome spinels. As the octahedral site preference energy of Ti^{4+} is considerably lower than elements such as Cr^{3+} (Burns, 1970) it should by virtue of its lower distribution coefficient become enriched in melt relative to the solid phase during crystallization

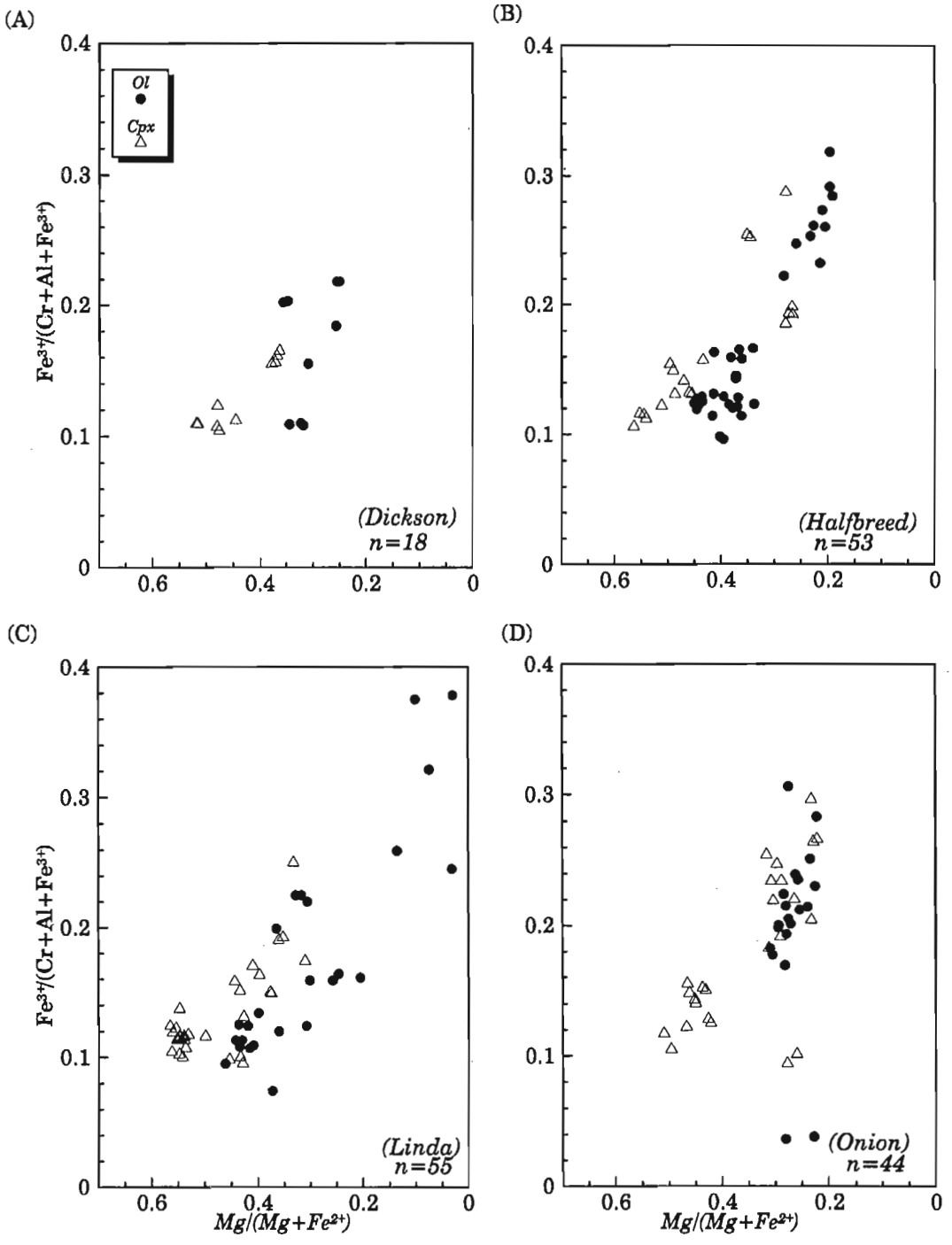

Figure 67 (A-D). *$Fe^{3+}/(Cr+Al+Fe^{3+})$ vs. $Mg/(Mg+Fe^{2+})$ compositional data for chromite from the Dickson, Halfbreed, Linda, and Onion complexes and property relative to host silicate. Ol = olivine, Cpx = clinopyroxene.*

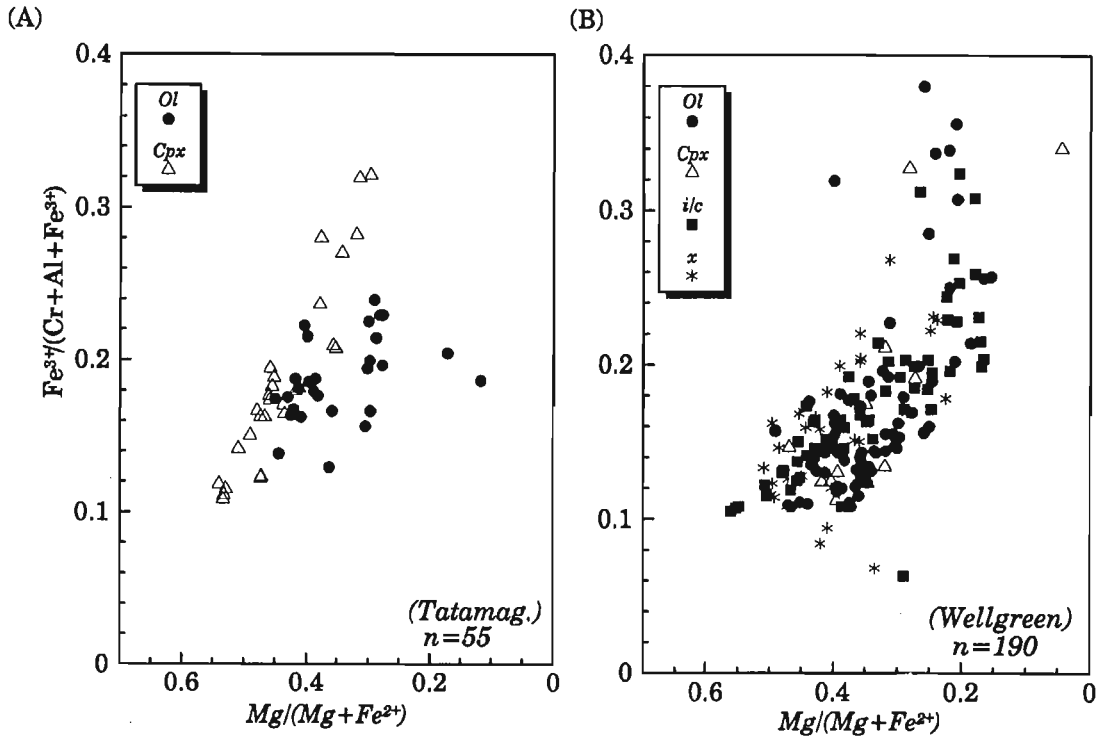

Figure 68 (A-B). *$Fe^{3+}/(Cr+Al+Fe^{3+})$ vs. $Mg/(Mg+Fe^{2+})$ compositional data for chromite from the Tatamagouche Creek and Wellgreen property of the Quill Creek Intrusive Complex relative to host silicate. Ol = olivine, Cpx = clinopyroxene, i/c = intercumulus, x = not recorded.*

(Eales and Reynolds, 1981). A decrease in temperature during fractional crystallization at a fixed fO_2 will enrich the residual magma in Fe_2O_3 relative to FeO and in TiO_2 (Hill and Roeder, 1974; Eales and Reynolds, 1981; El Goresy et al., 1976).

Scowen et al. (1991) documented that chromite totally enclosed in olivine could change its solidus composition by diffusion through olivine even in slowly cooled magmas. However, they found that the Ti content of spinel is a reliable indicator of parental magma chemistry since the diffusivity of Ti^{+4} in olivine is relatively slow. Arai (1992) investigated chromite compositions in volcanic rocks, and associated ultramafic cumulates, from three main volcanic group settings: arc magmas (basalt and andesite), ocean-floor basalt (MORB), and intraplate basalts. High-magnesium andesite and boninite were included in the arc magma grouping. He found that the three groups of magmas can be distinguished to some extent from each other by the chromite Ti contents; the contents increase from island arc magma to intraplate basalt via ocean-floor basalt for a particular $Mg/(Mg+Fe^{2+})$ ratio, and are consistent with the relative TiO_2 abundances of the magma.

As the $Fe^{3+}/(Cr+Al+Fe^{3+})$ ratio of spinel is strongly dependant on the degree of differentiation of the host magma (e.g. Arai and Takahashi, 1987) the TiO_2 content should be compared with respect to this. The chromite compositional plots of Arai (1992, i.e. Fig. 4, 6, 7) indicate that chromite from the oceanic intraplate basaltic environments are clearly distinguished from other groups by their high TiO_2 contents. Ultramafic cumulates (dunite) from this environment have up to 7.0 wt.% TiO_2 and chromite from oceanic plateau basalts plot in a distinctly lower-TiO_2 area than from intraplate basalt. The oceanic plateau basalt is treated as a subgroup of the intraplate basalt because of the lower Ti content of associated chromite, and the depleted nature of incompatible elements relative to other intraplate basalt. Based on the Arai's findings, the high TiO_2 contents of Kluane chromite suggests that the parental magma(s) and setting for the Kluane mafic-ultramafic complexes and coeval Nikolai basalt volcanism was akin to that of intraplate basalt.

Therefore, there appears to be a unique set of conditions giving rise to the Fe^{3+} and TiO_2-enriched chromite in the Kluane Belt: (1) the initial control appears to be related to the magmatic setting (i.e. intraplate basalt magmatism) and the relatively high TiO_2 content of such magmas, (2) crystallization from more evolved magma batches or differentiates with a higher ulvöspinel molecule component in the successive liquids took place within some complexes (i.e. Quill Creek, Tatamagouche), and (3) conditions giving rise to sulphide immiscibility (i.e. increased fO_2 resulting from crustal contamination) would increase the Fe^{3+} of the magma and correspondingly the $Fe^3/(Cr+Al+Fe^3)$ ratio of the nucleating chromite and the amount of Ti^{4+} it could accommodate.

Kluane chromite compositional fields and trends, expressed in terms of the ternary components Cr-Al-Fe^{3+}, are shown in Figure 71. The chromite shows a systematic increase of Fe^{3+} with decreasing Cr and relatively constant Al content. Chromite also displays differences in composition based on the nature of the host silicate. Chromite from the Quill Creek and Tatamagouche Creek complexes demonstrate the greatest degree of iron (Fe^{3+}) enrichment, as was also shown to be the case for the associated mafic silicates.

A systematic investigation of chromite compositions, with respect to TiO_2, NiO, and ZnO and the ratios $Mg/(Mg+Fe^{2+})$ and $Al/(Al+Fe^{3+}+Cr)$, was conducted through the Arch intrusion

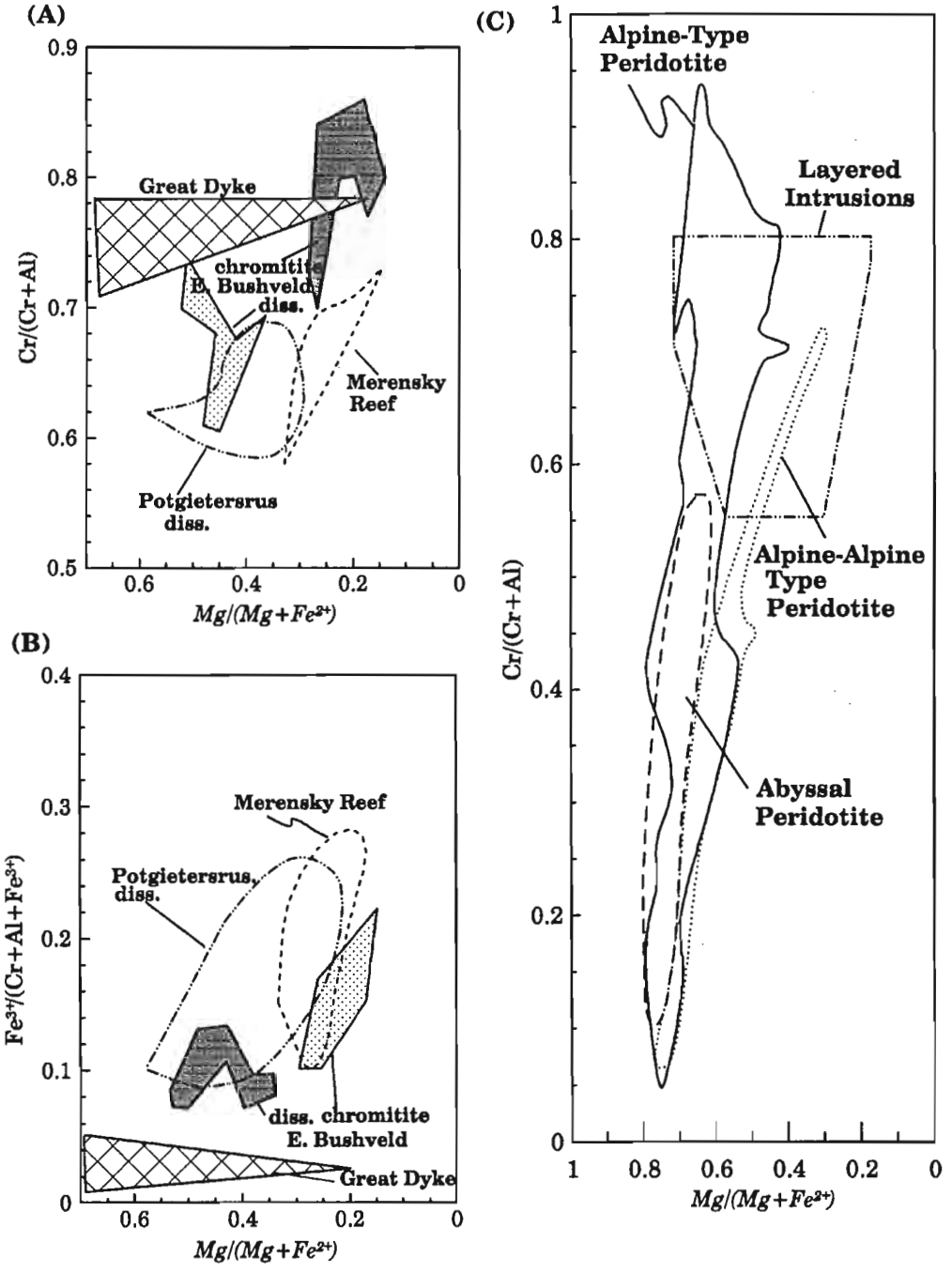

Figure 69 (A-C). *Cr/(Cr+Al) and $Fe^{3+}/(Cr+Al+Fe^{3+})$ vs. $Mg/(Mg+Fe^{2+})$ plots for comparison showing chromite fields associated with other well documented mafic-ultramafic complexes.*

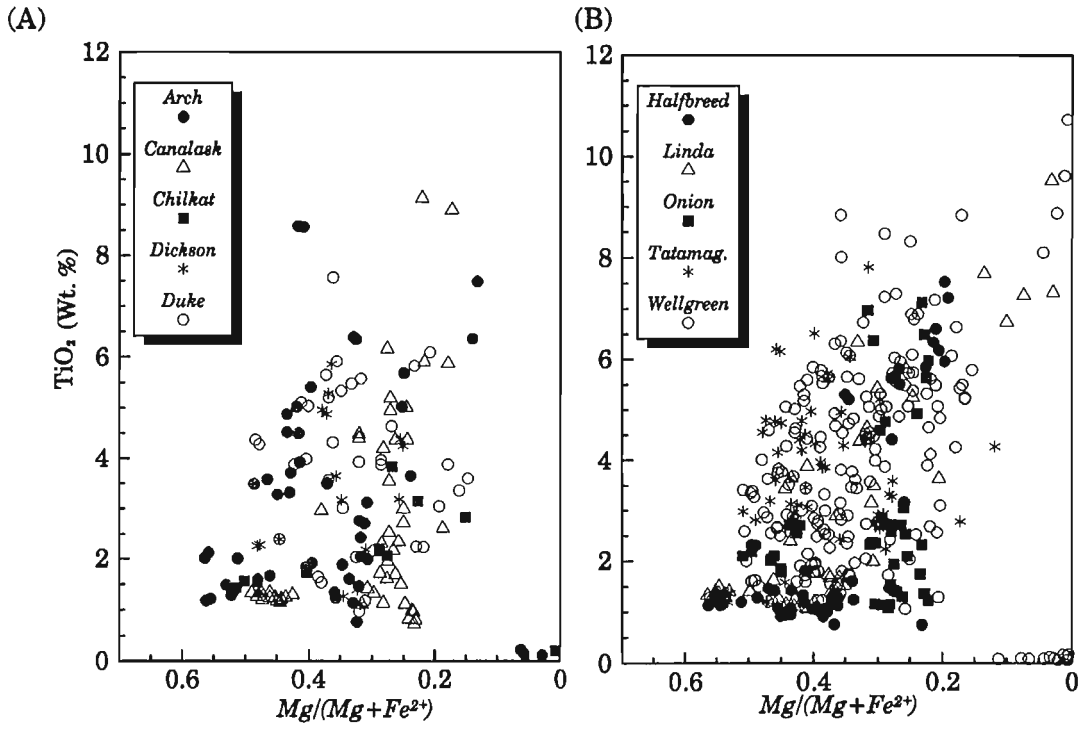

Figure 70 (A-B). TiO_2 (wt.%) vs. $Mg/(Mg+Fe^{2+})$ compositional data for chromite from different intrusive complexes and properties in the Kluane Belt.

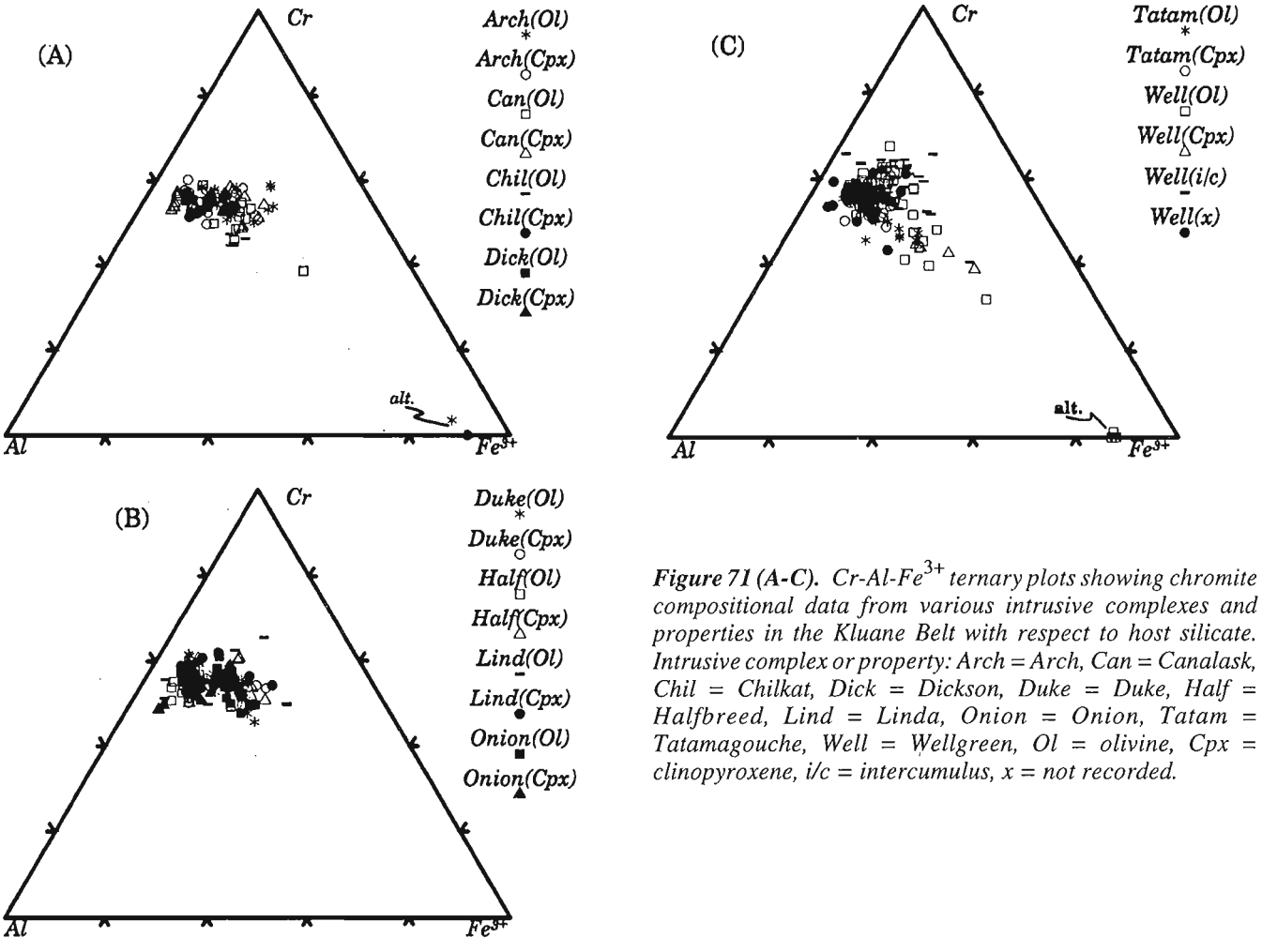

Figure 71 (A-C). Cr-Al-Fe^{3+} ternary plots showing chromite compositional data from various intrusive complexes and properties in the Kluane Belt with respect to host silicate. Intrusive complex or property: Arch = Arch, Can = Canalask, Chil = Chilkat, Dick = Dickson, Duke = Duke, Half = Halfbreed, Lind = Linda, Onion = Onion, Tatam = Tatamagouche, Well = Wellgreen, Ol = olivine, Cpx = clinopyroxene, i/c = intercumulus, x = not recorded.

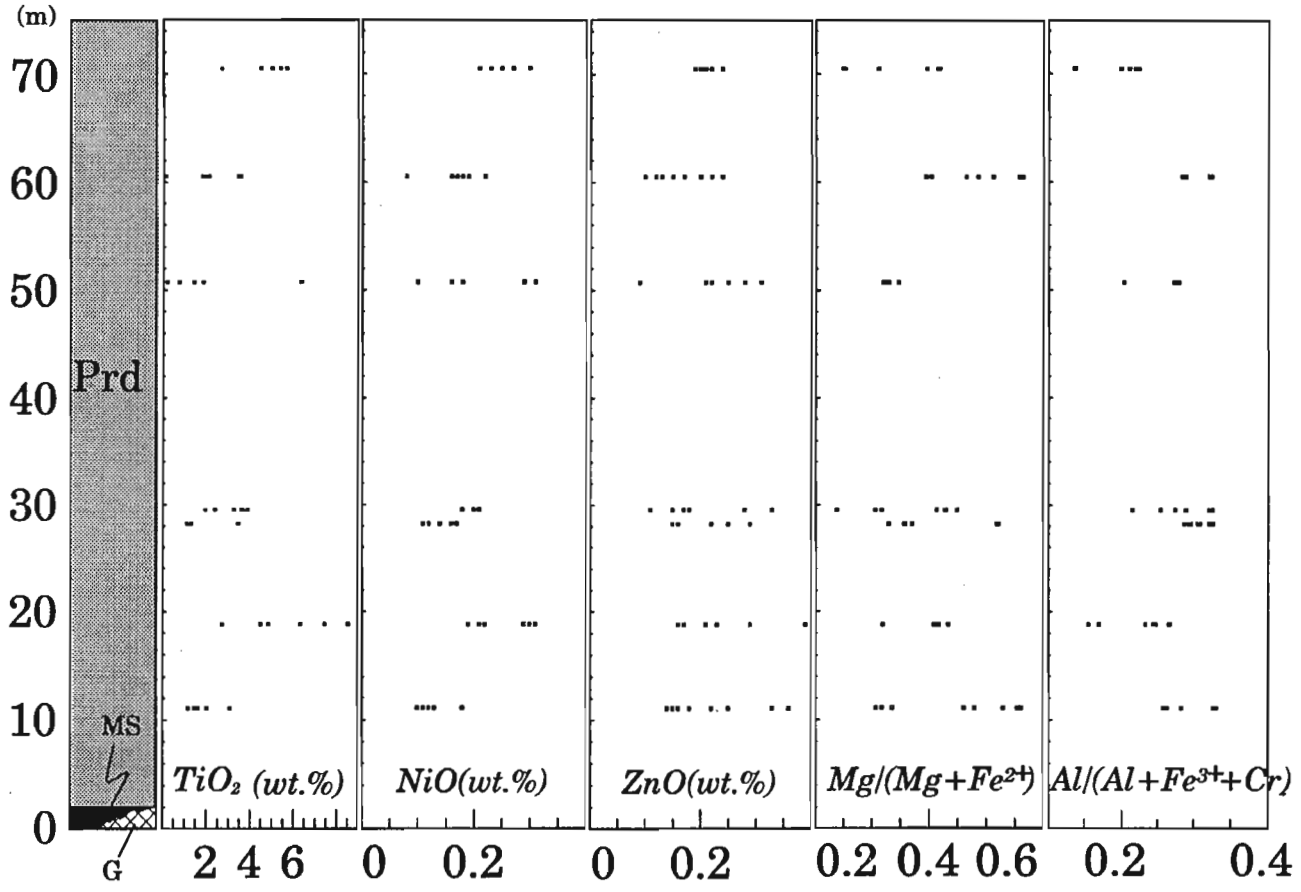

Figure 72. *Detailed investigation of chromite compositions through a 70 m diamond-drill hole intersection of the Arch Creek Intrusive Complex. Prd = peridotite, MS = massive sulphide, G = gabbro.*

(Fig. 72). There is considerable range in compositions (due to the influence of host silicate) with elemental association trends observed. The behaviour of TiO_2 and NiO (and to a lesser degree ZnO) are similar through the 70 m interval. The $Al/(Al+Fe^{3+}+Cr)$, and to a lesser degree $Mg/(Mg+Fe^{2+})$, tend to mirror that of TiO_2 and NiO. The basal 2 to 20 m interval of the ultramafic section contains 2 to 5% disseminated sulphides, whereas the remaining interval generally contains 1 to 2% sulphide. The correlation between NiO and TiO_2 and attainment of the highest values in this sulphide-enriched basal portion of the ultramafic interval warrant further investigation.

GEOCHEMISTRY OF SELECTED KLUANE MAFIC-ULTRAMAFIC INTRUSIONS

Ultramafic, gabbroic, country rock lithologies, and massive and semi-massive sulphide concentrations associated with the Kluane Belt mafic-ultramafic intrusive complexes were geochemically investigated to establish the range, maximum concentration, and trends associated with the elements: S, Ni, Cu, Co, As, Ba, Se, Bi, Sb, Te, Ba, Pt, Pd, Au, Rh, Ru, Ir, Os, Re, and their sulphur isotope compositions (Fig. 73 to 128). In addition, platinum-group element and gold ratios, ternary plots, and chondrite normalized PGE+Au profiles in 100% sulphide are given in Figures 129 to 165. Although the salient features with respect to these elements and the sulphur isotope compositions have been mentioned in previous discussions related to the Ni-Cu±PGE mineralization associated with each complex, concentrations and trends specific to each complex are not reiterated, as the focus is on regional geochemical patterns and characteristics. Geochemical diagrams with a similar format are presented collectively in this section to facilitate expeditious comparisons and act as a compendium of important metal and isotope data. Some plots may show no obvious geochemical trends, but nonetheless they provide a rapid overview of concentration ranges and associations of interest to explorationists and mineral rights holders. Due to the large size of the database, the tables of the geochemical data are generally not presented.

Nickel, copper, cobalt, and arsenic

Nickel, copper, cobalt, and arsenic concentrations and trends with respect to sulphur and the various intrusive complexes are presented in Figures 73 to 84.

Ni and Co commonly display smooth, curved (concave-up) trends with increasing S content. The inflection point for these curves generally occurs near the 1% sulphur (approximately 2.6% sulphide) concentration.

In the <0.01 to 1.0% S range, ultramafic rocks from known mineralized properties (Onion, Canalask, Arch, Wellgreen, and Linda) and complexes have average Ni and Co contents of 2000 and 130 ppm, respectively. However, ultramafic rocks from unmineralized (i.e. Halfbreed and Chilkat) complexes have significantly lower average concentrations (900 and 100 ppm, respectively) in rocks containing similar sulphur concentrations. Complexes with sporadic weakly mineralized ultramafic lithologies (Duke, Tatamagouche) have values that fall between these two extremes. Thus it would appear that

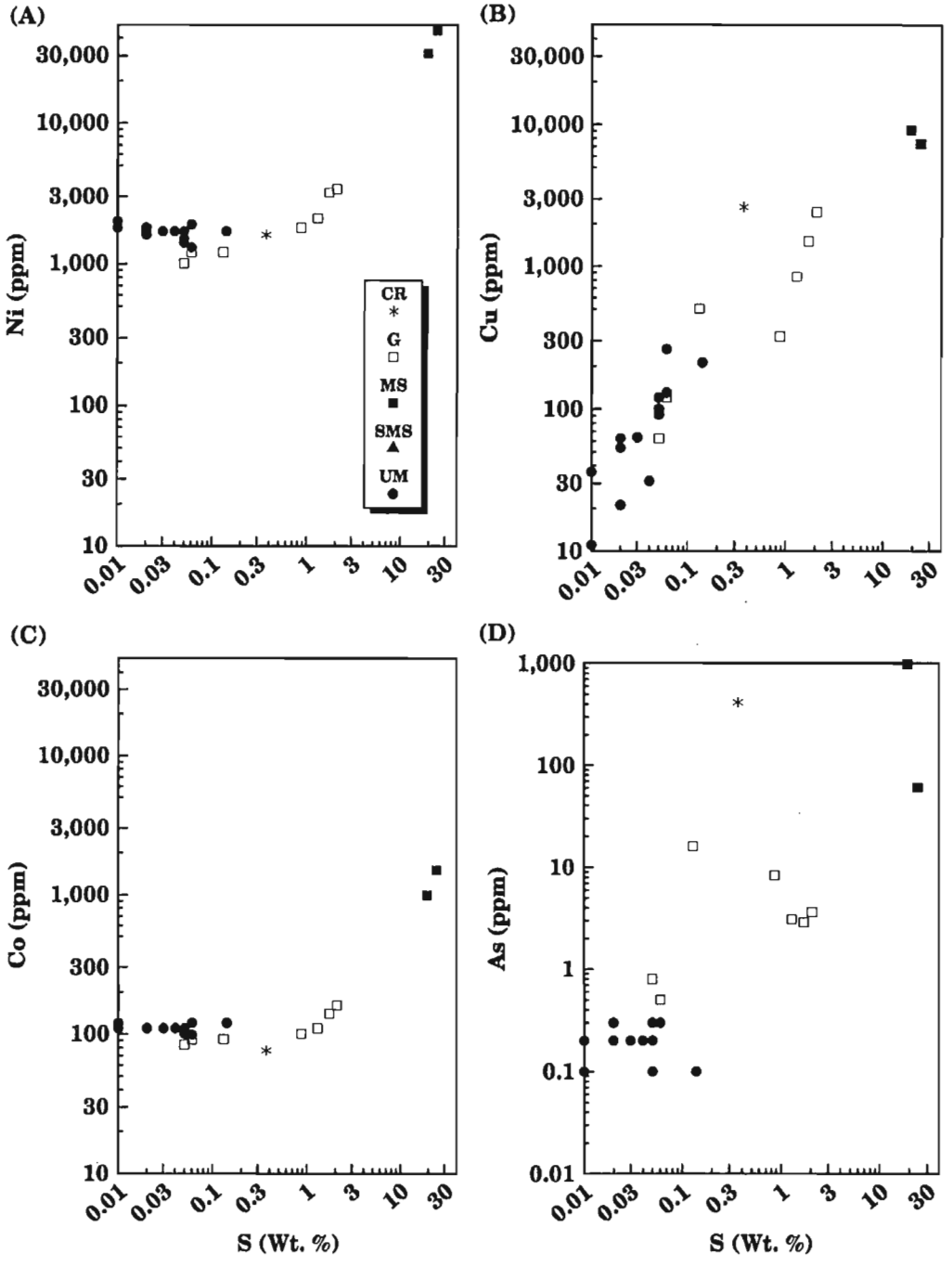

Figure 73 (A-D). *Ni, Cu, Co, As vs. S (wt.%) plots of elemental concentrations associated with ultramafic (UM), gabbroic (G), massive sulphide (MS), semi-massive sulphide (SMS), and country rock (CR) lithologies from the Onion property of the White River Intrusive Complex.*

the macroscopically unmineralized ultramafic lithologies from known mineralized intrusions contain approximately twice the background levels of Ni as their barren counterparts. As significant massive and semi-massive basal sulphide concentrations are associated with intrusions that have ultramafic rocks with anomalous Ni contents (although they appear macroscopically unmineralized), such a geochemically diagnostic feature could be a useful exploration guide. The flat Ni vs. S and Co vs. S trend in the <0.01 to 1.0% S range implies that sulphide had little influence on the overall Ni and Co concentrations within this range. It appears that the original silicate and oxide (chromite), and possibly sulphide, mineralogy making up these ultramafic rocks was enriched in Ni and Co relative to similar phases from barren and sporadically mineralized bodies. The relationship between increasing NiO content accompanying TiO_2 enrichment in chromite, in the

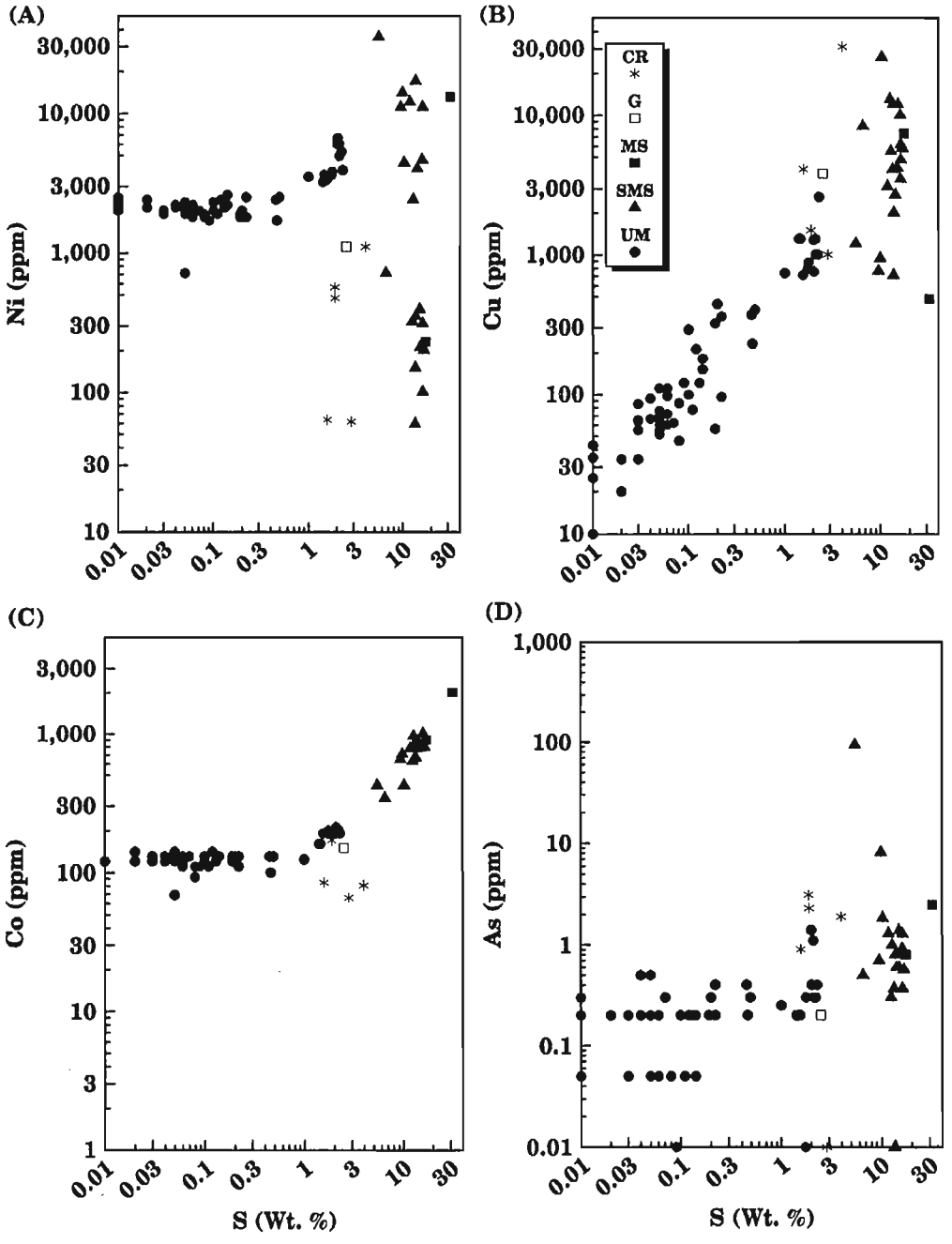

Figure 74 (A-D). Ni, Cu, Co, As vs. S (wt.%) plots of elemental concentrations associated with ultramafic (UM), gabbroic (G), massive sulphide (MS), semi-massive sulphide (SMS), and country rock (CR) lithologies from the Canalask property of the White River Intrusive Complex.

Arch Complex, and the association of TiO_2-rich chromite with ultramafic-hosted sulphide mineralization may explain part of this cryptic chemical relationship. The presence of fine secondary magnetite with a relatively high NiO content (trevorite-component) in the serpentinized ultramafic rocks from the Quill Creek Complex may also contribute to the higher whole rock Ni contents. Higher Ni content in this phase would reflect a higher original, primary Ni content in the host rock, regardless of its mineralogical source.

A similar, but somewhat more disperse, curved trend also exists for Ni and Co in gabbroic rocks containing <1.0% S; however, both curved (Onion) and to lesser degree Quill

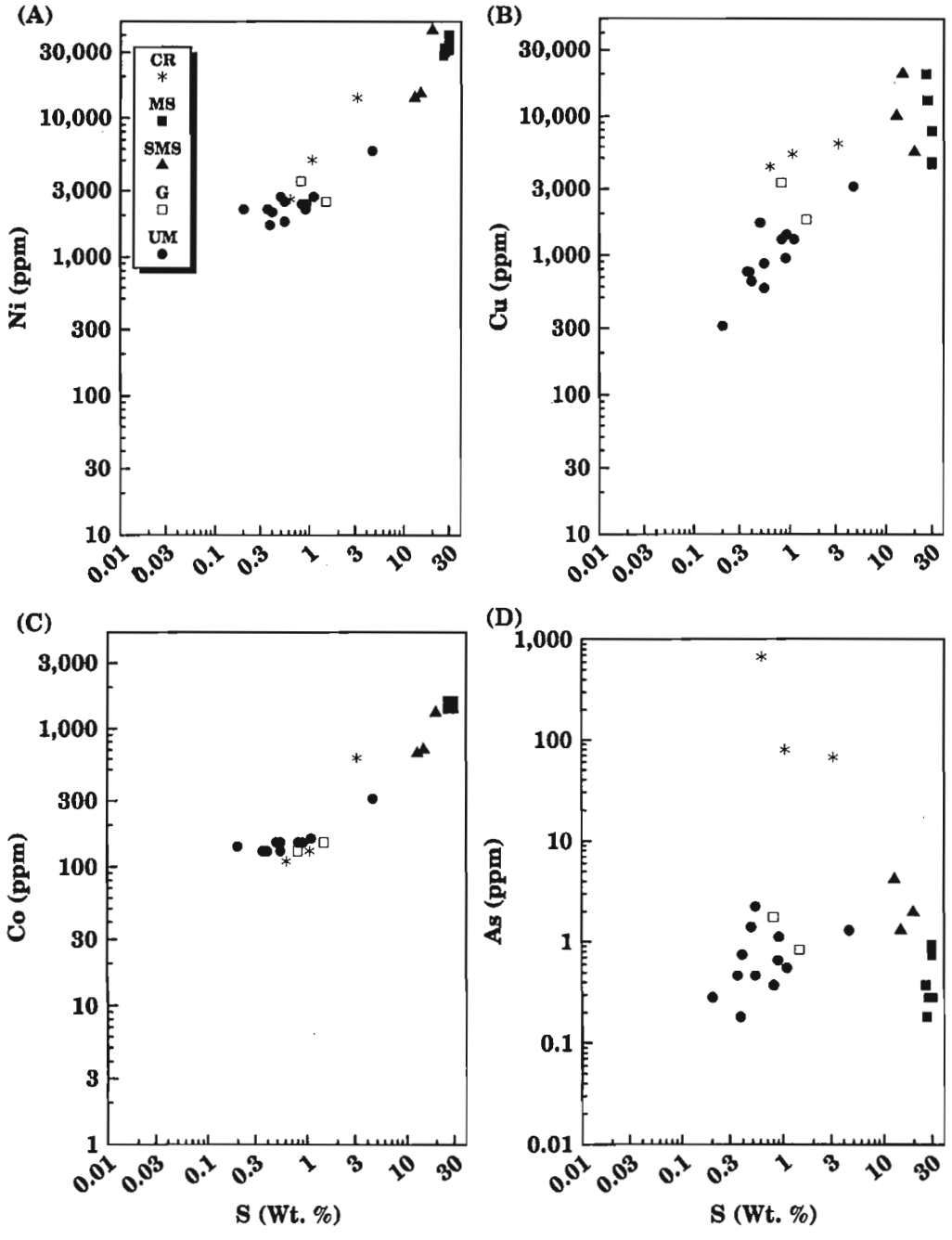

Figure 75 (A-D). *Ni, Cu, Co, As vs. S (wt.%) plots of elemental concentrations associated with ultramafic (UM), gabbroic (G), massive sulphide (MS), semi-massive sulphide (SMS), and country rock (CR) lithologies from the Arch Creek Intrusive Complex.*

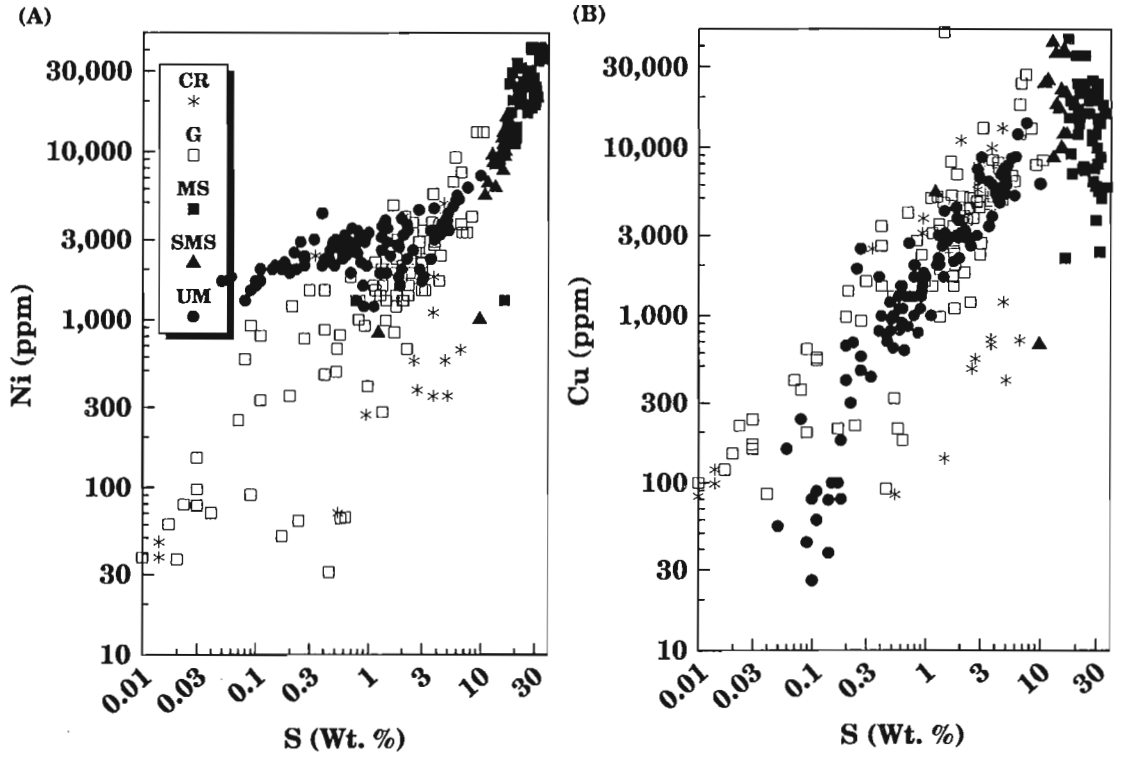

Figure 76 (A-B). *Ni, Cu vs. S (wt.%) plots of elemental concentrations associated with ultramafic (UM), gabbroic (G), massive sulphide (MS), semi-massive sulphide (SMS), and country rock (CR) lithologies from the Quill Creek Intrusive Complex.*

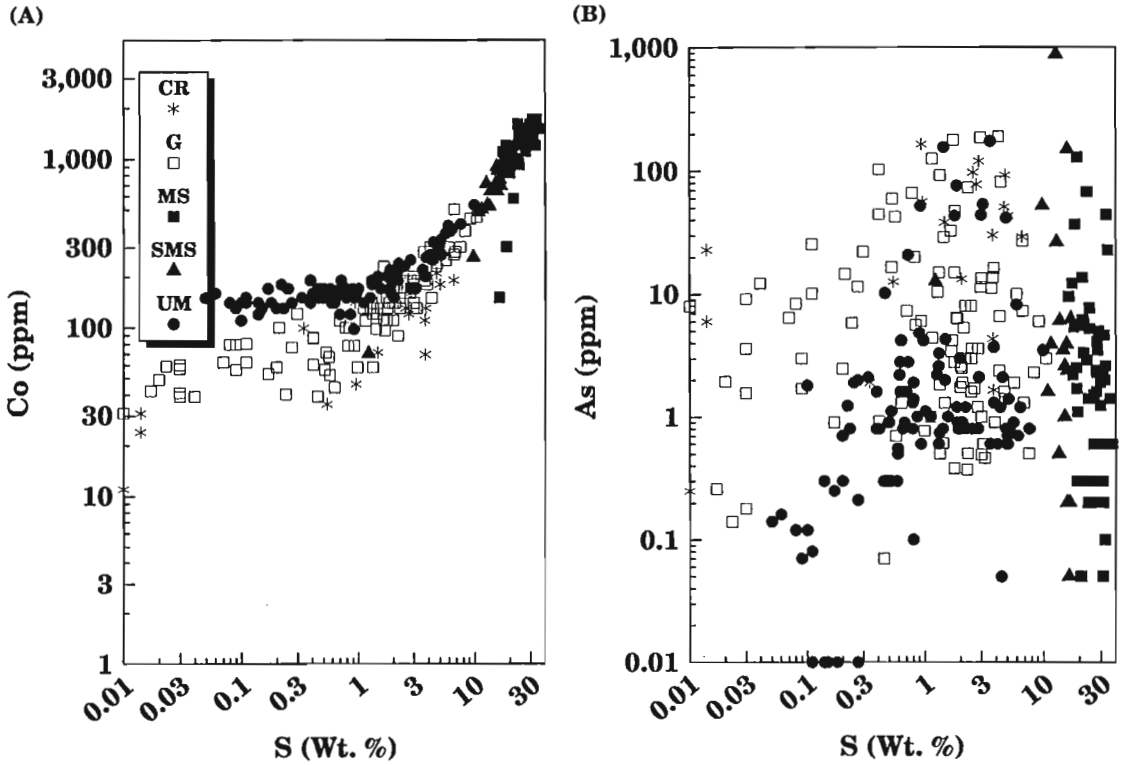

Figure 77 (A-B). *Co, As vs. S (wt.%) plots of elemental concentrations associated with ultramafic (UM), gabbroic (G), massive sulphide (MS), semi-massive sulphide (SMS), and country rock (CR) lithologies from the Quill Creek Intrusive Complex.*

Creek Complex (Wellgreen) and linear (Linda, Wellgreen, Tatamagouche, Dickson and Chilkat) trends occur in gabbro throughout the belt with respect to Ni. The curved trend in the <0.01 to 1.0 wt.% S range at the Onion and Wellgreen properties demonstrate that the bulk of the Ni is partitioned into silicate and oxide phases in rocks demonstrating this relationship. The observation that some of the sulphur-poor (0.03 to 0.10% S) marginal gabbro can have high Ni contents (700 to 1000 ppm range) suggests that some parental magmas were fairly Ni-rich. Linear gabbro-hosted Ni vs. S trends clearly demonstrate the influence of sulphide on the wholerock Ni content. This is particularly apparent for the marginal gabbro samples from

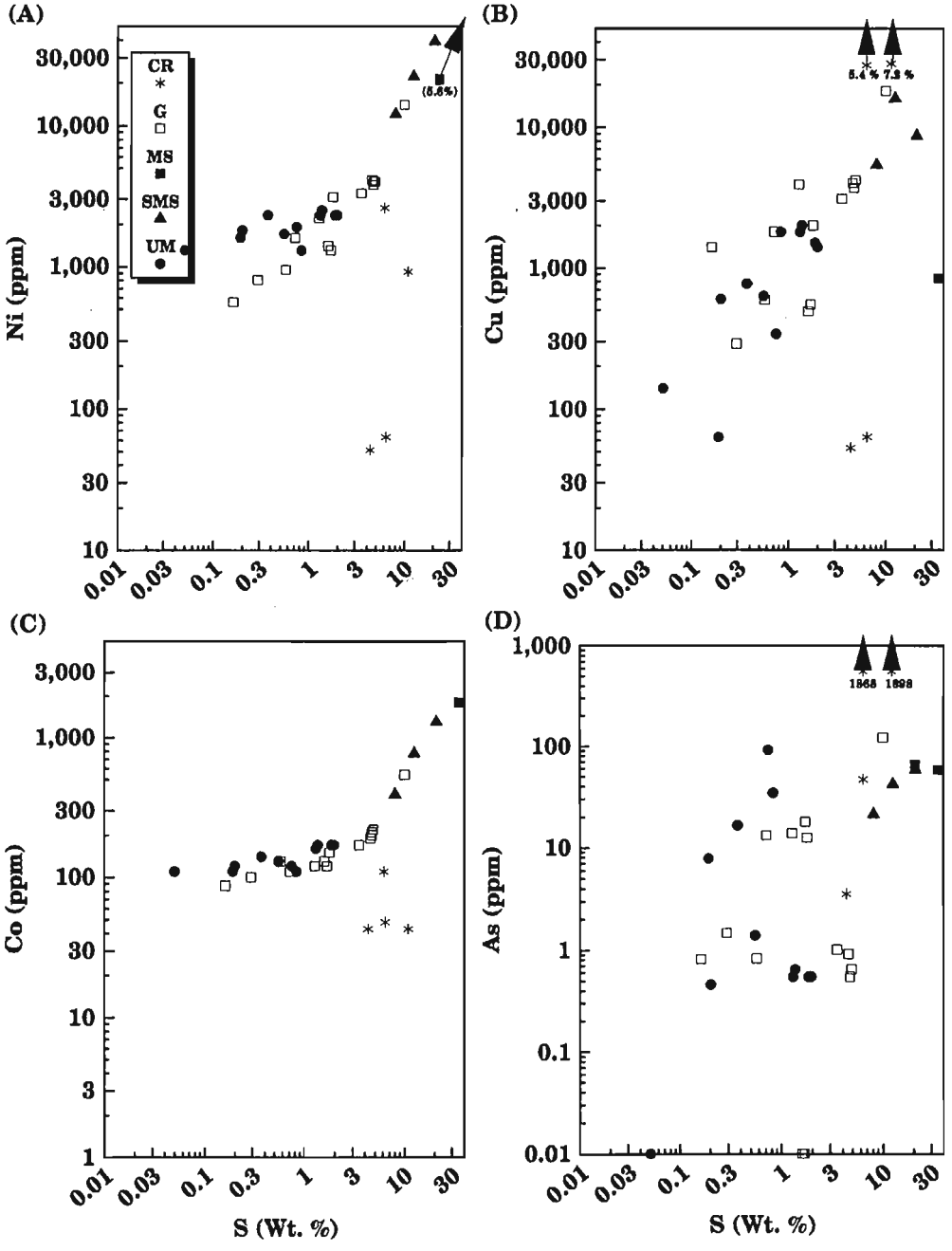

Figure 78 (A-D). Ni, Cu, Co, As vs. S (wt.%) plots of elemental concentrations associated with ultramafic (UM), gabbroic (G), massive sulphide (MS), semi-massive sulphide (SMS), and country rock (CR) lithologies from the Linda Creek Intrusive Complex.

Linda, Quill Creek (Wellgreen) and Tatamagouche. Continuity of this trend in the 0.03 to 1.0% S range with that of the mineralized gabbro, semi-massive and massive sulphide samples in the 1.0 to 37.5 wt. % S range confirms the sulphide control and the comagmatic nature of Ni in all these diverse lithologies. Deviations in the Ni and Co trends are associated with: (1) samples containing high Ni (120 to 700 ppm) and low S (<0.01%) in olivine gabbro cumulates from the Tatamagouche and Duke River complexes, (2) samples with very low Ni contents (<100 ppm) designated as belonging to the Maple Creek gabbro from Tatamagouche and the Duke River complexes, although they have not been divided, and (3) the low

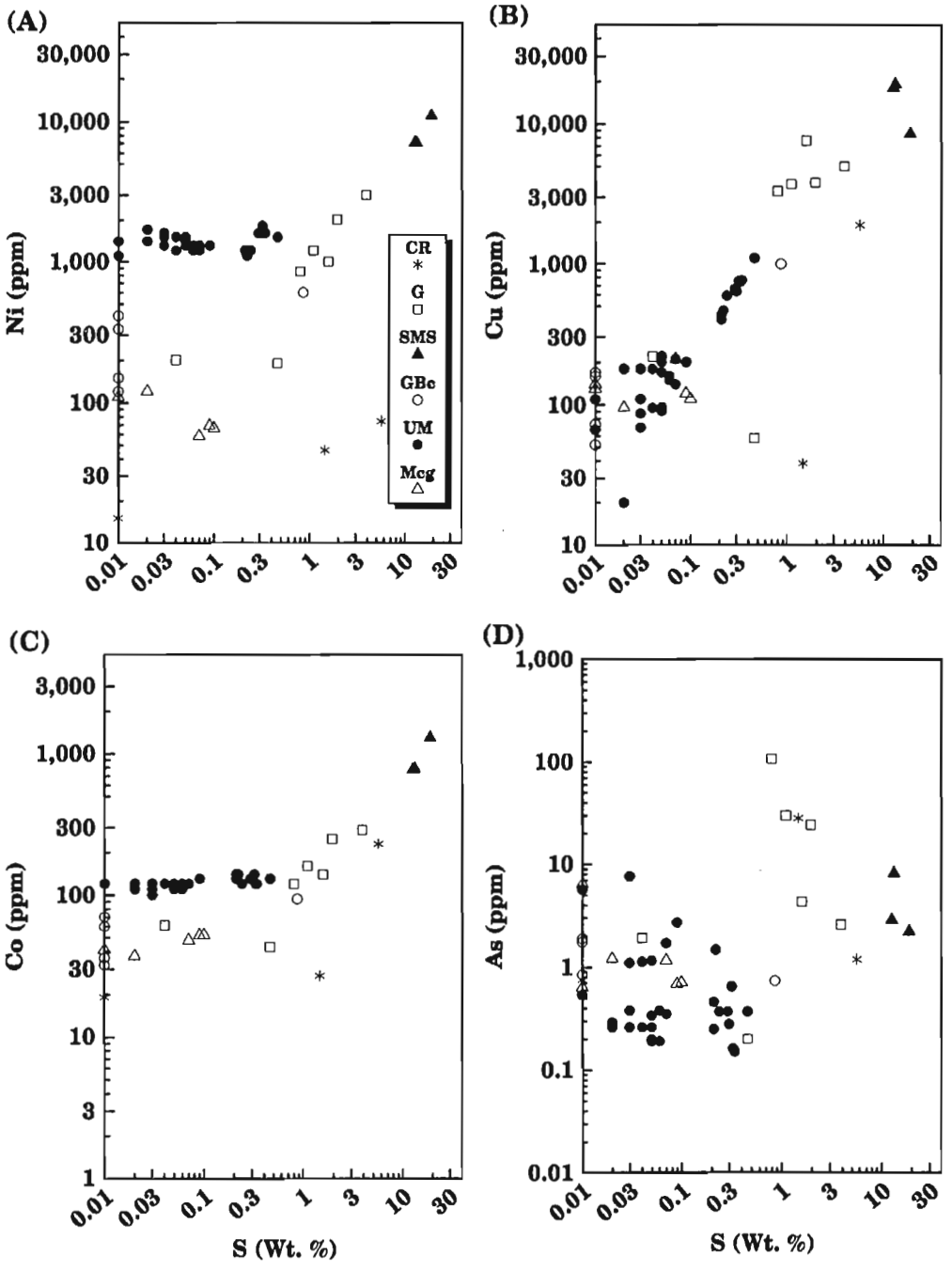

Figure 79 (A-D). Ni, Cu, Co, As vs. S (wt.%) plots of elemental concentrations associated with ultramafic (UM), gabbroic (G), basal gabbro (Gbc), Maple Creek gabbro (Mcg), massive sulphide (MS), semi-massive sulphide (SMS) and country rock (CR) lithologies from the Tatamagouche Creek Intrusive Complex.

Ni content (<70 ppm) in mineralized gabbro (1.0 to 3.0% S) from the Duke River, Halfbreed, and Dickson Creek complexes is a consequence of sulphide immiscibility resulting from localized crustal contamination and subsequent restricted communication with the magma.

Some massive and semi-massive sulphide mineralization from the Kluane Belt has economically desirable Ni grades and some interesting trends locally. Representative massive sulphide accumulations (Arch, Linda, Quill Creek or Wellgreen and Rainbow Mountain) associated with the basal contact of the intrusions generally have Ni grades in the 2.0 to

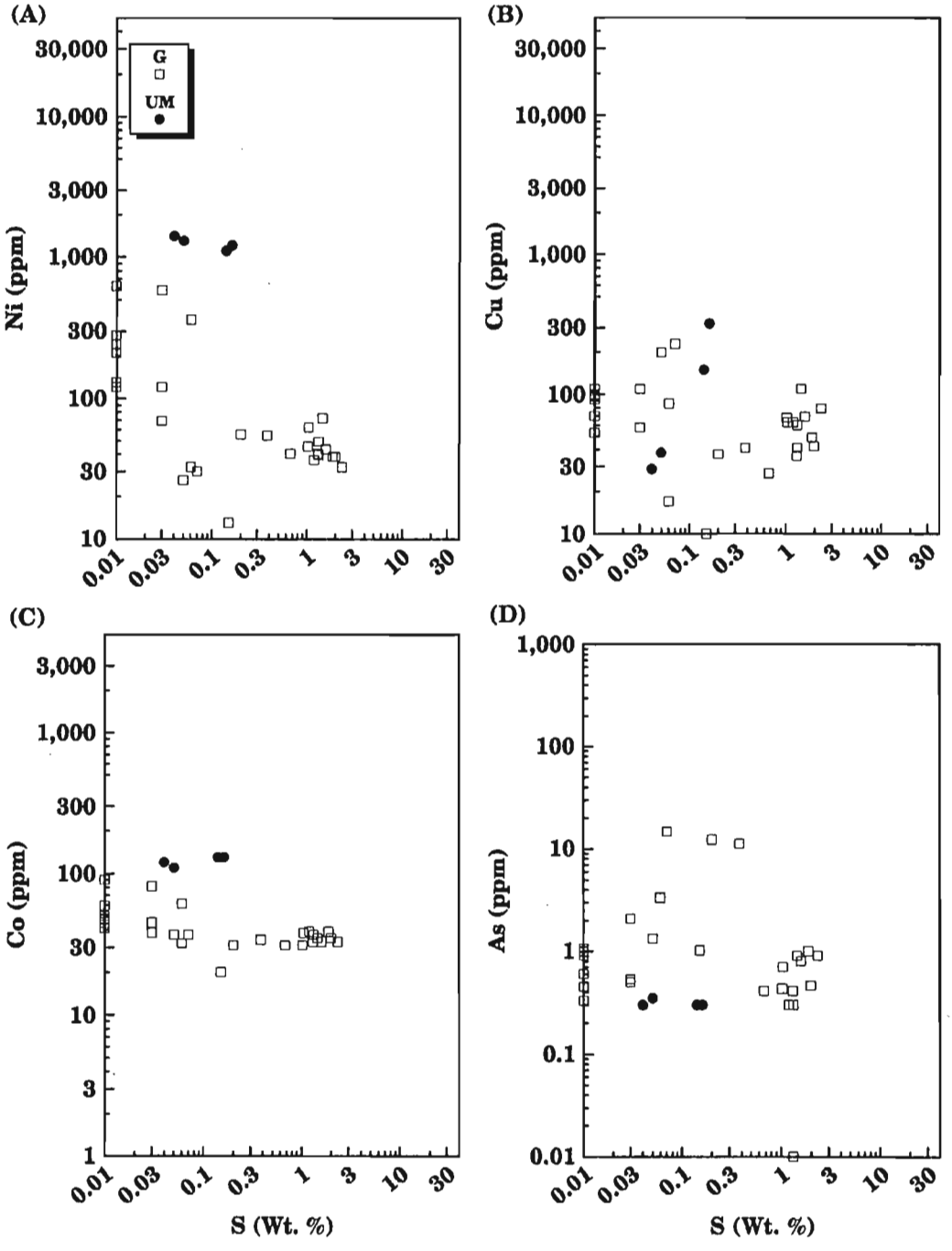

Figure 80 (A-D). *Ni, Cu, Co, As vs. S (wt.%) plots of elemental concentrations associated with ultramafic (UM) and gabbroic (G) lithologies from the Duke River Intrusive Complex.*

4.0 wt.% range (Fig. 75, 76, 78, 84); however, values of up to 5.6% have been obtained from the Linda Complex. Associated semi-massive concentrations generally contain 1.0 to 2.0% Ni. Atypical Ni vs. S trends associated with massive and semi-massive sulphides occur at Canalask, Dickson Creek, and to a lesser extent Tatamagouche Creek (Fig. 74, 82, and 79, respectively). Semi-massive and massive sulphides from Canalask demonstrate two conspicuous Ni groupings for samples containing >15% S (Fig. 74). The Ni-depleted group generally has concentrations similar to the weakly mineralized country rock sediments (<400 ppm). The Ni-enriched group contains between 2000 and 15 000 ppm Ni. Lower Ni values (<150 ppm) are associated with the massive and semi-massive sulphides from the Dickson Creek Complex (Fig. 82);

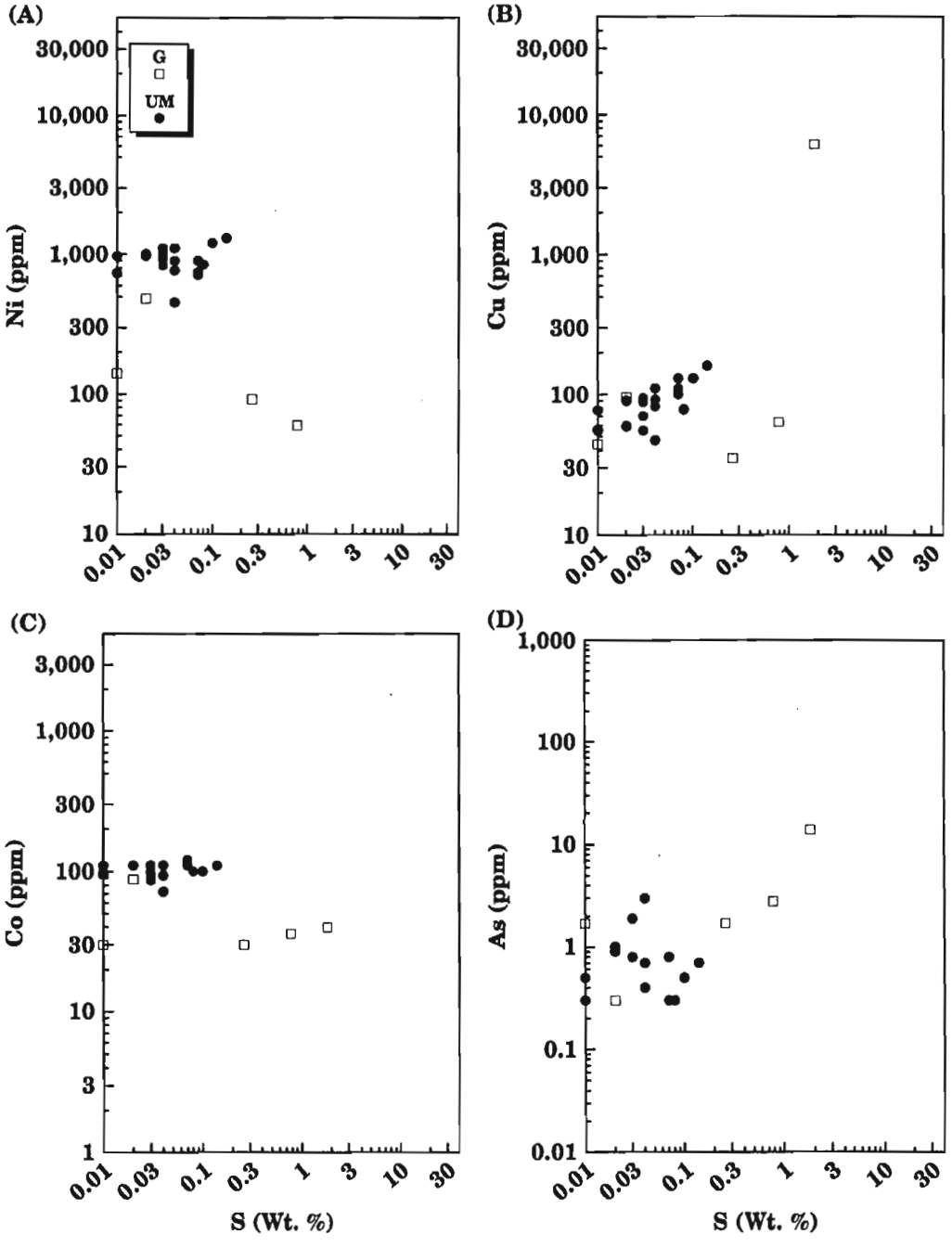

Figure 81 (A-D). *Ni, Cu, Co, As vs. S (wt.%) plots of elemental concentrations associated with ultramafic (UM) and gabbroic (G) lithologies from the Halfbreed Creek Intrusive Complex.*

however, corresponding Co concentrations are not far removed from those of Ni-enriched mineralization. This could indicate that significant levels of Co are associated with the proximal country rock contaminant at this locality. The slightly lower Ni content at Tatamagouche may be the result of Ni leaching due to the highly weathered nature of these sulphide samples. The Ni-depleted nature of semi-massive sulphide mineralization at the Canalask and Dickson Creek properties, and the extreme ^{32}S-enrichment associated with these sulphides (-14.5 to -17.2 and -28.4 to -29.9‰, $\delta^{34}S$, respectively), suggest that the Ni content of the sulphides is governed by the mass of silicate melt the sulphides

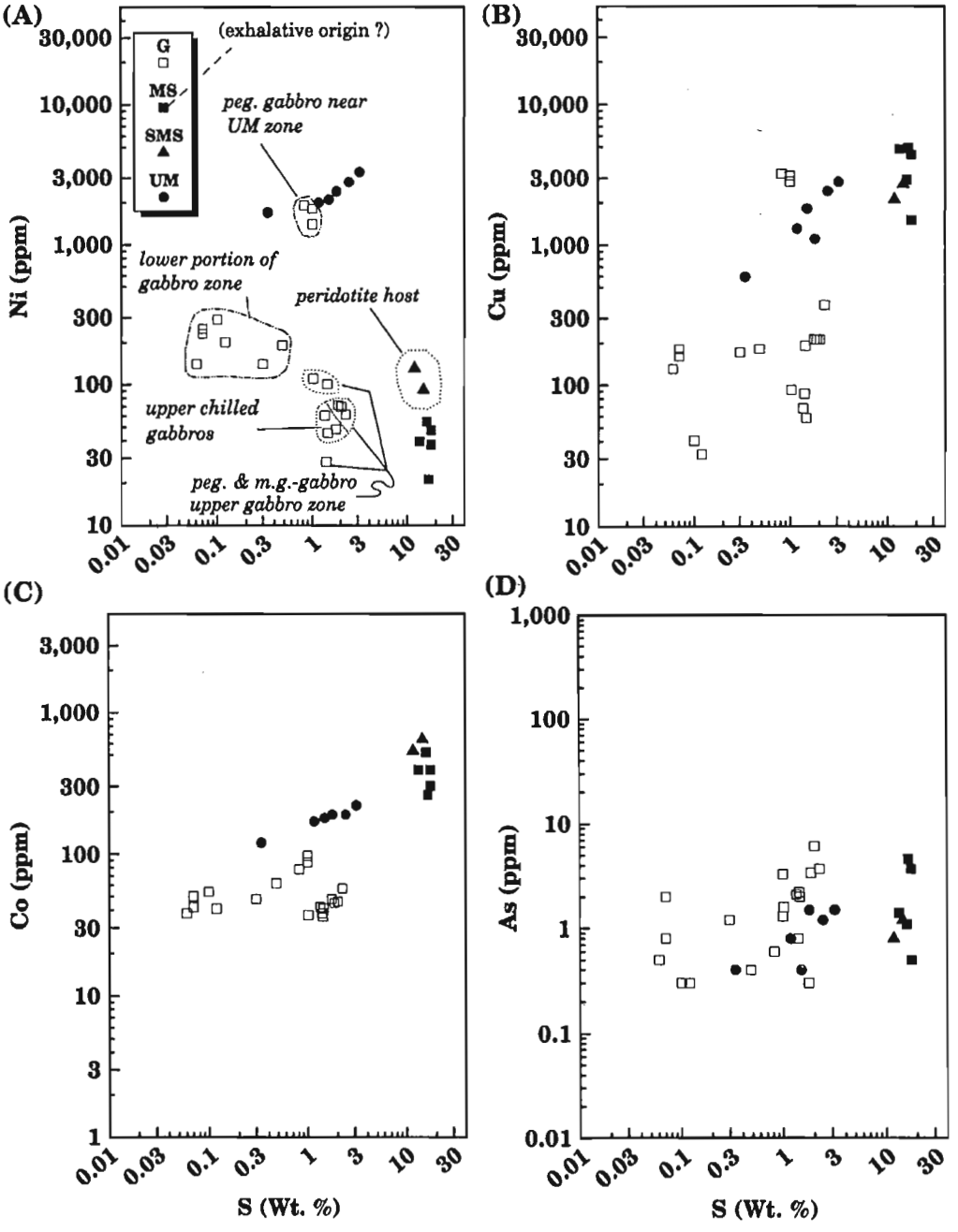

Figure 82 (A-D). Ni, Cu, Co, As vs. S (wt.%) plots of elemental concentrations associated with ultramafic (UM), gabbroic (G), massive country rock (exhalative ?) sulphide (MS), semi-massive sulphide (SMS) lithologies from the Dickson Creek Intrusive Complex.

equilibrated with or the R-Factor (Campbell et al., 1983). If so, then it is apparent that the Ni content of sulphide mineralization is a reliable indicator of the degree of crustal contamination and subsequent communication the sulphides experienced with the surrounding magmas.

Copper has a strong chalcophile character and thus the concentration of this element is a reliable monitor of the amount of Cu-sulphide present in the sample. Semi-massive sulphide commonly has the same range of Cu concentrations as the associated massive sulphides (4000 to 40 000 ppm), but most Ni-rich (>3.0%) massive sulphides generally contain the lowest Cu grades (4000 to 12 000 ppm).

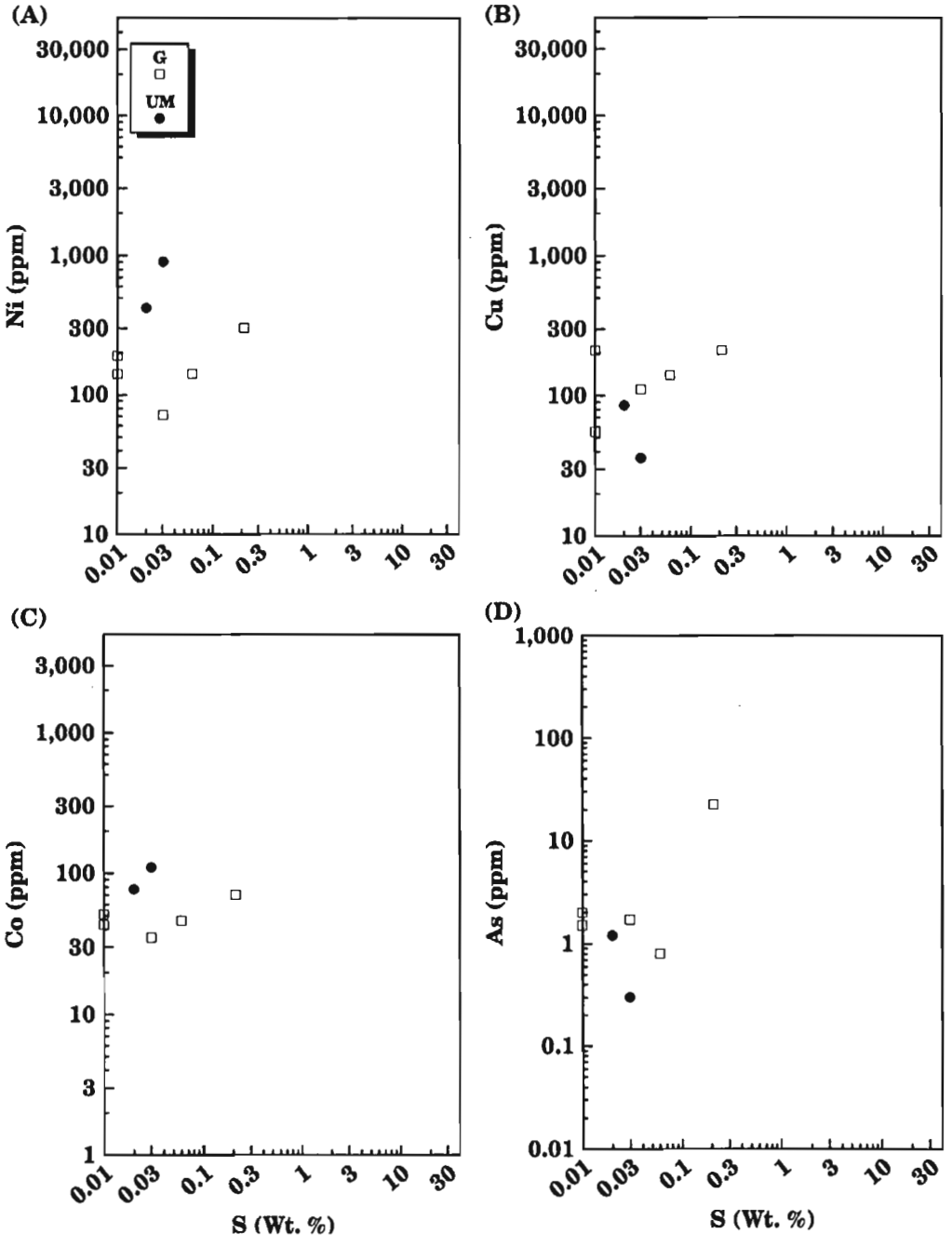

Figure 83 (A-D). *Ni, Cu, Co, As vs. S (wt.%) plots of elemental concentrations associated with ultramafic (UM) and gabbroic (G) lithologies from the Chilkat Intrusive Complex.*

Nevertheless, the highest Cu concentrations (5.4 to 7.9 wt.%) are associated with the most Ni-rich sulphides from the Linda Complex. Unlike Ni, with its chalcophile and lithophile character, the strictly chalcophile nature of Cu does not give rise to diverse geochemical trends that can be used to decipher various metallogenic processes.

Arsenic contents are highly variable and generally confined to the 0.1 to 100 ppm range. Inspection of Figures 73D to 83D also discloses that the As concentration is normally independent of host lithology; however, the country rock sediments locally can contain relatively high concentrations of As (i.e. Onion, Arch, Linda).

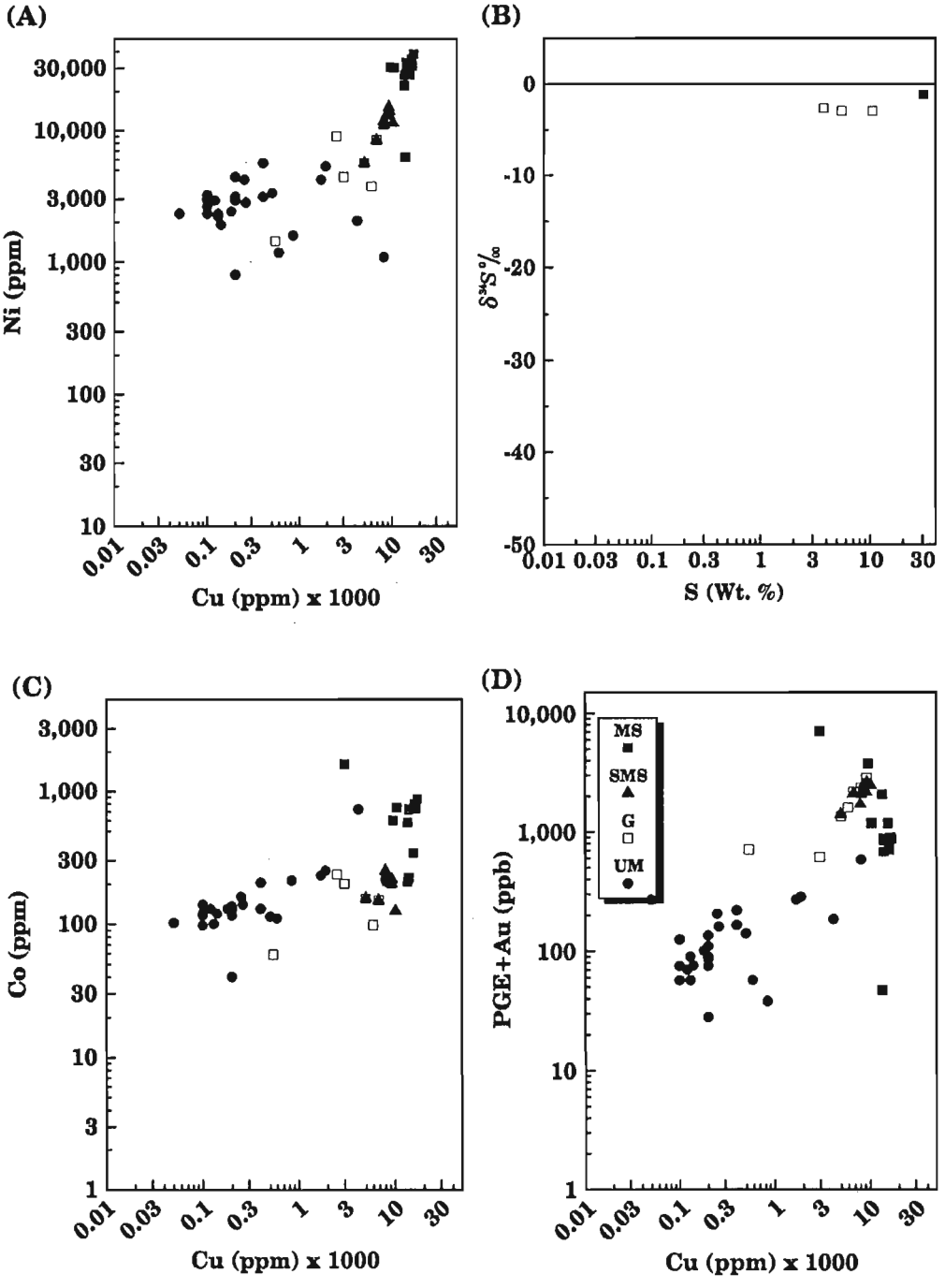

Figure 84 (A-D). Ni, Co, PGE+AU vs. Cu and $\delta^{34}S‰$ vs. S (wt.%) plots of elemental concentrations and isotopic compositions associated with ultramafic (UM), gabbroic (G), massive sulphide (MS), and semi-massive sulphide (SMS) lithologies from the Rainbow Mountain Intrusive Complex, Alaska.

Selenium, bismuth, antimony, and tellurium

Selenium, bismuth, antimony, and tellurium concentrations and behaviour have been investigated at a number of complexes within the belt. Concentrations and trends relative to the associated sulphur contents are represented in Figures 85 to 95, inclusive.

Of these four elements, Se demonstrates the most coherent geochemical trends with respect to associated S contents. The moderate to strong correlation with S, as depicted by the Se vs. S trends in Figures 85 to 95, demonstrates the chalcophile nature of Se. Paktunc et al. (1990) conducted a proton microprobe investigation of pentlandite, pyrrhotite, and chalcopyrite

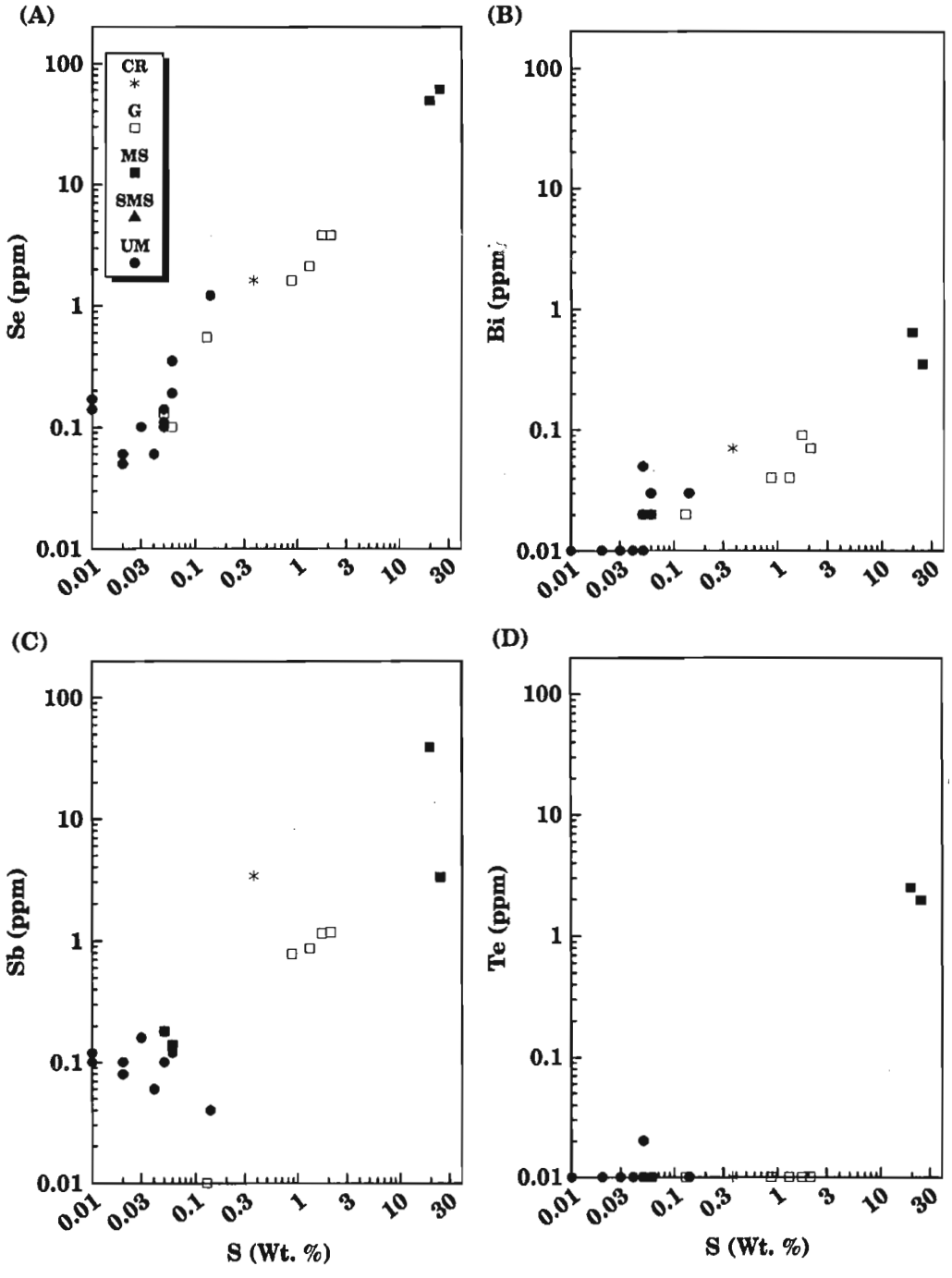

Figure 85 (A-D). *Se, Bi, Sb, Te vs. S (wt.%) plots of elemental concentrations associated with ultramafic (UM), gabbroic (G), massive sulphide (MS), semi-massive sulphide (SMS), and country rock (CR) lithologies from the Onion property of the White River Intrusive Complex. Values plotting along the base of the diagram represent concentrations at the detection limit of the analytical method.*

from the Wellgreen deposit and found the all three phases generally contain 95 to 130 ppm Se in solid solution. The highest Se contents are generally associated with massive and semi-massive sulphides except those from the Dickson Creek Complex which are clearly impoverished in this element. Mineralized gabbro from the Onion, Arch, Wellgreen, Linda, and Tatamagouche properties contain the next highest levels of Se, whereas macroscopically similar mineralized gabbro (i.e. in the 1 to 3% S range from the Duke River and Dickson Creek properties, Fig. 92, 94) generally contains less Se. Inspection of the Se:S trends associated with the various complexes suggests that ultramafic rocks generally contain

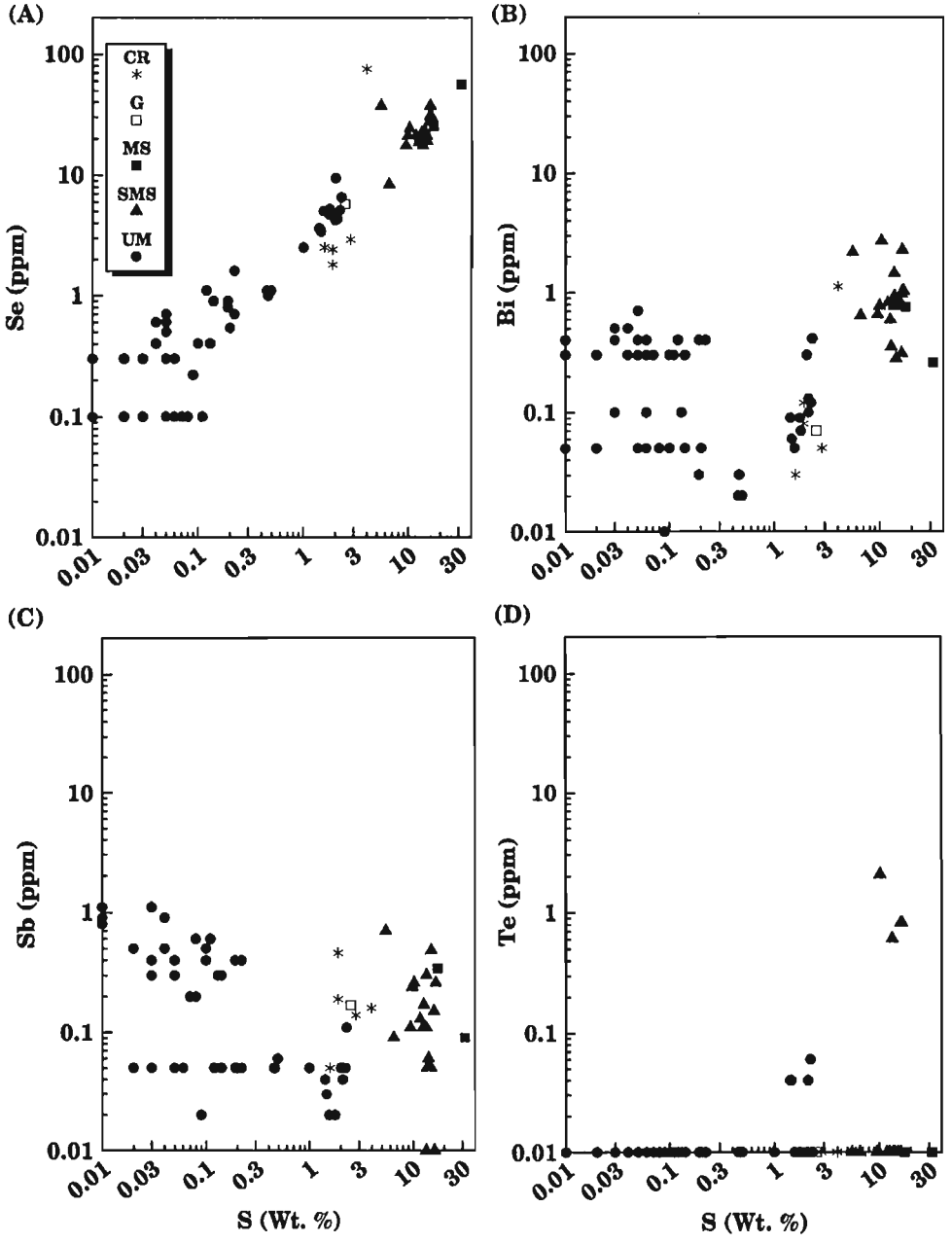

Figure 86 (A-D). Se, Bi, Sb, Te vs. S (wt.%) plots of elemental concentrations associated with ultramafic (UM), gabbroic (G), massive sulphide (MS), semi-massive sulphide (SMS), and country rock (CR) lithologies from the Canalask property of the White River Intrusive Complex. Values plotting along the base of the diagram represent concentrations at the detection limit of the analytical method.

more Se than their gabbroic counterparts with equal amounts of S. It is difficult to ascertain if this relationship is the result of a primary magmatic control (i.e. different distribution coefficients for Se), or a secondary process such as S-loss accompanying serpentinization. The latter process is more likely to have influenced the rocks with low S contents (<0.30 wt.%).

Although not as pronounced, Bi displays a moderate linear correlation with amount of S contained in the rock (Onion, Arch, Linda, Tatamagouche, and Dickson Creek properties) and thus demonstrates the rather chalcophile nature of Bi within these intrusions. However, at other localities (Canalask and Wellgreen) this is not the case and considerable scatter is associated with this plot. Ultramafic rocks from these two localities also have elevated Bi contents relative to those from other complexes. The highest Bi concentrations are associated with the massive and semi-massive sulphides.

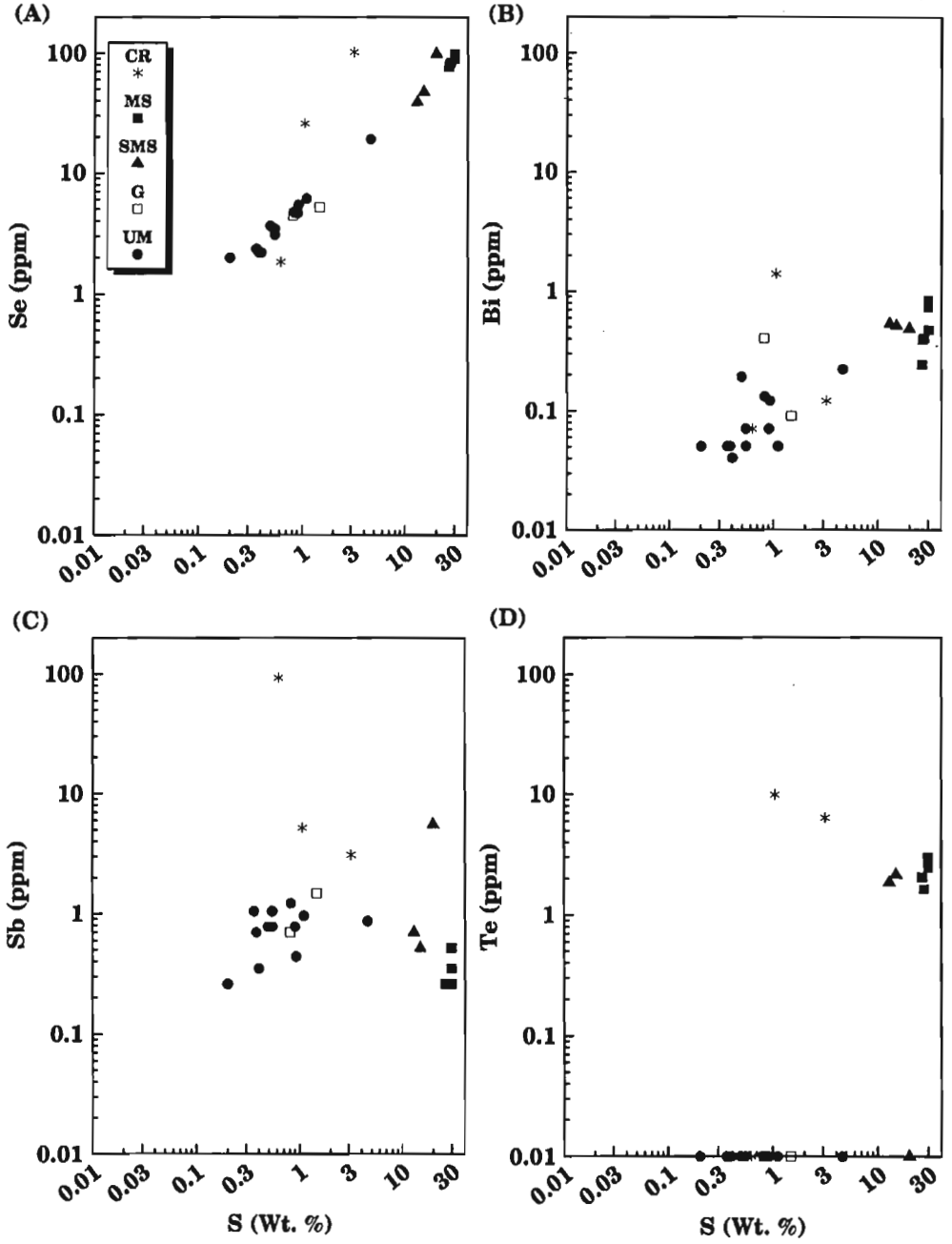

Figure 87 (A-D). *Se, Bi, Sb, Te vs. S (wt.%) plots of elemental concentrations associated with ultramafic (UM), gabbroic (G), massive sulphide (MS), semi-massive sulphide (SMS), and country rock (CR) lithologies from the Arch Creek Intrusive Complex. Values plotting along the base of the diagram represent concentrations at the detection limit of the analytical method.*

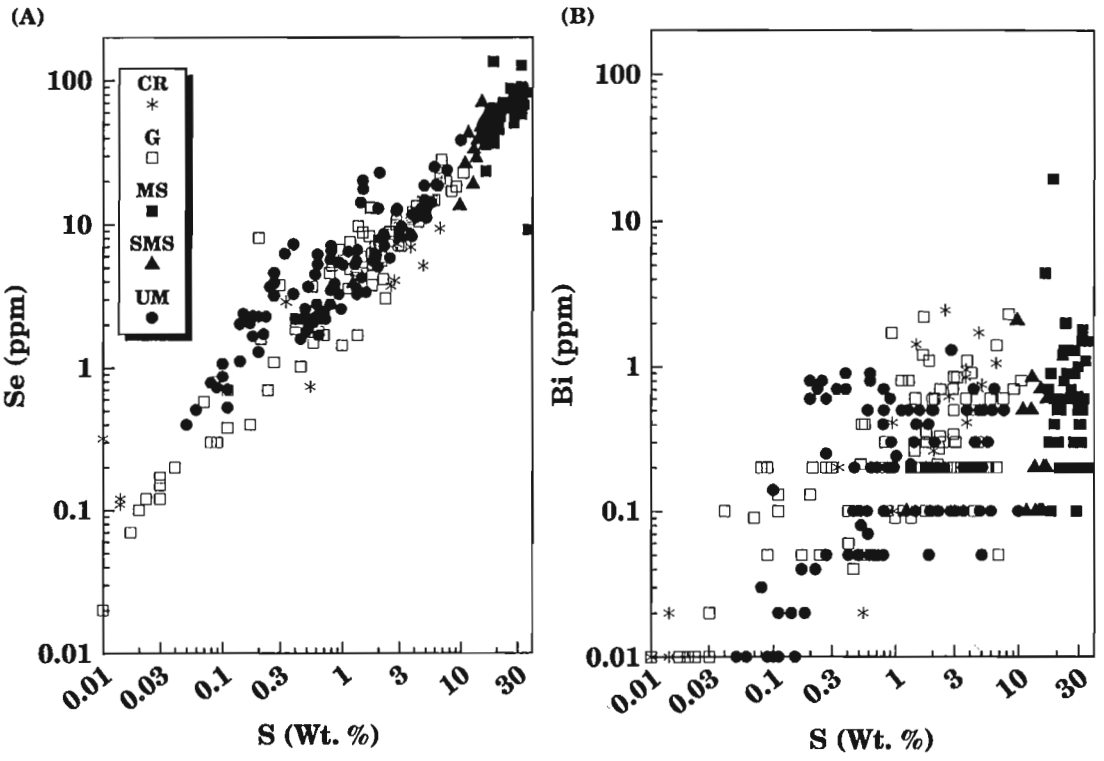

Figure 88 (A-B). *Se, Bi vs. S (wt.%) plots of elemental concentrations associated with ultramafic (UM), gabbroic (G), massive sulphide (MS), semi-massive sulphide (SMS), and country rock (CR) lithologies from the Quill Creek Intrusive Complex. Values plotting along the base of the diagram represent concentrations at the detection limit of the analytical method.*

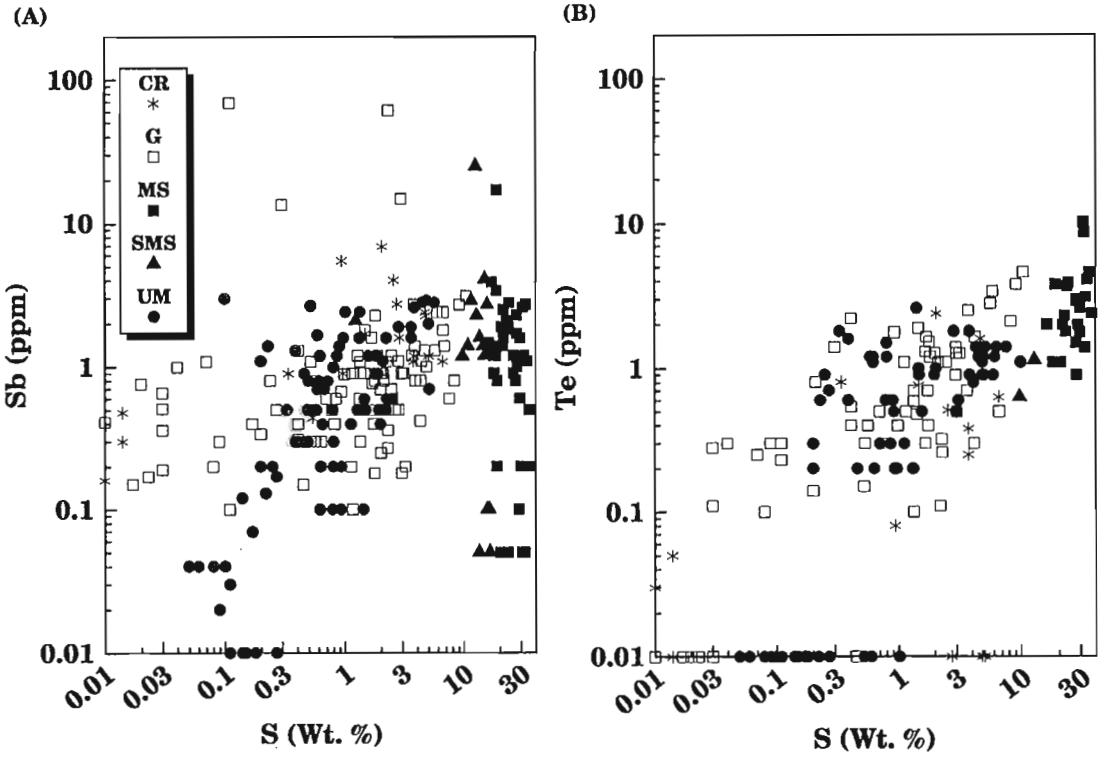

Figure 89 (A-B). *Sb, Te vs. S (wt.%) plots of elemental concentrations associated with ultramafic (UM), gabbroic (G), massive sulphide (MS), semi-massive sulphide (SMS), and country rock (CR) lithologies from the Quill Creek Intrusive Complex. Values plotting along the base of the diagram represent concentrations at the detection limit of the analytical method.*

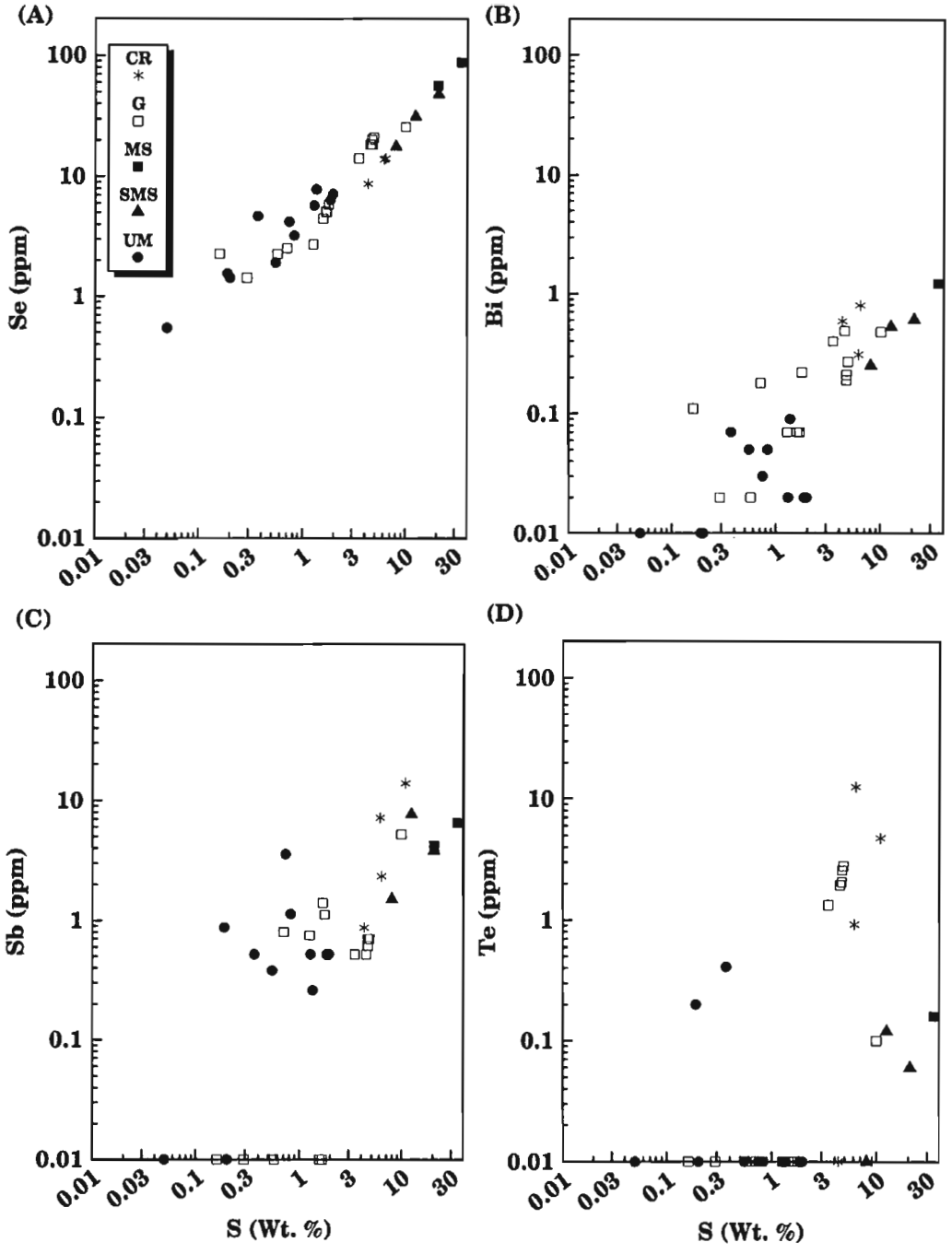

Figure 90 (A-D). *Se, Bi, Sb, Te vs. S (wt.%) plots of elemental concentrations associated with ultramafic (UM), gabbroic (G), massive sulphide (MS), semi-massive sulphide (SMS), and country rock (CR) lithologies from the Linda Creek Intrusive Complex. Values plotting along the base of the diagram represent concentrations at the detection limit of the analytical method.*

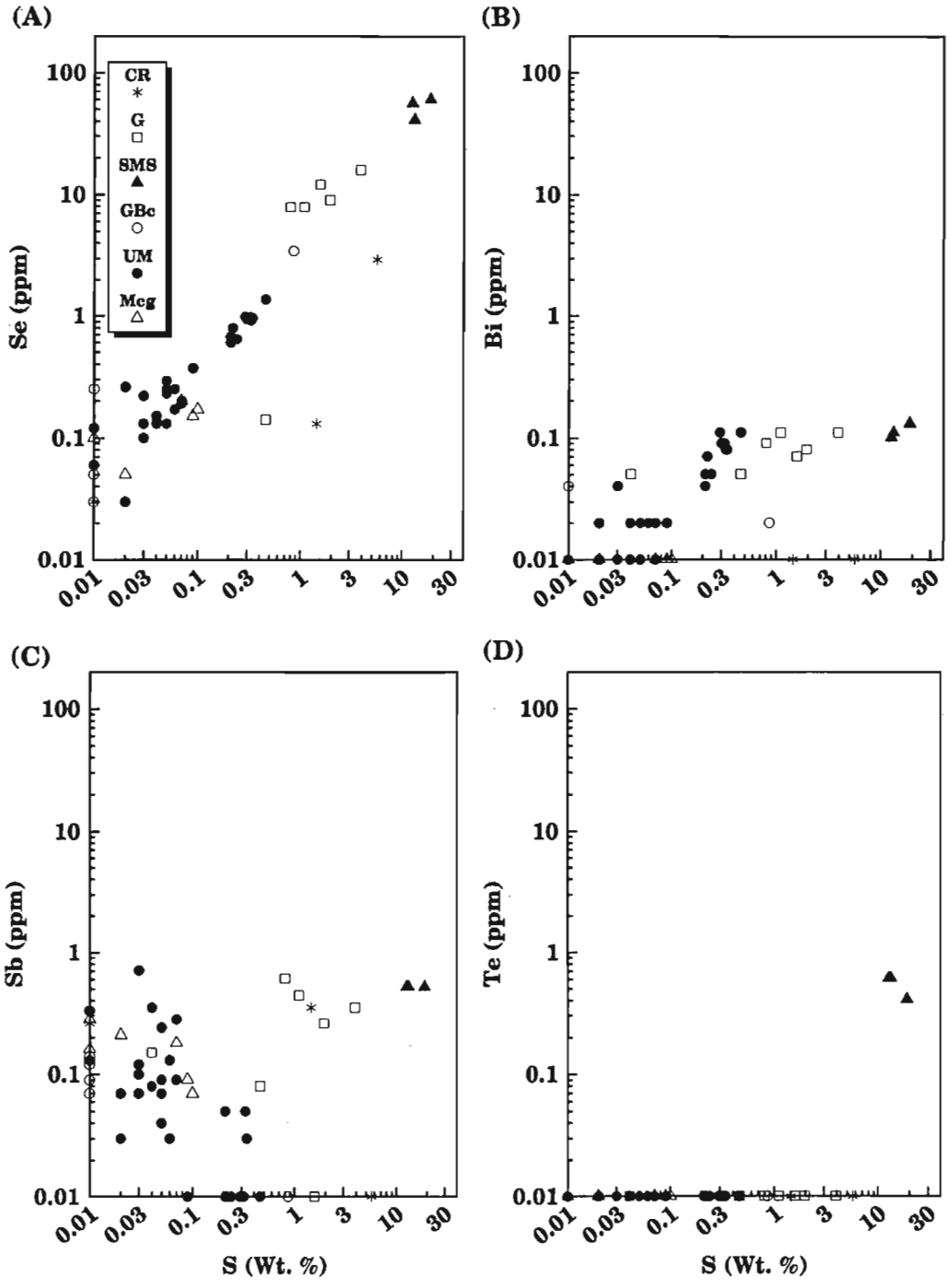

Figure 91 (A-D). *Se, Bi, Sb, Te vs. S (wt.%) plots of elemental concentrations associated with ultramafic (UM), gabbroic (G), Maple Creek gabbro (Mcg), basal gabbro (GBc), semi-massive sulphide (SMS), and country rock (CR) lithologies from the Tatamagouche Creek Intrusive Complex. Values plotting along the base of the diagram represent concentrations at the detection limit of the analytical method.*

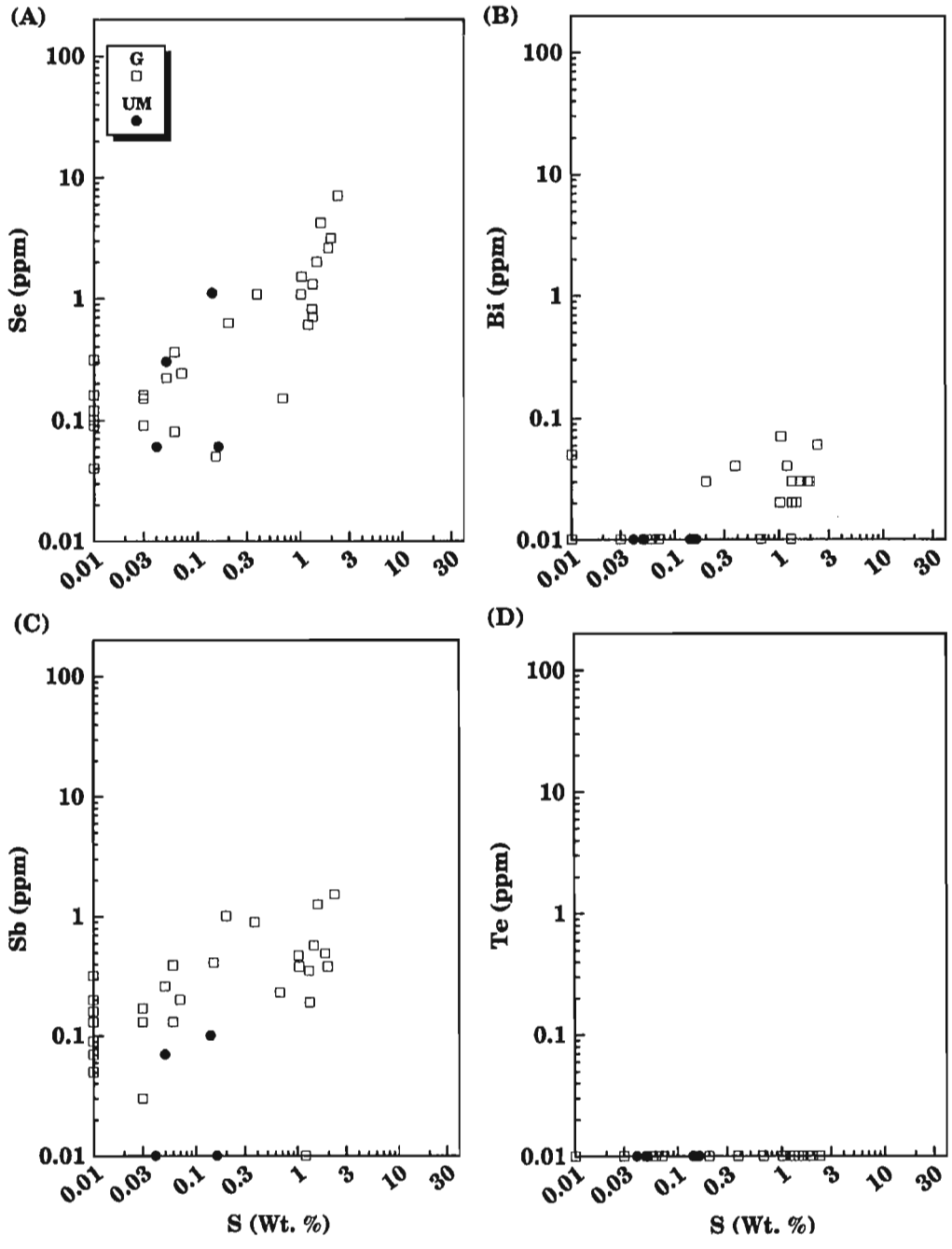

Figure 92 (A-D). *Se, Bi, Sb, Te vs. S (wt.%) plots of elemental concentrations associated with ultramafic (UM) and gabbroic (G) lithologies from the Duke River Intrusive Complex. Values plotting along the base of the diagram represent concentrations at the detection limit of the analytical method.*

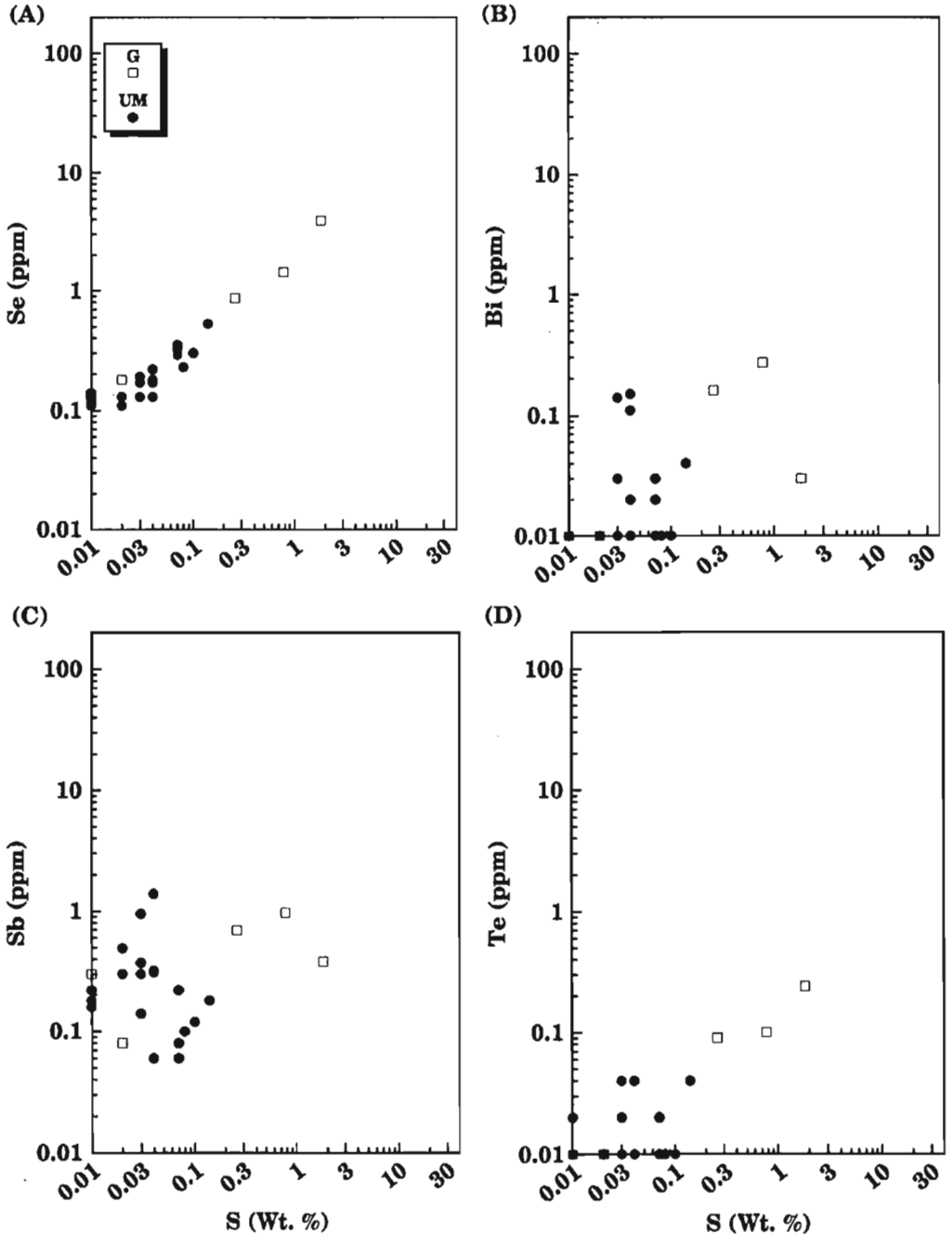

Figure 93 (A-D). *Se, Bi, Sb, Te vs. S (wt.%) plots of elemental concentrations associated with ultramafic (UM) and gabbroic (G) lithologies from the Halfbreed Creek Intrusive Complex. Values plotting along the base of the diagram represent concentrations at the detection limit of the analytical method.*

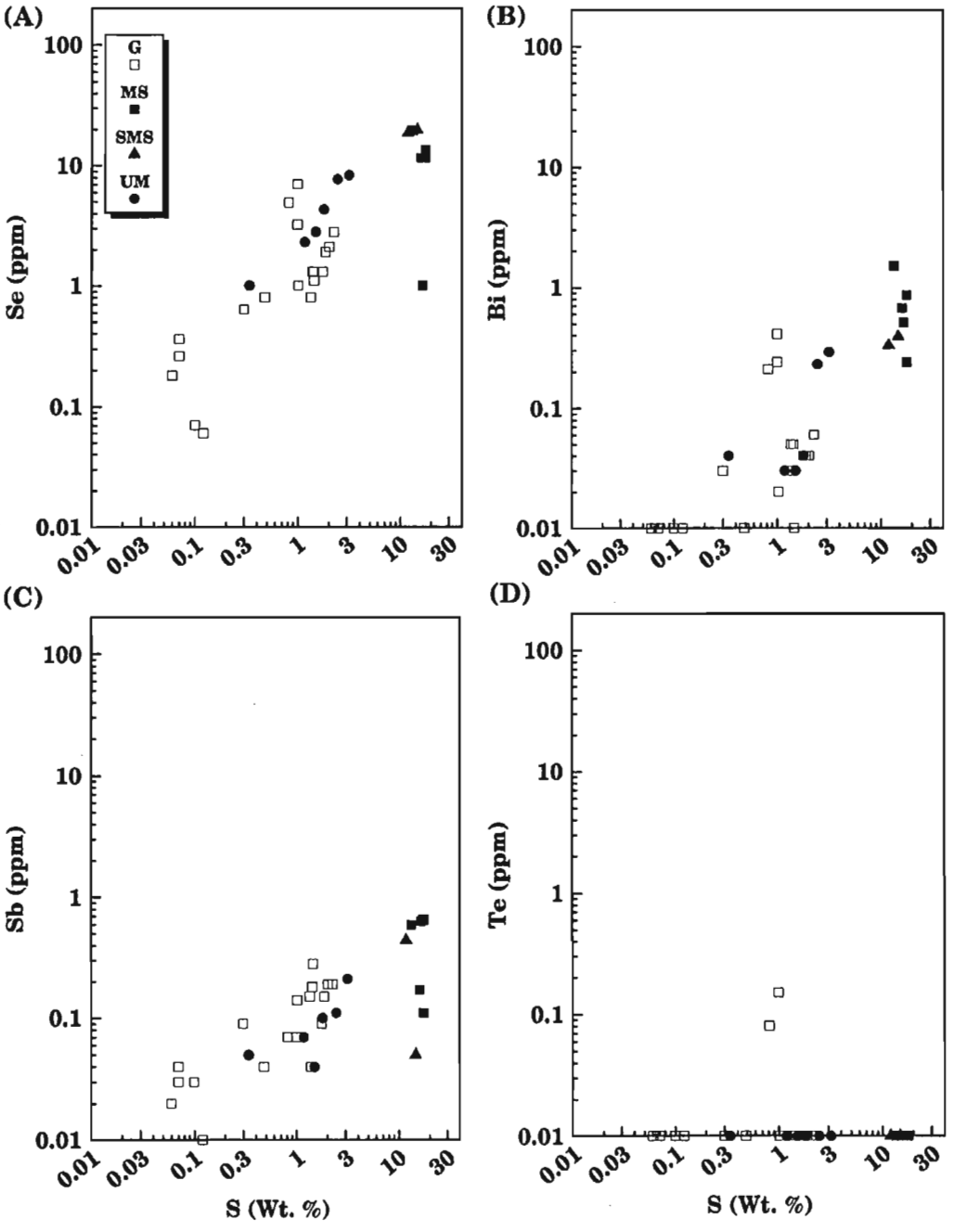

Figure 94 (A-D). *Se, Bi, Sb, Te vs. S (wt. %) plots of elemental concentrations associated with ultramafic (UM), gabbroic (G), massive country rock (exhalative ?) sulphide (MS), and semi-massive sulphide (SMS) lithologies from the Dickson Creek Intrusive Complex. Values plotting along the base of the diagram represent concentrations at the detection limit of the analytical method.*

Sb demonstrates a weak to moderate linear correlation with S at some localities (Onion, Linda, Duke River, and Dickson Creek), whereas at others (Canalask, Wellgreen, Tatamagouche, and Halfbreed Creek) no correlation exits. A high degree of variability exists in the massive and semi-massive sulphides with respect to the Sb concentration. An order of magnitude, and in some cases as much as two orders of magnitude, variation can be associated with these sulphide lithologies. Sb depletion in massive and semi-massive sulphides tends to be associated with the more Ni-rich samples. In many intrusions the silicate-rich rocks have Sb concentrations equivalent if not greater than the mineralized samples.

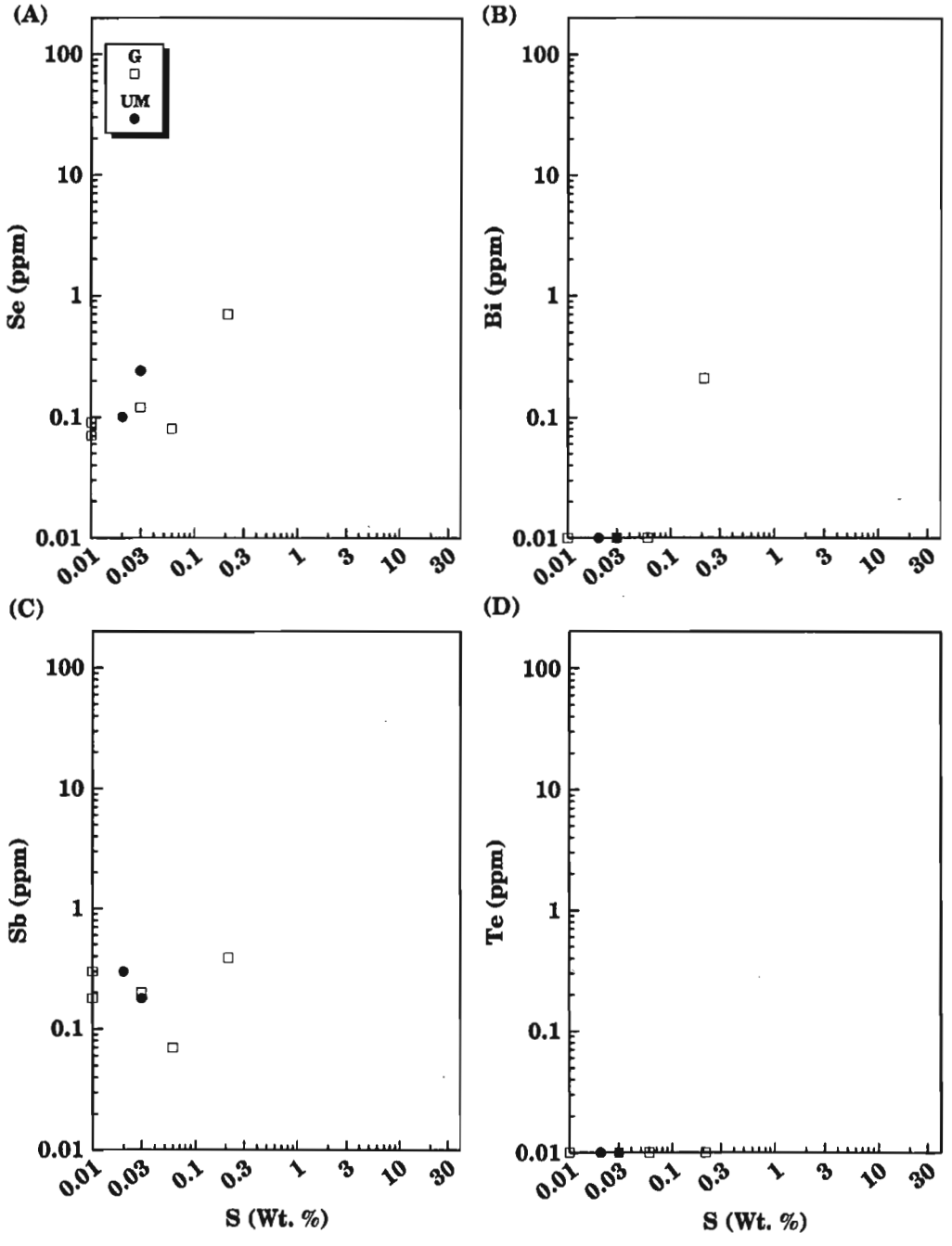

Figure 95 (A-D). *Se, Bi, Sb, Te vs. S (wt.%) plots of elemental concentrations associated with ultramafic (UM) and gabbroic (G) lithologies from the Chilkat Intrusive Complex. Values plotting along the base of the diagram represent concentrations at the detection limit of the analytical method.*

Te concentrations are highly variable but the highest are generally associated with the massive and semi-massive sulphides at most localities except Linda and Dickson Creek. High Te values generally correlate with Ni-rich sulphide mineralization. Paktunc et al. (1990) found that Quill Creek Complex (Wellgreen) pyrrhotite contains 28 ± 8 ppm Te and Cabri et al. (1993) discovered that altaite (PbTe) and hessite (Ag_2Te) are associated with the Quill Creek sulphide mineralization.

Sulphur/selenium ratio, barium, and sulphur isotope

S/Se ratios, barium concentrations and sulphur isotope compositions ($\delta^{34}S‰$) were investigated whenever possible to constrain a metallogenic model for the Ni-Cu and Fe-sulphide mineralization within the various Kluane mafic-ultramafic complexes. Due to the ^{32}S-rich nature of the surrounding Permian sedimentary rocks ($\delta^{34}S$ = -26 to -19‰ in the north and central sections of the belt respectively, and -39.6‰ in the southern section), crustal contamination is relatively easy to assess if sulphides can be extracted from the samples. Unfortunately, this approach cannot be used in intrusions devoid of or poor in sulphides (i.e. Chilkat and Halfbreed Creek); therefore, other elements and their ratios (Ba and S/Se) have been assessed as possible indicators of crustal contamination. Due to the common interdependence of S/Se ratios and compositions in sedimentary-derived sulphides, these two variables are examined collectively.

Although not well established, it is believed that mantle-derived sulphides have S/Se ratios of ≤3333 (McDonough and Sun, 1995) and sedimentary sulphides generally have higher S/Se ratios (Rankama and Sahama, 1950; Loftus-Hills and Solomon, 1967). It is known that primary sedimentary S/Se ratios can be variable even within a limited stratigraphic interval. Hulbert et al. (1992b) demonstrated that in Devonian black shale from the Yukon, this ratio varied from <1000 to 6000 within an 80 m stratigraphic interval. However, low S/Se ratios in sedimentary environments tend only to be associated with black shale due to their Se-rich nature relative to other sediments. In contrast, Thompson (1982) found that sulphide-bearing calc-silicate and pelitic schist from the Lower Devonian Hildreths Formation of Maine had a mean S/Se ratio of 40 000.

At the Canalask property sedimentary sulphides have S/Se ratios from 6280 to 10556, $\overline{X}$ = 8608, whereas mineralized calc-silicate adjacent the Quill Creek Complex has values of approximately 9200. Permo-Pennsylvanian sedimentary and sedimentary exhalative country rock from Tatamagouche Creek range from 19 381 to 111 538. Some gabbroic rocks from the Dickson Creek Complex have S/Se ratios of 20 000, thus the contaminating sediments must of had ratios greater than this value. Therefore, based on inspection of S/Se values associated with the various intrusions, and the limited data for sulphidic sedimentary country rocks, values of 10 000 to 20 000 represent the average range in S/Se ratios in the country rock throughout the belt.

Samples with S/Se ratios <2000 are generally associated with ultramafic, and to a lesser extent some gabbroic rocks, that have low sulphur contents (<3.0%). These unusually low values may be attributed to greater sulphur loss relative to Se accompanying serpentinization and alteration. At the Canalask property (Fig. 97A, C) sulphide-poor peridotite can have S/Se ratios up to 11 000; however, most of the better mineralized samples have ratios in the 3000 to 4500 range. Even within this limited S/Se range (3000 to 4500) a roughly 5‰ sulphur isotope variation was recorded. This demonstrates the influence of extraneous (country rock) sulphur on the associated S/Se ratios of the sulphides. The similarity in ratios for the country rock samples and the sulphide-poor peridotite with high ratios suggest that a much higher proportion of its sulphur is country rock derived than that associated with the better mineralized samples. This same influence occurs in the mineralized ultramafic rocks from the Quill Creek Complex (Fig. 99A, 100). The corresponding difference between the S/Se ratio and sulphur isotope composition within an intrusion can best be explained by magma mixing processes, but the extreme range in compositions encountered in the belt would also suggest that a high degree of S/Se variability, and in some cases even incongruous relationships, may be expected. This unusual relationship (i.e. decreasing S/Se ratio associated with increasing ^{32}S) occurs in the mineralized pegmatitic gabbro from the Linda Complex (Fig. 101A, C) with sulphide compositions of -10.6‰ but sulphides from the same gabbro have low S/Se ratios of about 2500. This could indicate that some of the assimilated sediments must have been enriched in Se relative to other sediments. The expected relationship is best illustrated in the Dickson Creek Complex (Fig. 105A, C) where mineralized gabbro varied from low S/Se ratios (1500 to 1700) with relatively heavy sulphur (-5.5 to -6.8‰) to high S/Se (>10 000) with very light sulphur (-28.4 to -29.9‰). This relationship is also well illustrated in the Duke River Complex (Fig. 103A, C).

Massive and semi-massive sulphides from the various complexes also demonstrate considerable range in the S/Se ratio (values up to 8000) and sulphur isotope composition (up to 8‰), and are due to factors similar to those mentioned above.

All mineralized and unmineralized mafic-ultramafic rocks from the Kluane Belt record anomalously high and variable Ba concentrations. The high Ba contents and associated variability appear to be a distinctive geochemical feature of not only the gabbro and ultramafic rocks, but also the semi-massive and massive sulphides in the belt. As Ba is commonly associated with the felsic constituents of tholeiitic rocks, the gabbro, ultramafic, and sulphide-rich samples from the Kluane Belt should contain successively lower Ba concentrations, respectively, and thus should be depleted in Ba relative to most tholeiitic rocks (if one assumes that the distribution and concentration of this element are controlled entirely by closed system crystallization conditions). Holm (1985) conducted a survey of Ba and the other hygromagmatophile element abundances in tholeiitic rocks and basaltic andesite and found the following mean concentrations (in ppm): ocean-island tholeiite (143), continental tholeiite (234), ocean floor tholeiite; N-MORB, (29), low-K tholeiite from Benioff zones (99), E-MORB (174), mean of oceanic and continental back-arc tholeiite (55), and initial rifting tholeiite in continental settings (163).

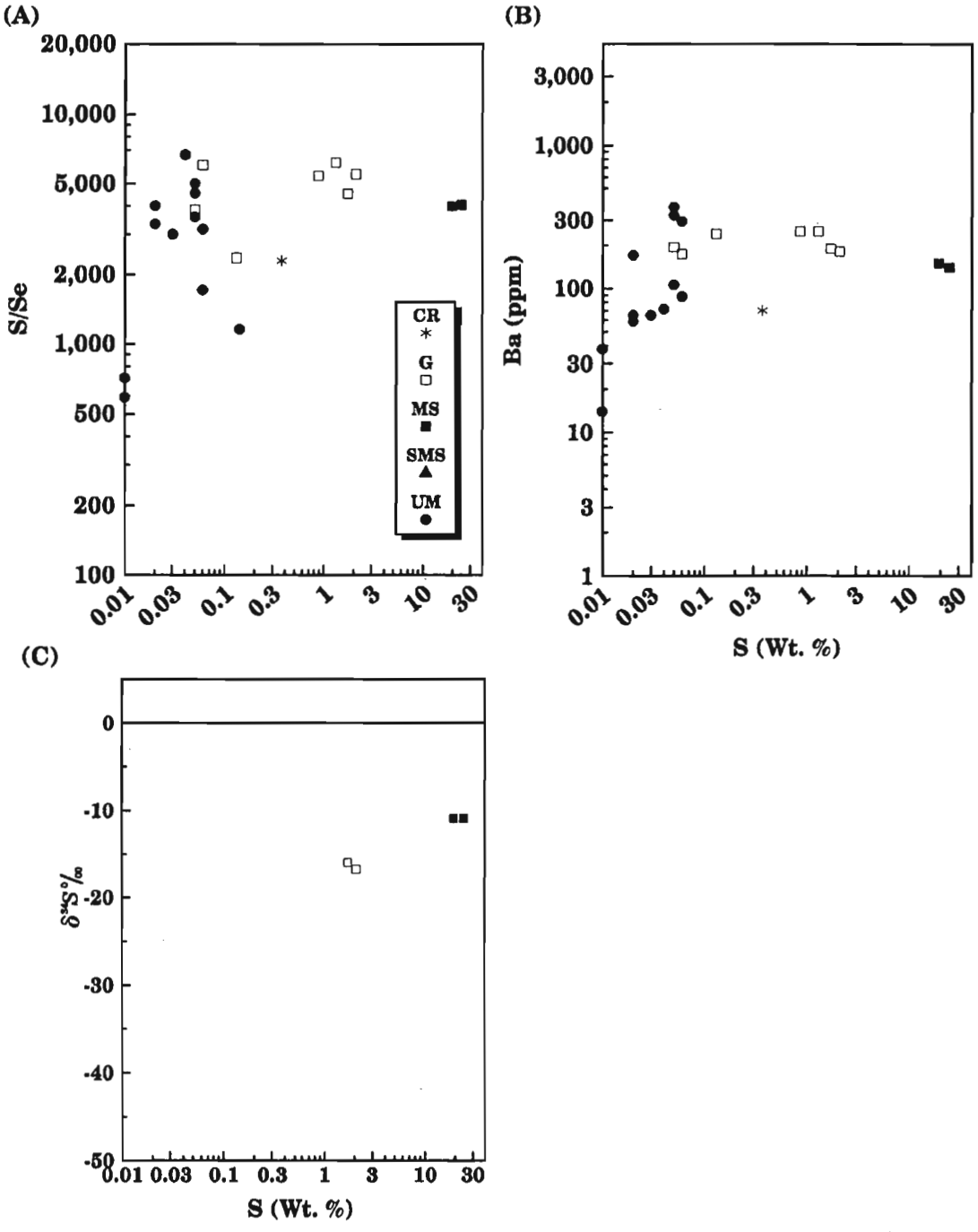

Figure 96 (A-C). *S/Se, Ba, $\delta^{34}S$‰ vs. S (wt.%) plots of elemental ratios, concentrations and isotopic compositions associated with ultramafic (UM), gabbroic (G), massive sulphide (MS), semi-massive sulphide (SMS), and country rock (CR) lithologies from the Onion property of the White River Intrusive Complex.*

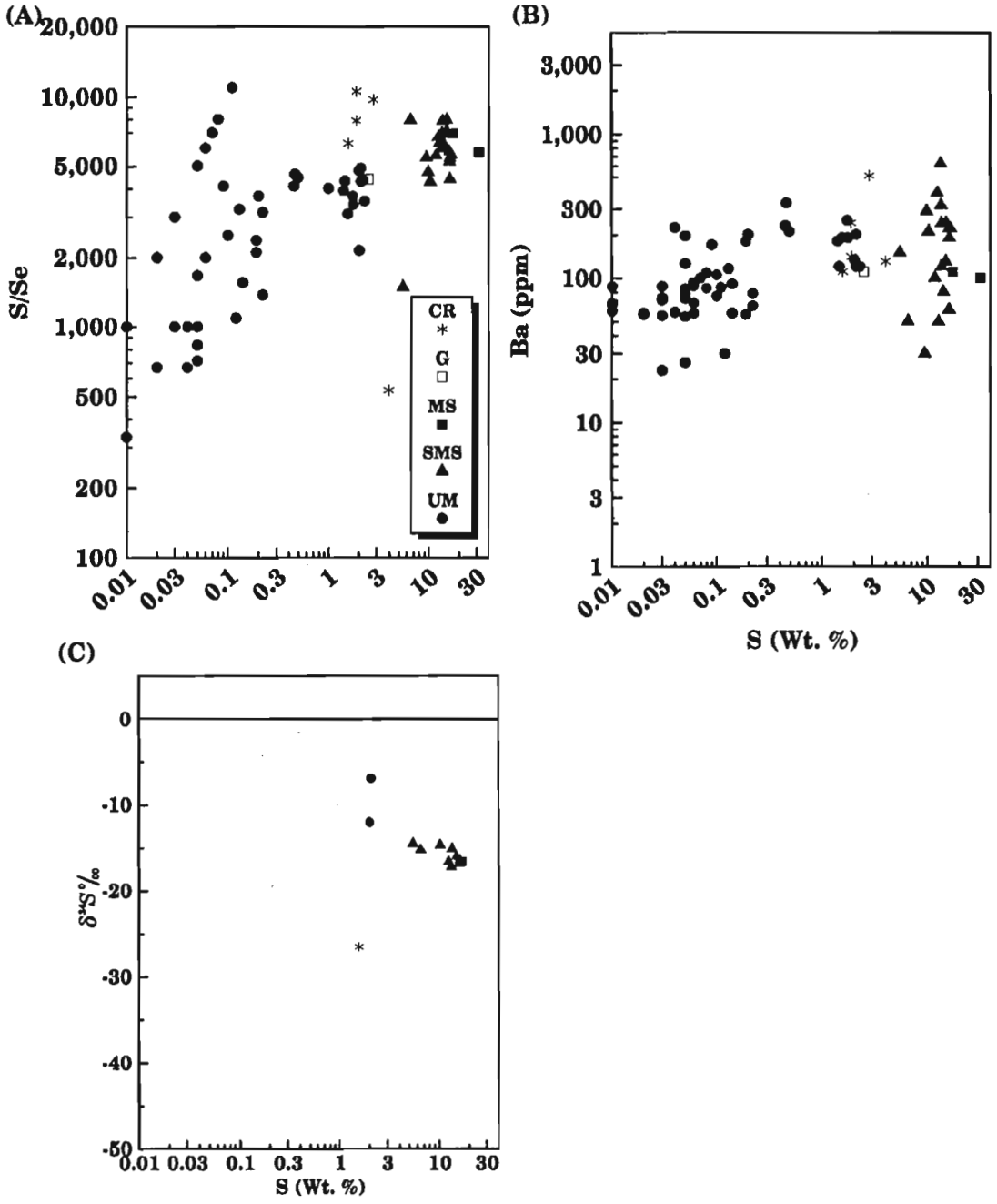

Figure 97 (A-C). S/Se, Ba, $\delta^{34}S$‰ vs. S (wt.%) plots of elemental ratios, concentrations and isotopic compositions associated with ultramafic (UM), gabbroic (G), massive sulphide (MS), semi-massive sulphide (SMS), and country rock (CR) lithologies from the Canalask property of the White River Intrusive Complex.

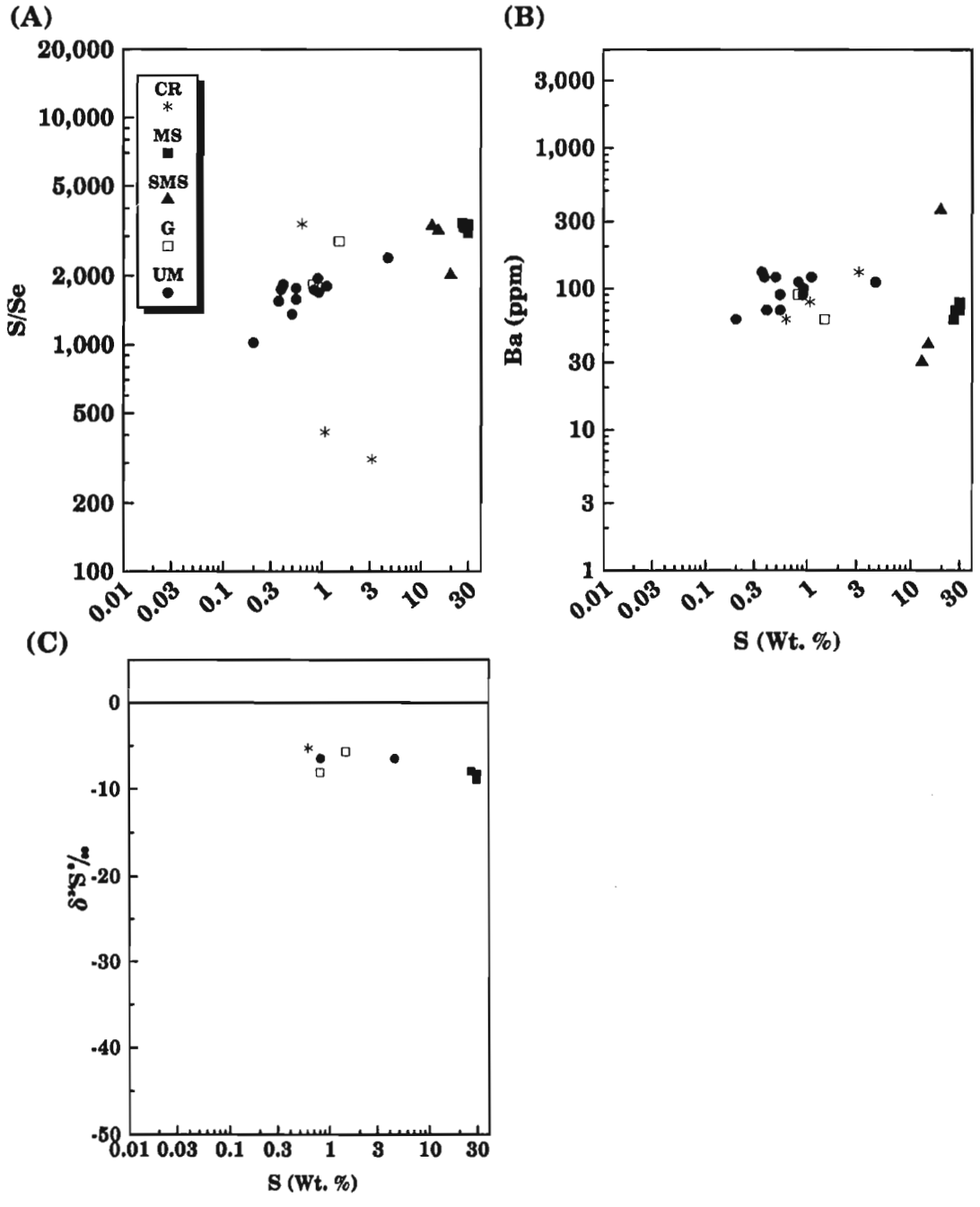

Figure 98 (A-C). *S/Se, Ba, $\delta^{34}S‰$ vs. S (wt.%) plots of elemental ratios, concentrations and isotopic compositions associated with ultramafic (UM), gabbroic (G), massive sulphide (MS), semi-massive sulphide (SMS), and country rock (CR) lithologies from the Arch Creek Intrusive Complex.*

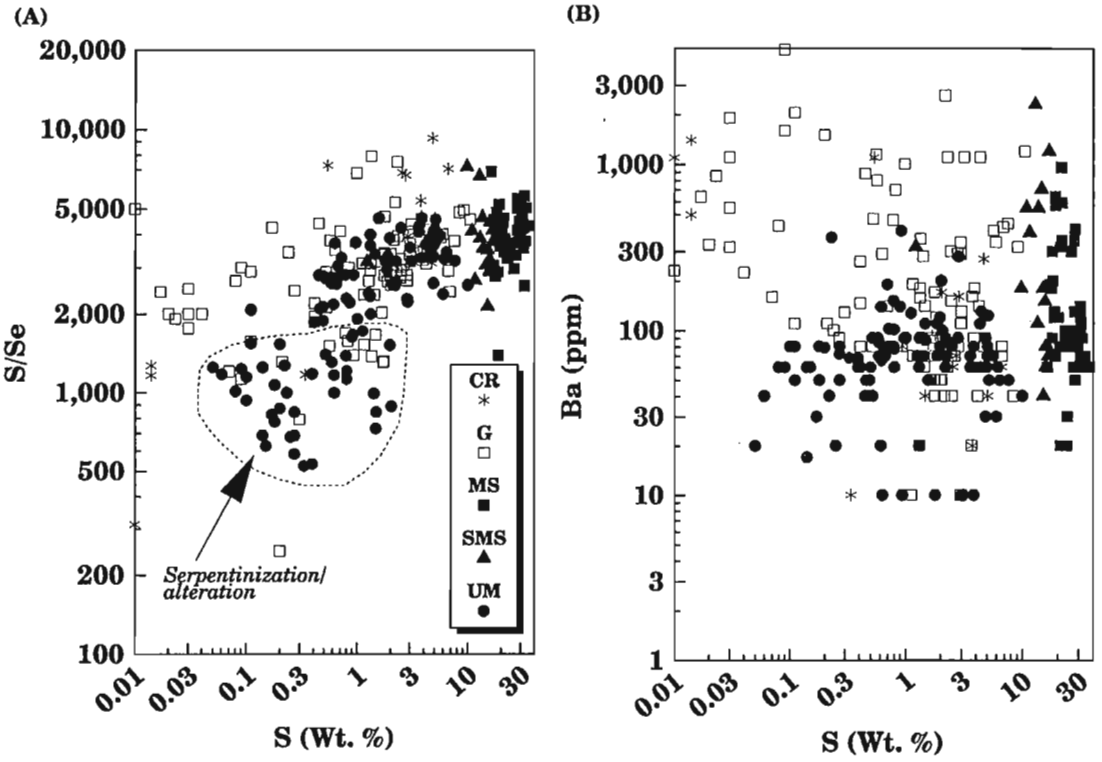

Figure 99 (A-B). *S/Se and Ba vs. S (wt.%) plots of elemental ratios, and concentrations associated with ultramafic (UM), gabbroic (G), massive sulphide (MS), semi-massive sulphide (SMS), and country rock (CR) lithologies from the Quill Creek Intrusive Complex.*

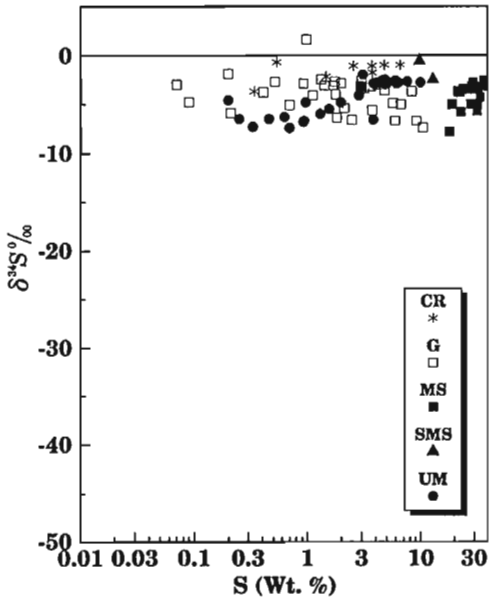

Figure 100.

$\delta^{34}S$‰ vs. S (wt.%) plots of isotopic compositions associated with ultramafic (UM), gabbroic (G), massive sulphide (MS), semi-massive sulphide (SMS), and country rock (CR) lithologies from the Quill Creek Intrusive Complex.

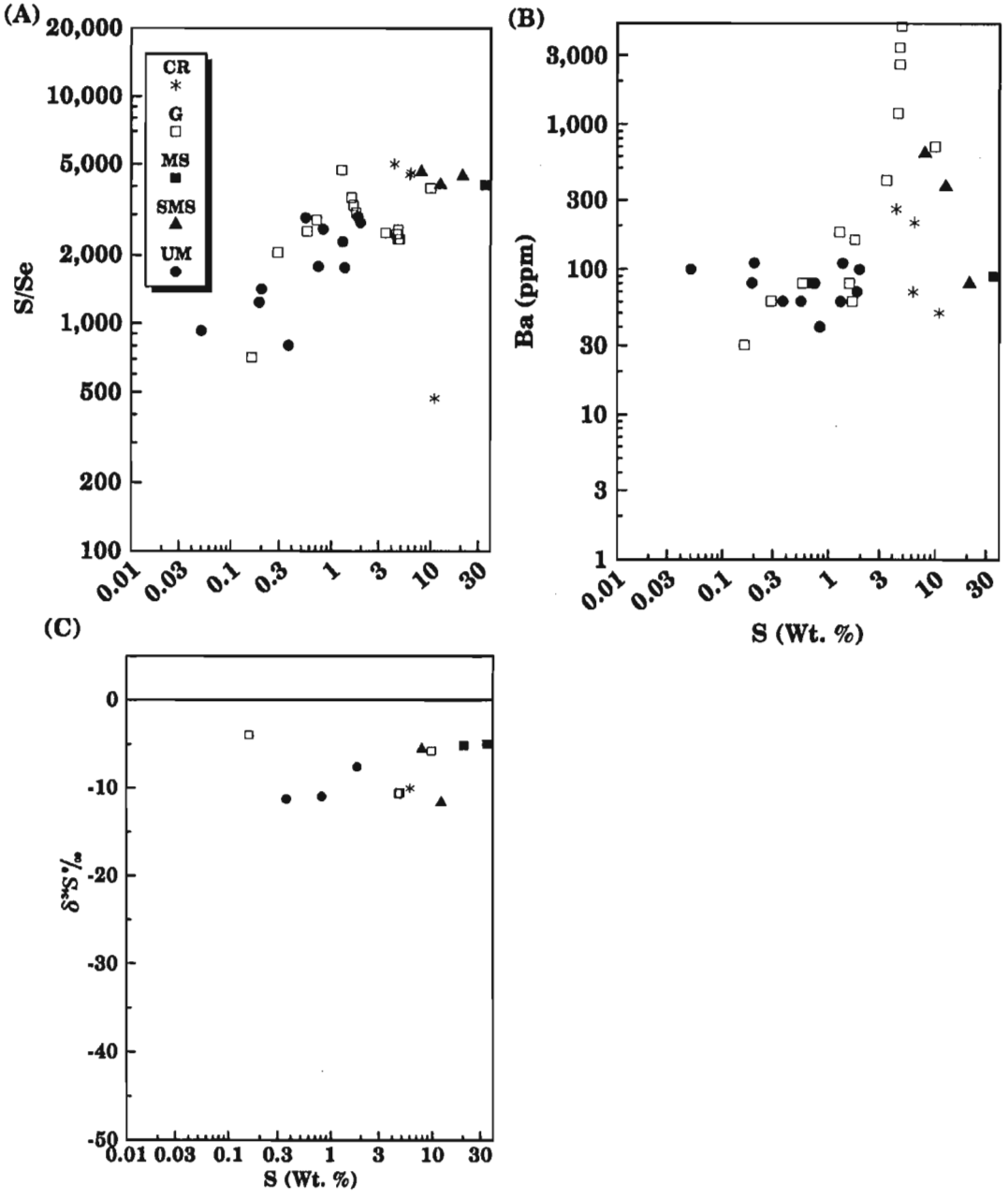

Figure 101 (A-C). *S/Se, Ba, $\delta^{34}S$‰ vs. S (wt.%) plots of elemental ratios, concentrations and isotopic compositions associated with ultramafic (UM), gabbroic (G), massive sulphide (MS), semi-massive sulphide (SMS), and country rock (CR) lithologies from the Linda Creek Intrusive Complex.*

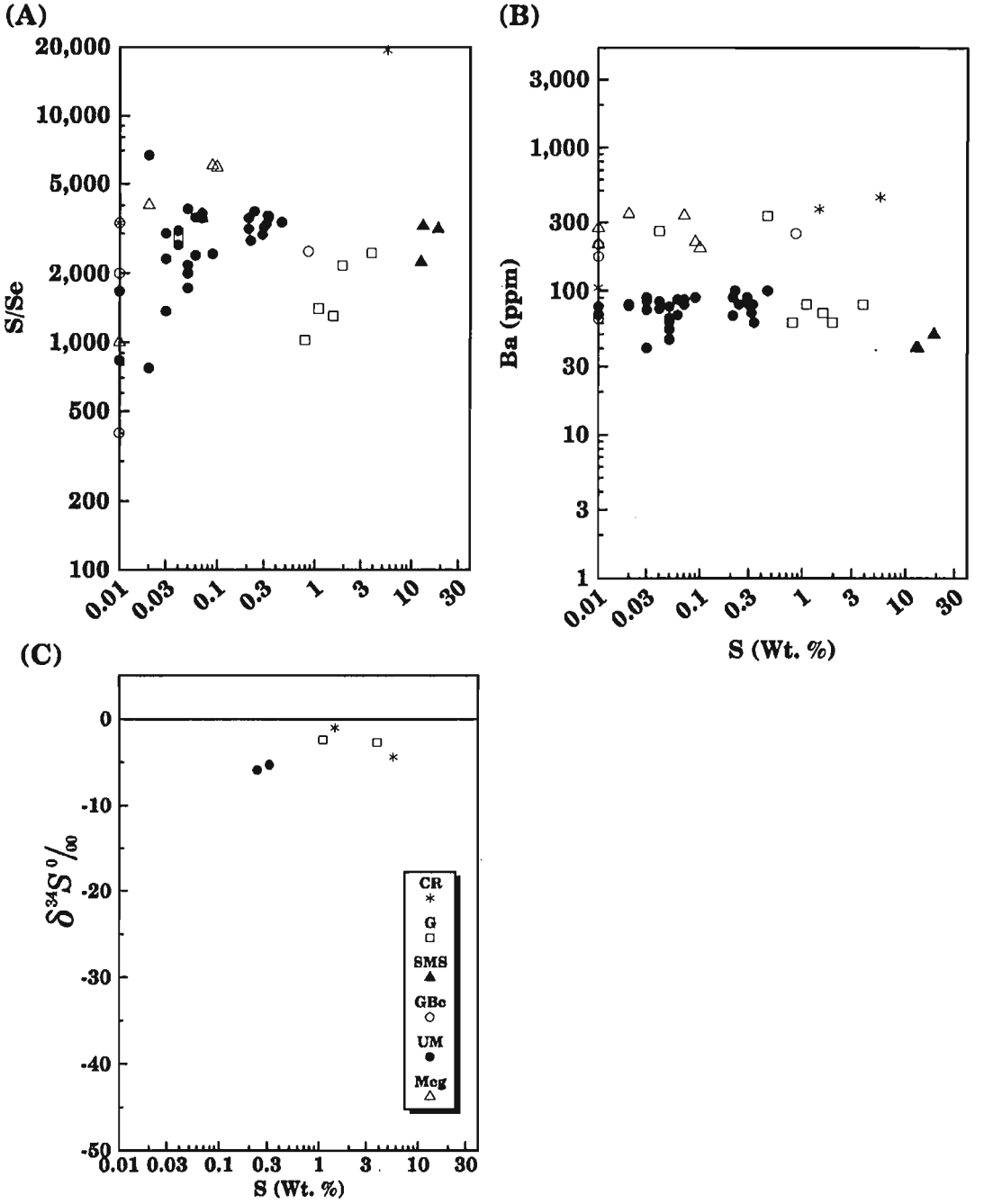

Figure 102 (A-C). S/Se, Ba, $\delta^{34}S‰$ vs. S (wt.%) plots of elemental ratios, concentrations and isotopic compositions associated with ultramafic (UM), gabbroic (G), basal gabbro (GBc), semi-massive sulphide (SMS), Maple Creek gabbro (Mcg), and country rock (CR) lithologies from the Tatamagouche Creek Intrusive Complex.

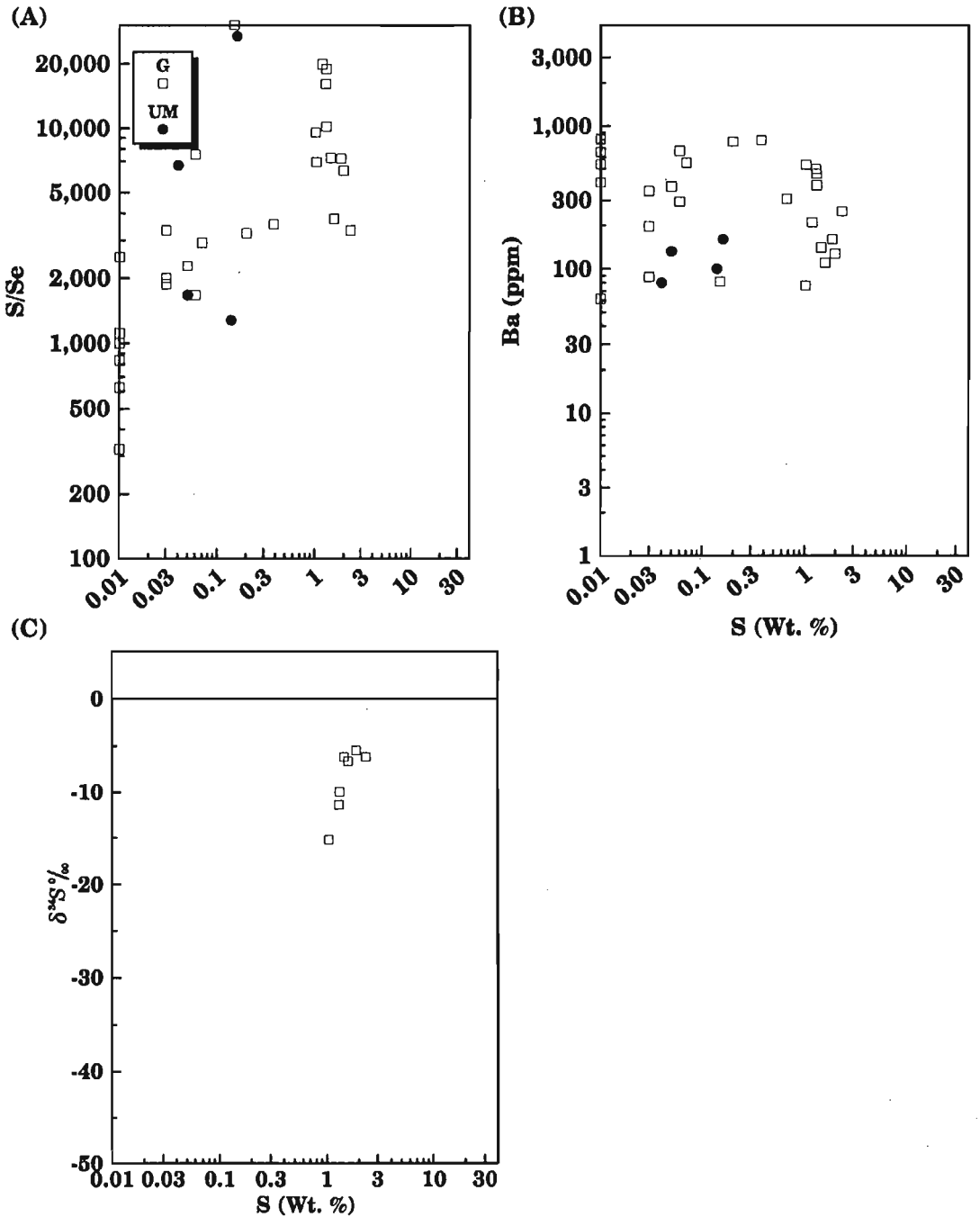

Figure 103 (A-C). *S/Se, Ba, $\delta^{34}S‰$ vs. S (wt.%) plots of elemental ratios, concentrations and isotopic compositions associated with ultramafic (UM) and gabbroic (G) lithologies from the Duke River Intrusive Complex.*

Coeval Triassic basalts from the Queen Charlotte Islands and Vancouver Island (Karmutsen basalt, n = 11, Barker et al., 1989) and the Chilkat Peninsula of Alaska (Nikolai basalt, n = 7, Davis and Plafker, 1985) have Ba concentrational ranges and means of 21 to 210, $\overline{X}$ = 81 ppm and 28 to 113, $\overline{X}$ = 80 ppm, respectively, in rocks with Mg# ranging from 0.51 to 0.63. The lowest Ba contents are in rocks with the highest Mg#. Consanguineous Nikolai basalt from the central portion of the Kluane Belt (Campbell, 1981) has Ba contents that varied from 12 to 192 ppm ($\overline{X}$ = 89 ppm, n = 8). Therefore it would appear that the Triassic mafic, ultramafic, and sulphide-rich lithologies within the Kluane Belt should have <210 ($\overline{X} \approx$ 85) ppm Ba if this element were purely of a mantle origin.

Inspection of Ba concentrations from the various complexes (Fig. 96B to 106B) demonstrates that ultramafic rocks contain as little as 10 or as high as 400 ppm Ba, but in general the samples concentrate in the 60 to 150 ppm range. In the Quill Creek Complex (Wellgreen) primary intercumulus Ba-feldspar has been identified in some of the ultramafic rocks. Gabbroic rocks demonstrate much wider ranges in Ba concentration (60-400 ppm) with many falling in the 200 to 2000 ppm range. As with the ultramafic rocks the Ba content is independent of S content. It is also interesting to note that some of the ultramafic rocks can contain more Ba than their gabbroic counterparts with equivalent sulphide (sulphur) contents. Gabbroic rocks from the Linda and Dickson Creek complexes indicate the origin of the anomalous Ba concentrations. In the Linda Complex the mineralized pegmatitic gabbro has Ba concentrations that range from about 1100 to 4000 ppm and $\delta^{34}S$ composition of -10.7‰. The association of high Ba concentrations with ^{32}S enriched sulphide mineralization, and the obvious macroscopic reaction features resulting from contamination of the magma by the Hasen Creek calcareous sediments imply that the country rock sediments have contributed Ba as well as S to the magmas. The mineralogical source of the Ba may originally have been sedimentary barite. A country rock source for the Ba-enrichment in the Dickson Creek gabbro is clearly illustrated in Figure 105B. Pegmatitic gabbro with 200-370 ppm Ba is associated with the least contaminated sulphides (-5.5 to -6.8‰), whereas similar gabbro with 1000 to 2000 ppm Ba is associated with sulphides having S isotope compositions of -28.4 to -29.9‰.

Ba contents associated with massive and semi-massive sulphide are also highly variable (i.e. Canalask (30-500 ppm), Arch (30-350 ppm), Quill Creek (30-2500 ppm), Linda (80-500 ppm), and Dickson Creek (50-800 ppm). Detailed mineralogical studies at Quill Creek showed that some of the Ba exists in a newly discovered Cu-Fe-Ba sulphide, whereas the remainder is associated with barite (Cabri et al., 1993). Both Cu-Fe-Ba sulphide and barite were also discovered in mineralized "West zone" chilled and pegmatitic gabbro. Typical low-grade gabbro and clinopyroxenite from the West zone and clinopyroxene-rich peridotite from the East zone all contain minor to trace amounts of barite. Variations are believed to be due to the contamination process (i.e. Hasen Creek Formation sediments with differing Ba concentrations and subsequent magma mixing constraints).

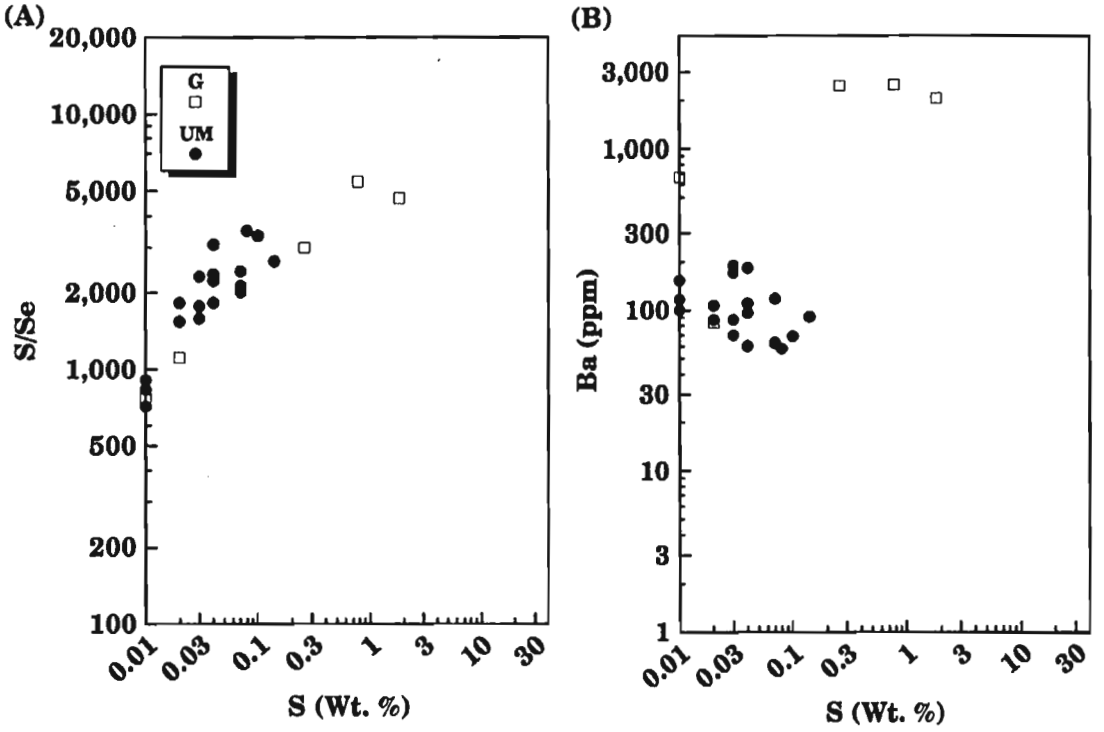

Figure 104 (A-B). *S/Se, Ba vs. S (wt.%) plots of elemental ratios, and concentrations and associated with ultramafic (UM) and gabbroic (G) lithologies from the Halfbreed Creek Intrusive Complex.*

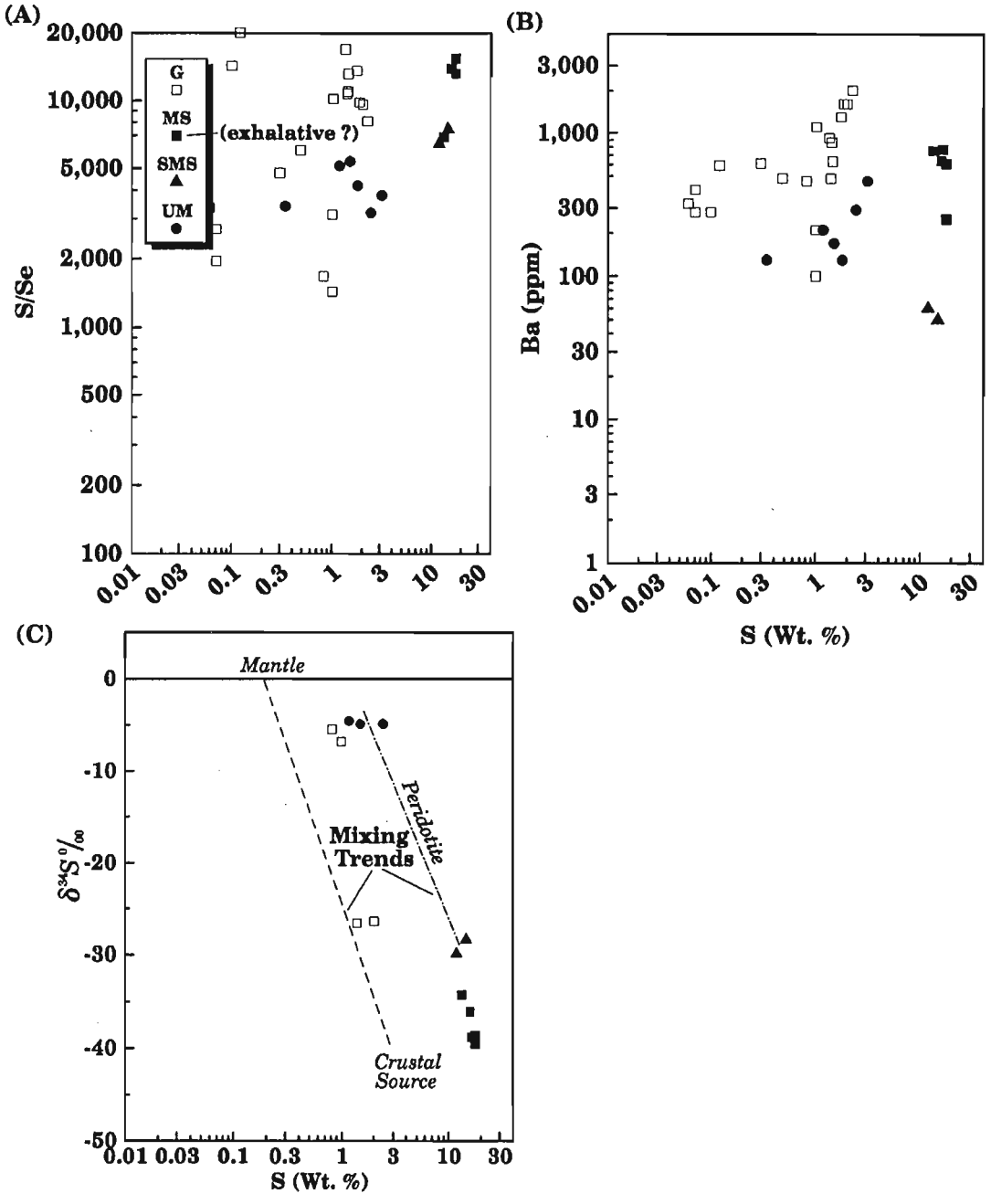

Figure 105 (A-C). *S/Se, Ba, $\delta^{34}S‰$ vs. S (wt.%) plots of elemental ratios, concentrations and isotopic compositions associated with ultramafic (UM), gabbroic (G), massive country rock (exhalative ?) sulphide (MS), and semi-massive sulphide (SMS) lithologies from the Dickson Creek Intrusive Complex.*

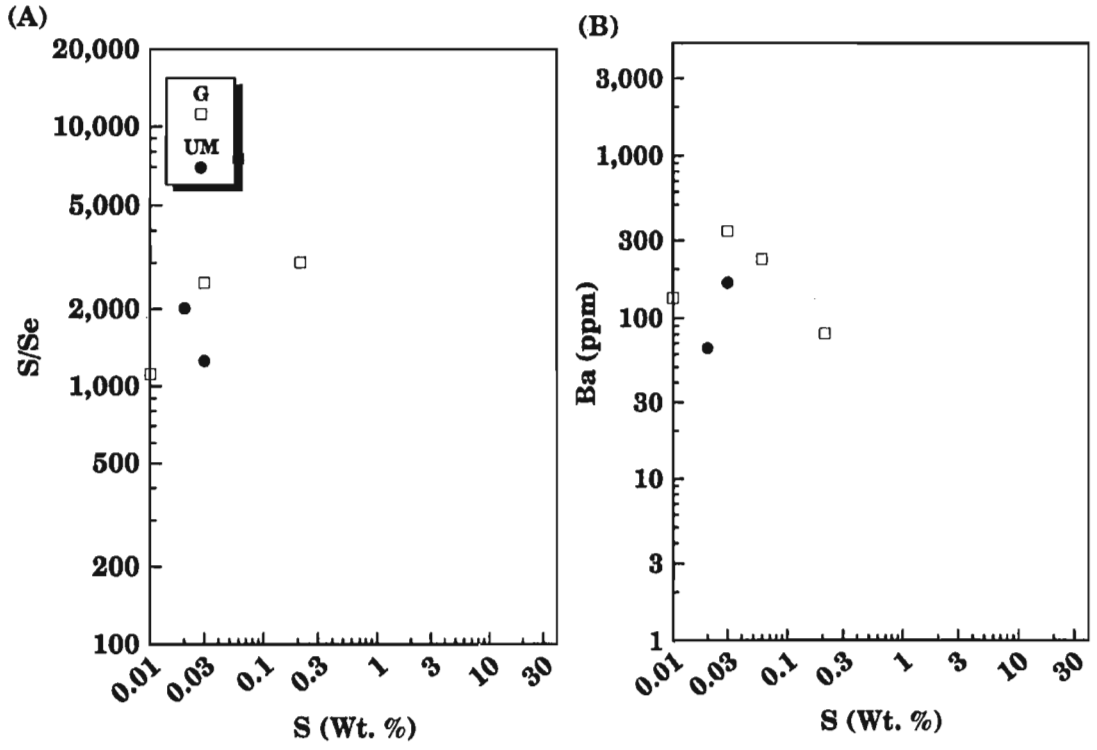

Figure 106 (A-B). *S/Se, Ba vs. S (wt.%) plots of elemental ratios and concentrations associated with ultramafic (UM) and gabbroic (G) lithologies from the Chilkat Intrusive Complex.*

From the above discussions it is apparent that the anomalous Ba levels (>210 ppm maximum) associated with many of the Kluane Belt gabbro, ultramafic and sulphide accumulations are the product of assimilation of Ba-rich sediments.

Platinum, palladium, gold, and rhodium

Platinum, palladium, gold, and rhodium within most Kluane mafic-ultramafic complexes display pronounced chalcophile trends (Fig. 107 to 118). However, at some localities this relationship does not hold (Canalask, Duke River, and Dickson Creek) and thus provides further evidence to support the magmatic contamination theory and its control on the grade of the associated mineralization.

Ultramafic rocks from the Kluane Belt display the best constrained chalcophile element trends. Not only are the ultramafic-hosted platinum and palladium values less dispersed than associated gabbro within a similar S concentrational interval, they also typically display parallel and higher Pt vs. S and Pd vs. S trends. The highest Pt and Pd values recorded in the ultramafic rocks (Quill Creek or Wellgreen) with disseminated sulphide mineralization (3.0% S) is 1700 and 1100 ppb, respectively. Some thin massive sulphide lenses within ultramafic rocks contain approximately 3000 ppb Pt and 1500 ppb Pd. Probably the most significant finding related to the Pt vs. S and Pd vs. S plots is that ultramafic samples with low (≤0.20 wt.%) S contents can be used to discriminate mineralized from non-mineralized intrusions. Figures 107A and B to 118A and B clearly demonstrate that unmineralized samples from the White River Complex (Onion, Canalask), Quill Creek Complex (Wellgreen), Arch and Linda Creek complexes and to a lesser extent the Tatamagouche Creek Complex (known to contain economically significant Ni-Cu sulphide accumulations) contain noticeably higher Pt and Pd concentrations than their counterparts from the apparently uneconomic Halfbreed Creek and Duke River complexes. Limited ultramafic material from the Chilkat Complex prevents such a comparison.

Due to the higher content of disseminated sulphides in some gabbroic rocks, this lithological group generally contains Pt and Pd concentrations spanning the interval between ultramafic and semi-massive to massive sulphides. Unlike ultramafic rocks which were accessible at each complex, the absence of gabbroic rocks at some localities does not allow similar mineral potential discriminations. The highest Pt and Pd concentrations occur in the 3 to 10 wt.% S range. High values of 1000 to 1300 ppb each for Pt and Pd are not uncommon within this S interval at Wellgreen (Quill Creek Complex) where the gabbroic rocks have been most throughly studied. The Pt- and Pd-depleted nature of gabbroic and ultramafic rocks from the Dickson Creek Complex and their enrichment relative to decreasing ^{32}S isotopic compositions demonstrate the role and mechanics of the magma mixing process on the precious metal grade of the associated sulphides. Pt and Pd concentrations for the country rock samples can be highly variable (≤2 to 2500 ppb) due to the diverse nature of this mineralization. Country rocks with high PGE values clearly reflect mobilization of these elements into the adjacent sediments.

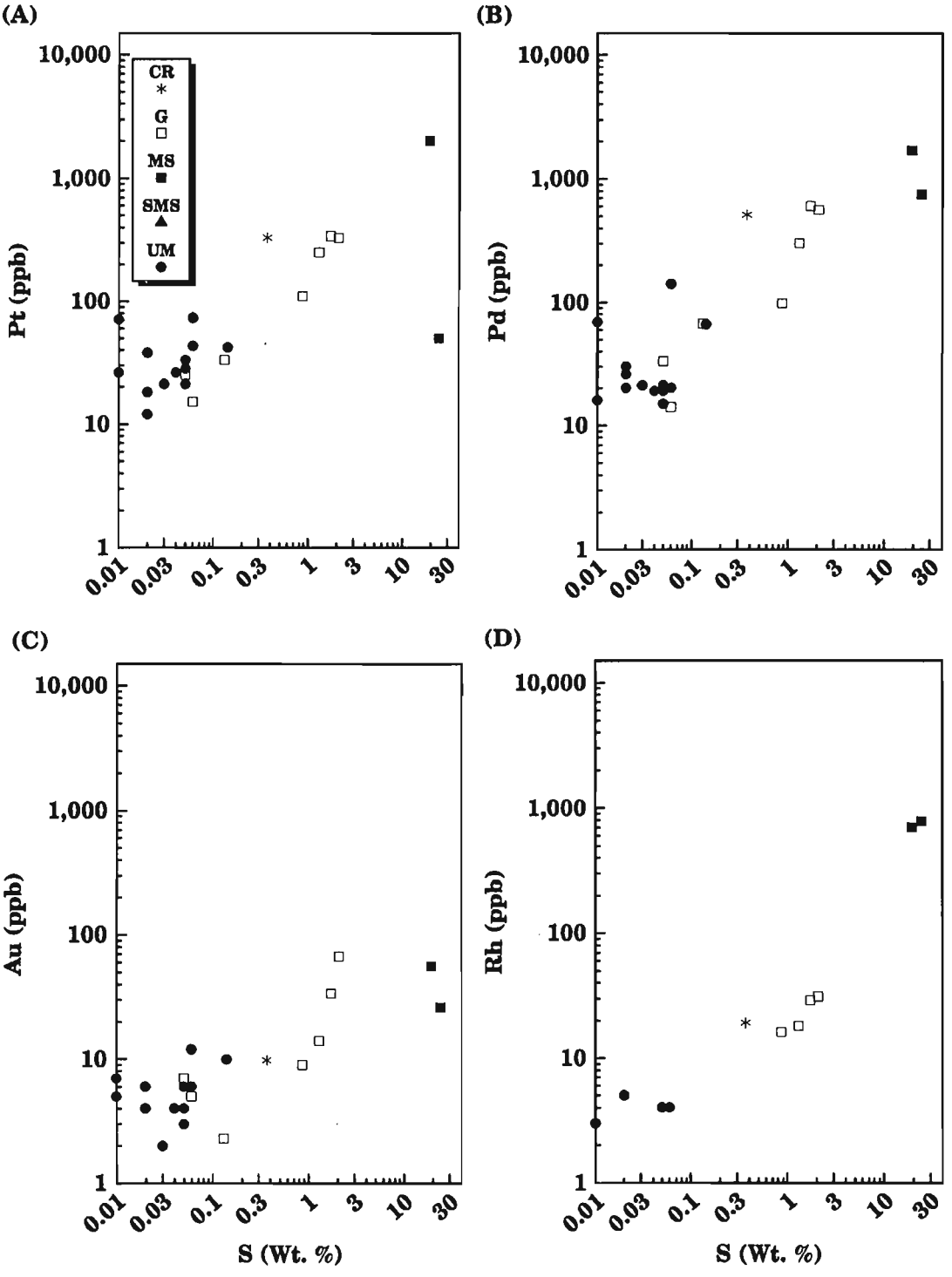

Figure 107 (A-D). *Pt, Pd, Au, Rh vs. S (wt.%) plots of elemental concentrations associated with ultramafic (UM), gabbroic (G), massive sulphide (MS), semi-massive sulphide (SMS), and country rock (CR) lithologies from the Onion property of the White River Intrusive Complex.*

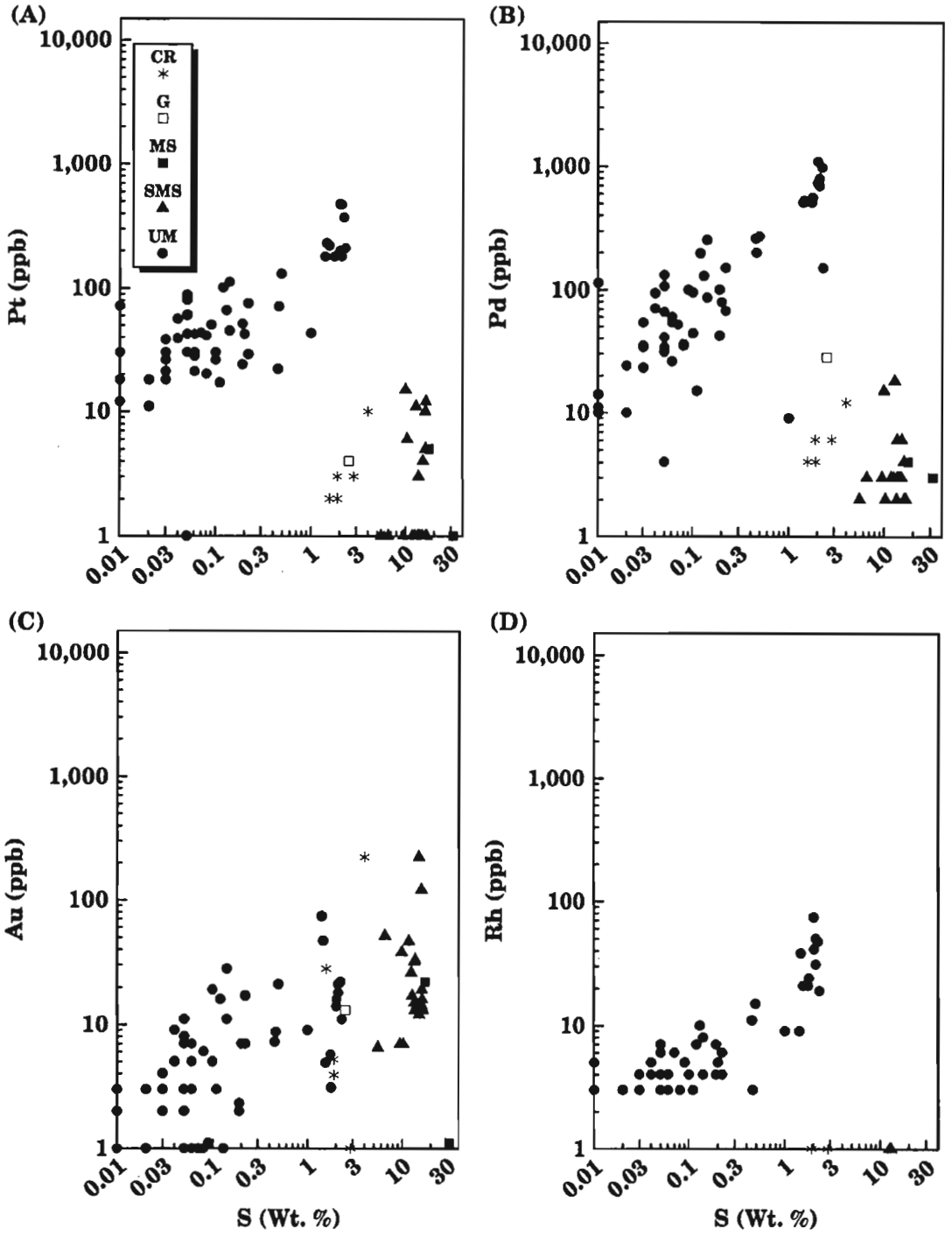

Figure 108 (A-D). *Pt, Pd, Au, Rh vs. S (wt.%) plots of elemental concentrations associated with ultramafic (UM), gabbroic (G), massive sulphide (MS), semi-massive sulphide (SMS), and country rock (CR) lithologies from the Canalask property of the White River Intrusive Complex. Values plotting along the base of the diagram represent concentrations at the detection limit of the analytical method.*

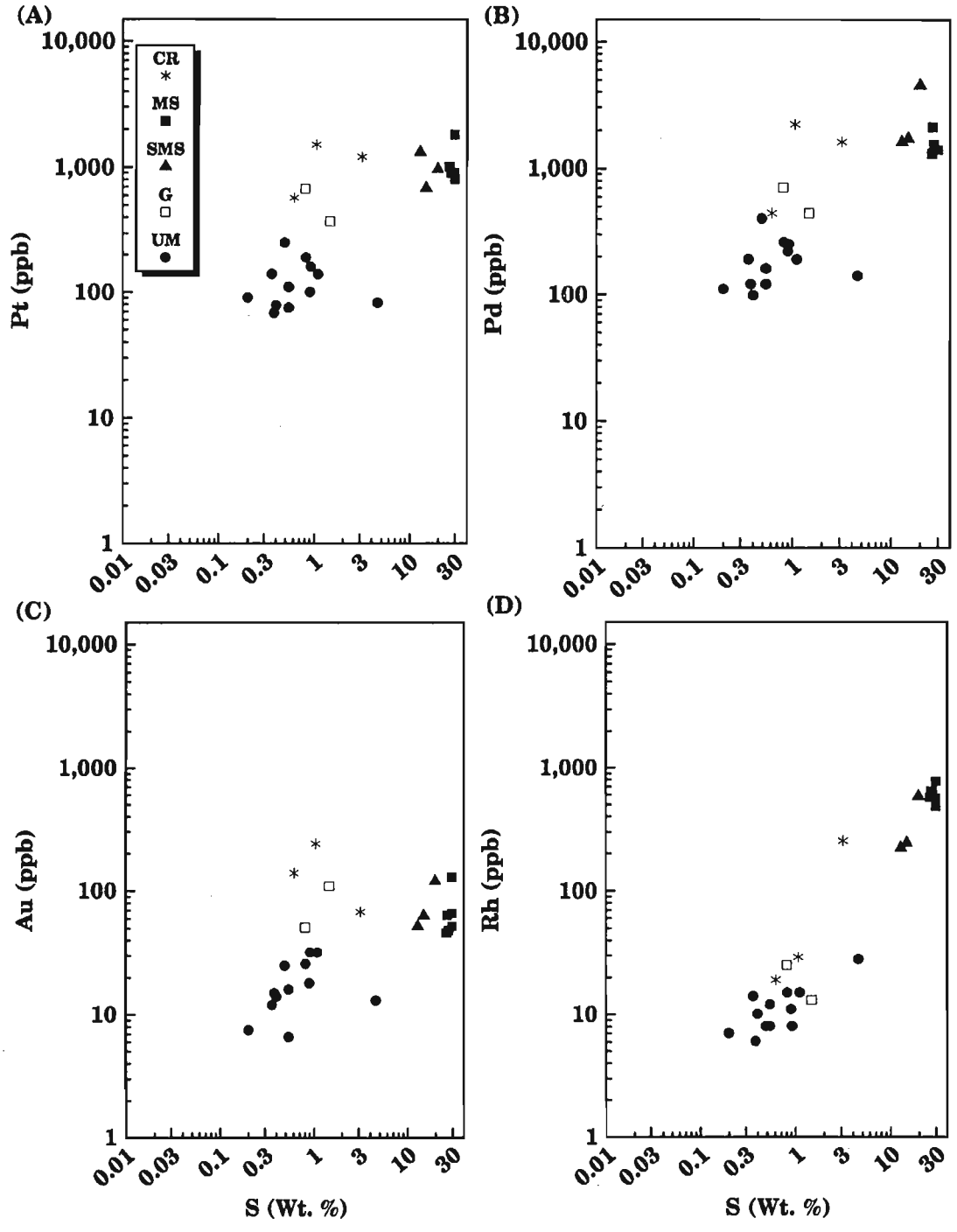

Figure 109 (A-D). Pt, Pd, Au, Rh vs. S (wt.%) plots of elemental concentrations associated with ultramafic (UM), gabbroic (G), massive sulphide (MS), semi-massive sulphide (SMS), and country rock (CR) lithologies from the Arch Creek Intrusive Complex.

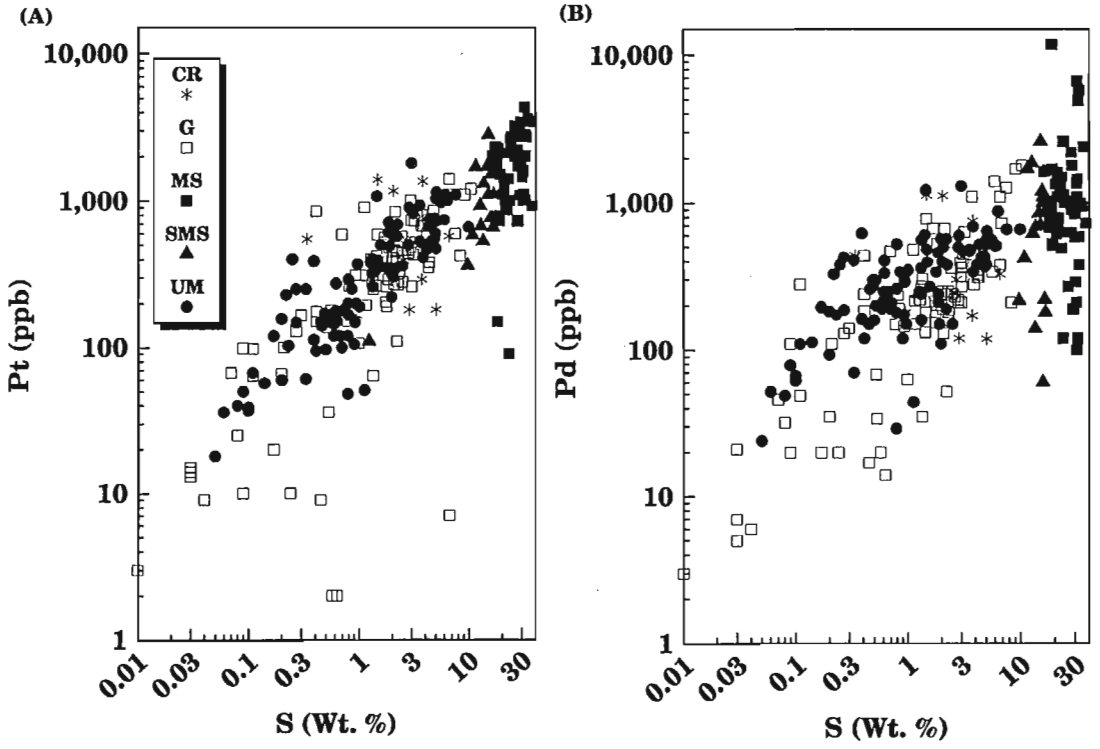

Figure 110 (A-B). *Pt, Pd vs. S (wt.%) plots of elemental concentrations associated with ultramafic (UM), gabbroic (G), massive sulphide (MS), semi-massive sulphide (SMS), and country rock (CR) lithologies from the Quill Creek Intrusive Complex.*

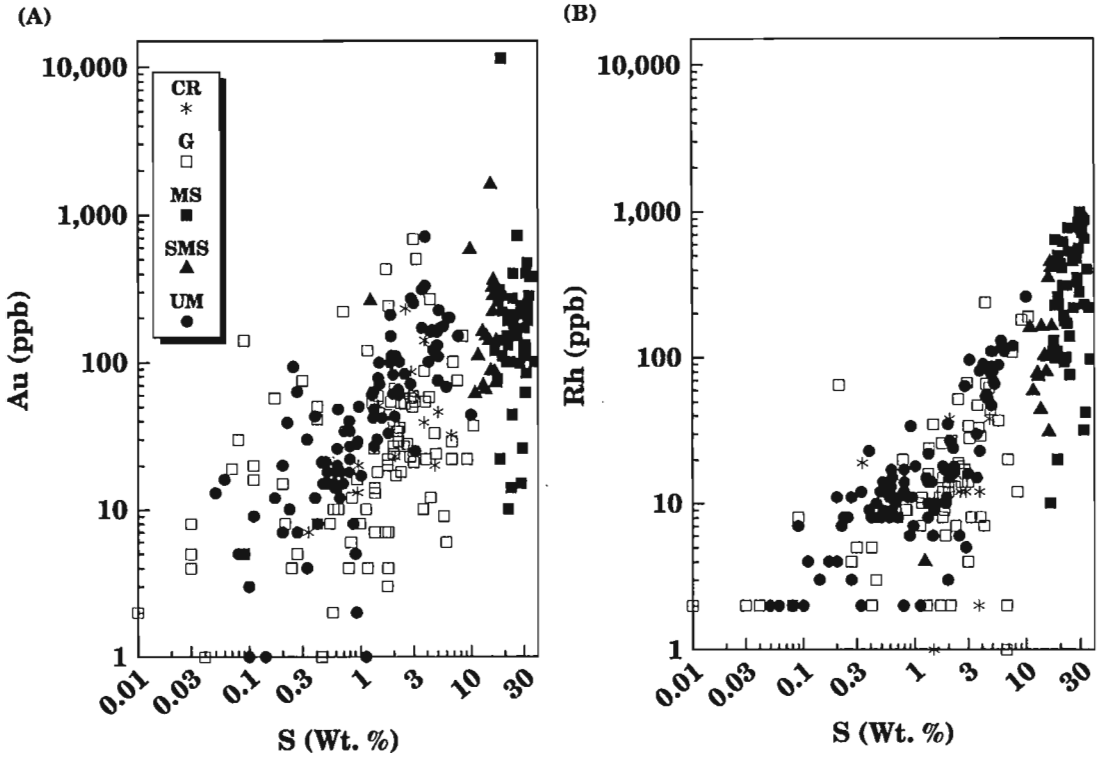

Figure 111 (A-B). *Au, Rh vs. S (wt.%) plots of elemental concentrations associated with ultramafic (UM), gabbroic (G), massive sulphide (MS), semi-massive sulphide (SMS), and country rock (CR) lithologies from the Quill Creek Intrusive Complex. Values plotting along the base of the diagram represent concentrations at the detection limit of the analytical method.*

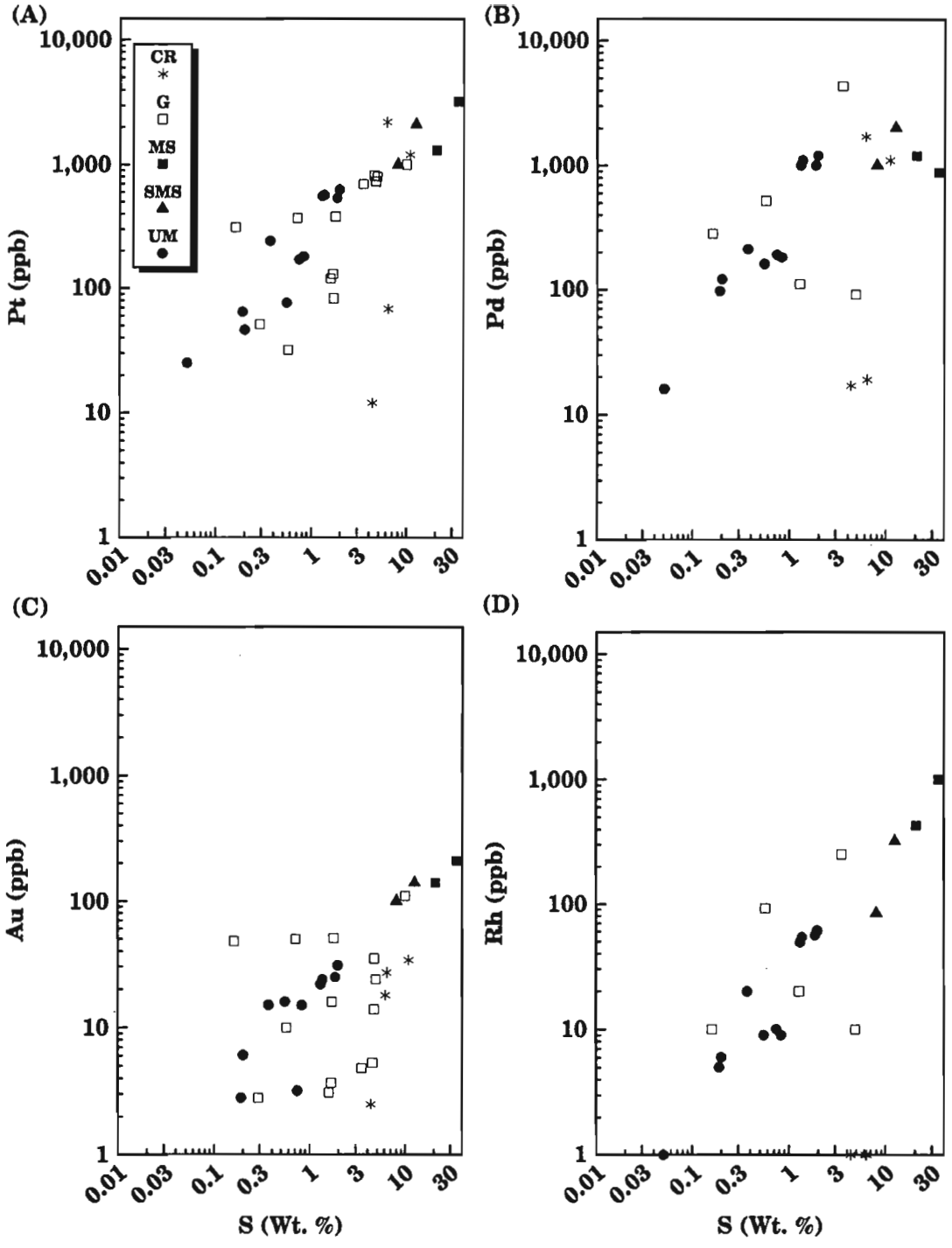

Figure 112 (A-D). *Pt, Pd, Au, Rh vs. S (wt.%) plots of elemental concentrations associated with ultramafic (UM), gabbroic (G), massive sulphide (MS), semi-massive sulphide (SMS), and country rock (CR) lithologies from the Linda Creek Intrusive Complex. Values plotting along the base of the diagram represent concentrations at the detection limit of the analytical method.*

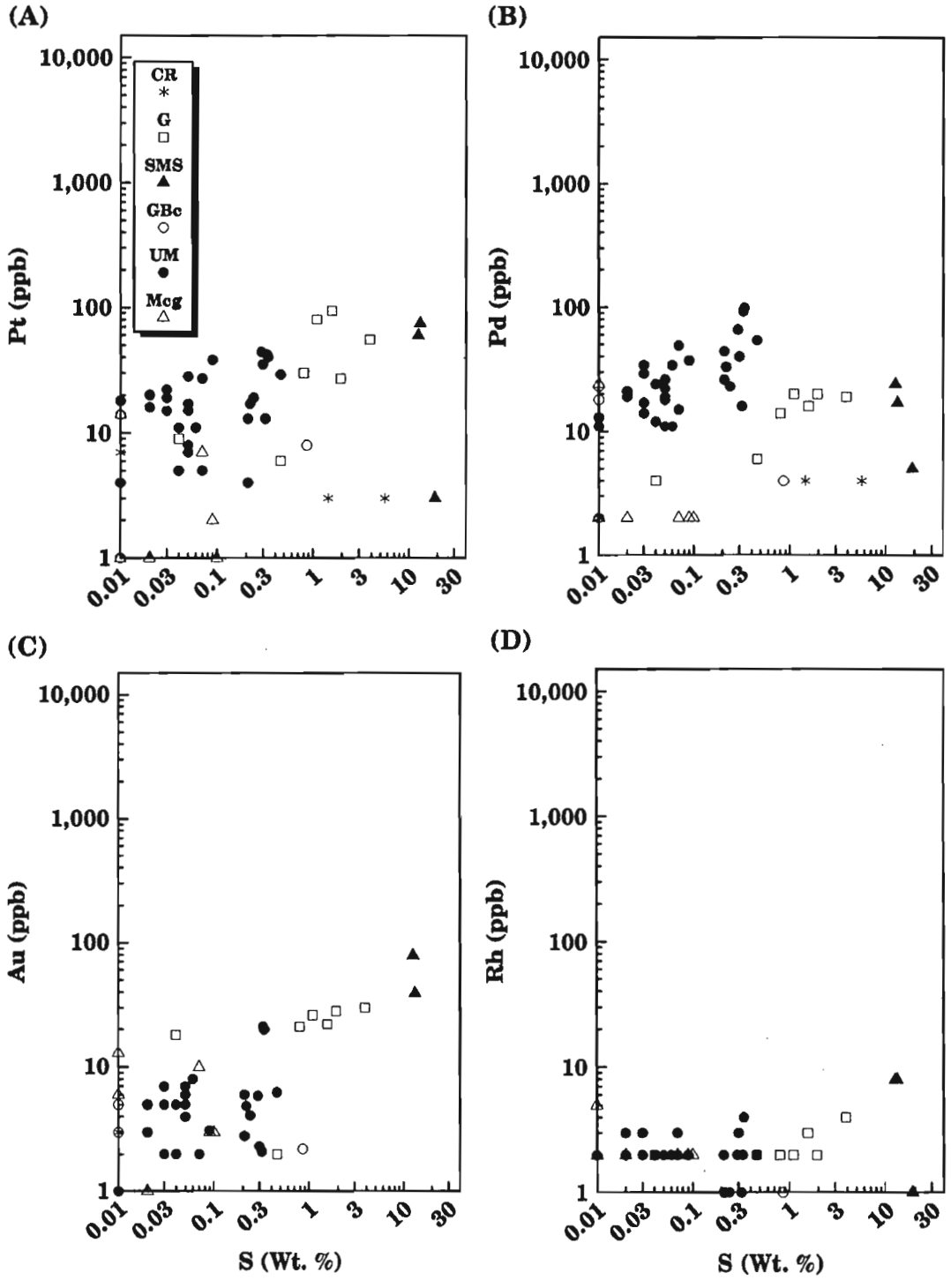

Figure 113 (A-D). Pt, Pd, Au, Rh vs. S (wt.%) plots of elemental concentrations associated with ultramafic (UM), gabbroic (G), semi-massive sulphide (SMS), basal gabbro (GBc), Maple Creek gabbro (Mcg), and country rock (CR) lithologies from the Tatamagouche Creek Intrusive Complex. Values plotting along the base of the diagram represent concentrations at the detection limit of the analytical method.

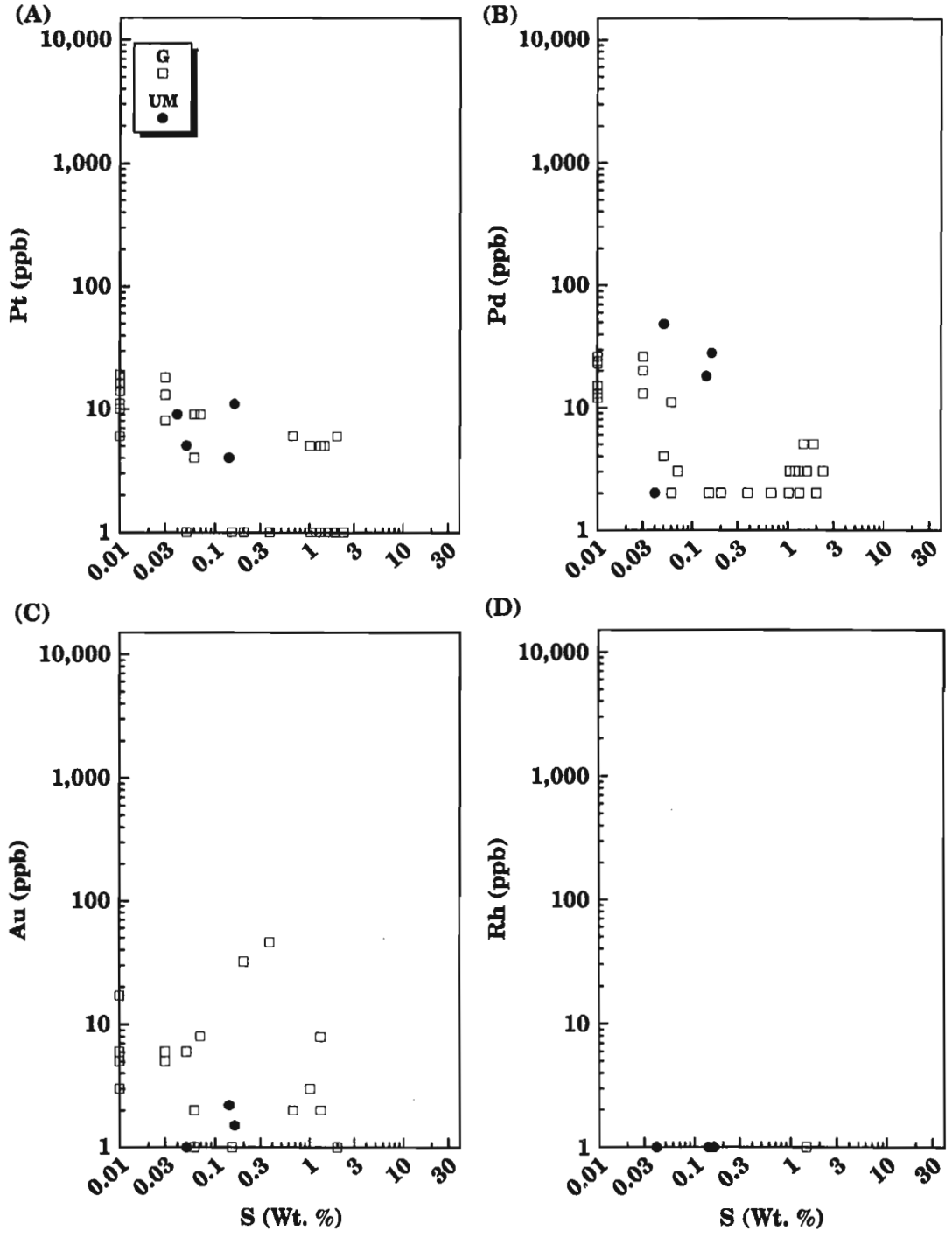

Figure 114 (A-D). *Pt, Pd, Au, Rh vs. S (wt.%) plots of elemental concentrations associated with ultramafic (UM) and gabbroic (G) lithologies from the Duke River Intrusive Complex. Values plotting along the base of the diagram represent concentrations at the detection limit of the analytical method.*

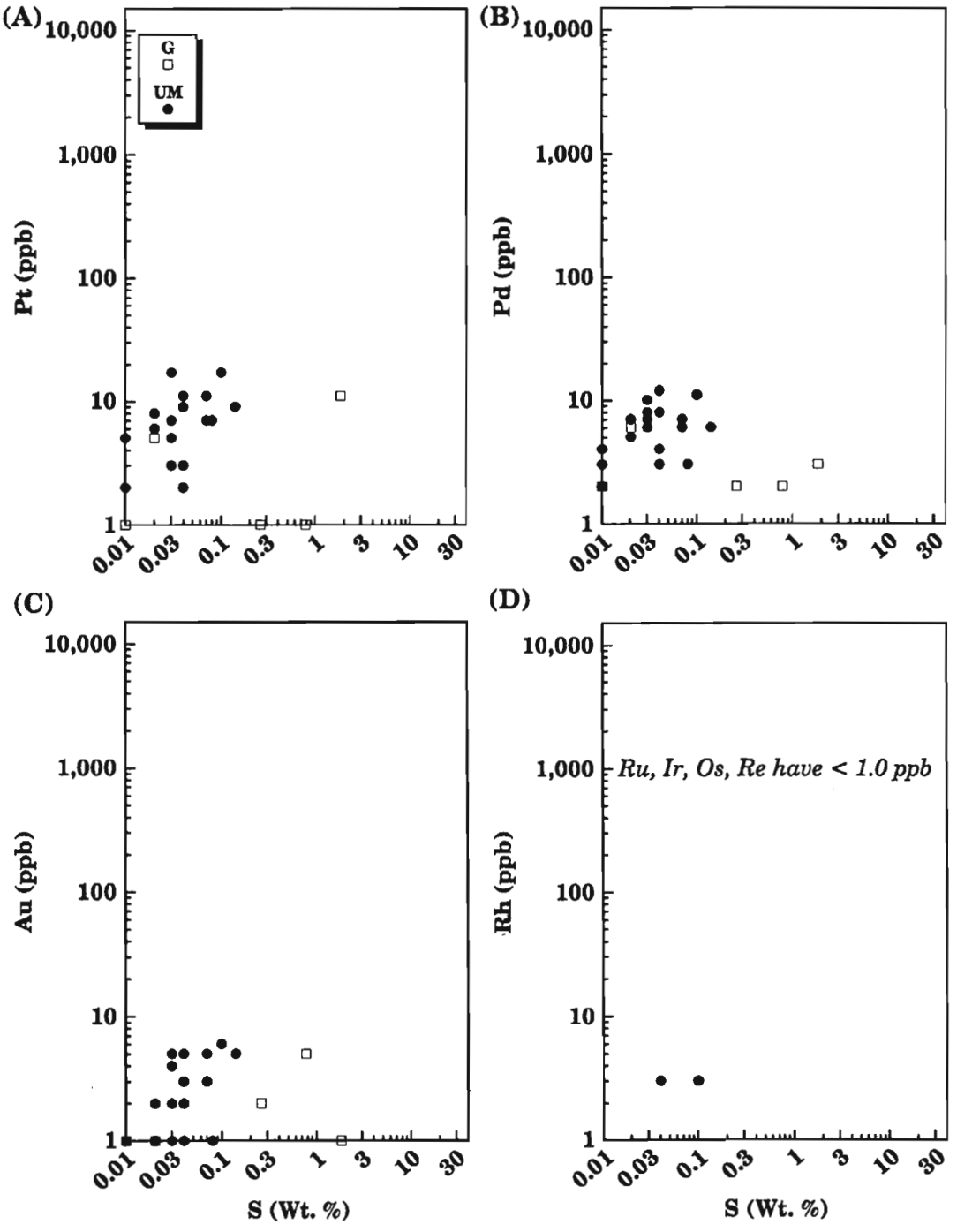

Figure 115 (A-D). *Pt, Pd, Au, Rh vs. S (wt.%) plots of elemental concentrations associated with ultramafic (UM) and gabbroic (G) lithologies from the Halfbreed Creek Intrusive Complex. Values plotting along the base of the diagram represent concentrations at the detection limit of the analytical method.*

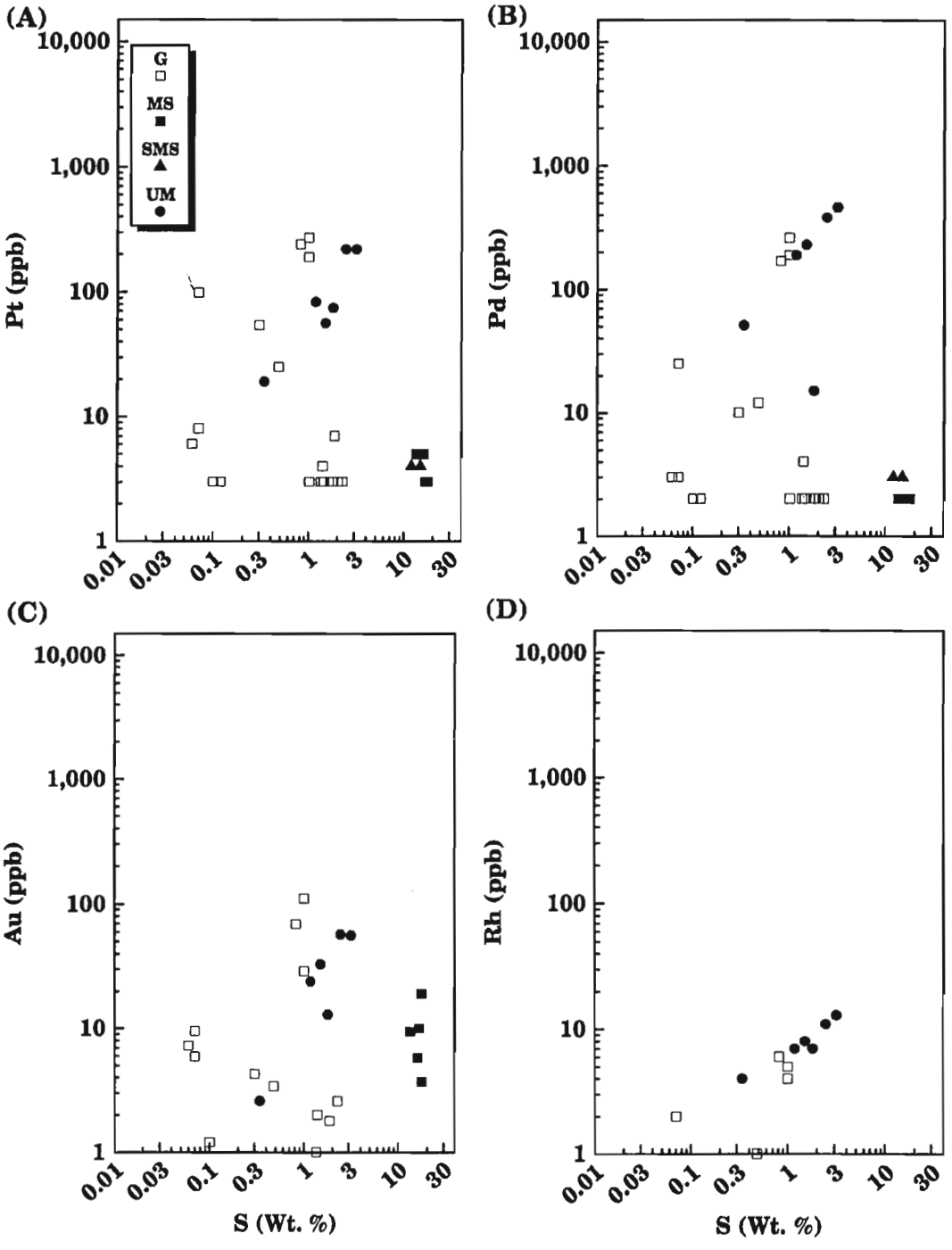

Figure 116 (A-D). *Pt, Pd, Au, Rh vs. S (wt.%) plots of elemental concentrations associated with ultramafic (UM), gabbroic (G), massive country rock (exhalative ?) sulphide (MS), and semi-massive sulphide (SMS) lithologies from the Dickson Creek Intrusive Complex. Values plotting along the base of the diagram represent concentrations at the detection limit of the analytical method.*

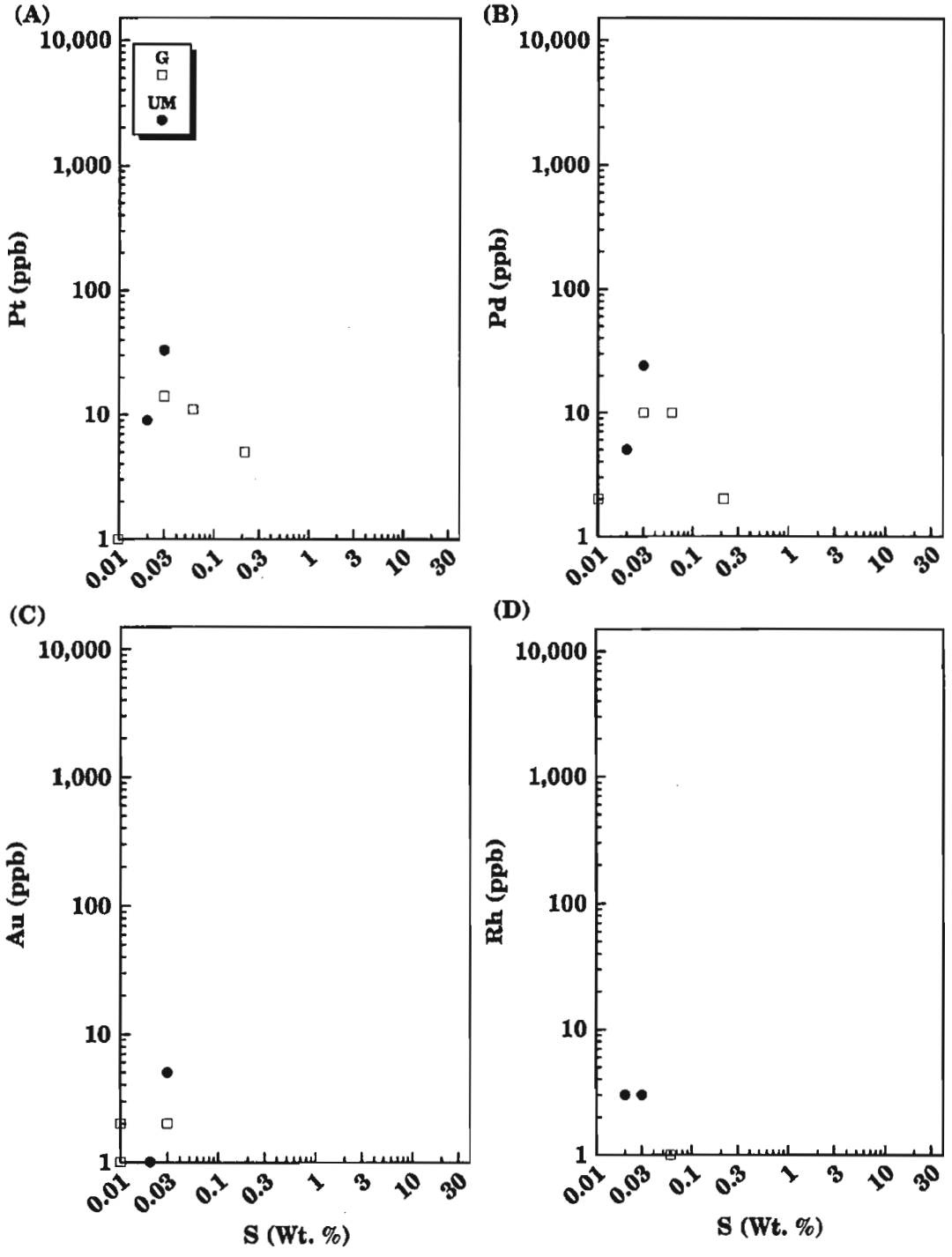

Figure 117 (A-D). Pt, Pd, Au, Rh vs. S (wt.%) plots of elemental concentrations associated with ultramafic (UM) and gabbroic (G) lithologies from the Chilkat Intrusive Complex. Values plotting along the base of the diagram represent concentrations at the detection limit of the analytical method.

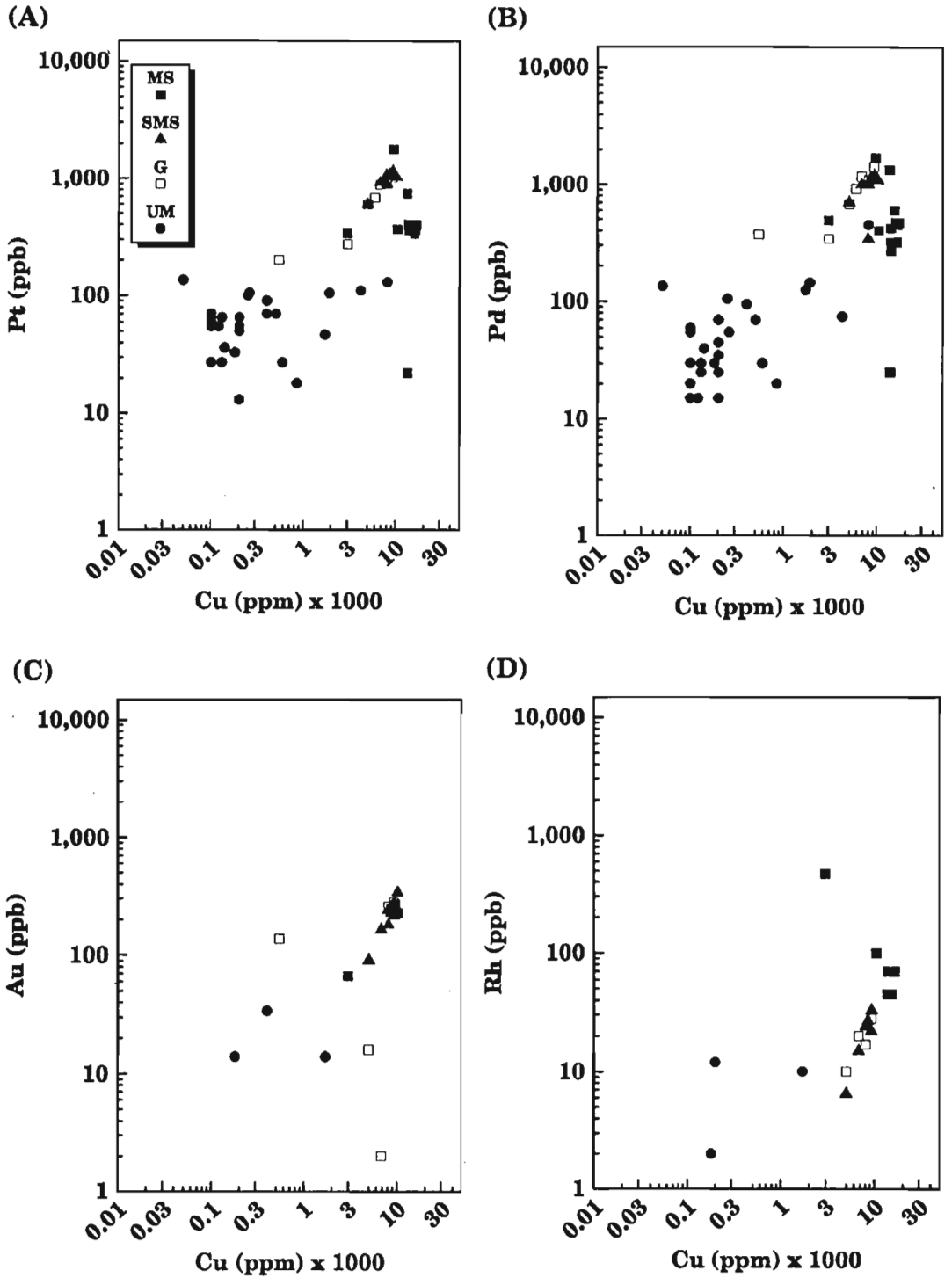

Figure 118 (A-D). *Pt, Pd, Au, Rh vs. Cu (ppm) plots of elemental concentrations associated with ultramafic (UM), gabbroic (G), massive sulphide (MS), and semi-massive sulphide (SMS) lithologies from the Rainbow Mountain Intrusive Complex, Alaska.*

Massive and semi-massive sulphides from the Kluane Belt display the greatest degree of variability. Unmodified magmatic sulphide accumulations generally have Pt and Pd concentrations in the 1000 to 3000 ppb range, but values as high as 5000 and 10000 ppb have been recorded for Pt and Pd at the Arch and Wellgreen properties, respectively (Fig. 109, 110). High Pt grades tend to be associated with the very Ni-rich samples, whereas high Pd can be associated with Ni-rich and/or Cu-rich samples. In the Quill Creek Complex (Wellgreen) Pt tends to display less spread, and a more coherent trend, with respect to the other magmatic lithologies, than Pd, regardless of its massive or semi-massive character. This may represent varying degrees of mobility as the samples with anomalously low concentrations represent remobilized sulphide concentrations. These low values are still approximately an order of magnitude higher than those from the Canalask deposit, and almost two orders of magnitude greater than those from Dickson Creek. Impoverishment of Pt and Pd is congruent with other magmatic element depletions noted previously for these occurrences, and are also believed to be a consequence of contamination and magma mixing processes.

Gold (Fig. 107C to 118C) also displays a chalcophile character in the Kluane magmatic mineralization, but this trend is somewhat more diffuse than that for Pt and Pd. Where comparisons can be made ultramafic rocks generally contain more Au than gabbroic rocks with similar S content. In the massive and semi-massive sulphide concentrations there appears to be an inverse relation between the Ni/Cu ratio and the Au content.

Rhodium also demonstrates a chalcophile geochemical affinity within the Kluane Belt (Fig. 108D to 118D). In fact, high Rh (as well as Os, Ir, Ru, and Re) content of typical Kluane Ni-Cu sulphide mineralization is one of the diagnostic features of sulphide mineralization from this belt. There appears to be less spread in the Rh vs. S trend associated with ultramafic than with gabbroic rocks, although the former tends to have slightly higher overall Rh concentrations for rocks of equivalent S content. Concentrations of Rh up to 1000 ppb at the Wellgreen, Arch, and Linda properties are not uncommon; however, similar lithologies at Canalask and Dickson Creek show marked depletion in this element (<1 ppb), and the impoverishment is again attributed to contamination and magma mixing processes.

Ruthenium, iridium, osmium, and rhenium

Ruthenium, iridium, and osmium (Fig. 119 to 128) also demonstrate a moderate to strong chalcophile geochemical character similar to that of Pt, Pd, Au, and Rh; therefore, discussions of these trends are not repeated here. Inspection of the Ru, Ir, Os, Re vs. S plots demonstrate that ultramafic rocks generally have higher levels of these PGEs and Re, at similar S contents than associated gabbroic rocks. The most remarkable feature pertaining to these elements is the exceptionally high absolute concentrations associated with the massive and semi-massive sulphide samples. Ru, Ir, and Os contents in the 500 to 2000 ppb range are not uncommon at Onion, Arch, Linda, and Wellgreen properties. Compared to other Ni and Ni-Cu ores, typical Kluane massive and semi-massive sulphide accumulations are exceptionally rich in these rarer PGEs. Nevertheless, at some localities in the belt similar mineralization can be exceptionally depleted in these elements (Canalask and Dickson Creek massive and semi-massive sulphides have concentrations less than 1.0 ppb). As these PGEs are generally regarded as mantle-derived magmatophile elements it is inferred that the Ru, Ir, and Os impoverished mineralization from Canalask and Dickson Creek is a consequence of localized sulphide immiscibility and limited magma mixing resulting from proximal crustal contamination. The restrictive nature of this sulphide generating process would limit the ability of the segregated sulphides to mix with a significant volume of silicate magma from which to expropriate these elements, thus accounting for the exceptionally low grades associated with this mineralization.

Rhenium is present in anomalous concentrations in all massive and semi-massive sulphide occurrences in the Kluane Belt. Experience with Ni, Ni-Cu deposits and occurrences elsewhere in Canada and abroad has shown that this element is seldom present in concentrations exceeding the lower limit of detection (3.0 ppb) of the analytical method Instrumental Neutron Activation Analyses – Nickel Sulphide (INAA-NiS) used to measure the concentration of this element. Re concentrations (ppb) fall within the following range with a high proportion of the samples occurring near the upper end of the range: Onion (20-120), Canalask (6-300), Arch (6-240), Wellgreen (20-900), Linda (10-550), Rainbow Mountain (≈400), Tatamagouche (<3), and Dickson Creek (<3). Hulbert et al. (1992b) showed that Re occurs in exceptionally high concentrations (9600-61 000 ppb) in sedimentary Ni-Zn-PGE mineralization of Devonian black shale from the Yukon. Recent literature pertaining to this element also demonstrates that unexpectedly high concentrations of Re tend to be associated with organic-rich shale: Central Asia (2.4 to 2.6 ppm, Poplavko et al., 1977), Black Sea sediments (41 to 83 ppb, Ravizza et al., 1988), Devonian Bakken Shale (55 to 285 ppb, Ravizza and Turekian, 1989). A survey (Koide et al., 1987) of the Re content of oxic (<0.1 ppb) and anoxic sediments (1.8 to 127 ppb) showed exceptional enrichment in anoxic sediments, especially those associated with hydrothermal sulphides (0.8-273 ppb). Their survey also demonstrated that Re levels were commonly depleted (relative to crustal abundances) in sediments that accumulate under oxidizing conditions. From this and the Kluane data, one may deduce that the high Re contents are due to the selective assimilation of Hasen Creek sediments with a significant organic-rich shale component that is also enriched in Re. The shale may not be unlike that of the Bakken Shale. Re-Os isotopic investigations conducted on Wellgreen mineralization and calc-silicate material derived from the Hasen Creek Formation demonstrated that some of these sediments can have high Re (34.08 ppb) contents. The low Re contents associated with the Dickson Creek mineralization and adjacent country rock exhalative massive sulphides (<3.0 ppb) probably reflects the low Re content of these contaminants due to redox conditions not favouring the sequestering of Re from seawater or hydrothermal conditions at the time of its formation.

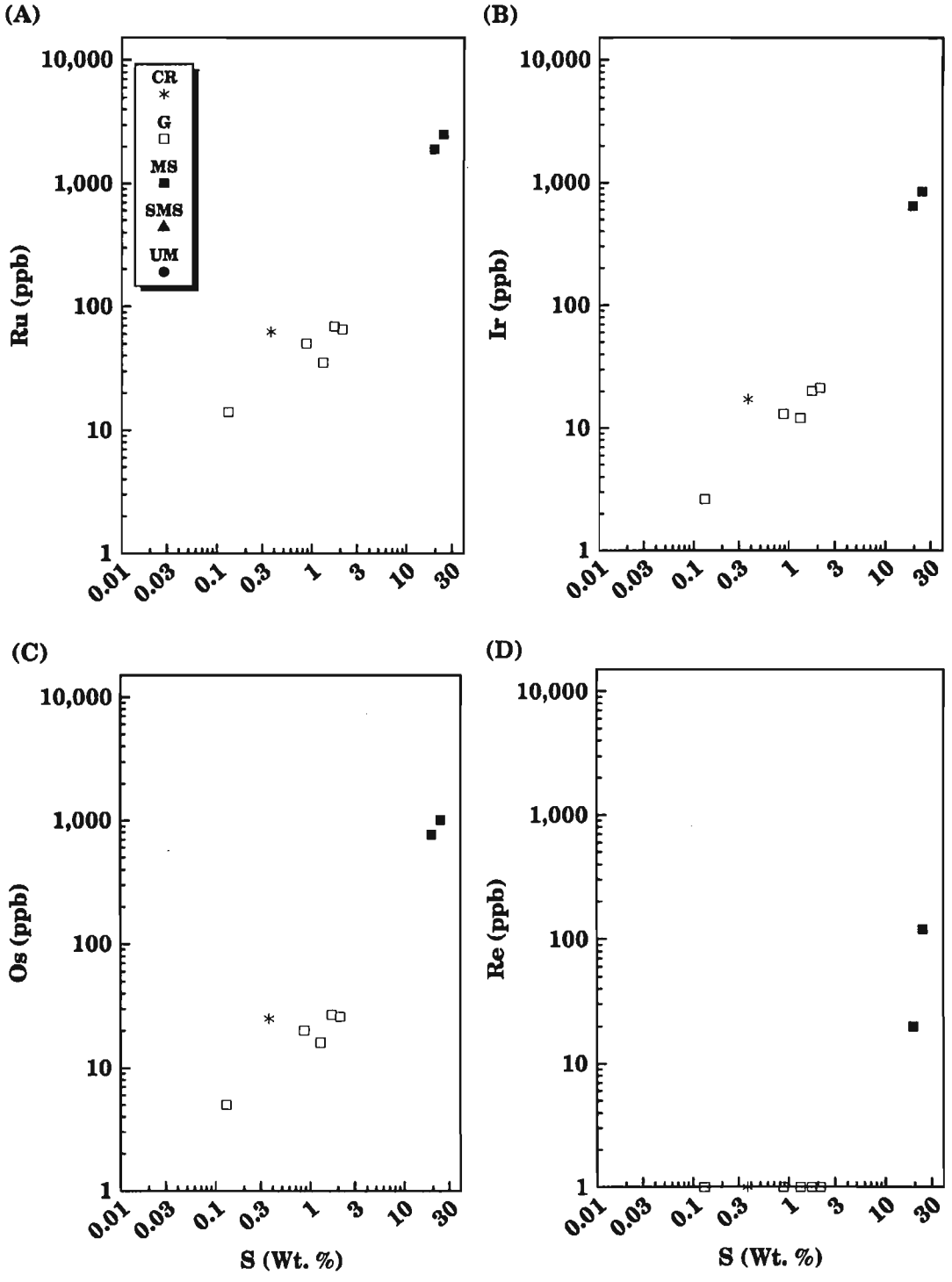

Figure 119 (A-D). *Ru, Ir, Os, Re vs. S (wt.%) plots of elemental concentrations associated with ultramafic (UM), gabbroic (G), massive sulphide (MS), semi-massive sulphide (SMS), and country rock (CR) lithologies from the Onion property of the White River Intrusive Complex. Values plotting along the base of the diagram represent concentrations at the detection limit of the analytical method.*

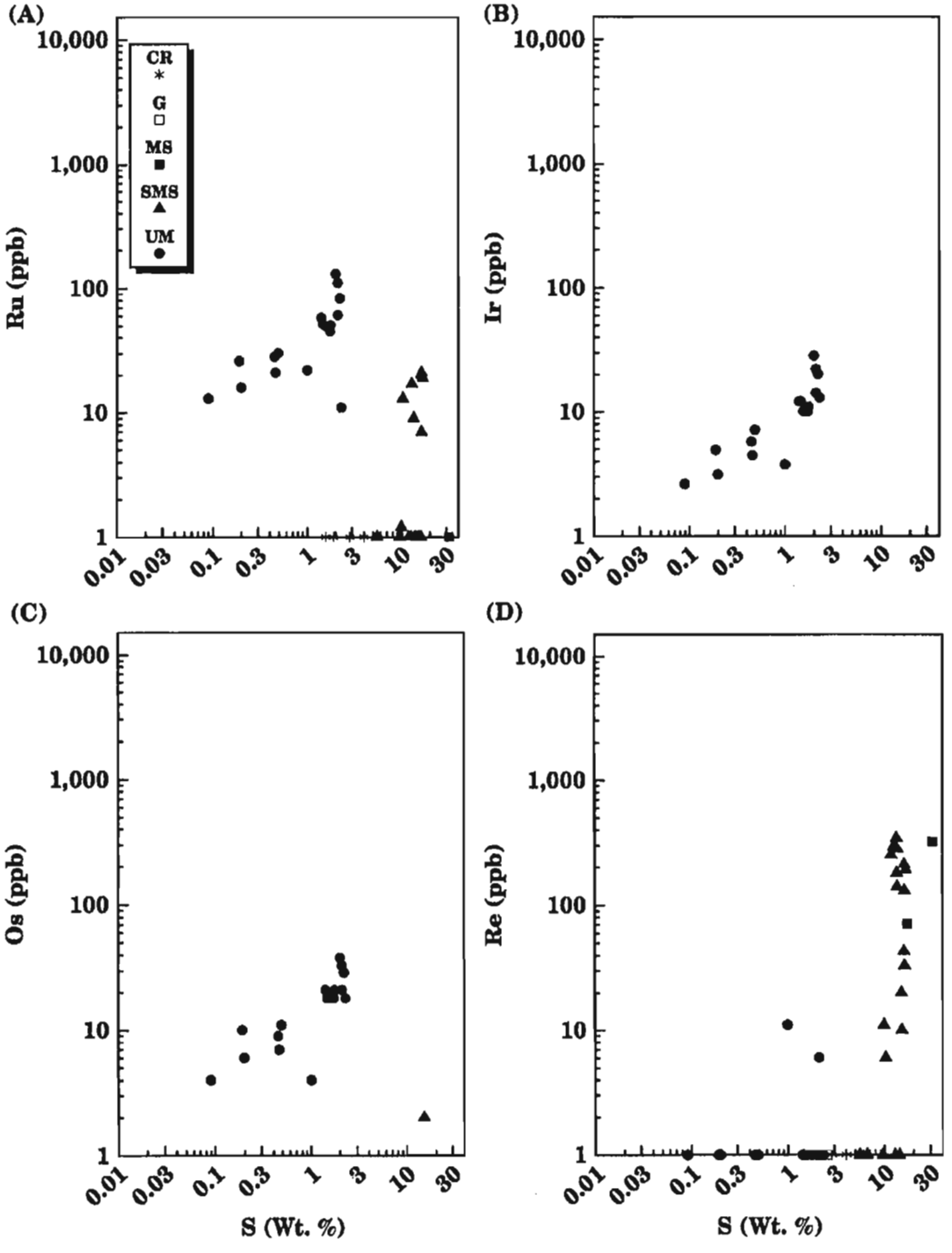

Figure 120 (A-D). *Ru, Ir, Os, Re vs. S (wt.%) plots of elemental concentrations associated with ultramafic (UM), gabbroic (G), massive sulphide (MS), semi-massive sulphide (SMS), and country rock (CR) lithologies from the Canalask property of the White River Intrusive Complex. Values plotting along the base of the diagram represent concentrations at the detection limit of the analytical method.*

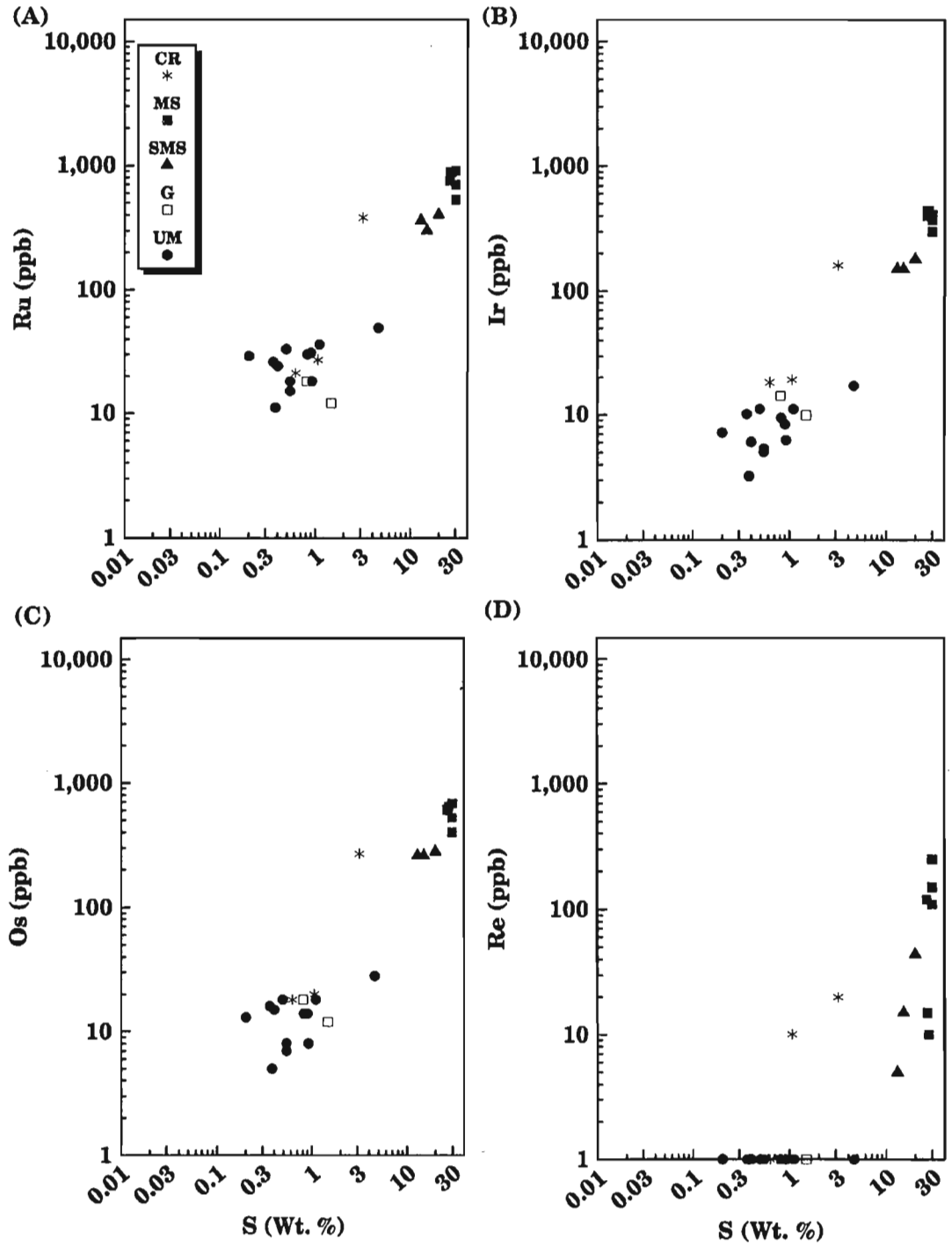

Figure 121 (A-D). Ru, Ir, Os, Re vs. S (wt.%) plots of elemental concentrations associated with ultramafic (UM), gabbroic (G), massive sulphide (MS), semi-massive sulphide (SMS), and country rock (CR) lithologies from the Arch Creek Intrusive Complex. Values plotting along the base of the diagram represent concentrations at the detection limit of the analytical method.

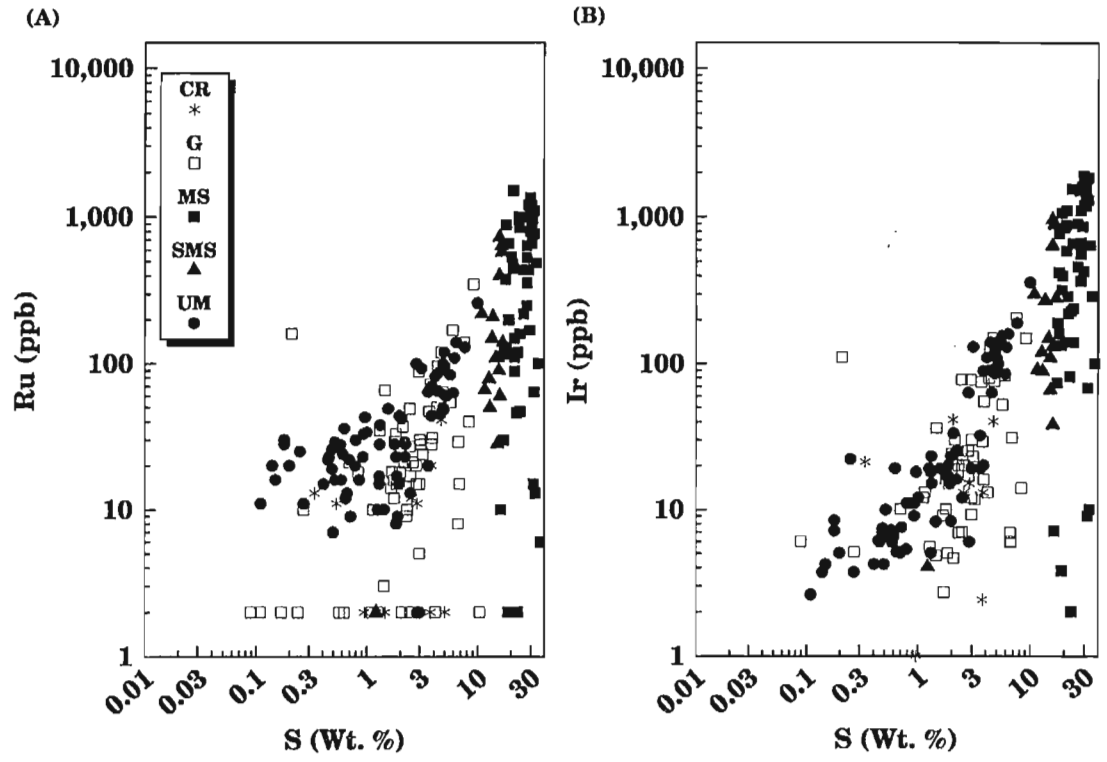

Figure 122 (A-B). Ru, Ir vs. S (wt.%) plots of elemental concentrations associated with ultramafic (UM), gabbroic (G), massive sulphide (MS), semi-massive sulphide (SMS), and country rock (CR) lithologies from the Quill Creek Intrusive Complex.

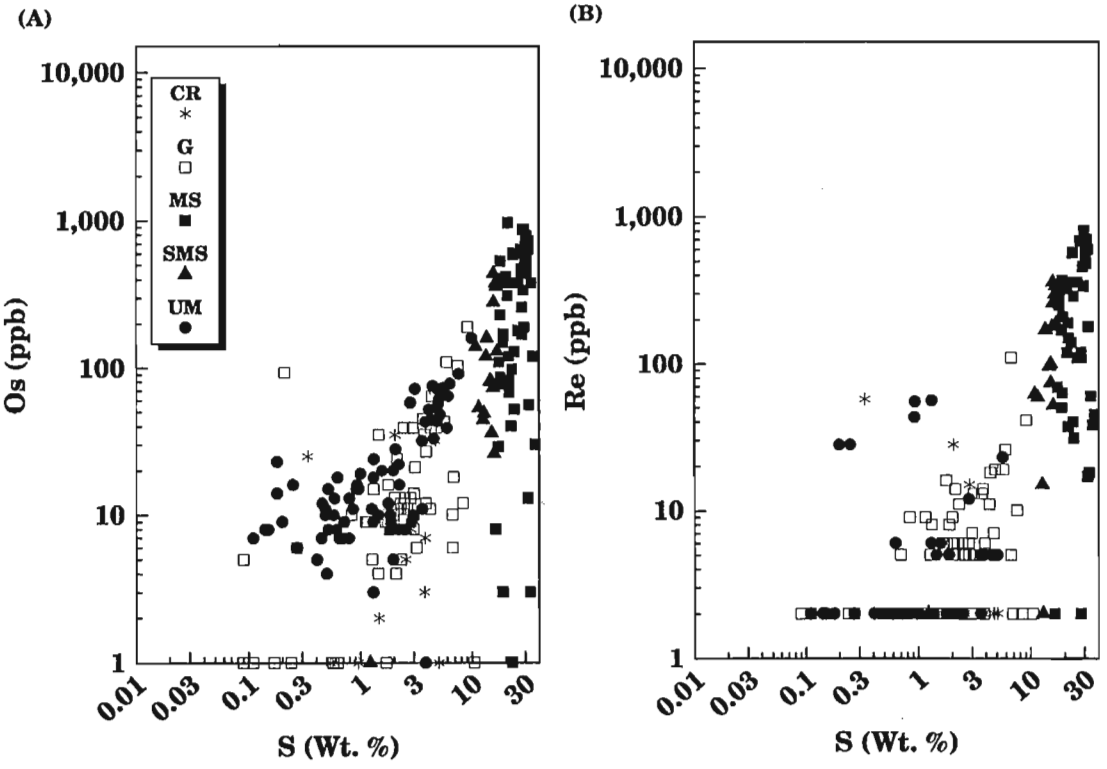

Figure 123 (A-B). Os, Re vs. S (wt.%) plots of elemental concentrations associated with ultramafic (UM), gabbroic (G), massive sulphide (MS), semi-massive sulphide (SMS), and country rock (CR) lithologies from the Quill Creek Intrusive Complex. Values plotting along the base of the diagram represent concentrations at the detection limit of the analytical method.

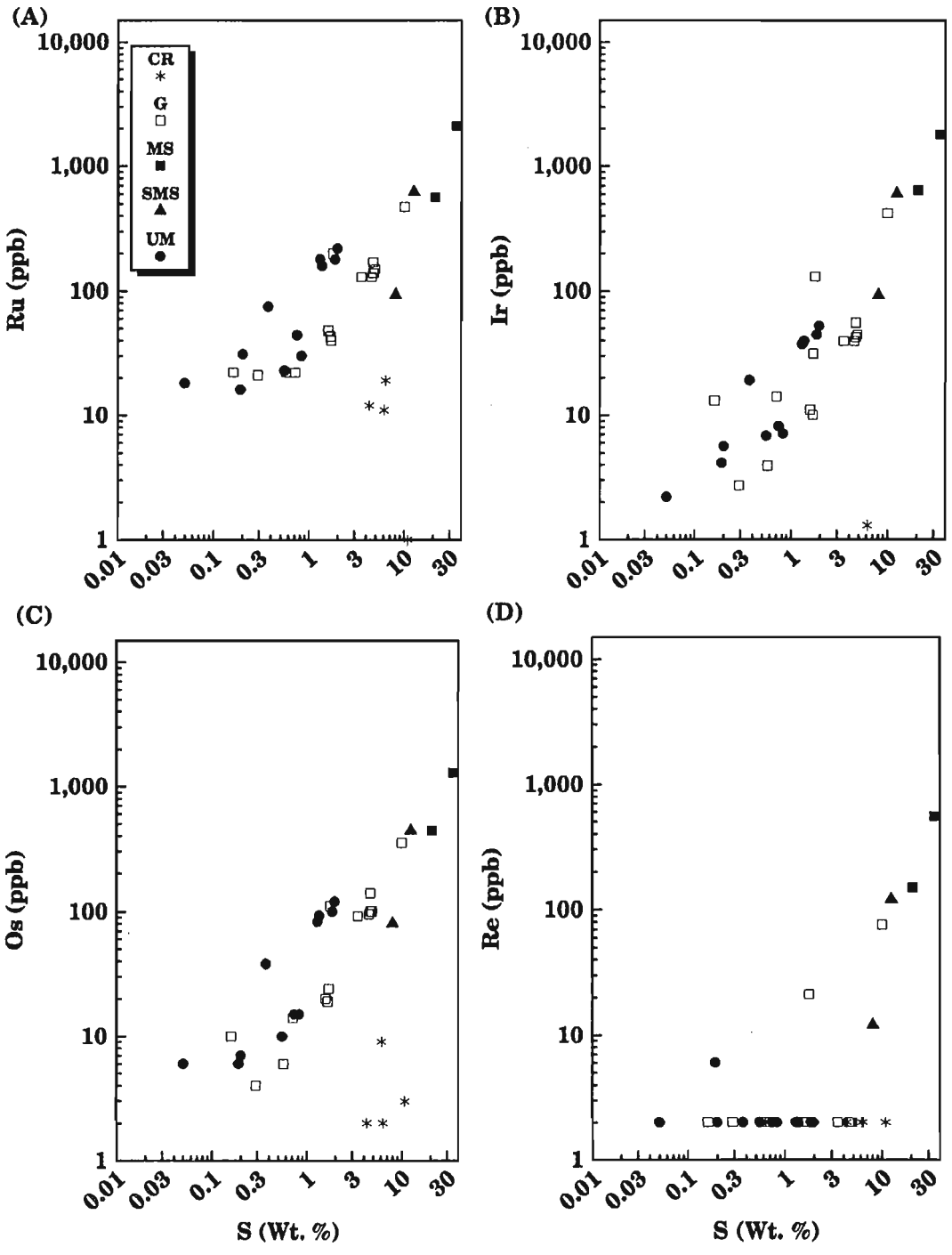

Figure 124 (A-D). *Ru, Ir, Os, Re vs. S (wt.%) plots of elemental concentrations associated with ultramafic (UM), gabbroic (G), massive sulphide (MS), semi-massive sulphide (SMS), and country rock (CR) lithologies from the Linda Creek Intrusive Complex.*

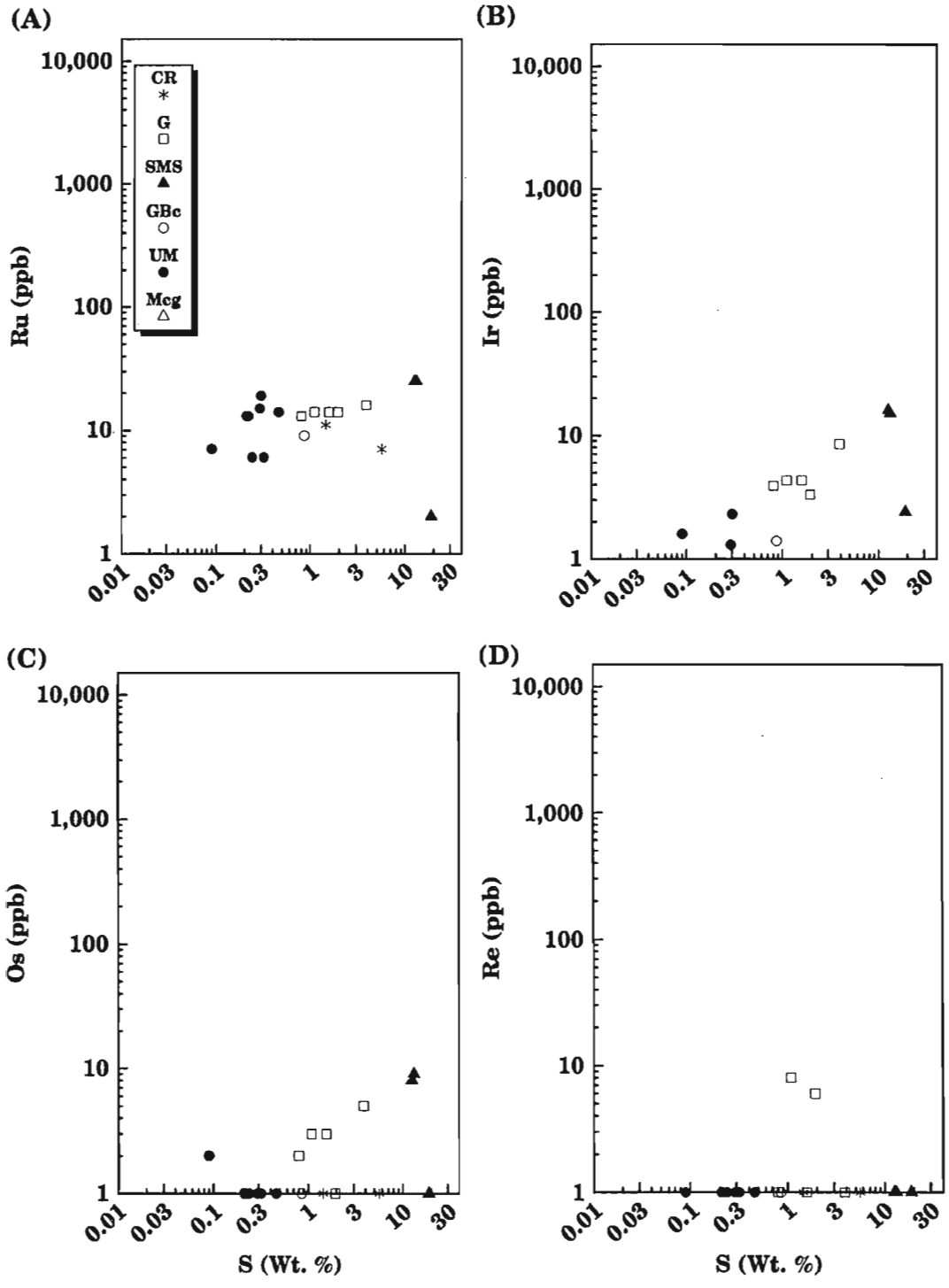

Figure 125 (A-D). *Ru, Ir, Os, Re vs. S (wt.%) plots of elemental concentrations associated with ultramafic (UM), gabbroic (G), basal gabbro (GBc), semi-massive sulphide (SMS), Maple Creek gabbro (Mcg), and country rock (CR) lithologies from the Tatamagouche Creek Intrusive Complex. Values plotting along the base of the diagram represent concentrations at the detection limit of the analytical method.*

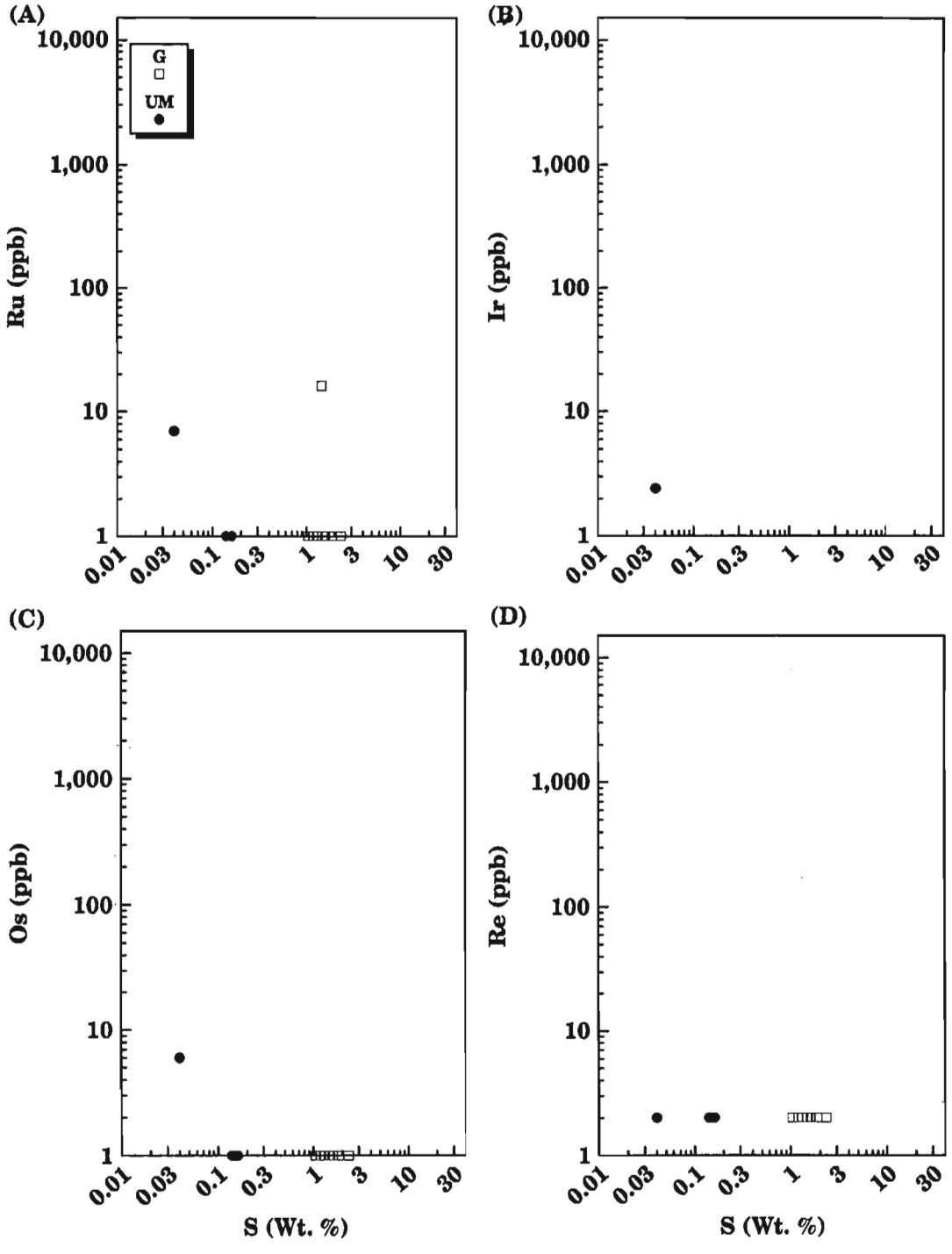

Figure 126 (A-D). Ru, Ir, Os, Re vs. S (wt.%) plots of elemental concentrations associated with ultramafic (UM) and gabbroic (G) lithologies from the Duke River Intrusive Complex. Values plotting along the base of the diagram represent concentrations at the detection limit of the analytical method.

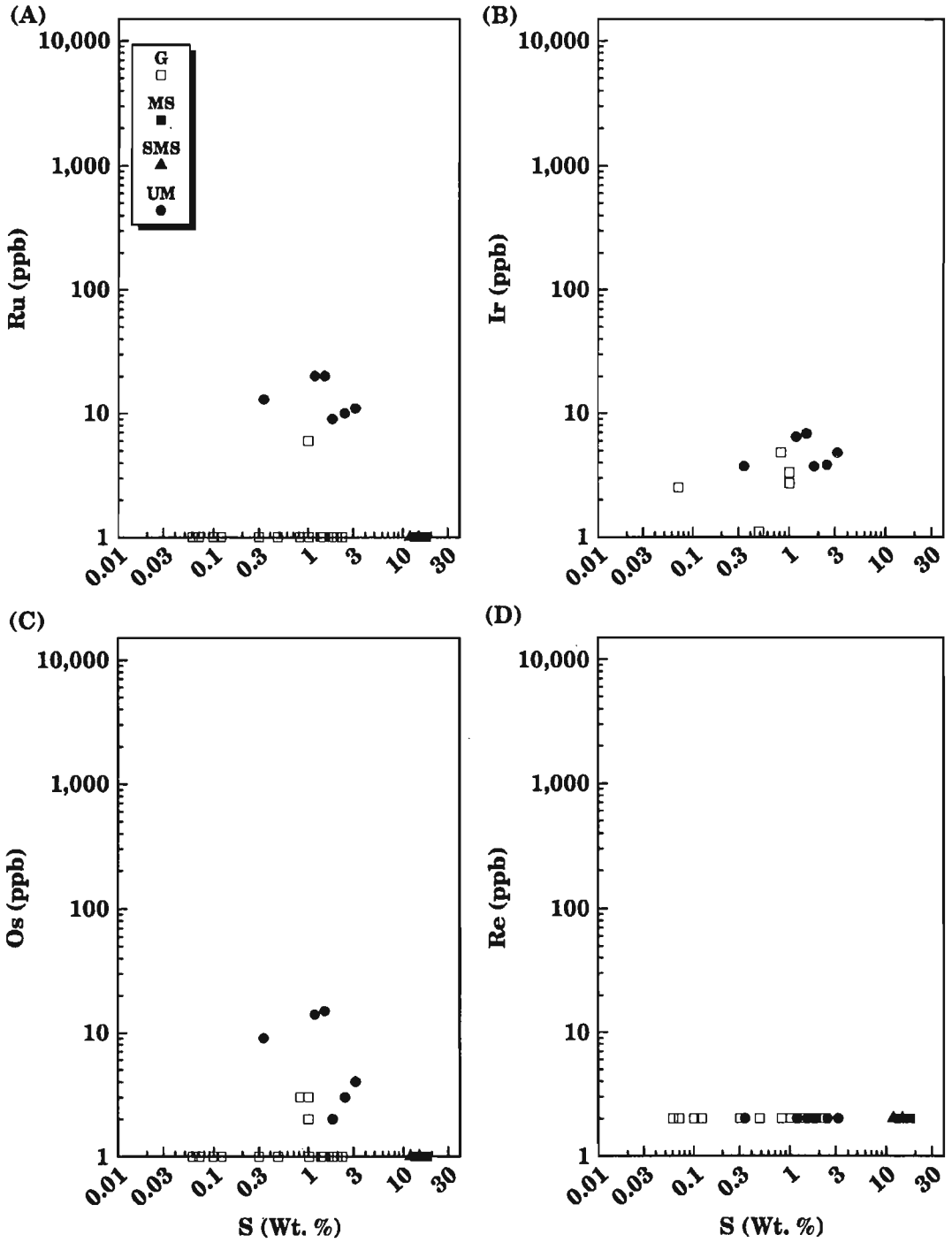

Figure 127 (A-D). *Ru, Ir, Os, Re vs. S (wt.%) plots of elemental concentrations associated with ultramafic (UM), gabbroic (G), massive country rock (exhalative ?) sulphide (MS), and semi-massive sulphide (SMS) lithologies from the Dickson Creek Intrusive Complex. Values plotting along the base of the diagram represent concentrations at the detection limit of the analytical method.*

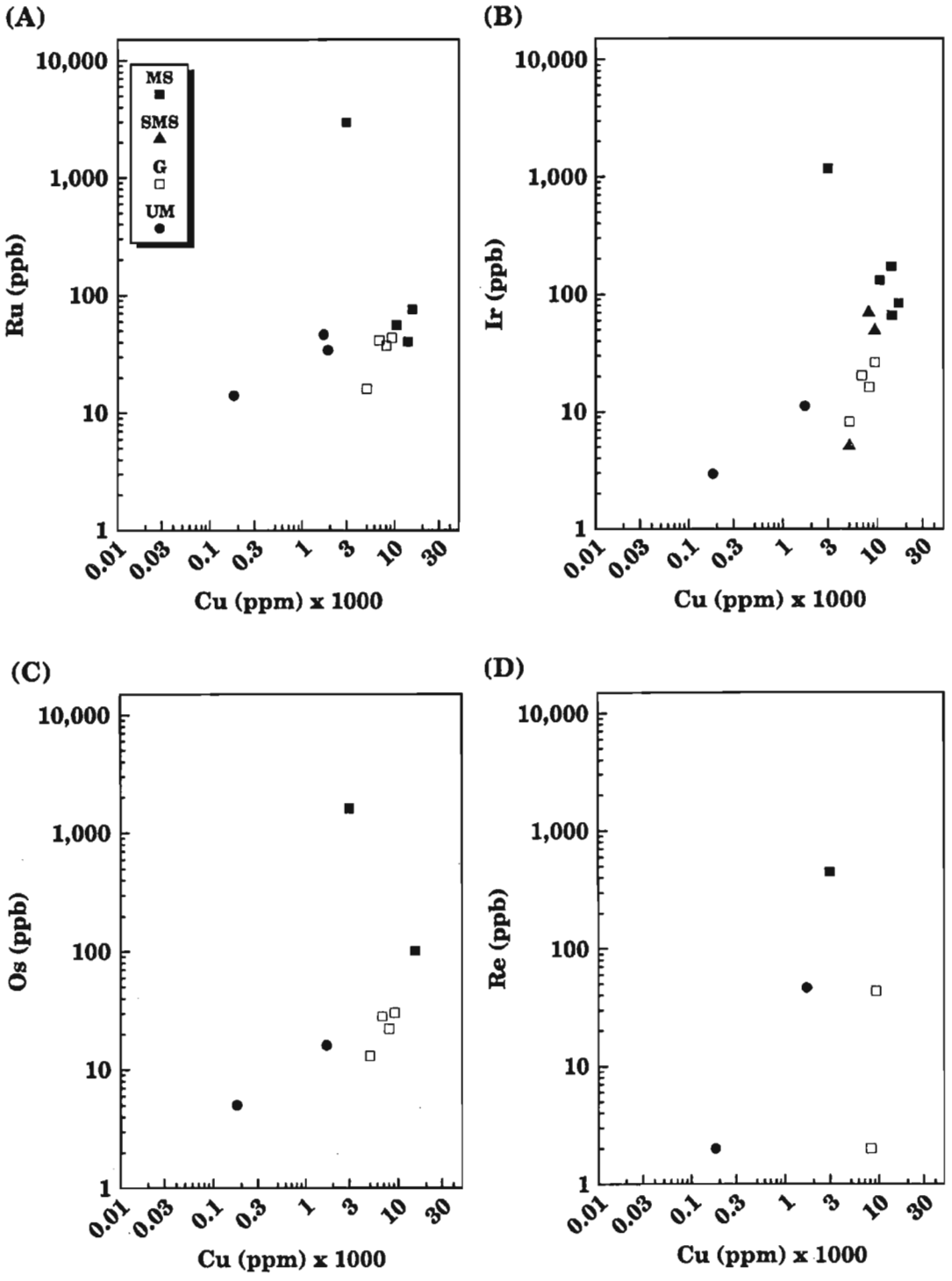

Figure 128 (A-D). Ru, Ir, Os, Re vs. Cu (ppm) plots of elemental concentrations associated with ultramafic (UM), gabbroic (G), massive sulphide (MS), and semi-massive sulphide (SMS) lithologies from the Rainbow Mountain Intrusive Complex, Alaska.

Low Re contents in the Tatamagouche samples are more difficult to explain but this gossanous material has been leached, and Re is known to be highly mobile in aqueous environments (Koide et al., 1987), thus some of the Re may have been removed. Within the massive and semi-massive sulphide mineralization Re occurs both as a solid solution in sulphide phases and locally as a rare unidentified Re-sulphide.

Noble metal concentrations and elemental ratios

Platinum group element and gold (PGE+Au) concentrations of samples from the investigated intrusive complexes are summarized in Figures 129A to 139A relative to the amount of S in the sample. This gives an accurate assessment of the concentrations associated with each lithology, as well as what could be expected with future discoveries of similar

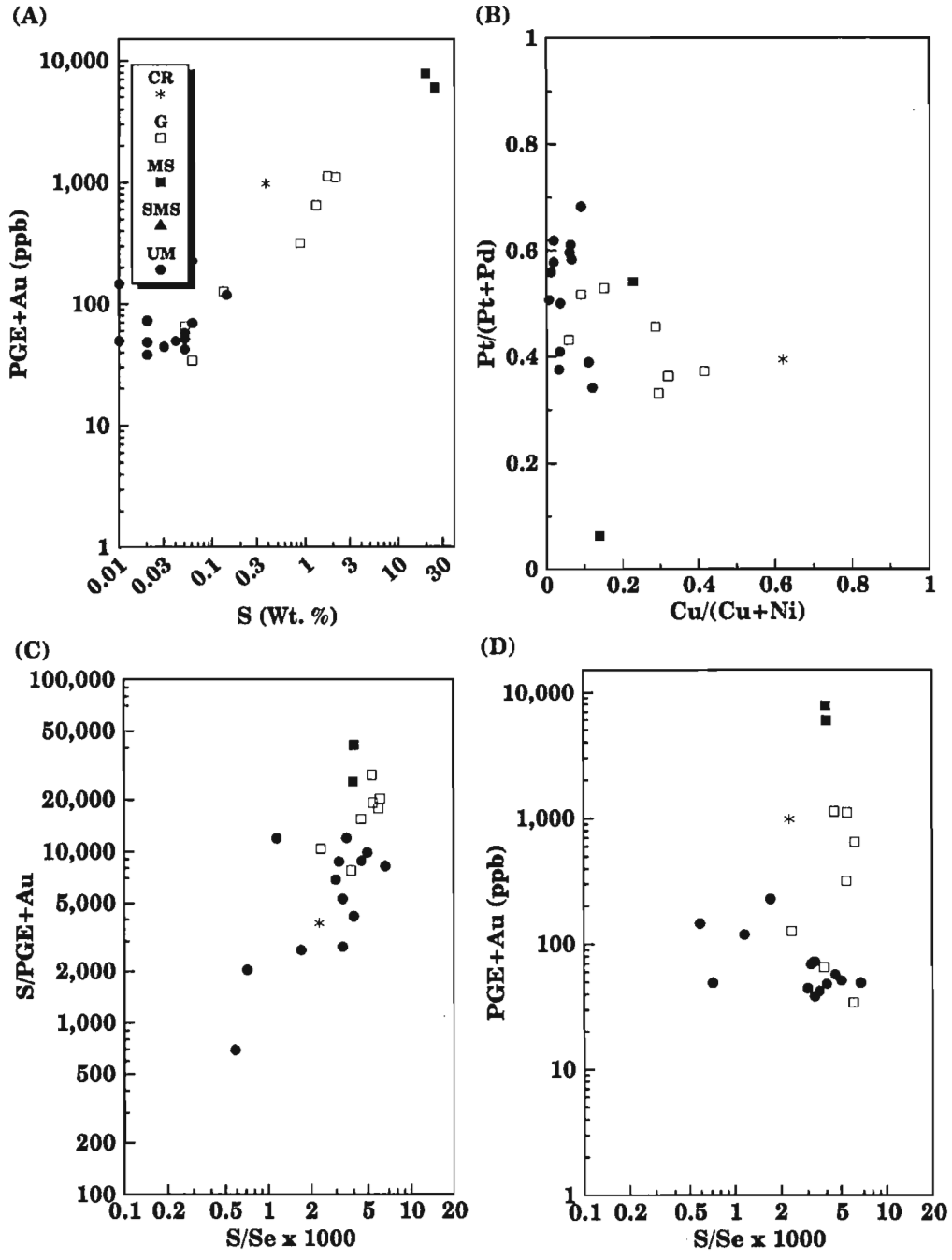

Figure 129 (A-D). PGE+Au vs. S (wt.%), Pt/(Pt+Pd) vs. Cu/(Cu+Ni), S/PGE+Au vs. S/Se, and PGE+Au vs. S/Se plots of elemental ratios and concentrations associated with ultramafic (UM), gabbroic (G), massive sulphide (MS), semi-massive sulphide (SMS), and country rock (CR) lithologies from the Onion property of the White River Intrusive Complex.

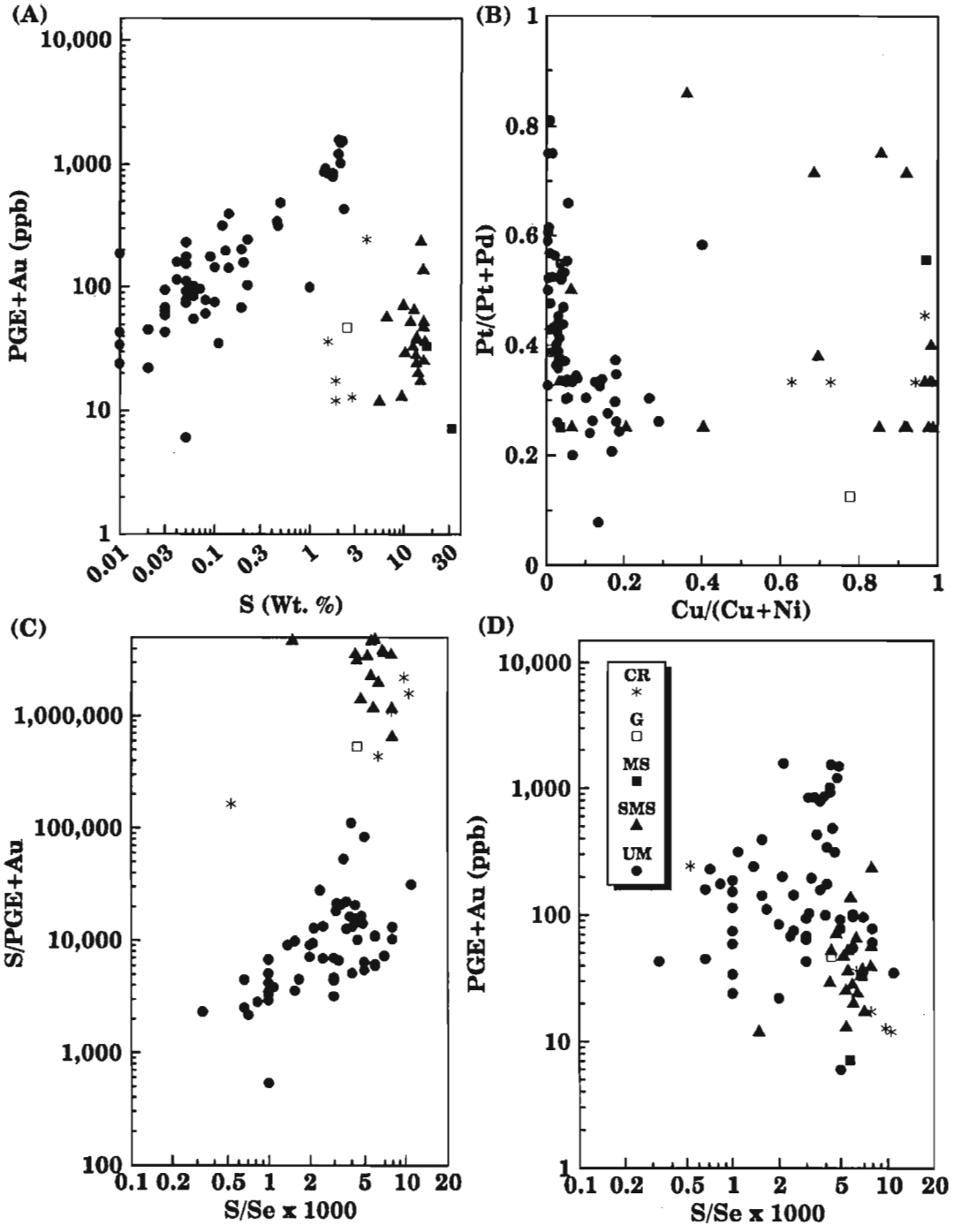

Figure 130 (A-D). *PGE+Au vs. S (wt.%), Pt/(Pt+Pd) vs. Cu/(Cu+Ni), S/PGE+Au vs. S/Se, and PGE+Au vs. S/Se plots of elemental ratios and concentrations associated with ultramafic (UM), gabbroic (G), massive sulphide (MS), semi-massive sulphide (SMS), and country rock (CR) lithologies from the Canalask property of the White River Intrusive Complex.*

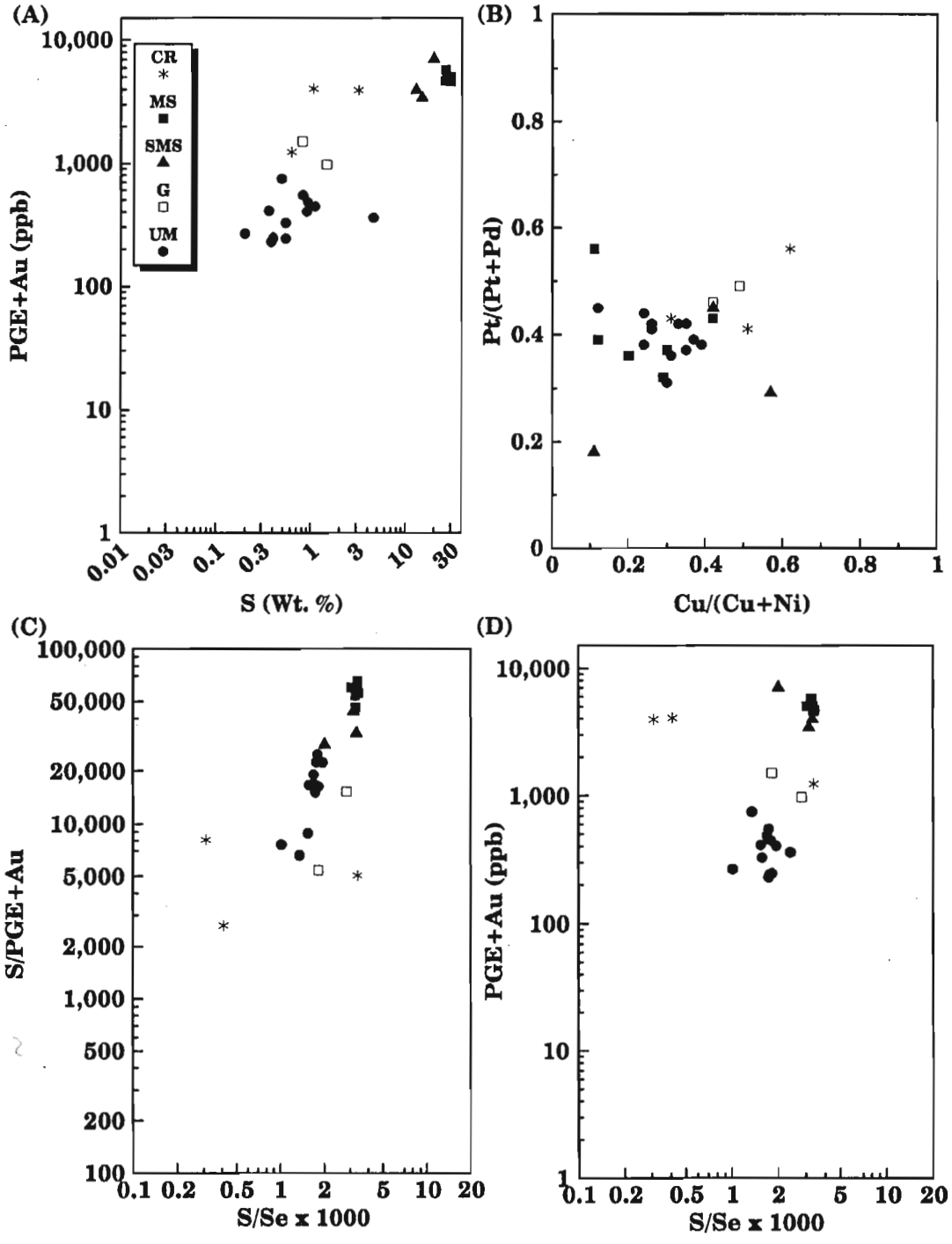

Figure 131 (A-D). PGE+Au vs. S (wt.%), Pt/(Pt+Pd) vs. Cu/(Cu+Ni), S/PGE+Au vs. S/Se, and PGE+Au vs. S/Se plots of elemental ratios and concentrations associated with ultramafic (UM), gabbroic (G), massive sulphide (MS), semi-massive sulphide (SMS), and country rock (CR) lithologies from the Arch Creek Intrusive Complex.

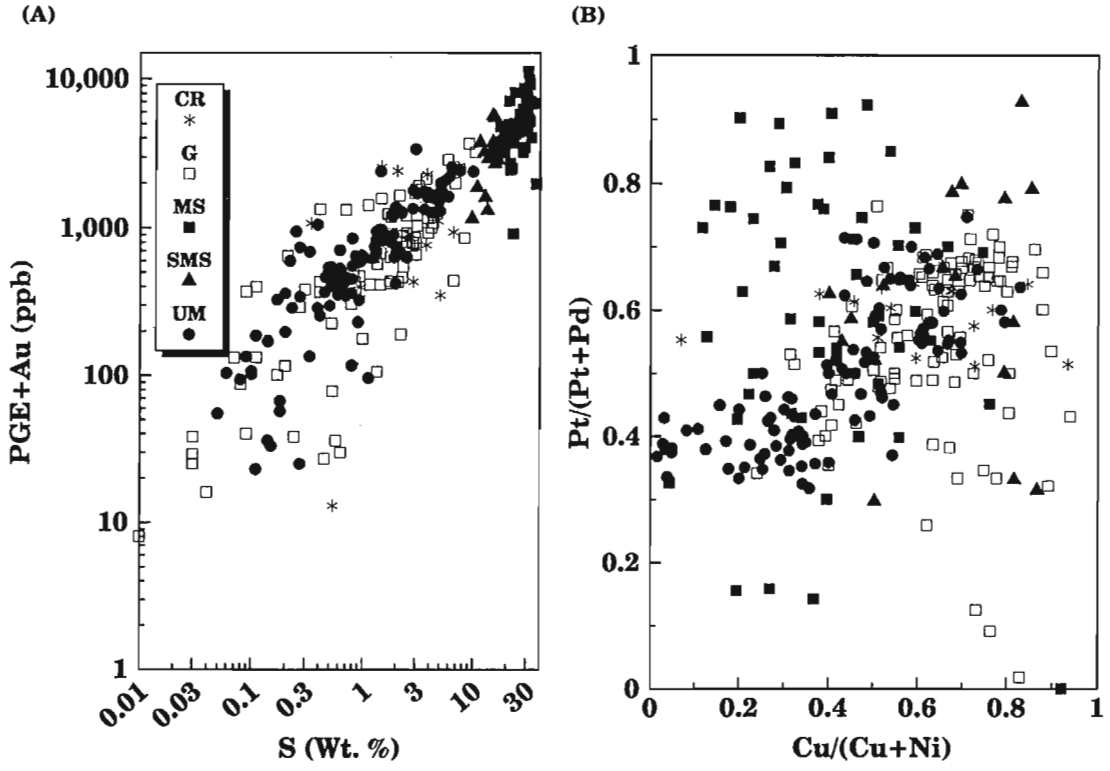

Figure 132 (A-B). PGE+Au vs. S (wt.%) and Pt/(Pt+Pd) vs. Cu/(Cu+Ni) plots of elemental ratios and concentrations associated with ultramafic (UM), gabbroic (G), massive sulphide (MS), semi-massive sulphide (SMS), and country rock (CR) lithologies from the Quill Creek Intrusive Complex.

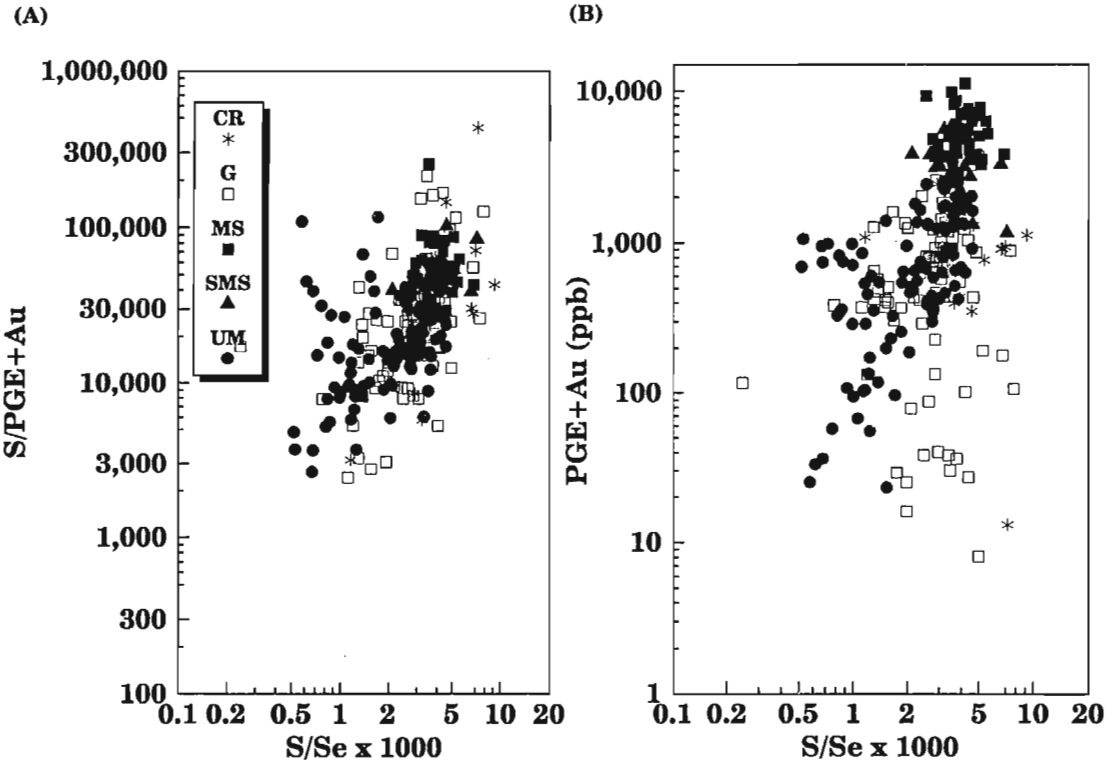

Figure 133 (A-B). S/PGE+Au vs. S/Se and PGE+Au vs. S/Se plots of elemental ratios and concentrations associated with ultramafic (UM), gabbroic (G), massive sulphide (MS), semi-massive sulphide (SMS), and country rock (CR) lithologies from the Quill Creek Intrusive Complex.

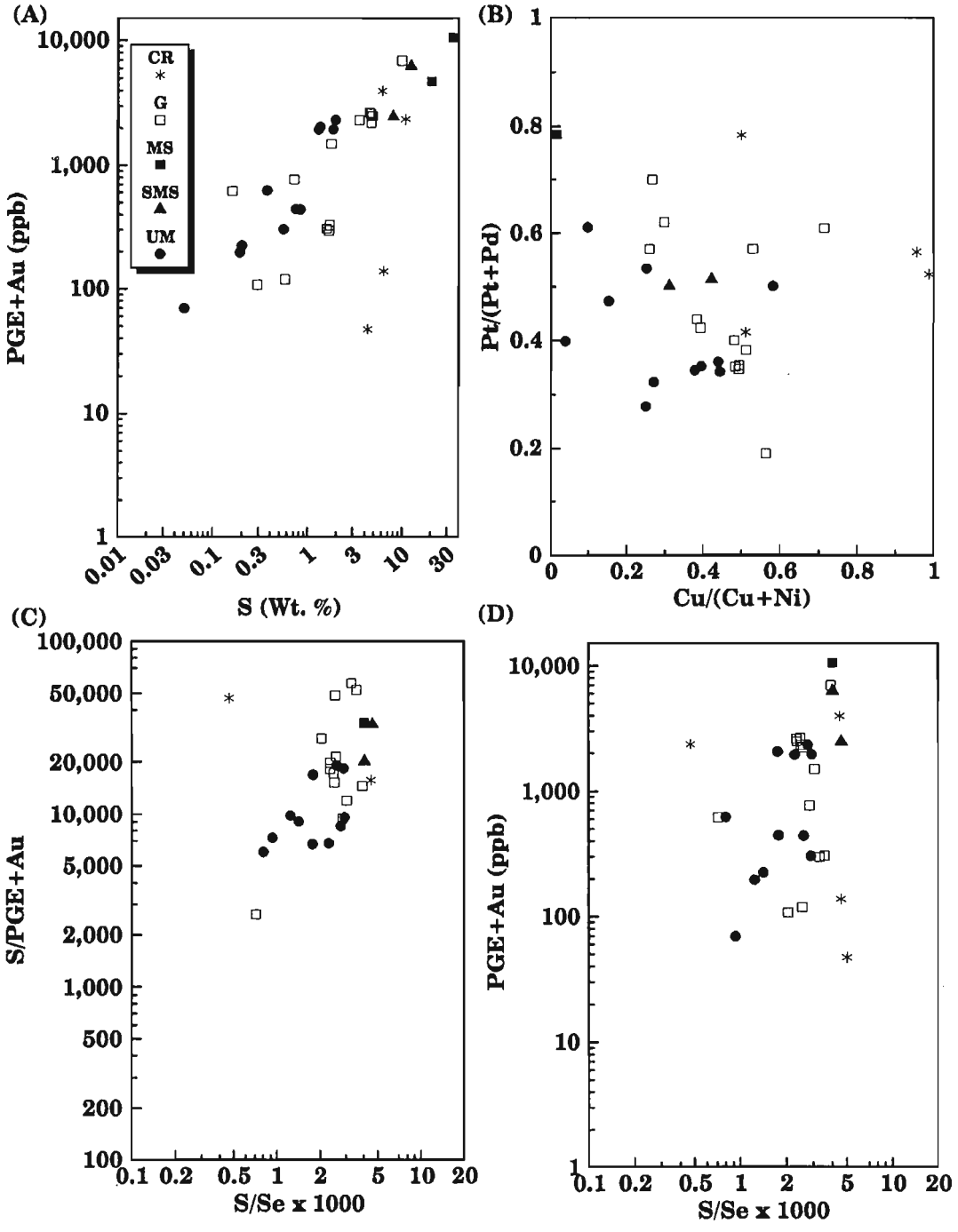

Figure 134 (A-D). *PGE+Au vs. S (wt.%), Pt/(Pt+Pd) vs. Cu/(Cu+Ni), S/PGE+Au vs. S/Se and PGE+Au vs. S/Se plots of elemental ratios and concentrations associated with ultramafic (UM), gabbroic (G), massive sulphide (MS), semi-massive sulphide (SMS), and country rock (CR) lithologies from the Linda Creek Intrusive Complex.*

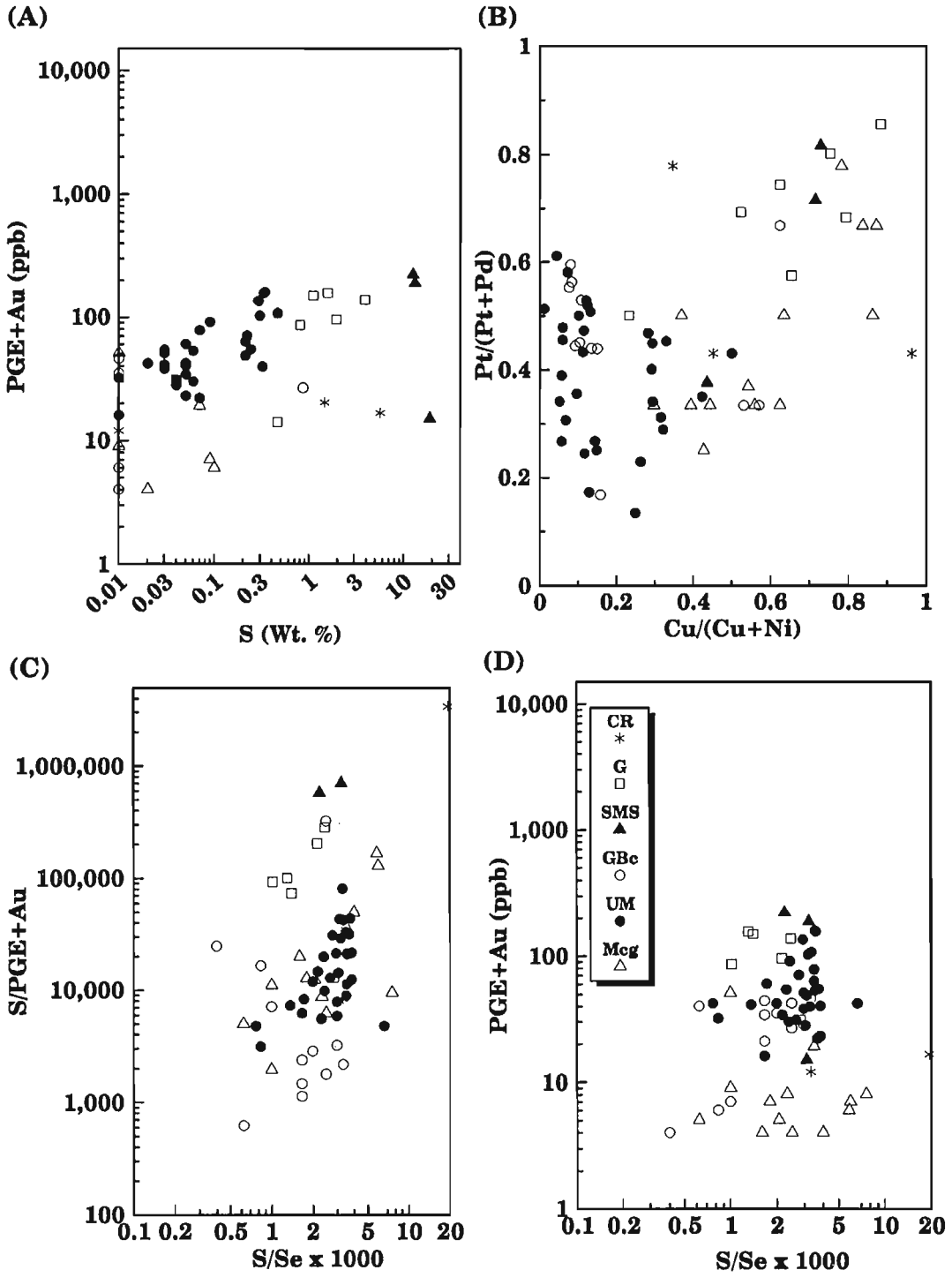

Figure 135 (A-D). *PGE+Au vs. S (wt.%), Pt/(Pt+Pd) vs. Cu/(Cu+Ni), S/PGE+Au vs. S/Se and PGE+Au vs. S/Se plots of elemental ratios and concentrations associated with ultramafic (UM), gabbroic (G), basal gabbro (GBc), Maple Creek gabbro (Mcg), semi-massive sulphide (SMS), and country rock (CR) lithologies from the Tatamagouche Creek Intrusive Complex.*

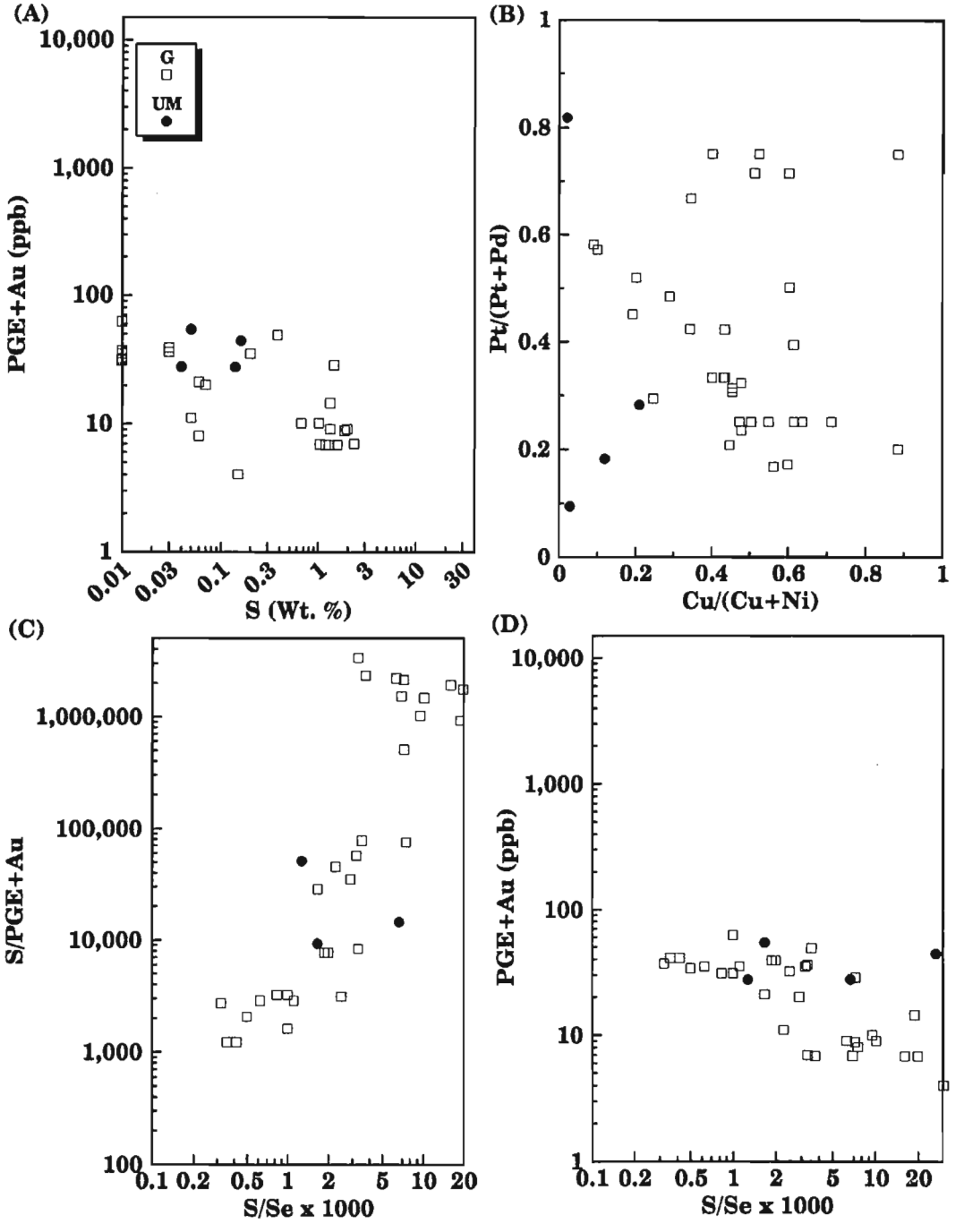

Figure 136 (A-D). *PGE+Au vs. S (wt.%), Pt/(Pt+Pd) vs. Cu/(Cu+Ni), S/PGE+Au vs. S/Se and PGE+Au vs. S/Se plots of elemental ratios and concentrations associated with ultramafic (UM) and gabbroic (G) lithologies from the Duke River Intrusive Complex.*

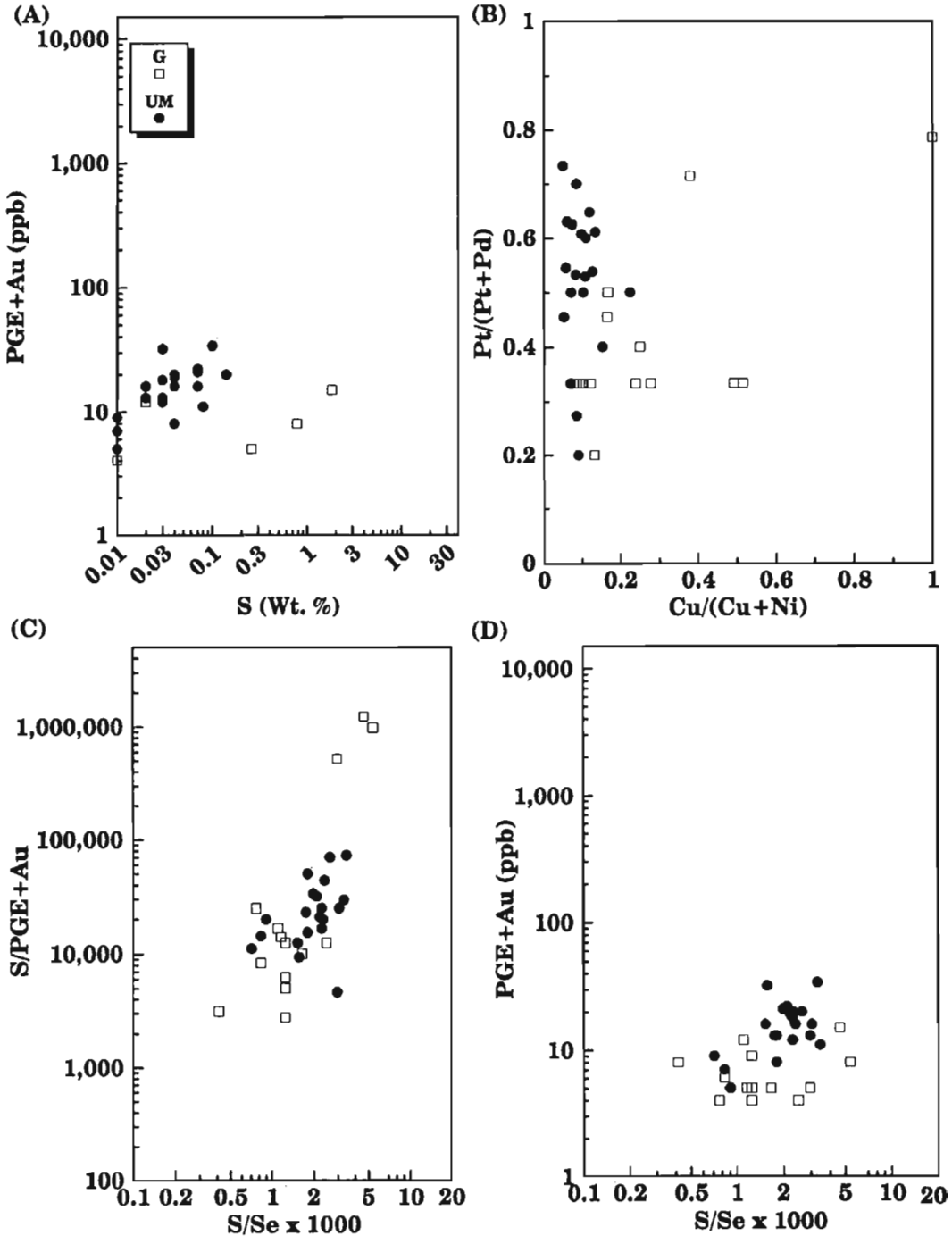

Figure 137 (A-D). *PGE+Au vs. S (wt.%), Pt/(Pt+Pd) vs. Cu/(Cu+Ni), S/PGE+Au vs. S/Se and PGE+Au vs. S/Se plots of elemental ratios and concentrations associated with ultramafic (UM) and gabbroic (G) lithologies from the Halfbreed Creek Intrusive Complex.*

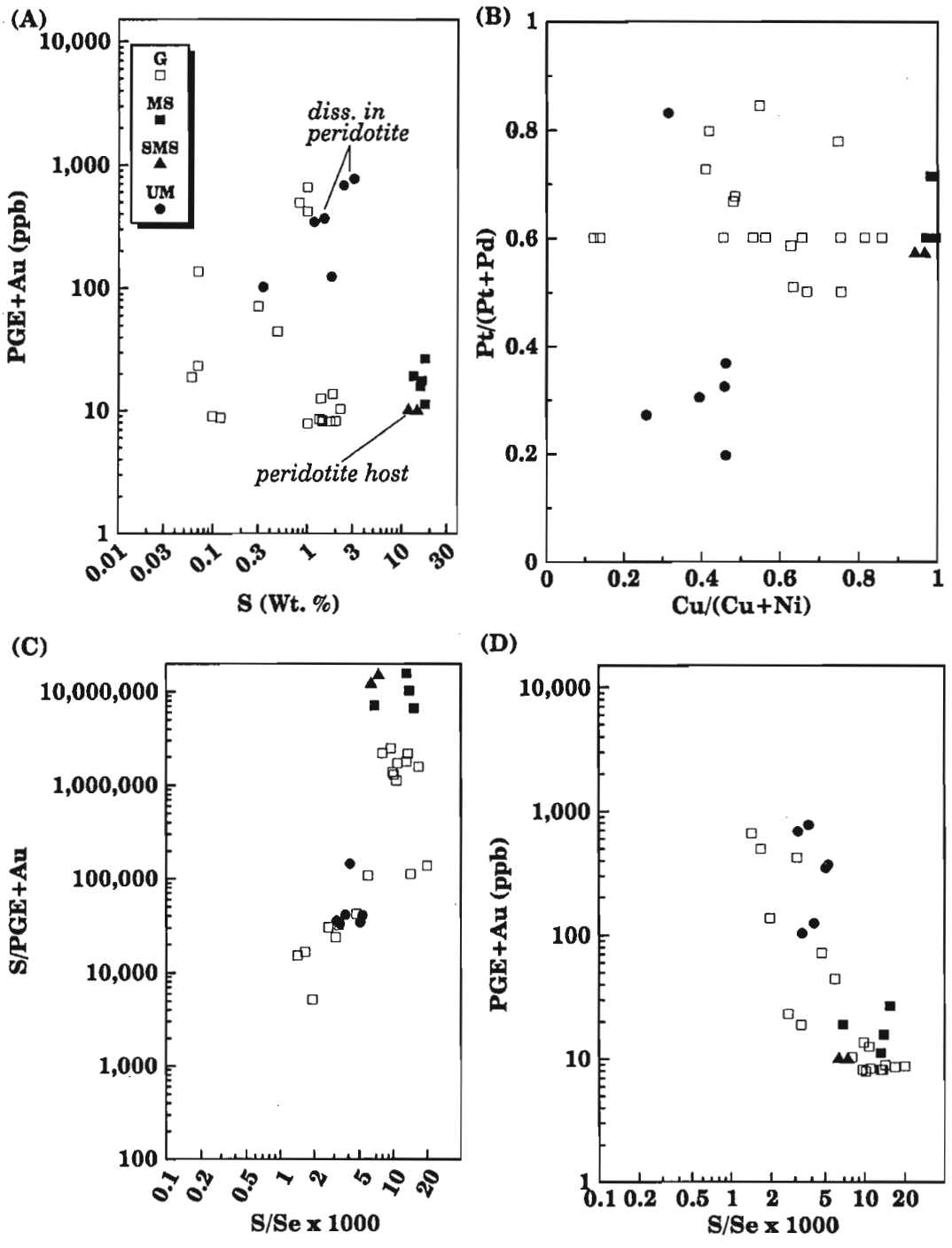

Figure 138 (A-D). *PGE+Au vs. S (wt.%), Pt/(Pt+Pd) vs. Cu/(Cu+Ni), S/PGE+Au vs. S/Se and PGE+Au vs. S/Se plots of elemental ratios and concentrations associated with ultramafic (UM), gabbroic (G), massive country rock (exhalative ?) sulphide (MS), and semi-massive sulphide (SMS) lithologies from the Dickson Creek Intrusive Complex.*

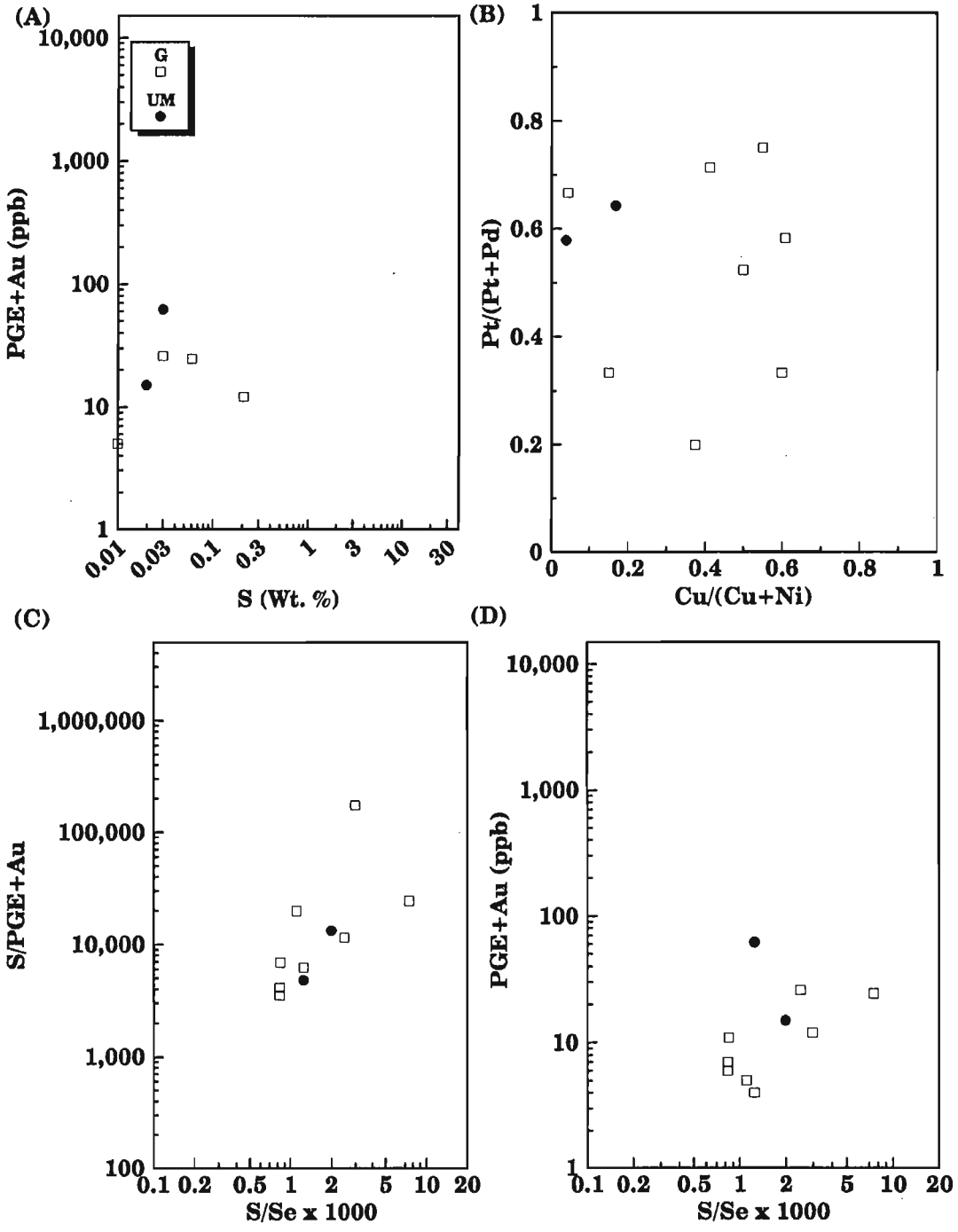

Figure 139 (A-D). *PGE+Au vs. S (wt.%), Pt/(Pt+Pd) vs. Cu/(Cu+Ni), S/PGE+Au vs. S/Se and PGE+Au vs. S/Se plots of elemental ratios and concentrations associated with ultramafic (UM) and gabbroic (G) lithologies from the Chilkat Intrusive Complex.*

mineralization, and the behavior of PGE+Au at each locality within the Kluane Belt. Similarly, in PGE+Au vs. S trends from the Onion, Arch, Linda and Wellgreen properties, massive and semi-massive basal sulphide compositions are congruous with trends established by both the gabbroic and ultramafic rocks from the same body. These trends and concentrations are significantly different from those established in what has proven to date to be less favourable complexes (Duke River and Halfbreed Creek). This relationship suggests that basal massive sulphide mineralization similar to that from the Wellgreen, Linda, and Arch properties could be expected at the base of the Canalask mafic-ultramafic section of the White River Complex. Future discoveries of this type of mineralization will be far superior, both in Ni and PGE+Au grades, to that of the presently known Canalask "offset mineralization". Structurally, it will also be more confined and predictable.

Another informative group of plots is that of the S/PGE+Au vs. S/Se x 1000 in Figures 129C to 139C. These plots demonstrate a strong positive correlation between these two ratios and indicate that the PGE+Au content associated with the sulphide phase increases in conjunction with increasing Se content of the sulphides. Samples with high S/PGE+Au and S/Se x 1000 ratios (i.e. Canalask and Dickson Creek massive and semi-masive sulphides and Duke River mineralized gabbro) are associated with other geochemical indicators (discussed previously) which suggest they are the result of extensive contamination from Se- and PGE-poor country rock sediments. The decreasing trend of these ratios indicates progressively less crustal contamination and increasing magmatic component in the sulphide fraction. Thus the most economically favourable lithologies appear to be those with the low S/Se x 1000 ratios (≈2 to 4); extremely low values (i.e. S/Se x 1000 <1) are probably artifacts of S-loss accompanying serpentinization.

The Pt/(Pt+Pd) vs. Cu/(Cu+Ni) and PGE+Au vs. S/Se x 1000 plots in Figures 129B and D to 139B and D are less informative because of the influence of the sulphide content on two of these variables. Nevertheless, the plots adequately represent ratios and PGE+Au concentrations associated with the semi-massive and massive sulphide samples, which are of most interest to explorationists, and illustrate how increasing silicate fractions (gabbro, ultramafic rocks) scatter these ratios due to the influence of non-recoverable silicate nickel. Massive and semi-massive sulphide concentrations show considerable variability at each locality, and within individual sulphide bodies (Fig. 29H), and it is clear that the massive and semi-massive sulphide concentrations are at opposite ends of the Cu/Cu+Ni range and cannot be used in conjunction with the Pt/Pt+Pd ratio to infer the nature of the parental magma as proposed by Naldrett (1981b). This relationship may be explained by the apparent pyrrhotite-pentlandite and chalcopyrite segregations observed within many of the basal sulphide bodies, and in the included gabbroic patches with disseminated chalcopyrite. The preferential association of chalcopyrite in the gabbroic fraction, and the engulfing massive sulphide intervals being almost exclusively the domain of pyrrhotite and pentlandite (Fig. 26A, B, C) is reminiscent of sulphide fractionation and sulphide-silicate immiscibility with the Cu-rich phase partitioning into the residual silicate melt.

PGE+Au ternary proportions

Platinum group elements plus gold trends, with respect to various ternary components (Pd:Pt:Au, Pd:Pt:Rh, Au:Pt:Rh, Au:Ir:Rh), have been examined from each complex with respect to the host lithology (Fig. 140 to 151). Examination of the Pd:Pt:Au plots suggest that the Pt:Pd ratio is highly variable, but there appears to be a systematic increase in the Au content from ultramafic to gabbroic and finally semi-massive sulphide samples. The Au enrichment is most pronounced in the semi-massive and massive sulphides from Canalask and Dickson Creek relative to other localities. The Au enrichment trends in the semi-massive and massive sulphides at these two localities are believed to represent a significant crustal (sediments) contribution relative to Pt and Pd. Increased Au content in the gabbroic rocks from throughout the belt is probably the result of sulphide fractionation. At many localities there is also a suggestion of Pt enrichment relative to Pd in the gabbroic rocks relative to the ultramafic rocks. Examination of these elements and trends with respect to gabbroic, olivine pyroxenite, peridotite, and dunite from the Quill Creek Intrusive Complex demonstrates an increase in the Au content from dunite to peridotite, olivine pyroxenite, and gabbro accompanying a general Pt increase, respectively (Fig. 145A). The Pd/Pt ratio increases from gabbroic to ultramafic rocks and is in concert with the lithological succession encountered. This relationship could be expected by fractionating successive sulphide melts that were evolving away from the base of the complex. Nevertheless, some gabbroic samples also contain amongst the lowest Au contents encountered within the sulphide-poor rocks. The only Rh trends that can be discerned with respect to Pd and Pt in Figures 140B to 150B is that of enrichment in massive sulphide samples, in particular where the Pd:Pt ratio is ≥0.5. Ultramafic rocks from the Quill Creek Complex (Fig. 145C) appear to show a slight Rh enrichment from dunite to olivine pyroxenite and peridotite, which also tends to accompany an increase in Pt. No trend is apparent for Rh in the gabbroic rocks.

Plots of Au:Pt:Rh in Figures 140C to 150C are devoid of significant compositional trends other than the preferential clustering near the Pt end member, except at Canalask and Dickson Creek where compositions tend to be continuous from Au to Pt due to the crustal contamination of Au. Au:Ir:Rh plots (Fig. 140D to 150D) are noteworthy because of the lack of Ir and Rh in some of the massive sulphides (Dickson Creek, Canalask) and the increased proportion of Ir:Rh at the Wellgreen and Linda properties compared to that at Canalask and Arch.

Chondrite normalized PGE+Au profiles in 100% sulphide

Platinum-group elements and gold concentrations from the various mineralized lithological groups in each complex have been normalized to 100% sulphide and divided by the concentration present in C1 chondritic meteorite (Naldrett et al., 1979).

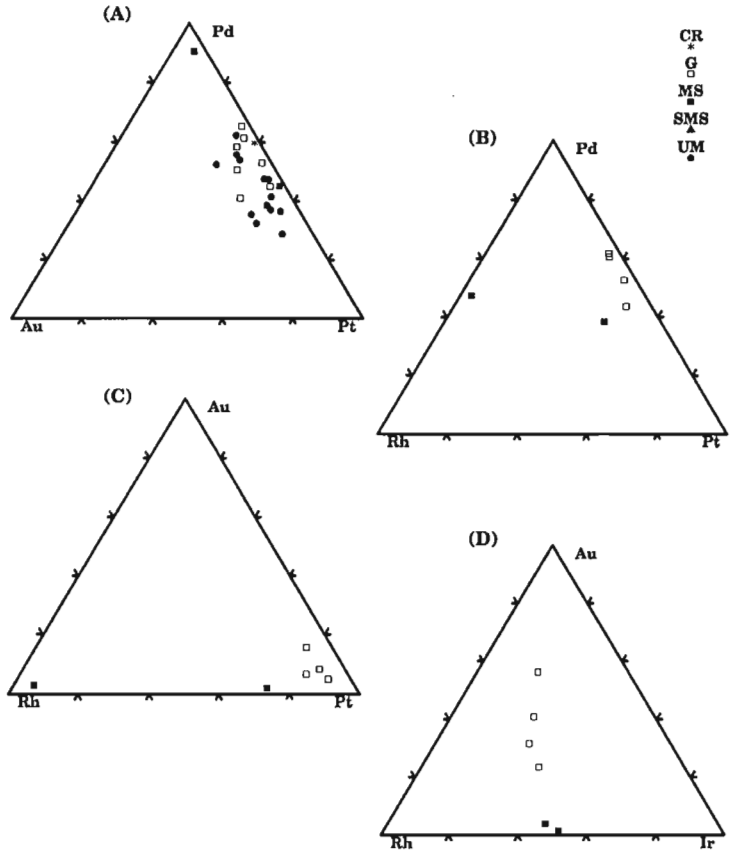

Figure 140 (A-D).

Pd-Au-Pt, Pd-Rh-Pt, Au-Rh-Pt, and Au-Rh-Ir ternary compositions of ultramafic (UM), gabbroic (G), massive sulphide (MS), semi-massive sulphide (SMS), and country rock (CR) lithologies associated with the Onion property of the White River Intrusive Complex.

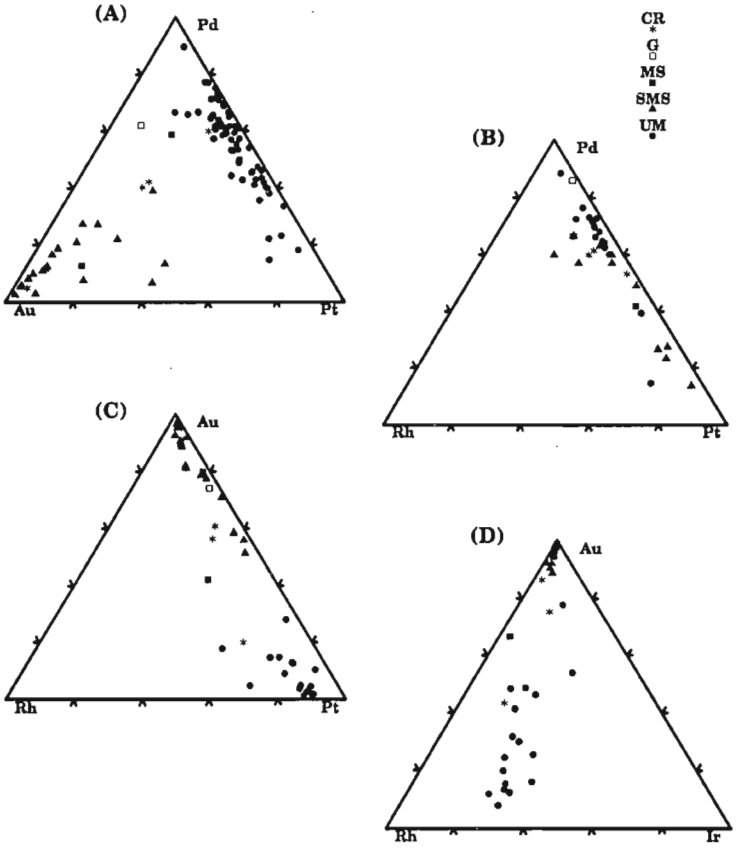

Figure 141 (A-D).

Pd-Au-Pt, Au-Rh-Pt, and Au-Rh-Ir ternary compositions of ultramafic (UM), gabbroic (G), massive sulphide (MS), semi-massive sulphide (SMS), and country rock (CR) lithologies associated with the Canalask property of the White River Intrusive Complex.

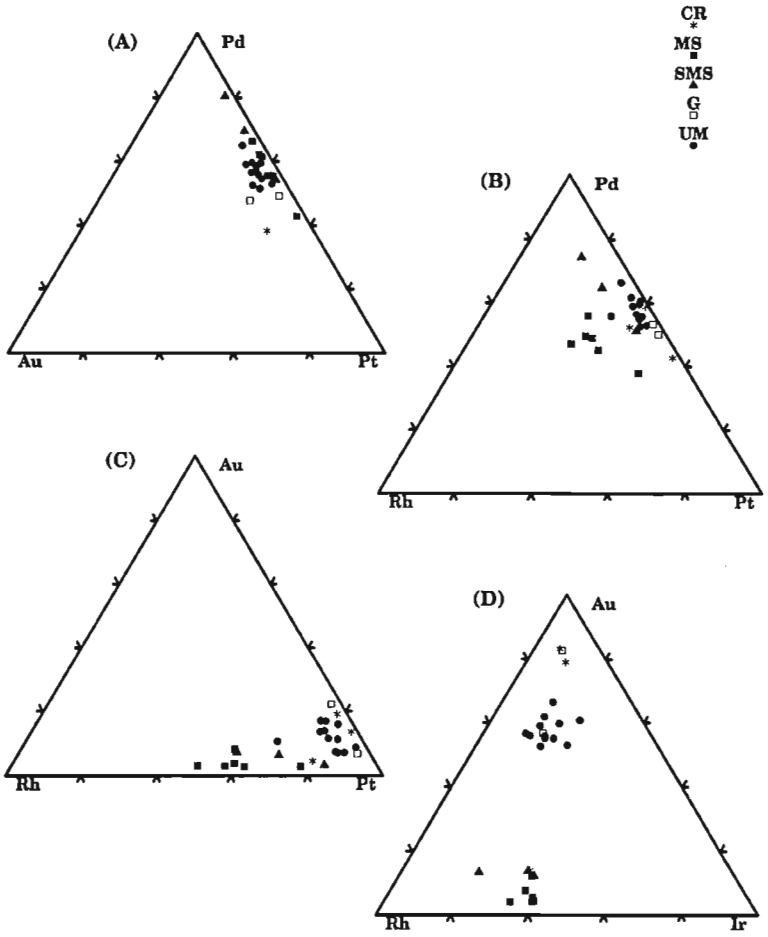

Figure 142 (A-D).

Pd-Au-Pt, Pd-Rh-Pt, Au-Rh-Pt, and Au-Rh-Ir ternary compositions of ultramafic (UM), gabbroic (G), massive sulphide (MS), semi-massive sulphide (SMS), and country rock (CR) lithologies associated with the Arch Creek Intrusive Complex.

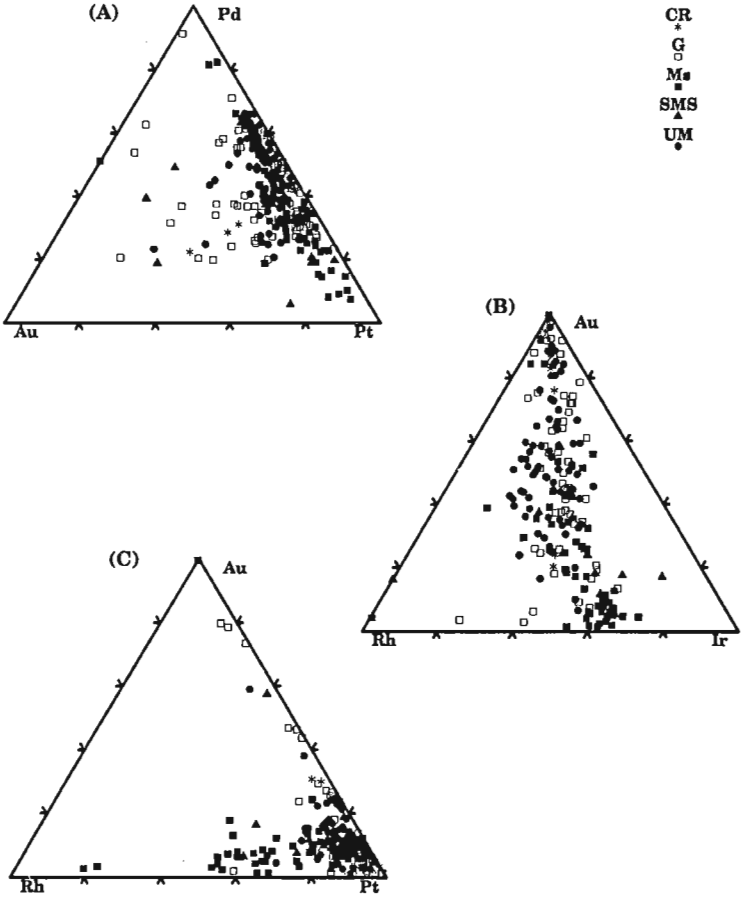

Figure 143 (A-C).

Pd-Au-Pt, Au-Rh-Ir, and Au-Rh-Pt ternary compositions of ultramafic (UM), gabbroic (G), massive sulphide (Ms), semi-massive sulphide (SMS), and country rock (CR) lithologies associated with the Quill Creek Intrusive Complex.

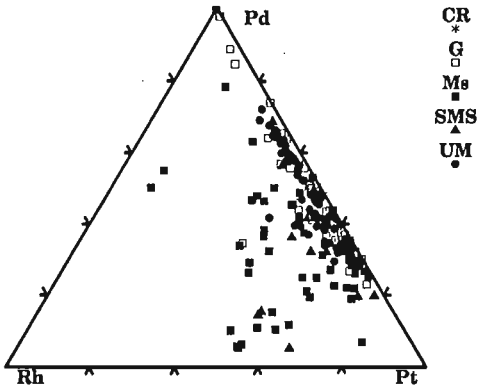

Figure 144. *Pd-Rh-Pt ternary compositions of ultramafic (UM), gabbroic (G), massive sulphide (Ms), semi-massive sulphide (SMS), and country rock (CR) lithologies associated with the Quill Creek Intrusive Complex.*

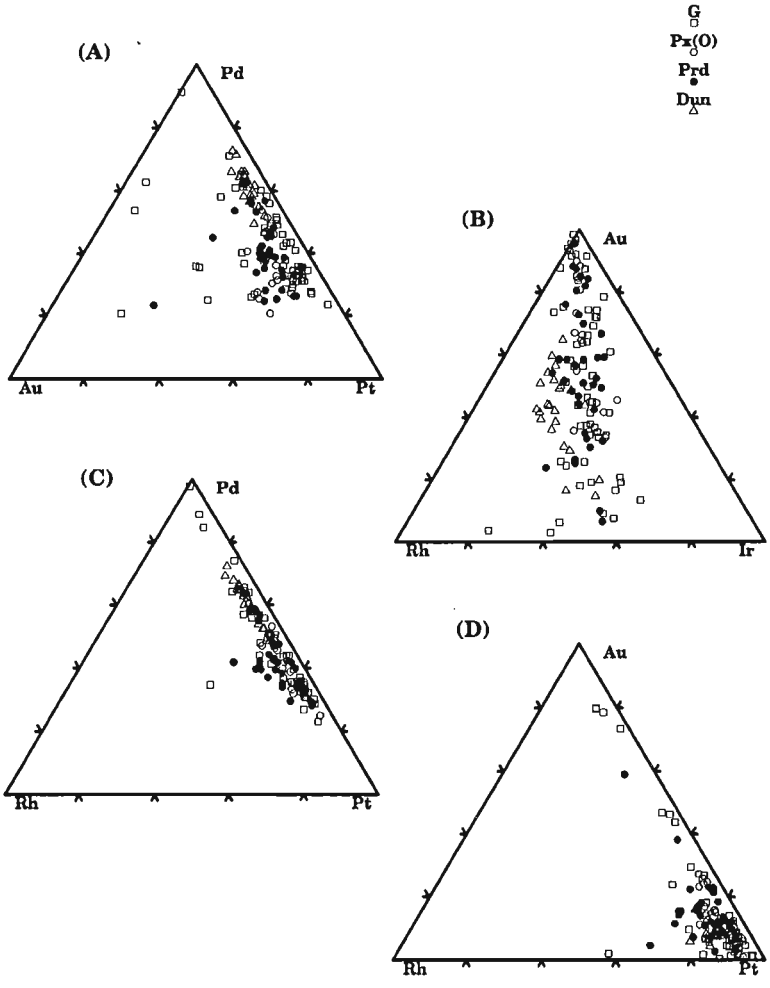

Figure 145 (A-D).

Pd-Au-Pt, Au-Rh-Ir, Pd-Rh-Pt, and Au-Rh-Pt ternary compositions of gabbroic (G), olivine pyroxenite (Px(O)), peridotite (Prd), and dunite (Dun) lithologies associated with the Quill Creek Intrusive Complex.

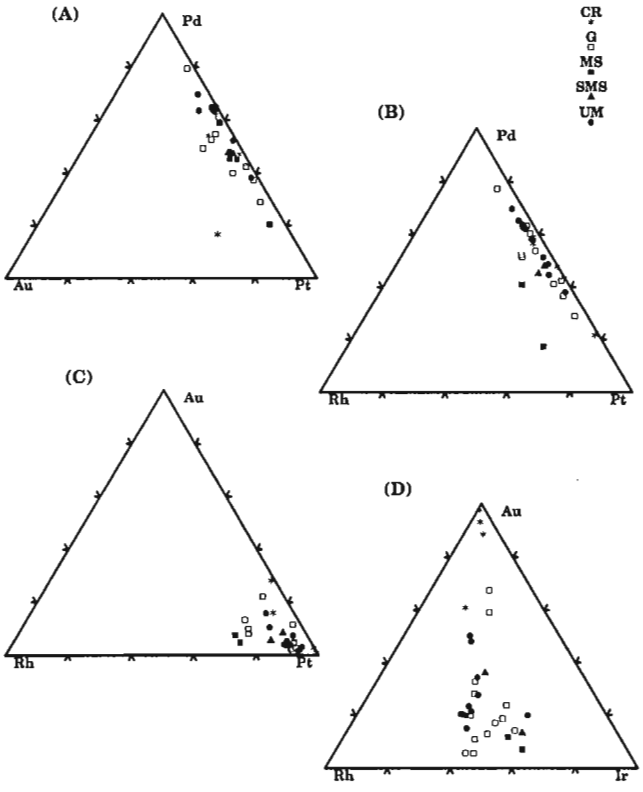

Figure 146 (A-D).

Pd-Au-Pt, Pd-Rh-Pt, Au-Rh-Pt, and Au-Rh-Ir ternary compositions of ultramafic (UM), gabbroic (G), massive sulphide (MS), semi-massive sulphide (SMS), and country rock (CR) lithologies associated with the Linda Creek Intrusive Complex.

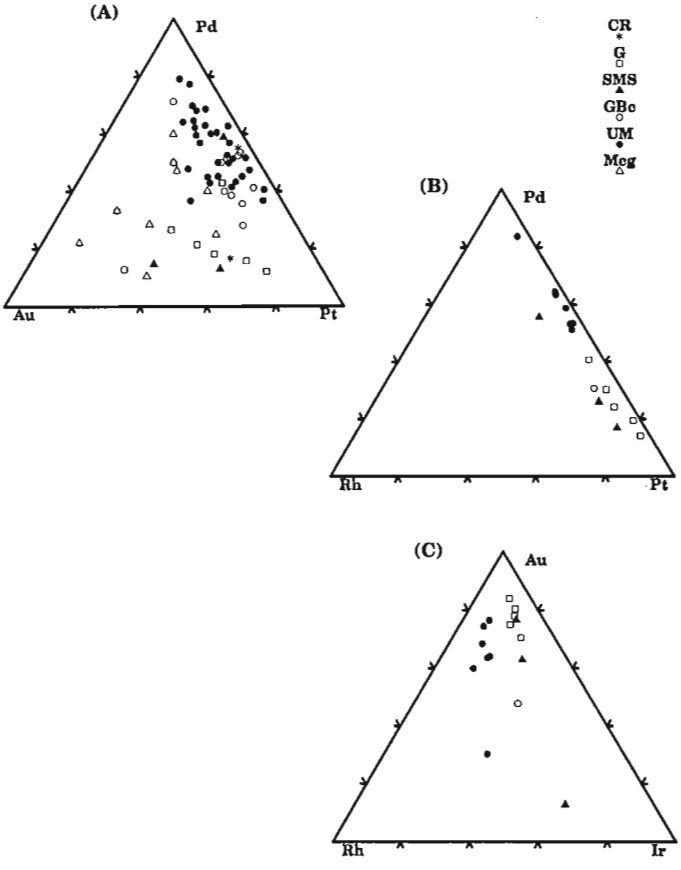

Figure 147 (A-C).

Pd-Au-Pt, Pd-Rh-Pt, and Au-Rh-Ir ternary compositions of ultramafic (UM), gabbroic (G), basal gabbro (GBc), Maple Creek gabbro (Mcg), semi-massive sulphide (SMS), and country rock (CR) lithologies associated with the Tatamagouche Creek Intrusive Complex.

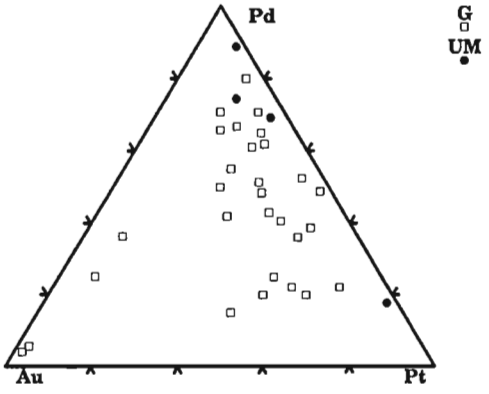

Figure 148. Pd-Au-Pt ternary compositions of ultramafic (UM) and gabbroic (G) lithologies associated with the Duke River Intrusive Complex.

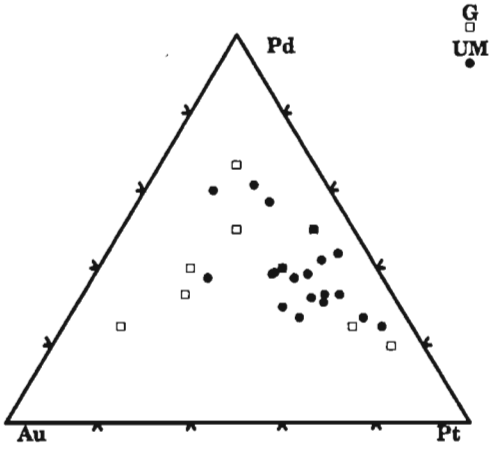

Figure 149. Pd-Au-Pt ternary compositions of ultramafic (UM) and gabbroic (G) lithologies associated with the Halfbreed Creek Intrusive Complex.

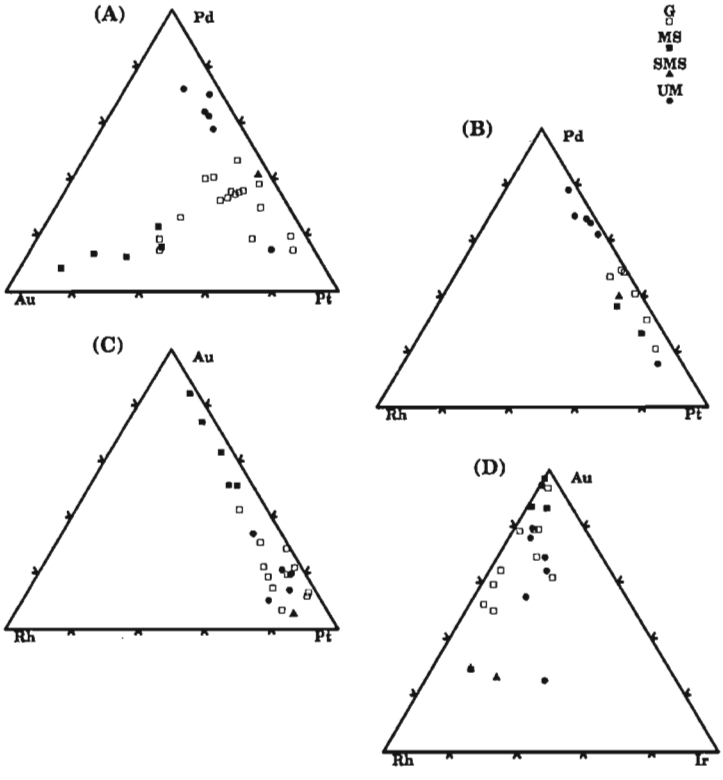

Figure 150 (A-D).

Pd-Au-Pt, Pd-Rh-Pt, Au-Rh-Pt, and Au-Rh-Ir ternary compositions of ultramafic (UM), gabbroic (G), massive country rock (exhalative ?) sulphide (MS), and semi-massive sulphide (SMS) lithologies associated with the Dickson Creek Intrusive Complex.

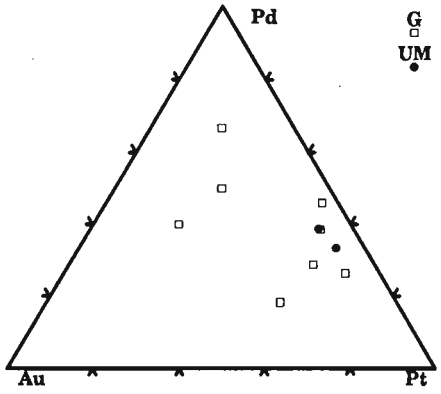

Figure 151. Pd-Au-Pt ternary compositions of ultramafic (UM) and gabbroic (G) lithologies associated with the Chilkat Intrusive Complex.

This chondrite normalizing process allows comparison of profiles from different complexes and lithologies and is independant of sulphide content. Profiles for the various lithological groups from the respective complexes are summarized in Figures 152 to 164. For comparison, profiles from other well documented Ni and Ni-Cu sulphide deposits are also given (Fig. 165, Naldrett, 1981b). It is generally believed that these profiles can be used to characterize the nature of the parental magma from which the sulphides have segregated, but this study demonstrates that such an assumption is incorrect and that profiles indicative of ophiolite, komatiite, continental flood basalt (tholeiite), stratiform layered intrusions, and even hydrothermal mineralization can be found in a single massive sulphide body. In many cases early segregating sulphides have radically different profiles than subsequent sulphides segregating from the same magma batch and mineralizing event comprising a sulphide body.

Massive sulphides from the Kluane Belt are characterized by four different chondrite normalized PGE+Au profiles (Fig. 152A to 164A). A few profiles have moderate to strong negative slopes resulting from Rh, Pt, Pd, and Au depletion relative Os, Ir, and Ru, and are best displayed in samples from the Onion property (Fig. 152A) and the Rainbow Mountain Complex (Fig. 164A). These so-called primitive profiles are characteristic of chondrite normalized PGE+Au profiles from ophiolite (Page et al., 1982a, b, 1983, 1986; Page and Talkington, 1984). The negative profiles may represent the very first immiscible sulphides to segregate from the magma as detailed sampling through massive sulphide lenses at Quill Creek Complex (Wellgreen) demonstrated that the earliest sulphides, which occur in the lower portions of most of these lenses, are very rich in Os, Ir, and Ru relative to the upper portions (Fig. 27D, E). In other lenses the concentration of Os, Ir, and Ru remain very high through the entire lens and in some cases exceed the levels of Pt, Pd, and Au (Fig. 29D, E, F). It is proposed that "in situ fractionation of sulphides" gave rise to the observed profiles.

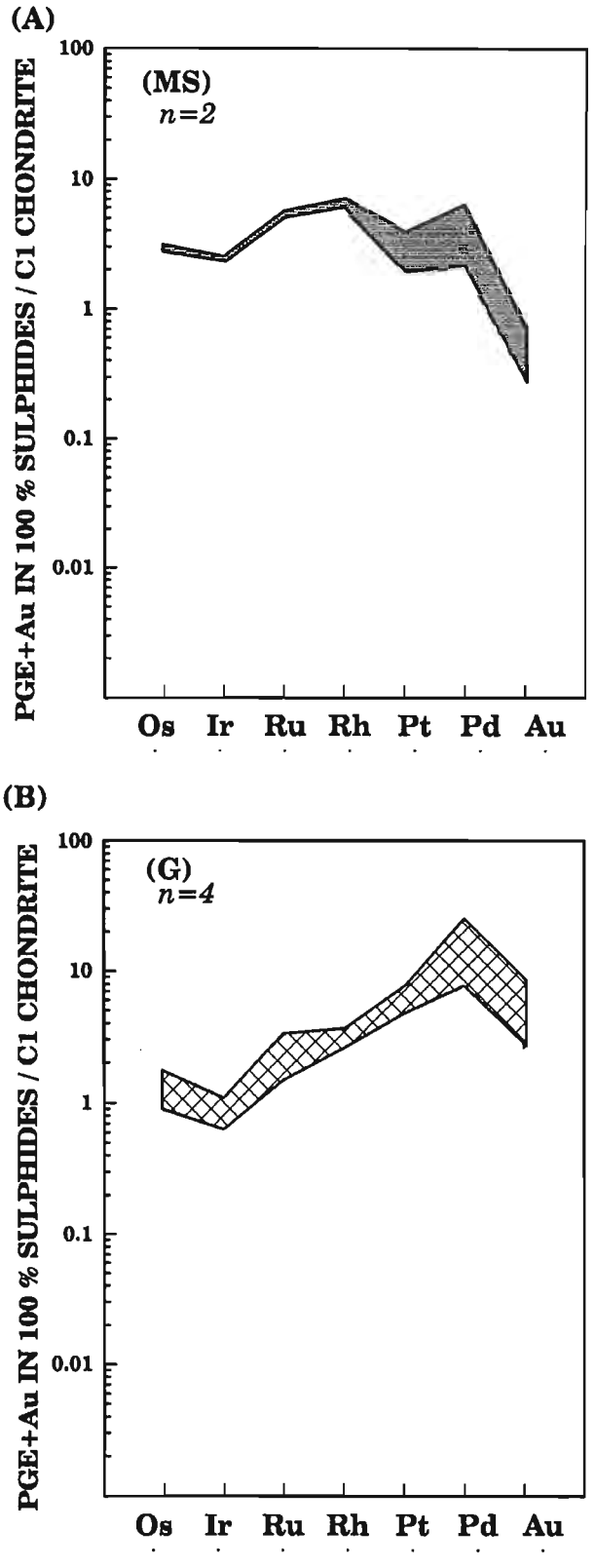

Figure 152 (A-B). Chondrite-normalized PGE+Au profiles in 100% sulphide from mineralized massive sulphide (MS) and gabbroic (G) lithologies associated with the Onion property of the White River Intrusive Complex. n = number of samples.

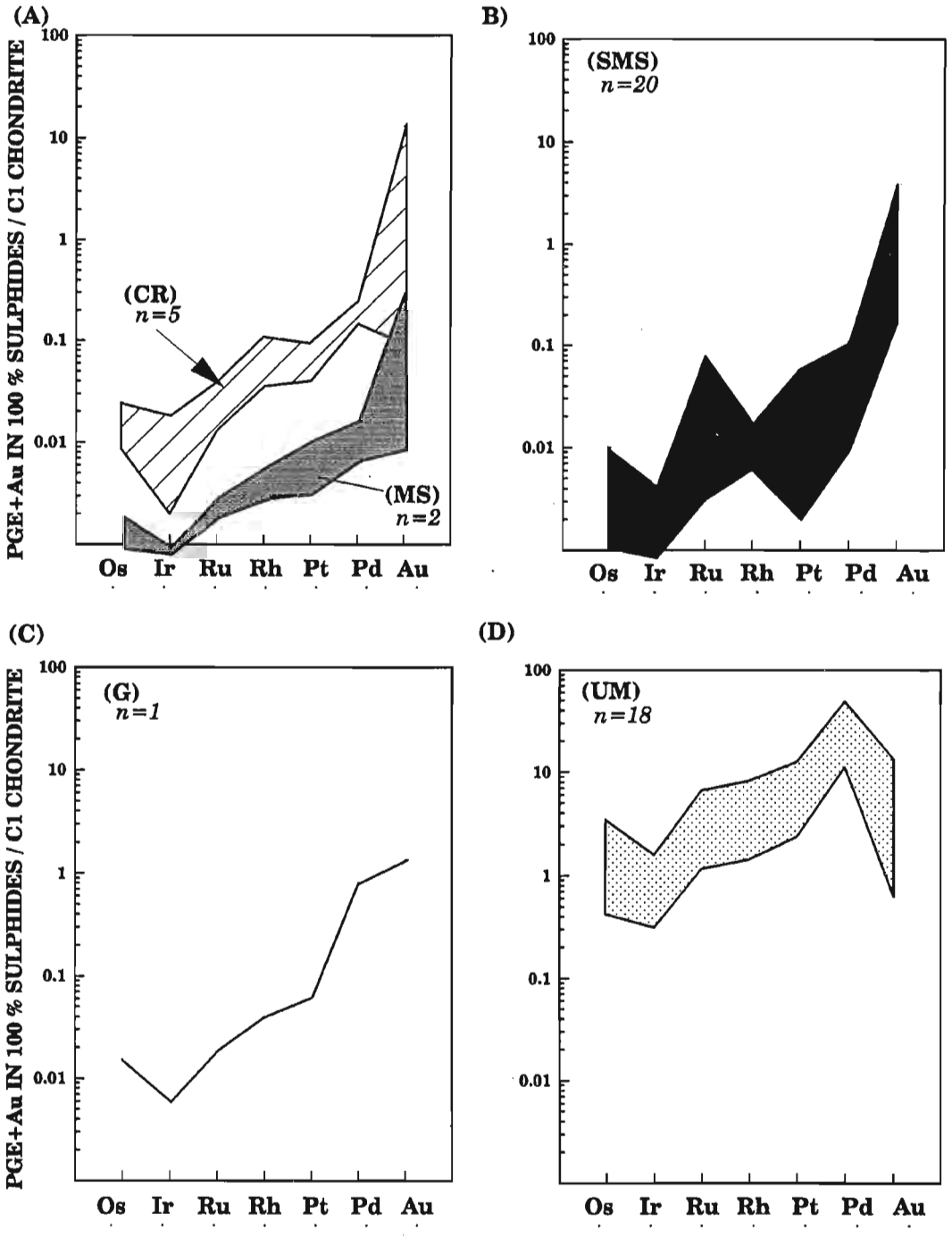

Figure 153 (A-D). *Chondrite-normalized PGE+Au profiles in 100% sulphide from mineralized country rock (CR), massive sulphide (MS), semi-massive sulphide (SMS), gabbroic (G), and ultramafic (UM) lithologies associated with the Canalask property of the White River Intrusive Complex. n = number of samples.*

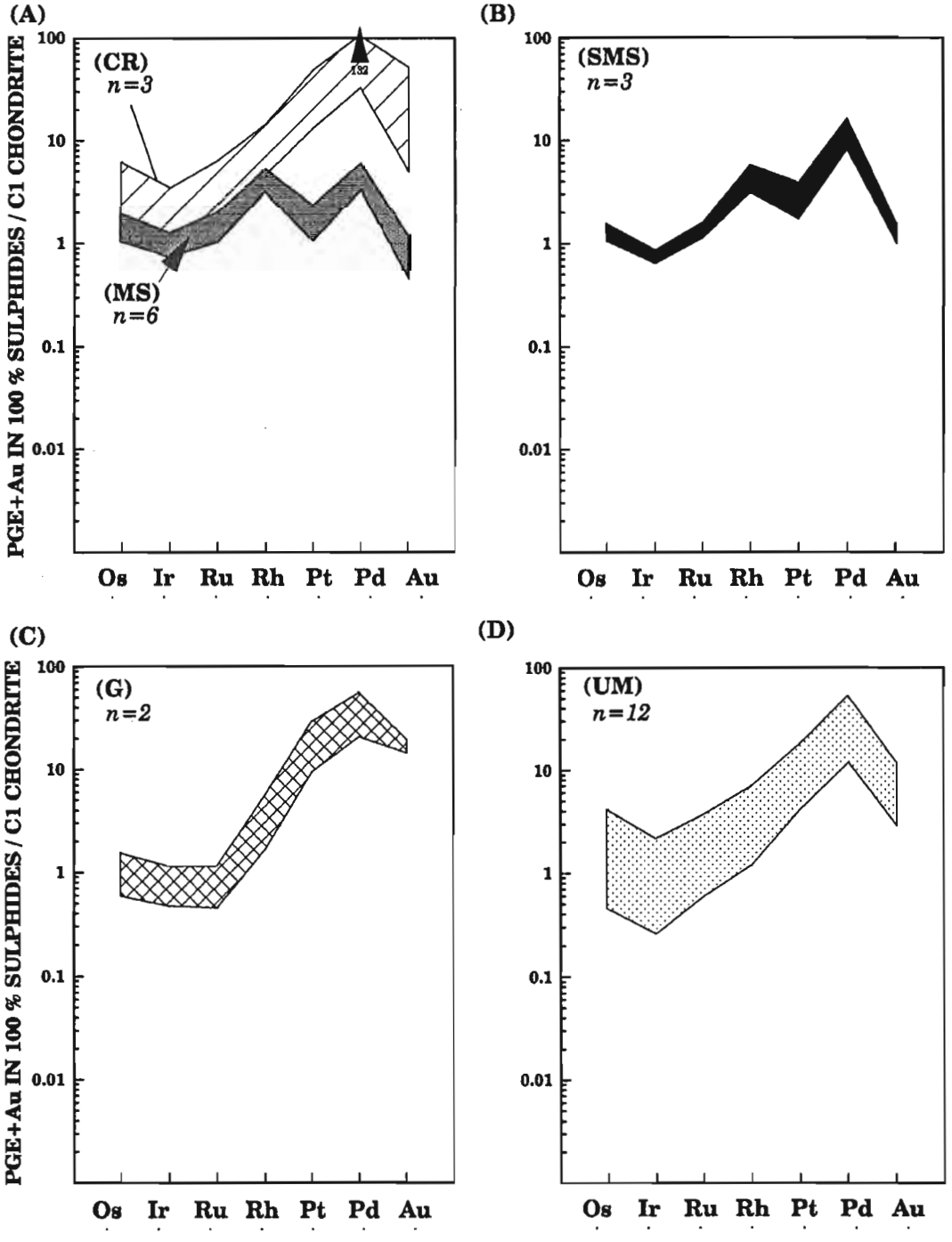

Figure 154 (A-D). Chondrite-normalized PGE+Au profiles in 100% sulphide from mineralized country rock (CR), massive sulphide (MS), semi-massive sulphide (SMS), gabbroic (G), and ultramafic (UM) lithologies associated with the Arch Creek Intrusive Complex. n = number of samples.

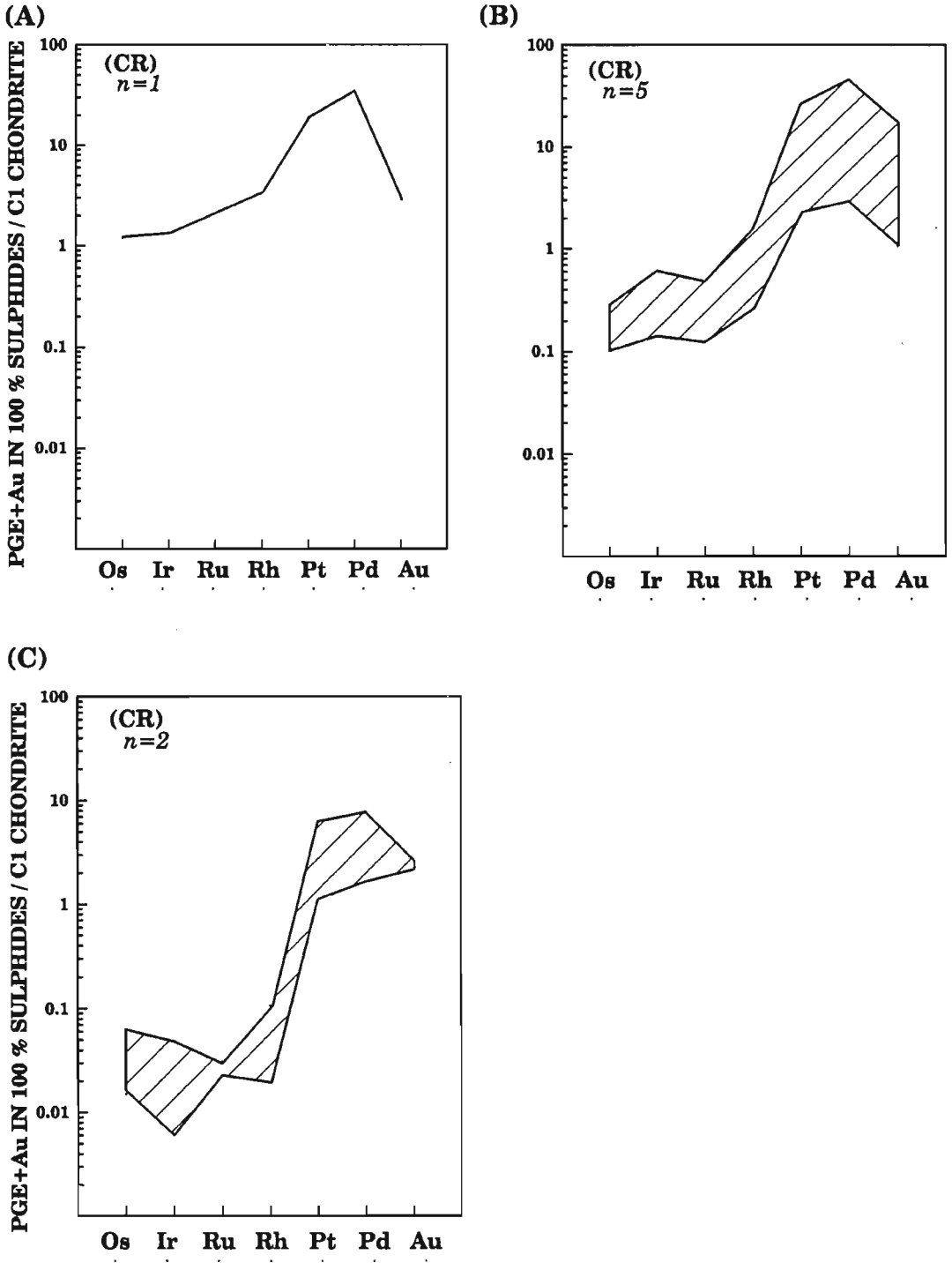

Figure 155 (A-C). *Chondrite-normalized PGE+Au profiles in 100% sulphide from mineralized country rock (CR) lithologies associated with the Quill Creek Intrusive Complex. n = number of samples. The mineralized samples have been divided into three groups on the basis of their chondrite normalized Os ratio in 100% sulphide: (**A**) = flat to weakly negative profiles: (Os/C1)n ≥ 1.0; (**B**) flat to weakly positive profiles: (Os/C1)n ≥ 0.1 and ≤ 1.0; (**C**) moderate to steeply dipping positive slopes: (Os/C1)n ≤ 0.1.*

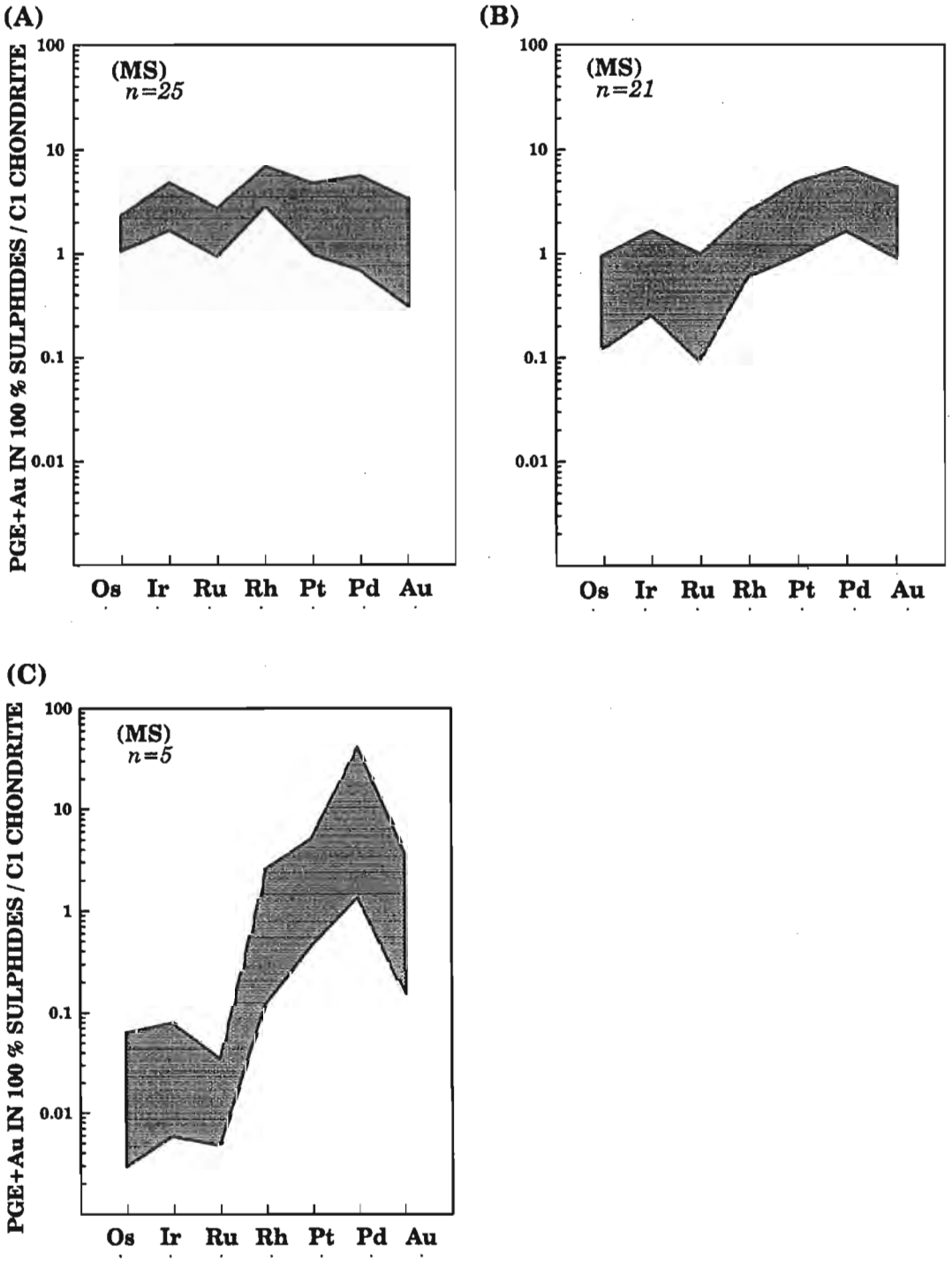

Figure 156 (A-C). *Chondrite-normalized PGE+Au profiles in 100% sulphide from massive sulphide (MS) lithologies associated with the Quill Creek Intrusive Complex. n = number of samples. The mineralized samples have been divided into three groups on the basis of their chondrite normalized Os ratio in 100% sulphide: (**A**) = flat to weakly negative profiles: (Os/C1)n ≥ 1.0; (**B**) flat to weakly positive profiles: (Os/C1)n ≥ 0.1 and ≤ 1.0; (**C**) moderate to steeply dipping positive slopes: (Os/C1)n ≤ 0.1.*

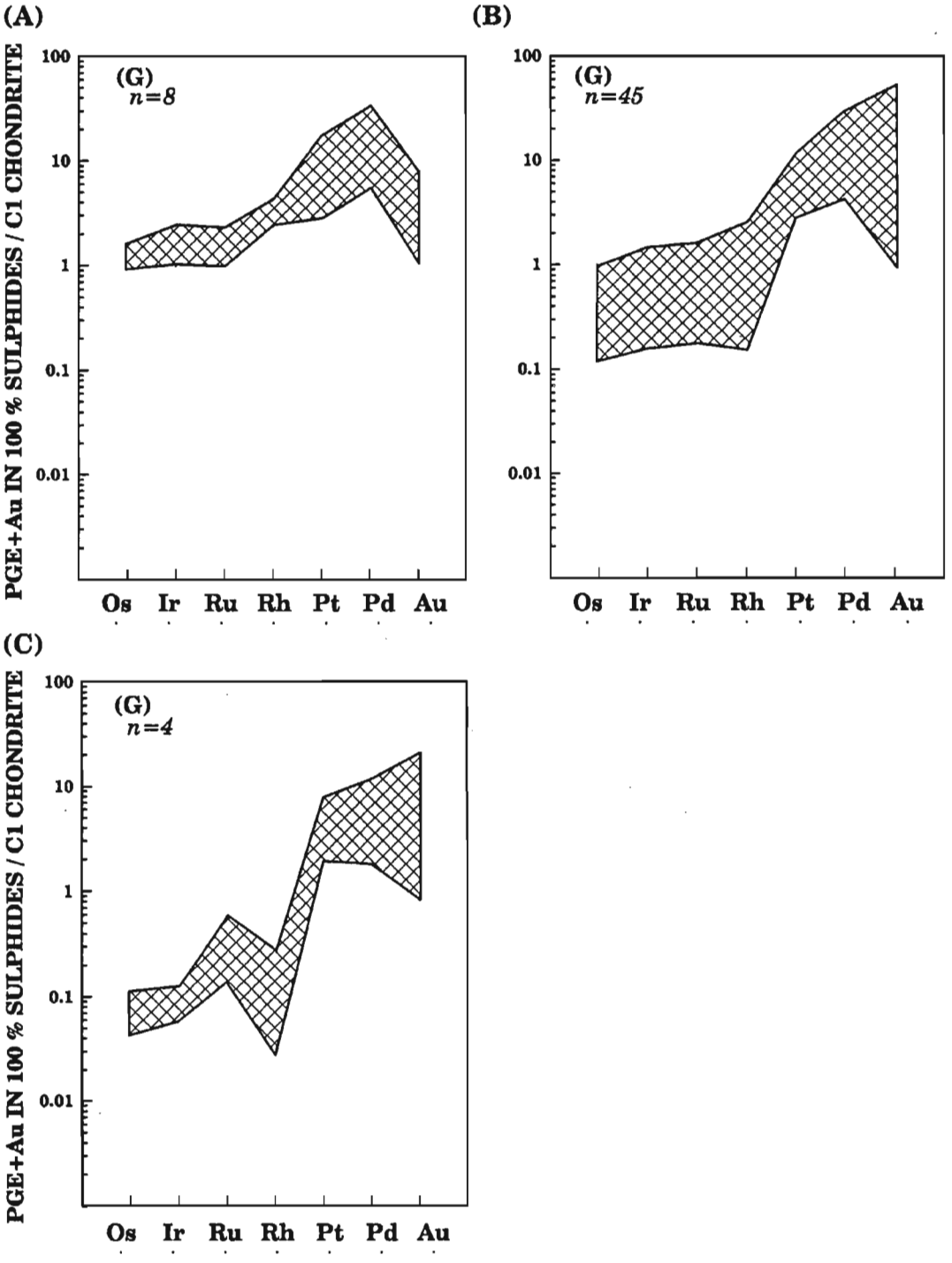

Figure 157 (A-C). *Chondrite-normalized PGE+Au profiles in 100% sulphide from mineralized gabbroic (G) lithologies associated with the Quill Creek Intrusive Complex. n = number of samples. The mineralized samples have been divided into three groups on the basis of their chondrite normalized Os ratio in 100% sulphide: (**A**) = flat to weakly negative profiles: (Os/C1)n ≥ 1.0; (**B**) flat to weakly positive profiles: (Os/C1)n ≥ 0.1 and ≤ 1.0; (**C**) moderate to steeply dipping positive slopes: (Os/C1)n ≤ 0.1.*

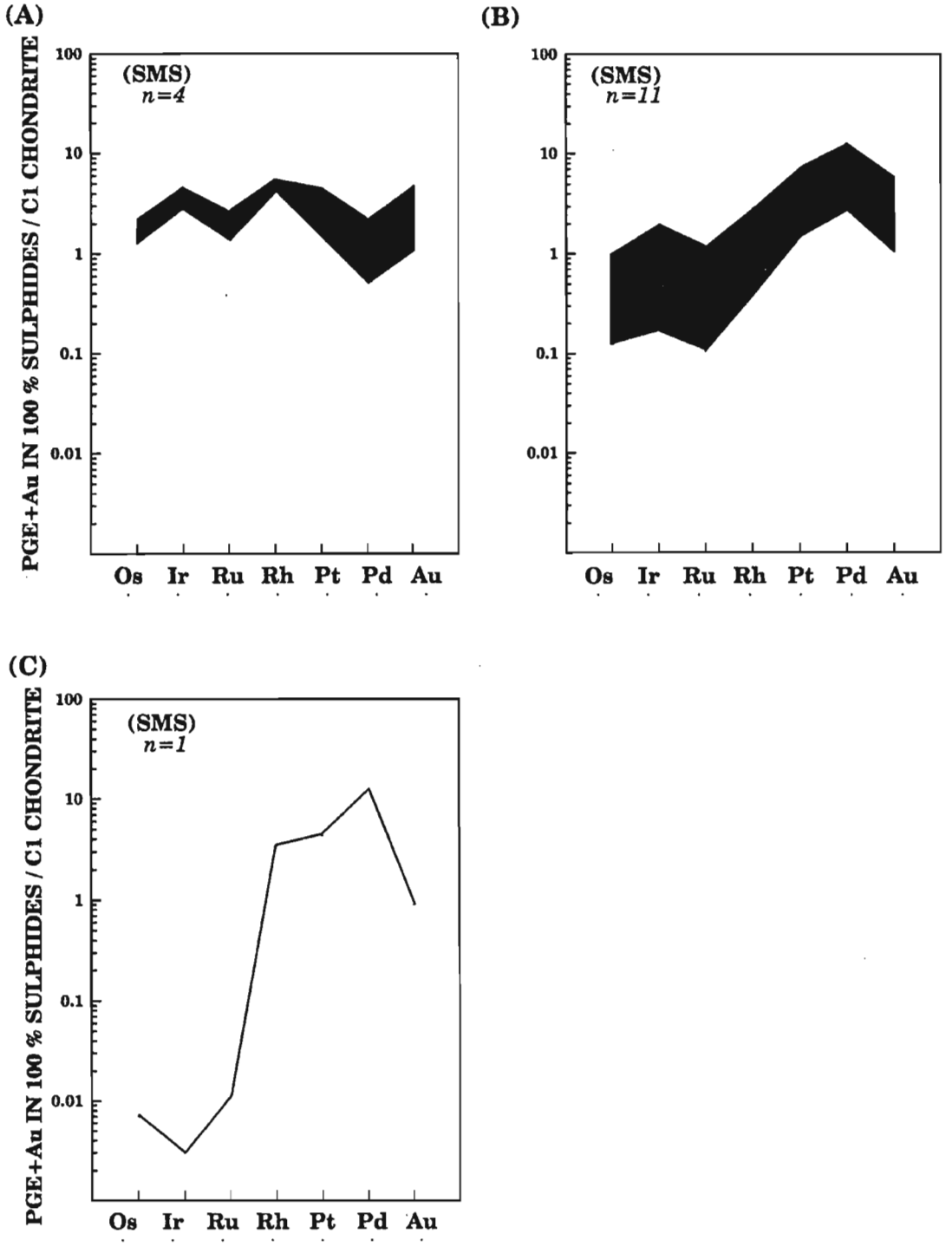

Figure 158 (A-C). *Chondrite-normalized PGE+Au profiles in 100% sulphide from semi-massive sulphide (SMS) lithologies associated with the Quill Creek Intrusive Complex. n = number of samples. The mineralized samples have been divided into three groups on the basis of their chondrite normalized Os ratio in 100% sulphide: (**A**) = flat to weakly negative profiles: (Os/C1)n ≥ 1.0; (**B**) flat to weakly positive profiles: (Os/C1)n ≥ 0.1 and ≤ 1.0; (**C**) moderate to steeply dipping positive slopes: (Os/C1)n ≤ 0.1.*

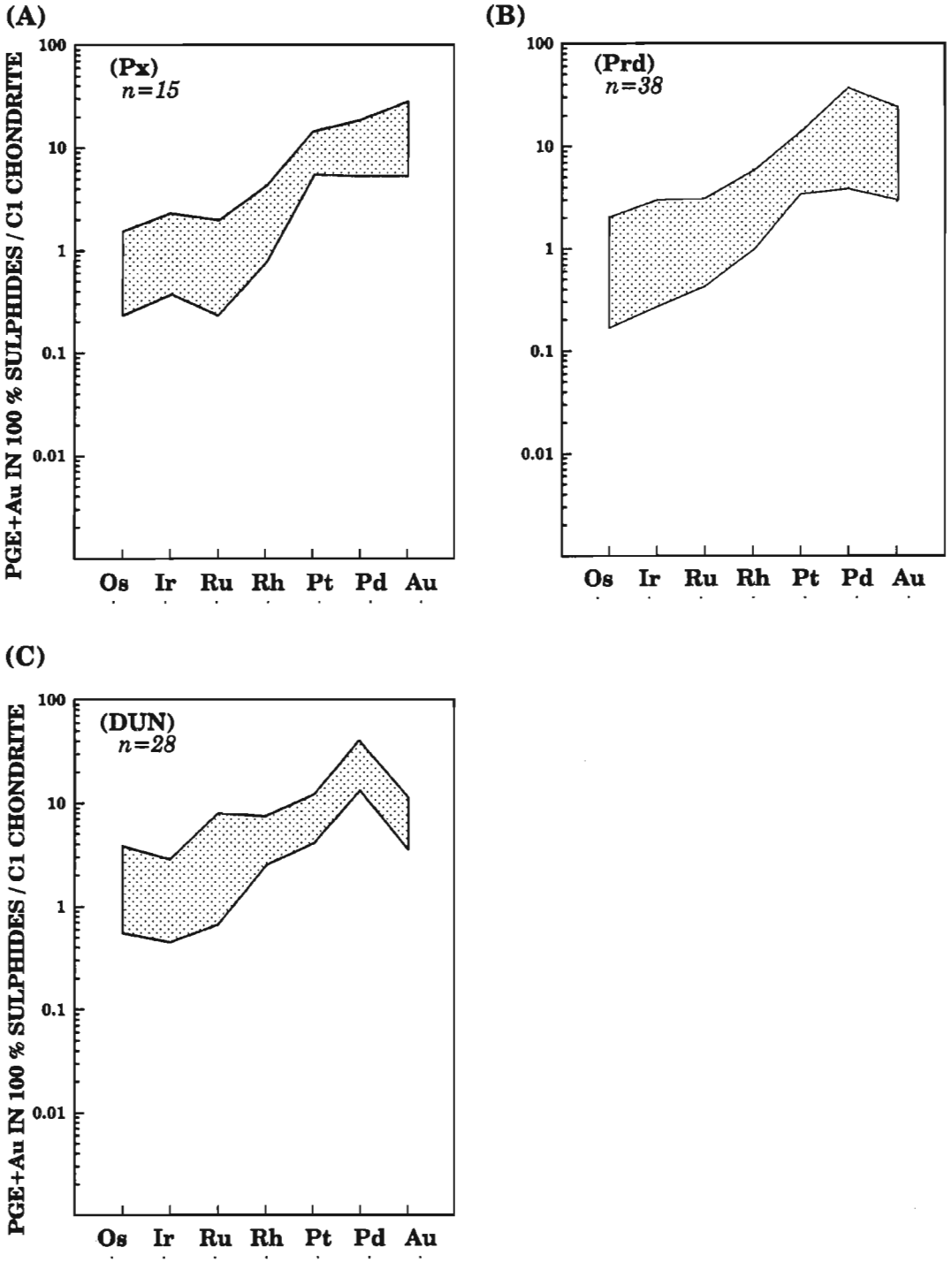

Figure 159 (A-C). *Chondrite-normalized PGE+Au profiles in 100% sulphide from mineralized ultramafic lithologies: clinopyroxenite, olivine clinopyroxenite (Px), peridotite (Prd), and dunite (DUN) lithologies associated with the Quill Creek Intrusive Complex. n = number of samples.*

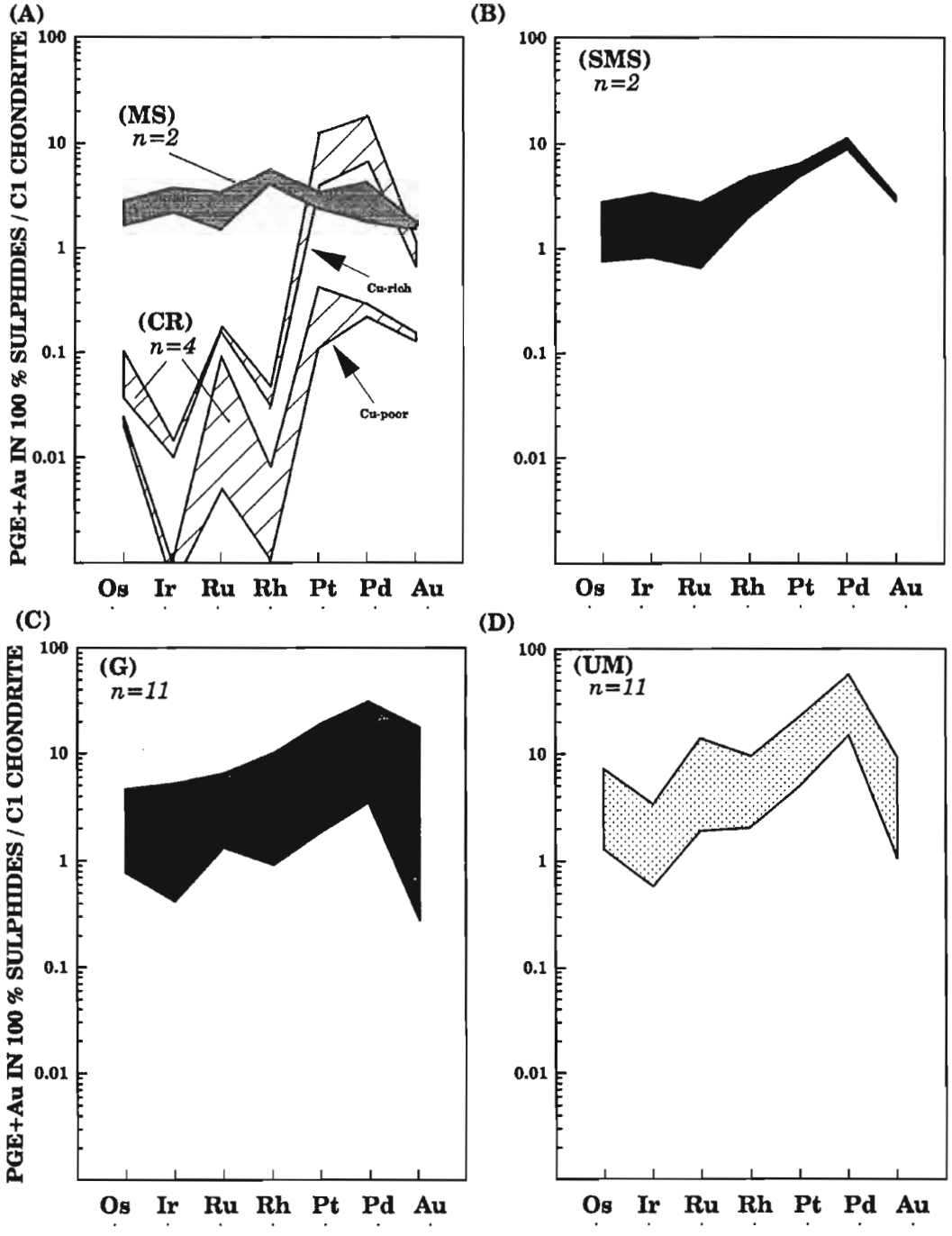

Figure 160 (A-D). *Chondrite-normalized PGE+Au profiles in 100% sulphide from mineralized massive sulphide (MS) and country rock (CR), semi-massive sulphide (SMS), gabbroic (G), and ultramafic (UM) lithologies associated with the Linda Creek Intrusive Complex. n = number of samples.*

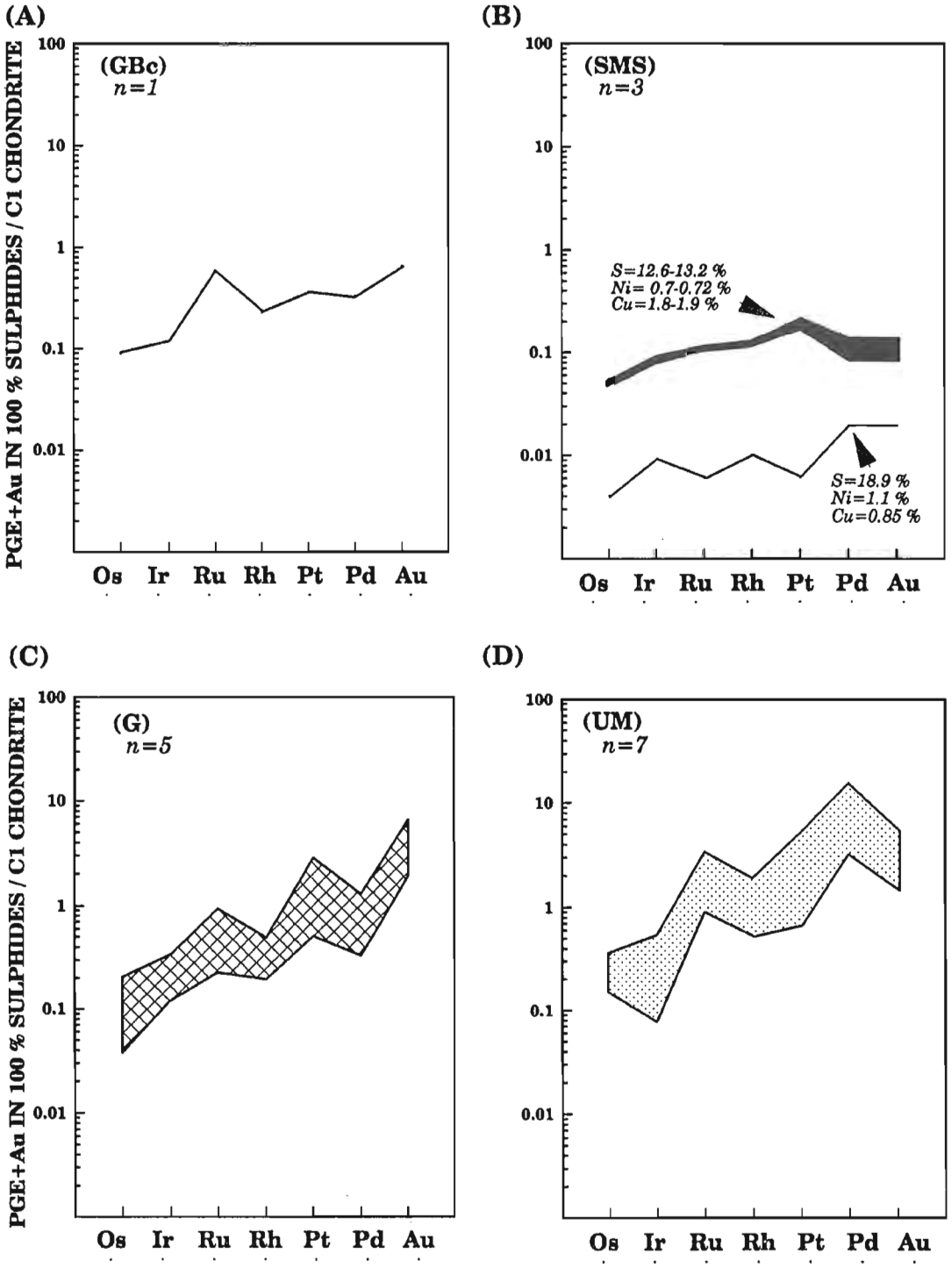

Figure 161 (A-D). *Chondrite-normalized PGE+Au profiles in 100% sulphide from mineralized gabbro cumulate (GBc), semi-massive sulphide (SMS), gabbroic (G), and ultramafic (UM) lithologies associated with the Tatamagouche Creek Intrusive Complex. n = number of samples.*

During the crystallization of the sulphide melt the monosulphide solid solution (which is the first phase to crystallize) prefers to accommodate the Ir-group (Os, Ir, Ru) over the Pd-group (Rh, Pt, Pd, Au) noble metals (Distler et al., 1977; Naldrett et al., 1982; Barnes and Naldrett, 1987). The monosulphide solid solution settles to the bottom of the sulphide liquid thereby depleting the remaining sulphide melt in Ir-group elements. Flat chondrite normalized PGE+Au profiles similar to those in Figures 154A, 156A, B, and 160A are common in the massive sulphide lenses from the Arch, Wellgreen, and Linda properties. At Wellgreen, extensive detailed sampling of massive sulphides, as well as other mineralized lithologies, provided an opportunity to study the factors controlling the distribution of the PGE+Au and the resulting chondrite normalized profiles in 100% sulphide.

Massive sulphides (as well as semi-massive sulphides, mineralized gabbro, and country rock material) can be divided into three groups on the basis of their chondrite normalized Os ratio in 100% sulphide, $(Os/C1)_n$: (1) flat to weakly negative profiles, $(Os/C1)_n \geq 1.0$; (2) flat to weakly positive sloping profiles, $(Os/C1)_n \geq 0.1$ and ≤ 1.0, and (3) moderate to steeply dipping positive slopes $(Os/C1)_n \leq 0.1$. Massive sulphides from Wellgreen (Quill Creek Complex) divided on this basis are shown in Figure 156. The shape of these profiles is generally a function of sample location within the sulphide lenses, which in turn is controlled by fractional crystallization of the evolving sulphide melt. Massive sulphides with $(Os/C1)_n \geq 1.0$ tend to be the most Ni-rich samples. The profiles in Figure 156 could be considered representative of the lower, intermediate, and upper portions of some sulphide lenses, respectively. Steep positive profiles, similar to Figure 156C, are associated with massive sulphide segregations injected into the footwall. Some massive sulphides (Canalask and Dickson Creek, Fig. 153, 163) are extremely impoverished in all PGE+Au and have positive slopes similar to that of the semi-massive sulphide samples, but they are also anomalously enriched in Au.

Semi-massive sulphides are generally enriched in Rh, Pt, Pd, and Au relative to their massive counterparts (Arch, Wellgreen, Linda, Canalask). Detailed sampling and classification on the basis of $(Os/C1)_n$ and a large number of samples at Wellgreen also indicate that both flat and moderately positive sloping profiles occur not only within the same deposit, but also in the same orebody or sulphide lens (Fig. 158). Rare, very steeply trending profiles (Fig. 158C) tend to be associated with footwall segregations, but in some cases they appear to be late stage primary magmatic Cu-rich differentiates. Although present in lower absolute concentrations, semi-massive, primary, magmatic sulphides from Tatamagouche (Fig. 161B), and those hosted in ultramafic rocks at Dickson Creek (Fig. 163B) also display relatively flat profiles. Copper-rich (1.8-1.9 wt.%) samples from Tatamagouche have profiles that are an order of magnitude higher than that associated with the relatively Cu-poor (0.85%) sample. With the exception of the Canalask massive and semi-massive "offset" mineralization, Kluane massive and semi-massive sulphide mineralization generally has flat to moderately positive sloping chondrite normalized PGE+Au profiles.

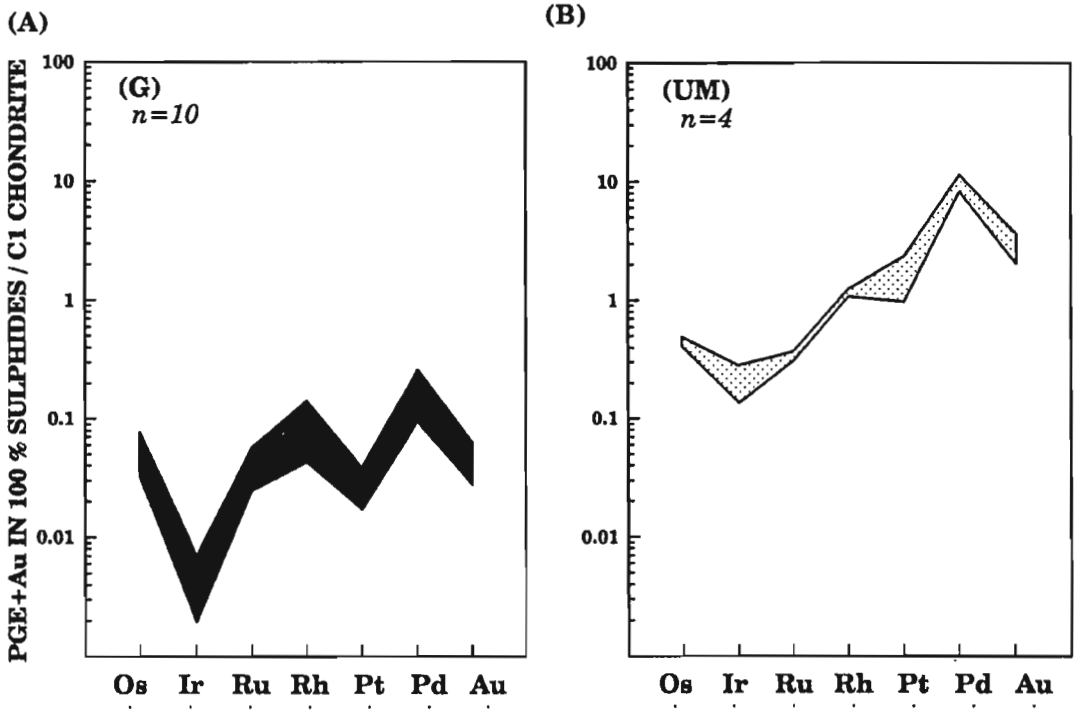

Figure 162 (A-B). Chondrite-normalized PGE+Au profiles in 100% sulphide from mineralized gabbroic (G) and ultramafic (UM) lithologies associated with the Duke River Intrusive Complex. n = number of samples.

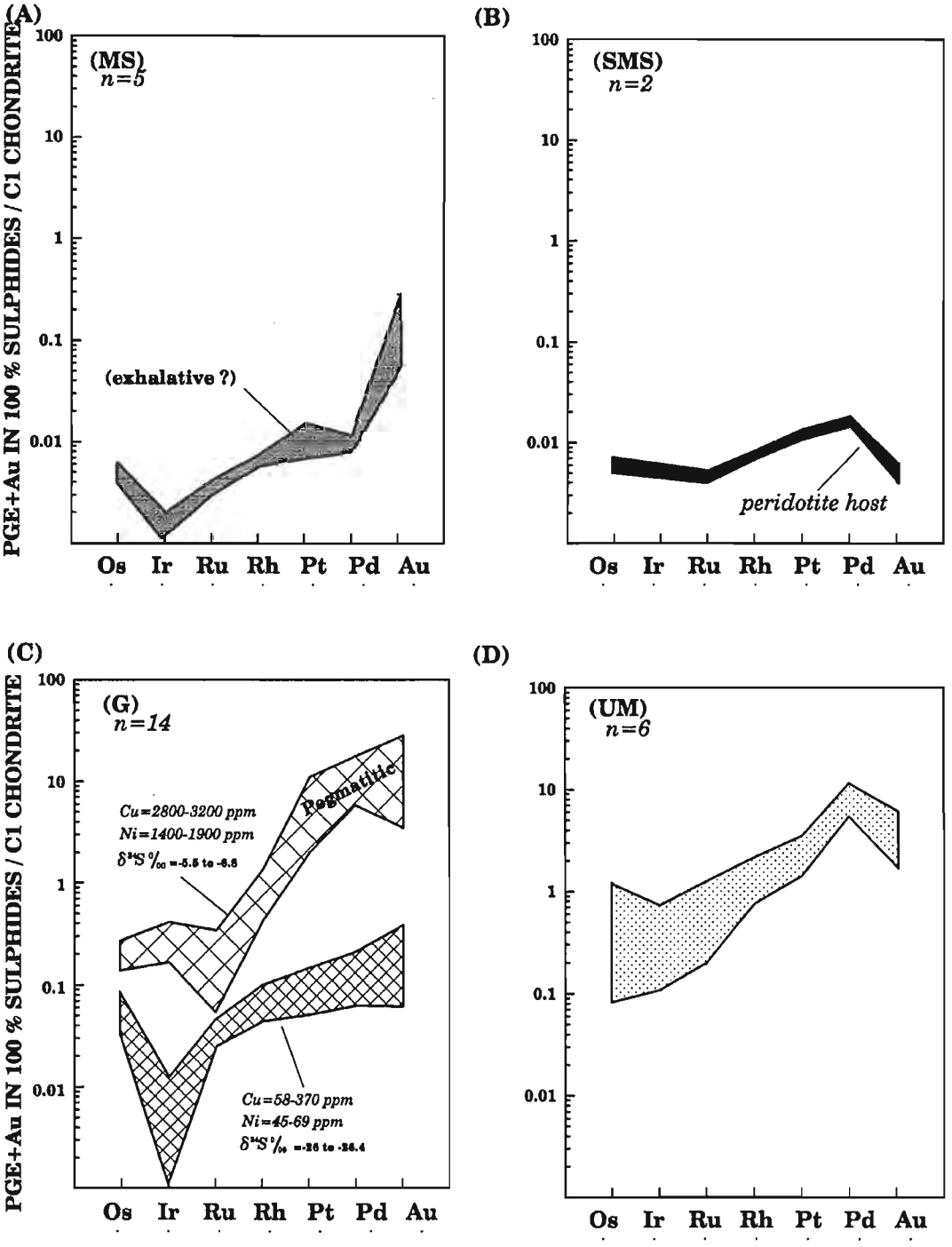

Figure 163 (A-D). Chondrite-normalized PGE+Au profiles in 100% sulphide from mineralized massive country rock (exhalative ?) sulphide (MS), semi-massive sulphide (SMS), gabbroic (G), and ultramafic (UM) lithologies associated with the Dickson Creek Intrusive Complex. n = number of samples.

These profiles are most similar to those established for komatiite-hosted Ni-sulphide ores (Fig. 165A) but the noble metal grades for representative Kluane mineralization are superior to those of typical komatiite. The Os, Ir and Ru, Rh and Pt levels for the Kluane mineralization are also higher than that of the pyroxenitic komatiite from the Cape Smith Belt of Ungava, but the latter have distinctively higher Pd contents. Nevertheless, based on the Mg# of the chilled margins and the consanguineous Nikolai volcanic rocks, the composition of olivine, clinopyroxene, and chromite, the REE profiles, and other geochemical constraints, it is apparent that the parental magma to the Kluane mafic and ultramafic complexes was tholeiitic in character. Discussions related to the nature of the parental magma are given in a subsequent section. Examination of Figure 165C also demonstrates the higher PGE tenor of the Kluane ores relative to typical Sudbury ore.

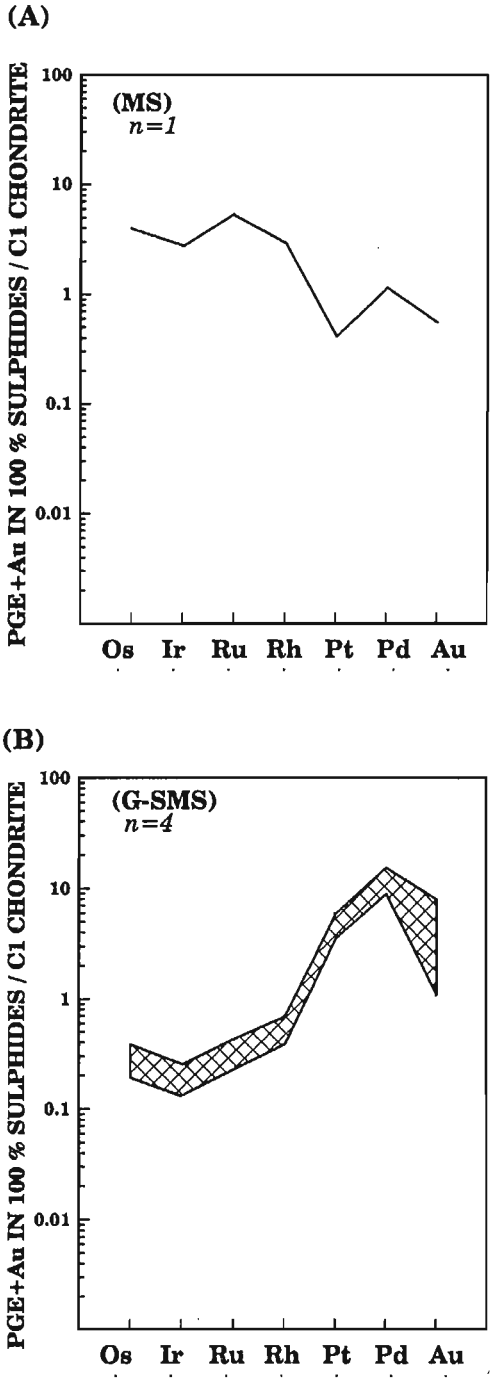

Figure 164 (A-B). *Chondrite-normalized PGE+Au profiles in 100% sulphide from mineralized massive sulphide (MS) and gabbroic semi-massive sulphide (G-SMS) lithologies associated with the Rainbow Mountain Intrusive Complex, Alaska. n = number of samples.*

Mineralized gabbroic rocks generally have steeper positive sloping profiles than associated semi-massive and massive sulphides. The profiles shown in Figures 152, 154, 160, 161, 162, 163, and 164 demonstrate that they are not as steep as those for the sulphide ores from Minnamax and Great Lakes Nickel deposits (related to the Proterozoic Keweenawan continental flood basalt province of Lake Superior), but are closer to those of the Permo-Triassic continental flood basalt related Oktyabr'sk-Talnakh ores from the Noril'sk-Talnakh mining camp of Siberia. The normalized concentration for these gabbroic rocks spans that established for the Minnamax-Great Lakes Nickel and Oktyabr'sk-Talnakh ores shown in Figure 165B. As was the case with the semi-massive and massive sulphides from Wellgreen, gabbroic rocks from this locality can be divided on the basis of similar $(Os/C1)_n$ values established for the sulphide-rich samples (Fig. 157). Samples with $(Os/C1)_n \geq 1.0$ (Fig. 157A) are enriched in Os, Ir, Ru, Rh, and Pt whereas samples with ratios ≤ 1.0 are notably enriched in Au and have steeper profiles. Mineralized gabbroic rocks from Dickson Creek also demonstrate some interesting trends and features (Fig. 163C). The lower profile is associated with pegmatitic and medium-grained gabbro from the upper contact zone. These rocks are not unlike those represented by the upper profile (both contain 1-2% S) apart from being slightly more pegmatitic. However, the comparably mineralized gabbro from the lower profile is poor in Cu (58-370 ppm) and Ni (45-69 ppm) relative to the gabbro representative of the upper profile (Cu = 2800-3200, Ni = 1400-1900 ppm). Also, mineralization representative of the upper profile contains significantly more mantle-derived sulphur ($\delta^{34}S$ = -5.5 to -6.8‰) than the mineralization from the lower depleted profile ($\delta^{34}S$ = -26.0 to -26.4‰). This relationship suggests that comparable levels of sulphides from the upper profile have equilibrated with a larger volume of magma in which to scavenge PGE+Au as well as Ni and Cu.

Ultramafic rocks tend to have the most characteristic chondrite-normalized PGE+Au profiles with respect to slope and pattern, although the concentration levels vary noticeably (Fig. 153, 154, 159, 160, 161, 162, 163). The profiles for the Canalask, Linda, Arch, and Quill Creek (Wellgreen) ultramafic rocks indicate that the sulphide fraction is enriched in PGE+Au relative to similar rocks from the Tatamagouche, Dickson Creek, and Duke River localities, but all show the distinctive Au-depletion trend. At many localities ultramafic profiles are similar to their gabbroic counterparts. The large number of ultramafic samples obtained from Quill Creek Complex (Wellgreen) allowed this group to be divided on the basis of pyroxenite (olivine clinopyroxenite), peridotite, and dunite (Fig. 159).

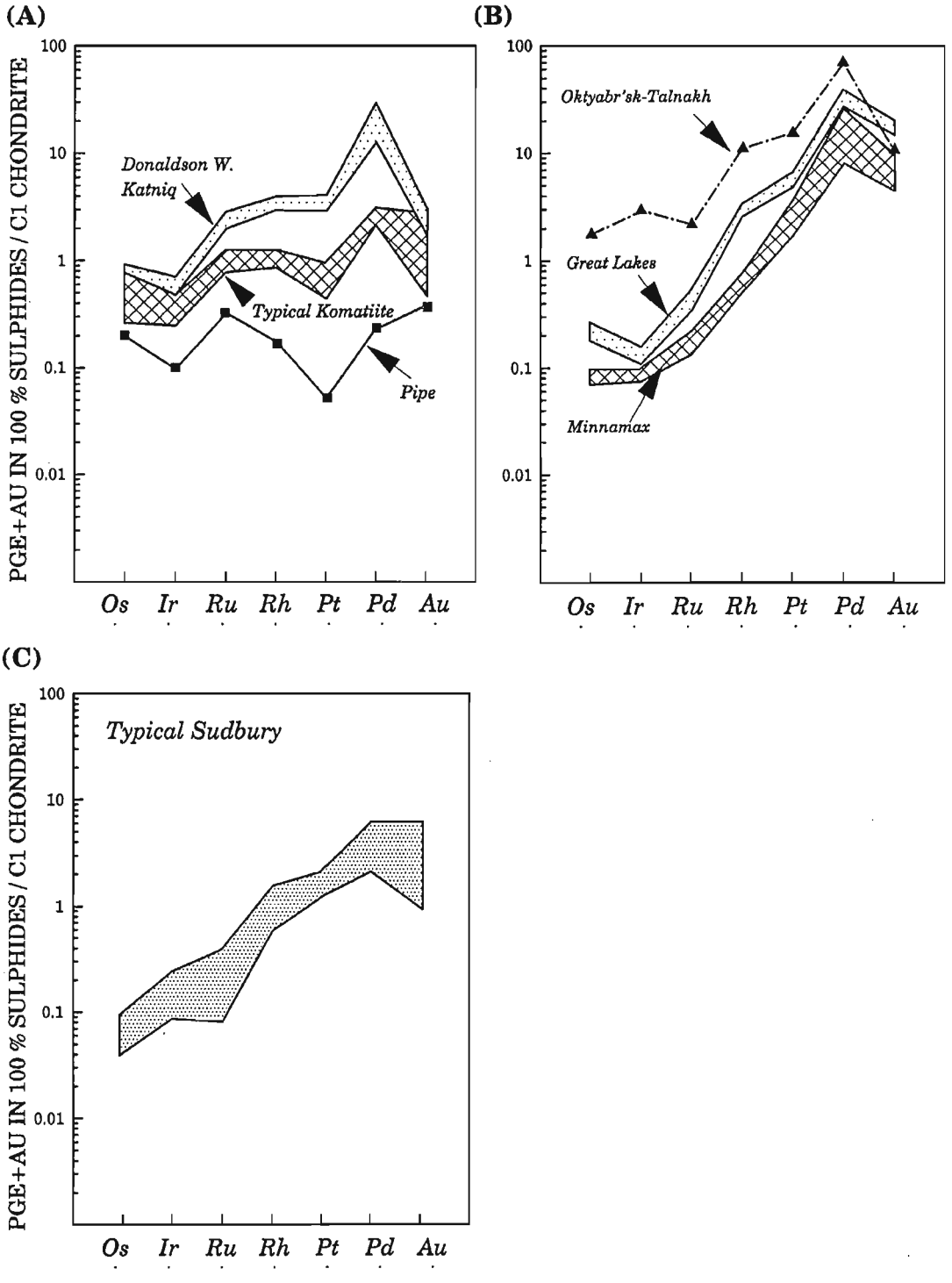

Figure 165 (A-C). *Chondrite-normalized PGE+Au profiles in 100% sulphide from other well-studied mineralized mafic-ultramafic intrusions (Naldrett, 1981) for comparison with the Kluane Belt profiles.*

From these profiles the pyroxenite sub-group displays a Au-enrichment trend and has a profile similar to the gabbro with $(Os/C1)_n$ ratios in the 0.1 to 1.0 range. Profiles for peridotite demonstrate a moderate Pd anomaly and Au-depletion trend. This trend and anomaly become even more pronounced as the ultramafic rocks progress from peridotite to dunite. In addition, as the ultramafic lithologies progress from pyroxenite to dunite, the Ir content decreases markedly. This decreasing Ir trend is accompanied by an increase in Pd, and can best be explained by fractionation of the evolving sulphide liquid. Barnes and Naldrett (1987) proposed a similar process to explain the variation in the Pd/Ir ratio of sulphides in komatiite from the Abitibi Greenstone Belt of northern Ontario.

Sulphide mineralization hosted in the adjacent country rocks generally has chondrite normalized profiles similar to that of the igneous-hosted mineralization (Fig. 153A, 154A, and 155), and thus reveals the source of these metals. Sulphides that have migrated farthest from the intrusion tend to be enriched in Pt, Pd, and Au and relatively depleted in the less mobile Ir-group (Os, Ir, Ru) elements. PGE+Au appear to be more mobile in Cu-rich than Cu-poor sulphides as shown for the remobilized country rock-hosted sulphides at the Linda property (Fig. 160A).

In conclusion, it would appear that the chondrite-normalized PGE+Au profiles in 100% sulphide is determined by in situ fractionation of the evolving sulphide melt.

WRANGELLIA: PARENTAL MAGMA(S), TECTONOMAGMATIC-STRATIGRAPHIC SETTING, AND GEOCHRONOLOGY

One of the greatest challenges encountered during the investigation of the Kluane mafic-ultramafic complexes was to establish: (1) the relationship between the intrusive complexes and the proximal Nikolai volcanic rocks and Maple Creek gabbro, (2) the nature of the parental magma and magmatic setting (i.e. oceanic; island-arc, back-arc, ocean island, etc. ? or continental), and (3) unequivocally that the terrane is part of Wrangellia. Initially terrane authenticity was complicated by recognition of macroscopic and geochemical characteristics also common to other Triassic basalt sequences in the region: Nicola, Takla, Stuhini, and Lewes River groups (Monger, 1977b; Souther, 1977; Preto, 1977; Mortimer, 1986) and Middle Tats volcanic rocks (Peters et al., in prep.) from the Stikinia-Quesnellia and Alexander terranes to the south, respectively. The Stikinia and Quesnellia volcanic terranes appear to be laterally conformable and are not far removed from the southern end of the Nikolai volcanic terrane. As the principal unifying characteristic of Wrangellia is the thick Middle to Upper Triassic tholeiitic basalt sequence, which is disconformably overlain by calcareous sediments of Carnian or earliest Norian time, any doubt concerning authenticity of the so-called Nikolai volcanic sequence questions the authenticity of the terrane. In addition, the lack of reported mafic-ultramafic intrusive complexes, and associated Ni-Cu-±PGE mineralization, from the western portion of Wrangellia, and the initially inferred primitive nature of the parental magma(s) to complexes in the Kluane Ranges (based on chondrite normalized PGE+Au profiles for sulphide mineralization) did little to corroborate this then "suspect" terrane. As a result of these concerns the author conducted a number of detailed geochemical, isotopic, and geochronological investigations. The findings, in conjunction with the pioneering "terrane" work of Read and Monger (1976) in the Kluane Ranges, have finally and unequivocally demonstrated that the study area is indeed part of Wrangellia. However, unlike previous hypothesis for the Triassic tholeiitic volcanic rocks, the present study proposes a new magmatic setting for the volcanics, a rather distinctive geochemical signature, and a precise age for the onset of Nikolai volcanism and coeval magmatism within Wrangellia.

Parental magma compositions and tectonomagmatic constraints

Petrology and geochemistry of the coeval Nikolai basalt, Maple Creek gabbro and selected chilled margins from Kluane mafic-ultramafic complexes

Field relationships, geochemical, mineralogical, petrological, and geochronological studies indicate that the Kluane mafic-ultramafic complexes, Maple Creek gabbro suite (dykes and sills), and the Nikolai volcanic rocks are coeval and related to Middle Triassic magmatism that commenced 232 ± 1 Ma. In the past, however, Kluane mafic-ultramafic complexes were considered to be of a komatiitic origin (Campbell, 1981) because of the large proportion of ultramafic constituents associated with the intrusions. As a result considerable confusion arose over the nature of the parental magma(s) and its association, or lack of, with the proximal tholeiitic Nikolai volcanic rocks. To resolve this quandary chilled margins from the various mafic-ultramafic intrusive complexes are compared with quenched equivalents from the Maple Creek gabbro dykes and Nikolai volcanic rocks. In addition, the magnesium content of the parental magmas that gave rise to the coeval ultramafic suites was constrained by employing the compositions of the associated olivine. Although many of the chilled margins have been extensively altered, a number of relatively unaltered sample localities were discovered and data obtained from these samples are presented. The unusually high concentration of Ba, Na, and K in the Kluane basaltic suites (more characteristic alkali basalt than tholeiite) also complicated the geochemical interpretation. Anomalous concentrations of alkalies, however, are the product of crustal contamination rather than primary melt composition. To constrain the nature of the Kluane parental magma(s), therefore, different petrological, mineralogical, and geochemical studies are presented.

Petrology

Maple Creek gabbro. Dyke and plug-like bodies of gabbroic material commonly intrude the mafic-ultramafic complexes (i.e. Quill Creek, Arch), and at some localities (Tatamagouche Creek) are recognized as feeders to the overlying Nikolai volcanic rocks. Figure 166 contains a series of photomicrographs of samples obtained from Maple Creek gabbro intrusions cutting the Quill Creek (DDH-87-94; 1235L-6B-A-C) and Arch

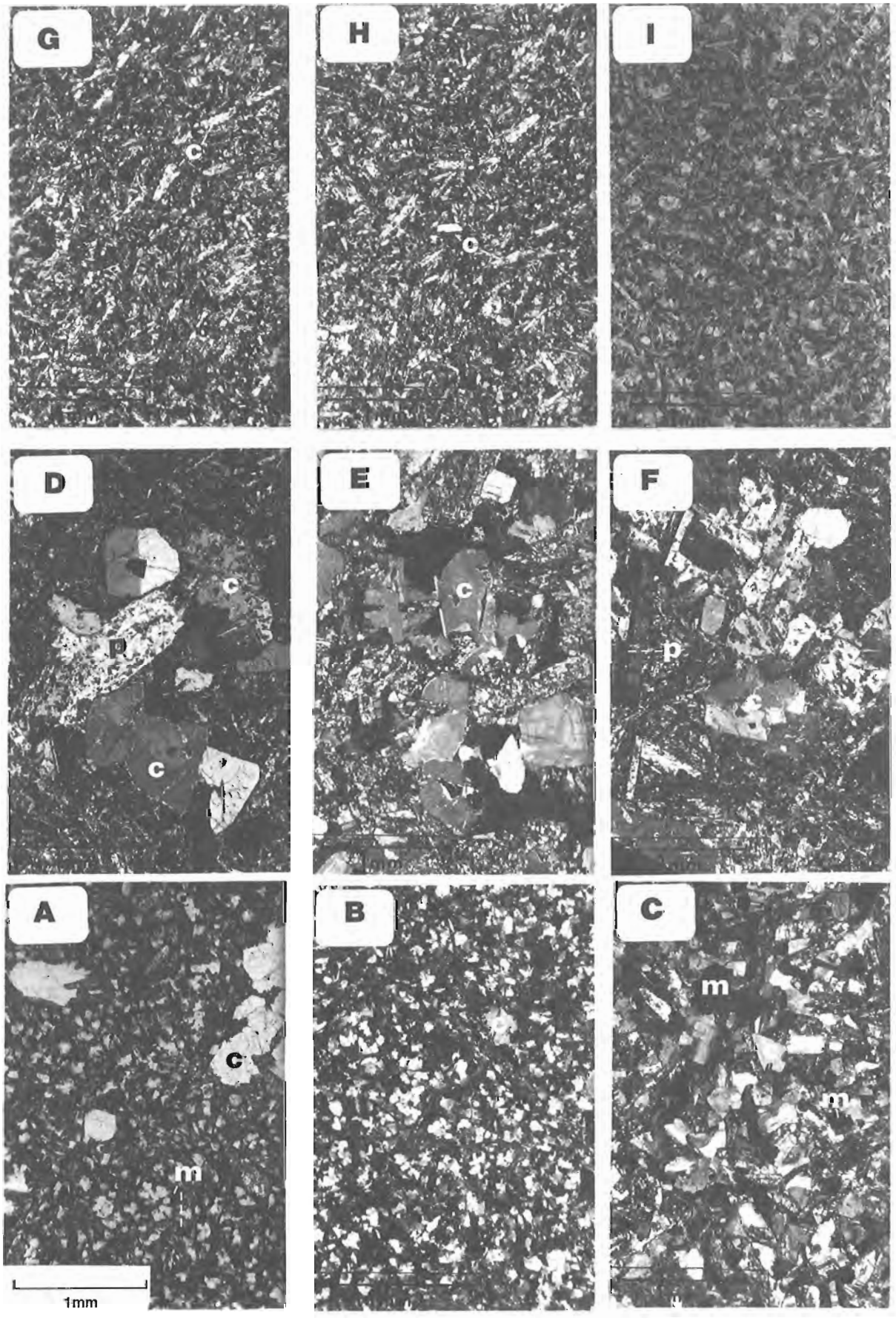
G
c
H
c
I
D
c
p
c
E
c
F
p
A
c
m
1mm
B
C
m
m

Creek (HDB-88-ARC-12C) complexes. Figure 166(A, B, C) displays textural variations encountered in DDH-87-94, which intersected one of these plug-like bodies. One of the more common microfabrics associated with these bodies (i.e. microcrystalline hypidiomorphic inequigranular) from the more slowly cooled central portion of these bodies, is shown in Figure 166A. This textural variety has a pronounced porphyritic texture due to the presence of clinopyroxene phenocrysts set in a finer-grained groundmass of augite, altered plagioclase and abundant Fe-Ti-oxides. The finest grained rocks occur at the intrusive contact and characteristically have a microcrystalline hypidiomorphic equigranular texture consisting of augite, altered plagioclase, oxides, and minor amounts of devitrified glass (Fig. 166B). Away from the intrusive contact zone the very fine-grained gabbro coarsens and develops a subophitic texture with interseptal augite (Fig. 166C).

Thinner Maple Creek gabbro dykes from the 1235 Level of the Wellgreen mine (<200 m from DDH-87-94 locality) have pronounced glomerophyric and cumulophyric textures (Fig. 166D-F). Glomerophyric clots of augite and plagioclase (Fig. 166D) are less common than the cumulophyric clots of augite in Figure 166(D, E, F). These clots are considerably coarser grained than their groundmass, and the clinopyroxene characteristically displays the same strong optical (as well as chemical) zoning and twinning found in the marginal zone gabbro from the same complex they intrude. Other portions of the same dyke are strongly microcrystalline equigranular, lack glomero- and cumulophyric textures, and are reliable indicators of the parental melt composition (Fig. 166G, H). Similar microcrystalline equigranular material from dykes intrude the Arch Creek Complex, but these also contain minor amounts of altered olivine phenocrysts (Fig. 166I).

Nikolai volcanic rocks. Extensive areas of these rocks outcrop throughout the eastern arm of Wrangellia. The best exposed and preserved localities in the study area are located west of Kluane Lake (Fig. 169). Maroon to dark green amygdaloidal basalt, similar to that in Figure 167A, is not only the most common, but also the most altered variety of Nikolai extrusive rocks in the area. The amygdules generally consist of carbonate with lesser amounts of prehnite-pumpellyite facies burial metamorphic mineral constituents. The groundmass in the amygdaloidal variety is generally more altered than that of other Nikolai volcanic rocks. Cumulophyric varieties with clots of plagioclase (Fig. 167B), and porphyritic types with large subhedral (Fig. 167C, E) and rounded (Fig. 167D) augite crystals in a finer-grained matrix are present. Acicular augite with primary amphibole rims has also been observed (Fig. 167D) in the same samples. Iddingsite pseudomorphs after olivine (Fig. 167F) occur in some samples and bear a striking resemblance to the olivine-bearing Maple Creek gabbro dykes. Devitrified glass occurs in a few samples, but due to the similarity in appearance with that of pervasively altered plagioclase (with its dark turbid appearance), the former is generally difficult to distinguish. In some samples plagioclase crystals are skeletal and contain glass-filled cores (Fig. 167C), making recognition even more difficult. Nikolai volcanic rocks closely associated with Maple Creek gabbro feeders tend to display a coarser groundmass with a distinctive ophitic to subophitic texture (Fig. 167C, F, G).

Kluane mafic-ultramafic complex chilled margins. Due to the recessive nature of intrusive contacts, chilled margins are generally difficult to find on surface. Diamond drilling along the basal contact of the Quill Creek, and to a lesser extent, the Arch and Linda Creek complexes, has sampled the chilled margins.

The best example of quenched material representative of the earliest parental magma from which immiscible sulphides segregated and the marginal zone of the Quill Creek Complex crystallized is shown in Figure 168A. This sample was taken within 0.5 cm of a basal massive sulphide body and characteristically contains curved acicular clinopyroxene. This curved, quenched growth feature, along with the hypocrystalline nature of the groundmass, clearly indicates rapid cooling

Figure 166. *Photomicrographs of representative lithologies associated with the Maple Creek gabbro suite. GSC-106H (**A**) DDH-87-94-67. Coarser-grained central portion of gabbroic plug. Note the porphyric clinopyroxenes set in a finer-grained matrix of clinopyroxene, altered plagioclase, and Fe-Ti oxides. Quill Creek Intrusive Complex. Plane-polarized light. (**B**) DDH-87-94-24. Fine-grained chilled margin from intrusive contact of the same body. Quill Creek Intrusive Complex. Crossed-polarized light. (**C**) DDH-87-94-61.3. Gabbro with typical subophitic texture developed in the more slowly cooled areas between localities in A and B. Quill Creek Intrusive Complex. Cross-polarized light. (**D**) 1235L-66a. Glomerophyric plagioclase-clinopyroxene clots in finer-grained gabbroic matrix. Quill Creek Intrusive Complex. Cross-polarized light. (**E**) 1235L-66b. Cumulophyric clots of clinopyroxene set in a coarser grained matrix of altered plagioclase. Note the zoned nature of some of the clinopyroxenes. Quill Creek Intrusive Complex. Cross-polarized light. (**F**) 1235L-66c. Cumulophyric clots of clinopyroxene in a finer-grained gabbroic matrix. Quill Creek Intrusive Complex. Cross-polarized light. (**G**) 1235L-66d. Chilled margin of the same dyke that hosts the textural varieties shown in D, E, and F. Quill Creek Intrusive Complex. Plane-polarized light. (**H**) 1235L-66e. Similar chilled marginal gabbro showing typical quench fabric. Quill Creek Intrusive Complex. Plane-polarized light. (**I**) HDB-88-Arc-12c. Quenched intrusive contact of dyke cutting Arch Creek Intrusive Complex. Note the altered round pseudomorphs of iddingsite after olivine in the very fine-grained gabbroic matrix. Plane-polarized light. m = magnetite (Fe-Ti oxides), c = clinopyroxene, p = plagioclase, o = olivine.*

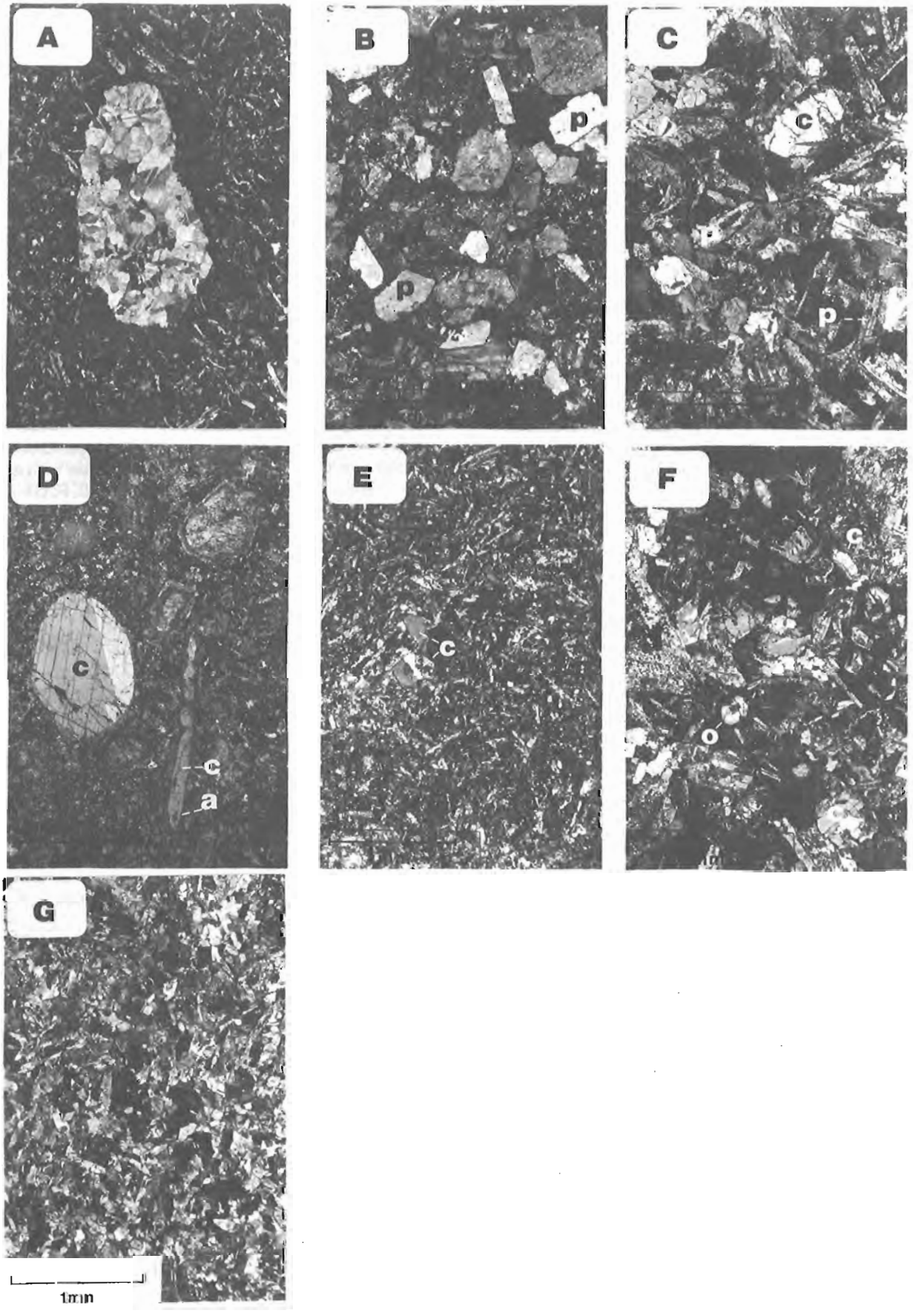
A
B
p
p
C
c
p
D
c
c
a
E
c
F
c
o
G
1mm

of this initial melt. A fine dusting of sulphides is also dispersed through the groundmass. A coarser-grained equivalent of this quench growth feature, in a sulphide-poor environment, was also found at the Linda Creek Complex (Fig. 33B). Additional examples of quench textured chills (without sulphides) have textures similar to that shown in Figures 168C, acicular clinopyroxene and ilmenite, and skeletal plagioclase set in an altered hypocrystalline groundmass. Under slower cooling conditions away from the intrusive contact, seriate texture develops with the gradual increase in the size of the main constituents (clinopyroxene and plagioclase). Elongated crystals of plagioclase, with or without glass filled cores, become partially enclosed in enlarged interstitial augite giving rise to a subophitic texture (Fig. 168D, E). Finer-grained, microcrystalline, inequigranular chill facies gabbro with microphenocrysts of a telluric origin are also present (Fig. 168G, H); however, the presence of clinopyroxene of an intratelluric origin cannot be ruled out.

A summary of petrographic differences between tholeiitic and alkali basalts, as outlined by Hughes (1982, Table 9.5, p. 297), corroborates the tholeiitic character of the Kluane magmatic event based on the nature of the phenocrysts, groundmass, and associated rock types. Phenocrysts of olivine are rare, clinopyroxene is pale brown, and plagioclase is fairly common and occurs early in the crystallization sequence of Kluane suites, unlike alkali basalt. Groundmass of the quenched Kluane suites is relatively fine grained, lacks groundmass olivine, alkali feldspar, or analcite, and interstitial glass is relatively common. Associated rocks like ultramafic xenoliths of dunite and wehrlite, fairly common to the alkalic basalt suite, are absent from the Kluane Belt.

Detailed petrographic investigation of the cumulates and quenched initial melts revealed the following crystallization order: olivine (±chromite±sulphide) : clinopyroxene : plagioclase : orthopyroxene : Fe-Ti-oxides.

Although orthopyroxene is a relatively common normative component in these rocks, it is characteristically absent as a primary crystallization product, and where present occurs only in trace amounts as a late stage intercumulus phase. In addition to its presence as an intercumulus mineral, orthopyroxene is also present as an exsolution phase in clinopyroxene. The characteristic absence of this phase as a primary constituent in these rocks requires explanation as the major normative composition of these Triassic magmas is: plagioclase, clinopyroxene, olivine, and orthopyroxene.

Compositional and mineralogical variations within this magmatic system are best examined with the aid of a modification of O'Hara's CaO-MgO-Al_2O_3-SiO_2 (CMAS) system to construct the tetrahedron plagioclase, olivine, diopside, and silica as outlined by Walker et al. (1979). Proximity of the projected quenched compositions to the 1 atmosphere boundary curve, rather than the 4.5 kbar boundary curve, confirms the low pressure crystallization conditions operative in these subvolcanic magma chambers. This low pressure regime is an additional factor influencing the scarcity of orthopyroxene from these magmas as the orthopyroxene volume expands considerably with increasing pressure (i.e. doubles from 1 atm. to 9 kbar, Irvine, 1970, Fig. 16).

Mineralogy

Clinopyroxene compositions from a number of chilled margins associated with the Quill Creek (Wellgreen), Linda Creek, and Dickson Creek complexes, as well as samples of Maple Creek gabbro dykes and Nikolai volcanic rocks were determined by electron microprobe analyses (Fig. 53C, 59B). The degree of $Mg/(Mg+Fe^{2+})$ variability appears to decrease in the following order: Quill Creek Complex (Wellgreen chills), Maple Creek gabbro dykes, Nikolai volcanic rocks, Dickson Creek and Linda chilled margins. Although most samples retain their primary igneous compositions, the variation encountered should sound as a precaution to those attempting to interpret the composition of the initial magma(s) based on pyroxene compositions from sulphide-bearing samples. Significant compositional variations (up to 10%) of pyroxene cores were noted within a single polished thin section depending on proximity of the pyroxene to sulphide concentrations. Extreme normal zoning was encountered in the clinopyroxene from the Quill Creek (Wellgreen) chilled gabbro (0.710 to 0.460). However, clinopyroxene from sulphide-poor chilled gabbro generally has core compositions in the 0.788 to 0.710 range, with an average core $Mg/(Mg+Fe^{2+})$ value of 0.720, and rim compositions that are generally 10% or atomic units richer in iron. The most common $Mg/Mg+Fe^{2+}$-rich clinopyroxene falls in the 0.788 to 0.764

Figure 167. *Photomicrographs of representative lithologies associated with the Nikolai basalt suite from the Tatamagouche Creek area. GSC 1995-106I (**A**) HDB-88-TAT-63. Typical maroon amygdaloidal basalt with carbonate vesicular fillings set in a very fine-grained, altered (carbonate, albite, epidote) basaltic matrix. Cross-polarized light. (**B**) HDB-88-TAT-66a. Cumulophric basalt with clots of plagioclase. Cross-polarized light. (**C**) HDB-88-TAT-61. Porphyritic basalt with clinopyroxene phenocrysts and skeletal plagioclase with dark, altered glass filled cores. Cross-polarized light. (**D**) HDB-88-TAT-65ba. Rounded and acicular clinopyroxene phenocrysts set in a very fine-grained basaltic matrix. Some of the phenocrysts have rims of primary magmatic amphibole. Cross-polarized light. (**E**) HDB-88-TAT-65ba. Clinopyroxene microphenocrysts in a very fine-grained quenched basaltic matrix. Cross-polarized light. (**F**) HDB-88-TAT-61. Olivine-bearing basalt with iddingsite pseudomorphs after olivine. Cross-polarized light. (**G**) HDB-88-TAT-58j. Equigranular, fine-grained basalt that appears to coarsen and pass into a Maple Creek gabbro sill. Some of these flows are clearly fed and pass into sills along strike. Cross-polarized light. c = clinopyroxene, p = plagioclase, o = olivine.*

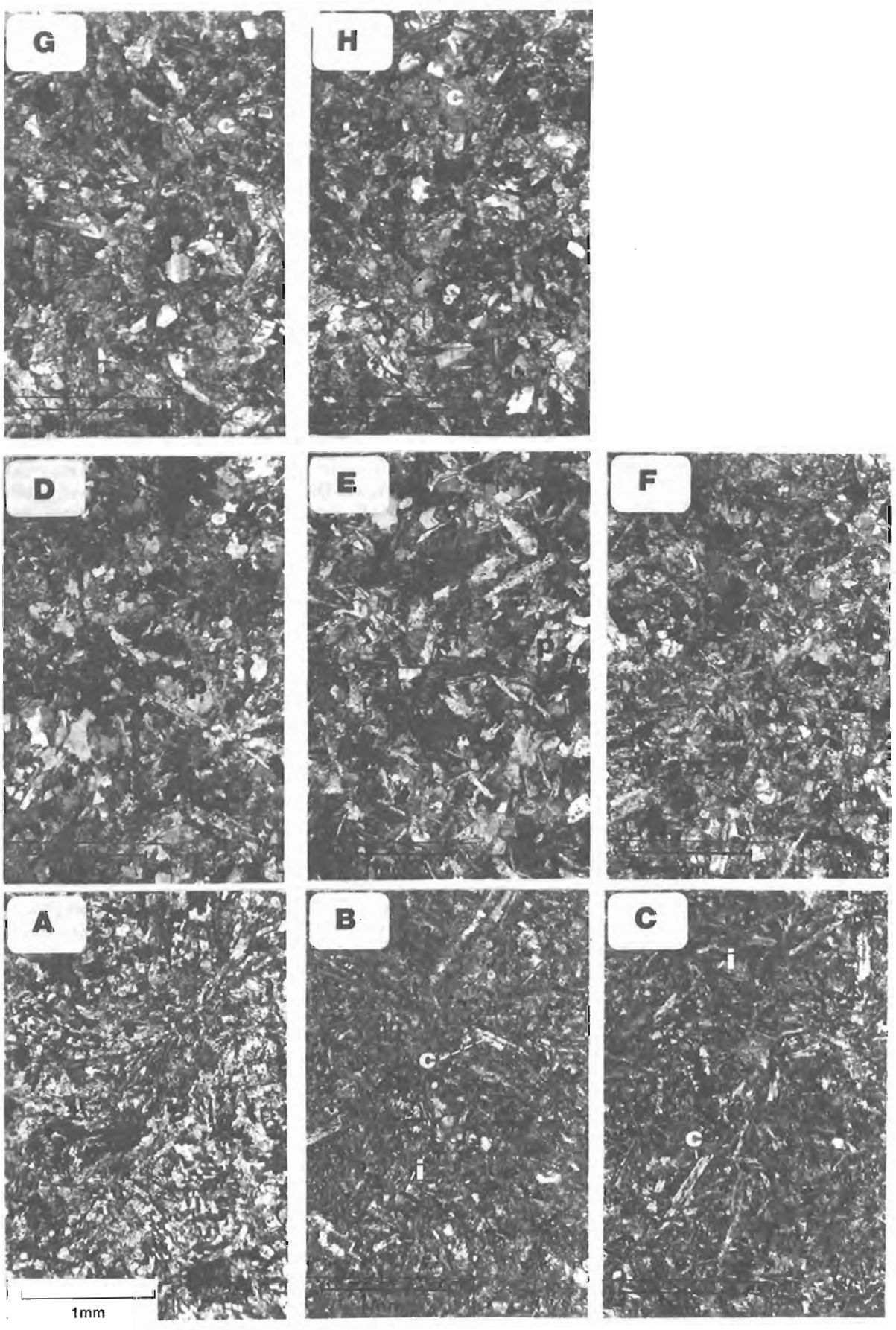
G
c
H
c
s
D
p
E
p
F
A
1mm
B
c
i
C
i
c

range and generally has rims enriched in iron (1 to 2%). These values are similar to those in clinopyroxene cores from chilled margins of Maple Creek gabbro dykes (0.787) that cut the complex. Rims of the same pyroxene are generally enriched in iron (2.0%) due to normal zoning, but rim compositions with 6 to 7% more iron have been noted. Dykes represent the most fractionated Maple Creek gabbro suite generally have whole rock Mg#s of 0.506. Similar dykes cutting the Arch Complex have clinopyroxene with noticeably higher $Mg/(Mg+Fe^{2+})$ core compositions (0.847 to 0.825) with less than 0.5% Fe enrichment on the rims. These initial clinopyroxene compositions (based on chilled margins of Maple Creek gabbro dykes in the Arch Complex) are similar to those measured in chilled margin material from the Linda Complex (0.827 to 0.815) and to the Mg-rich group from Quill Creek Complex ($Mg/(Mg+Fe^{2+}) = 0.870$ to 0.805). The more primitive pyroxene compositions are also associated with chills that have noticeably higher whole rock Mg#s: Maple Creek gabbro dykes cutting the Arch (0.621), Linda Creek (0.653), and primitive Quill Creek (0.679) complexes. Differences in clinopyroxene composition from chilled margins of Maple Creek gabbro dykes and the complexes they intrude, suggest that at least two batches of basaltic magma were emplaced during the evolution of many of these mafic-ultramafic complexes. This mineralogical evidence supports earlier suggestions for at least two pulses of magma. Although limited, investigation of the Nikolai volcanic rocks demonstrated two groups of clinopyroxene based on their $Mg/(Mg+Fe^{2+})$ ratios. Those with ratios in the 0.805 to 0.750 range represent the compositions of cumulophyric clinopyroxene, whereas compositions in the 0.750 to 0.705 range are indicative of clinopyroxene groundmass compositions.

Pyroxene from the fine-grained chilled margins at Wellgreen, Linda, and Dickson properties, as well as Maple Creek gabbro dykes and Nikolai volcanic rocks, demonstrates a greater compositional range than that from the cumulate intrusive sequences and non-chilled gabbroic intervals (Fig. 56 to 59, 59B). This is due to the range in composition of the respective magmas and differing crystallization conditions (i.e. equilibrium crystallization in the chills and fractional crystallization conditions in the cumulates). Nevertheless, it is clear from the confines of the clinopyroxene fields and trends (in particular the chilled samples, Fig. 59B) that the pyroxene belongs to a tholeiitic basalt rather than alkali basalt suite (Wilson, 1989, p. 259). The low TiO_2 ($\overline{X} = 0.53$) and Na_2O ($\overline{X} = 0.20$) contents (wt.%) of the quenched clinopyroxene also confirm the tholeiitic rather than alkalic basalt lineage of these magmas, as does the presence of normative hypersthene in concentrations up to 20% in over 90% of the analyzed samples.

In addition to field evidence, it is apparent from clinopyroxene compositions obtained from the respective quenched suites that magma ingressions of varying composition have

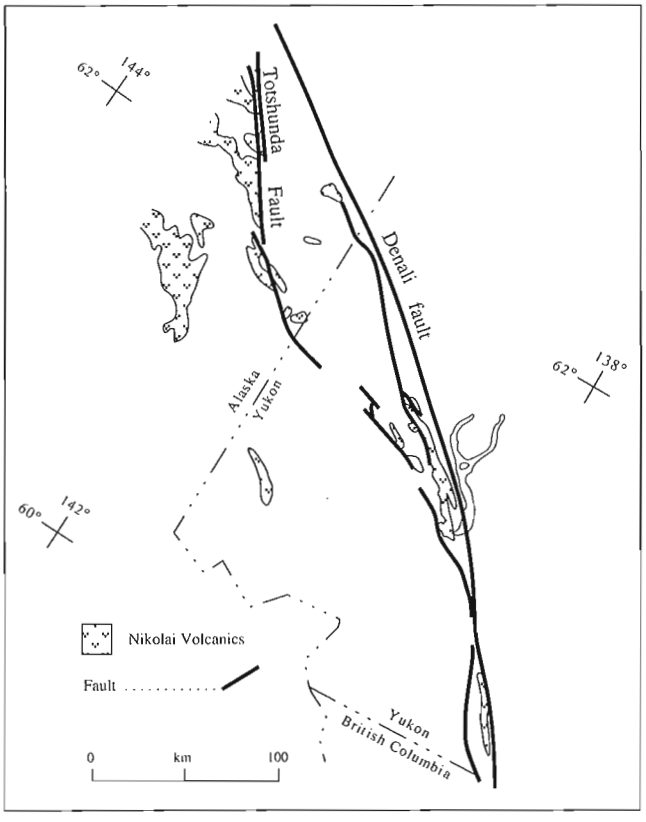

Figure 169. *Geological outline map showing the main areas of Nikolai basalt exposures in eastern Wrangellia.*

Figure 168. *Photomicrographs of representative lithologies associated with chilled margins or quench facies rocks of the Quill Creek Intrusive Complex. GSC 1995-106G (**A**) U382-76.5. Quenched gabbroic rock associated with early, basal massive sulphide mineralization in the Wellgreen deposit. Note the characteristic curved, acicular clinopyroxene quenched growth fabric and the fine dusting and disseminations of sulphide in the rock matrix. Plane-polarized light. (**B**) U490-29.9. Acicular clinopyroxene and ilmenite, and skeletal plagioclase set in an altered hypocrystalline groundmass. Plane-polarized light. (**C**) U490-29.9. Acicular clinopyroxene, ilmenite, and skeletal plagioclase set in an altered hypocrystalline groundmass. Plane-polarized light. (**D**) DDH-87-105-148.3. Fine-grained subophitic gabbro from the chilled facies. Cross-polarized light. (**E**) DDH-87-105-148.3. Same chill sample but with more acicular or elongated clinopyroxene domains. Cross-polarized light. (**F**) DDH-87-104-125. Intermediate grain size between that shown in B and E. Cross-polarized light. (**G**) DDH-87-107-128. Fine-grained microcrystalline, inequigranular chill facies gabbro with microphenocrysts of telluric clinopyroxene. Cross-polarized light. (**H**) DDH-87-105-147.5. Similar microphenocryst-bearing chill facies rock from different drill hole. c = clinopyroxene, i = ilmenite, p = plagioclase.*

occurred during this Triassic magmatic event. The more primitive suites have compositions similar to those of MORB clinopyroxene phenocrysts (diopsidic augite) which generally have a restricted chemical composition, clustering around $Wo_{35-40}En_{50}Fs_{10-15}$ with subcalcic augite and Mg-pigeonite being rare (Wilson, 1989). The composition of the parental melt that gave rise to the olivine-rich ultramafic sequences has to be constrained to clearly establish the magnesium content of the parental magma(s) to these early mineralized sub-volcanic magma chambers. Fe-Mg partitioning between crystallizing olivine and silicate melt provides the most direct constraints on the magnesium content of the liquids. Roeder and Emslie (1970) established that Fe-Mg partitioning between olivine and basaltic melt was relatively insensitive to temperature, liquid composition, or the ferric iron content of the melt. The distribution coefficient (K_D) for this relationship was 0.30 ± 0.03 for basaltic rocks:

$$K_D = (Mg / Fe^{2+})_{melt} \times (Fe^{2+} / Mg)_{olivine}$$

Employing this relationship, one can calculate the $Mg/(Mg+Fe^{2+})$ ratio or Mg# of the parent magma from which the cumulus olivine crystallized. As we would like to know the maximum Mg#, or most primitive magma to have crystallized within each complex, the maximum $Mg/(Mg+Fe^{2+})$ ratio of olivine from peridotite (ortho and mesocumulates) is used to set an upper limit on the Mg# of the magma. Olivine compositions from dunite were not employed due to the adcumulate nature of these rocks and associated postcumulus compositional modifications. The following is a list of maximum $Mg/(Mg+Fe^{2+})$ ratios encountered in olivine from each complex or property: Onion (0.870), Canalask (0.855), Arch (0.840), Quill Creek or Wellgreen (0.863), Linda (0.847), Tatamagouche (0.865), Duke (0.842), and Halfbreed Creek (0.865). The computed maximum Mg# of the parental magma for these complexes are: 0.667, 0.629, 0.611, 0.648, 0.611, 0.648, 0.611, and 0.648, respectively. The average $Mg/(Mg+Fe^{2+})$ ratio for olivine from the Kluane Belt is 0.840, and would have crystallized from a basaltic magma with a Mg# of 0.611. These calculations clearly demonstrate that the primitive chills in the Quill Creek (0.679) and Linda Creek (0.653) complexes have quenched rock compositions (Mg#) compatible with the most primitive melt requirements based on the associated olivine compositions. In fact, the Mg# of the more primitive Maple Creek gabbro suite (0.621) and the average Nikolai basalt (0.629) is compatible with the average Kluane parental magma composition (0.611) based on the average olivine composition (0.840).

Relict igneous plagioclase associated with the Maple Creek gabbro dykes is the most representative plagioclase associated with the initial magmas. Core compositions generally have a Ca# in the 0.55 to 0.52 range. Plagioclase compositions in this range are more compatible with a tholeiitic basalt than alkali basalt suite, as is the appearance of plagioclase as a common phenocryst phase.

Geochemistry

The geochemistry of chilled margins from the Quill Creek (Wellgreen), Chilkat, and Dickson Creek complexes, Maple Creek gabbro intrusives, and quenched material from the Nikolai volcanic rocks are represented in terms of each suites: Mg# vs. Ni, Cr, Cu, Co, V, Zn, Zr, Ba, and PGE+Au concentrations and trends, chondrite normalized PGE+Au profiles, chondrite normalized Rare Earth Element (REE) profiles and hygromagmatophile element (H-Element) profiles in Figures 170 to 177. In addition to employing the Mg#s of the chill and volcanic rocks as a measure of the primitiveness of the respective suites, whole rock MgO (wt.%) and normative olivine contents are discussed. Comparison of the Mg#s of the various suites and compatibility with the calculated Mg# of the melt that fractionated olivine from the various complexes are further discussed to assess the authenticity of the chills as bona fide representatives of parental magma compositions.

Mg#, MgO and normative olivine content of quenched material. During investigation of quenched rocks from the Maple Creek gabbro dykes, Kluane intrusive complexes marginal zones, and Nikolai volcanic rocks, it became evident from both field observations and petrographic studies that at least two major ingressions of basaltic magma could be recognized within each of the quenched suites. Examination of diamond-drill core from the thin marginal zone at the Wellgreen Mine provided the most direct evidence for more than one pulse of gabbroic (basaltic) magma to give rise to the marginal zone. In addition, petrographic identification of both olivine- and non-olivine-bearing Maple Creek gabbro and Nikolai volcanic suites provides corroborating evidence for magmatic injection of both relatively primitive and evolved, olivine-phyric and olivine-aphyric basaltic magmas during the evolution of Triassic magma. It is envisaged that repeated ingressions of basaltic magma, of equivalent or marginally higher Mg#s and with progressively more phenocrysts of olivine, gave rise to the successively more olivine-rich ultramafic horizons within the intrusive complexes.

Chemical analyses of a number of unequivocal chilled margins obtained from drill core intersecting the basal contact of the Quill Creek and Linda Creek complexes suggest at least two different basaltic suites. Other representative chilled margins were obtained from the Dickson Creek Complex (Fig. 46A,B), however, the presence of anomalous sulphides (0.90 to 1.34 wt.% S) and contamination features makes petrogenetic interpretations more equivocal.

The most primitive and probably representative quenched material from chilled marginal zones of Kluane mafic-ultramafic intrusions is represented in the photomicrographs in Figures 33B and 168(D, E) from the Linda and Quill Creek complexes, respectively. The quenched material from the Linda Complex (88LO3-97.26) has 7.86% MgO (wt.%), a Mg# of 0.653, S-content of 0.010 (wt.%), and a normative olivine content of 15.2%. This is fairly similar to the Quill Creek Complex chill (sample DDH-87-105-148) which contains 8.53% MgO, has a Mg# of 0.679, 0.012% S, and 20.6% normative olivine. As primitive basaltic magmas that have

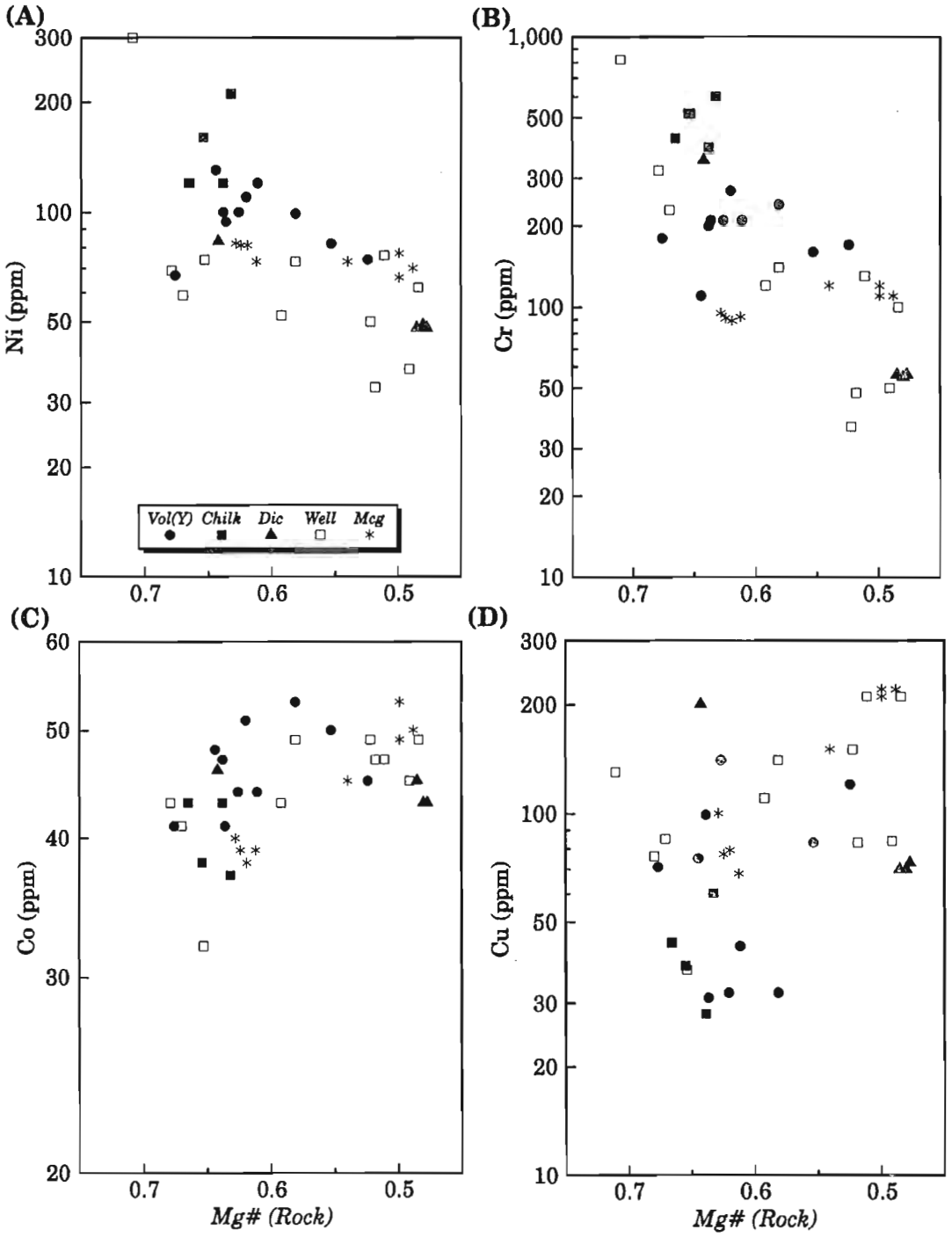

Figure 170 (A-D). *Ni, Cr, Co, Cu, vs. Mg# (Mg/(Mg+Fe^{2+})) plots of elemental concentrations associated with Nikolai basalt from the Yukon (Vol(Y)) and the Chilkat Peninsula of Alaska (Chilk) and chilled marginal gabbro associated with the Dickson Creek Complex (Dic), Quill Creek Complex (Well), and Maple Creek gabbro intrusions (Mcg).*

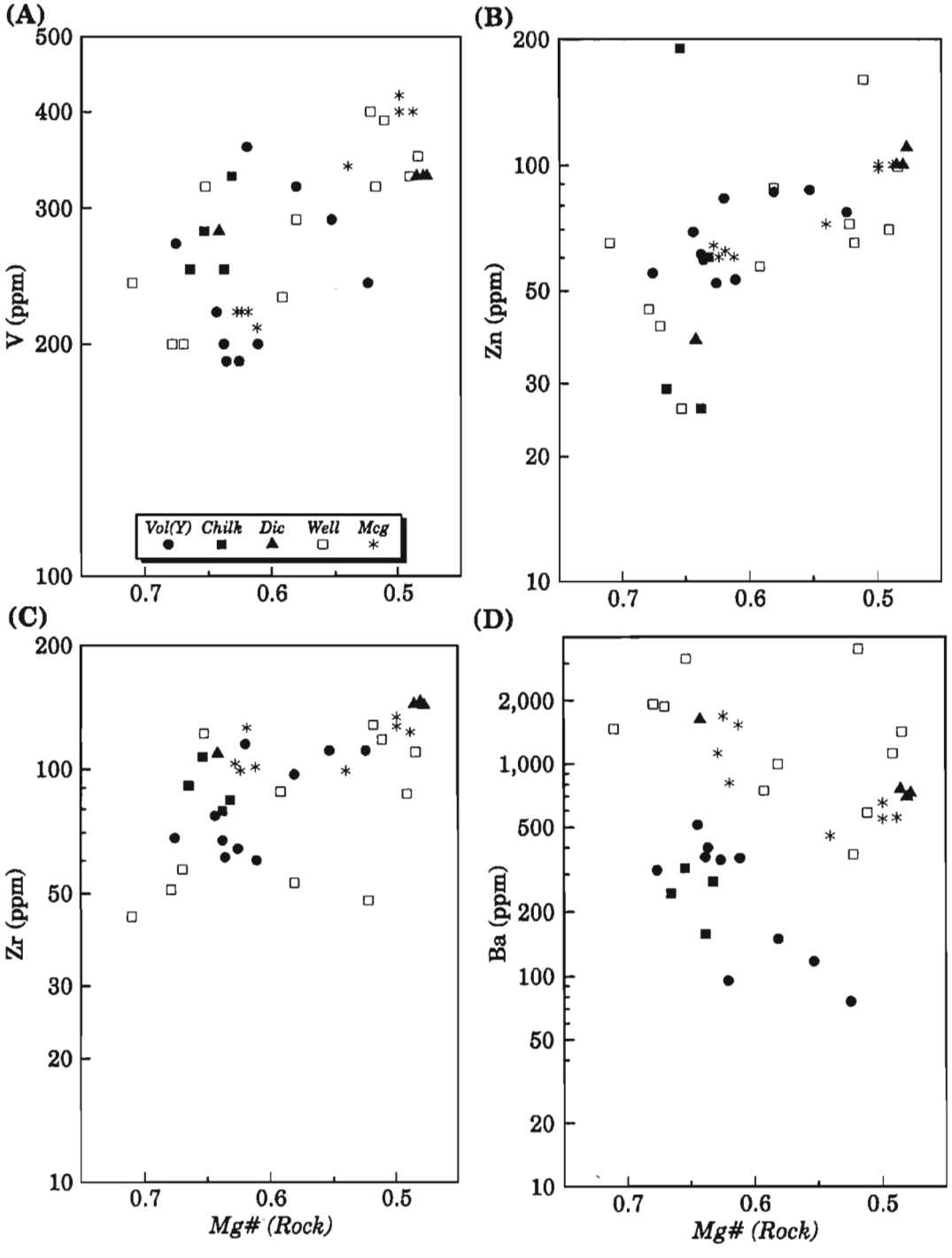

Figure 171 (A-D). *V, Zn, Zr, Ba vs. Mg# (Mg/(Mg+Fe^{2+})) plots of elemental concentrations associated with Nikolai basalt from the Yukon (Vol(Y)) and the Chilkat Peninsula of Alaska (Chilk) and chilled marginal gabbro associated with the Dickson Creek Complex (Dic), Quill Creek Complex (Well), and Maple Creek gabbro intrusions (Mcg).*

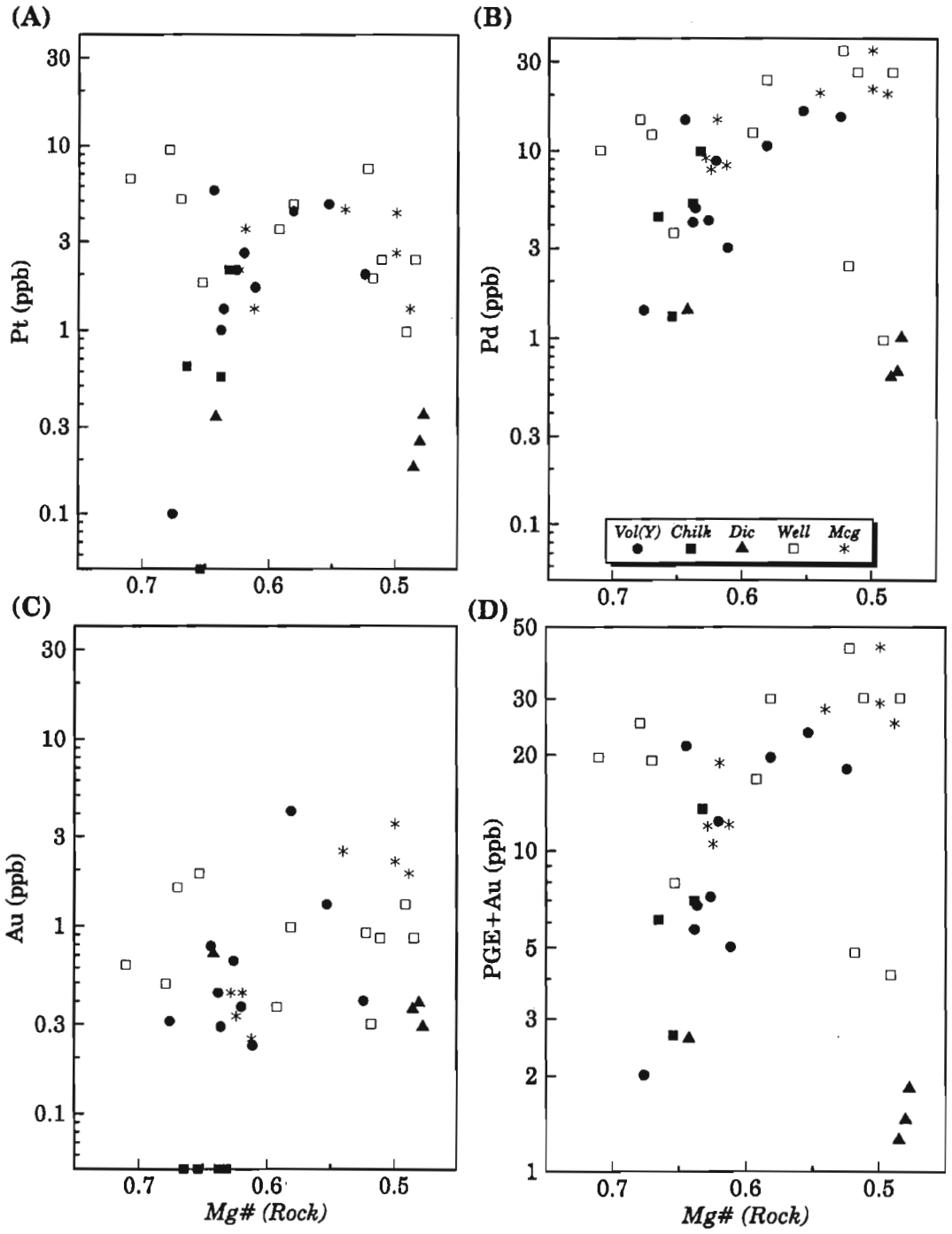

Figure 172 (A-D). *Pt, Pd, Au, PGE+Au vs. Mg# (Mg/(Mg+Fe^{2+})) plots of elemental concentrations associated with Nikolai basalt from the Yukon (Vol(Y)) and the Chilkat Peninsula of Alaska (Chilk) and chilled marginal gabbro associated with the Dickson Creek Complex (Dic), Quill Creek Complex (Well), and Maple Creek gabbro intrusions (Mcg).*

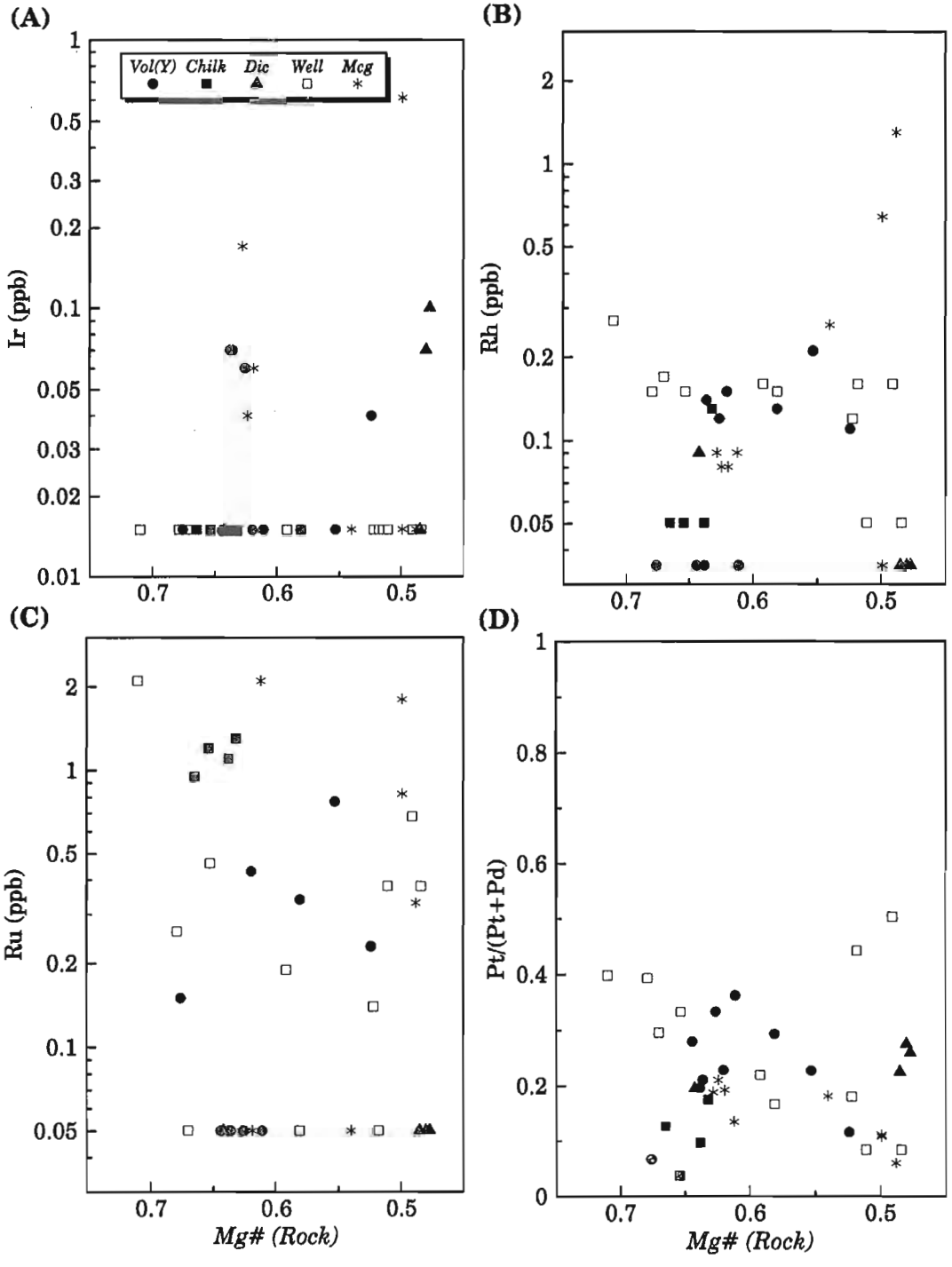

Figure 173 (A-D). *Ir, Rh, Ru, Pt/(Pt+Pd) vs. Mg# ($Mg/(Mg+Fe^{2+})$) plots of elemental concentrations and ratios associated with Nikolai basalt from the Yukon (Vol(Y)) and the Chilkat Peninsula of Alaska (Chilk) and chilled marginal gabbro associated with the Dickson Creek Complex (Dic), Quill Creek Complex (Well), and Maple Creek gabbro intrusions (Mcg).*

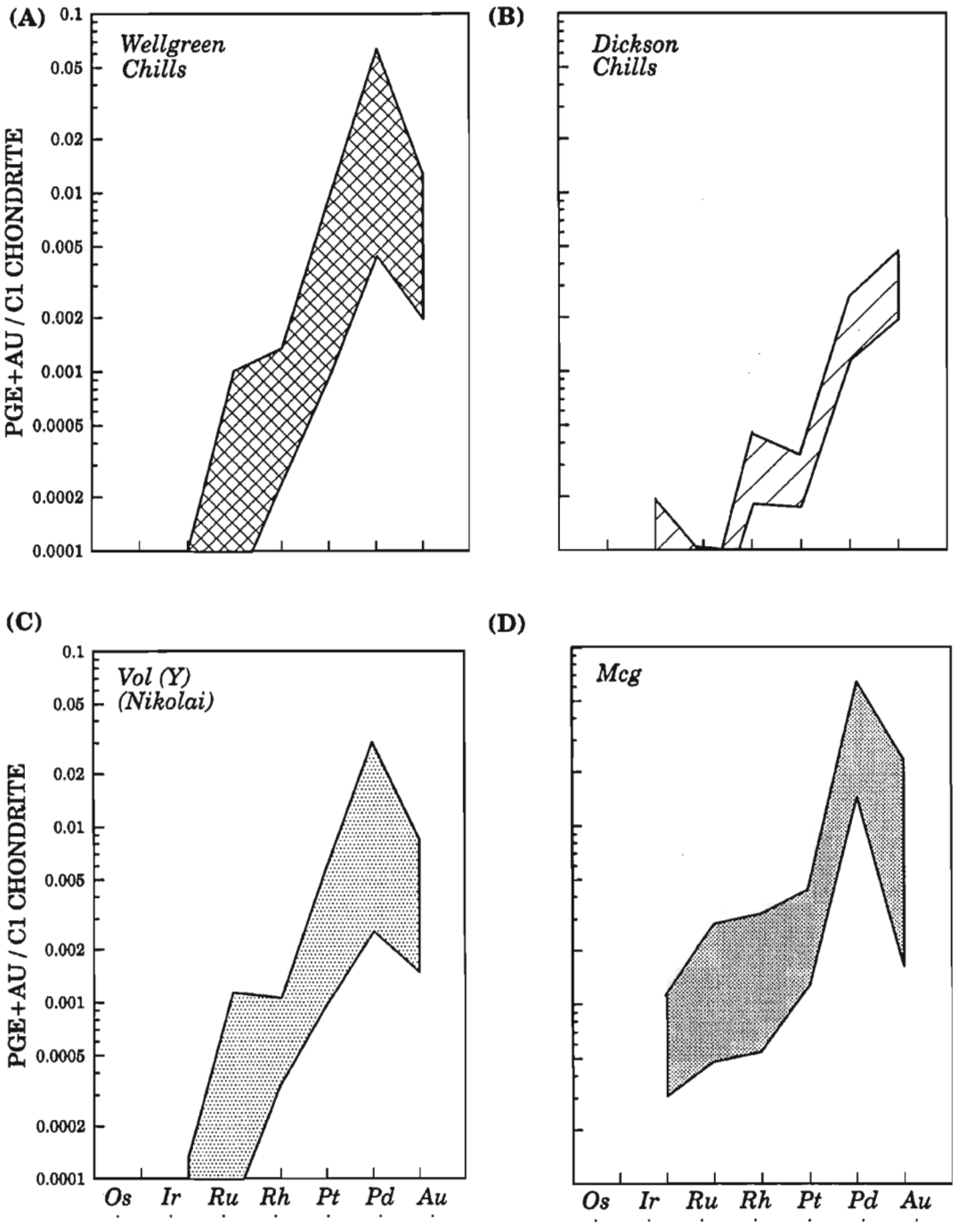

Figure 174 (A-D). *Chondrite normalized PGE+Au profiles for quenched basalt and intrusive chills associated with Nikolai basalt from the Yukon (Vol(Y)), Dickson Creek Complex (Dickson), Quill Creek Complex (Wellgreen), and Maple Creek gabbro intrusions (Mcg).*

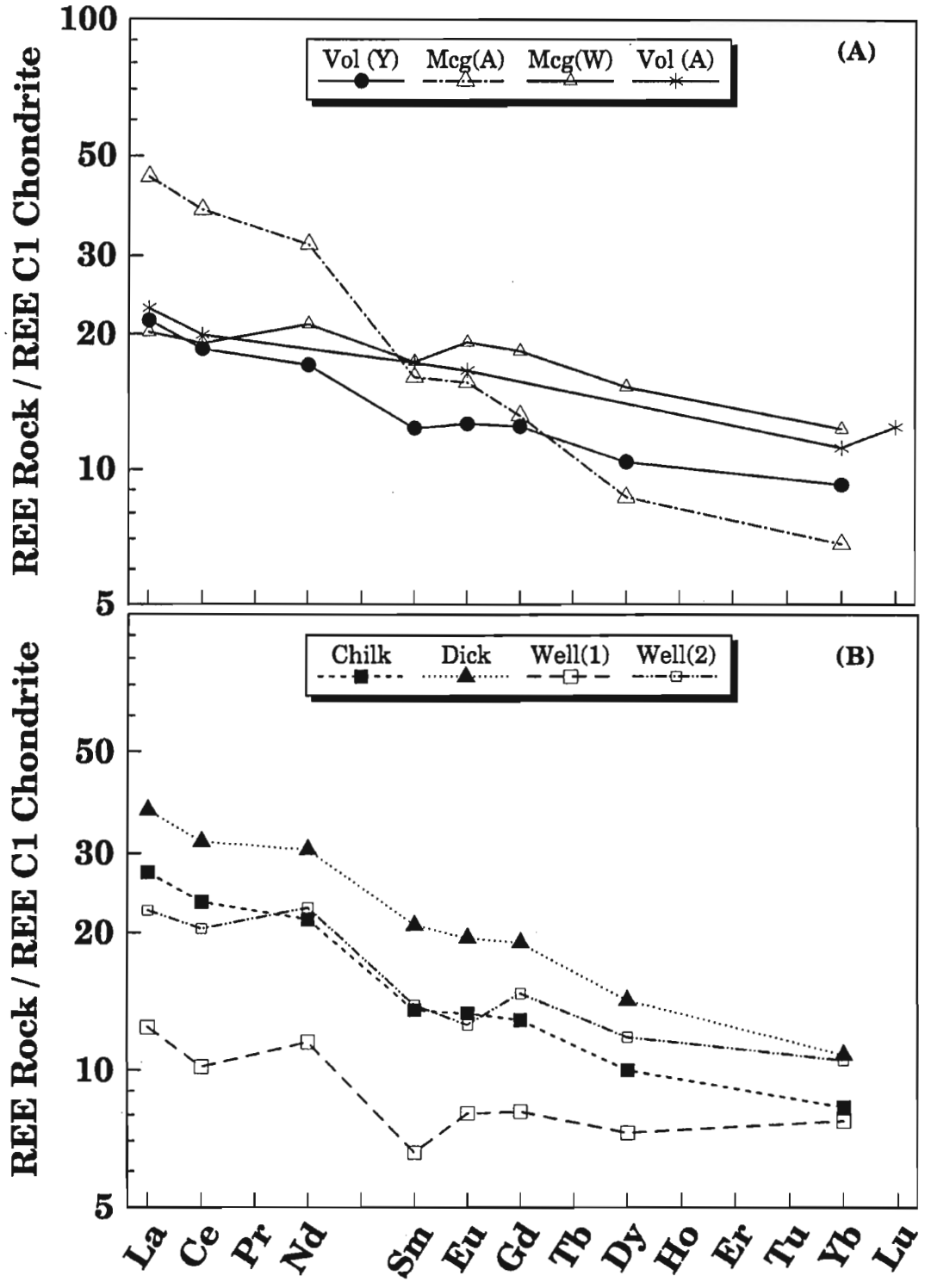

Figure 175. *Chondrite normalized rare earth element (REE) profiles for: (**A**) Nikolai basalt from the Yukon (Vol(Y)), n = 8; Alaska (Vol(A)), n = 9; and Maple Creek gabbro intrusions cutting the Arch Creek Complex (Mcg(A)), n = 4 and Wellgreen property of the Quill Creek Complex (Mcg(W)), n = 4, and (**B**) primitive, Well(1), n = 2; evolved, Well(2), n = 5, Quill Creek Complex and Chilkat (Chilk), n = 4 and Dickson Creek (Dick), n = 4, Complex chills. Chondrite normalizing values from Nakamura (1974).*

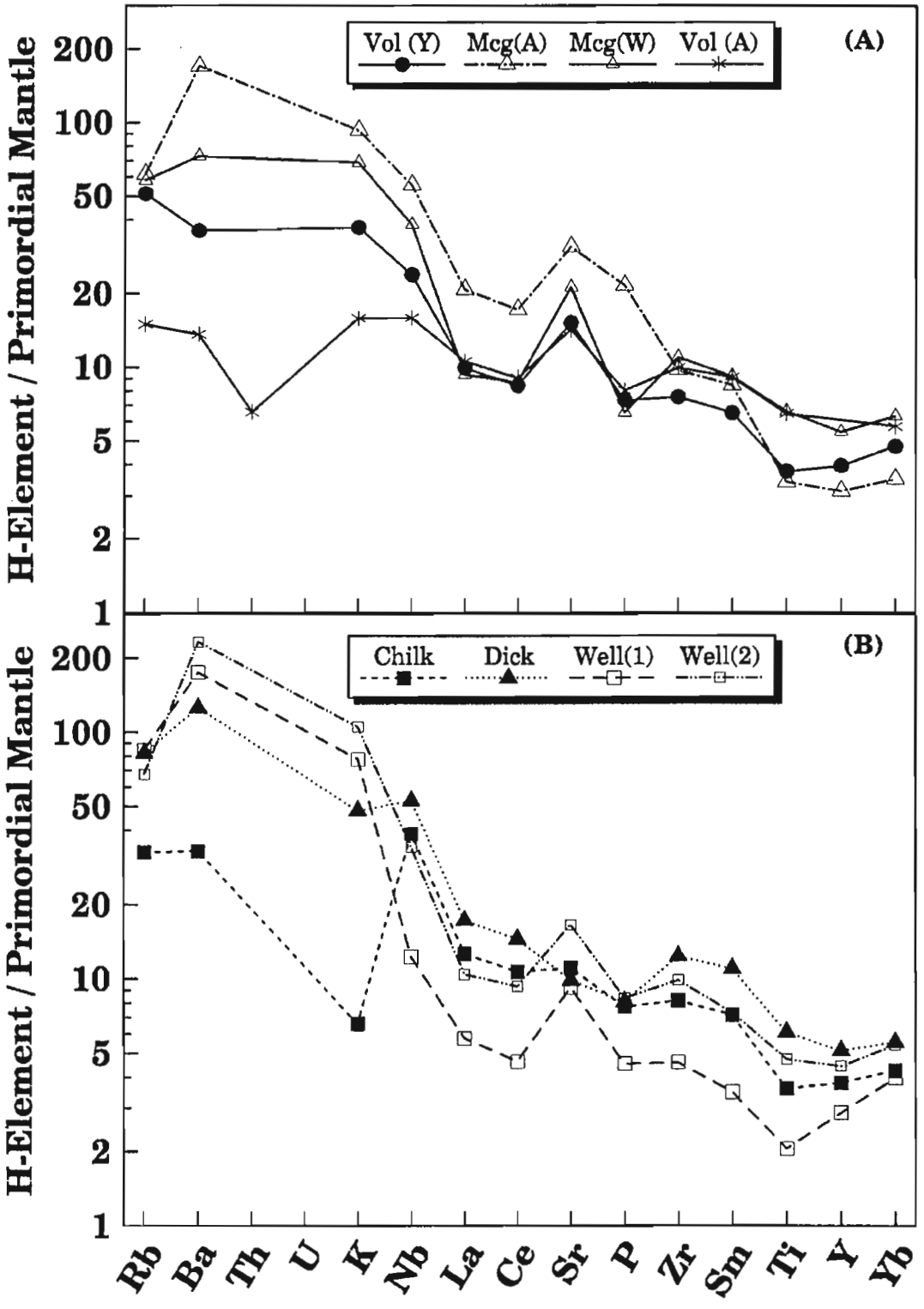

Figure 176 (A-B). *Hygromagmatophile element profiles. Same sources and abbreviations, and number of samples for each profile as in Figure 175.*

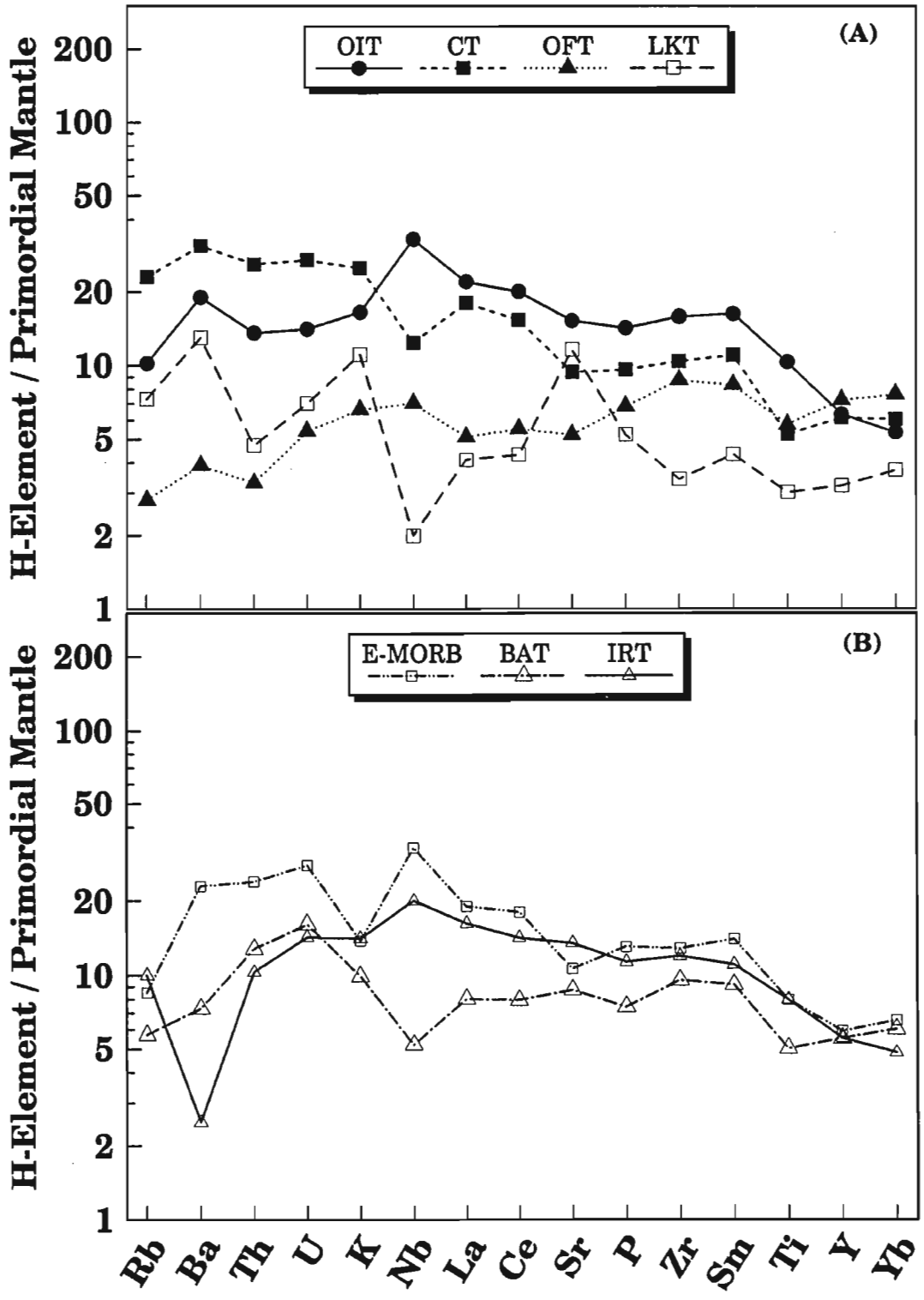

Figure 177. *Hygromagmatophile element profiles for other basaltic environments for comparison. OIT = ocean-island tholeiite, CT = continental tholeiite, LKT = low-K tholeiite from Benioff zones, OFT = N-MORB, E-MORB = enriched MORB-types, BAT = oceanic and back-arc tholeiite, IRT = initial rift tholeiite in continental setting. For details see Holm (1985).*

equilibrated with mantle peridotite require Mg#s of 0.68 to 0.75, for melts generated by up to 30% partial melting (Frey et al., 1978), it is clear that the most primitive chills associated with the Kluane intrusive complexes (Linda and Quill Creek) represent primary partial melts that have experienced little or no fractionation since they segregated from the mantle. Barnes and Picard (1993) suggested that Mg#s greater than 0.66 could be considered as primary partial melts. The high normative olivine content associated with quenched chills devoid of olivine may be due to the elevated $aSiO_2$ accompanying crustal contamination.

Other more abundant quenched material, that macroscopically appears similar to the above, defines a chemically distinct, less primitive, suite for the Quill Creek Complex. Photomicrographs of this type material are shown in Figure 168(C, H). The compositional ranges and means for this material are: MgO (5.9-6.8%, $\overline{X}$ = 6.2%), Mg# (0.484-0.581, $\overline{X}$ = 0.523), normative olivine (9.87-17.26%, $\overline{X}$ =12.79%). The more abundant nature of this type of material, and contact relationships, suggest that it represents the initial pulse of gabbroic magma. The more evolved nature of this initial pulse of magma may represent the first pulse of magma that was tapped off the top of a fractionating, density stratified, master magma chamber at depth. Subsequent pulses of more primitive magma (Mg#s of 0.653-0.679) probably represent the true composition of later ingressions of magma emplaced into these subvolcanic magma chambers (Quill Creek, Linda Creek complexes, etc.).

Petrographic and geochemical studies also suggest the presence of different generations of Maple Creek gabbro dykes. The most primitive variety (represented by the HDB-88-ARC12) has a restricted MgO content (6.4-6.7%), Mg# (0.619-0.628, $\overline{X}$ = 0.621), and 0.10-0.02 wt.% S. This variety is distinquished from the more fractionated Maple Creek gabbro suite by its high normative olivine content (16.2-17.3%) and actual presence of rare olivine grains. This olivine-bearing suite may be part of a distinct feeder system to overlying olivine-bearing Nikolai basalt similar to that of sample HDB-TAT-61 with a Mg# of 0.620 and a normative olivine content of 20.2%, or to other olivine-bearing Nikolai basalt horizons. Although all remaining Nikolai volcanic rocks are olivine free, they nevertheless have correspondingly high Mg#s (0.581 to 0.676, $\overline{X}$ = 0.629) and normative olivine contents (15.9-20.7%, $\overline{X}$ = 19.1%), and could have been fed by olivine fractionated Maple Creek gabbro dykes not too unlike the more primitive suite mentioned above. On the basis of the more evolved compositions (Mg# = 0.506) and lower normative olivine contents (9.0%) associated with the Maple Creek gabbro dykes intruding the eastern portion of the Quill Creek Complex, it is inferred that these dykes acted as feeders to more fractionated Nikolai volcanic rocks not encountered during this study. Such evolved feeders would be more akin to Nikolai volcanic rocks from the Chilkat Peninsula and Wrangell Mountains of Alaska (Davis and Plafker, 1985) with the following compositions: Mg# (0.481-0.638, $\overline{X}$ = 0.555), MgO (5.8-8.8%, $\overline{X}$ = 7.07%) and normative olivine contents of 0-18.8%, $\overline{X}$ = 10.0%. Due to the limited investigation of the Nikolai volcanic rocks during the present study, it is difficult to ascertain whether the more primitive basaltic compositions in this portion of Wrangellia are representative, or just artifacts of the limited sampling. Analyses of Nikolai volcanic rocks by Campbell (1981) also demonstrated that relatively primitive basaltic compositions prevail in the study area. It is more than coincidental that the most primitive and olivine normative Triassic basalt overlies the only area within Wrangellia known to have olivine-rich, subvolcanic, ultramafic intrusions. An interesting economic analogue to this relationship also occurs associated with the Lower Triassic Noril'sk-Talnakh Cu-Ni camp of the Siberian flood basalt province – "although the magmatic activity is very widespread, olivine-rich basalts tend to concentrate in the Noril'sk region" and " sill-like tholeiitic intrusions, varying in composition from subalkaline dolerite to gabbro-dolerite, were emplaced contemporaneously with, and were, in part, feeders to, the extrusive activity" (Naldrett, 1989, p. 103). The presence of this relationship in two different Triassic, flood basalt terranes, of near identical age, and their affiliation with the largest known period of Cu-Ni-PGE metallogenesis since Precambrian has to be more than coincidental.

Mg# vs. Ni, Cr, Co, Cu, V, Zn, Zr, Ba. Examination of the geochemical behaviour of Ni, Cr, Co, Cu, V, Zn, Zr and Ba with respect to the Mg# (Fig. 170, 171) of the associated quenched samples reveals some interesting relationships. With the exception of one sample (Mg# > 0.70) with an inferred cumulative component, all analyzed samples have Mg#s ≤ 0.679.

Nickel concentrations associated with the chilled margins from the Quill Creek Complex (≈ WELL in plots), and to a lesser extent the Dickson Creek Complex, display pronounced depletions relative to the other quenched suites. Also, the Nikolai volcanic rocks from the Yukon (82-120; $\overline{X}$ = 94 ppm) and Maple Creek gabbro dykes (66-82; $\overline{X}$ = 75 ppm), regardless of Mg# (Fig. 170A), are noticeably depleted in Ni when compared to their coeval basaltic equivalents from the western limb of Wrangellia: Karmutsen (64-345, $\overline{X}$ = 136 ppm), Chilkat (96-150, $\overline{X}$ = 152 ppm) and Nikolai (100-160, $\overline{X}$ = 124 ppm) (Davis and Plafker, 1985; Barker et al., 1989). The depleted samples generally have ≤70 ppm Ni. The more primitive Quill Creek (Wellgreen) samples are equivalent in magnesium composition to normal and enriched MORB basalts which generally have Ni contents of 177 and 132 ppm, respectively, (Wilson, 1989), or the average primitive (*g#* = 0.60 to 0.70) "normal" (132-214 ppm), "plume" (104-143 ppm), and "transitional" (94-146 ppm) MORB-types from the Mid-Atlantic Ridge (Schilling et al., 1983). Island-arc tholeiitic rocks generally have very low (≤27 ppm) Ni contents suggesting that they are not primary magmas but have undergone olivine fractionation en route to surface (Wilson, 1989). Reference to these non-Yukon basaltic terranes clearly demonstrates how depleted this quenched Kluane material is. The most evolved compositions from the Quill Creek Complex have Mg#s in the 0.484 to 0.522 range and can have Ni contents as low as 33 ppm.

The more primitive (Mg# = 0.612 to 0.628) Maple Creek gabbro dyke suite is only marginally more enriched in Ni (73-82, $\overline{X}$ = 79 ppm) than its fractionated counterpart (Mg# = 0.488 to 0.540) with 66-77, $\overline{X}$ = 71 ppm Ni, the difference is

related to fractional crystallization. With the exception of one relatively primitive sample with a Mg# of 0.676, the Nikolai volcanic rocks display a general Ni depletion trend accompanying differentiation (decreasing Mg#) (Fig. 170A). The fine-grained gabbroic samples from the Chilkat Complex contain the highest Ni contents; however, the quenched nature of these samples is somewhat equivocal. Nevertheless, it is apparent from the Ni vs. Mg# trends associated with the extrusive and feeder dyke suites in Figure 170A, and the Ni contents of basaltic rocks of comparable Mg# from other basaltic terranes, that chills from mineralized intrusions demonstrate pronounced Ni depletion. The most plausible explanation for this depletion is attributed to Ni scavenging by cotectic or prior immiscible Fe-Ni-Cu sulphide melts. This relationship requires further investigation as it suggests that whole rock Ni depletion associated with chilled margins, and the coeval volcanic suites, may prove to be a useful exploration tool in evaluating other complexes and volcanic terranes for their Ni-Cu-PGE potential. A similar approach has been used to evaluate mafic and ultramafic magmas and komatiite for Ni sulphide potential (Duke and Naldrett, 1978; Duke, 1979). The abnormally low Ni content of the weakly mineralized (0.90 to 1.30% S) and the fractionated Dickson Creek chill may also be a consequence of Ni scavenging by sulphide as abnormal concentrations of barren sulphides are associated with the weakly sulphidic chilled margin specimens. Remarkable Ni and Cu depletion in Triassic basalt has also been recorded from the Noril'sk-Talnakh Ni-Cu-PGE mining camp of Siberia, Russia. At Noril'sk, the 3500 m thick volcanic sequence consists of 11 different suites. The extrusive suite associated with the sulphide mineralized subeconomic and economic intrusions demonstrate pronounced Ni (12-38, $\overline{X}$ = 23 ppm) and Cu depletion (9-53, $\overline{X}$ = 33 ppm) in basalt with Mg#s of 0.56 to 0.61, and significant crustal contamination (Ce/Yb = 15-19), relative to the non-contaminated extrusive suite (Ce/Yb = 6-9) with normal Ni (79-134, $\overline{X}$ = 87 ppm) and Cu (54-151, $\overline{X}$ = 113 ppm) contents in basalt with Mg#s of 0.51 to 0.59 and no known association with Ni-Cu sulphide mineralized intrusions (Fedorenko, 1992; Naldrett et al., 1992; Naldrett, 1992). With the exception of three suites, Naldrett (1992) found that the Mg# of the basalt is relatively constant throughout, but Ni and Cu contents show a sharp drop, coincident with increased in La/Sm ratios. The jump in the La/Sm, while retaining low Gd/Yb, is suggestive of major crustal contamination. This is corroborated by an accompanying marked increase in SiO_2 and $(^{87}Sr/^{86}Sr)_{initial}$ (Naldrett et al., 1992). Explanation for the chalcophile element depletion in some volcanic suites is due to strong enrichment of Ni, Cu, and PGEs in sulphides associated with the ore-bearing intrusions in which these metals came from magma that is now represented by the basalt magma with which the sulphides have come into contact. Naldrett et al. (1992) estimated that this magma has lost about 75% of its Ni and Cu and essentially all of its PGEs. The conspicuous Ni and Cu depletion associated with the Triassic basaltic magmas from the eastern limb of Wrangellia, relative to its western counterpart, is remarkably similar to that observed in the Triassic basalt from the Noril'sk region.

The chromium depletion trend, accompanying decreasing Mg#s in Figure 170B, demonstrates the compatible geochemical behaviour of Cr in a differentiating basaltic magma due to Mg-Cr diadochy. In general the Cr concentrations for the Karmutsen (109-49, $\overline{X}$ = 253 ppm), Chilkat (160-220, $\overline{X}$ = 172 ppm), and Nikolai (120-260, $\overline{X}$ = 191 ppm) basalts from the western limb of Wrangellia (Davis and Plafker, 1985; Barker et al., 1989) are similar to those of the Nikolai volcanic rocks (180-270, $\overline{X}$ = 205 ppm) in the study area. Nevertheless, Maple Creek gabbro dykes, Dickson Creek chills, and most of the Quill Creek quenched samples, especially the more differentiated variates, are relatively depleted in Cr.

Cobalt tends to display an inverse relationship to that of Ni when compared to the evolving Mg# (Fig. 170C) of the various suites. This relationship is to be expected since the Ni/Co ratio of the melt decreases with fractionation, and any influence exerted by Ni sulphide would be offset by a proportional depletion in Co since Ni and Co are present as solid solution end-members in the Ni-sulphide (pentlandite).

Copper trends are somewhat more erratic, but the more fractionated Maple Creek gabbro dyke suite is considerably enriched in Cu relative to the earlier more primitive suite. Cu contents also tend to be higher in the most fractionated Quill Creek chills. The depletion and scatter of Cu values associated with the Nikolai volcanic rocks, may be due to remobilization of Cu accompanying metamorphism. The Nikolai basalt from the study is exceptionally depleted in Cu when compared with the Karmutsen basalt (155-1122, $\overline{X}$ = 343 ppm) data of Barker et al. (1989). Unfortunately, Cu data are not available for the Chilkat or Nikolai basalt from Alaska. Due to the chalcophile nature of Cu, and the depletion associated with fresh chills, as well as the relatively fresh nature of the Nikolai basalt used in this study, one can only attribute the Cu depletion to extraction by sulphides.

Vanadium appears to have a similar distribution pattern to Cu, and thus would appear to be geochemically similar.

Zinc concentration increases considerably, and is relatively well defined, with differentiation (Fig. 171B), particularly in the extrusive and dyke suites, and to a lesser extent in the Quill Creek quenched suite. This coupled increase of Zn and Fe clearly demonstrates the geochemical evolution of these fractionating magmas, and the increasing solid solution component of Zn in mafic phases with differentiation.

Zirconium contents within the Nikolai volcanic (60-110, $\overline{X}$ = 85 ppm) and Quill Creek chill suites (45-130 ppm) increase considerably with differentiation, however, there is only a marginal increase associated with the Maple Creek gabbro dyke suites (Fig. 171C). The Zr concentrations for the coeval basalt from the western limb of Wrangellia are considerably higher: Karmutsen basalt (72-152, $\overline{X}$ = 102 ppm), Chilkat basalt (91-168, $\overline{X}$ = 122 ppm), and Nikolai basalt (90-134, $\overline{X}$ = 109 ppm) with the lowest Zr contents always being associated with the most primitive basalt samples (Davis and Plafker, 1985; Barker et al., 1989). The most primitive, and probably representative, Quill Creek parental liquids contain 51 to 56 ppm Zr which is considerably less

than that associated with "normal" (85 ppm) and "enriched" (75 ppm) MORB samples, within-plate tholeiite (149 ppm), and back-arc tholeiite (130 ppm) (Wilson, 1989), but only marginally less than that associated with the most primitive Nikolai volcanic rocks (68 ppm).

The low Zr contents associated with the primitive (Mg# = 0.60 to 0.70) Quill Creek quenched samples, and the Nikolai volcanic rocks from the Yukon, are believed to indicate magmas derived by relatively high degrees of partial melting. The Zr content of the most primitive chilled margins and volcanic material can be used to estimate the degree of partial melting (estimated by averaging Zr(mantle) / Zr(primitive melt) and Ti(mantle) / Ti(primitive melt) in a manner similar to that used by Barnes and Picard (1993). The most primitive (Mg# = 0.679) parental magma from the Quill Creek Complex is estimated to be the result of about 24% partial melting of the mantle, whereas the most primitive Nikolai volcanic (Mg# = 0.676) could have resulted from subsequent partial melting but to a lesser degree (≈17%). The lower Zr content associated with the primitive Kluane parental magmas is believed to represent relatively higher degrees of partial melting when compared with other magmas of comparable MgO content (Wilson, 1989), particularly the coeval Karmutsen, Chilkat, and Nikolai basalts from the western limb of Wrangellia. The increase in Zr content with differentiation from the most primitive to the most evolved compositions demonstrates the incompatible behaviour of Zr with fractional crystallization.

Barium has a considerable range (75-3300 ppm) in concentrations. Ba concentrations in the Nikolai volcanic and Maple Creek gabbro suites decrease with differentiation (Fig. 171D). The decreasing Ba content could be attributed to plagioclase fractionation accompanying differentiation of its parental magma as Ba and Sr substitute for Ca in the plagioclase lattice (Deer et al., 1970), and the Ca content of plagioclase is known to decrease with differentiation. With the exception of one sample (Mg# = 0.520), the Quill Creek quenched suite also decreases in Ba content accompanying differentiation. Note that the intrusive quenched suites have much higher Ba concentrations than the extrusive suite. Regardless of this association, the Kluane quenched melts are considerably enriched in Ba relative to comparable tholeiitic suites: Normal MORB (4.2-10.7 ppm), Plume MORB (36-149 ppm), Transitional MORB (14.3-39.8 ppm), Schilling et al. (1983); ocean-island tholeiite (70-200 ppm), Basaltic Volcanism Study Project (1981); within plate tholeiite (100 ppm), Pearce (1982); back-arc tholeiite (77 ppm) and island-arc tholeiite (110 ppm), Hawkesworth et al. (1977). Other tholeiitic suites, south-west Pacific island-arc (364 ppm), Andean basalt (345 ppm), Ewart (1982) have relatively high Ba (and other trace element) concentrations due to the combined effects of derivation from an enriched mantle source and contamination, and from enriched subcontinental lithosphere sources. Continental flood basalts of comparable MgO content have the following Ba contents: Snake River Plain (298-464 ppm) and Deccan (239 ppm), Thompson et al. (1983) and Parana (280-413 ppm), Bellieni et al. (1986). The Ba concentrations of the Kluane basaltic magmas are anomalously enriched even when compared to known Ba-rich, unrelated, within plate alkalic (380 ppm) and island arc calc-alkaline (300 ppm) basalts (Sun, 1980). Comparison with coeval Karmutsen, Chilkat, and Nikolai basalt equivalents from the western limb of Wrangellia is also very informative: Karmutsen (21-210, $\overline{X}$ = 81 ppm), Chilkat (28-122, $\overline{X}$ = 80 ppm), Nikolai (15-236, $\overline{X}$ = 103 ppm) (Davis and Plafker, 1985; Barker et al., 1989).

This indicates that the primitive intrusive suites (Mg# 0.60-0.70) within the Kluane Belt are considerably enriched (up to nearly an order of magnitude) in Ba relative to their extrusive equivalents. Based on the distribution of Ba concentrations in the 320 to 510 ppm range for the primitive members of the Nikolai basalt suite, it is inferred that the early Nikolai magma had Ba contents of approximately 380 ppm. This value is also similar to that for comparable continental flood basalt (Thompson et al., 1983; Bellieni et al., 1986), but nonetheless is still approximately four times the level in average basalt with comparable Mg#s from the western limb of Wrangellia. Due to the nature of emplacement of these magmas through narrow dykes, plugs, and hypabyssal sills, many of which are concentrated within or proximal to the mafic-ultramafic complexes, the extrusive suite would be less prone to country rock contamination during ascent to surface than the sill-like intrusive bodies. Nevertheless, comparison with its western counterparts demonstrates that significant Ba contamination has also occurred in the Nikolai basalt within the study area relative to the rest of Wrangellia. The sill-like subvolcanic intrusive complexes would be extremely prone to country rock contamination as a consequence of the nature of their emplacement, repeated replenishment events, higher temperature initial magmas, and longer crystallization interval for heat retention. All of these factors favour magma contamination. The preferential association of the best immiscible sulphide segregations proximal to Hasen Creek Formation carbonate sequences, the discovery of a Cu-Fe-Ba sulphide and barite in the sulphide mineralization, and pronounced Ba enrichments in the mineralized pegmatitic gabbro or so-called "skarn" rock where the intrusion is in contact with carbonate provide strong evidence for Ba contamination from the Permian Hasen Creek Formation strata. Unfortunately, detailed petrographic and geochemical studies of the Hasen Creek strata are not available thus the presence of barite or some other Ba mineral is not unequivocal. However, argillaceous and carbonate Phanerozoic sequences both within and outside the Yukon generally contain high background Ba concentrations and there appears to be little doubt that the elevated concentrations associated with the intrusive suites are the product of country rock contamination. It would appear, therefore, that Ba may prove to be a useful exploration pathfinder element in the mafic-ultramafic intrusions within Kluane Belt.

PGE+Au concentrations and profiles. Platinum group elements and gold also demonstrate concentrational groupings, differentiation trends (Fig. 172, 173), and chondrite normalized profiles characteristic of tholeiitic magmas (Fig. 174). Unlike other chalcophile and siderophile elements, the PGEs generally appear not to be depleted, but exceptions occur locally.

Platinum shows a subtle decreasing trend with differentiation for the Wellgreen suite (Fig. 172A) with the most primitive samples (Mg# > 0.65) containing approximately 5 ppb, and the most evolved (Mg# 0.49 to 0.52) about 2 ppb. The Nikolai volcanic suite tends to cluster in the 1 to 5.5 ppb range within its differentiation interval, but one exceptionally low value (0.1 ppb) was encountered and is associated with weak Ni, Cr, and Cu depletion. The primitive Maple Creek gabbro suite contains marginally less Pt (1.3-3.5 ppb) than its fractionated equivalent (1.3-4.6 ppb), which was unexpected as the former contains more S (401-640 ppm) than the latter (144-220 ppm). Although they have relatively high S contents (9026-12 542 ppm) the Dickson Creek chills are exceptionally impoverished in Pt (0.18-0.34 ppb), regardless of associated Mg#s.

Palladium (Fig. 172B) displays the most coherent trends with differentiation of all the PGEs. However, pronounced Pd depletion is associated with the Dickson Creek suite and some of the Wellgreen chills, and may be the result of earlier Pd scavenging by sulphide melts. Brugmann et al. (1991) found that the PGEs behave in a similar, but somewhat more extreme manner than Ni and Cu, in basalt suites from the Noril'sk region of Russia. Although PGE depletion in some Kluane suites is apparent, the depletion is not as obvious as for Ni and Cu, and is partly due to the relatively large database for these metals compared to that of the PGE data which are restricted to Yukon suites. Excluding one sample, the Quill Creek suite defines a coherent trend that increases from 10 to 20 ppb with differentiation. The Nikolai volcanic (1.4-16.3 ppb) and Maple Creek gabbro suites (≈8-20 ppb) also establish well constrained, increasing concentrational trends with differentiation.

Gold concentrations (Fig. 172C) increase only within the differentiated Maple Creek gabbro suite relative to its more primitive counterpart, whereas no coherent trends were observed with respect to the other suites. PGE+Au concentrations increase with differentiation (Fig. 172C) in a manner similar to that established by Pd (Fig. 172B).

Iridium levels in over half the analyzed samples fall below the lower limit of detection (0.03 ppb). Nevertheless, some noteworthy features can be seen in Figure 173A. It is apparent that the primitive Maple Creek gabbro suite (0.04-0.17 ppb) is enriched in Ir relative to the more differentiated suite (≤0.03 ppb). The Ir enrichment associated with the Dickson Creek chills, and comparable enrichment associated with primitive Maple Creek gabbro suite suggest that Ir is also present in the mafic silicates, and behaved as a compatible element with differentiation. Nikolai basalt data points occurring above the lower limit of detection are limited (three), nevertheless, they suggest a compatible geochemical nature for this element. This relationship suggests that the primitive Wellgreen chills should have comparable if not greater concentrations of Ir. The Ir-rich character of the Wellgreen Ni-Cu ores and low concentrations of Ir in all Wellgreen chills suggest that cotectic or prior sulphide immiscibility has depleted the Quill Creek or Wellgreen chills in Ir.

Rhodium concentrations clearly increase with differentiation in the Maple Creek gabbro and Nikolai volcanic suites (Fig. 173B). This geochemical behaviour demonstrates the incompatible nature of this element with differentiation. However, the Rh vs. Mg# trend established by some of the Quill Creek (Wellgreen) chills, the extreme Rh depletion associated with the Dickson Creek and some Wellgreen chills, and the Rh-rich character of the Wellgreen Ni-Cu ores illustrate the influence of immiscible sulphides. The greater influence of sulphides on the Rh content of the basaltic melts, relative to that of Pd (Fig. 172B), is probably related to the higher distribution coefficient ($D_{sul/sil}$) of Rh for sulphide melt than that of Pd (i.e. $D^{Os} > D^{Ir} > D^{Ru} > D^{Rh} > D^{Pt} > D^{Pd}$). Although D^{Rh} is not precisely known it is will probably be intermediate between that of $D^{Ir} = 10^3$ and $D^{Pd} = 10^2$, but even these values may be low (Barnes et al., 1985). Regardless of the precise value, D^{Rh} will probably be at least half an order of magnitude greater than D^{Pd}, and any sulphide fractionation would have a pronounced influence on the Rh contents of successive differentiated magmas.

Ruthenium (Fig. 173C) generally ranges in concentration from ≤0.05 to approximately 2 ppb but no compositional grouping or trend exists.

Pt/(Pt+Pd) ratios (Fig. 173D) for the Nikolai volcanic, Maple Creek gabbro, and Wellgreen suites display a striking decreasing trend with differentiation, and is distinct from that associated with the mineralized Dickson Creek and some of the Quill Creek chills.

Chondrite normalized PGE+Au profiles for the Quill Creek, Dickson Creek, Maple Creek gabbro chills, and the Nikolai volcanic rocks (Fig. 174) have steep profiles characteristic of continental tholeiite (Barnes et al., 1985) or their mineralized equivalents (Fig. 165B, C), and thus further confirms the tholeiitic parentage of Triassic magmatism within Wrangellia.

Pd/Ir ratios can be used as a measure of the primitiveness of the associated magmas. Barnes et al. (1985) found that peridotitic magmas have Pd/Ir = 10, pyroxenitic komatiite is slightly more fractionated (Pd/Ir = 30) and both continental and ocean-floor basalts are highly fractionated (Pd/Ir = 100). Unfortunately many of the analyzed quenched suites from the Kluane Belt have Ir concentrations <0.03 ppb, therefore only a minimum Pd/Ir ratio was obtained. Nevertheless, all samples have Pd/Ir ratios considerably greater than 100 thus corroborating the basaltic nature of the parental magma.

Rare earth element investigations. Chondrite-normalized REE patterns are shown in Figure 175 for volcanic suites from the Yukon and Alaska, the Maple Creek gabbro suites at Arch Creek, and Wellgreen, primitive and fractionated chills from the Quill Creek Complex, as well as from the Chilkat and Dickson Creek complexes. Each profile represents the average trend based on all available representative samples for that suite (see figure caption for number of samples). Chondrite normalizing values are from Nakamura (1974). The Triassic suites all have concentrations between 12 to 44 times chondrite with moderate to steep patterns, and light-REE (LREE) enrichment.

When the most primitive chills (Well(1)) are compared to the more evolved chills (Well(2)) from the Quill Creek Complex subtle differences between the profiles appear apart

from the obvious difference in absolute concentrations of the REEs (Fig. 175B). The primitive chills appear to have a flat to slightly decreasing heavy-REE (HREE) trend, LREE enrichment, and absolute REE abundances equivalent to half that of the more evolved suite. The evolved suite generally displays flat HREE trends, a distinctive Eu anomaly, a lower degree of LREE enrichment, and lower $(La/Sm)_{cn}$ ratios. The slight negative slope of the HREE associated with the primitive suite may be due to depletion of these elements as a consequence of a small amount of prior partial melting in the mantle source.

The negative Sm anomaly could be the product of clinopyroxene fractionation. Samarium preferentially partitions into clinopyroxene ($D_{cpx/melt} = 0.291)_{Sm}$, only marginally less than that of Ti ($D_{cpx/melt} = 0.384)_{Ti}$ (Hart and Dunn, 1993), therefore fractionation of clinopyroxene would give rise to both negative Sm and Ti anomalies. The presence of cumulophyric clots of clinopyroxene in some chills may corroborate this. $(D_{cpx/melt})_{Sm}$ is known to increase from 0.250 ± 0.009 at 2.35% partial melting of garnet lherzolite to 0.310 ± 0.008 at 37.5% melting (Harrison, 1981), therefore clinopyroxene in the more primitive Kluane melts would be expected to have higher Sm concentrations and any removal of this phase would give rise to more pronounced Sm depletion than the less primitive melts. The negative Eu anomaly associated with the more fractionated or evolved Wellgreen suite suggests fractionation of plagioclase which reduces the LREE/HREE ratio of the melt and causes a negative Eu anomaly in the more evolved melts (Haskins and Paster, 1984). Apart from the Eu anomaly, the Chilkat and Dickson Creek chills have chondrite-normalized REE profiles similar to that of the fractionated suite from Quill Creek Complex (Wellgreen), but with higher abundances, respectively. The lower total REE contents of the primitive Wellgreen chills relative to that of the fractionated chills could be generated by higher degrees of partial melting of a relatively homogenous source (Wilson, 1989). The slight to progressive LREE depletion associated with the fractionated Wellgreen chill, Chilkat and Dickson Creek chills, fractionated Maple Creek gabbro suite and ultimately the volcanic suites from the Yukon and Alaska relative to that of the primitive Quill Creek chill suggest that the successive LREE-depleted patterns are the result of previous depletions of the mantle source. Thus large variations in the LREE in tholeiite are usually attributed to variations in the LREE content of the source. Fractional crystallization of plagioclase, pyroxene, or olivine from the tholeiite does not result in much of a change in the REE content unless the degree of crystallization is large.

Unfortunately, the only available REE data from the western limb of Wrangellia are those from the Chilkat Peninsula of southern Alaska (Davis and Plafker, 1985), and this data set is rather incomplete as several REEs were not analyzed. Nevertheless, this limited data set does suggest that the heavy and intermediate REEs from the western limb are present in higher abundances, but the LREEs are not too unlike those from the study area in the eastern limb of Wrangellia. Intermediate and heavy REE concentrations for basalt suites from Alaska appear to be intermediate between that of the Nikolai suite from the Yukon and the fractionated Maple Creek gabbro suite. Similarity in the LREE from these suites would suggest similar to slightly lower degrees of partial melting gave rise to the Alaskan suite, and that crustal contamination has not seriously influenced the REE patterns.

The steep LREE-enriched profile associated with the less evolved Maple Creek gabbro suite requires explanation. LREE enrichment in this suite, relative to its fractionate counterpart, could suggest derivation from a relatively LREE-enriched mantle source. It is inferred that this chill suite and the primitive Wellgreen suite were derived from a LREE-enriched, garnet-bearing mantle source, whereas subsequent less primitive melts were derived from a garnet-free, possibly plagioclase-bearing, mantle source. Partial melting in the presence of residual source garnet leads to less enrichment of the heavy REEs in the magma, relative to melts derived from garnet-free mantle sources.

Regardless of the nature of the mantle source, the chondrite-normalized REE patterns in Figure 175 indicate that the parental magmas to Triassic magmatism in the Kluane Belt were of a tholeiitic, and not komatiitic lineage. The patterns closely match those of oceanic island tholeiitic basalt (i.e. Kilauea and Mauna Loa tholeiites, Basaltic Volcanism Study Project, 1981). Apart from the negative Sm anomaly, the REE profile for the primitive Wellgreen chilled suite is similar to that of E-MORB basalt. Temporal, regional, and even local (i.e. central section of Kluane Belt) variations in the REE distribution patterns are not unusual and usually reflect variation in magma composition and the nature of the underlying mantle.

Hygromagmatophile element profiles. To understand other trace element patterns and abundances in the successive basaltic parental magmas, it is necessary to have a frame of reference to which elemental abundances can be compared. This approach was used previously for plotting chondrite-normalized REE patterns and is extended using "spiderdiagrams" in which the abundances of a range of incompatible trace elements are normalized to estimates of their abundances in the primordial earth. The plotted elements all behave incompatibly (i.e. have $D < 1$) during most partial melting and crystallization processes. Exceptions to this are Sr which may be compatible in plagioclase, Y and Yb in garnet, and Ti in magnetite. Once these effects have been taken into consideration the slopes and curvature, peaks and troughs provide valuable information concerning crystal-liquid equilibria: (1) troughs at Sr probably result from the fractional crystallization of plagioclase from the melts, and (2) troughs at Th and Rb combined with one at Nb-Ta suggest contamination by lower continental crustal rocks. The use of such diagrams, normalized to primordial mantle, was first proposed by Wood et al. (1979) who replaced the nondescript term "incompatible" and the frequently misused term "large ion lithophile" with the term "hygromagmatophile" (H-) for those trace elements with bulk distribution coefficients (D) of less than one. Holm (1985) modified this plot to exclusively fingerprint tholeiitic basalt and basaltic andesite from different tectonomagmatic environments to reduce ambiguity introduced when alkali basalt is present in the discriminating

plots. He believed that the disturbing effects of crustal contamination and hydrothermal alteration on the hygromagmatophile (H-) element patterns are of minor significance in recognition of plate tectonic settings.

The H-element profiles (based on mean composition of representative samples) for quenched magmas from the Yukon and Alaska mentioned previously are represented in Figure 176. Profiles for typical ocean-island tholeiite, continental tholeiite, low-K tholeiite from Benioff zones, N-MORB types, enriched MORB-types, oceanic and continental back-arc tholeiites, and initial rifting tholeiite in continental settings are shown in Figure 177 for comparison. The patterns for MORB and ocean-island basalts are considered to be products of relatively large degrees of partial melting, therefore their trace element patterns should reflect those of their mantle source. In general, the less compatible elements on the right side of the H-element spiderdiagram pattern should be less enriched during partial melting, tilting the curve up and to the left. The profile should be tilted up even farther towards the left with fractional crystallization subsequent to melt segregation. The only known mechanism for tilting the curve down to the left is due to depletion resulting from partial melting events.

Although not shown, it is worth mentioning that alkalic ocean island basalt shows extreme degrees of incompatible element enrichment, relative to MORB, with a peak at Nb-Ta, suggesting the source may also be enriched in incompatible elements. Compared to N-MORB and ocean-island tholeiite profiles, that of subduction-related basalt is strongly spiked (positively) due to components added to the mantle source of basalt by subduction zone fluids. Volcanic arc basalt has a marked Nb-Ta trough which is believed to be due to retention of these elements in the source during partial melting (Wilson, 1989). A similar trough is also a feature of basalt that has experienced crustal contamination, and caution must be exercised when interpreting this sort of pattern. H-element spiderdiagrams are not only useful for comparing the trace element characteristics of various volcanic rocks, but they can also be used to characterize the trace element signature of contaminated magmas (Wilson, 1989). Continental crustal rocks are variably enriched in a whole range of elements from Rb to Hf relative to ocean floor tholeiite (MORB) and variably depleted in the elements Ti to Yb, therefore the latter should be examined to see through the contamination process to trace element characteristics of the primary mantle derived magmas. It is believed that the Kluane magmas were derived by partial melting of asthenospheric upper mantle, and did not interact with continental crust rocks en route to surface. Contrasting H-element profiles from the Yukon with that of relatively uncontaminated basaltic counterparts from Alaska should help identify some of the trace elements in the contaminant, and allow us to see through the contamination.

The H-element profile of Nikolai basalt from the Chilkat Peninsula, Alaska (Fig. 176A) appears to be most similar to the primary profiles of E-MORB ocean floor tholeiite and continental tholeiite. Unfortunately, research quality U analyses are not available for the Yukon suites, as are the Alaskan equivalents, but this does not seriously hamper comparison of H-element profiles. The profiles for the elements Nb to Yb are very similar for both the Yukon and Alaskan suites. There is also a marked increase in the level of the elements Rb to K for the successive Yukon suites (Fig. 176). The pronounced hump (anomaly) in the profile, encompassing the elements Rb, Ba, and K, is uncharacteristic of tholeiitic basalt, as well as most other basalt types, and is typically associated with crustal contamination (Holm, 1985, p. 315, Fig. 12 and Wilson, 1989, p. 96, Fig. 4.13). The Ba peak associated with this hump, and the strong evidence for Ba contamination from the Hasen Creek Formation calcareous and argillaceous sediments mentioned previously support the hypothesis that this curvature in the H-element profile is the product of crustal contamination rather than a primary mantle-derived characteristic. The magnitude of this anomaly decreases from: sills to hypabyssal dykes, plugs to volcanic rocks, an effect of decreasing contamination. A distinctive Sr anomaly (spike) occurs in all suites (including the Alaskan volcanic suite) and thus is unlikely to be the product of contamination, but rather the result of plagioclase accumulation as cumulophyric plagioclase clots have been noted in many of the quenched suites. Another interesting trend in the profiles concerns the elements Ti to Yb (Fig. 176B). In the Alaskan volcanic rocks there is a negative slope from Ti to Yb, whereas in most Yukon suites, particularly the more primitive suites (i.e. Fig. 176; Well(1) and Mcg(A)), there is a positive slope from Ti to Tb. This positive slope indicates Ti depletion in most of the Yukon magmas. This depletion is best explained by removal of clinopyroxene or ilmenite from the melts prior to quenching. Primary ilmenite is a common feature in the chills from the Wellgreen property (Fig 168B, C) and the presence of cumulophyric clinopyroxene in some of the quenched suites does not rule out the prior removal of significant quantities of clinopyroxene by cumulate activity in master magma chambers at depth.

Comparison of the generalized profiles for tholeiite in Figure 177 suggests that Triassic magmatism and volcanism within Wrangellia could not belong to: (1) ocean-island tholeiites because of its inverted U-shape pattern with minor anomalies, positive Nb anomaly, and the distinctive negative slope from Sm-Yb, (2) continental tholeiites with its negative Nb anomaly, (3) ocean-ridge and floor basalts with its positive slope that flattens out from left to right, (4) tholeiite from island arcs and continental margins with several distinctive major anomalies, the pronounced negative Nb anomaly being important. Tholeiite from subenvironments like back-arc or marginal basins with their generally rather flat slope, a positive gradient for the segment Rb-Ba-Th-U and negative Nb anomalies. The negative slope for initial rift tholeiites, especially for the interval Sm to Yb, distinquishes this ambiguous tectonic setting from the Wrangellia tholeiite. Thus it would appear that enriched-MORB (E-MORB) ocean floor tholeiite has H-element profiles closest to those that gave rise to Triassic magmas in Wrangellia, if one does not consider the anomalous concentrations of Rb and Ba in the latter.

Although the Kluane magmas have anomalous Rb and Ba concentrations this suite should not be confused with shoshonitic magmas as the Kluane magmas are: (1) not associated with calc-alkalic volcanic rocks, (2) did not form in an island-arc setting, (3) have far too low K_2O (<1%) contents relative to associated SiO_2, (4) have a scarcity of orthopyroxene and amphibole, particularly as phenocryst phases, (5) lack alkali

feldspar and feldspathoids, (6) have an abundance of ilmenite coexisting with magnetite as opposed to the absence of ilmenite in the low TiO_2 island-arc magmas, (7) contain low gold concentrations in contrast to the high gold contents of shoshonite, and (8) formed during the Early Triassic whereas shoshonitic terranes in the North American Cordillera are Late Triassic to Early Jurassic (Mortimer, 1986; Barrie, 1993).

Tectonomagmatic setting

During the past two decades many tectonomagmatic geochemical discriminant diagrams have been created and are now widely used to reconstruct paleotectonic environments. Such diagrams have been used during this study in an attempt to understand many of the ambiguities associated with the Triassic magmatism and volcanism in Wrangellia. However, inconsistent results from regions with known tectonic settings has become apparent from other studies (Wang and Glover, 1992), as is the case of the present study. Although the results of basalt geochemistry from various intrusive and extrusive suites within Wrangellia are to be discussed, it should be stressed that "reconstruction of paleotectonic settings should not be done by using geochemistry alone, but instead tectonostratigraphic analysis based on knowledge of field relations, structure and petrology of epiclastic, volcaniclastic and igneous protoliths is an essential adjunct to geochemistry in determining ancient tectonic environments" (Wang and Glover, 1992). Detailed stratigraphic relationships and comparisons of three Triassic volcano-sedimentary sections from widely separated localities within Wrangellia are described in subsequent discussions.

At present more than 14 tectonomagmatic geochemical discriminant diagrams are in use (Wang and Glover, 1992), however, only those shown in Figures 178, 179, and 180 are used in this study because of geochemical limitations (lack of certain elements and required lower limits of detection) and the inappropriate nature of some plots. In the past, similar diagrams have been employed by other authors (Davis and Plafker, 1985; Barker et al., 1989) attempting to reconstruct the paleoenvironment of the volcanic sequence in the western portion of Wrangellia. In many respects these discriminant diagrams are discussed concerning the erroneous, rather than substantive, conclusions they produce, and how extreme caution should be employed when using them.

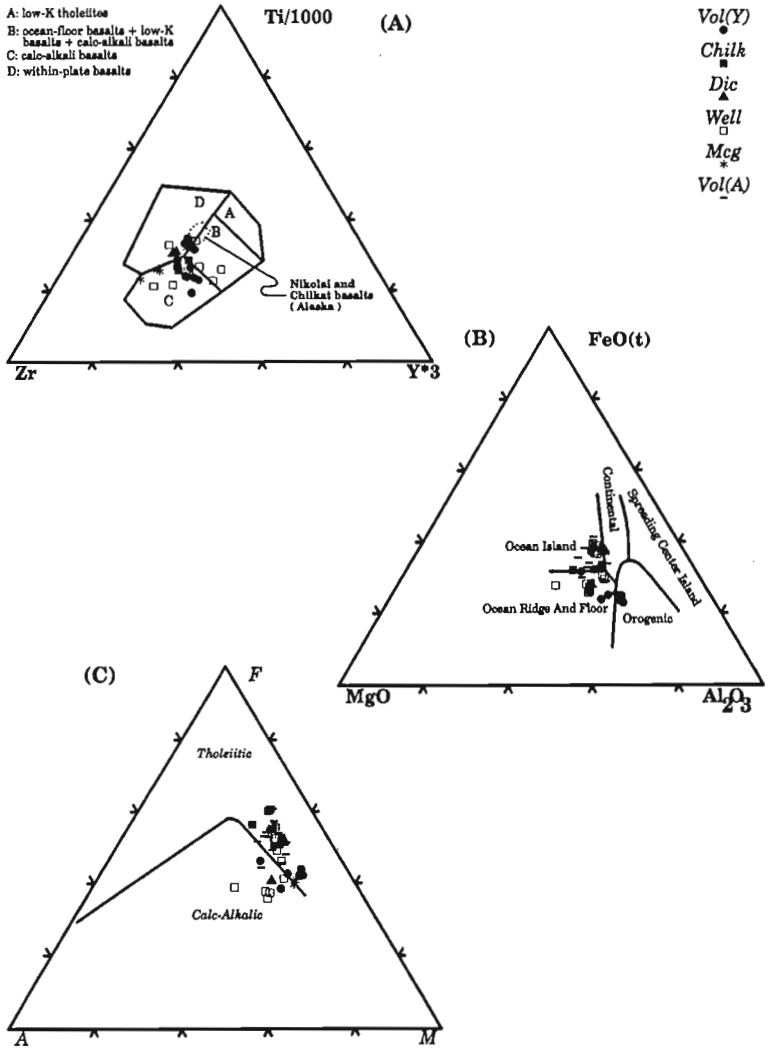

Figure 178 (A-C).

*Ti/1000-Zr-Y*3, FeO(t)-MgO-Al_2O_3, and A-F-M tectonomagmatic ternary discriminant diagrams showing the composition fields occupied by Nikolai basalt from the Yukon (Vol(Y)) and Alaska (Vol(A)), the Chilkat Peninsula of Alaska (Chilk), and chilled marginal gabbro associated with the Dickson Creek Complex (Dic), Quill Creek Complex (Well), and Maple Creek gabbro intrusions (Mcg).*

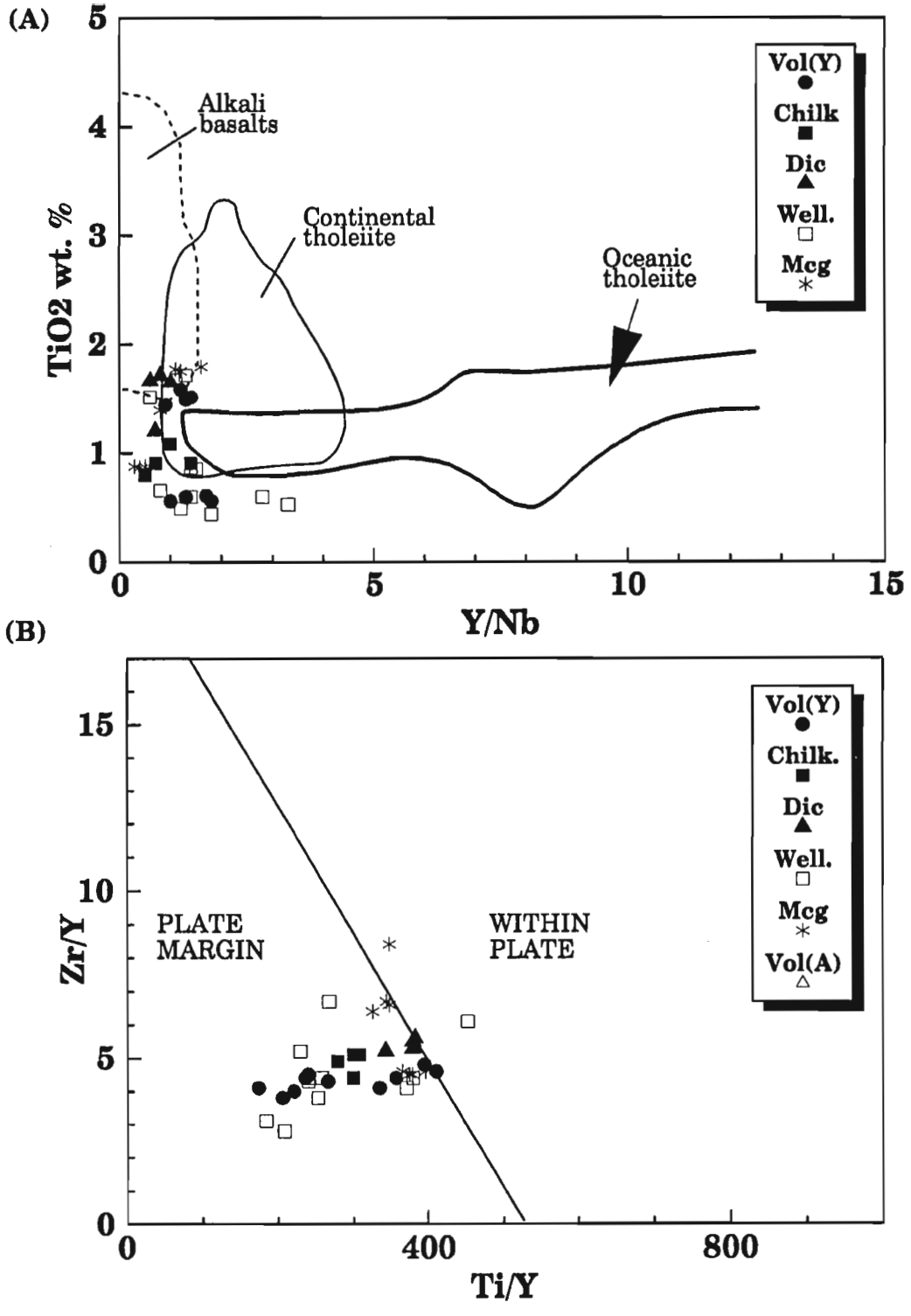

Figure 179. *(**A**) TiO_2 vs. Y/Nb and (**B**) Zr/Y vs. Ti/Y (after Pearce and Gale, 1977) tectonomagmatic discriminant diagrams showing the composition fields occupied by Nikolai basalt from the Yukon (Vol(Y)), and Alaska (Vol(A)), the Chilkat Peninsula of Alaska (Chilk), and chilled marginal gabbros associated with the Dickson Creek Complex (Dic), Quill Creek Complex (Well), and Maple Creek gabbro intrusions (Mcg).*

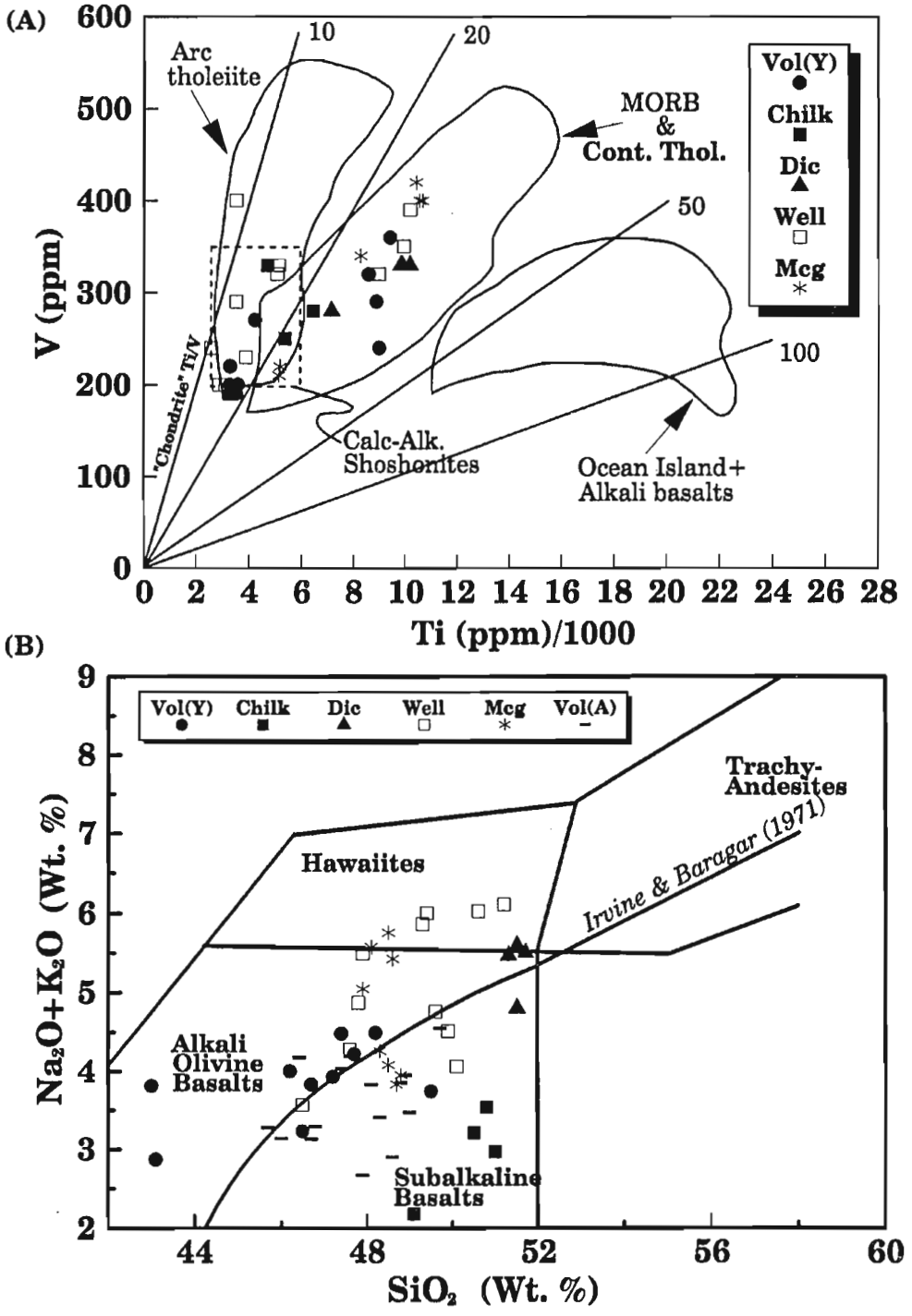

Figure 180. (A) V vs. Ti/1000 tectonomagmatic discriminant diagrams and (B) Na_2O+K_2O vs. SiO_2 basalt compositional fields occupied by Nikolai basalt from the Yukon (Vol(Y)), and Alaska (Vol(A)), the Chilkat Peninsula of Alaska (Chilk), and chilled marginal gabbros associated with the Dickson Creek Complex (Dic), Quill Creek Complex (Well), and Maple Creek gabbro intrusions (Mcg).

*Ti/100-Zr-Y*3 ternary plot*

This plot (Fig. 178A) was created by Pearce and Cann (1971) and is amongst the most commonly used discriminant diagram. Davis and Plafker (1985) also used this plot in examining the Triassic basalt from the Chilkat Peninsula, Alaska. Quenched basaltic material from the Yukon falls within the fields: B (ocean-floor basalt+low-K basalt+calc-alkali basalt but this field is also that of MORB basalt), C (calc-alkali basalt), and D (within-plate basalt). The Alaskan samples straddle fields B and D. It is apparent this diagram is of little practical use in discriminating the tectonomagmatic environment nor petrological association of basaltic rocks from Wrangellia. Based on a more comprehensive study of this discriminant plot Wang and Glover (1992) found that: 1) the diagram could not discriminate ocean island basalt from continental basalt which is a serious concern, 2) back arc basalt is treated as ocean floor basalt, 3) greater than 80% of the ocean floor basalt defining this field is from the Gulf of Aden and Mid-Atlantic, and 4) over 60% of the database for continental basalt is from the Deccan and Karoo basalts, and many plot out of the within-plate basalt field with the majority in the ocean floor basalt and calc-alkali basalt fields. This is a major concern as the diagram was originally designed to separate within-plate basalt from other types.

$FeO(t)$-MgO-Al_2O_3 ternary plot

As proposed by Pearce et al. (1977) this diagram (Fig. 178B) is designed for non-alkaline basaltic andesite (SiO_2 = 51-56%), with no or a fairly low degree of metamorphism or alteration. The diagram is very sensitive to the effect of crystal fractionation because it uses Fe and Mg as discriminants. With only a few exceptions this diagram clearly discriminates the Wrangellia basaltic material as belonging to an oceanic setting rather than continental, orogenic, or spreading centre as nearly all of the samples from the Yukon and Alaska fall in either the ocean island or ocean ridge and floor fields. One of the major concerns of this diagram is that the discriminant fields are so small that the accuracy of data may affect the result of the discrimination.

AFM (Na_2O+K_2O-MgO-$FeO(t)$ ternary plot

The AFM plot (Fig. 178C) with the solid line to separate tholeiitic and calc-alkaline fields (Irvine and Baragar, 1971) demonstrates the tholeiitic rather than calc-alkaline character of most of the Triassic basaltic samples from Wrangellia. As the majority of the samples that fall within the calc-alkaline field are from the Yukon intrusive suite, which is believed to have been contaminated with Ba and alkalis upon emplacement, these so-called calc-alkaline samples are merely alkali-contaminated tholeiite. Davis and Plafker (1985) found that the vast majority of coeval Triassic volcanic rocks from Alaska fall within the tholeiitic field, and Barker et al. (1989) found that all Karmutsen basalt falls within the tholeiite field. This plot also clearly distinguishes the Triassic tholeiitic within Wrangellia from that of the macroscopically similar Late Triassic subduction-related Takla Group and Nicola Group mafic lavas from the Quesnellia terrane. Tholeiite from this group is associated with a more voluminous calc-alkalic group which displays extreme alkali enrichment (Mortimer, 1987).

TiO_2-Y/Nb plot

Ti, Y, and Zr are generally considered to be immobile during alteration processes, therefore it should be possible to distinguish between magma types in ancient basic volcanic rocks that have been subject to low grade alteration, as has been the case for the Triassic volcanic rocks from the Yukon and Alaska. In the TiO_2-Y/Nb plot (Fig. 179A), as proposed by Floyd and Winchester (1975), a Y/Nb ratio of 1 provides a convenient divider of tholeiitic and alkali basalts although some overlap is apparent. Although no distinction can be made between continental and oceanic tholeiites for Wrangellia, a clear distinction can be made with the alkali basalt. As these basalts are not of a continental origin, this additional geochemical constraint (Fig. 179A) further corroborates that these basaltic rocks are not of a alkali basalt lineage even though they have high Rb and Ba concentrations.

Zr/Y-Ti/Y plot

The preferential clustering of data points in the "plate margin" field in Figure 179B (diagram after Pearce and Gale, 1977) also confirms the non-continental geochemical character of the quenched basaltic suites from the Yukon and Alaska.

V -Ti/1000 plot

This diagram, created by Shervais (1982), is intended to separate MORB, arc basalt, and alkalic basalt (Fig. 180A). Wang and Glover (1992) had serious concerns relating to: (1) MORB, back-arc basin basalt and continental flood basalt plot in the same field (i.e. Ti/V = 20-50), (2) some arc-basalts, especially differentiated ones, plot in the MORB and continental flood basalt field, and (3) calc-alkaline arc basalts plot in both MORB and arc-tholeiite fields. Many of the basaltic rocks from Wrangellia fall within the confines of the MORB and continental tholeiite field, but some samples also fall within the lower portion of the arc-tholeiite field where the two fields overlap. This same area can also be occupied by calc-alkali and shoshonite but other lines of evidence indicate that such lithologies are not present. Clinopyroxene fractionation may be an important variable giving rise to these acute trends as this phase incorporates Ti and fractionation of clinopyroxene or spinel will cause curved fractionation trends that cross the constant Ti/V ratio lines at a low angle (Shervais, 1982). Ti depletion associated with the H-element plots mentioned previously for certain Yukon suites tends to support this explanation. The one unequivocal finding from this plot is that none of the Wrangellian basaltic suites are of an alkalic character. This is important because the conventional Na_2O+K_2O-SiO_2 plot (Fig. 180B) of Irvine and Baragar (1971) suggests that approximately half the samples have an alkalic parentage, but the anomalous alkalis are clearly a product of contamination and alteration.

Geochronology

Although generally assumed to be broadly comagmatic with the proximal Nikolai Group volcanic rocks, the only direct age determinations for the mafic-ultramafic intrusive complexes consist of a small number of relatively imprecise K-Ar ages. These data, together with field observations, indicate that the main mafic-ultramafic intrusive event in the Kluane Belt occurred prior to the onset of mafic volcanism. The present geochronological study was undertaken to resolve two important questions: (1) the age for the onset of Nikolai volcanism, and (2) was there a significant hiatus between the emplacement of the inferred subvolcanic mafic-ultramafic intrusives and the main Nikolai extrusive event?

Prior to this study only two radiogenic age determinations were made on selected mafic-ultramafic intrusions in the Kluane Belt. Campbell (1981) reported K-Ar ages of 224 ± 16 and 225 ± 14 Ma for intercumulus phlogopite separated from peridotite at Tatamagouche Creek and White River intrusive complexes, respectively. The K-Ar ages only represent cooling ages through the closure temperature of the K-Ar system in phlogopite (≈280°C). However, if these intrusions are subvolcanic, then they should have cooled relatively rapidly, and the K-Ar ages may closely approximate the actual emplacement age. Nevertheless, an error of ±15 Ma is far too large (≥60% of the Triassic period, Hartland et al., 1989) to accurately record the onset of Triassic mafic magmatism in the Kluane Belt since it could imply that magmatism was initiated either during the Anisian stage of the Middle Triassic (epoch = Tr2) at 240 Ma or during the end of the Norian stage (epoch = Tr3) of the Late Triassic at 210 Ma.

Field relationships at Tatamagouche Creek provided a unique opportunity to date unequivocally both the Maple Creek gabbro and Nikolai basalt emplacement ages, respectively, and place a minimum age on the Tatamagouche Creek mafic-ultramafic complex. Along the south side of Tatamagouche Creek, 4.2 km upstream from the confluence with Burwash Creek, a Maple Creek gabbro sill intrudes the western end of the Tatamagouche Creek mafic-ultramafic complex (Fig. 36, 37). The sill has a maximum strike length of 2 km, and attains an average thickness of 120 m. East and northeast of the Tatamagouche fault and Tatamagouche Creek similar thin dykes and sills can clearly be seen as feeders to the Nikolai volcanic rocks in the area.

The sill sampled for this geochronological investigation consists of variably textured, greyish-black, oxide-rich gabbro. Grain size varies considerably within the body, but most rock types present are fine- to medium-grained with a well developed ophitic texture. Fine-grained chilled margins have been observed near the top of the intrusion (Fig. 37) where the body intrudes the Station Creek Formation tuff. Irregular, very coarse-grained pockets and segregations of oxide-rich gabbro are scattered throughout the sill. These pegmatitic areas are up to several metres thick and tens of metres long. In the coarser-grained facies, augite crystals 2-4 cm x 0.5-1.0 cm are not uncommon. Large skeletal Fe-Ti oxide patches of similar dimensions are also present. Apart from their coarse grain size, the pegmatitic material resembles the enveloping host rock. Mineralogically the rock generally contains: plagioclase (49%), augite (38%), ilmenite (6%), magnetite (2%), quartz (1%), apatite (0.5%), and pyrite, biotite, titanite, leucoxene, and zircon making up the remainder. Compositionally the Mg# of the clinopyroxene varies from 0.64 to 0.67, and associated plagioclase has a Ca# of 0.60.

Zircon was separated from a 3 kg sample of pegmatitic gabbro using conventional Wilfley table and heavy liquids. All zircon fractions were abraded prior to dissolution. $^{207}Pb/^{206}Pb$ ages for the three zircon fractions (stubby to elongate, clear, colourless to medium-brown prisms) give an average age of 232.3 ± 1.0 Ma (Fig. 181). Further details concerning the analytical techniques and results are given in Mortensen and Hulbert (1991).

The U-Pb zircon age for the Maple Creek gabbro provides a minimum age for the Kluane mafic-ultramafic intrusive complexes, and corroborates the earlier less precise K-Ar

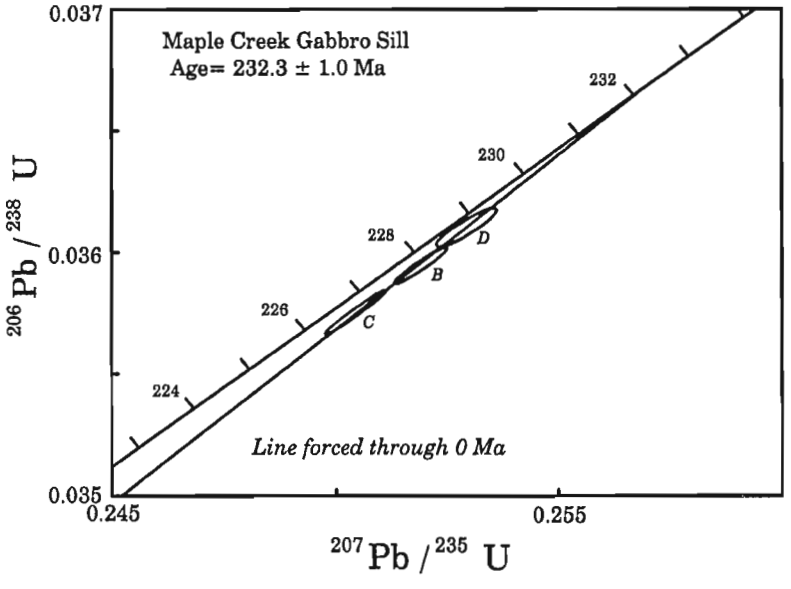

Figure 181.

U-Pb isochron for zircon extracted from a Maple Creek gabbro sill, Tatamagouche Creek.

ages determined for two of these complexes. This new age determination demonstrates that Nikolai Group volcanism began in the Carnian, and not Norian stage of the Triassic as previously believed (Read and Monger, 1976; Campbell, 1981). Conodonts from limestone beds within the Nikolai Group indicate that Nikolai volcanism continued into at least the Early Norian stage (Campbell, 1981). These age brackets indicate that volcanism spanned a period of at least 9 to 10 Ma.

Neodymium, strontium, oxygen, and osmium isotope geochemistry

Radiogenic isotopic variations frequently survive chemical fractionation events which accompany the formation and evolution of magmas. During partial melting, therefore, a magma inherits the isotopic composition of its source which remains constant during subsequent fractional crystallization events as long *as the magma does not become contaminated by isotopically distinct country rocks* or other batches of magma. A detailed Nd, Sr, Os, and O isotopic study of material from the Quill Creek Complex was undertaken. In addition, Os isotopic analyses of a Nikolai basalt from Tatamagouche Creek area and a Permian sedimentary country rock (contaminant ?) from the White River area were also investigated. The study investigated the isotopic character of various lithological suites (ultramafic cumulates, basal gabbroic marginal rocks, chills, associated sulphide segregations, and contemporaneous Nikolai basalts), and the proximal wall rock contaminants. In addition, Nd and Sr isotopic data from other lithological domains from the western limb of Wrangellia are compared with that from the study area to further constrain the isotopic character of Triassic magmatism within Wrangellia, the tectonomagmatic setting, and the influence of crustal contamination on the isotopic systematics and metallogenesis. The influence of late magmatic hydrothermal and postmagmatic alteration (deuteric and serpentinization) fluids on the various isotope systems are also discussed. The results of the isotopic study are given in Tables 4, 5, and 6, and Figures 182 to 188.

Rb, Sr, Sm, and Nd isotopes were determined on the same sample powders for which Re and Os results were obtained. All isotopic data reported from this study were analyzed at the Lamont-Doherty Earth Observatory of Columbia University (Marcantonio et al., 1993). Appendix 1 describes analytic methods.

Rubidium-strontium isotopes

Ratios and isotope dilution concentration data for the investigated samples are displayed in Table 4 and Figure 182A. Regression of the $^{87}Sr/^{86}Sr$ and $^{87}Rb/^{86}Sr$ data for the gabbro in Figure 182A indicates a weak to moderate linear correlation ($r = 0.559$) with a suggested initial Sr ratio of 0.7059. Initial Sr ratios calculated for the peridotite (wehrlite) are meaningless (initial ratios <0.700) and indicate that a significant amount of Rb has been added to these samples, possibly during the serpentinization stage. Calculated initial Sr ratios are variable and range from 0.7044 to 0.7062 in the gabbro. The range in initial $^{87}Sr/^{86}Sr$ ratios for Karmutsen and Chilkat Peninsula basalts (western limb of Wrangellia) are 0.70312 to 0.70400 (Samson et al., 1990; Andrew et al., 1991). Although the $^{87}Sr/^{86}Sr$ ratio of the Quill Creek Complex (Wellgreen) gabbroic rocks has been modified by crustal contamination, and in some cases late deuteric or hydrothermal fluids, it would appear that the least modified Wellgreen gabbroic material had an initial $^{87}Sr/^{86}Sr$ ratio of 0.7044 which is similar to the highest values from the western limb of Wrangellia.

Neodymium and samarium isotopes

Nd and Sm concentrations are presented in Table 5. The Nd isotopic results are not as variable as those for Sr. The measured $^{143}Nd/^{144}Nd$ ratios range from 0.51266 to 0.51278, corresponding to ε_{Nd} (232 Ma) of +2.3 to +4.5. The relatively young age of the complex, and lack of spread in Sm/Nd ($^{147}Sm/^{144}Nd$ = 0.125 to 0.165), preclude calculation of a meaningful Sm-Nd age. With one exception, the gabbro is more "enriched" (lower ε_{Nd} (232 Ma)) than the associated

Table 4. Rb, Sr and O isotope systematics from the Wellgreen property of the Quill Creek Intrusive Complex.

Sample Number	$^{87}Sr/^{86}Sr^{a}$ (measured)	$^{87}Rb/^{86}Sr$	Rb (ppm)	Sr (ppm)	$^{87}Sr/^{86}Sr_{(i)}$ (t = 232 Ma)[b]	$\delta^{18}O‰$	Lithology
HDB-87-18	0.706215	0.0068	1.83	773.2	0.70619	7.6	Gab.
U391-60-67	0.706062	0.4986	5.89	34.16	0.70442	7.9	Gab.
U382-79	0.706602	0.2433	2.18	25.95	0.70580	7.7	Gab.
HDB-87-13	0.705708	0.2128	1.42	19.26	0.70501	7.6	Gab.
87-98-119.58	0.705870	0.1257	1.33	30.62	0.70546		Gab.
HDB-87-27	0.707183	0.5847	3.34	16.50	0.70525	7.9	Gab.

[a] $^{87}Sr/^{86}Sr$ data were normalized to a value of 0.70807 for the E & A standard, which repeated to within 0.0032%

[b] $^{87}Sr/^{86}Sr$ based on the 232 Ma zircon age and using $\lambda^{87}Rb = 1.42 \times 10^{-11}$

Table 5. Nd and Sm isotope systematics from the Wellgreen property of the Quill Creek Intrusive Complex.

Sample Number	$^{143}Nd/^{144}Nd$[a] (measured)	$^{147}Sm/^{144}Nd$	Sm (ppm)	Nd (ppm)	$^{143}Nd/^{144}Nd_{(I)}$ (t=232Ma)[b]	ε_{Nd} (t=232Ma)	Lithology
HDB-87-18	0.512706	0.1355	1.975	8.782	0.512500	3.14	Gab.
U391-60-67	0.512749	0.1645	1.532	5.610	0.512499	3.12	Gab.
U382-79	0.512743	0.1490	1.998	8.083	0.512517	3.46	Gab.
HDB-87-13	0.512677	0.1438	1.434	6.007	0.512459	2.33	Gab.
87-98-119.58	0.512696	0.1551	1.034	4.020	0.512461	2.37	Gab.
HDB-87-27	0.512664	0.1458	1.369	5.663	0.512443	2.02	Gab.
U391-67-70	0.512779	0.1537	1.644	6.440	0.512546	4.03	Perid.
U441-45	0.512759	0.1247	1.076	5.201	0.512570	4.49	Perid.
U441-40	0.512740	0.1664	1.082	3.920	0.512487	2.89	Perid.

[a] Nd data required no normalization as repeat analyses of La Jolla Nd standard yielded an average $^{143}Nd/^{144}Nd$ of 0.5118433 with a reproducibility of 0.0025%.
[b] $^{87}Sr/^{86}Sr$ based on the 232 Ma zircon age and using $\lambda^{147}Sm = 6.54x10^{-12}$

Table 6. Re and Os isotope systematics from the Wellgreen property of the Quill Creek Intrusive Complex and surrounds.

Sample Number	$^{187}Os/^{186}Os$ (measured)	$^{187}Re/^{186}Os$	Os (ppb)	Re (ppb)	$^{187}Os/^{186}Os^{(b)}$ (t=232Ma)[b]	γ_{Os} (t=232Ma)	Lithology
HDB-87-18	2.349	161.0	11.00	42.99	1.735	66.91	Gab.
87-98-119.58	1.268	29.6	41.60	30.29	1.155	10.48	Gab.
U391-60-67	1.204	25.9	62.60	39.80	1.106	5.21	Gab.
HDB-87-13	1.231	26.2	82.30	53.04	1.131	8.15	Gab.
HDB-87-27	2.131	166.8	24.50	99.10	1.495	27.28	Gab.
U382-79	1.373	55.90	27.77	38.12	1.160	12.47	Gab.
U441-45	1.152	21.40	39.70	20.97	1.071	3.44	Perid.
U391-67-70	1.197	36.2	31.73	28.30	1.058	1.46	Perid.
HDB-87-21	1.152	23.9	23.75	14.00	1.061	1.53	Perid.
U441-40	1.210	26.9	22.50	14.90	1.108	5.90	Perid.
HDB-87-4	1.192	16.1	28.90	11.50	1.131	8.01	Calc-Sil.
WMS-1	1.479	90.50	114.1	254.0	1.134	8.37	MSS
483-84.3	1.353	23.7	355.6	207.4	1.263	20.66	MSS
88-CAN15A	17.75	1658	1.05	34.08	11.43		Hasen Ck.
87-104-125	20.87	2122	0.039	1.56	12.78		Chill.
TAT-65b	3.58	348.8	0.021	0.177	2.25		Nikolai

[b] $^{187}Os/^{186}Os$ based on the 232 Ma zircon age and using $\lambda^{187}Re = 1.64x10^{-11}$ (Lindner et al., 1989)
Gab. = gabbro, Perid. = peridotite, Calc-Sil. = calc-silicate, MSS = massive sulphide, Chill. = chilled gabbroic margin, Nikolai = Nikolai basalt, Hasen Ck. = Hasen Creek Formation sediment.

peridotite. A plot of $^{143}Nd/^{144}Nd$ and $^{147}Sm/^{144}Nd$ data for the gabbroic and ultramafic samples from the Wellgreen property is shown in Figure 182B.

To compare differences between $^{143}Nd/^{144}Nd$ ratios of igneous rocks, including those from Wrangellia, with CHUR (Chondritic Uniform Reservoir), the epsilon parameter ε_{Nd} of DePaolo and Wasserburg (1976) is used. This parameter expresses deviations from the chondritic curve. A positive ε_{Nd} value implies that the magmas were derived from depleted mantle (higher Sm/Nd), whereas a negative value indicates that they were derived from a mantle source more enriched (lower Sm/Nd) than CHUR. In general, the earth's upper mantle or juvenile continental crust displays positive ε_{Nd} values during and subsequent to the Archean, whereas older, recycled continental crust displays lower positive or negative ε_{Nd} values.

Figure 182C presents the range in ε_{Nd} values for gabbroic and ultramafic rocks from the Wellgreen property; rhyodacite and andesite from the Karmutsen Formation (Andrew et al., 1991); Karmutsen basalt (Samson et al., 1990; Andrew et al., 1991),

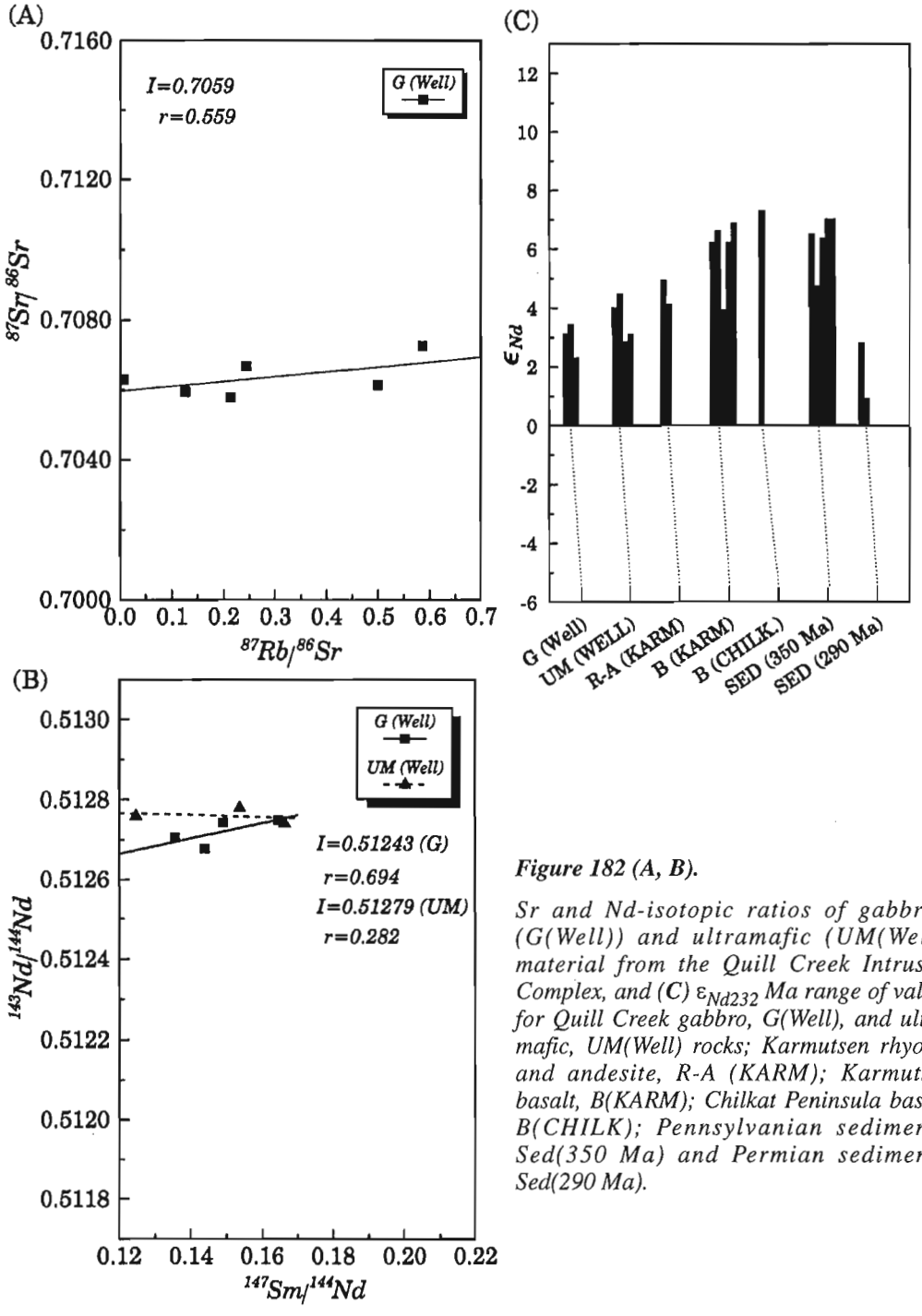

Figure 182 (A, B).

Sr and Nd-isotopic ratios of gabbroic (G(Well)) and ultramafic (UM(Well)) material from the Quill Creek Intrusive Complex, and (C) ε_{Nd232} Ma range of values for Quill Creek gabbro, G(Well), and ultramafic, UM(Well) rocks; Karmutsen rhyolite and andesite, R-A (KARM); Karmutsen basalt, B(KARM); Chilkat Peninsula basalt, B(CHILK); Pennsylvanian sediments, Sed(350 Ma) and Permian sediments, Sed(290 Ma).

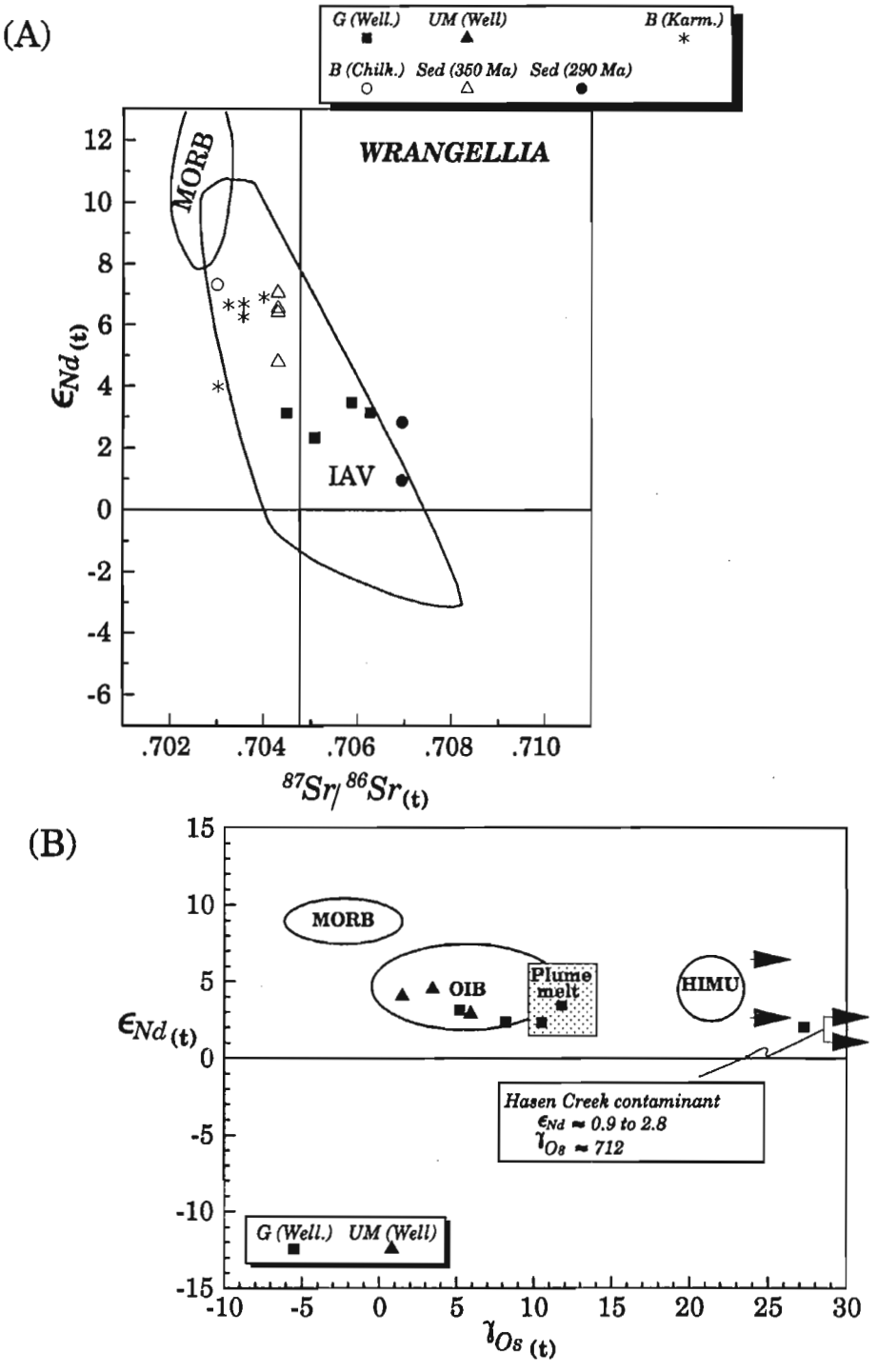

Figure 183. *(**A**) Nd-Sr and (**B**) Nd-Os isotopic compositions of gabbroic, G(Well.), and ultramafic, UM(Well), material from the Quill Creek Intrusive Complex; Karmutsen rhyolite and andesite, R-A (Karm); Karmutsen basalt, B(Karm.); Chilkat Peninsula basalt, B(Chilk.); Pennsylvanian sediments, Sed(350 Ma) and Permian sediments, Sed(290 Ma), relative to different tectonomagmatic environments; OIB = ocean-island tholeiite, IAV = island-arc volcanic. Nd-Os plot modified after Ellam et al. (1992).*

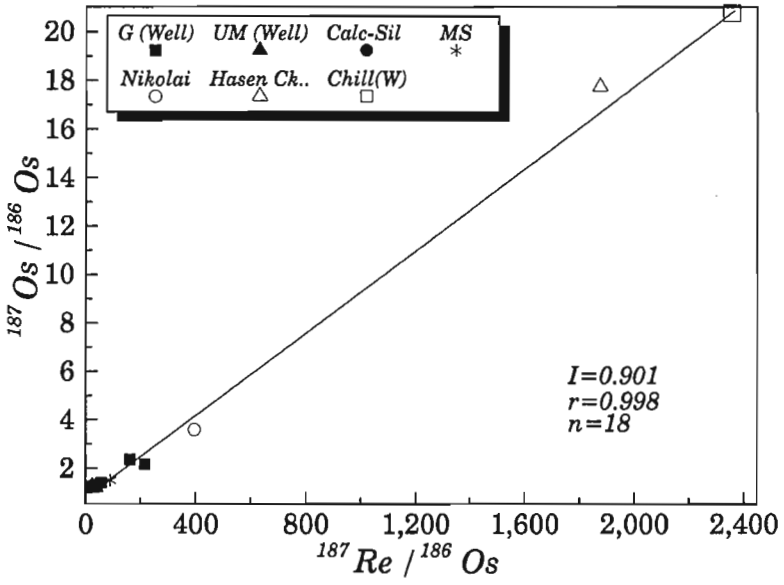

Figure 184.

$^{187}Os/^{186}Os$ vs. $^{187}Re/^{186}Os$ plot of isotopic compositions of mineralized gabbroic, G(Well) and ultramafic, UM(Well), rocks; massive sulphide, MS; mineralized calc-silicate, Calc-Sil, and chilled gabbro, Chill (W), from the Quill Creek Intrusive Complex as well as a Hasen Creek sedimentary rock, Hasen Ck., and a Nikolai basalt, Nikolai. I = calculated initial composition, r = Pearson correlation coefficient of data regression line (shown), n = number of samples.

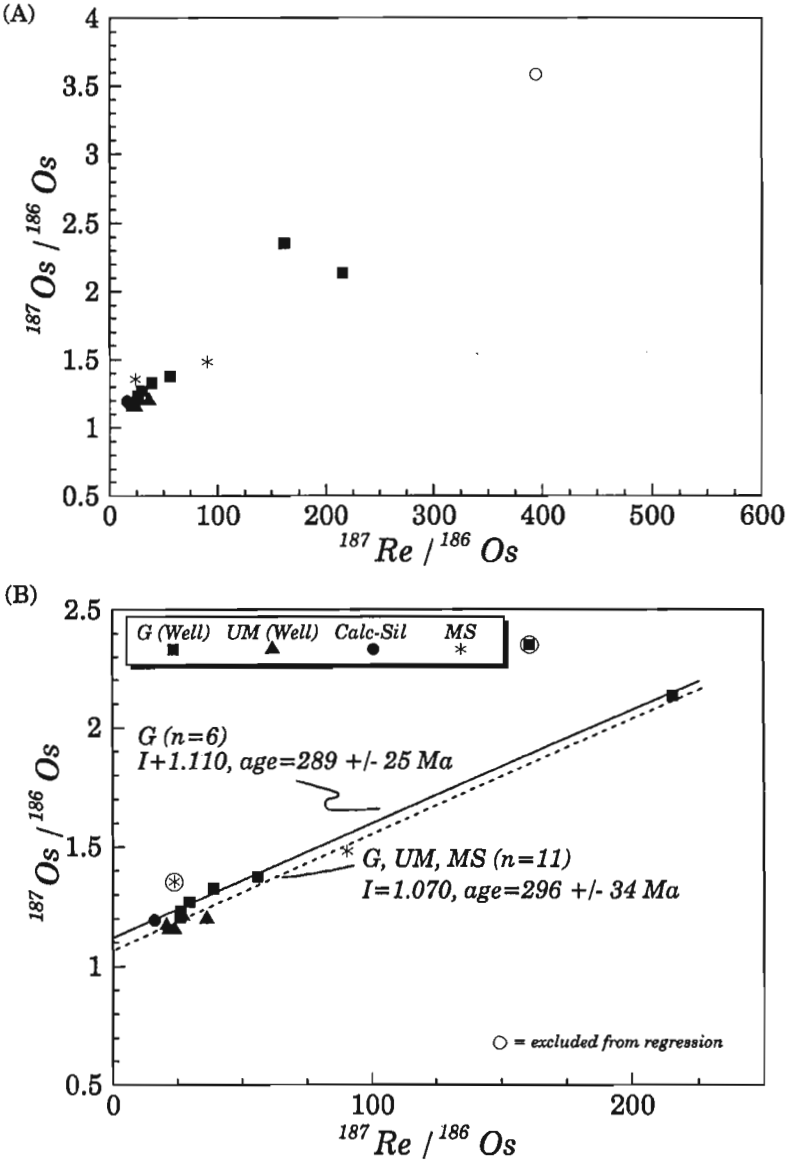

Figure 185.

(A) Same as Figure 184 except at a reduced scale to emphasize differences between the various data sets. (B) Re-Os systematics for gabbroic samples (n = 6) and all gabbroic, ultramafic, and massive sulphide samples (n = 11) at a reduced scale. I = computed initial isotopic composition based on a regression of each data set. The computed age, based on each data set, is also given. Note that samples excluded from the data sets and calculations are encircled. G, G(Well) = gabbroic, UM, UM(Well) = ultramafic, Calc-Sil = mineralized calc-silicate, MS = massive sulphide.

basalt from the Chilkat Peninsula, Alaska (Samson et al., 1990); and 350 Ma and 290 Ma mudstones from Wrangellia (Samson et al., 1990). The combination of intrusive, extrusive, and sedimentary samples of known isotopic composition from Wrangellia is useful in that it can provide different but complementary information. Unfortunately, Nd and Sr isotopic data are not available for the Nikolai basalt or the Hasen Creek Formation sediments from the study area. Nevertheless, the subvolcanic mafic-ultramafic bodies can provide important information concerning the source of the magma, and unexposed crust through which the magma passed. Comagmatic extrusive rocks should experience less crustal contamination and monitor the character of successive magma pulses. The sedimentary rocks provide valuable information about a large crustal area exposed at the time of sedimentation and the isotopic character of potential magma contaminants.

Basaltic rocks from the western limb of Wrangellia (i.e. Karmutsen and Chilkat Peninsula basalts) generally have ε_{Nd} values in the +6.2 to +7.3 range. The less voluminous Karmutsen rhyodacite and andesite have values of +5.0 and +4.1, respectively. These more acidic derivatives may be a product of siliceous crustal contamination. It is clear from Figure 182C that contamination of these magmas by the 350 Ma sediments would have little effect on the values of the basaltic magmas, but the same cannot be said for the 290 Ma (Permian) sediments (Butte Lake Formation) with values ranging from +0.9 to +2.8. Although Nd isotopic data for the inferred Permian contaminants from the Wellgreen area are not available and it is assumed to be similar to the Butte Lake Formation, then it is not difficult to envisage how assimilation of such material could lower the primary ε_{Nd} signature from approximately +6.9 to +2.3. This contamination hypothesis is also corroborated by the

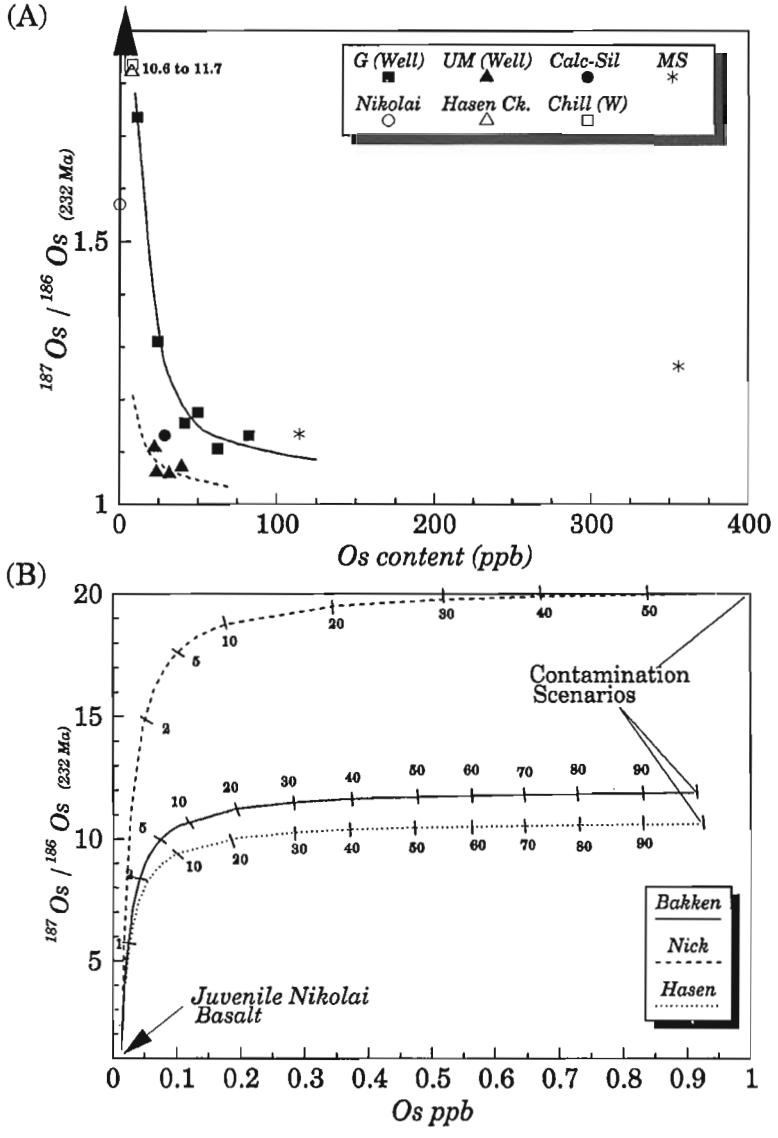

Figure 186.

(A) Plot of $^{187}Os/^{186}Os_{(232\ Ma)}$ vs. Os (ppb) of mineralized gabbroic, G(Well), and ultramafic, UM(Well), rocks; massive sulphide, MS; mineralized calc-silicate, Calc-Sil, and chilled gabbro, Chill (W) from the Quill Creek Intrusive Complex as well as a Hasen Creek sedimentary rock, Hasen Ck., and a Nikolai basalt, Nikolai. The plot demonstrates that the gabbroic suite displays a hyperbolic correlation with respect to these two variables, and that the most radiogenic samples are generally associated with the chilled margin and Nikolai basalt samples which also contain the lowest Os concentrations. (B) $^{187}Os/^{186}Os_{(232\ Ma)}$ vs. Os (ppb) magma-country rock mixing (contamination) models based on three different sedimentary contaminants (i.e. Bakken shale, Nick-type sedimentary nickeliferous sulphides, Hasen Creek sediments) and an initial basaltic magma with Os concentrations similar to that of the Nikolai basalt and a primary $^{187}Os/^{186}Os_{(232\ Ma)}$ ratio similar to that of juvenile mantle derived magmas (1.047) of that age.

noticeably more positive ε_{Nd} values associated with the ultramafic rocks (+2.89 to +4.49) relative to the marginal zone gabbroic rocks (+2.02 to +3.46) which are commonly juxtaposed Permian Hasen Creek Formation sediments. Marginal gabbroic rocks are commonly assimilating and reacting with the Hasen Creek Formation sediments, whereas similar intrusive reactions are not apparent in the overlying ultramafic rocks which appear to be buffered from the country rock contaminants more than the gabbro. The ε_{Nd} values of the Triassic basalt from the western portion of Wrangellia are similar to the value calculated by DePaolo (1981) for depleted mantle of the same age. The high positive values indicate that the terrane is an isotopically unevolved juvenile crustal fragment (Samson et al., 1990). These signatures also indicate that the mantle beneath Wrangellia was LREE depleted rather than LREE enriched, and that other related Triassic magmas from the eastern limb of the terrane have ε_{Nd} values far too low to be pristine melts derived from a depleted mantle. These eastern magmas must have incorporated older crustal material (i.e. Permian (290 Ma) sediments) with lower ε_{Nd} values as previously suggested. Andrew and Godwin (1989) suggested that Karmutsen volcanic rocks display evidence of sediment contamination based on initial Pb isotope ratios. Mixing of crustal sediment with oceanic basaltic magmas is possible, but only a maximum of just a few per cent of an evolved sedimentary component is allowed by the Nd and Sr isotopic data (Samson et al., 1990). Samson et al. (1989) pointed out that just a few per cent of continent-derived sediment mixed with terrane-derived sediment would give lower ε_{Nd} values because of the very negative ε_{Nd} value of average crustal sediment. Similarly small amounts of contamination have been inferred for the Quill Creek Intrusive Complex and the associated Wellgreen mineralization based on S and Os isotope mixing models. However, with the exception of the Permian (290 Ma) sediments, the ε_{Nd} values for most Wrangellian sedimentary rocks are high, illustrating their juvenile nature.

The ε_{Nd} vs. $^{87}Sr/^{86}Sr_{(i)}$ plots (Fig. 183A) have conventionally been used for tectonomagmatic interpretations but they are used in this study to demonstrate the influence of contamination on the Wellgreen samples, and how selective sedimentary contamination can lead to erroneous tectonomagmatic inferences. Unfortunately, $^{87}Sr/^{86}Sr$ analyses are not available for corresponding sedimentary samples from Wrangellia with known ε_{Nd} data (Samson et al., 1990). If these samples are assumed to have $^{87}Sr/^{86}Sr$ values similar to siltstone (0.70695) of comparable age and ε_{Nd} signatures

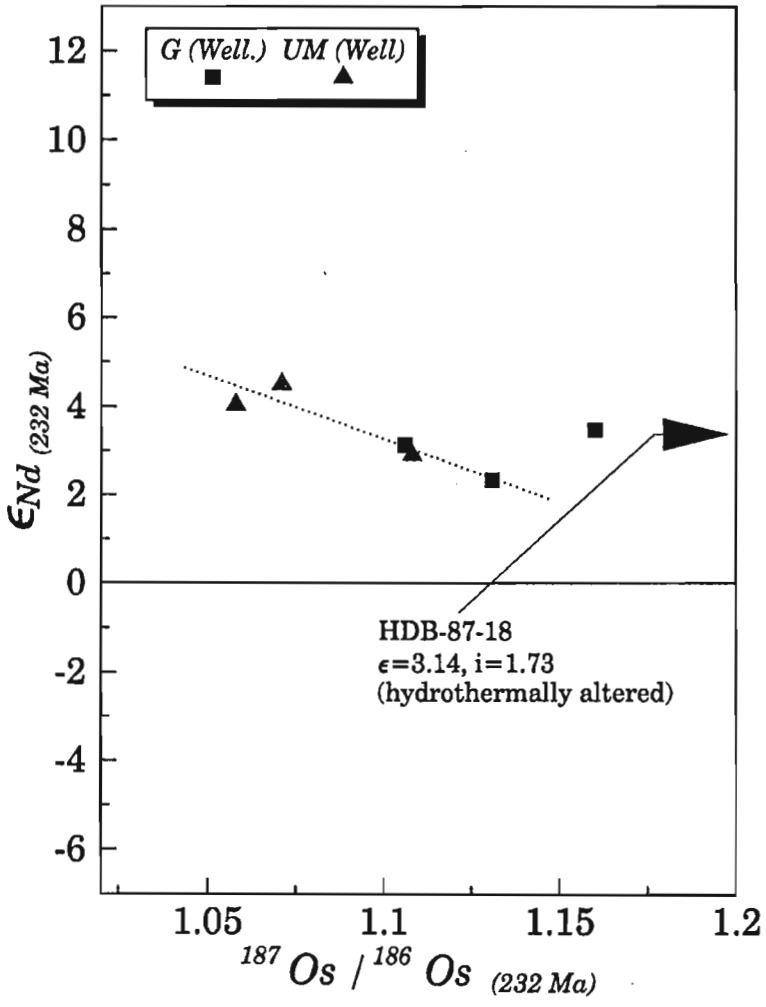

Figure 187.

$\varepsilon_{Nd232Ma}$ vs. $^{187}Os/^{186}Os_{(232\ Ma)}$ plot of gabbroic (G(Well.)) and ultramafic (UM(Well)) lithologies from the Wellgreen deposit of the Quill Creek Intrusive Complex, illustrating the more chondritic nature of the ultramafic rocks and how decreasing values are associated with samples (gabbro) containing increasingly more radiogenic Os.

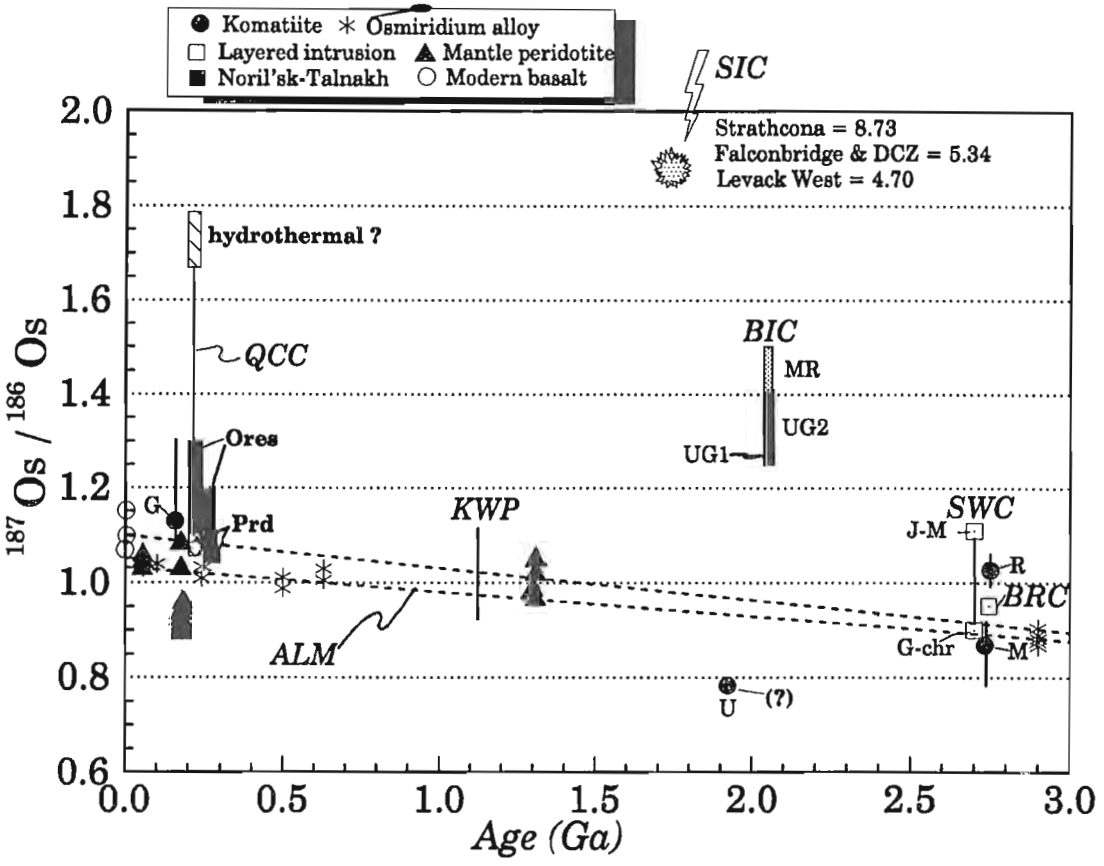

Figure 188. *Initial $^{187}Os/^{186}Os$ vs. time of formation plot; data from GSC studies and from the available literature showing the QCC, Quill Creek Complex (Wellgreen deposit) (Marcantonio et al., 1991) data relative to other associations. R, Rankin Inlet; BRC, Bird River Sill; M, Munro Township komatiite (Walker et al., 1988); SWC, Stillwater Complex (J-M, J-M Reef; G-chr, G-chromitite) (Martin, 1989; Lambert et al., 1989); BIC, Bushveld Igneous Complex (MR, Merensky Reef; UG2, UG2 chromitite; UG1, UG1 chromitite) (McCandless and Ruiz, 1990; Ruiz and McCandless, 1990; Hart and Kinloch, 1989); U, Ungava Ni-sulphide ore (Luck and Allègre, 1984); KWP, Keweenawan picrite (Shirey and Carlson, 1991); G, Gorgona komatiite (Walker et al., 1991b); SIC, Sudbury Igneous Complex (Walker et al., 1991a) osmiridium alloys (from youngest to oldest: Borneo, Columbia, Tulameen, B.C., Australia, Japan, Tasmania and Witwatersrand, RSA) (Allègre and Luck, 1980; Hattori et al., 1991; Hattori and Hart, 1991; Hart and Kinloch, 1989); Noril'sk-Talnakh, Russia (Horan et al., 1991; Walker et al., 1992); mantle peridotite: S.W. Indian Ridge, Zabargad Island (Red Sea), Zambales ophiolite, Philippines, Kaapvaal craton, RSA and Ronda Complex, Spain (Martin 1991; Reisberg et al., 1991; Walker et al., 1989). Modern basalt: Hawaii, Iceland, East Pacific Rise (Martin, 1991). The two broken curves in the lower half of the diagram represent the osmium isotopic evolution of the mantle 1) the lower curve (ALM) is the evolution curve for the mantle source of osmiridium alloys based on the findings of Allègre and Luck (1980) recently published data on Hattori et al. (1991), Hattori and Hart (1991), and Hart and Kinloch (1989), 2) the upper curve passes through the meteorite initial composition at 4.55 Ga (Luck and Allègre, 1983; Walker and Morgan, 1989) and undifferentiated mantle follows an Os isotopic evolution with $^{187}Re/^{186}Os$ of 3.3 giving a present-day $^{187}Os/^{186}Os$ of 1.06 which is typical of present day values measured for carbonaceous chondrite (Walker and Morgan, 1989).*

from the Alexander Terrane, then it becomes apparent how crustal contamination of a pristine Karmutsen (or Nikolai) basalt by Permian (290 Ma) sediments can give rise to isotopic signatures characteristic of Wellgreen gabbro. Under these conditions the significance of the island arc volcanic (IAV) field boundary becomes somewhat questionable particularly when ε_{Nd} vs. γ_{Os} data plot both in the ocean island basalt (OIB) field and plume melt field (Fig. 183B).

Oxygen isotope

Results are also reported in Table 4. The data show little variation within the same rock type or between different rock types with a total range of $\delta^{18}O$ from 7.3 to 7.9‰. The limited range of the isotopic compositions is believed to represent the isotopic signature of one fluid event passing through these rocks.

Rhenium-osmium isotopes

Results of samples from the Wellgreen property of the Quill Creek Complex are presented in Table 6 (see Appendix 1 for analytical methods). Measured $^{187}Os/^{186}Os$ ratios range from 1.15 to 2.35 in the mineralized rocks, whereas Re and Os concentrations ranged from 11.5 to 254 ppb and 11.0 to 356 ppb, respectively. The initial Os ratios (age-corrected using the U-Pb zircon age of 232 Ma) for the same samples are variable and range from 1.06 to 1.82. Age corrections are made using the most recent, directly determined ^{187}Re decay constant of 1.64×10^{-11} (Lindner et al., 1989). Re-Os data for some unmineralized rocks that are associated with, or in the vicinity of, the Wellgreen property are also given in Table 5. A fine-grained unmineralized quenched gabbroic sample from the chilled margin occurs at the base of the mineralized gabbroic unit. This chill is characterized by a low Os concentration (0.039 ppb), comparable to basaltic values, but is extremely radiogenic ($^{187}Os/^{186}Os_{(232\ Ma)} = 12.8$). Permian siliceous carbonate of the Hasen Creek Formation contains surprisingly high concentrations of Os (1.05 ppb) and is very radiogenic ($^{187}Os/^{186}Os_{(232\ Ma)} = 11.4$). The one sample of Nikolai basalt analyzed had a radiogenic initial Os ratio of 2.25 and a low Os concentration (0.021 ppb).

A plot of the present day $^{187}Os/^{186}Os$ and $^{187}Re/^{186}Os$ ratios for the different sample populations, at varying scales, is shown in Figures 184 and 185(A, B). Figure 184 shows that the lowest ratios are associated with the ultramafic rocks, mineralized and weakly mineralized gabbro, and massive sulphide. The highest ratios are associated with samples from the basal intrusive contact zones (i.e. chilled margin to the Quill Creek Complex, and the weakly sulphidic Permian Hasen Creek carbonate strata, from the immediate footwall contact of the White River Complex at the Canalask property). With one exception (Nikolai basalt from Tatamagouche Creek), these samples also contain the lowest concentrations of Os (0.039 to 1.05 ppb) encountered in the study. This relationship between the most radiogenic samples being associated with the least mineralized samples (containing the lowest Os concentrations) suggests the influence of either crustal contamination or the mobility of Os in either hydrothermal fluids resulting from the emplacement of the intrusion, or subsequent deuteric fluids generated during the cooling history of the intrusion. Figure 185(A, B) shows the different trends and anomalous values that emerge when the scale is decreased, and the radiogenic unmineralized chill, Hasen Creek Formation contact rock, and Nikolai basalt samples are excluded. Figure 185B reveals different radiogenic populations and trends. Ultramafic rocks from Wellgreen clearly have lower $^{187}Os/^{186}Os$ ratios than the gabbroic rocks. With the exception of one excluded (circled) gabbroic rock, the gabbroic population ($n = 6$) defines an isochron with an initial $^{187}Os/^{186}Os$ ratio (I) = 1.110, an age of 289 ± 25 Ma and a MSWD = 0.82. Another isochron is calculated for the gabbroic, ultramafic, and massive sulphide samples ($n = 11$) collectively about the broken line with an initial $^{187}Os/^{186}Os$ ratio of 1.07, an age of 296 ± 34 Ma, and a MSWD = 2.33. These age determinations indicate that Re-Os geochronology is both less precise and reliable than U-Pb dating of zircons (Fig. 181).

The potential effects of the Os mobility must be carefully evaluated prior to invoking crustal contamination to explain variable and radiogenic Os initial ratios in mafic-ultramafic igneous rocks and layered intrusions. A plot of $^{187}Os/^{186}Os_{(232\ Ma)}$ vs. Os content (Fig. 186) for the Wellgreen gabbroic suite and associated chilled margin along with the bordering Hasen Creek sediment, demonstrates a hyperbolic correlation. The samples with the most radiogenic Os generally contain the lowest concentration of Os, suggesting either extreme crustal contamination of the initial chilled magma from the intruded Hasen Creek sediments, or that the Os mobility accompanying alteration has primarily affected samples with the low-Os levels. The decreasing $^{187}Os/^{186}Os_{(232\ Ma)}$ ratio with increasing Os concentration also generally reflects increasing sulphide content of the associated gabbroic rocks. Massive sulphides hosted in the gabbroic rocks are least radiogenic and contain the highest Os content. Ultramafic rocks maintain their unradiogenic Os isotopic compositions although they contain relatively little Os compared to the gabbro. Therefore the Os isotopic compositions of the gabbro are disturbed to a greater degree than the overlying ultramafic rocks. One may argue that this is consistent with the more altered state of the gabbro, or conversely that the degree of magma assimilation of Hasen Creek sediments diminishes upwards from the chilled margin, through the overlying gabbro towards the ultramafic horizons.

The role of assimilation is compelling when one considers the three different contamination scenarios shown in Figure 186B. There is very little information pertaining to the Os-Re isotopic compositions and elemental concentrations of sedimentary rocks that could be considered as potential contaminants to the basic magmas. Hulbert et al. (1992b), Horan et al. (1994), and Ravizza and Turekian (1989) demonstrated that Devonian black shale and associated nickeliferous sulphide from the Yukon and the extensive coeval Bakken Shale within the Williston Basin of North America, contained sediments with high Os concentrations and elevated $^{187}Os/^{186}Os$ ratios at 232 Ma. Figure 186B demonstrates that a juvenile Nikolai magma with an initial $^{187}Os/^{186}Os_{(232\ Ma)}$ ratio of 1.047, and Os and Re concentrations of 0.0214 and 0.177 ppb, respectively, could be elevated

to a ratio of 10 with less than 1.5% contamination of "Nick"-type sulphidic sediment. Contamination from unmineralized "Bakken"-type black shale would only require 5% contamination to elevate the $^{187}Os/^{186}Os_{(232\ Ma)}$ ratio of the magma to 10. Assimilation of "Hasen"-type sediment would require approximately 20% contamination. The elevated Os content of the chilled margin from Wellgreen, relative to that of the juvenile Nikolai magma, is also in accord with the modelling. Although the contamination model is compelling, a postcrystallization fluid-assisted disturbance of the Re-Os systematics could conceivably have occurred *via* Os mobilization.

Quill Creek samples from the Wellgreen Ni-Cu-PGE deposit in Figure 188 facilitate comparison with other mineralized and unmineralized ultramafic and mafic bodies. This figure shows the osmium isotopic evolution of the mantle and the isotopic composition of various magmatic rocks and ores at a given time, based on a compilation of available Re-Os isotope data to date. The lower curve is the evolution curve for the mantle source of osmiridium alloys based on the findings of Allègre and Luck (1980) and recently published data of Hart and Kinloch (1989), Hattori et al. (1991), and Hattori and Hart (1991). The upper curve passes through the meteorite initial composition at 4.55 Ga (Walker and Morgan, 1989; Luck and Allègre, 1983). The undifferentiated mantle follows an Os isotopic evolution with $^{187}Re/^{186}Os$ of 3.3 giving rise to a present-day $^{187}Os/^{186}Os$ of 1.06, which is typical of present-day values measured for carbonaceous chondrites (Walker and Morgan, 1989).

The Re depleted nature of the Munro samples is demonstrated in Figure 188, as well as by their negative γ_{Os} values. Samples of the Munro Township komatiite (Walker et al., 1988) have ε_{Nd} values of +2 to +3 indicating a LREE-depleted mantle source region for these magmas. It is possible that the LREE depletion was accompanied by depletion in Re as a result of melt extraction. The existence of a Re- and LREE-depleted mantle in the source region for the Stillwater Complex ultramafic series (which hosts the G-chromite layer) has been suggested by Lambert et al. (1989). Magmas from these early times could be derived from either depleted or chondritic sources. Mantle peridotite derived from both suboceanic and subcontinental mantle (Walker et al., 1989; Martin, 1991; Reisberg et al., 1991) appears to have been derived from a reservoir that was relatively Re depleted since Precambrian time (Fig. 188).

The chondritic to slightly Re-depleted nature of most pristine mantle-derived magmas establishes a baseline from which one can interpret the Re-Os isotope systematics in other ultramafic and mafic bodies, and to evaluate the potential of Os isotopes as an exploration tool to characterize contaminated magmas, which have a greater potential to produce Ni-Cu±PGE deposits, than uncontaminated magmas. The Re-enriched nature of the Quill Creek ore and gabbro (cross-hatched area, Fig. 188) clearly distinquishes it from other sulphide-barren, age-equivalents. A similar relationship exists for the Rankin Inlet komatiite-hosted Ni deposit (Hulbert and Grégoire, 1993) and the contemporaneous Re-depleted Munro Township komatiite examined by Walker et al. (1988). Figure 188 suggests that mafic-ultramafic intrusions that host ore-grade Ni-Cu-PGE mineralization have anomalous to extreme $^{187}Os/^{186}Os$ ratios (Re enriched), regardless of age. Examples include Quill Creek Complex which hosts the Wellgreen Ni-Cu deposit (Marcantonio et al., 1991), Noril'sk-Talnakh deposit (Horan et al., 1991; Walker et al., 1992), Ungava (Ungava or Cape Smith ore, Luck and Allègre, 1984), Bushveld Igneous Complex (Hart and Kinloch, 1989; McCandless and Ruiz, 1990; Ruiz and McCandless, 1990), Stillwater Complex (Martin, 1989; Lambert et al., 1989), and Sudbury Igneous Complex (Walker et al., 1991a). Unmineralized ultramafic rocks and chromitite from the 2745 ± 5 Ma stratiform Bird River Complex, Manitoba (analyzed at the GSC by isotope dilution and inductively coupled plasma mass spectroscopy) have higher $^{187}Os/^{186}Os$ ratios than contemporaneous mantle. Two small Ni-Cu deposits occur at the base of this large stratiform intrusion.

Many of the economic ores in these mafic-ultramafic bodies (Fig. 188) are hosted in the gabbroic or more feldspathic portions of the intrusions, and contain the highest $^{187}Os/^{186}Os$ values. One of the most unusual features of these intrusions is the more chondritic character (lower $^{187}Os/^{186}Os$ ratios) of the barren to weakly mineralized ultramafic portions. Such a relationship may imply that the gabbro and contained sulphides have enriched $^{187}Os/^{186}Os$ ratios due to assimilation of crustal material (as the sulphur-isotope and S/Se data from many of these intrusions also suggest) whereas the magmas that gave rise to the ultramafic rocks have not interacted significantly with the crust and thus retain a nearly chondritic character. If this is the case, it seems clear that significant degrees of crustal contamination are required to generate ore-grade sulphide and PGE deposits. This may also have petrogenetic implications concerning the origin of feldspathic (gabbroic) sequences in stratiform intrusions. Could the later gabbroic differentiates represent nothing more than ingressions of more contaminated coeval magma with an initial composition similar that which gave rise to the underlying ultramafic sequence, rather than new magma derived from partial melting of a different source? Whatever the genetic explanation, intrusions hosting economic concentrations of Ni-Cu and PGE mineralization are significantly enriched in $^{187}Os/^{186}Os$ relative to chondritic mantle of the same age and the Re-Os isotopic character of the Quill Creek Complex is an excellent example of this relationship.

Tectonostratigraphic comparisons and proposed magmatic setting

To present a tectonomagmatic and metallogenic model for Triassic magmatism within Wrangellia it is necessary to examine stratigraphic correlations from the western and eastern portions of this terrane. Figure 189 illustrates generalized stratigraphic type sections (modified from Read and Monger, 1976 and Jones et al., 1977) from various localities within Wrangellia. Apart from variations in thickness (not illustrated) the stratigraphic sections look remarkably similar considering the vast distances between various areas. The Vancouver Island section is approximately 1800 km south of the Wrangell Mountains section in Alaska. The eastern limb of Wrangellia, which contains the Quill-Burwash Creek section in the Yukon, is approximately 250 km to the east.

One of the most striking differences between eastern and western Wrangellia is related to the thickness and nature of the Triassic volcanic rocks. On Vancouver Island, Karmutsen basalt is approximately 6000 m thick and consists predominantly of pillow basalt. A submarine setting is suggested for most of these lavas. Only locally do the upper more massive lavas appear to have been emergent (Barker et al., 1989). On the other hand, the Nikolai basalt from the Wrangell Mountains and Quill-Burwash Creek sections is considerably thinner (i.e. approximately 3500 m and 1000 m thick, respectively). Also, Nikolai basalt is largely subaerial and only pillowed near its base. Therefore, Triassic basalt from the western limb differs from its eastern counterpart not only with respect to thickness but also the environment of deposition (i.e. the former contains a much higher percentage of pillow basalt and aquagene tuff indicative of formation under water whereas the latter formed mainly in a subaerial environment). Although both areas have subjacent comagmatic diabase (gabbroic) sills, and lack extensive dyke systems or sheeted dykes, the western limb of Wrangellia is characteristically devoid of comagmatic ultramafic intrusions, whereas ultramafic cumulates are one of the hallmark features of eastern Wrangellia.

The huge thickness and vast extent of this rapidly erupted basalt has no obvious analogue or explanation in terms of plate boundary volcanism such as island arc formation or seafloor spreading (Richards et al., 1991) and thus remains enigmatic (Barker et al., 1989). As continentally derived clastic material is wholly lacking in the Wrangellian sequence, deposition in an oceanic setting seems imperative (Ben-Avraham et al., 1981). This finding is supported by Nd and Sr isotopic studies of Sampson et al. (1990), who found that Wrangellia contained unevolved, juvenile material and suggested that the terrane probably resided in an intra-oceanic environment until its accretion to North America.

Ocean basins contain a number of large basaltic plateaus of uncertain origin. More than 100 present-day oceanic plateaus are known and they are particularly abundant in the western Pacific and Indian oceans. They are also found in the Atlantic Ocean, and Caribbean and Mediterranean seas. Oceanic plateaus are anomalously high parts of the seafloor that are not at present part of continents, active spreading ridges, or active volcanic arcs. Rises that have been described as extinct arcs, extinct spreading ridges, detached and submerged continental fragments, anomalous volcanic piles, or uplifted oceanic crust have been included (Ben-Avraham et al., 1981). Most plateaus rise thousands of metres above the surrounding seafloor. The Ontong-Java Plateau is 1500-2000 m below sea level whereas others like the Seychelles Bank rise above sea level. Most of the plateaus are moving with the oceanic plates in which they are embedded. Plateaus similar to those that exist in the ocean basins today also existed in ancient ocean basins. Ancient plateaus can now be recognized only by their remanents that have been incorporated into continental masses in the form of allochthonous terranes. Possibly one of the best exposed of these plateaus is Wrangellia.

Earlier suggestions (Davis and Plafker, 1985; Barker et al., 1989) to explain the origin of the Triassic magmatism share a common rifting property of a Paleozoic island arc

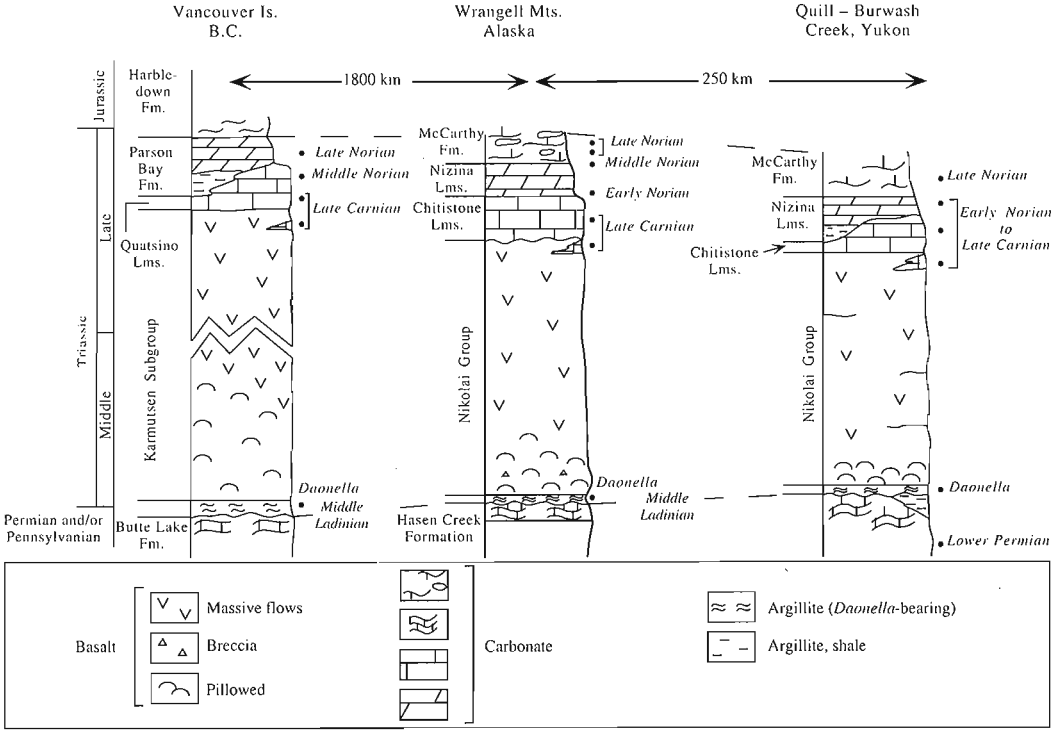

Figure 189. *Generalized stratigraphic type sections from widely separated localities within Wrangellia including the Quill-Burwash Creek section from the study area (modified from Read and Monger, 1976; Jones et al., 1977).*

complex, or rifting of an adjacent, contemporaneous island arc, analogous to the tectonic evolution of the Marianas volcanic arc and back-arc rift system. Such models are inadequate because: (1) convincing evidence is lacking for large amounts of crustal extension and graben formation (normal faulting), or significant tilting of the older strata, but instead the basalt flows appear to be flat lying and conformable with the underlying sediments; (2) the widespread emplacement of gabbroic (diabasic) sills rather than dykes, and the lack of sheeted dyke complexes also imply that the crust did not undergo significant extension associated with the magmatism; nevertheless, minor extension must have occurred for the basalt to have been erupted through the crust; (3) one would expect subsidence and submarine volcanism at depths comparable to those of mid-ocean ridges during the rifting of an island arc complex, but the Triassic volcanism is largely subaerial or of a shallow submarine nature; and (4) rifting of an adjacent, active arc does not explain evidence (sills and dykes) that the Triassic basalt erupted through the underlying sedimentary rocks. Therefore, a petrotectonic model not emphasizing rifting is proposed to explain the huge volume of tholeiitic magmatism associated with Wrangellia during the Triassic. Richards et al.(1991) proposed a *"mantle plume initiation model"*, which does not emphasize rifting, to explain the enormous outpouring of Triassic basalt and the preceding rapid uplift, and subsequent gradual subsidence of the plateau. A slightly modified version of this model has been developed by the author and is used, in conjunction with Figure 190, to reconstruct a particular sequence of geological events that evolved in Wrangellia preceding and during the late Triassic.

Prior to Triassic magmatism and marine sedimentation Wrangellia (Fig. 190A) consisted of a Paleozoic marine sequence that includes a Pennsylvanian island arc complex whose last activity predated the Triassic basalt by more than 80 million years, and postarc sedimentary rocks consisting of Lower Permian shallow water fossiliferous limestone, sandstone, shale, and locally mid-Upper Permian deep water argillite and radiolarian chert. This stratigraphic sequence suggests that cooling and gradual subsidence followed the cessation of arc volcanism at approximately 285 Ma. Terminal Permian deposition occurred at depths of at least 1 km, based on the calcium carbonate compensation depth for that time, and suggest a minimum subsidence rate of ≈40 m/Ma (Richards et al., 1991).

During Middle Triassic (Middle Ladinian, 238 to 236.5 Ma) a thin (<100 m) conformable, discontinuous black argillite, containing abundant bivalves of *Daonella* was deposited in a deep water (<1 km) basinal environment. Contemporaneously, or possibly slightly earlier, a large hot diapir of deep mantle material (starting plume) rose beneath the oceanic lithosphere of Wrangellia. Plume heads may be as large as 1000 km in diameter and give rise to a rapid uplift of the ocean floor. The sudden onset of a huge partial melt event of both deep (enriched) mantle and thermally entrained (depleted) upper mantle material, and perhaps pre-existing oceanic lithosphere and island arc crustal material, gave rise to a flood basalt volcanic sequence (Richards et al., 1991). Volcanism commenced at 232 ± 1 Ma and lasted until Late Carnian (227 to 223.4 Ma) time (Fig. 3, 190B).

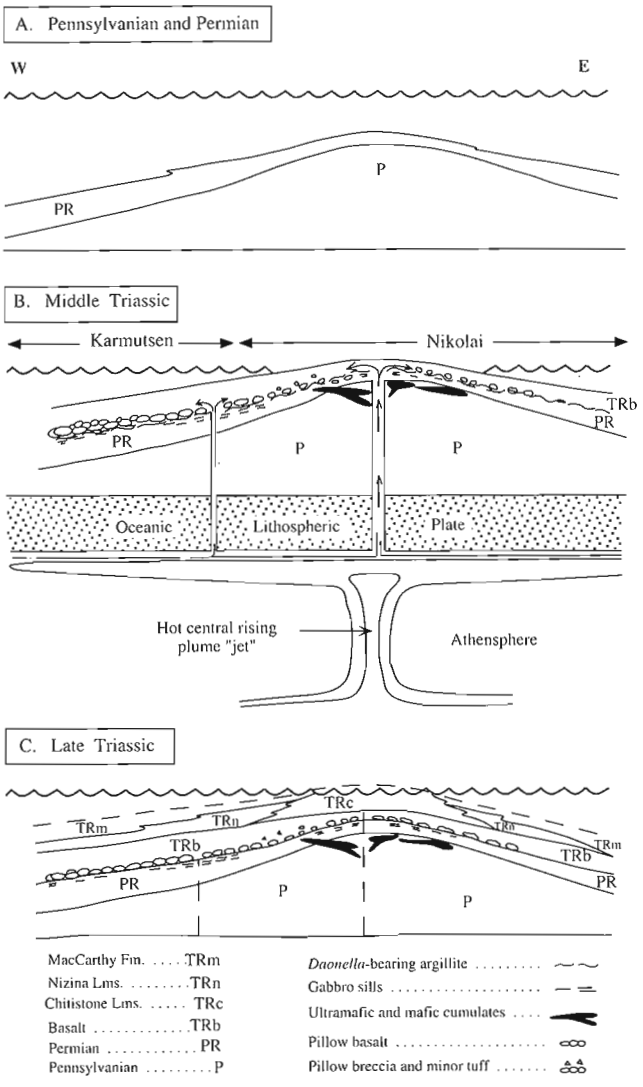

Figure 190. *Tectonomagmatic model for the evolution of Triassic magmatism within Wrangellia. (**A**) Development of a Paleozoic marine sequence consisting of a Pennsylvanian island arc complex (P) and postarc Permian sedimentary rocks (PR). (**B**) Deep water basinal deposition of a black argillite containing bivalves of* Daonella *during the Middle Triassic. Contemporaneous, or possibly slightly earlier, development of a large hot mantle plume beneath the oceanic lithosphere of Wrangellia that gave rise to the extensive Nikolai and Karmutsen flood basalt sequence. The regional development of normative olivine-rich basalt, and mafic and ultramafic cumulate intrusions exclusively in eastern Wrangellia may be a consequence of spatially having formed over or near the hotter "axial jet" domain of the mantle plume; whereas the less olivine normative and ultramafic deficient western portions of Wrangellia formed in the cooler more flanking regions of the plume. (**C**) Post flood basalt formations (i.e. Chitistone, Nizina and MacCarthy) record progressive subsidence of the lithosphere during the Late Triassic due to gradual thermal abatement following cessation of basalt volcanism. Modified after Richards et al. (1991).*

It is envisaged that the more olivine normative volcanic rocks and abundant ultramafic cumulate intrusions confined to the eastern limb of Wrangellia may represent extrusive and intrusive domains that were originally centred over the hotter (central) axial "train" or "jet" of the plume, whereas the relatively olivine-poor volcanic rocks from the western limb tapped magma from a cooler non-axial portion of the plume head. Fluid dynamic studies by Campbell et al. (1989) showed that a starting plume consists of a hot axial jet, capped by a large head into which cooler surrounding mantle is entrained. The subaerial nature of the Nikolai volcanic rocks from the eastern limb, in conjunction with the more primitive nature of their parental magmas and abundance of ultramafic intrusions, could imply that the axial portion of the plume has domed the immediately overlying crust. Doming in this area may also have been amplified by the existence of a paleotopographic high (Paleozoic island arc complex), giving rise to a thickened and more elevated portion of the crust in eastern Wrangellia relative to that which existed in western part of the terrane (Fig. 190B). Upper Triassic, post flood basalt sediments (Chitistone, Nizina, and MacCarthy) record progressive subsidence due to gradual thermal abatement of the lithosphere following cessation of basaltic volcanism (Fig. 190C).

In conclusion, the synchronous nature and similarity of Triassic magmatism, followed by slow subsidence throughout Wrangellia resulting in deposition over most of the area of inner-platform, and eventual finer-grained detrital deep-water basinal deposits must imply a deep-seated mantle control – possibly of a mantle plume origin.

KLUANE BELT MAGMATIC AND METALLOGENIC MODEL

Any model for the Kluane mafic-ultramafic intrusive complexes and affiliated PGE+Au-rich Ni-Cu mineralization must rationalize the following characteristics: (1) the distinctive lithological zoning of the mafic-ultramafic sill to lens-like bodies, consisting of a core of dunite contained within a sheath of peridotite which in turn passes into olivine-clinopyroxenite, clinopyroxenite, and chilled gabbro near the margins of the intrusion (Fig. 191); (2) the preferential emplacement of these intrusions at the sulphidic "Transition zone" or contact between the Station Creek and Hasen Creek formations; (3) the presence of basal accumulations of sulphides which appear to have formed by sulphide immiscibility and gravitational setting; (4) the association of "skarn-type" Ni-Cu-PGE mineralization juxtaposed the Hasen Creek Formation carbonates; (5) variable grades and noble metal concentrations; (6) reappearance of significant sulphide mineralization (as disseminated sulphide and net-textured sulphides) within ultramafic rocks located above the marginal gabbro-ultramafic zone contact along with a concomitant decrease in the amount of mineralization towards the core of the intrusion; (7) pronounced Ba anomalies and ^{32}S-enriched sulphides associated with the mineralized intrusions; (8) gradation within the ultramafic zone from an olivine-enriched core (dunitic) with adcumulate textures, to members containing progressively less olivine (peridotite to olivine clinopyroxenite), with meso- and orthocumulate textures, towards the outer confines of this zone; and (9) komatiitic-like Os, Ir, Ru group, noble metal-enriched sulphide mineralization with Ni/Cu ratios characteristic of tholeiitic magmas.

Lithological zonation and intrusive horizons

With the exception of the marginal zone being gabbroic, the distinctive lithological zoning of the Kluane intrusions from olivine-rich cores to olivine-poor marginal zones, and the nature and distribution of sulphide mineralization are characteristic features of komatiitic ultramafic bodies (i.e. Raglan horizon, Cape Smith Belt, Quebec, Barnes et al. (1982); Thompson Ni Belt, on-going research of author; Six-mile deposit at Yakabindie, Western Australia, Naldrett and Turner (1977). The zonation within the Cape Smith Belt sills has been attributed to flow differentiation of a phenocryst-charged magma (Wilson et al., 1969; Barnes et al., 1982). This mechanism has been proven in quasi-scale model experiments by Bhattacharji (1967) and demonstrated to be conceivable in narrow intrusions (Komar, 1972a, b). However, Barrière (1976) demonstrated that the process is rather limited to flow channels <10 m wide. As individual ultramafic zones within intrusions from the Kluane Belt and the Cape Smith Belt (Barnes et al., 1982) may exceed 100 m, the amount of inward transport of suspended olivine phenocrysts due to flow differentiation in channels of this width would be slight. Therefore, an alternative process is required to explain the olivine distribution within these zoned sills.

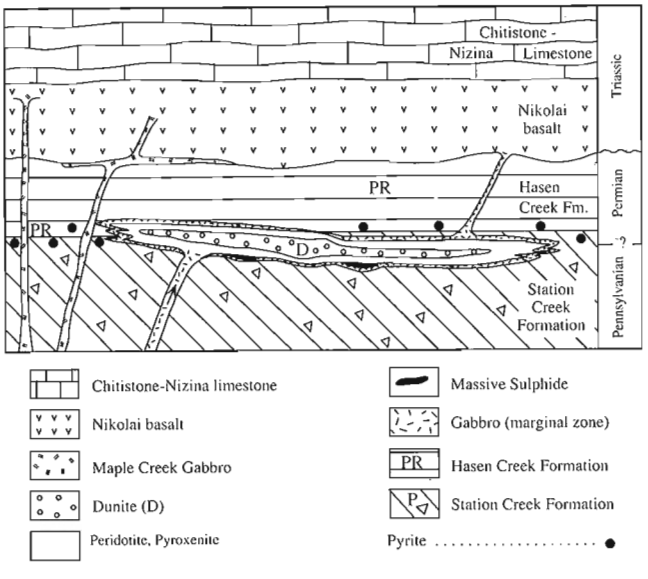

Figure 191. *Schematic section of typical Kluane mafic-ultramafic intrusive complex (pre-deformation) showing the outer marginal gabbroic envelope, and the zonal development of progressively more ultramafic rocks (i.e. pyroxenite, peridotite, and dunite, respectively) towards the core of the intrusion. Note the massive sulphide concentrations at the base of the complex and the intrusions preferential emplacement at or near the pyritic Station Creek-Hasen Creek formations contact zone.*

The model presented for the Kluane intrusions envisages the initial emplacement of an olivine phenocryst-free tholeiitic magma, now represented by the marginal zone gabbro (Fig. 191). This initial gabbroic pulse probably represents relatively fractionated magma from the top of a density-stratified master magma chamber at depth. Reaction between the hot gabbroic magma and the sulphidic "Transition zone" and Hasen Creek sediments gave rise to significant degrees of crustal contamination and sulphide immiscibility. Rapid cooling of this contaminated initial magma developed a protective, insulating envelope about the intrusion thus inhibiting subsequent pulses of magma from the same degree of heat loss and contamination. These subvolcanic magma chambers are envisaged as open magmatic systems that sustained the surface Nikolai volcanism, and were periodically purged of their residual melts. Essential elements of this model are that successive batches of progressive more primitive tholeiitic magma were introduced into the sills due to successive tapping of deeper levels of a density-stratified magma within a master chamber at depth, and that olivine was on the liquidus at the time of intrusion. If this were so, phenocrysts of olivine would settle relative to the magma, and lag behind the upward flowing magma ascending along the deep feeder system. Consequently, successive batches of magma would become progressively enriched in accumulated phenocrysts of olivine. It is believed that the transition from the inwardly cooling gabbroic marginal zone to the pyroxenitic, peridotitic, and dunitic members of the ultramafic zone records the ingression of successive magma pulses progressively enriched in accumulated olivine phenocrysts more magnesian in composition.

The olivine is believed to have settled from the melt as the phenocryst-charged suspension flowed over top the accumulating pile and expelled most of the residual melt to surface. After the olivine settled the resulting cumulus material would behave as a crystal mush and the remaining intercumulus magma would crystallize in situ giving rise to oikocrysts of clinopyroxene and a finer-grained groundmass consisting of a clinopyroxene-plagioclase-phlogopite-orthopyroxene intergrowth. The change in cumulate textures from orthocumulates and mesocumulates, associated with olivine clinopyroxenite and peridotite near the base of the ultramafic zone, to adcumulates in the dunitic core of the intrusion, also suggests that more residual liquid was retained in the outer portions of the ultramafic zone than in its core. This may be a consequence of progressive volumes of intercumulus melt being purged from the hotter, more slowly cooling central portions of the intrusion along which magma would be constantly flowing relative to the faster cooling outer portions of the ultramafic zone. The thickness of the sill increased with each new ingression of magma as the pressure of the intruding magma lifts the overlying country rocks. An analogous model had been proposed by Barnes et al. (1982) for the komatiitic Katiniq sill from the Cape Smith Belt.

Recently, a new interpretation for the Katiniq and some other komatiitic ultramafic bodies has been proposed (Barnes et al., 1988; Hill et al., 1989; Barnes and Barnes, 1990) that envisages the bodies as having developed in a lava lake above a volcanic vent. This interpretation is conceivable in the above komatiitic terranes where the ultramafic bodies are juxtaposed against comagmatic flows. However, an extrusive origin for the zoned Kluane mafic-ultramafic bodies (and similarity zoned ultramafic bodies from the Thompson Ni belt) is inconceivable due to the considerable thicknesses that separate these bodies from their overlying coeval volcanic rocks.

The preferential emplacement of the Kluane mafic-ultramafic bodies in the so-called "Transition zone" of the Station Creek Formation and contact zone between the Station Creek and Hasen Creek formations may be a consequence of a significant change in the mechanical competency and permeability of strata within these horizons relative to that of the underlying Station Creek Formation (Fig. 191). Strata below the "Transition zone" consist almost exclusively of massive, competent volcanic flows and pyroclastic rocks, whereas strata from within and above comprise rather fissile, permeable, and mechanically incompetent argillaceous rocks and carbonate. The presence of the heterogeneous layered sedimentary rocks of variable competency within and above the "Transition zone" would have an influence on the emplacement level and form (i.e. sills or dykes) of these intrusions (Bradley, 1965). Although mechanical competency is an important variable, Anderson (1951) and Gretener (1969) demonstrated that the ambient stress field in the host rock is the most important factor controlling the form of the intrusions. As dykes and sills represent material originating from the mantle or base of the crust, they must be fed by dyke- or plug-like bodies, and the formation of a sill represents a major re-orientation of the form of the intrusion. Dykes and sills are envisaged to intrude by a process analogous to "hydraulic fracturing" (Hubbert and Willis, 1957) and align themselves perpendicular to the least principal stress. It would appear that the principal horizontal stresses are greater than the vertical principal stresses within or above the "Transition zone" and thus the fractures that formed are horizonal and as a result sill-like bodies form.

Sulphide mineralization: types, controls, and grades

Different types of Ni-Cu-PGE mineralization are associated with the intrusive activity of the Kluane mafic-ultramafic complexes during the Middle Triassic. The most important types are: (1) accumulations of immiscible sulphides which appear to have formed by gravity settling in the basal portion of the gabbroic marginal zone following emplacement and crustal contamination of the initial magma(s), and (2) sulphides associated with the encroachment of subsequent olivine phenocryst-rich pulses of magma that gave rise to the ultramafic zone.

Structural evidence suggests that massive sulphide concentrations in the Wellgreen deposit of the Quill Creek Intrusive Complex are the result of riffling of sulphide-bearing magma flowing over irregularities along the base of the complex. These irregularities appear to be the result of intrusive "plucking" of floor rocks along pre-ore joints and faults. This, in conjunction with the presence of sulphide mineralization associated with structural depressions in the basal portions of the White River Complex (Onion and Canalask properties), suggests that footwall topography is the primary controlling factor for the localization of massive sulphides within the Kluane Belt. Concentration of sulphide

by footwall topography is a characteristic feature in a number of other important nickel sulphide deposits (e.g. Katiniq, Ungava, Barnes et al., 1982; the 2-3 sill, Ungava, Miller, 1977; Kambalda, Australia, Ross and Hopkins, 1975; Shangani, Zimbabwe, Williams, 1979; Langmuir, Canada, Green, 1978; Dundonald, Canada, Muir and Comba, 1979; Rankin Inlet, Canada, Hulbert and Grégoire, 1993).

The near ubiquitous presence of disseminated, net-textured, and in some cases very thin massive sulphide concentrations, in the early ultramafic members suggests that the parental magmas were also carrying immiscible sulphides during much of the ultramafic zones crystallization history. Decreasing sulphide content towards the dunitic core, and the presence of minor thin massive sulphide segregations and disseminations higher up within the ultramafic zone, suggest that sulphide accumulations probably originated by settling of sulphide liquid introduced in subsequent pulses of magma that gave rise to the ultramafic zone. Increasing disseminations of sulphides towards the base or outer portion of the ultramafic zone, and the heterogenous nature of the mineralization, suggest that sulphide melt had to percolate through the pore space of the cumulate olivine crystal mush and thus concentration would be less efficient as a result of incomplete settling. The most effective concentration of sulphide would have occurred at an early stage from phenocryst-poor magma.

The presence of massive and semi-massive sulphides, in sizeable concentrations and in some cases with economic grades, within the ultramafic zones of the Dickson Creek and Rainbow Mountain intrusive complexes indicate that the ultramafic portions of all intrusive complexes in the belt should be re-examined for their massive sulphide potential.

The remaining types of Ni-Cu-PGE mineralization (i.e. "skarn", hydrothermal, and remobilized sulphides) are related to the interaction of contact metasomatic and postmagmatic fluids with the country rock.

Although there are a number of types of lower grade sulphide and noble metal mineralization associated with the emplacement and cooling history of these intrusions (discussed previously), recent assessment reveals that only the massive sulphide concentrations are economically feasible under present day market conditions. The discovery of excellent massive sulphide ores associated with these intrusions, the larger size of most of the intrusions (White River Complex, 16 km x 250 m; Quill Creek Complex, 4.2 km x 600 m; Tatamagouche Complex, 17 km x 3 km) when compared to those from the Cape Smith Belt of Ungava (where the ultramafic sills that host the Ni-Cu-PGE deposits of the Raglan Horizon are generally thinner than 150 m and can be traced for only a few kilometres at most, Giovenazzo et al., 1989), clearly substantiates the exploration potential of these intrusive complexes. When one considers this, and the fact that most of these intrusions were originally much larger (pre-tectonism and erosion) than at present, and that associated Ni-Cu-PGE mineralized occurrences can be traced intermittently along strike for approximately 600 km, the exploration potential of this newly recognized belt becomes unequivocal.

Geochemical and sulphur-isotope investigations of mafic-ultramafic igneous rocks and associated mineralization reveal that crustal contamination of the "Kluane" parental magmas by S- and Ba-rich sediments lowered the solubility of sulphur within these magmas and triggered sulphide immiscibility. The Ba-enriched nature of the mineralized and unmineralized gabbroic and ultramafic rocks and Ni-Cu-PGE ores is uncharacteristic of pristine tholeiitic melt products, as are the S/Se and $\delta^{34}S‰$ signatures of the magmatic sulphides shown in Figures 192 and 193 with respect to the mineralization from the Quill Creek, White River, and Dickson Creek complexes. Modelling the amount of contamination in Figures 192 and 193 is based on the assumption that the pristine Kluane parental magmas had a $\delta^{34}S$ signature of 0‰ and a S/Se ratio of 3500, whereas the Hasen Creek contaminating sediments had corresponding values of -19‰ and 20 000. A value of -39‰ was used in the model for the contaminating country rock sulphur (Permian tuffaceous sediments) assimilated by the Dickson Creek magma.

Calculations for the mineralized ultramafic rocks, gabbro, and massive sulphides from the Wellgreen deposit (Fig. 192A) indicate that gabbro and gabbro-hosted massive sulphides have experienced about 3.5 to 10% and 2.5 to 8.3% crustal contamination, respectively, whereas the ultramafic rock has experienced 1.5 to 9% contamination. Similar calculations based on mineralized specimens from the White River Complex (Fig. 192B) demonstrate significantly higher degrees of crustal contamination than that experienced by the Quill Creek magma. The ultramafic, and massive and semi-massive "offset" mineralization from the Canalask property has resulted from 5 to 11% and 16 to 25% contamination, respectively. Limited data from the Onion property massive sulphide and mineralized gabbro suggest approximately 9% and 18% contamination. The most extreme examples of crustal contamination are clearly associated with the Dickson Creek magma (Fig. 193). This plot demonstrates that the degree of contamination can vary significantly even within the same intrusion. Disseminated and net-textured sulphides associated with the ultramafic and gabbroic rocks from the lower portion of the intrusion appear to have experienced approximately 2% and 3% contamination, respectively. Mineralized gabbro from the upper contact, proximal to the pyrrhotite-rich exhalative massive sulphide body within the Permian tuffaceous sediments, has experienced approximately 18% crustal contamination. Barren semi-massive sulphides within ultramafic rocks from this intrusion have been generated from magmas that have experienced 30-35% contamination from the mineralized Permian tuff.

Comparing the calculated degrees of contamination (Fig. 192, 193) associated with the various types of mineralization and the associated PGEs, Ni, Cu, and Co assays, it becomes clear that the grade of the mineralization is a function of the degree of contamination experienced by the parental magma. Sulphide resulting from the lowest degrees of contamination are most enriched in Ni, Cu, Co, and PGEs, whereas those generated from magma that has experienced the most contamination are clearly the most depleted (barren) with respect to these elements. This relationship suggests that although an external source of sulphur is necessary to trigger

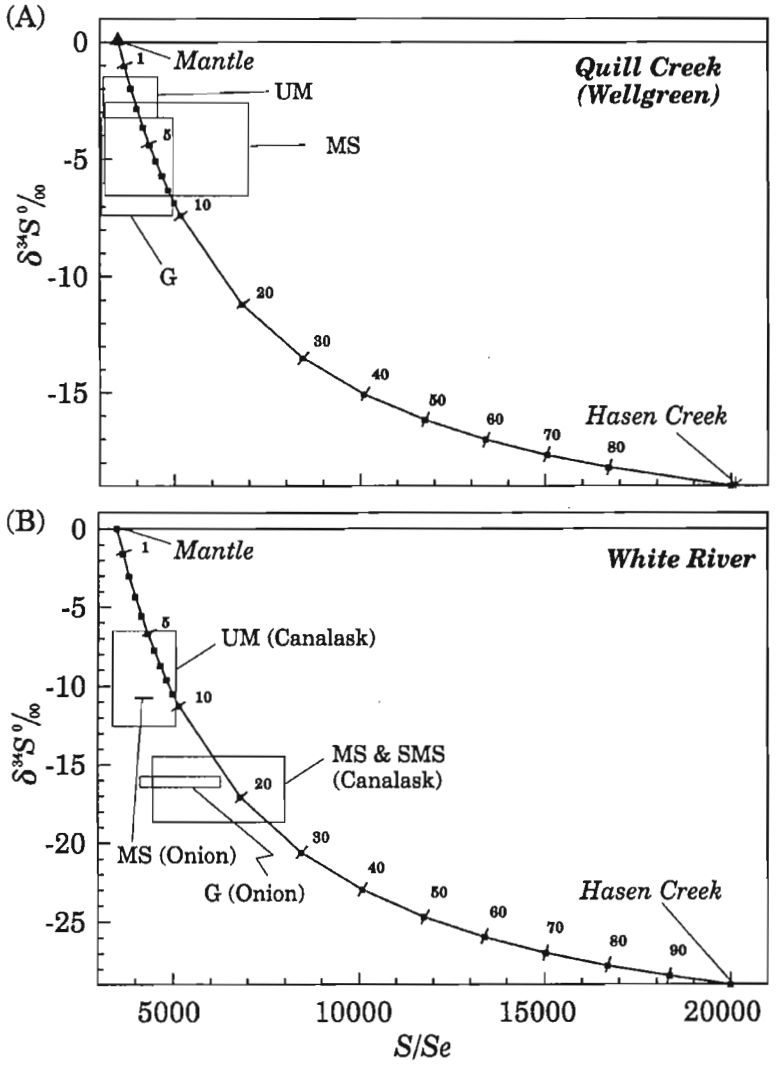

Figure 192.

*$\delta^{34}S‰$ vs. S/Se plot modelling the amount of crustal contamination required to produce the gabbro (G), ultramafic (UM), massive sulphide (MS), and semi-massive sulphide (SMS) mineralization in (**A**) the Quill Creek Complex and (**B**) the White River Complex, assuming the source of contamination is the Hasen Creek Formation.*

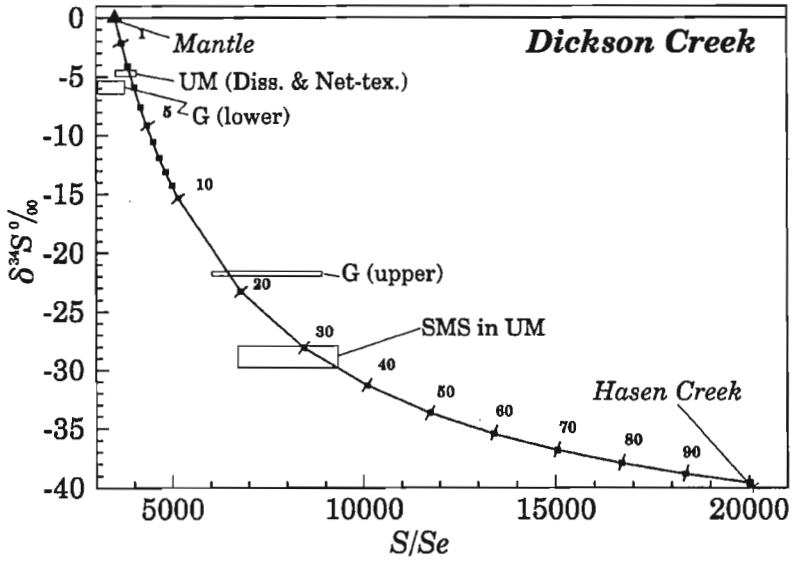

Figure 193.

$\delta^{34}‰$ vs. S/Se plot modelling the amount of crustal contamination required to produce the gabbro (G), ultramafic (UM), and semi-massive sulphide (SMS) mineralization in the Dickson Creek Complex assuming the source of contamination is the Hasen Creek Formation.

sulphide immiscibility within the Kluane parental magma, too much local sulphur contamination promotes relatively rapid sulphide immiscibility and gravitational settling. As a consequence the sulphides have not had an opportunity to equilibrate with a significant mass of magma from which they can sequester Ni, Cu, Co, and PGEs.

Campbell et al. (1983) presented a model to show the effects of various silicate magma/sulphide liquid mass ratios on the concentration of Ni, Co, and Pt of sulphides in equilibrium with basaltic magma containing typical concentrations of these elements. This relationship is given by the general expression:

$$Y_i = \frac{D_i x C_{oi} x (R+1)}{(R+d_i)}$$

where Y_i is the concentration of any metal i in the sulphide melt (Y), by the partition coefficient D_i (sulphide/silicate), R is the ratio of the mass of silicate magma to the mass of sulphide, and C_{oi} is the initial concentration of the metal i equilibrating with it. This expression demonstrates that where R is low, in the range 100 to 2000, the Ni and Co contents of sulphides will be typical of most Ni sulphide ores and the Pt values will be relatively low, and would be less than or equal to those values observed in normal Sudbury ores. R values in the 10 000 to 100 000 range will have Ni and Co contents not much higher than at lower R values, but the Pt concentration will be much higher and in the range characterizing those of the Merensky and J-M reefs.

Mineralized ultramafic (peridotite) and massive sulphide samples from the Wellgreen, Canalask, and Dickson Creek deposits demonstrate this relationship when the concentrations of the elements (Ni, Cu, Se, Pt, Pd) are recast in terms of concentration in 100% sulphide, and the *R*-factor is computed (Table 7). Mineralized samples with nearly identical sulphur contents were selected from the database for each deposit to minimize possible erroneous effects due to the normalization of metal concentrations of samples with significantly different S contents. In the *R*-factor calculations it was assumed that the silicate magma had a composition similar to a Nikolai basalt from the base of the volcanic sequence: S (112 ppm), Ni (110 ppm), Cu (32 ppm), Pt (2.6 ppb), and Pd (8.8 ppb). Palladium was used to calculate the *R*-factor as its partition coefficient (Bezmen et al., 1994) is the most accurately known of all the PGEs, it partitions only into sulphide, and it is the noble metal that allows the most precise and accurate analytical determinations.

Comparison of the concentration of metals and *R*-factors (Table 7) in the Wellgreen massive sulphide and the ultramafic representatives demonstrates that the ultramafic-hosted sulphides have approximately double and triple the amount of Ni, Cu and Pt, Pd, respectively, as the massive sulphides. The *R*-factor for the ultramafic sulphide is approximately triple that of the massive sulphide and suggests that the former has been in equilibrium with almost three times as much silicate magma as the latter. An *R*-factor of 0 for the Pt (3 ppb) and Pd (9 ppb) barren Canalask massive sulphide mineralization reveals that these sulphides have not equilibrated with the parental magma from which they segregated. They are also conspicuous by their low Cu and Se contents when compared to their counterparts from the Wellgreen deposit. The high *R*-factor (1381) associated with the Canalask ultramafic disseminated sulphides implies that these sulphides have equilibrated with an enormous mass of silicate magma compared to that for the massive sulphide.

Although the Pd and Ni concentrations and computed R-factor for the Wellgreen and Canalask ultramafic sulphides are the same, some conspicuous differences are apparent and warrant explanation. These differences also characterize the Canalask massive sulphides. The most unique features of the Canalask sulphides are: unusually high Ni/Cu ratios (3.8-4.3), low Se concentrations (approximately half that of Wellgreen), Pt depletion, and similar high Pd/Pt ratios in the various types of mineralization. These similar geochemical features suggest that the Canalask sulphides have inherited these chemical traits from similar parental magmas, whereas, differences between

Table 7. Computed metal contents in 100% sulphide and *R*-factors for mineralization from the Wellgreen, Canalask and Dickson Creek properties.

Material	Ni (%)	Cu (%)	Se (ppm)	Pt (ppb)	Pd (ppb)	*R* (Pd)
Wellgreen MS	4.09	3.46	102	4096	4096	468
Wellgreen UM	8.20	7.59	266	12514	11693	1361
Canalask MS	3.81	0.98	67	3.1	9.5	0
Canalask UM	8.05	1.86	110	3813	11864	1381
Dickson SMS	0.04	0.66	58	12.6	9.4	0
Dickson UM	5.75	2.63	103	1774	359	40

MS= massive sulphides, UM= ultramafic (peridotite), *R*= *R*-factor or mass of silicate magma in equilibrium with the mass of sulphide melt. D_{Pd}= 5.5 x 10^4 (Bezmen et al., 1994).

Wellgreen and Canalask sulphides suggest that the varying base metal and noble metal concentrations and ratios are inherent geochemical characteristics associated with parental magmas from the different complexes. The elevated Ni/Cu ratios are incompatible with the high Pd/Pt and Pd/Ir ratios, as a measure of the primitiveness of the Canalask magmas. Therefore, it would appear more likely that differences between the Wellgreen and Canalask mineralization may be a consequence of early Canalask magmas having segregated a significant quantity of Cu-sulphides enriched in Pt and Se subsequent to the fractionation of the sulphide melts.

Table 7 reveals that the barren and depleted sulphides from the Dickson Creek mineralized occurrences are directly related to the *R*-factor. The massive sulphides, which occur in peridotite, are effectively barren of Ni, Pt, and Pd as they have communicated with a very limited mass of magma as indicated by the extremely low *R*-value (0). The relatively elevated Cu content of the massive sulphide is due to the enriched nature of this element in the country rock contaminant. In contrast, disseminated and net-textured sulphides segregating from the ultramafic had an opportunity to communicate with at least 40 times the mass of magma available to the massive sulphides.

R-factor and metal content in 100% sulphide calculations have been statistically analyzed. Samples included in the data set (n=390) were mineralized specimens that contained >0.50% S. Very strong correlation coefficients (r, @ $\rho \leq 0.05$) occur between the computed *R*-factor and: Ni (0.70), Pd (0.97), Pt (0.94), Au (0.49), Rh (0.66), Os (0.55), and to a much weaker extent Ir (0.16). There was no significant correlation with As, the S/Se ratio or the $\delta^{34}S$ value of the sulphides. A very strong correlation also exists between the Ni-content of the sulphide and Pd (0.75), Pt (0.80), Au (0.67), and Rh (0.67). A stronger correlation exists between Se and Cu (0.49) than for Ni (0.32) and may corroborate the earlier suggestion of prior Cu sulphide segregation at the Canalask deposit. From the above, and Figures 192 and 193, it is clear that crustal contamination of the Kluane magmas is essential to initiate sulphide immiscibility; however, the amount of communication the sulphides have experienced with the surrounding magma determines the grade of the ores. Also, as pointed out previously (Fig. 27, 28, 29), fractionation of the sulphide melts with respect to PGE+Au can also have a pronounced influence on the noble metal content and profiles.

REFERENCES

Allègre, C.J. and Luck, J.-M.
1980: Osmium isotopes as petrogenetic and geologic tracers; Earth and Planetary Science Letters, v. 48, p. 148-154.

Anderson, E.M.
1951: The Dynamics of Faulting and Dyke Formation with Application to Britain; 2nd revised edition, Oliver and Boyd, London, 206 p.

Andrew, A. and Godwin, C.I.
1989: Lead and strontium isotope geochemistry of the Karmutsen Formation, Vancouver Island, British Columbia; Canadian Journal of Earth Sciences, v. 26, p. 908-919.

Andrew, A., Armstrong, R.L., and Rundle, D.
1991: Neodymium-strontium-lead isotopic study of Vancouver Island igneous rocks; Canadian Journal of Earth Sciences, v. 28, p. 1744-1752.

Arai, S.
1992: Chemistry of chromium spinel in volcanic rocks as a potential guide to magma chemistry; Mineralogical Magazine, v. 56, p. 173-184.

Arai, S. And Takahashi, N.
1987: Petrographical notes on deep-seated and related rocks: (5) Compositional relationships between olivine and chromium spinel in some volcanic rocks from Iwate and Rishiri volcanoes, NE Japanese Arc; Annual Report of the Institute of Geosciences, University of Tsukuba, v. 13, p. 110-114.

Armstrong, A.K., MacKevett, E.M., and Silberling, N.J.
1969: The Chitistone and Nizina Limestones of part of the southern Wrangell Mountains, Alaska – a preliminary report stressing carbonate petrography and depositional environments; United States Geological Survey, Professional Paper 650-D, p. D49-D62.

Atkins, F.B.
1969: Pyroxenes of the Bushveld Intrusion, South Africa; Journal of Petrology, v. 10, p. 222-249.

Barker, J. C.
1988: Distribution of platinum-group elements in an ultramafic complex near Rainbow Mountain, east-central Alaska Range; in Process Mineralogy VII; The Metallurgical Society, p. 197-220.

Barker, F., Southerland Brown, A., Budahn, J.R., and Plafker, G.
1989: Back-arc with frontal-arc component origin of Triassic Karmutsen basalt, British Columbia, Canada; Chemical Geology, v. 75, p. 81-102.

Barnes, S-J. and Naldrett, A.J.
1987: Fractionation of platinum-group elements and gold in some komatiites of the Abitibi Greenstone Belt, northern Ontario; Economic Geology, v. 82, p. 165-183.

Barnes, S-J. and Picard, C.P.
1993: The behaviour of platinum-group elements during partial melting, crystal fractionation, and sulphide segregation: An example from the Cape Smith Fold Belt, northern Quebec; Geochimica et Cosmochimica Acta, v. 57, p. 79-87.

Barnes, S-J., Naldrett, A.J., and Gorton, M.P.
1985: The origin of the fractionation of platinum-group elements in terrestrial magmas; Chemical Geology, v. 53, p. 303-323.

Barnes, S.J. and Barnes, S-J.
1990: A new interpretation of the Katiniq nickel deposit, Ungava, Northern Quebec; Economic Geology, v. 85, p. 1269-1272.

Barnes, S.J., Coats, C.J., and Naldrett, A.J.
1982: Petrogenesis of a Proterozoic nickel sulphide-komatiite association: the Katiniq sill, Ungava, Quebec; Economic Geology, v. 77, p. 413-429.

Barnes, S.J., Hill, R.E.T., and Gole, M.J.
1988: The Perserverence ultramafic complex, Western Australia: the product of a komatiite lava river; Journal of Petrology, v. 29, p. 305-331.

Barrie, C.T.
1993: Petrochemistry of shoshonitic rocks associated with porphyry copper-gold deposits of central Quesnellia, British Columbia, Canada; Journal of Geochemical Exploration, v. 48, p. 225-258.

Barrière, M.
1976: Flowage differentiation; limitation of the "Bagnold Effect" to the narrow intrusions; Contributions to Mineralogy and Petrology, v. 55, p. 139-145.

Basaltic Volcanism Study Project
1981: Basaltic Volcanism on the Terrestial Planets; Pergamon Press, New York, 1286 p.

Bellieni, G.P., Comin-Chiaramonti, Marques, L.S., Melfi, A.J., Nardy, A.J.R., Papatrechas, C., Piccirillo, E.M., Roisenberg, A., and Stolfa, D.
1986: Petrogenetic aspects of acid and basaltic lavas from the Parana Plateau (Brazil): geological, mineralogical and petrological relationships; Journal of Petrology, v. 27, p. 915-944.

Ben-Avraham, Z., Nur, A., Jones, D., and Cox, A.
1981: Continental accretion: from oceanic plateaus to allochthonous terranes; Science, v. 213, p. 47-54.

Berg, H.C., Jones, D.L., and Richter, D.H.
1972: Gravina-Nutzotin belt- tectonic significance of an upper Mesozoic sedimentary and volcanic sequence in southern and southeastern Alaska; United States Geological Survey, Professional Paper 800-D, p. D1-D24.

Bezmen, N.I., Asif, M., Brügmann, G.E., Romanenko, I.M., and Naldrett, A.J.
1994: Distribution of Pd, Rh, Ru, Ir, Os and Au between sulphide and silicate metals; Geochimica et Cosmochimica Acta, v. 58, no. 4, p. 1251-1260.

Bhattacharji, S.
1967: Scale model experiments on flowage differentiation in sills; in Ultramafic and Related Rocks, P.J. Wyllie (ed.); John Wiley and Sons, New York, p. 69-70.

Bostock, H.S.
1952: Geology of the northwest Shakwak Valley, Yukon Territory; Geological Survey of Canada, Memoir 267.

Bradley, J.
1965: Intrusion of major dolerite sills; Transactions of the Royal Society of New Zealand, v. 3, no. 4, p. 27-55.

Brooks, C., Hart, S.R., and Wendt, I.
1972: Realistic use of two-error regression treatment as applied to rubidium-strontium data; Reviews of Geophysics and Space Physics, v. 10, p. 551-577.

Brown, G.M. and Vincent, E.A.
1963: Pyroxenes from late stages of fractionation of the Skaergaard Intrusion, East Greenland; Journal of Petrology, v. 4, p. 175-197.

Brügmann, G.E., Asif, M., Naldrett, A.J., Gorbachev, N.S., Federenko, V.A., and Lightfoot, P.C.
1991: Distribution of siderophile and chalcophile elements in the Siberian traps near Noril'sk; American Geophysical Union, Fall Meeting, San Francisco, December 1991, Abstracts with Programs, p. 571.

Buchanan, D.L.
1979: A combined transmission electron microprobe and electron microprpbe study of Bushveld pyroxenes from the Bethal area; Journal of Petrology, v. 20, p. 327-354.

Burns, R.G.
1970: Mineralogical applications of crystal field theory; Cambridge University Press, London, 244 p.

Cabri,L.J., Hulbert, L.J., Laflamme, J.H.G., Lastra, R, Sie Soey H., Ryan, C.G., and Campbell, I.J.
1993: Process mineralogy of samples from the Wellgreen Cu-Ni-Pt-Pd deposit, Yukon; Exploration and Mining Geology, v. 2, no. 2, p. 105-119.

Cabri, L.J., Laflamme, J.H.G., and Lastra, R.
1991: Process mineralogy of samples from the Wellgreen Cu-Ni-Pt-Pd deposit, Yukon; CANMET Report MSL 91-8 (CR) prepared for Galactic Resources Ltd., p. 1-37.

Cairnes, D.D.
1915: Upper White River district, Yukon; Geological Survey of Canada, Memoir 50, 175 p.

Campbell, I.H.
1973: Aspects of the petrology of the Jimberlana Layered Intrusion of Western Australia; Ph.D thesis, University of London, United Kingdom.

Campbell, I.H., Naldrett, A.J., and Barnes, S.J.
1983: A model for the origin of the platinum-rich sulphide horizons in the Bushveld and Stillwater Complexes; Journal of Petrology, v. 24, p. 133-165.

Campbell, I.H., Griffiths, R.W., and Hill, R.I.
1989: Melting in an Archean mantle plume: heads it's basalts, tails it's komatiites; Nature, v. 339, p. 697-699.

Campbell, S.W.
1981: Geology and genesis of copper deposits and associated host rocks in and near the Quill Creek area, southwestern Yukon; Ph.D. thesis, University of British Columbia, Vancouver, British Columbia, 215 p.

Cameron, E.N.
1975: Postcumulus and subsolidus equilibrium of chromite and existing silicates in the eastern Bushveld Complex; Geochimica et Cosmochimica Acta, v. 39, p. 1021-33.

Cameron, E.N. (cont.)
1977: Chromite in the central sector of the eastern Bushveld Complex; American Mineralogist, v. 62, p. 1082-1096.

Carne, R.C.
1987: Report on 1987 exploration for copper-nickel-platinum group elements, Wellgreen property, Southwestern Yukon Territory, for Hudson-Yukon Mining Company, Ltd., Chevron Minerals Ltd. and All-North Resources Ltd.; Archer, Cathro & Associates (1981) Limited, p. 1-51.
1989: Report on proposed 1989 exploration: Canalask property latitude 61°57'N; longitude 140°32'W, NTS 115F/15 for Kluane Joint Venture; Archer, Cathro & Associates (1981) Limited, p. 1-12.

Christopher, A., White, W.H., and Harakal, J.E.
1972: K-Ar dating of the Cork (Burwash Creek) Cu-Mo prospect, Burwash Landing Area, Yukon Territory; Canadian Journal of Earth Sciences, v. 9, p. 918-921.

Clark, T.
1978: Oxide minerals in the Turnagain ultramafic complex, northwestern British Columbia; Canadian Journal of Earth Sciences, v. 15, p. 1893-1903.

Clayton, R.N. and Mayeda, T.K.
1963: The use of bromine pentafluoride in the extraction of oxygen from oxide and silicates for isotopic analyses; Geochimica et Cosmochimica Acta, v. 27, p. 43-52.

Creaser, R.A., Papanastassiou, D.A., and Wasserburg, G.J.
1991: Negative thermal ion mass spectrometry of osmium, rhenium, and iridium; Geochimica et Cosmochimica Acta, v. 5, p. 397-401.

Crocket, J.H.
1981: Geochemistry of platinum-group elements; in Platinum-Group Elements: Mineralogy, Geology, Recovery, L.J. Cabri (ed.); Canadian Institute of Mining and Metallurgy, Special Volume 23, p. 47-64.

Csejtey, B., Cox, D.P., Evarts, R.C., Stricker, G.D., and Foster, H.I.
1982: The Cenozoic Denali fault system and Cretaceous accretionary development of southern Alaska; Journal of Geophysical Research, v. 87, p. 3741-3754.

Davis, A. and Plafker, G.
1985: Comparative geochemistry and petrology of Triassic basaltic rocks from the Taku terrane on Chilkat Peninsula and Wrangellia; Canadian Journal of Earth Sciences, v. 22, p. 183-194.

Davis, D.C. and Main, C.A.
1988: Geological, geophysical, geochemical and trenching report at the Mansfield and Chilkat properties, Tatshenshini River area, B.C.; Archer, Cathro & Associates (1981) Limited, p. 1-36.

Deer, W.A., Howie, R.A., and Zussman, J.
1970: An introduction to the rock forming minerals; Longman Group Ltd., London, 528 p.

DePaolo, D.J.
1981: Neodymium isotopes in the Colorado Front Range and crust-mantle evolution in the proterozoic; Nature, v. 291, p. 193-196.

DePaolo, D.J. and Wasserburg, G.J
1976: Nd isotopic variations and petrogenetic models; Geophysical Research Letters, v. 4, p. 249-252.

Dick, H.J.B. and Bullen, T.
1984: Chromian spinel as a petrogenetic indicator in abyssal and alpine-type peridotites and spatially associated lavas; Contributions to Mineralogy and Petrology, v. 86, p. 54-76.

Distler, V.V., Malevsky, A.Y., and Laputina, I.P.
1977: Distribution of platinoids between pyrrhotite and pentlandite in crystallization of a sulphide melt; Geochemical International, v. 11, p. 30-40.

Duchesne, J.C.
1972: Pyroxenes et olivines dans le massit de Bjerkrem-Sognal (Norvege meridionate) Contribution a l'etude de la serie anorthosite-mangerite; Rapport du 24^{e} Congrès géologique international, Section 2, p. 320-328.

Duke, J.M.
1979: Computer simulation of the fractionation of olivine and sulphide from mafic and ultramafic magmas; Canadian Mineralogist, v. 76, p. 507-514.

Duke, J.M. and Naldrett, A.J.
1978: A numerical model of the fractionation of olivine and molten sulphide from komatiite magma; Earth and Planetary Science Letters, v. 39, p. 255-266.

Eales, H.V. and Reynolds, I.M.
1981: Factors influencing the composition of chromite and magnetite in some southern African rocks; 1st International Congress on Applied Mineralogy, Proceedings, Geological Society of South Africa, Johannesburg, p. 1-49.

Eaton, W.D.
1987: Report on prospecting and geochemical program Duke 1-16 claims (YB06331-YB06346), Duke 17-24 claims (YB06904-YB06911), Duke 25-28 claims (YB06347-YB06350), Duke 29-44 claims (YB06912-YB06927); for Rockridge Mining Corporation; Archer, Cathro & Associates (1981) Limited, p. 1-10.
1988a: Summary report on 1988 exploration, Linda property (KLU 1-71 claims); performed for 2001 Resource Industries Ltd., Rockridge Mining Corporation and Kluane Joint Venture; Archer, Cathro & Associates (1981) Limited, p. 1-22,
1988b: Summary report on 1988 exploration, Arch property (Barny, Mus, Amp and Eugene claims); performed for Pak-Man Resources Inc., Rockridge Mining Corporation and Kluane Joint Venture; Archer, Cathro & Associates (1981) Limited, p. 1-20.

Eckstrand, O.R. and Hulbert, L.J.
1987: Selenium and the source of magmatic nickel and platinum deposits; Geological Association of Canada/Minerological Association of Canada, Joint Annual Meeting, Abstracts with Programs, v. 12, p. 40.

Eisbacher, G.H.
1976: Sedimentology of the Dezadeash flysch and its implications for strike-slip faulting along the Denali fault, Yukon Territory and Alaska; Canadian Journal of Earth Sciences, v. 13, p. 1495-1513.

Ellam, R.M., Carlson, R.W., and Shirey, S.B.
1992: Evidence from Re-Os isotopes for plume-lithosphere mixing in Karoo flood basalt genesis; Nature, v. 359, p. 718-721.

Evans, B.W. and Wright, T.L.
1972: Composition of liquidus chromite from the 1959 (Kilauea Iki) and the 1965 (Makaopuhi) eruptions of Kilauea, volcano, Hawaii; American Mineralogist, v. 57, p. 217-230.

Ewart, A.
1982: The mineralogy and petrology of Tertiary-Recent orogenic volcanic rocks: with special reference to the andesitic and basaltic compositional range; in Andesites: Orogenic Andesites and Related Rocks, R.S. Thorpe (ed.); Wiley, Chichester, p. 26-87.

Fayak, M.
1989: The petrology, geochemistry, and economic geology of the pegmatitic gabbro and skarn rock from the Wellgreen deposit, Yukon Territory; B.Sc. thesis, Carleton University, Ottawa, Ontario, 118 p.

Fedorenko, V.A.
1992: Evolution of Permian-Triassic mafic-ultramafic magmatism in the Noril'sk region (abstract); Canadian Mineralogist, v. 30, pt. 2, p. 475-476.

Floyd, P.A. and Winchester, J.A.
1975: Magma type and tectonic discrimination using immobile elements; Earth and Planetary Science letters, v. 27, p. 211-218.

Forbes, R.B., Smith, T.E., and Turner, D.L.
1974: Comparative petrology and structure of the Maclaren Ruby Range, and Coast Range belts. Implications for offset along the Denali fault system; Geological Society of America, Abstracts with Programs, 6, p. 177.

Frey, F.A., Green, D.H., and Roy, S.D.
1978: Integrated model of basalt petrogenesis: A study of quartz tholeiites to olivine melilites from South Eastern Australia utilizing geochemical and experimental petrological data; Journal of Petrology, v. 19, p. 463-513.

Genkin, A.D., Distler, V.V., Gladyshev, G.D., Filimonova, A.A., Evstigneeva, T.L., Kovalenker, V.A., Laputina, I.P., Smirnov, A.V., and Grokhovskaya, T.L.
1981: Copper-nickel sulphide ores of the Noril'sk deposits; a translation of "Sul'fidnye medno-nikelevye rudy Noril'skikh mestorozhdenii", Akademiya Nauk SSSR, Tyvestiya, Nauka, Moskva, 446 p.

Giovenazzo, D., Picard, C., and Guha, K.
1989: Tectonic setting of Ni-Cu-PGE deposits in the central part of the Cape Smith Belt; Geoscience Canada, v. 16, no. 3, p. 134-136.

Goresy, A., EL, Printz, M., and Ramdohr, P.
1976: Zoning in spinels as an indicator of crystallization histories of mare basalts; Proceedings of 7th Lunar Science Conference, p. 1261-1279.

Green A.H.
1978: Evolution of Fe-Ni sulphide ores associated with Archean ultramafic komatiites, Langmuir Township, Ontario; Ph.D. thesis, University of Toronto, Toronto, Ontario, 340 p.

Grégoire, D.C.
1988: Determination of platinum, palladium, ruthenium and iridium in geological material by inductively coupled plasma mass spectrometry with sample introduction by electrothermal vaporisation; Analytical Chemistry, v. 58, p. 616-620.

Gretener, P.E.
1969: On the mechanics of the intrusion of sills; Canadian Journal of Earth Sciences, v. 6, p. 1415-1420.

Hall, G.E.M., MacLaurin, A.I., and Vaive, J.
1986: The analysis of geological materials for fluorine, chlorine, and sulphur using pyrohydrolysis and ion chromatograph; Journal of Geochemical Exploration, v. 26, p. 177-186.

Harrison, W.J.
1981: Partitioning of REE between minerals and coexisting melts during partial melting of a garnet lherzolite; American Mineralogist, v. 66, p. 242-259.

Hart, S.R. and Kinloch, E.D.
1989: Osmium isotope systematics in Witwatersrand and Bushveld ore deposits; Economic Geology, v. 84, p. 1651-1655.

Hart, S.R. and Dunn, T.
1993: Experimental cpx/melt partitioning of 24 trace elements; Contributions to Mineralogy and Petrology, v. 113, p. 1-8.

Hartland, W.B., Armstrong, R.L., Cox, A.V., Craig, L.E., Smith, A.G., and Smith, D.G.
1989: A geologic time scale: 1989; Cambridge University Press, Cambridge, 263 p.

Haskins, L.A. and Paster, T.P.
1984: Geochemistry and mineralogy of the rare earths; in Rare Earth Element Geochemistry, Developments in Geochemistry, P. Henderson (ed.); Elsevier, p. 1-109.

Hattori, K. and Hart, S.R.
1991: Osmium-isotope ratios of platinum-group minerals associated with ultramafic intrusions: Os-isotope evolution of the oceanic mantle; Earth and Planetary Science Letters, v. 107, p. 499-514.

Hattori, K., Cabri, L.J., and Hart, S.R.
1991: Osmium isotope ratios of PGM grains associated with the Freetown layered complex, Sierra Leone, and their origin; Contributions to Mineralogy and Petrology, v. 109, p. 10-18.

Hawkesworth, C.J., O'Nions, R.K., Pankhurst, R.J., Hamilton, P.J., and Evensen, N.M.
1977: A geochemical study of island-arc and back-arc tholeiites from the Scotia Sea; Earth and Planetary Science Letters, v. 36, p. 253-262.

Henderson, P.
1975: Reaction trends shown by chrome-spinels of the Rhum layered intrusion; Geochimica et Cosmochimica Acta, v. 39, p. 1035-1044.

Hill, R. and Roeder, P.L.
1974: The crystallization of spinel from basaltic liquid as a function of oxygen fugacity; Journal of Geology, v. 82, p. 709-729.

Hill, R.E.T., Gole, M.J., and Barnes, S.J.
1989: Olivine adcumulates in the Norsemen-Wiluna greenstone belt, Western Australia: implications for the volcanology of komatiites; in Magmatic Sulphides, The Zimbabwe Volume, M.D. Prendergast and M.J. Jones (ed.); Institute of Mining and Metallurgy, p. 189-206.

Himmelberg, G.R. and Ford, A.B.
1976: Pyroxenes of the Dufek Intrusion, Antartica; Journal of Petrology, v. 62, p. 623-633.

Hoffman, E.L., Naldrett, A.J., Van Loon, J.C., Hancock, R.G.V., and Manson, A.
1978: The determination of all the platinum group elements and gold in rocks and ore by neutron activation analysis after preconcentration by nickel sulphide fire-assay technique on large samples; Analytical Chimistry Acta, v. 102, p. 157-166.

Holm, P.E.
1985: The geochemical fingerprints of different tectonomagmatic environments using hygromagmatophile element abundances of tholeiitic basalts and basaltic andesites; Chemical Geology, v. 51, p. 303-323.

Horan, M.F., Morgan, J.W., and Foose, M.P.
1991: Rhenium-osmium isotope systematics of ores rich in platinum-group elements, Noril'sk-Talnakh district, Siberia (abstract); Eos, v. 72, p. 517.

Horan, M.F., Morgan, J.W., Grauch, R.I., Coveney, R.M. Jr., Murowchick, J.B., and Hulbert, L.J.
1994: Rhenium and osmium isotopes in black shales and Ni-Mo-PGE-rich sulphide layers, Yukon Territory, Canada, and Hunan and Guizhou province, China; Geochimica et Cosmochimica Acta, v. 58, p. 257-265.

Hubbert, M.K. and Willis, D.G.
1957: Mechanics of hydraulic fracturing; Journal of Petrology, v. 9, p. 153-168.

Hughes, C.J.
1982: Igneous petrology; Elsevier, New York, 551 p.

Hulbert, L.J.
1983: A petrological investigation of the Rustenburg Layered Suite and associated mineralization south of Potgietersrus; D.Sc. thesis, University of Pretoria, 512 p.

Hulbert, L.J. and Grégoire, D.C.
1993: Re-Os isotope systematics of the Rankin Inlet Ni ores: an example of the application of ICP-MS to investigate Ni-Cu-PGE mineralization, and the potential us of Os isotopes in mineral exploration; Canadian Mineralogist, v. 31, p. 861-876.

Hulbert, L.J. and Sharpe, M.R.
1981: Stop 1: andalusite-biotite-cordierite-muscovite hornfels, Faugha Ballagh; in Third International Platinum Symposium Excursion Guidebook, C.F. Vermaak and G. Von Gruenewaldt (ed.); p. 39-41.

Hulbert, L.J., Duke, J.M., Eckstrand, O.R., Lydon, J.W., Scoates, R.F.J., Cabri, L.J., and Irvine, T.N.
1988: Geological Environments of the Platinum Group Elements; Geological Survey of Canada, Open File 1440, 148 p.

Hulbert, L.J., Duke, J.M., Eckstrand, O.R., Scoates, R.F.J., Theriault, R.J., LeCheminant, G.M., Kyser, T.K., Grinenko, L.N., Williamson, B., Gallagher, M., and Gunn, G.
1992a: Metallogenesis and geochemical evolution of cyclic unit 1, lower Eastern Layered Series, Rhum; in Mineral Deposit Modelling in Relation to Crustal Reservoirs of the Ore Forming Elements, R.P. Foster (ed.); Institute of Mining and Metallurgy, Extended Abstracts.

Hulbert, L.J., Grégoire, D.C., Paktunc, D., and Carne, R.C.
1992b: Sedimentary nickel, zinc, and platinum-group element mineralization in Devonian black shales at the Nick property, Yukon Canada: a new deposit type; Exploration and Mining Geology, v. 1, no. 1 p. 39-62.

Irvine, T.N.
1970: Crystallization sequences in the Muskox intrusion and other layered intrusions; Transactions of the Geological Society of South Africa, Special Publication 1, p. 441-474.
1982: Terminology for layered intrusions; Journal of Petrology, v. 23, part 2, p. 127-162.

Irvine, T.N. and Baragar, W.R.A.
1971: A guide to the chemical classification of the common volcanic rocks; Canadian Journal of Earth Sciences, v. 8, p. 523-548.

Jones, D.L., Silberling, N.J., and Hillhouse, J.
1977: Wrangellia- A displaced terrane in northwestern North America; Canadian Journal of Earth Sciences, v. 14, p. 2565-2577.

Koide, M., Hodge, V., Yang, Jae S., and Goldberg, E.D.
1987: Determination of rhenium in marine waters and sediments by graphite furnace atomic absorption spectrometry; Analytical Chemistry, v. 59, p. 1802-1805.

Komar, P.D.
1972a: Mechanical interaction of phenocrysts and flow differentiation of igneous dikes and sills; Geological Society of America Bulletin, v. 83, p. 973-988.
1972b: Flow differentiation in igneous dikes and sills – profiles of velocity and phenocryst concentration; Geological Society of America Bulletin, v. 83, p. 3443-3448.

Lambert, D.D., Morgan, J.W., Walker, R.J., Shirey, S.B., Carlson, R.W., Zientek, M.L., and Koski, M.S.
1989: Rhenium-osmium and samarium-neodymium isotopic systematics of the Stillwater Complex; Science, v. 244, p. 1169-1174.

Lightfoot, P.C. and Naldrett, A.J.
1983: The geology of the Tabankulu section of the Insizwa Complex, Transkei, Southern Africa, with reference to the nickel sulphide potential; Transactions of the Geological Society of South Africa, v. 86, p. 169-187.

Lindner, M., Leich, D.A., Russ, G.P., Bazan, D., and Borg, R.J.
1989: Direct determination of the half-life of ^{187}Re; Geochimica et Cosmochimica Acta, v. 53, p. 1597-1606.

Loftus Hills, G. and Solomon, M.
1967: Cobalt, nickel and selenium in sulphides as an indicator of ore genesis; Mineralium Deposita, v. 2, p. 228-242.

Luck, J.-M. and Allègre, C.J.
1983: Rhenium and osmium systematics in meteorites and cosmochemical consequences; Nature, v. 302, p. 130-132.
1984: ^{187}Re-^{187}Os investigation in sulphide from Cape Smith komatiite; Earth and Planetary Science Letters, v. 68, p. 205-208.

MacKevett, E.M., Jr.
1971: Stratigraphy and general geology of the McCarthy C-5 quadrangle, Alaska; United States Geological Survey, Bulletin 1321, 35 p.

Main, C.A. and Davis, D.C.
1989: Report on geophysical and geochemical surveys: Onion 1-13, Onion 14-25, NTS 115F/15 and 115k/2 latitude 62°00'N; longitude 140°37'W; performed for Rexford Minerals Ltd. and Kluane Joint Venture; Archer, Cathro & Associates (1981) Limited, p. 1-21.

Mainwaring, P.F.
1975: The petrology of a sulphide-bearing layered intrusion at the base of the Duluth Complex, St. Louis County, Minnesota; Ph.D. thesis, University of Toronto, Toronto, Ontario, p. 253.

Marcantonio, F., Reisberg, L., Zindler, A., Hulbert, L.J., England, J., and Wyman, D.
1991: Re-Os isotope evidence for the genesis of the Wellgreen Ni-Cu-PGE deposit (abstract); Eos, v. 72, p. 530.

Marcantonio, F., Reisberg, L., Zindler, A., Wyman, D., and Hulbert, L.J.
1993: An isotopic study of the Ni-Cu-PGE-rich Wellgreen intrusion of the Wrangellia Terrane: evidence for hydrothermal mobilization of Re and Os; Geochimica et Cosmochimica Acta, v. 58, p. 1007-1017.

Martin, C.E.
1989: Re-Os isotope investigation of the Stillwater Complex, Montana; Earth and Planetary Science Letters, v. 93, p. 336-344.
1991: Osmium isotopic characteristics of mantle-derived rocks; Geochimica et Cosmochimica Acta, v. 55, p. 1421-1434.

McCallum, I.S., Raedeke, L.D., and Mathez, E.A.
1980: Investigation of the Stillwater Complex: Part I. Stratigraphy and structure of the banded zone; American Journal of Science, v. 280-A, p. 59-87.

McCandless, T.E. and Ruiz, J.
1990: Osmium isotope characteristics of the UG-2 and UG-1 chromitites, Bushveld Igneous Complex, South Africa (abstract); Eos, v. 71 (43), p. 1421.

McConnell, R.G.
1905: The Kluane mining district; Geological Survey of Canada, Annual Report, 1904, v. 16, p. 1A-18A.

McDonough, W.F. and Sun, S.-S.
1995: The composition of the Earth; Chemical Geology, v. 120, p. 223-253.

Merkle, R.
1986: Compositional variation of Co-rich pentlandite: Relation to the evolution of the upper zone of the western Bushveld Complex, South Africa; Canadian Mineralogist, v. 24, p. 529-546.

Miller, A.
1977: Petrogenesis of the 2-3 sill and related rocks, New Quebec; PhD. thesis, University of Western Ontario, London, Ontario, 218 p.

Miller, S.
1991: Geology, petrology and geochemistry of the host rocks and associated Ni-Cu-PGE disseminated mineralization of the Wellgreen deposit, Kluane Ranges, Yukon Territory; M.Sc. thesis, McMaster University, Hamilton, Ontario, 249 p.

Monger, J.W.H.
1977a: Upper Paleozoic rocks of the western Canadian Cordillera and their bearing on Cordilleran evolution; Canadian Journal of Earth Sciences, v. 14, p. 1832-1859.
1977b: The Triassic Takla Group in McConnell Creek map-area, north-central British Columbia; Geological Survey of Canada, Paper 76-29, 45 p.
1984: Cordilleran tectonics: a Canadian perspective; Sociète géologique de France, Bulletin (7) XXXVI, no. 2, p. 255-278.

Mortensen, J.K and Hulbert, L.J.
1991: A U-Pb zircon age for a Maple Creek gabbro sill, Tatamagouche Creek area, southwest Yukon Territory; in Radiogenic Age and Isotopic Studies: Report 5; Geological Survey of Canada, Paper 91-2, p. 175-179.

Mortimer, N.
1986: Late Triassic arc-related, potassic igneous rocks in the North American Cordillera; Geology, v. 14, p. 1035-1038.
1987: The Nicola Group: Late Triassic and Early Jurassic subduction-related volcanism in British Columbia; Canadian Journal of Earth Sciences, v. 24, p. 2521-2536.

Muir, J.E. and Comba, C.D.A.
1979: The Dundonald deposit- an example of volcanic-type nickel-sulphide mineralization; Canadian Mineralogist, v. 17, p. 351-359.

Muller, J.E.
1967: Kluane Lake map-area, Yukon Territory (115G, 115F/E 1/2); Geological Survey of Canada, Memoir 340, 137 p.

Nakamura, N.
1974: Determination of REE, Ba, Fe, Mg, Na, and k in carbonaceous and ordinary chondrites; Geochimica et Cosmochimica Acta, v. 38, p. 757-775.

Naldrett, A.J.
1981a: Nickel sulphide deposits: Classification, composition and genesis; Economic Geology, 75th Anniversary Volume, p. 628-685.
1981b: Pt group element deposits; in Platinum Group Elements: Mineralogy, Geology, Geochemistry, L.C. Cabri, (ed.); Canadian Institute of Mining and Metallurgy, Special Volume 23, p. 197-232.
1989: Ores associated with flood basalts; in Ore Deposits Associated with Magmas, J.A. Whitney and A.J. Naldrett (ed.); Reviews in Economic Geology, v. 4, p. 103-118.
1992: A model for the Ni-Cu-PGE ores of the Noril'sk region and its application to other areas of flood basalt; Economic Geology, v. 87, no. 8, p. 1945-1962.

Naldrett, A.J. and Turner, A.R.
1977: The geology and petrogenesis of a greenstone belt and related nickel sulphide mineralization at Yakabindie, Western Australia; Precambrian Research, v. 5, p. 43-103.

Naldrett, A.J., Bray, G., Gasparrini, E.L., Podolsky, T., and Rucklege, J.C.
1970: Cryptic variation and petrology of the Sudbury Nickel Irruptive; Economic Geology, v. 65, p. 122-155.

Naldrett, A.J., Innes, D.G., Sowa, J., and Gorton, M.P.
1982: Compositional variations within and between five Sudbury ore deposits; Economic Geology, v. 77, p. 1519-1534.

Naldrett, A.J., Hoffman, E.L., Green, A.H., Chou, C.L., Naldrett, S.R., and Alcock, R.A.
1979: The composition of Ni-sulphide ores, with particular reference to their PGE and Au; Canadian Mineralogist, v. 17, p. 403-416.

Naldrett, A.J., Lightfoot, P.C., Fedorenko, V., Doherty, W., and Gorbachev, N.S.
1992: Geology and geochemistry of intrusions and flood basalts of the Noril'sk region, USSR, with implications for the origin of the Ni-Cu ores; Economic Geology, v. 87, no. 4, p. 975-1004.

O'Hara, M.J.
1968: The bearing of phase equilibria studies in synthetic and natural systems on the origin and evolution of basic and ultrabasic rocks; Earth Science Reviews, v. 4, p. 69-133.

Page , N.J. and Talkington, R.W.
1984: Palladium, platinum, rhodium, ruthenium and iridium in peridotites and chromitites from ophiolite complexes from Newfoundland; Canadian Mineralogist, v. 22, p. 137-149.

Page, N.J., Aruscavage, P.J., and Haffty, J.
1983: Platinum-group elements in rocks from the Voikar-Syninsky ophiolite complex, Polar Urals, USSR; Mineralium Deposita, v. 18, p. 443-455.

Page, N.J., Cassard, D., and Haffty, J.
1982a: Palladium, platinum, rhodium, ruthenium and iridium in chromitites from the Massif du Sud and Teibaghi Massif, New Caledonia; Economic Geology v. 77, p. 1571-1577.

Page, N.J., Pallister, J.S., Brown, M.A., Smewing, J.D., and Haffty, J.
1982b: Palladium, platinum, rhodium, iridium and ruthenium in chromite-rich rocks from the Samail Ophiolite, Oman; Canadian Mineralogist, v. 20, p. 537-548.

Page, N.J., Singer, D.A., Moring, B.C., Carlson, C.A., McDade, J.M., and Wilson, S.A.
1986: Platinum-group element resources in podiform chromitites from California and Oregon; Economic Geology, v. 81 p. 1261-1271.

Paktunc, A.D., Hulbert, L.J., and Harris, D.C.
1990: Partitioning of the platinum-group and other trace elements in sulphides from the Bushveld Complex and other Canadian occurrences of nickel-copper sulphides; Canadian Mineralogist, v. 28, p. 475-488.

Pearce, J.A.
1982: Trace element characteristics of lavas from destructive plate boundaries; in Andesites: Orogenic Andesites and Related Rocks, R.S. Thorpe (ed.); Wiley, Chichester, p. 525-548.

Pearce, J.A. and Cann, J.R.
1971: Ophiolite origin investigated by discriminant analysis using Ti, Zr and Y; Earth and Planetary Science Letters, v. 12, p. 339-349.

Pearce J.A. and Gale, G.H.
1977: Identification of ore deposition environments from trace element geochemistry of associated igneous host rocks; in Volcanic Processes in Ore Genesis; Institute of Mining and Metallurgy, London, p. 14-24.

Pearce, T.H., Gorman, B.E., and Birkett, T.C.
1977: The relationship between major element chemistry and tectonic environment of basic and intermediate volcanic rocks; Earth and Planetary Science Letters, v. 36, p. 121-132.

Poplavko, Ye. M., Ivanov, V.V., Longinova, L.G., Orekhov, V.S., Miller, A.D., Nazarempl, I.I., Nishankhodzhayev, R.N., and Tarkhov, Yu. A.
1977: Behaviour of rhenium and other metals in combustible central Asian shales; Geokhimiya, v. 2, p. 273-283.

Preto, V.A.
1977: The Nicola group: Mesozoic volcanism related to rifting in southern British Columbia; in Volcanic regimes in Canada, W.R.A. Baragar, L.C. Coleman, and J.M. Hall (ed.); Geological Association of Canada, Special Paper 16, p. 39-57.

Rankama, K. and Sahama, Th.G
1950: Geochemistry; University of Chicago Press, Chicago, U.S.A., 912 p.

Ravizza, G. and Turekian, K.K.
1989: Application of ^{187}Re-^{187}Os system to black shale geochemistry; Geochimica et Cosmochimica Acta, v. 53, p. 3257-3262.

Ravizza, G., Hay, B.J., and Turekian, K.K.
1988: Re and Os geochemistry in Black Sea sediments (abstract); Eos, v. 69, p. 1242.

Read, P.B. and Monger, J.W.H.
1976: Pre-Cenozoic volcanic assemblages of the Kluane and Alsek Ranges, southwestern Yukon Territory; Geological Survey of Canada, Open File 381, 96 p.

Reisberg, L.C., Allègre, C.J., and Luck, J.-M.
1991: The Re-Os systematics of the Ronda ultramafic complex of southern Spain; Earth and Planetary Science Letters, v. 105, p. 196-213.

Reisberg, L., Zindler, A., Marcantonio, F., White, W., Wyman, D.A., and Weaver, B.
1993: Os isotope systematics in ocean island basalts; Earth and Planetary Science Letters, v. 120, no. 3-4, p. 149-167.

Richards, M.A., Jones, D.L., Duncan, R.A., and DePaolo, D.J.
1991: A mantle plume initiation model for the Wrangellia flood basalt and other oceanic plateaus; Science, v. 254, p. 263-267.

Richter, D.H., Lanphere, M.A., and Matson, N.A., Jr.
1975: Granitic plutonism and metamorphism in the eastern Alaska Range; United States Geological Survey, Professional Paper 975, p. 68.

Richter, D.H. and Dutro, J.T., Jr.
1975: Revision of the type Mankomen Formation (Pennsylvanian and Permian) Eagle Creek Area, eastern Alaska Range, Alaska; United States Geological Survey, Bulletin 1396-B, B25 p.

Roach, T.A.
1992: Formation and evolution of the Main Chromitite, Muskox layered intrusion, Northwest Territories; M.Sc. thesis, Queen's University, Kingston, Ontario, 155 p.

Roeder, P.L. and Campbell, I.H.
1985: The effects of postcumulus reactions on compositions of chrome-spinels from the Jimberlana Intrusion; Journal of Petrology, v. 26, p. 763-786.

Roeder, P.L. and Emslie, R.F.
1970: Olivine-liquid equilibrium; Contributions to Mineralogy and Petrology, v. 29, p. 275-282

Ross, J.R. and Hopkins, G.M.F.
1975: Kambalda nickel sulphide deposits; in Economic Geology of Australia and Papua New Guinea, I., Metals, C.F. Knight (ed.); Australasian Institute of Mining and Metallurgy, Melbourne, Monograph 5, p. 100-121.

Rousseau, R.M.
1989a: Concepts of influence coefficients in XRF analysis and calibration; Advances in X-Ray Analysis, v. 32, p. 77-82.
1989b: Painless XRF analysis using new generation computer programs; Advaces in X-Ray Analysis, v. 32, p. 69-75.

Ruiz, J. and McCandless, T.E.
1990: Osmium isotope systematics in the Bushveld Complex; in Seventh International Conference on Geochronology, Cosmochronology and Isotope Geology; Abstracts with programs, Geological Society of Australia, v. 27, p. 86.

Sabine, P.A.
1974: How should rocks be named?; Geological Magazine, v. 111 (2), p. 165-176.

Samson, S.D., McClelland, W.C., Patchett, P.J., Gehrels, G.E., and Anderson, R.G.
1989: Evidence from neodynium isotopes for mantle contributions to Phanerozoic crustal genesis in the Canadian Cordillera; Nature, v. 337, no. 23, p. 705-709.

Samson, S.D., Patchett, P.J., Gehrels, G.E., and Anderson, R.G.
1990: Nd and Sr isotopic characterization of the Wrangellia Terrane and implications for crustal growth of the Canadian Cordillera; Journal of Geology, v. 98, p. 749-762.

Schilling, J.-G., Zajac, M., Evans, R., Johnston, T., and White, W.
1983: Petrologic and geochemical variations along the Mid-Atlantic Ridge from 27°N to 73°N; American Journal of Science, v. 283, p. 510-586.

Scowen, P.A.H., Roeder, P.L., and Helz, R.T.
1991: Re-equilibration of chromite within Kilauea Iki lava lake, Hawaii; Contributions to Mineralogy and Petrology, v. 107, p. 8-20.

Sen Gupta, J.G. and Grégoire, D.C.
1989: Determination of ruthenium, palladium, and iridium in 27 international reference silicate and iron-formation rocks, ores and related materials by inductively-coupled plasma mass spectrometry; Geostandards Newsletter, v. 13, p. 197-204.

Sharp, R.P.
1943: Geology of the Wolf Creek area, St. Elias Range, Yukon Territory, Canada; Bulletin of the Geological Society of America, v. 54, p. 625-649.

Shervais, J.W.
1982: Ti-V plots and the petrogenesis of modern and ophiolitic lavas; Earth and Planetary Science Letters, v. 59, p. 101-118.

Shirey, S.B. and Carlson, R.W.
1991: The Re-Os isotopic system: new applications in geochemistry at DTM; Carnegie Institute Washington, Year Book 90, p. 58-75.

Smith, J.G. and MacKevett, E.M., Jr.
1970: The Skolai Group in the McCarthy B-4, C-4, and C-5 quadrangles, Wrangell Mountains, Alaska; United States Geological Survey, Bulletin 1274-Q, p. Q1-Q26.

Smol'kin, V.F. and Pakhomovskiy, Ya. A.
1985: The petrogenetic significance of the olivine-chrome spinelide assemblage in Pechenga ultramafics; International Geological Reviews, v. 27, p. 709-726.

Souther, J.G.
1977: Volcanism and tectonic environments in the Canadaian Cordillera – A second look; in Volcanic Regimes in Canada, W.R.A. Baragar, L.C. Coleman, and J.M. Hall, (ed.); Geological Association of Canada, Special Paper 16, p. 3-24.

Sun, S.-S.
1980: Lead isotopic study of young volcanic rocks from mid-ocean ridges, ocean islands and island arcs; Philosphical Transactions of the Royal Society of London, v. A297, p. 409-445.

Thompson, J.F.H.
1982: The intrusion and crystallization of mafic magmas, central Maine and genesis of their associated sulphides; Ph.D. thesis, University of Toronto, Toronto, Ontario.

Thompson, M. and Walsh, J.N.
1983: A Handbook of Inductively Coupled Plasma Spectrometry; Blackie & Sons Ltd., Glasgow, Scotland, 273 p.

Thompson, R.N., Morrison, M.A., Dicken, A.P., and Hendry, G.L.
1983: Continental flood basalts... arachnids rule OK?; in Continental Basalts and Mantle Xenoliths, C.J. Hawksworth and M.J. Norry (ed.); Nantwich, Shiva., p. 158-85.

Tipper, H.W.
1981: Offset of an upper Pliensbachian geographic zonation in the North American Cordillera by transcurrent faulting; Canadian Journal of Earth Sciences, v. 18, p. 1788-1792.

Tozer, E.T.
1982: Marine Triassic faunas of North America: their significance in assessing plate and terrane movements; Geologische Rundschau, v. 17, p. 1077-1104.

Ulff-Møller, F.
1985: Solidification history of the Kitdlît Lens; Immiscible metal and sulphide liquids from a basaltic dyke on Disko, central West Greenland; Journal of Petrology, v. 26, part 1, p. 64-91.

Wager, L.R. and Brown, G.M.
1968: Layered igneous rocks; Oliver and Boyd, London, 588 p.

Walker, D., Shibata, T., and DeLong, S.E.
1979: Abyssal tholeiites from the Oceanographer Fracture Zone; Contributions to Mineralogy and Petrology, v. 70, p. 111-125.

Walker, R.J. and Morgan, J.W.
1989: Rhenium-osmium systematics of carbonaceous chondrite; Science, v. 243, p. 519-522.

Walker, R.J., Carlson, R.W., Shirey, S.B., and Boyd, F.R.
1989: Os, Sr, Nd, and Pb isotope systematics of southern African peridotite xenoliths: Implications for the chemical evolution of subcontinental mantle; Geochimica et Cosmochimica Acta, v. 53, p. 1583-1595.

Walker, R.J., Echeverría, L.M., Shirey, S.B., and Horan, M.F.
1991b: Re-Os isotopic constraints on the origin of volcanic rocks, Gorgona Island, Columbia: Os isotopic evidence for ancient heterogeneities in the mantle; Contributions to Mineralogy and Petrology, v. 107, p. 150-162.

Walker, R.J., Morgan, J.W., Horan, M.F., Czamanske, G.K., Likhachev, A.P., and Kunilov, V.E.
1992: Rhenium-osmium isotopic systematics of ores rich in platinum-group elements, Noril'sk – Talnakh district, Siberia (abstract); Canadian Mineralogist, v. 30, p. 408-409.

Walker, R.J., Morgan, J.W., Naldrett, A.J., Li, C., and Fassett, J.D.
1991a: Re-Os systematics of Ni-Cu sulphide ores, Sudbury Igneous Complex, Ontario: evidence for a major crustal component; Earth and Planetary Science Letters, v. 105, p. 416-429.

Walker, R.J., Shirey, S.B., and Stecher, O.
1988: Comparative Re-Os, Sm-Nd and Rb-Sr isotope and trace element systematics for Archean komatiite flows from Munro Township, Abitibi Belt, Ontario; Earth and Planetary Science Letters, v. 87, p. 1-12.

Wang, P. and Glover, L., III
1992: A tectonic test of the most commonly used geochemical discriminant diagrams and patterns; Earth Science Reviews, v. 33, p. 111-131.

Whittaker, P.J.
1982: Chromite occurrences in ultramafic rocks in the Mitchell Range, central British Columbia; in Current Research, Part A; Geological Survey of Canada, Paper 82-1A, p. 239-245.
1984: Origin of chromite in dunitic layers of the Mt. Sydney-Williams ultramafic rock complex, British Columbia; Ottawa-Carleton Centre for Geoscience Studies, Paper 08-84, p. 217-228.

Whittaker, P. and Watkinson D.H.
1981: Chromite in some ultramafic rocks of the Cache Creek Group, British Columbia; in Current Research, Part A; Geological Survey of Canada, Paper 81-1A, p. 349-355.

Williams, D.A.C.
1979: The association of some nickel sulphide deposits with komatiitic volcanism in Rhodesia; Canadian Mineralogist, v.17, p. 337-349.

Wilson, A.H.
1982: The geology of the Great Dyke, Zimbabwe: the ultramafic rocks; Journal of Petrology, v. 23, p. 240-92.

Wilson, H.D.B., Kilburn, L.C., Graham, A.R., and Ramlal, K.
1969: Geochemistry of some Canadian nickeliferous ultramafic intrusions; Economic Geology, Monograph 4, p. 294-309.

Wilson, M.
1989: Igneous Petrogenesis; Unwin Hyman Ltd., London. 466 p.

Wood, D.A., Joron, J.L., and Treuil, M.
1979: A reappraisal of the use of trace elements to classify and discriminate between magma series erupted in different tectonic settings; Earth and Planetary Science Letters, v. 45, p. 326-336.

Zindler, A., Staudigel, H., and Batiza, R.
1984: Isotope and trace element geochemistry of young pacific seamounts: implications for the scale of upper mantle heterogeneity; Earth and Planetary Science Letters, v. 70, p. 175-195.

Appendix 1

Analytical Methods

Major element oxides and the trace elements (Ba, Nb, Rb, Sr, Y, and Zr) were determined by XRF, following the procedure of Rousseau (1989a,b), whereas Be, Co, Cr, La, Ni, Pb, V, Yb, and Zn were analyzed by inductively coupled plasma emission spectrometry (ICP-ES) following the methods of Thompson and Walsh (1983). Standard chemical methods were used to analyze for FeO, $H_2O(t)$, and CO_2. Trace-element data are generally accurate to within ±5% of the given concentration, except that Pb is accurate to ±10%. F, Cl, and S were analyzed using pyrohydrolysis and ion chromatography (Hall et al., 1986). The limits of detection are 50, 100, and 50 ppm, respectively, and have precision averages of ±5% relative standard deviation at levels greater than 100 ppm up to per cent amounts. The metalloids As, Bi, Sb, Se, and Te were analyzed by hydride generation quartz-tube atomic absorption spectrophotometry (AAS) following digestion in aqua regia and separation from potentially interfering base metals by co-precipitation with $La(OH)_3$. This method has a detection limit of 0.01 ppm. Rare earth elements were analyzed by ICP-MS and have a detection limit of 20 ppb.

Initially, all samples for PGE analyses were crushed and ground into rock powder (<300 mesh) at the GSC chemical preparation laboratories. Subsequent PGE+Au analyses were performed at two different laboratories. Pt, Pd, Au, and Rh analyses, using ICP-MS after preconcentration in a 10 g sample in a Pb bead by fire-assay techniques was undertaken at Acme Laboratories Ltd., Vancouver. The limits of detection for Pt, Pd, Au, and Rh are 1, 1, 1 and 2 ppb, respectively. Mineralized samples from this group were also analyzed for Os, Ir, Ru, Rh, Pt, Pd, Au, and Re by INAA subsequent to preconcentration in a Ni-sulphide bead by fire-assay techniques (Nuclear Activation Services Ltd., Hamilton) according to the method of Hoffman et al. (1978). Limits of detection for this method are 3, 0.1, 5, 1, 5, 5, 2, and 5 ppb respectively. Within the constraints imposed by the various analytical detection limits for the various PGEs, more than 95% of the samples were in excellent agreement. Unmineralized basalt and chilled margin material were analyzed at the GSC by isotope-dilution ICP-MS techniques following an HF-aqua regia digestion and Te co-precipitation (Grégoire, 1988; Sen Gupta and Grégoire, 1989). Limits of detection for Pt, Pd, Ru, Ir, Rh, and Au are 0.1, 0.01, 0.05, 0.05, 0.1, and 0.15 ppb.

Mineralogical identifications and compositions were determined on a Cameca, CAMEBAX-electron microprobe by wavelength-dispersion, using synthetic and natural mineral standards, and pure metals for Ni and Co. Operating conditions were 15kV accelerating voltage, at a regulated beam current of 39 nA. Counting time of 10 seconds was extended to 20 seconds for Ni to improve the detection limits. The major element oxides: SiO_2, Al_2O_3, Cr_2O_3, FeO, MgO, CaO, Na_2O, K_2O, MnO, and TiO_2 were determined on all phases. In addition NiO, CoO, ZnO, and V_2O_3 analyses were conducted on spinels; BaO, SrO, and Fe_2O_3 analyses on feldspar, NiO and CoO on pyroxene and olivine.

Bulk pyrrhotite-pentlandite-chalcopyrite concentrates were extracted from mineralized samples by a combination of magnetic and heavy-liquid separations. The concentrates were then analyzed at the Ottawa-Carleton-GSC Centre for Geoscience Studies (OCCGS/GSC) stable isotope laboratory, and have a precision of 0.2‰.

Rb, Sr, Sm, and Nd isotopes were determined on the same sample powders for which Re and Os results were obtained. All isotopic data reported from this study were analyzed at the Lamont-Doherty Earth Observatory of Columbia University (Marcantonio et al., 1993). The analytical techniques used are the same as those described by Zindler et al. (1984) and Reisberg et al. (1993).

The Re-Os results from all samples from the Wellgreen property of the Quill Creek Complex were analyzed at the Lamont-Doherty Earth Observatory of Columbia University (Marcantonio et al., 1993). Single aliquots of the same sample were often analyzed several times on the mass spectrometer to test the reproducibility of the negative thermal ionization mass spectrometric (NTIMS) technique (Creaser et al., 1991). For practical reasons not all of the data appear in Table 6 (see Appendix I of Marcantonio et al., 1993 for full details). Different splits of the same sample have somewhat different concentrations of Re and Os (up to 59% in Os and 31% in Re). However, where the Re/Os ratio in one split was higher than another, the measured $^{187}Os/^{186}Os$ ratio was also higher. This sample heterogeneity is representative of the so-called "nugget effect" seen by many workers in the field (e.g. Walker et al., 1988; Walker and Morgan, 1989; Lambert et al., 1989). This "nugget effect" is a reasonable expectation for the Wellgreen samples because

the sulphides contain high Re and Os concentrations and may not be evenly distributed among the rock powder aliquots. Replicate initial Os isotope ratios (measured on separate powder aliquotes), however, are always reproducible to better than 5%.

Oxygen isotopic studies were performed on seven selected whole rock powders (mineralized gabbro and peridotite (wehrlite)) at the University of Saskatchewan stable isotope laboratory under the direction of T.K. Kyser. Oxygen was extracted from 10 mg samples by reaction with BrF_5 (Clayton and Mayeda, 1963). The $\delta^{18}O$ values, reported relative to Standard Mean Ocean Water (SMOW), have a precision of ±0.2‰.

Appendix 2

List of abbreviations in text and diagrams

Pl = plagioclase, Ol = olivine, Cpx = clinopyroxene, Opx = orthopyroxene, Chr = chromite, Q = quartz

Mg# = $Mg/(Mg+Fe^{2+})$; Ca# = Ca/(Ca+Na+K) in plagioclase

CIPW = Cross-Iddings-Pearson-Washington norm calculation

PGE = Platinum Group Element; PGM = Platinum Group Mineral

ppm = parts per million; ppb = parts per billion; ‰ = per mil; % = per cent

ID = isotope dilution

ICP-MS = inductively coupled plasma mass spectrometry

ICP-ES = inductively coupled plasma emission spectrometry

R = silicate magma/sulphide liquid mass ratio (Campbell et al., 1983)

S/Se x 1000= the absolute S/Se value is equal to the x-axis value times 1000

REE = Rare Earth Element; LREE (light-REE); HREE (heavy-REE)

cn = chondrite normalized REE

H- = hygromagmatophile element patterns (Holm, 1985)

CMAS = tetrahedral system $CaO-MgO-Al_2O_3-SiO_2$ (O'Hara, 1968)

(*r*) = statistical correlation coefficient (Pearson)

(*n*) = number of samples; vol.= volume; wt. = weight

D = distribution coefficient for chemical elements

$\overline{X}$ = arithmetic mean

m/Ma = metres per million years

ε_{Nd} = epsilon Nd (DePaolo and Wasserburg, 1976); percentage difference between the Nd isotopic composition at any time (T) and a reference mantle value at that time.

γ_{Os} = gamma Os (Walker et al., 1989); percentage difference between the Os isotopic composition at any time (T) and a reference mantle value at that time.

CHUR = chondritic uniform reservoir; I or (i)= initial isotopic ratio.

ALM = Os isotopic evolution curve of the mantle based on osmiridium alloy (Allègre and Luck, 1980).

MSWD = mean square of weighted deviations (Brooks et al., 1972); a measure of the goodness of fit of isotopic data points about a regression curve. If MSWD is ≥ 2.5 data points represent an errorchron and ≤ 2.5 an isochron.

Quill Creek Complex (*QCC*), Ungava (*U*) (Ungava or Cape Smith), Bushveld Igneous Complex *(BIC)*, Stillwater Complex (*SWC*), Sudbury Igneous Complex (*SIC*), Bird River Complex (*BRC*).

GSC = Geological Survey of Canada.

OIT = ocean-island tholeiite; CT = continental tholeiite; OFT = ocean-ridge and floor basalt; LKT = tholeiite from island arcs and continental margins; BAT = back-arc tholeiite; IRT = initial rift tholeiite; MORB = mid-ocean ridge basalt; E-MORB = enriched MORB.

Well = Wellgreen deposit; Mcg = Maple Creek gabbro (A, W, intruding Arch and Wellgreen, respectively); Vol = Nikolai volcanic rocks (A, Y, from Alaska and Yukon, respectively).

DDH = diamond-drill hole.

Metres (m); kilometre (km); millimetre (mm); micron (μm).

Abbreviations used in diagrams for ages and lithology

Miocene to Pliocene – Wrangell lava (Mw): basaltic to andesitic flows with minor acidic pyroclastic rocks.

Paleocene – Amphitheatre Formation (Os): sandstone, siltstone, and conglomerate.

Oligocene – felsite (O): felsite and latite porphyry (f).

Cretaceous – Kluane Range intrusions (K): diorite (di), granodiorite (g).

Jurassic/Cretaceous – Dezadeash Group (JKD): greywacke, sandstone, and siltstone.

Triassic – McCarthy Formation: argillaceous limestone and argillite (m).

Nikolai Group (TR): basalt (b), argillite (a); Maple Creek gabbro (Mcg): spotted anorthositic gabbro (Gs), coarse-grained to pegmatitic gabbro (Gp).

Kluane mafic-ultramafic intrusions: dunite (D), peridotite (Prd), feldspathic peridotite (Pf), olivine clinopyroxenite and clinopyroxenite (Cp), marginal gabbro (G), basal gabbro (GBc); gabbroic cumulate from basal portion of ultramafic zone of the Tatamagouche Creek Complex, SK (skarn).

Permian – Hasen Creek Formation (PR): limestone (c), argillite (a), siltstone (s), tuff (tq), chert (q).

Pennsylvanian – Station Creek Formation (P): basaltic agglomerate or breccia (ag), tuff (t), chert (q), andesitic flows (av).

Devonian – (D): marble/limestone (c), phyllite and greenstone (cp).

Abbreviations used in diagrams

Ultramafic, UM; gabbro, G; olivine gabbro, Gb(O); massive sulphide, MS; semi-massive sulphide, SMS; magnetite gabbro, Gb(mag); anorthositic gabbro, An(G); gabbroic anorthosite, Gb(An); mineralized gabbro, G(Min); pegmatitic gabbro, Gb(P); melanocratic gabbro, Gb(Mel); Maple Creek gabbro dyke, Mcg(d); country rock, CR; intercumulus, i/c; unknown, x; alteration, alt.